University of Bath

PHD

Near-ultraviolet radiation-induced lipid peroxidation and membrane effects in Escherichia coli and human skin fibroblasts

Chamberlain, Jacqueline

Award date:
1987

Awarding institution:
University of Bath

Link to publication

General rights
Copyright and moral rights for the publications made accessible in the public portal are retained by the authors and/or other copyright owners and it is a condition of accessing publications that users recognise and abide by the legal requirements associated with these rights.

- Users may download and print one copy of any publication from the public portal for the purpose of private study or research.
- You may not further distribute the material or use it for any profit-making activity or commercial gain
- You may freely distribute the URL identifying the publication in the public portal ?

Take down policy
If you believe that this document breaches copyright please contact us providing details, and we will remove access to the work immediately and investigate your claim.

Download date: 13. May. 2019

NEAR-ULTRAVIOLET RADIATION-INDUCED LIPID PEROXIDATION AND MEMBRANE EFFECTS IN *ESCHERICHIA COLI* AND HUMAN SKIN FIBROBLASTS

Submitted by Jacqueline Chamberlain, B.Sc.

for the degree of Doctor of Philosophy

of the University of Bath

1987

This research has been carried out in the School of Pharmacy and Pharmacology of the University of Bath under the supervision of S.H. Moss, M.Sc., Ph.D., M.P.S.

Copyright

Attention is drawn to the fact that copyright of this thesis rests with its author. This copy of the thesis has been supplied on condition that anyone who consults it is understood to recognise that its copyright rests with its author and that no quotation from the thesis and no information derived from it may be published without the prior written consent of the author.

This thesis may be made available for consultation within the University Library and may be photocopied or lent to other libraries for the purposes of consultation.

SIGNED: J Chamberlain

UMI Number: U002765

All rights reserved

INFORMATION TO ALL USERS
The quality of this reproduction is dependent upon the quality of the copy submitted.

In the unlikely event that the author did not send a complete manuscript
and there are missing pages, these will be noted. Also, if material had to be removed,
a note will indicate the deletion.

UMI U002765
Published by ProQuest LLC 2013. Copyright in the Dissertation held by the Author.
Microform Edition © ProQuest LLC.
All rights reserved. This work is protected against
unauthorized copying under Title 17, United States Code.

ProQuest LLC
789 East Eisenhower Parkway
P.O. Box 1346
Ann Arbor, MI 48106-1346

UNIVERSITY OF BATH
LIBRARY
93
- 7 JUL 1988
PHARM
5022340

To **my family**

CONTENTS

ACKNOWLEDGEMENTS

I would like to thank my supervisor, Dr. S.M. Moss for giving me the opportunity to do this research and for his guidance during the work.

I thank all my friends and colleagues for moral support, constructive discussion and criticism during the course of this work. Also I thank the technical staff in the School of Pharmacy for their assistance, Miss K. Powell for her advice and help with the electron microscopy, Mr. R. Sadler for the photography and Mrs J. Harbutt for typing this thesis.

This research was funded by the Science and Engineering Research Council, to which I express my gratitude.

Especially I wish to thank my husband Philip for his encouragement and full support in looking after our son Lloyd. To Lloyd I give my special thanks for being so patient when I was not there, and for realising how important this is to me.

SUMMARY

The Introduction to this thesis consists of a review of the current evidence concerning the effects of near-ultraviolet radiation on cells, emphasis being given to effects on the cell membrane. The generation and reactivity of oxygen species and free radicals, with particular reference to lipid peroxidation, are considered as possible mediators of near-ultraviolet-induced effects. Cellular defense against oxidative attack is described.

The experimental work, the broad aim of which is to expand existing knowledge of the effects of near-ultraviolet radiation that may lead to cell lethality, has fallen into three parts.

The first part examines the response of an unsaturated fatty acid auxotroph, Escherichia coli K1060 to broad-band near-UV radiation. Sensitivity, lipid peroxidation and leakage of rubidium from irradiated cells were found to increase with increasing unsaturation of membrane fatty acids. The involvement of singlet oxygen was implicated by an increase in sensitivity, lipid peroxidation and leakage of rubidium following irradiation in deuterium oxide. Some factors influencing survival following irradiation were investigated, where lower growth rates were shown to enhance survival.

In the second part the study was extended to human fibroblasts where a normal human skin fibroblast strain, GM730 and a strain derived from an actinic reticuloid patient, AR6LO, are compared. Lipid peroxidation was measured in both cell lines following broad-band near-UV irradiation. Membrane activity, as assessed by

the pinocytic uptake of ^{14}C-sucrose and its subsequent release from the cell, was measured. Near-UV irradiation was found to increase such activity in both strains. Vitamin E and Trolox-C were found to decrease this response in AR6LO but not GM730 cells.

The final part consists of preliminary investigations into the near-UV induced peroxidation of fatty acids and liposomes, and the subsequent increase in the level of hydroperoxides in the hours following irradiation.

INTRODUCTION

ORIGINS OF THE PRESENT WORK

In 1943 Alexander Hollaender reported important differences in the response of Escherichia coli to near- and far-ultraviolet (UV) radiations. The appreciation of such differences is crucial to our understanding of the damaging effects of the environmentally relevant components of solar radiation. Nevertheless with the availability of far-UV-emitting sources, which are economical and easily utilized, much research has concentrated on these shorter wavelengths. As a result our understanding of far-UV-induced effects is well established, and such knowledge can be usefully applied to the effects of mid-UV radiation where, as nucleic acids begin to absorb, sunburn and skin cancer are most effectively produced. This absorption is much less significant in the near-UV region, so that a wide variety of other chromophores become important, producing a range of biological effects. Such effects, often requiring considerably higher fluences than those required for killing by far-UV radiation, may either be lethal to the cell or may result in sub-lethal lesions with evident detriment to the physiology of the cell.

In recent years, with the use of sources emitting longer wavelengths, differences between the damage initiated by these and shorter wavelengths have become a focus of interest. The direction of much of this research, reviewed by Jagger (1985), may be attributed to the pioneering work of Hollaender, in particular his finding that irradiated E. coli cells were sensitive to salt solution, indicating an effect on the ion permeability of the cell membrane. Similar effects were later demonstrated in yeast cells,

while the induction of salt-sensitivity in bacteria was re-investigated and the importance of membrane damage in terms of permeability and damage to transport systems was established. When the oxygen- dependence of near-UV killing was subsequently demonstrated, the role of active oxygen species and their targets, such as the unsaturated fatty acyl components of membrane lipids, became widely considered topics for investigation.

The major part of early work was carried out using micro-organisms, not only because of the ease with which they may be used experimentally, but also because ultraviolet light penetrates the whole organism. The results of work in this field are not easily applied to mammalian cells, where the complexity of cellular organization presents a different picture of targets and defences. More applicable are techniques of cell culture, now widely used, facilitating the study of the effects of near-UV radiation at a cellular level.

In the work presented here, attention has been focussed on the cell membrane as a target for near-UV radiation-induced effects, and in particular on the unsaturated fatty acid component of the *E. coli* membrane. Attention is therefore given in the Introduction to the structure and functions of cell membranes and how near-UV radiation may damage them. The peroxidation of membrane lipids and its effects on the cell are discussed, together with the various reactive oxygen species which may be involved in the attack on membranes.

ULTRAVIOLET (UV) RADIATION

Ultraviolet radiation represents a small portion of the electromagnetic spectrum, and is defined usefully in terms of its biological effects as shown below:

Far-UV - wavelengths between 190 and 290 nm.

Mid-UV - wavelengths between 290 and 320 nm.

Near-UV - wavelengths between 320 and 400 nm.

The environmentally relevant wavelengths are those above 290 nm, since shorter wavelengths are absorbed by the ozone in the upper atmosphere. This protection of the biosphere from far-UV radiation is essential to its continuing existence, since both DNA, crucial in its genetic role, and proteins, absorb these wavelengths strongly. The mid-UV represents a region of transition, where although the absorption by DNA is poor, it is in this region that the most deleterious effects of sunlight on humans, such as sunburn and skin cancer, are found.

The near-UV represents a region where the biological mechanisms for radiation-induced damage are varied, as are the targets, and differ in several respects from those of the more energetic shorter wavelengths. The biological effects of radiation are concerned with the deposition of energy within target molecules. The relationship between energy and wavelength is given by the following expression:

$$E = \frac{h \times c}{\lambda}$$

where: E = energy of the quantum in Joules

h = Planck's constant (6.624×10^{-34} Js^{-1})

c = velocity of light (3×10^{10} $cm\ s^{-1}$)

λ = wavelength in cm

DIFFERENCES BETWEEN NEAR-UV KILLING AND FAR-UV KILLING

Fundamental differences are evident between near-UV and far-UV killing, as indicated below:

1. Survival curves usually show more pronounced 'shoulders' following near-UV irradiation (Hollaender, 1943; review by Webb, 1977).
2. Fluences required for near-UV killing are from 4 to 6 orders of magnitude higher than those required in the far-UV, as shown in Fig. 1 (from Webb and Brown, 1979, but first reported by Hollaender, 1943). This difference is also evident in human cells as demonstrated by Keyse et al. (1983).
3. Near-UV killing is strongly dependent upon oxygen, as demonstrated in bacterial cells by Webb and Brown (1979), shown in Fig. 1, and in mammalian cells by Danpure and Tyrrell (1976). Such an oxygen-dependence indicates the action of photodynamic processes, as discussed subsequently.
4. Photoreactivation is not demonstrable in most cases following near-UV irradiation at low fluence rates and at room temperature, but is following far-UV irradiation (Webb, 1978).

SOME TARGETS FOR NEAR-UV RADIATION

1. DNA

Far-UV irradiation results in the formation of a variety of photoproducts, the most important of which is the pyrimidine dimer in DNA. The importance of such dimers at wavelengths above 320 nm where absorption by DNA is poor, has been the subject of debate and is reviewed together with other lethal lesions in DNA by Jagger

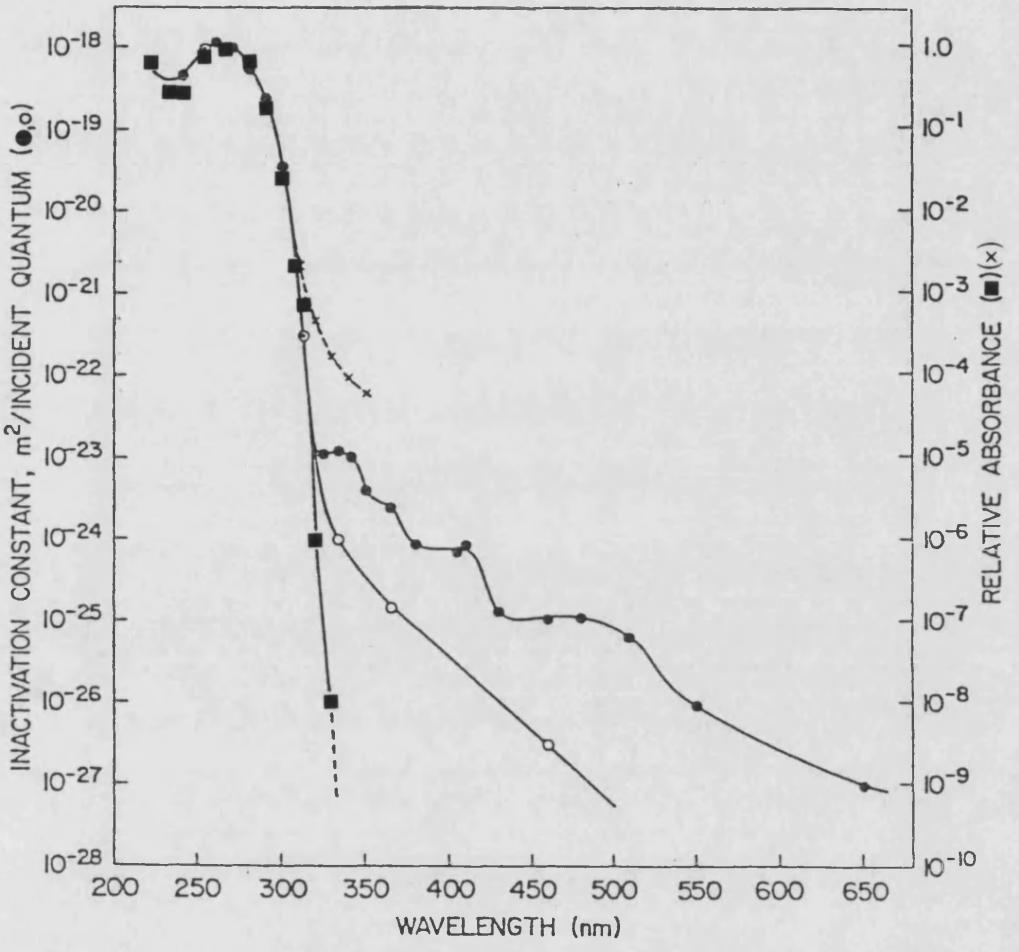

Figure 1 Action spectra for killing of stationary-phase *E. coli* WP2s *uvrA* irradiated at 25°C in the presence (●) and absence (○) of oxygen (Webb and Brown, 1979). Also shown are the absorption spectra of thymidine in M9 buffer at pH 7(■) (Webb and Brown, 1979) and of *E. coli* DNA (Sutherland and Griffin, 1981)(×)

1983; 1985). Single strand breaks (ssb) of DNA are produced with approximately the same efficiency as pyrimidine dimers by 366 nm radiation (Tyrrell, 1979). Action spectra have been obtained by Peak and Peak (1982) for B. subtilis in the 254-434 nm range, and in human fibroblasts by Rosenstein and Ducore (1983). Single strand break induction is enhanced in the presence of oxygen by 365 nm radiation (Tyrrell et al., 1974; Peak and Peak, 1982).

2. DNA Repair Systems

The systems concerned with both enzymatic photoreactivation and dark repair are inactivated by high near-UV fluences. Evidence for this includes work by Tyrrell (1979). For the E. coli K-12 wild type, Tyrrell estimated that the break in the shoulder of the survival curve for log-phase cultures of 366 nm occurs at 10^6 Jm^{-2}, at which fluence approximately 30 ssb have been produced in the DNA of a completely dark-repair-deficient system. These breaks are presumed to be repaired in the wild-type strain at lower fluences, but the sharp drop in survival observed at the higher fluences is thought to reflect the destruction of the repair systems.

3. Membranes

Since Hollaender's demonstration of salt-sensitivity in irradiated E. coli cells the membrane has been examined as a target for near-UV-induced damage in both prokaryotic and eukaryotic cells, not only in terms of ion permeability but more widely with respect to membrane function. The evidence for near-UV-induced membrane effects is presented in a subsequent section of this

Introduction, following an account of the structure and functions of membranes in bacterial and mammalian cells.

THE ABSORPTION OF ENERGY

Before a biological effect is possible in any part of the cell, radiation must be absorbed. Molecules or molecular groups absorbing radiation are called chromophores, and consideration is given here to some chromophores believed to be important in the near-UV region.

The absorption spectrum for the killing of E. coli (Webb and Brown, 1979) shown in Fig. 1 is due to the absorption by component nucleotides such as thymidine, and since this is effective up to 320 nm, DNA is considered to be the major chromophore in both the far- and mid-UV regions for cell killing. Sutherland and Griffin (1981) measured the absorption spectra of DNA from various sources using procedures which separate optical density due to true absorption from that due to the turbidity of the solution. The absorption spectrum of E. coli DNA is superimposed on the data of Webb and Brown in Fig. 1. This illustrates that absorption may take place as far out as 350 nm, though the authors do not rule out the possibility of absorption by chromophores contaminating the DNA samples. Fig. 1 also illustrates that at wavelengths above which DNA effectively absorbs, killing is strongly dependent upon the presence of oxygen. Furthermore, plateaux in the action spectrum for aerobic killing of E. coli (Fig. 1) indicate the presence of chromophores absorbing radiation at those wavelengths. Such chromophores, it is suggested, absorb the incident radiation,

transferring its energy in the presence of oxygen to DNA. Such photodynamic action may involve chromophores bound to the DNA, however chromophores need not be so confined. Several membrane-bound chromophores have been suggested, including molecules of the electron transfer chains of bacteria and mitochondria, such as the porphyrins, flavins and quinones.

Amongst the quinones, naphthoquinone vitamin K1 has an absorption maximum at 334 and being extremely sensitive to near-UV radiation is considered as a potential chromophore, as are several other components of the oxidative phosphorylation system (reviewed by Jagger, 1985). Porphyrin derivatives have recently been implicated by Peak et al. (1987) in the killing of E. coli by 334 and 340 nm radiations. Riboflavin, absorbing at 375 and 450 nm, is known to cause the photosensitized oxidation of tryptophan and tyrosine during the broad-band near-UV irradiation of tissue culture medium (Stoein and Wang, 1974) and is a constituent of mammalian cells. Bilirubin, structurally related to the porphyrins, absorbs maximally at 450 nm and has been shown to sensitize the production of single-strand breaks in the DNA of human fibroblasts (Rosenstein et al., 1983).

Chromophores, often unidentified, have been implicated in the near-UV-induced damage to the systems involving the transport of ions, sugars and amino acids across the cell membranes (Jagger, 1983, 1985). In recent years the nucleoside 4-thiouridine (^{4}Srd) has been found to play an important role in the photobiological behaviour of the E. coli cells in which it is found. In vitro and in vivo correlations between the presence of ^{4}Srd and single-strand

DNA breakage strongly suggest that this nucleoside is responsible for a considerable fraction of the single-strand breakage observed in bacterial DNA following 340 nm irradiation and that this causes much of the near-UV killing. Such evidence includes the enhanced resistance of $^{4}Srd^{-}$ mutants relative to $^{4}Srd^{+}$ strains (Tsai and Jagger, 1981) and the in vitro enhancement of single-strand breaks observed in DNA irradiated in the presence of ^{4}Srd (Peak et al., 1984), and indeed in the presence of 2-thiouracil, another nucleoside, found in Drosophila tRNA (Peak et al., 1986). In the latter case, superoxide anion and singlet oxygen were implicated, while ^{4}Srd is known to produce singlet oxygen during near-UV irradiation (Salet et al., 1985). Other reactive oxygen species known to result from the near-UV irradiation of intracellular chromophores include superoxide anion, produced by the monochromatic near-UV irradiation of nicotinamide adenine dinucleotide in its reduced form (NADH), (Cunningham et al., 1985). Other cases of the production and involvement of reactive oxygen species are discussed subsequently.

Potential chromophores for near-UV radiation-induced effects are thus diverse and variously distributed within the cell and between different cell types, and their effects would be expected to differ as a consequence. Some examples of membrane-bound chromophores have been described, together with examples of chromophores elsewhere in the cell which may cause membrane damage through the production of reactive oxygen species following the absorption of radiation. In considering the effects of the absorption of radiation by chromophores, whatever their location,

on cellular membranes, the complexity of structure and function of membranes must be taken into account.

THE MOLECULAR ORGANIZATION OF MEMBRANES

The membranes of prokaryotic and eukaryotic cells have a common overall structure, consisting of assemblies of lipids and proteins held together by noncovalent forces. The Singer-Nicholson model postulates that the lipid bilayer exists in a relatively fluid state and that lipids in each monolayer can move laterally within the plane of the membrane. Various protein molecules are distributed on each surface of the lipid bilayer but protrude from one (periferal proteins) or both (integral proteins) surfaces. While proteins may move laterally within the plane of the lipid bilayer they rarely "flip-flop" to the other surface. Fig. 2 illustrates the structure proposed by this model and indicates the hydrophobic and hydrophilic interactions proposed as the predominant forces responsible. Hydrophobic interactions occur between non-polar residues of proteins and non-polar hydrocarbon chains of the phospholipid bilayer. Hydrophilic interactions involve the charged residues of amphipathic membrane proteins, polar heads of amphipathic phospholipids and the aqueous phases on each side of the membrane.

THE CELL ENVELOPE OF *E. COLI*

The cell envelope of Gram-negative organisms is considered to be composed of three regions, an inner cytoplasmic membrane, 7.5 nm in thickness, and two regions which constitute the cell wall; a

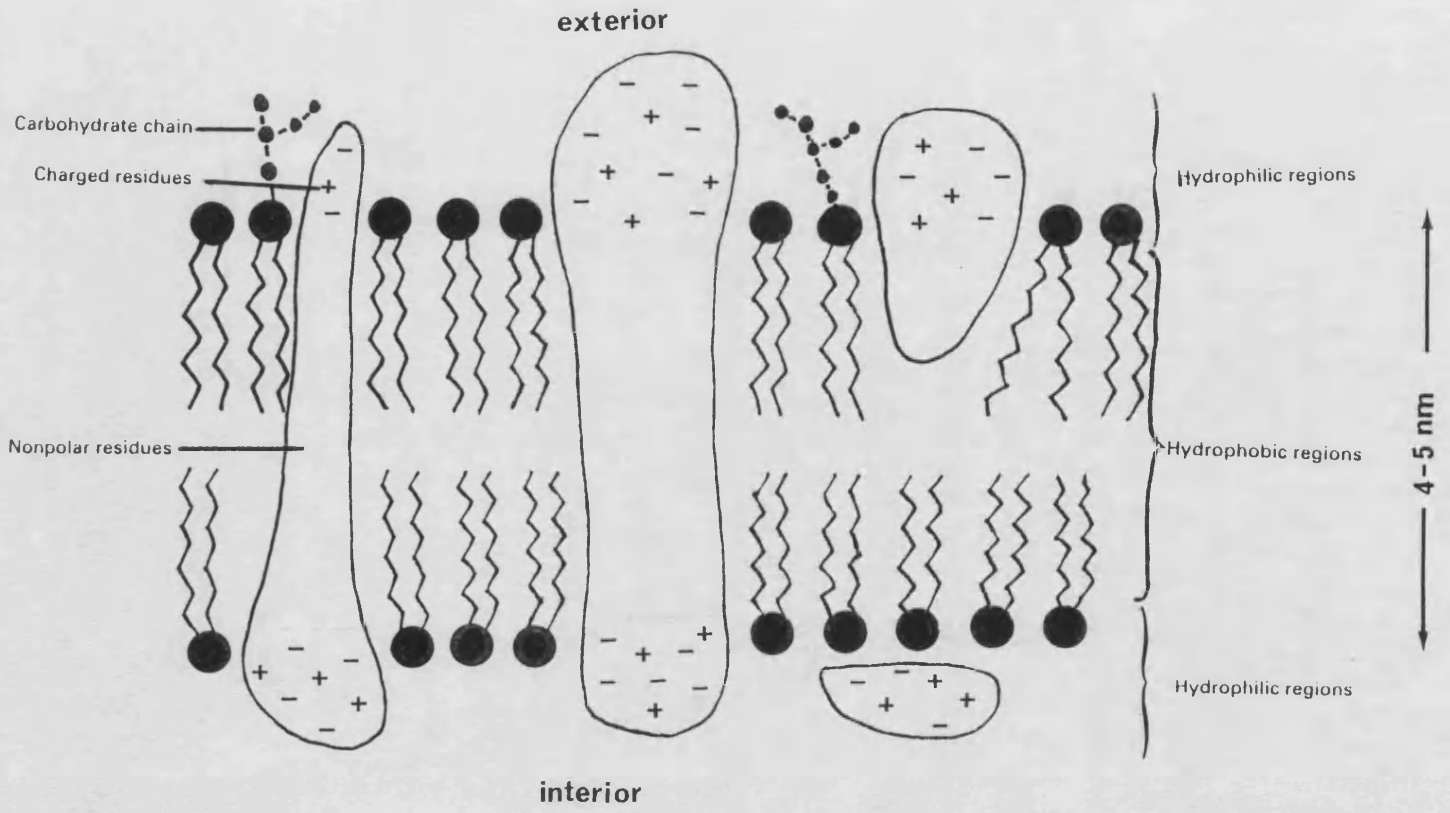

Figure 2
The molecular arrangement of membranes.

cytoplasmic space containing a very thin (1 nm) layer of peptidoglycan and an outer membrane, 7.5 nm thick, (shown diagramatically in Fig. 3.)

The entire lipid content of E. coli is found in the cell envelope and comprises about one-tenth the dry weight of the cell (Cronan and Vagelos, 1972). The outer membrane contains the greater proportion (approximately 60%) of the total lipid, having a higher lipid:protein ratio than the inner membrane which contains more enzymes and proteins such as the cytochromes; 60-70% of the cytoplasmic membrane is protein. A small amount of fatty acid is covalently bound to galactosamine moieties of the outer membrane polysaccharide, this being known as lipid A. The major outer membrane protein, murein lipoprotein, is found amide-linked to a fatty acid, predominantly palmitate, and thioester-linked to a diacylglycerol. However, the remaining lipids are phospholipids, synthesized within the cell envelope rather than in the cytoplasm. The phospholipid biosynthetic enzymes are found in the cell envelope fraction of disrupted cells, the acyl carrier protein (ACP) being located on the inner surface of the cell envelope. The biosynthetic pathway is shown in outline in Fig. 4.

Phospholipid Species found in E. coli

There are four groups of phospholipids, all derivatives of phosphatidic acid, found in E. coli as shown in Fig. 5. Phosphatidylethanolamine is the major phospholipid, particularly of the outer membrane, comprising 70-80% of the cellular phospholipid. The cytoplasmic membrane in addition contains the minor

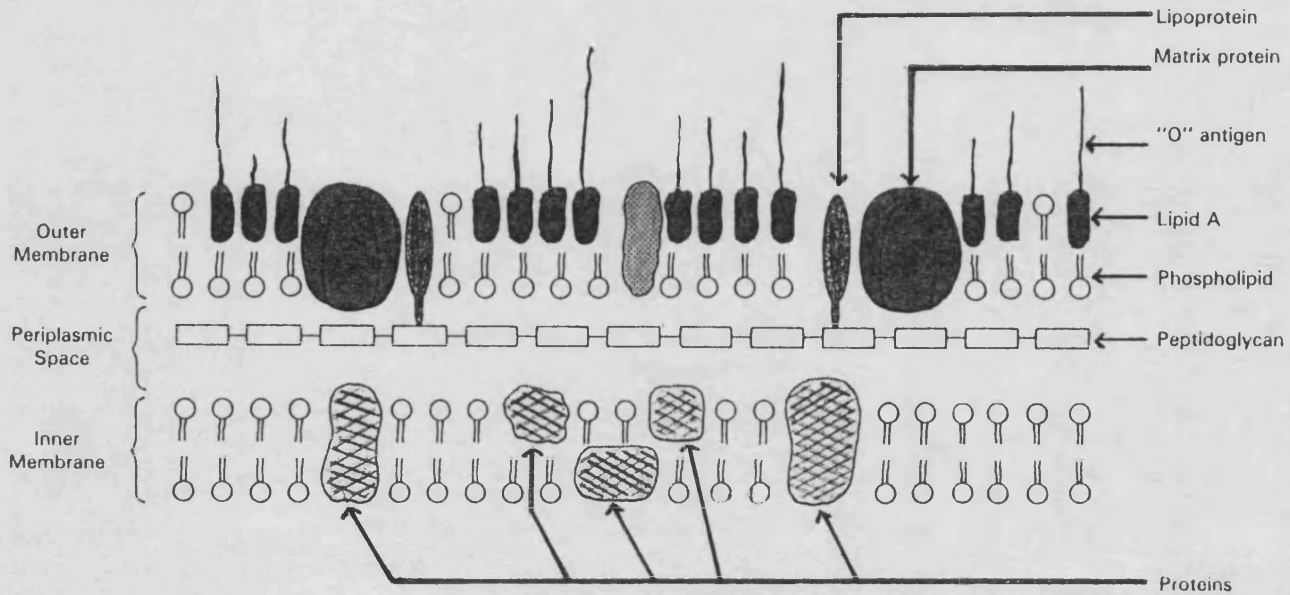

Figure 3
The E. coli cell envelope.
(Adapted from Davis et al. 1980)

Fig. 4. An outline of the biosynthesis of phospholipids of E. coli.

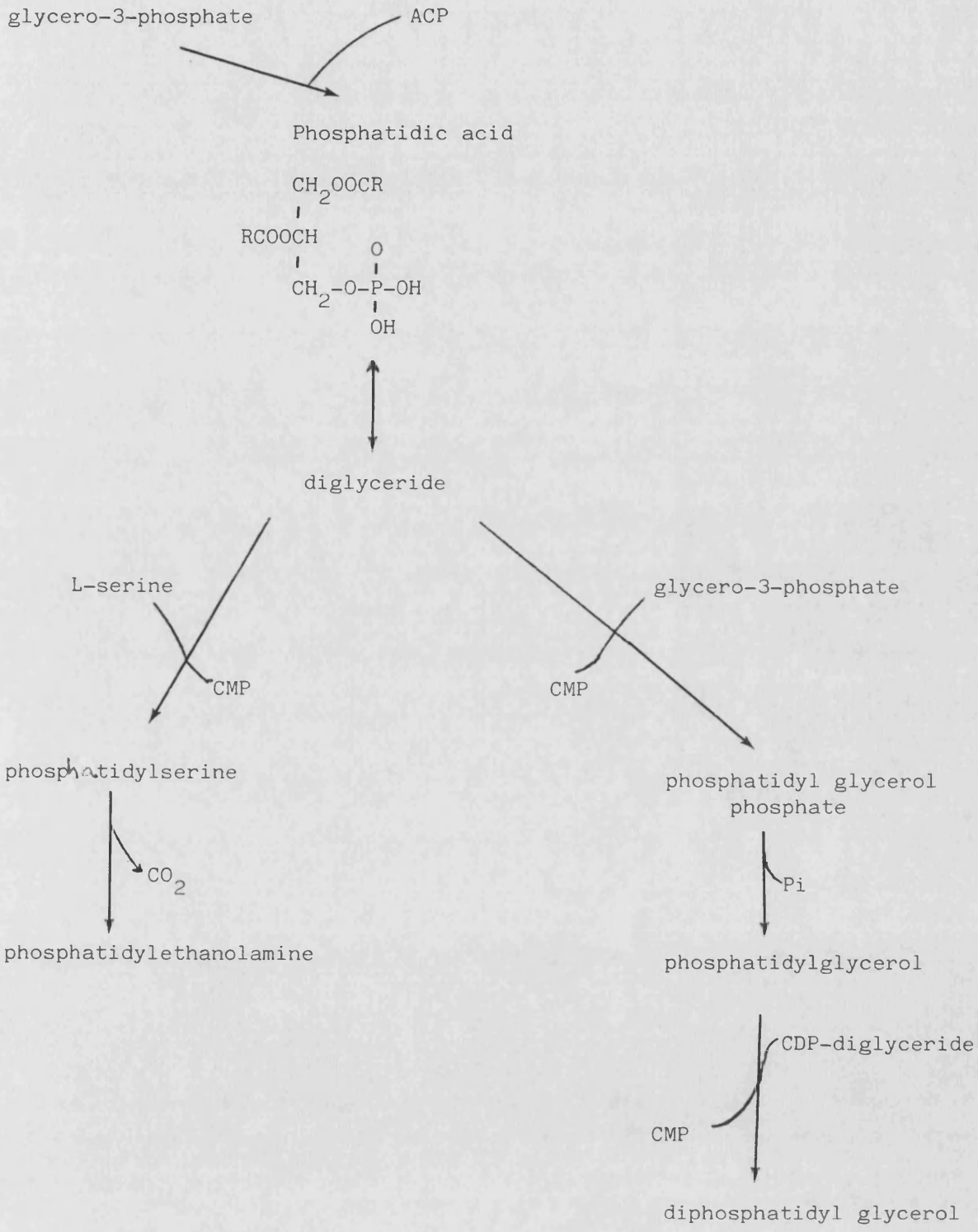

Adapted from Cronan and Vagelos (1972).

Fig. 5. Phospholipids found in E. coli.

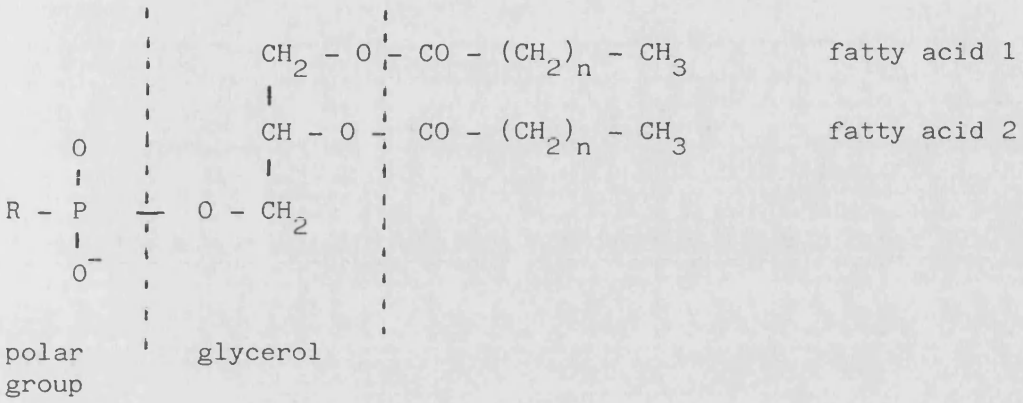

The R on the polar group may be any one of the following:

Phospholipid	R
phosphatidic acid	- H
phosphatidyl glycerol	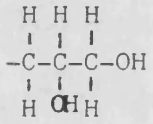
diphosphatidyl glycerol (cardiolipin)	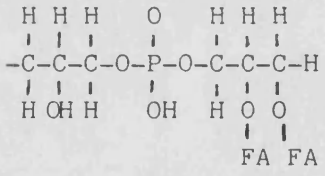
phosphatidylethanolamine	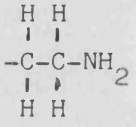

(FA = fatty acid)

phospholipids; phosphatidylglycerol, comprising 5-15%; diphosphatidylglycerol, also known as cardiolipin, comprising 5-15% and phosphatidic acid, found only in trace amounts (Cronan and Vagelos, 1972). As cultures undergo transition from exponential growth to the stationary phase there is an increase in cardiolipin and a decrease in phosphatidylglycerol (Cronan and Vagelos, 1972).

The Fatty Acids of the Phospholipids

Both saturated and unsaturated fatty acids are found in E. coli phospholipids is shown in Table 1. The outer membrane phospholipids are more saturated than those of the inner membrane, which is reflected in a higher viscosity as measured using electron spin resonance (Harwood, 1984). A phospholipid normally has one saturated and one unsaturated fatty acyl chain. Lipid A contains minimal amounts of unsaturated fatty acid, but a large proportion of β-hydroxymyristic acid. Variations in culture conditions will alter the fatty acid composition, for example as the growth temperature is lowered, the proportion of unsaturated fatty acids increases (Marr and Ingraham, 1962).

Saturated Fatty Acids

Palmitic acid (16:0) comprises the major saturated fatty acid, while small amounts of myristic (14:0) and trace amounts of stearic acid (18:0) are generally found (Cronan and Vagelos, 1972).

Unsaturated Fatty Acids

The unsaturated fatty acids of E. coli are all monoenes of the

Table 1. The fatty acid composition of phospholipids and lipid A of *E. coli*.

Fatty Acid	Fatty acid composition (% w/w) Total phospholipid	Inner membrane phospholipid	Outer membrane phospholipid	Lipid A
12:0	-	-	-	9
14:0	3	3	4	10
16:0	35	34	37	2
16:1	33	33	31	1
17:0 cyc	2	2	3	-
18:0	1	1	1	-
18:1	25	26	23	1
19:0 cyc	1	1	1	-
D-3-OH-14:0	-	-	-	77

Saturated fatty acids

12:0 Lauric acid: $CH_3(CH_2)_{10}COOH$

14:0 Myristic acid: $CH_3(CH_2)_{12}COOH$

16:0 Palmitic acid: $CH_3(CH_2)_{14}COOH$

18:0 Stearic acid: $CH_3(CH_2)_{16}COOH$

Unsaturated fatty acids

16:1 Palmitoleic acid: $CH_3(CH_2)_5CH{=}CH(CH_2)_7COOH$

18:1 Cis-vaccenic acid: $CH_3(CH_2)_5CH{=}CH(CH_2)_9COOH$

Cyclopropane fatty acids

17:0 $CH_3(CH_2)_5\underset{H\ H}{\overset{CH_2}{C\text{-}C}}(CH_2)_7COOH$

19:0 $CH_3(CH_2)_5\underset{H\ H}{\overset{CH_2}{C\text{-}C}}(CH_2)_9\ COOH$

Hydroxy fatty acid

D-3-OH.14:0: $CH_3(CH_2)_{10}CHOH\cdot CH_2.COOH$

From Harwood and Russell (1984)

cis configuration. Palmitoleic (16:1) and cis-vaccenic (18:1) are normally the only unsaturated fatty acids found in E. coli.

Cyclopropane Fatty Acids

The cyclopropane fatty acids of E. coli are formed by the methylation of the unsaturated fatty acids of the phospholipids. Thus palmitoleic acid is converted to cis-9,10-methylenehexadecanoic acid (17:0) and cis-vaccenic acid to cis-11,12-methyleneoctadecanoic acid (also called lactobacillic acid) (19:0). This change in lipid composition occurs as the cells approach the stationary phase of growth, and may contribute towards protection against oxidative damage. Normally 25-30% of unsaturated fatty acids are converted to their cyclopropane analogues during this phase of growth (Taylor and Cronan, 1976).

Unsaturated Fatty Acid Auxotrophs of E. coli

There are two classes of unsaturated fatty acid auxotrophs, known as fab A and fab B mutants. The fab A mutants are defective in the enzyme β-hydroxydecanoyl thioester dehydrase, catalysing the first committed reaction in the unsaturated fatty synthetic pathway (Fig. 6). The fab B mutants are defective in the enzyme β-ketoacyl-ACP synthetase (Rosenfeld and Vagelos, 1973). It is to this class of mutants that E. coli K1060 (Overath et al., 1970), a strain employed during research for this thesis, belongs. Mutations at the fad locus block the degradation or activation of fatty acids prior to incorporation into the phospholipid; K1060 is a double mutant having a mutation of the fad E type in addition to the fab B

Fig. 6. Fatty acid biosynthesis in E. coli indicating the positions of enzymes defective in fab A and fab B mutants.

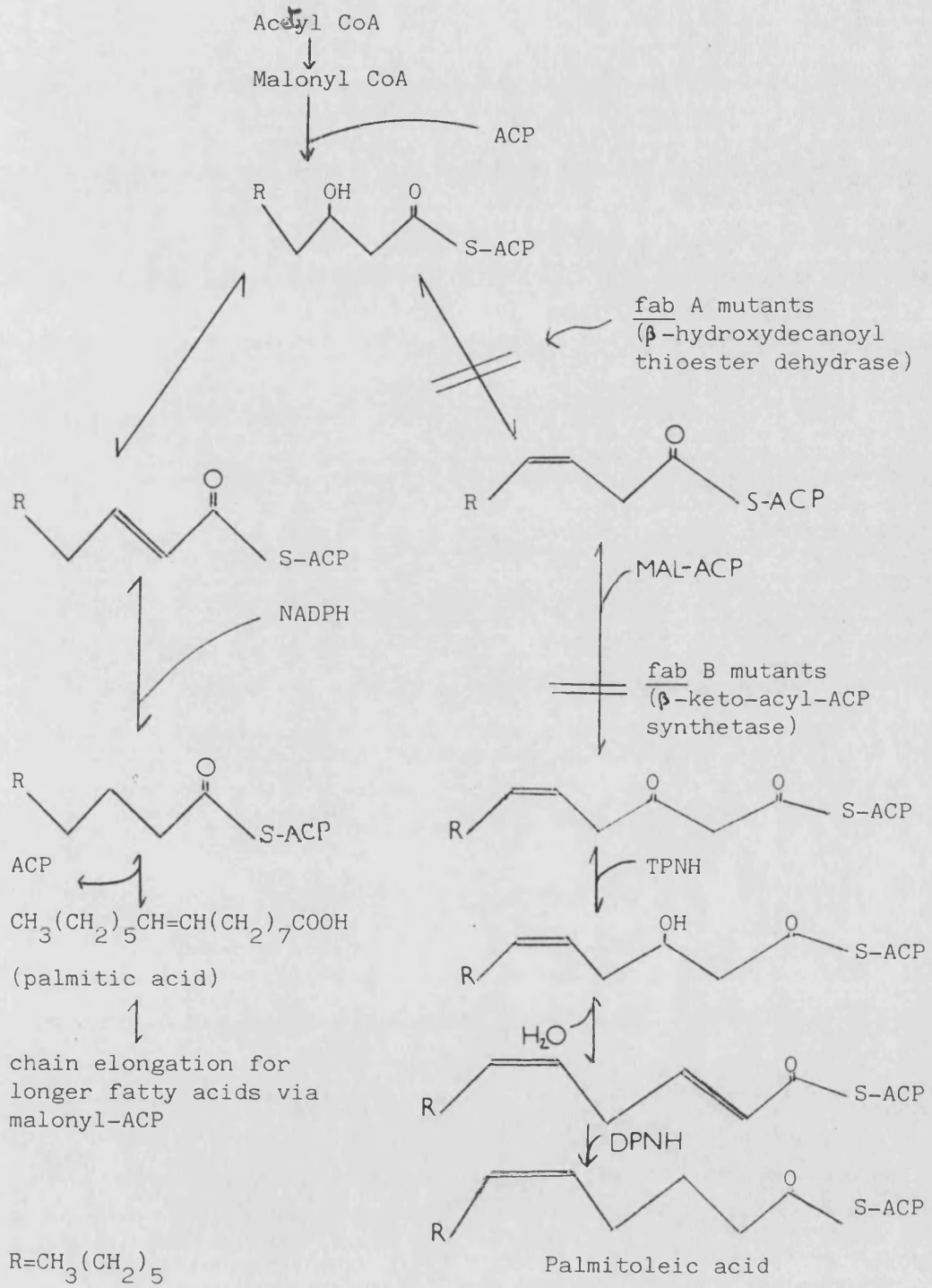

mutation. The fad E mutation results in an inability to degrade fatty acids via the β-oxidation pathway and consequently in the incorporation of exogenously supplied fatty acids, unchanged, into the phospholipids (Rock and Jackowski, 1985). E. coli K1060 is of considerable value in membrane studies since, because of its double mutation, it is able to incorporate only those unsaturated fatty acids supplied in the medium, being unable to change them or synthesize them de novo. The membrane may thus be manipulated to incorporate specific unsaturated fatty acids, the effects of which may be studied in relation to membrane function.

Membrane Function in E. coli

The cytoplasmic membrane provides an osmotic barrier, traversed at intervals by specific transport systems. Ions and non-ionized molecules larger than glycerol can penetrate only slowly except by utilization of specific transport systems, while metabolites are retained and larger external molecules are excluded. In contrast to the outer membrane, which incorporates enzymes concerned with catabolic processes, such as lipid degradation, the cytoplasmic membrane is rich in anabolic enzymes, such as those concerned with lipid synthesis, cell wall synthesis and DNA replication. Much like the eukaryotic endoplasmic reticulum system the membrane is concerned with protein secretion, binding a considerable fraction of the ribosomes. It also contains the enzymes and respiratory pigments of the electron transport system and respiration, in parallel with the mitochondrial membrane of eukaryotic cells.

The Association Between Membrane Function and Lipid Composition

A review by Ingledew and Poole (1984) considers many aspects of the respiratory chains in E. coli, including their modification under various growth conditions by alterations in the composition of cytochromes, quinones and dehydrogenases. It is a property of membrane enzymes, including some involved with respiration, that they depend upon their association with phospholipid for their activity. Some of these are listed in a review by Machtiger and Fox (1973). Variable dependence upon the fatty acid composition of membranous enzymes in E. coli has been reported by Mavis and Vagelos (1972) who described a heterogeneity in the relationship between such enzymes and membrane phospholipids. It is believed that local domains exist within the membrane, where the fatty acid composition of the phospholipids differs from the average composition of the membrane. Transport systems and membrane-associated enzymes may then be dependent upon the integrity of such domains.

Several lines of evidence suggest that unsaturated fatty acids are needed to support growth and cellular integrity. Unsaturated fatty acid auxotrophs, when starved of an appropriate fatty acid, ceased synthesis of DNA, RNA, protein and phospholipid; death and lysis followed (Henning et al., 1969). It was suggested that phospholipids were synthesized incorporating inappropriate fatty acids which failed to provide a stable membrane. Abnormally low concentrations of unsaturated fatty acids led to an unstable, fragile, membrane which is protected in osmotically stabilized conditions, allowing growth. Akamatsu (1974) demonstrated that

growth of an unsaturated fatty acid auxotroph was permitted in the absence of exogenous fatty acid in a medium containing 15 to 20% sucrose or 1.5% inorganic salts. These results were complicated by the inability of all the strains of unsaturated fatty auxotrophs tested to grow under such conditions, but Akamatsu concluded that unsaturated fatty acids in the membrane function to stabilize the membrane against osmotic stress. The osmolarity of the growth medium is also known to affect the turnover of phospholipids, where high osmolarity medium leads to a low turnover rate (Munro and Bell, 1973). More recently it has been demonstrated that phosphatidylglycerol is the key factor that stabilizes liposomes prepared from E. coli phospholipids against osmotic pressure (Yoshikawa et al., 1985); such a role may be considered in the bacterial membrane. However the peptidoglycan of the periplasmic space, while conferring rigidity on the cell wall, has an important function in preventing osmotic lysis. It has also been suggested that DNA replication occurs in association with a lipid site on the bacterial membrane, this site requiring unsaturated fatty acids (Fralick and Lark, 1973).

The Biological Importance of the Physical Properties of Membrane Lipids

Many of the examples above indicate that the functions of the bacterial membrane are related to its phospholipid or fatty acid composition. The unsaturation of the fatty acyl components is generally accepted to confer the required degree of fluidity on the membrane. The lipid bilayer is in a more fluid state when the

hydrocarbon chains are not packed tightly, this being achieved by the incorporation of fatty acids with either shorter or unsaturated hydrocarbon chains, or by a lower concentration of transmembrane proteins. A review of the biological relevance and regulation of the physical properties of membrane lipids is available (Cronan and Gelman, 1975), where lipid bilayer phase properties and the correlation between membrane-associated physiology and lipid physical properties are discussed. By comparing the survival of E. coli K1060 incorporating fatty acids with various degrees of unsaturation following γ-irradiation, at room or ice-bath temperatures, Yatvin (1976) demonstrated that membrane fluidity determined sensitivity. Under conditions where the membrane would be more fluid, the organism was more resistant to irradiation.

THE MAMMALIAN MEMBRANE

The organization of chemical activity in higher cells depends in large upon the compartmentation afforded by membranes. Embedded in the lipid matrix are the many different protein molecules which give each membrane its distinct identity and carry out its specialized functions. The cell itself is bounded by the plasma membrane, the complex nature of which is illustrated diagrammatically in Fig. 7, which moderates movement of molecules in both directions, maintaining the concentrations required for cellular function. Intracellular membrane-bound organelles include the nucleus, mitochondria, lysosomes, smooth and rough endoplasmic reticulum and the associated Golgi complex. While the bacterial cell envelope is multi-functional, the membranes of eukaryotic

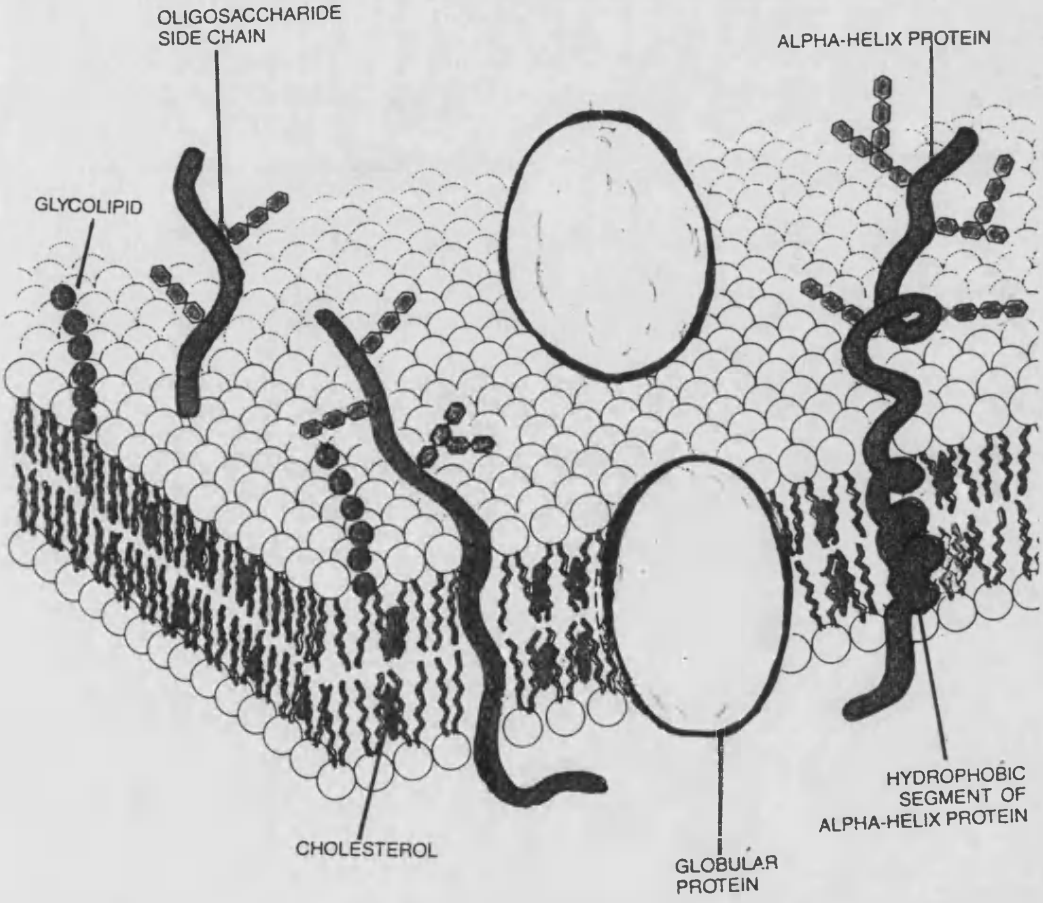

Figure 7
The mammalian plasma membrane

cells have evolved to serve specific functions, hence the mitochondrial membrane accommodates the respiratory enzyme complexes and the endoplasmic reticulum is concerned with protein synthesis, to give two examples. The structure of mammalian membranes follows the model illustrated in Fig. 2 and while there are many similarities with the bacterial membrane, some important differences are indicated in the following descriptions of their structure and function.

Amphipathic Lipids of Mammalian Membranes

The major phospholipids in mammalian membranes are phosphatidylcholine, phosphatidylethanolamine, phosphatidylinositol and phosphatidylserine, the structures of which are shown in Fig. 8. These phospholipids are distributed so that the bilayer is asymmetrical. In addition, many membranes contain glycolipids, also amphipathic lipids, resembling phospholipids but distinguished by the presence of one or more sugar residues as the polar head group. Recently glycosphingolipids have been studied in relation to membrane-related changes associated with the onset of cancer (Hakomori, 1986). Sphingolipids, such as sphingomyelin are also present in the membrane, these molecules possessing one fatty acyl chain and one sphingosine molecule bound to the polar head group (Fig. 8).

Cholesterol

Cholesterol is present in substantial amounts in mammalian cytoplasmic, and certain other membranes, the molecules being

Fig. 8. Amphipathic lipids of mammalian membranes

1. Phospholipids: these have the same structure as those shown in Fig. 5, the R residue of the polar head group may be one of the following.

Phospholipid	R
phosphatidylethanolamine	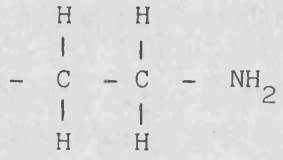
phosphatidylcholine	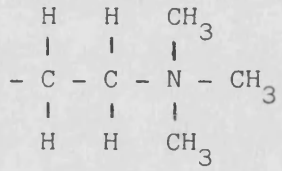
phosphatidylserine	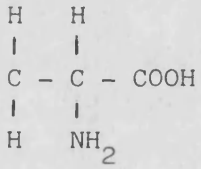
phosphatidylinositol	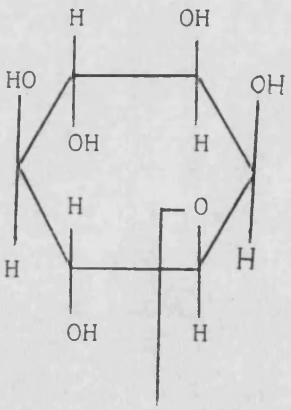

2. Glycolipid

e.g. glactocerebroside:

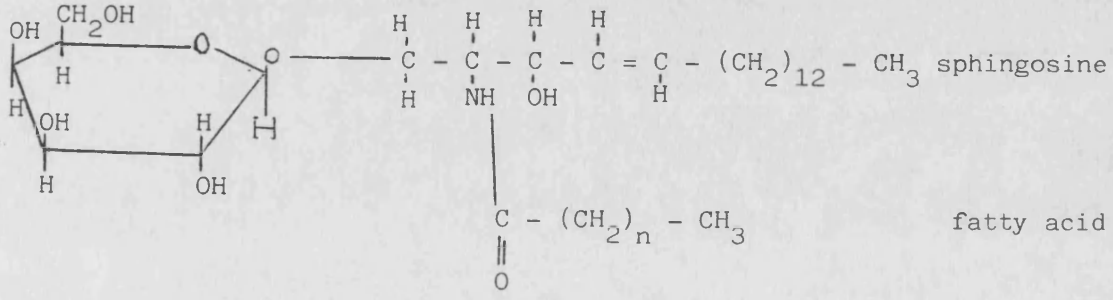

3. Sphingolipid

e.g. spingomyelin

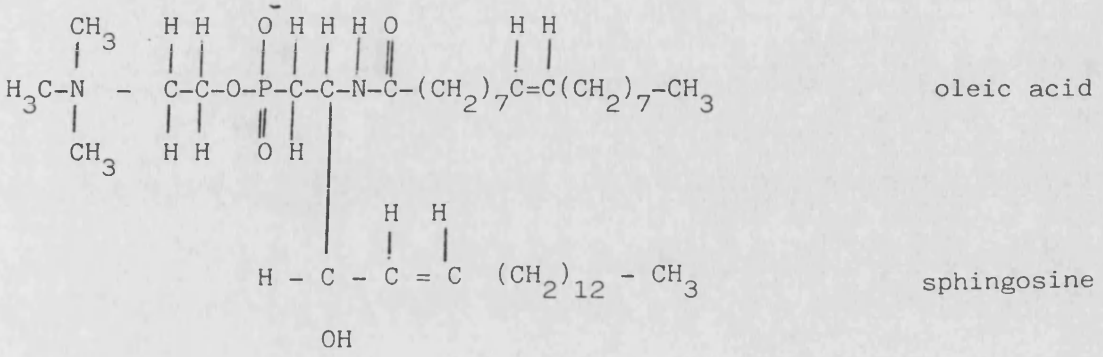

oriented in the bilayer in a way that contributes to membrane fluidity (Fig. 9). The steroid rings interact with those regions of the phospholipid and glycolipid hydrocarbon chains nearest the polar head groups, leaving the remainder of the chains flexible, and preventing their crystallization into a rigid aggregate. In addition, cholesterol is believed to contribute to the mechanical stability of the membrane.

The lipid composition of eukaryotic membranes is variable, one of the most notable differences being the mitochondrial membrane, which contains more than twice the amount of phosphatidylethanolamine found in other membranes, but very low amounts of cholesterol and no sphingomyelin. Various comparisons are available between various animal organelle membranes and bacterial membranes (e.g. Wolff, 1981).

The Fatty Acids of Mammalian Membranes

There is a wide variety of both saturated and unsaturated fatty acids present in membrane phospholipids. Chain length varies from the 14-carbon myristic acid to the 24-carbon nervonic acid. Degrees of unsaturation vary from monoenoic fatty acids such as oleic (18:1) and gadoleic (20:1) to the hexaenoic cervonic acid (22:6). A comprehensive review (Stubbs and Smith, 1984) describes constituent fatty acids of mammalian membranes, while describing how these may be varied by dietary modification (in the whole animal) or by manipulation of growth media and conditions (in cell culture). In general it may be stated that the eukaryotic membrane has a higher

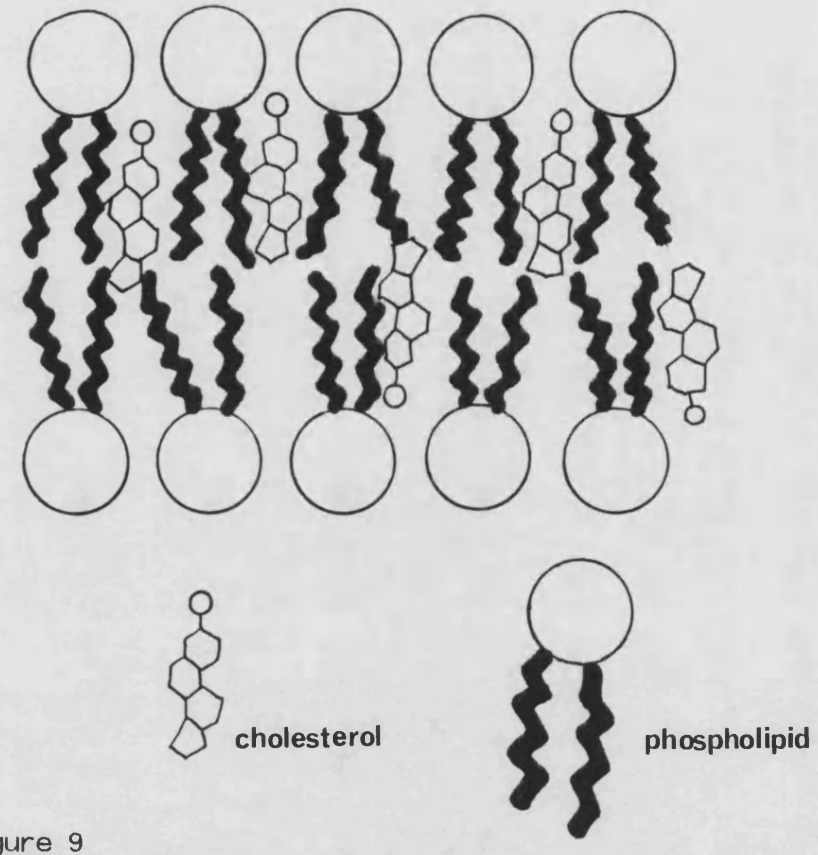

Figure 9
Cholesterol and its position in the phospholipid bilayer

unsaturation index (calculated by the molar proportion of each fatty acid multiplied by the number of double bonds it contains) than bacterial membranes, which will only contain monounsaturated fatty acids under normal culture conditions.

Both the fatty acids and polar head groups of membrane phospholipids are asymmetrically distributed. This serves, for example, to provide an appropriate physico-chemical environment for integral membrane enzymes, some of which will be required in the leaflet at the cytosolic side of the membrane, while others, requiring a different lipid domain, will be required at the leaflet on the side interior to the organelle (Stubbs and Smith, 1984).

Membrane proteins

Since many of the specific functions of cellular membranes are carried out by their constituent proteins, the types and amounts of proteins in a membrane reflect its functions. Hence the mitochondrial membrane contains about 75% protein, being enzymes and molecules associated with energy transduction. The plasma membrane contains about 50% protein, many of which are concerned with the selective transport of molecules across the membrane, by way of specific protein channels or pumps. In addition there are numerous specific protein receptors which are responsible for the receptor-mediated endocytosis of molecules from extracellular fluid into the cell. The activity of membrane-bound enzymes and other proteins is known to be critically dependent upon the lipid components of the membrane (Carruthers and Melchior, 1986), for example, by the specific organization of the lipids into domains necessary for the functioning of the proteins.

The Functions of the Plasma Membrane of Eukaryotic Cells

The plasma membrane serves as a dynamic, regulatory barrier to the entry and exit of molecules and particles. Substances cross the membrane barrier by three general routes: (1) by passive transport, that is the free diffusion or facilitated diffusion, of molecules along a concentration gradient; (2) by active transport, in which energy is expended as a substance moves against its concentration gradient; and (3) by the enclosure of substances in membranous vesicles so that they may enter a cell (endocytosis) or be expelled from the cell (exocytosis) with the expenditure of energy.

Passive Transport

Small hydrophobic and uncharged polar molecules diffuse rapidly across the bilayer, which is highly impermeable to charged molecules. Transport proteins, channel proteins and carrier proteins facilitate the diffusion of various molecules across the membrane (a situation also found in the bacterial cytoplasmic membrane).

Active Transport

The movement of ions and metabolites against their electrochemical gradients requires the expenditure of energy, a source of which is ATP. Membrane ATPases catalyze the release of free energy from ATP, and function as pumps, supplying the energy for the translocation of substances across the membrane. The Na^+-K^+-ATPase is one example of such a pump, which generates and maintains the membrane potential which is in turn responsible for driving the active transport of sugars and amino acids into the

cell. Active transport may be driven by the energy stored in ion gradients rather than by ATP hydrolysis. In such a system an ion and a metabolite are co-transported; in animal cells the ion is generally Na^+ (in bacterial cells it is usually H^+). The ion gradient produced by the movement of the ion across the membrane provides the energy for active transport of metabolites across this membrane. Many such pumps and transport systems are reviewed by Benga (1986).

Endocytosis

Endocytic activity has been traditionally divided into two categories, phagocytosis which describes the uptake of large, particulate, substances into the cell, and pinocytosis, which is used to describe the vesicular uptake of small particles, soluble macromolecules and extracellular fluid.

Pinocytosis may further be divided into fluid and receptor-mediated endocytosis, referring to the fact that substances can enter the cell in the fluid content of an endocytic vesicle or be bound to appropriate receptors on the membrane prior to vesicle formation.

Receptor-Mediated Endocytosis

Receptor-mediated endocytosis in particular has been the subject of much recent research which is well reviewed (for example, Goldstein *et al.*, 1979; Pearce and Bretscher, 1981; Steinman *et al.*, 1983; Pastan and Willingham, 1985). A summary of the pathway of receptor-mediated endocytosis is illustrated in Fig. 10. Briefly, the process involves the binding of a

macromolecule from the extracellular fluid to specific receptors which are localized in coated pits, where the membrane is indented and coated with clathrin on the cytoplasmic side. The pit then invaginates and breaks away from the plasma membrane, forming a coated vesicle. The clathrin coat is shed, and the vesicle fuses with an intracellular vesicle, forming a receptosome. This moves along tracks of microtubules, eventually coming into contact with the Golgi system or lysosomes, with which it fuses, thus delivering the ligand. The receptor is returned by the recycling of that membrane portion, to the plasmalemma, in the reverse process of exocytosis, while the ligand is utilized by the cell. Receptor-mediated endocytosis is known to be responsible for the uptake of, for example, extracellular yolk protein in developing chicken oocytes, and in cell culture for the uptake of low-density lipoprotein and epidermal growth factor.

Fluid-Phase Endocytosis

The uptake of extracellular fluid by cells grown in cell and tissue culture has been demonstrated by following the internalization of radioactively labelled substances, such as polyvinylpyrrolidine (Williams et al., 1977) or sucrose (Besterman et al., 1981), though its precise function is a matter for speculation. The process involves the invagination of the plasma membrane with the enclosure of a small volume of extracellular fluid. The vesicle so formed is thought to fuse with a lysosome, and while the nutrients so internalized are available for utilization by the cell, the membrane is returned to the cytoplasmic membrane (Fig. 11). In order to maintain the

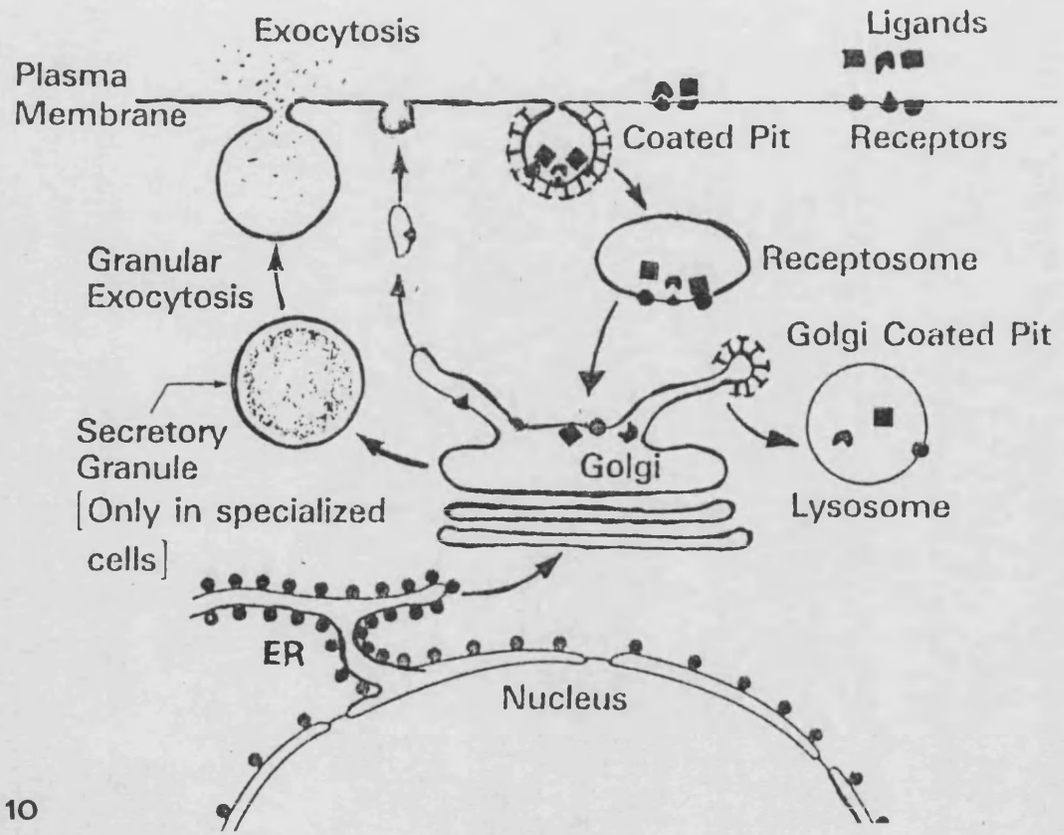

Figure 10

Receptor-mediated endocytosis and exocytosis: the pathway in cultured cells. The symbols represent ligands such as transferrin or epidermal growth factor. (Adapted from Pastan and Willingham, 1982)

homeostatic balance within the cell a continual process of exocytosis removes excess internalized material. Besterman et al. (1981) demonstrated that the process of fluid-phase pinocytosis and subsequent exocytosis apparently required the existence of at least two intracellular compartments in series, one being small, with a rapid turnover, (6-8 minutes in fibroblasts) and the other being larger and with a slow turnover (430-620 minutes). Their results indicated a rapid return of internalized fluid via exocytosis, commencing within minutes of the onset of endocytosis.

The Roles of Endocytosis and Exocytosis

Both receptor-mediated and fluid-phase endocytosis appear to be important in the uptake of macromolecules and nutrients as described above. With rapid internalization of plasma membrane it is evident that compensation must follow, a role fulfilled by exocytosis. Exocytosis has a role too in the secretion of cellular products, such as mucus, or histamine in an allergic reaction. It is also a well supported hypothesis that pinocytosis serves as a pathway for the continual turnover of plasma membrane lipid and/or protein, as addressed in reviews by Pearse and Bretscher (1981) and Steinman et al. (1983). Such a function would rationalize the rapid endocytic events which result in the internalization of extracellular substances to excess. It would also allow for the modification of transient membrane fractions by way of selective degradation of, for example, altered or damaged proteins, as they pass through the lysosomal system. Plasma membrane biogenesis could also proceed through a vacuolar intermediate rather than by direct transport from Golgi apparatus (Steinman et al., 1983).

Figure 11

Pathways which may be involved in the recycling of plasma membrane and solutes. (a) Plasma membrane and solute influx (b) Recycled membrane efflux (c) New membrane efflux The secondary lysosome (2lys) serves as an intermediate member of the vacuolar apparatus, accepting membrane and solutes from the extracellular environment and from endogenous synthetic sources. Primary lysosomes (1lys) may fuse immediately with the plasma membrane, or after fusion with the secondary lysosome.

(Adapted from Cohn and Steinman 1982)

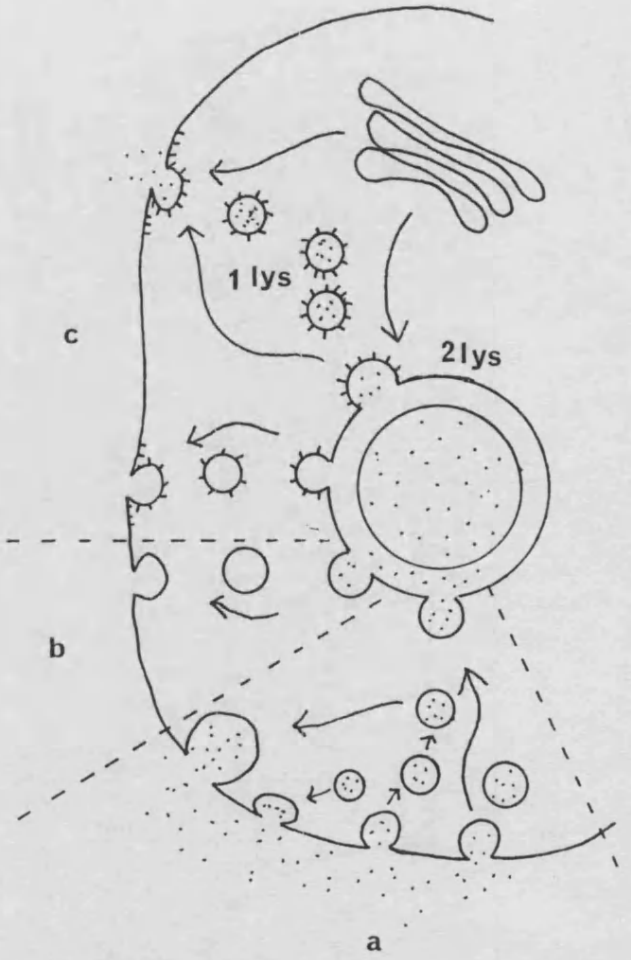

The extent of these processes can be gauged by measurements indicating that fibroblasts in culture interiorize 25% of their cell volume every 3-6 hours (Steinman et al., 1976), even though the lysosomal fraction of a cell constitutes only 1-10% of total cell volume, and is not changed during pinocytosis. In parallel, fibroblasts endocytose 186% of their cell surface area each hour, though total cell volume and surface area remain constant through the process (Steinman et al., 1976). It should be noted however, that the magnitude of pinocytosis alters with such factors as cell type, serum used in media, the phase of the cell cycle and density in culture (see Besterman and Low, 1983).

THE EVIDENCE FOR NUV RADIATION-INDUCED MEMBRANE DAMAGE

The cell membrane has been shown to have great complexity of both structure and function. Its integrity must be considered to be vital to the maintenance and survival of the cell so that events resulting in the impairment of any function may contribute to lethality.

Since the first report of near-UV radiation-induced salt sensitivity in E. coli (Hollaender, 1943), effects have been reported in four main areas of membrane function: (i) effects on membrane active uptake; (ii) effects on bacterial respiration; (iii) effects leading to cell lysis or changes in the permeability barrier and (iv) effects associated with membrane lipid composition.

A survey of work in these fields is presented below, together with effects which have been reported to be caused by the

peroxidation, induced by a variety of means including near-UV irradiation, of membrane lipids.

(i) Effects on membrane active uptake

Among the first indications of near-UV lability of membrane active transport systems, other than ion transport, was the report by Sprott *et al.* (1976) that monochromatic near-UV wavelengths down to 366 nm were more effective than visible light in inhibiting the uptake by *E. coli* of some amino acids and sugars, the effects being different for different groups of amino acids. A review of subsequent work in this field is available (Jagger, 1985).

(ii) Effects on bacterial respiration

Components of the electron-transport chain have been shown to be involved in near-UV radiation-induced biological effects. For example, Sprott and Usher (1977) have shown that at fluences above 1×10^6 Jm^{-2} of 366 nm radiation, where 80% inhibition of respiration is apparent, there is a rapid loss of the electrochemical proton gradient in *E. coli*. There is considerable evidence that isoprenoid naphthoquinones, which function in the electron-transport systems of oxidative phosphorylation, may be important near-UV targets. For example, Taber *et al.* (1978) showed naphthoquinones to be the chromophore and target in the near-UV-induced growth delay in *B. subtilis*.

Cytochromes and flavins are generally more resistant to near-UV than the quinones but there is some evidence that they may be involved in near-UV effects on oxidative phosphorylation (reviewed

by Jagger, 1985). More recently Tuveson and Sammartano (1986) demonstrated sensitization to the lethal effects of broad-band near-UV radiation (300-400 nm) of E. coli RT8 haem A8, a strain defective in δ-aminolevulinic acid (δ-ALA) synthesis when the cells were supplemented with δ-ALA, allowing porphyrin synthesis. The effect was proportional to the degree of supplementation and was not observed in far-UV-irradiated cells. It was subsequently shown by Peak et al. (1987) that the organism was inactivated more efficiently by monochromatic 334 and 405 nm radiations if supplemented with δ-ALA. The effect was enhanced by the presence of oxygen and both effects were larger at 405 nm than 334 nm. At the longer wavelength there was also a doubling in the accumulation of DNA breaks. Rubidium leakage caused by 405 nm radiation occurred at lower fluences in cells grown with higher levels of δ-ALA than in cells supplemented at lower levels. These results suggested to the authors that porphyrin derivatives may have a role in cell killing by near-UV radiations, and that damage to cytomembranes may be a critical lesion produced by these events, whereas DNA breakage may not. The location of the aerobic respiratory complexes of E. coli in the membrane (Jones, 1982) also helps to explain the relative importance of the membrane as a near-UV target.

(iii) Effects leading to cell lysis or changes in the permeability barrier

One method used in the investigation of UV-radiation-induced damage is to introduce irradiated cells into conditions of increased osmotic stress. Under these conditions membrane damage

may be seen to relate to cell death. This approach was originally used in the pioneering work of Hollaender (1943) and later by Moss and Smith (1981) who exposed near-UV-irradiated E. coli to hypertonic conditions. Moss and Smith demonstrated that a DNA repair-competent strain of E. coli K12 showed an increased sensitivity when plated on minimal media following broad-band (320-405 nm) irradiation at fluences resulting in little inactivation on complex media. This was related to the presence of relatively high concentrations of inorganic salts in the minimal media. Sensitivity was further increased by the addition of higher concentrations of salts to the media. An action spectrum for such salt sensitivity following monochromatic near-UV irradiation was produced by Kelland et al. (1983a). They demonstrated that at wavelengths betwen 254 nm and 310 nm lethality closely corresponded to the absorption spectrum of DNA, and there was no indication of membrane damage. Above 310 nm the direct absorption of radiation by DNA could not account for the sensitivity observed, and at wavelengths longer than 310 nm membrane damage was induced by an increasing factor up to a plateau at 334 nm. After 365 and 405 nm irradiation there was a decrease from this plateau. They concluded that at these wavelengths membrane damage could contribute significantly to near-UV radiation-induced lethality. It was subsequently shown that such membrane damage, following broad-band near-UV irradiation, was recoverable when irradiated E. coli K12 cells were held in a complex recovery medium (Kelland et al., 1983b). While neither penicillin nor chloramphenicol (inhibitors of cell wall synthesis and protein synthesis, respectively) prevented

recovery, incubation with bacitracin, which acts in part by inhibiting membrane synthesis, decreased the amount of recovery by irradiated cells. It was suggested that membrane synthesis was therefore required for recovery. Kelland et al. (1984) further showed that near-UV irradiated E. coli K12 cells leaked intracellular material as assessed by three methods; the leakage of 260 nm absorbing substances, [methyl-^{3}H] thymidine leakage, and $^{86}Rb^{+}$ leakage. As a control response, leakage was also demonstrated after mild heat treatment, known to result in membrane damage.

As shown in Fig. 12, an action spectrum for $^{86}Rb^{+}$ leakage was presented, showing leakage to occur at fluences equivalent to, or slightly less than fluences causing inactivation, at wavelengths above 305 nm. At lower wavelengths leakage could only be induced at fluences significantly greater than those required to cause cell inactivation.

Membrane damage has also been implicated in the inactivation by broad-band near-UV radiation of the yeast Saccharomyces cerevisiae (Ito and Ito, 1983). Exponentially growing yeast cells, but not stationary phase cells, were inactivated when placed in water following 300-380 nm broad-band irradiation. Cells were not inactivated in 0.1 M potassium phosphate buffer, nor following 254 nm irradiation. The membrane effects were oxygen-dependent with a low temperature dependence, consistent with the view that the effects were caused by photosensitization rather than enzymatic processes. Further examples of near-UV-irradiation-induced membrane leakiness are described in the section dealing with lipid peroxidation, where this was demonstrated to occur concomitantly.

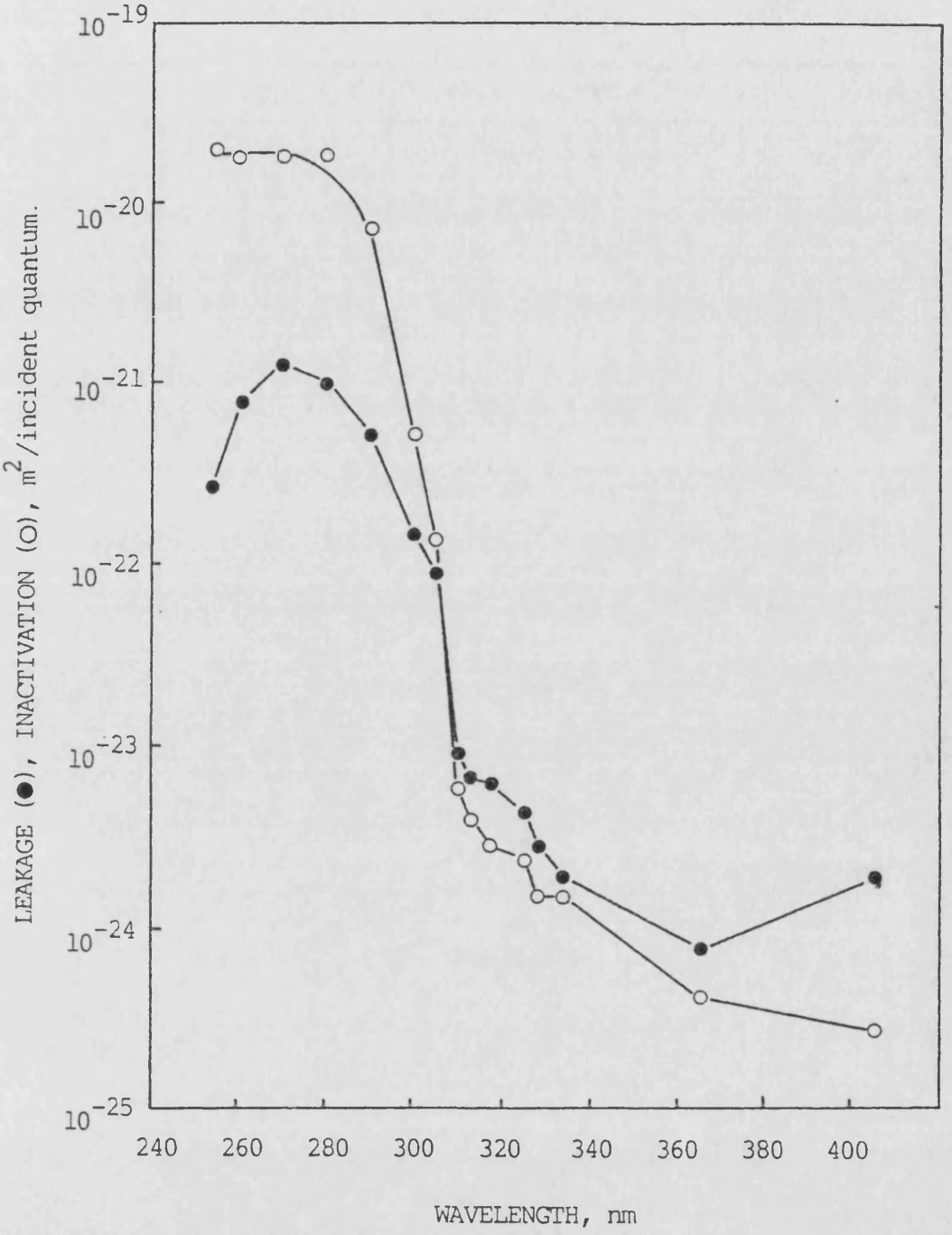

Figure 12
Action spectra for rubidium leakage (●) and lethality (o) for E. coli K12(SR385). (From Kelland, 1984)

(iv) The effects associated with membrane lipid composition

It has been shown that near-UV irradiation disturbs the equilibria between the phospholipids of E. coli B/r (Jacobson and Yatvin, 1976). In the period up to three hours following irradiation the proportion of cardiolipin rose, while levels of phosphatidylglycerol and phosphatidylethanolamine fell. There was an unidentified, new phospholipid which appeared and increased in amount during this period. Similar changes followed γ-irradiation.

The work by Klamen and Tuveson (1982) using the unsaturated fatty acid auxotroph E. coli K1060, provided evidence for unsaturated fatty acids of membrane phospholipids as targets for near-UV radiation. This organism is unable to synthesize or degrade unsaturated fatty acids and so incorporates them, unchanged as supplied in the growth medium. Manipulation of the membrane by the incorporation of fatty acids with various degrees of unsaturation resulted in an increase in sensitivity to broad band (300-400 nm) radiation as the degree of fatty acid unsaturation increased. Increasing the amount of unsaturated fatty acid by lowering of the growth temperature (as demonstrated by Cronan, 1968) had no such effect, indicating that it was the degree of unsaturation of the incorporated fatty acids which was important. They postulated that singlet oxygen, produced as a result of the absorption of radiation by endogenous photosensitizers, attacked the unsaturated carbon-carbon bonds of the fatty acyl chains of the membrane phospholipids. The consequent formation of peroxides or hydroperoxides would alter the hydrophobic character of the membrane, resulting in membrane destruction.

The correlation between fatty acid unsaturation and sensitivity was clearly evident in exponential phase cultures but only marginal in stationary phase cells, as shown in Fig. 13. Since K1060 does not efficiently convert unsaturated fatty acids to saturated cyclopropane analogues (13% instead of the expected 25-30%) it would be expected that stationary phase cell populations would be as sensitive as log phase cultures. They interpreted these results as meaning that the unsaturated bonds are more important in log phase cells than in stationary phase cells where other targets are more relevant.

Klamen and Tuveson's work with E. coli K1060 reflected similar results obtained by Redpath and Patterson (1978) showing a correlation between radiosensitivity and membrane fatty acid composition. Comparisons are frequently made between the effects of near-UV and ionizing radiations, as contrasts are made between near-UV and far-UV radiations. A review is available in which the membrane effects of ionizing radiation, including lipid peroxidation, membrane permeability and membrane fluidity are discussed (Leyko and Bartosz, 1986). An earlier review considers wider aspects of the effects of radiation on mammalian cell membranes (Patrick, 1977).

A direct action of mid-UV irradiation on the membranes of mouse fibroblasts and human keratinocytes has been implied by the rapid radiation-induced release of arachidonic acid from membrane phospholipids (DeLeo et al., 1984, 1985), an effect which occurred within 5 minutes of irradiation.

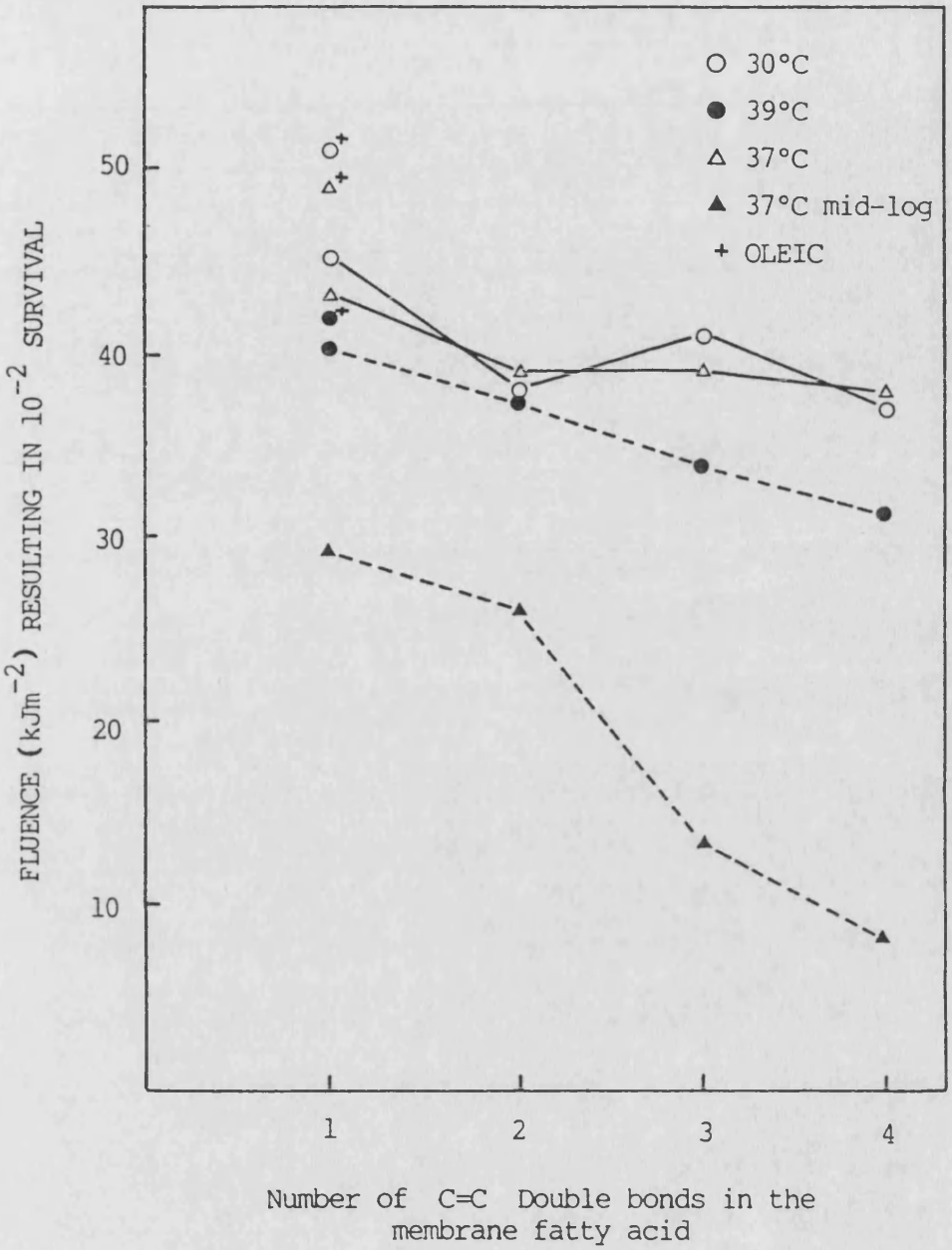

Figure 13

Dependence of fluence to give 1% survival for E. coli K1060 on the number of double bonds in the supplemented unsaturated fatty acids.

(From Klamen and Tuveson, 1982).

Proposed mechanisms for the near-UV-induced damage to membranes are frequently related to the peroxidation of membrane phospholipids, though general observations concerning the detection of lipid peroxidation products in UV-irradiated skin have been reported (Meffert et al., 1976).

THE EFFECTS OF LIPID PEROXIDATION ON CELL MEMBRANES

Lipid peroxidation, induced by a variety of treatments, is known to affect membrane properties in several ways. The liposomal membrane provides for the investigation of effects concerning only the lipid bilayer, without interference from proteins or nucleic acid. Liposomes were used, for example, in the demonstration that Vibrio cholerae and egg lecithin phospholipids were peroxidised following irradiation by 254 nm, 365 nm and sunlight. At the fluences used the liposomes also became leaky. The effect was greater when lower fluence rates were used, and the amount of leakiness was correlated with the degree of fatty acid oxidation (Mandal and Chatterjee, 1980). It was apparent that 365 nm radiation was more efficient than 254 nm radiation in producing these effects, where 1.2×10^3 Jm^{-2} of 365 nm radiation resulted in the same amount of lipid peroxidation as 6×10^3 Jm^{-2} of 254 nm radiation. Previous work by Roshchupkin et al. (1975) similarly demonstrated both far- and near-UV-induced lipid photoperoxidation in egg lecithin liposomes and erythrocyte membranes, though fluences of 10^3 Jm^{-2} of far-UV radiation were required. They demonstrated that lipid photolysis in erythrocyte membranes involved sensitization, probably by protoporphyrin, and that the

antioxidant α-tocopherol present in the membranes was directly photooxidised by 254 nm and 313 nm, thus allowing lipid peroxidation. Lipid peroxidation was discussed by both groups as the causative factor in the leakiness observed following irradiation. Indeed, lipid peroxidation induced by other means has been used to demonstrate membrane damage. Van der Zee et al. (1985) exposed erythrocytes to hydrogen peroxide or t-butyl hydroperoxide. The resulting lipid peroxidation was accompanied by leakage of potassium ions from the cells. In this case the involvement of -SH groups was also considered, since H_2O_2-induced damage was prevented by diamide, whereas the t-butyl hydroperoxide-induced damage was not. Photosensitized peroxidation of membrane phospholipids has also been shown to result in leakage from liposomes. Anderson and Krinsky (1973) used toluidine blue-photosensitized liposomes to investigate peroxidative damage leading to the leakage of glucose from the liposomes following visible light irradiation. Carotenoids, DABCO, BHT and α-tocopherol, used as singlet oxygen quenchers and free radical scavengers, protected the liposomes from the photodynamic damage. More recently, Girotti et al. (1985), showed that continuous blue-light irradiation of resealed erythrocyte ghosts in the presence of uroporphyrin or protoporphyrin as photosensitizers, resulted in singlet oxygen-mediated lipid peroxidation and membrane lysis as determined by glucose-6-P release, singlet oxygen involvement being implicated by the inhibiting action of azide. They showed that low concentrations of ascorbate enhanced the rates of both lysis and peroxidation, while high concentrations inhibited both processes.

Pro-oxidant activity was assumed to be favoured at low concentrations, where redox metal-mediated breakdown of photoperoxides occurred, amplifying peroxidation. At high concentrations the ascorbate was assumed to act as an antioxidant by scavenging or quenching activity.

In addition to causing lysis or leakage of membranes other effects of lipid peroxidation have been reported. Dearden and Hunter (1981) showed that singlet oxygen-mediated photooxidation of single bilayer vesicles caused a reduction in the microviscosity of the bilayer. The increase in chain fluidity resulting from the peroxidation of lipid double bonds was visualised as follows: the hydroperoxy group (-OOH) which is formed adjacent to the double bonds leads to breakdown products and to chain fissure. Such effects attack the integrity of the chain structure leading to a much more fluid environment. Alternatively the hydroperoxy group, being polar, will have a tendency to seek an environment less hydrophobic than the one in which it is situated. Configurational changes caused as the -OOH groups project towards the phospholipid head groups, would produce chain twisting and a more fluid environment. Interestingly, this increase in fluidity would lead to higher diffusive capabilities for oxygen and thus dissolved oxygen would show higher concentrations in such regions. This, being a continuous process, would lead to regions of high oxidation and large scale breakdown leading to loss of membrane integrity in certain regions. The application of the importance of processes such as this to a biological membrane must, however, take into account the more complex nature and incorporation of structural

protein in such a membrane. Dearden et al. (1985) further correlated the rate of photosensitized oxidation of microvesicles with the degree of unsaturation of the fatty acid chains.

The results of Dearden and Hunter (1981) conflict with those of other workers, including Dobretsov et al. (1977) and Eichenberger et al. (1982) where a decrease in membrane fluidity was demonstrated in liposomes and endoplasmic reticulum vesicles, and in microsomes respectively, and attributed to the lipid peroxidation induced.

In vivo lipid peroxidation and changes in membrane fluidity were linked by Sakanashi et al. (1986). Cultured melanoma cells exposed to UV-B (290-320 nm) radiation were found to undergo peroxidation. While no change in membrane fluidity was observed immediately after irradiation, it increased significantly 6 hours after exposure, by which time the lipid peroxidation products had been reduced to levels below that of controls. At the fluences chosen, resulting in only 10 per cent loss of viability, it was suggested that lipid peroxidation does not directly induce a significant alteration in membrane fluidity, but that delayed damage, or induced repair or metabolic processes involved in dealing with the peroxidative damage may result in such changes.

THE IMPORTANCE OF OXYGEN

The proposal that lipid peroxidation is a cause of near-UV-induced membrane damage necessitates demonstration that such effects are oxygen-dependent. It is a feature specific to near but not far-UV- induced effects that there is a strong dependence on

oxygen, which applies to cell killing in bacteria (Webb and Lorenz, 1970) and mammalian cells (Danpure and Tyrrell, 1976), in the enhancement of single strand break induction (Tyrrell et al., 1974; Peak and Peak, 1982) and the inactivation of transforming DNA (Peak et al., 1981).

The action spectra in Fig. 1 show the killing of stationary-phase E. coli WP2s uvr A following irradiation under aerobic and anaerobic conditions. Not only is sensitivity greater under aerobic conditions at wavelengths above 320 nm, but it is evident that distinct plateaux arise at 340, 365, 410 and 500 nm, interpreted as indicating chromophores absorbing radiation at these wavelengths. The inactivation of yeast cells (Ito and Ito, 1983) by broad-band near-UV radiation, considered to be due to membane damage, was reported to be oxygen-dependent, as was the inactivation of E. coli hem A8 (Peak et al., 1987). This study, discussed previously, also demonstrates membrane damage, while considering the role of porphyrin derivatives as possible endogenous photosensitizers.

Oxygen-dependence is evidently important in a variety of near UV-induced effects, and where lipid peroxidation is specifically demonstrated together with membrane damage the involvement of oxygen may be inferred without proof (Mandal and Chatterjee, 1970; Sakanashi et al., 1986). Lipid peroxidation-mediated effects may be modified by the addition of antioxidants (Anderson and Krinsky, 1973), prooxidants (Girotti et al., 1985), or by the exclusion of oxygen (Roshchupkin et al., 1975), or proposed without measurement (Klamen and Tuveson, 1982). Oxygen is therefore an important mediator of near-UV-induced effects; its mode of action may be

considered in relation to the formation of reactive oxygen species during irradiation and their subsequent activity within the cell.

The formation of reactive oxygen species

Oxygen in its ground state contains two unpaired electrons with parallel spins, imposing a restriction on electron transfer, slowing its reaction with non-radical species. The majority of oxygen effects are therefore thought to arise through more reactive species, namely superoxide anion, hydrogen peroxide, hydroxyl radicals and singlet oxygen.

The generation and reactivity of the superoxide radical ($O_2^{\cdot-}$)

If ground state oxygen accepts a single electron, the superoxide radical is formed, a process which takes place during the univalent reductions of oxygen to water in all aerobically respiring cells (Fridovich, 1975). This series of reactions results also in the generation of hydrogen peroxide and hydroxyl radicals.

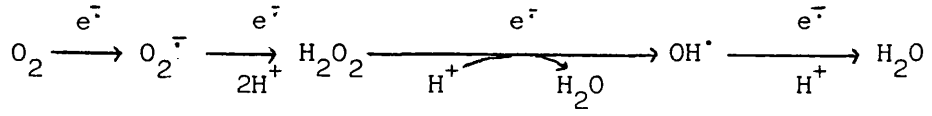

The reduced pyrimidine coenzymes NADPH and NADH have been shown to produce $O_2^{\cdot-}$ when irradiated by UV radiation extending from 290-405 nm (Cunningham et al., 1985), while these wavelengths have been shown to generate $O_2^{\cdot-}$ from other naturally occurring photosensitizers with quantum yields of about 10^{-7} to 10^{-9} molecules per photon (Peak et al., 1985). NADH has been used as a photosensitizer for the induction of DNA breakage by 334 nm

radiation (Peak et al., 1984), and $O_2^{\cdot-}$ has been implicated in the photosensitized breakage of DNA by 2 thio-uracil and 334 nm radiation (Peak et al., 1986). The superoxide ion is, however, considered by many to be too unreactive with biological targets to be of importance (Midden, 1985). Much of the $O_2^{\cdot-}$ generated within cells comes from membrane-bound systems, but while it will not diffuse through non-polar environments because of its charged nature, it is more stable in organic solutions and could destroy phospholipids, attacking the carbonyl groups of the ester bonds linking the fatty acids to the glycerol "backbone" of the phospholipids (Halliwell and Gutteridge, 1985).

In aqueous environments the radical undergoes dismutation reactions to produce hydrogen peroxide and oxygen:

$$HO_2^{\cdot} + HO_2^{\cdot} \longrightarrow H_2O_2 + O_2$$

$$HO_2^{\cdot} + O_2^{\cdot-} + H^+ \longrightarrow H_2O_2 + O_2$$

represented overall by:

$$O_2^{\cdot-} + O_2^{\cdot-} + 2H^+ \rightarrow H_2O_2 + O_2 \quad \text{(Fridovich, 1975)}$$

a reaction catalyzed by the superoxide dismutase (SOD) enzymes present in all cells.

Superoxide ion may be important in the metal-catalyzed Haber-Weiss reaction which results in the formation of potentially dangerous hydroxyl radicals:

$$Fe^{3+} + O_2^{\cdot-} \longrightarrow Fe^{2+} + O_2$$

$$Fe^{2+} + H_2O_2 \rightarrow Fe^{3+} + OH^{\cdot} + OH^-$$

represented overall by:

$$O_2^{\cdot-} + H_2O_2 \xrightarrow[\text{catalyst}]{Fe} O_2 + OH^{\cdot} + OH^-$$

It has also been suggested that toxicity due to the superoxide ion may be due to its conversion to the highly toxic singlet oxygen by electron transfer from superoxide to other electron acceptors such as disulphides or lipid peroxides. The role of SOD is then considered to be vital in catalyzing the dismutation reaction to yield the relatively harmless products before singlet oxygen can be formed (Midden, 1985).

While many deleterious effects of systems generating the superoxide radical have been reported, many such effects are reduced not only by superoxide dismutases, but also by catalase and hydroxyl radical scavengers indicating that H_2O_2 and/or hydroxyl radicals are important within such systems (Halliwell and Gutteridge, 1985).

The generation and reactivity of hydrogen peroxide (H_2O_2)

As shown above, H_2O_2 is produced as a result of the dismutation of superoxide ion, and as a normal metabolite of cells it is present at a concentration of 10^{-7} - 10^{-9} μM (Freeman, 1984). However, H_2O_2 is an important photoproduct of near-UV radiation (McCormick et al., 1976) and is known to be generated as the result of the near-UV irradiation of L-tryptophan, riboflavin and tyrosine, which are components of tissue culture medium (Stoien and Wang, 1974). In addition, H_2O_2 and near-UV radiation synergistically kill bacteria and phage (Hartman et al., 1979;

Hartman and Eisenstark, 1978), and there is evidence that the synergistic action is probably due to the NUV conversion of H_2O_2 to superoxide ion (Ahmad, 1977).

The presence of between 12 and 30 μM H_2O_2 is sufficient to reduce the survival of cold-shocked Salm. typhimureum and E. coli (Mackey and Derrick, 1986), while 20 μM kills more than 95 per cent of human fibroblasts after a 30 minute incubation at 37°C (Hoffmann and Meneghini, 1979). The incorporation of catalase (the enzyme responsible for catalyzing the dismutation of H_2O_2 to oxygen and water) in the plating medium has been shown to protect E. coli cells against the lethal and mutagenic effects of broad-band NUV radiation (Sammartano and Tuveson, 1984). The pretreatment of growing E. coli cells with non-lethal amounts of H_2O_2 has been shown to induce resistance not only to subsequent, higher doses of H_2O_2 but also to NUV radiation (Coombs and Moss, 1987; Sammartano and Tuveson, 1985; Tyrrell et al., 1985) leading to the suggestion that H_2O_2 (or NUV) pretreatment increases levels of enzymes that scavenge and degrade H_2O_2 and oxygen-related free radicals (Tyrrell, 1985; Sammartano and Tuveson, 1985). H_2O_2 is a weak oxidizing agent and can inactivate a few enzymes directly, usually by oxidation of essential thiol (-SH) groups. It can penetrate cell membranes rapidly and inside the cell it can probably react with Fe(II) or Cu(I) ions to form the hydroxyl radical:

$$Fe^{2+} + H_2O_2 \longrightarrow Fe^{3+} + OH^{\cdot} + OH^{-}$$

This is probably the origin of most of its toxic effects. Evidence for this theory comes from the ability of hydroxyl radical

scavengers to decrease the toxicity of H_2O_2 only if they are able to penetrate into the cell (Halliwell and Gutteridge, 1985). H_2O_2 has been shown to affect cell membranes directly, for example by causing an increase in membrane potential, followed by a massive depolarization as demonstrated by Scott et al. (1987) in renal epithelial cells, a change also brought about by superoxide ions. The prevention of cellular swelling which results from exposure to oxygen radicals reduces these membrane potential changes.

The generation and reactivity of hydroxyl radicals ($OH^{\cdot}$)

As previously stated, the hydroxyl radical is generated during the univalent reduction of oxygen to water and in the metal - catalysed Haber-Weiss reaction, while exposure of living cells to ionizing radiations results in $OH^{\cdot}$ production, due to the radiolysis of their water content. Endogenous H_2O_2 is photolysed by light of wavelengths below 350 nm to form two $OH^{\cdot}$ radicals (Czapski, 1984). The $OH^{\cdot}$ radical reacts with extremely high rate constants with almost every type of molecule found in living cells, such as sugars, amino acids, phospholipids, DNA bases and organic acids (Halliwell and Gutteridge, 1984, 1985). Its reactivity is such that, if $OH^{\cdot}$ is formed in living systems, it will react immediately with whatever biological molecule is in the vicinity, consequently diffusing only about 100 nm from its locus of production (Slater, 1976). Upon reaction it will form new radicals of varying reactivities; this is discussed in further detail in the context of lipid peroxidation. Reactions of $OH^{\cdot}$ with purine and pyrimidine bases present in DNA and RNA can severely damage the structure and

induce strand breakage, such events may be lethal or mutagenic. The modification of amino acid residues by $OH^{\cdot}$ reaction may affect enzyme activity, while proteins may be fragmented or crosslinked causing varied effects, including membrane disruption (Wolff et al., 1986).

Other free radical species

It is also important to note that free radical species may arise, during lipid peroxidation as discussed subsequently, and during ultraviolet radiation of skin. It has recently been shown by Koch and Chedekel (1987) that precursors of melanin present in the skin are photochemically unstable in the presence of mid- and near-UV radiation, and that ensuing photochemical processes involve free radical production. The authors demonstrated single strand break induction in DNA as a result of such free radicals and speculated upon their ability to damage proteins and initiate lipid peroxidation. Free radical reactions have been implicated in photocarcinogenesis, reviewed most recently by Black (1987), a review which also includes reference to other cutaneous damage mediated by free radical reactions in response to UV- irradiation.

Reactive free radicals may also damage cells through a pathway dependent essentially on membrane damage (Slater, 1984):

(a) by covalent binding of the free radical to membrane enzymes and/or receptors, thereby modifying the activities of membrane components.

(b) by covalent binding to membrane components, thereby changing the structure and producing effects on membrane function and/or

antigenic character.

(c) by disturbance of transport processes through covalent binding, thiol-group oxidation, or change in polyunsaturated fatty acid: protein ratios.

(d) by initiation of lipid peroxidation of polyunsaturated fatty acids with direct effects on membrane structure, and associated influences of the products of peroxidation on membrane fluidity, crosslinking, structure and function.

Potential effects from free radical attacks on biological membranes are shown diagrammatically in Fig. 14.

The generation of singlet oxygen ($^1O_2$)

One way of increasing the reactivity of oxygen is to move one of the unpaired electrons so that the spin restriction is alleviated. Singlet oxygen so formed has no unpaired electrons (and is therefore not a radical), and is considered to be the most important reactive species in biological systems. Singlet oxygen is formed when certain molecules absorb light of a specific wavelength, the absorbed energy raising the molecule to an 'excited state'. The excitation energy can then be transferred to an adjacent oxygen molecule, converting it to the singlet state, whilst the photosensitizer molecule returns to the ground state.

$$S + h\nu \longrightarrow {}^1S \rightsquigarrow {}^3S + {}^3O_2 \longrightarrow S + {}^1O_2$$

The singlet oxygen produced can react with other molecules present, or the photosensitizer molecule itself. The chemical

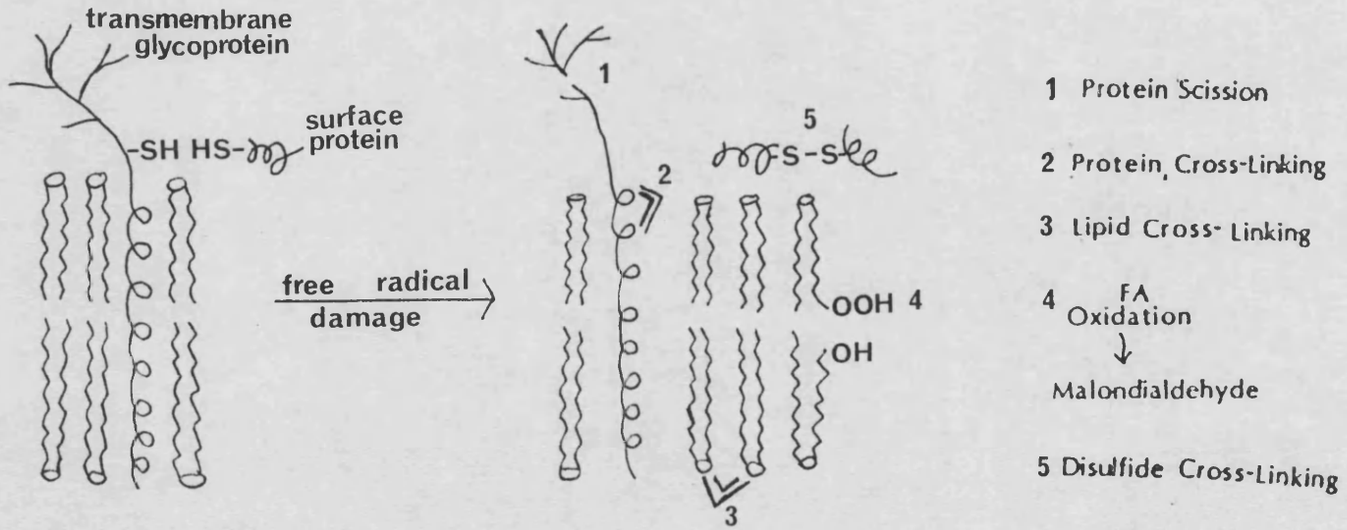

Figure 14

Potential effects resulting from free radical attack upon biological membranes. (Adapted from Black (1987)).

changes thereby produced are known as photodynamic effects, or type II photosensitizations.

The presence of suitable chromophores for singlet oxygen generation

Sensitizers which could produce singlet oxygen intracellularly include riboflavin and its derivative FMN (flavin mononucleotide) and FAD (flavin adenine dinucleotide), bilirubin, retinal and various porphyrins (Halliwell and Gutteridge, 1985). Intracellular flavins have been implicated as photosensitizers in the killing of lung fibroblasts and irradiation of cell homogenates in the presence of riboflavin have been shown to increase lipid peroxidation (Pereira et al., 1976). The base 4-thiouridine, found in many bacterial cells, with an absorption peak at 340 nm is discussed elsewhere as an important chromophore, however it has also been demonstrated to yield singlet oxygen when irradiated at 365 nm (Salet et al., 1985), causing oxidation of tryptophan and histidine, which may explain some of its biological relevance.

The reactivity of singlet oxygen

Singlet oxygen can interact with other molecules by combining chemically with them, or by transferring its excitation energy to them, returning to the ground state while leaving the molecule in an excited state (quenching). Compounds containing two double bonds separated by a single bond (i.e. conjugated double bonds) often react with singlet oxygen to give endoperoxides. If one double bond is present a hydroperoxide will be produced. These reactions are further discussed in the section describing lipid peroxidation.

Singlet oxygen may also damage proteins by the oxidation of the amino acid residues histidine, tryptophan, methionine and cysteine, while such biologically important molecules such as DNA, NADPH, cholesterol and vitamin E will also react (Halliwell and Gutteridge, 1985).

The probability of cellular damage mediated by singlet oxygen will depend upon the quantum yield of singlet oxygen production, the situation of the sensitizer, and the lifetime of the excited molecule. A longer lifetime will allow more time for reactions to take place and allow the excited oxygen molecule to diffuse further away from its source. If endogenous photosensitizers are situated in the cytosol, the lifetime of singlet oxygen will be in the order of 3 to 4 microseconds, and the mean diffusion distance before solvent quenching occurs will be about 0.06 - 0.1 microns (from a review by Valenzeno, 1987). The lifetime of this species is prolonged in a lipid environment, leading to an expected extended diffusion distance within the hydrophobic interior of a membrane of about 0.16 microns (Pooler and Valenzeno, 1979). There is no quantitative data relating to singlet oxygen penetrability through biological membranes but while membranes are freely permeable to ground state oxygen, and therefore presumably singlet oxygen, it does not necessarily follow that the latter would remain in the excited state after crossing the membrane interface (Valenzeno, 1987). Cellular and subcellular mechanisms of photodynamic action involving exogenous photosensitizers are reviewed by Ito (1978).

The detection of singlet oxygen in biological systems

Two approaches are frequently used to determine the involvement of singlet oxygen in a biological effect, though neither is specific to singlet oxygen and could indicate the involvement of other active oxygen species (Foote, 1979).

One method relies upon the use of singlet oxygen quenchers, such as DABCO, shown by Peak et al., in 1981, to protect transforming DNA against the inactivation due to near-UV irradiation. Other quenching molecules include sodium azide, β-carotene, α-tocopherol and histidine, the uses of which are compared by Ito (1978), and rate parameters for several quenchers has been described (Lindig and Rodgers, 1981).

Another approach relies upon the use of deuterium oxide (D_2O) in which the decay time of singlet oxygen is about 10 times slower than in H_2O (Merkel et al., 1972). An enhanced biological effect in a deuterated medium is taken as evidence for the participation of singlet oxygen in the damage, as shown for example by Peak et al. (1986) where the photosensitized breakage of DNA by 334 nm irradiation in the presence of 2-thiouracil was enhanced five times when D_2O replaced H_2O as the solvent. Complex results in this series of experiments, including the reduction of single strand breaks formed when superoxide dismutase was present, indicating the additional involvement of superoxide anion, made interpretation difficult.

If near-UV-induced membrane damage is to be attributed, at least in part, to active oxygen-mediated events, reference to research where membrane damage has resulted from the sensitized photomodification of membranes may be useful.

Evidence from sensitized photomodification of membranes

It has been suggested that near-UV irradiation of endogenous photosensitizers resulting in the production of singlet oxygen may be responsible for attacking a number of targets within the cell. If such photosensitizers are situated within the cytoplasmic membrane then locally produced $^1O_2$ may result in lipid peroxidation or modification of membrane proteins, resulting in perturbations in membrane function. The sensitized photomodification of biological membranes and model membrane systems may therefore help in the understanding of processes taking place during irradiation of natural membranes where endogenous photosensitizers are present.

Much work has been done in this field, where membrane damage has been demonstrated following the near-UV irradiation of photosensitized cells. Wagner et al. (1980) presented evidence that the broad-band near-UV irradiation of E. coli in the presence of acridine, a photosensitizer localizing in the hydrocarbon zones of membranes, damaged both DNA and membranes. Split-dose experiments indicated that recovery was possible during a 30 min incubation period, but that the sub-lethal damage from which recovery was possible was not associated with the reduced sedimentation properties of the cellular DNA. These authors demonstrated that E. coli K1060 (the unsaturated fatty auxotroph) was more sensitive to photosensitized irradiation when incorporating oleic acid rather than linoleic acid, and still more sensitive when incorporating elaidic acid. They interpreted these results as an indication that membrane fluidity was essential for resistance to the photo-sensitized damage. Membrane damage was implicated by the increased

sensitivity of irradiated cells grown in low osmolarity minimal medium and the increasing permeability to σ-nitrophenyl-D-β galatopyranoside, the β-galactosidase indicator. The outer membrane was shown to be damaged by the loss of ability to exclude lysozyme. Subsequent work indicated that split dose recovery: (a) did not require DNA synthesis, (b) was reduced by inhibition of electron transport or protein synthesis and (c) was eliminated by inhibition of phospholipid synthesis or cell wall synthesis (Wagner et al., 1982). That outer membrane proteins were selectively damaged by photosensitized near-UV irradiation was shown by changes in bacteriophage adsorption and gel electrophoretic analysis (Wagner and Snipes, 1982). While such evidence may be similar to events occurring during the irradiation of endogenous photosensitizers there are important differences. The membrane fatty acid-related effect described above is in direct contrast to the results observed by Klamen and Tuveson (1982) described previously where increasing unsaturation resulted in increasing near-UV sensitivity.

The involvement of protein synthesis in recovery processes described by Wagner et al. (1982) is also in contrast with the absence of such a requirement during the recovery by E. coli from near UV-induced salt-sensitivity described by Kelland et al. (1983b). Therefore results from photosensitized-irradiation experiments, while providing useful data, should be used with care when interpreting near-UV irradiation effects as being due to hypothetical endogenous sensitizers.

A review by Lamola (1977) considered the evidence for membrane damage in the photoinactivation of cells by near-UV and visible

light in the presence of naturally occurring and added photosensitizers. Ito has been prominent in the field of cell photosensitization, and some of his work is included in a review (Ito, 1983) where photodynamic agents are considered as tools for cell biology. More recently Valenzeno reviewed photomodification of biological membranes and model membranes with emphasis on singlet oxygen mechanisms (Valenzeno, 1987). Valenzeno describes the binding sites of various photosensitizers and the results of irradiation. Singlet oxygen is considered in terms of its diffusion through membranes, its lifetime and its role in photosensitization reactions. He emphasises that membrane photomodification cannot be understood based only on the properties of sensitizers and singlet oxygen in aqueous solution, but rather on the properties of sensitizers in association with membranes. These evidently are important considerations when formulating a hypothesis for membrane damage suffered as a result of the absorption of near-UV radiation by proposed endogenous photosensitizers.

THE PROCESS OF LIPID PEROXIDATION AND ITS CONSEQUENCES IN THE CELL

Lipids in cell membranes

The lipid bilayer is the basis for cell membrane structure (Fig. 2), where phospholipids are a major constituent. The general structure of a membrane phospholipid is shown in Figs. 5 and 8. It is important to note that one of the hydrocarbon chains (that on position 2) is normally unsaturated. In bacterial cells this residue would normally be mono-unsaturated, as 16:1 or 18:1 fatty

acids (Cronan and Vagelos, 1972). In mammalian cells polyunsaturated fatty acids are abundant, as 18:2, 18:3, 20:2, 20:4 and 22:6 residues (Lagarde et al., 1984).

When lipids are subjected to free radical attack the nature of the lipid will necessarily modify the properties of the free radicals formed, since radical centres will be formed in a non-aqueous environment and their arrangement within the lipid bilayer may permit maximum interaction of the individual molecules, as demonstrated in vitro by Sunamoto et al. (1985) using liposomal membranes. Such reactions in a cell membrane would maximize damage to the cell.

The Peroxidation Process

Lipid peroxidation has three discernible phases, namely initiation, propagation and termination.

The role of oxygen-derived species in the initiation of lipid peroxidation

Unlike ground-state oxygen, singlet oxygen can react rapidly with compounds containing C=C bonds to give hydroperoxides. If one double bond is present the ene-reaction can occur, where the singlet oxygen adds on and the double bond shifts to a different position, resulting in the production of a hydroperoxide:

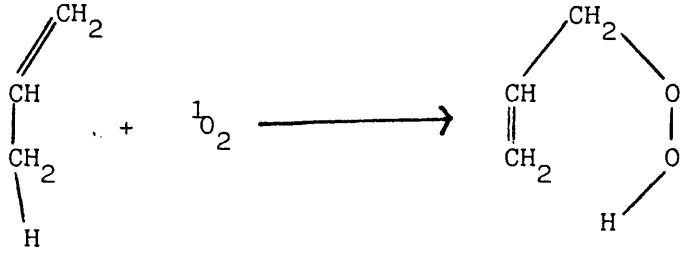

This reaction is so rapid that is has been postulated as a process initiating free radical autooxidation (Frankel, 1984). Where conjugated double bonds are present, an endoperoxide may result:

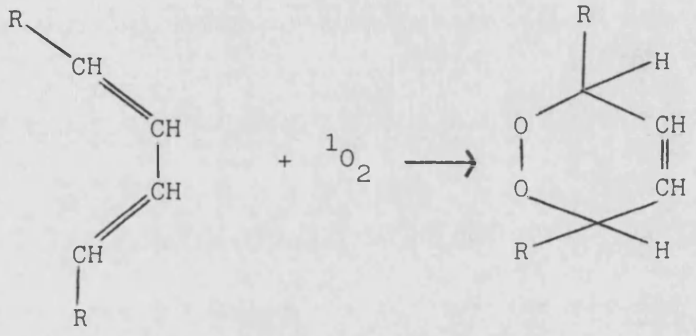

(from Halliwell and Gutteridge, 1985).

Such reactions may result from the production of singlet oxygen by near-UV irradiation of endogenous sensitizers, and cytochrome C has been shown to catalyze phospholipid oxidation via singlet oxygen production (Goni et al., 1985). A free radical sensitized process can also occur by a type I photo-oxidation, in which the sensitizer reacts directly with the substrate (Frankel, 1985). The hydroxyl radical ($OH^{\cdot}$) is an efficient initiator of lipid peroxidation (Raleigh and Kremers, 1978) and its generation and importance in radiation-induced events has been discussed. $OH^{\cdot}$ will react with unsaturated fatty acids by hydrogen abstraction from a methylene ($-CH_2-$) group, leaving an unpaired atom on the carbon ($-\dot{C}H-$) and forming a lipid radical:

$$\text{Lipid-H} + OH^{\cdot} \longrightarrow \text{Lipid}^{\cdot} + H_2O$$

This reaction is known to occur in membranes, the rate constant for the reaction of $OH^{\cdot}$ with artificial lecithin bilayers is about $5 \times 10^8\ M^{-1}s^{-1}$, and the reaction causes leakiness of the bilayer.

In contrast with this view a recent report by Minotti and Aust

(1987) concludes that, in the liposomal model which they used, lipid peroxidation is not initiated by $OH^{\cdot}$, but is dependent upon the Fe^{3+}:Fe^{2+} ratio. The peroxidation system they used involved Fe^{2+} and H_2O_2, where $OH^{\cdot}$ is normally considered to be the initiating species produced as a result of the iron-catalyzed Haber-Weiss reaction:

$$O_2^{\cdot-} + Fe^{3+} \longrightarrow O_2 + Fe^{2+}$$

$$2O_2^{\cdot-} + 2H^{+} \longrightarrow O_2 + H_2O_2$$

$$Fe^{2+} + H_2O_2 \longrightarrow Fe^{3+} + OH^{-} + OH^{\cdot}$$

Minotti and Aust found that while catalase and hydroxyl radical scavengers could inhibit the generation and detection of $OH^{\cdot}$ they could either stimulate or inhibit lipid peroxidation. This was interpreted as a specific alteration in the Fe^{3+}:Fe^{2+} ratio by these agents, and that this was the factor which determined whether lipid peroxidation would be initiated or inhibited.

Superoxide ion is insufficiently reactive to abstract $H^{\cdot}$ from membrane lipids, and in any case would not be expected to enter the membrane interior because of its charged nature. However, the protonated form, $HO_2^{\cdot}$ is more reactive and may attack fatty acids directly.

The propagation processes of lipid peroxidation

Following the formation of the lipid (alkyl) radical by hydrogen abstraction, the molecule tends to be stabilized by a molecular rearrangement to form a conjugated diene. This reacts easily with an oxygen molecule to give a peroxy radical ($L\text{-}OO^{\cdot}$). Peroxy radicals can abstract a hydrogen atom from an adjacent

unsaturated fatty acyl chain thus propagating the reaction. The peroxy radical combines with the hydrogen atom it abstracted, producing a lipid hydroperoxide (LOOH). This sequence is shown in Fig. 15.

Further reactions of the lipid hydroperoxide may be considered, since in the presence of small amounts of transition metal ions (such as Mn), lipid alkoxy ($LO^{\cdot}$) radicals and lipid peroxy ($LO_2^{\cdot}$) radicals are produced, which in turn can initiate hydrogen abstraction from the unsaturated fatty acid causing further initiation and propagation steps (Konings, 1984):

$$LOOH + Mn^{n+} \longrightarrow LO^{\cdot} + OH^{-} + Mn^{(n+1)+}$$

$$LOOH + Mn^{m+} \longrightarrow LO_2^{\cdot} + H^{+} + Mn^{(m-1)+}$$

Alternatively, hydroperoxides may decompose in a homolytic fashion to produce lipid alkoxy and hydroxyl radicals:

$$LOOH \longrightarrow LO^{\cdot} + OH^{\cdot}$$

Lipid hydroperoxides may also react with superoxide anion to produce alkoxy radicals which again initiate further reactions:

$$LOOH + O_2^{\cdot -} \longrightarrow O_2 + LO^{\cdot} + OH^{-}$$

(Thomas et al., 1978).

The termination of lipid peroxidation

When sufficient oxygen and suitable substrate (lipid) is present it can be assumed that most of the free radicals are in the form of the peroxy ($LO_2^{\cdot}$) radical (Konings, 1984).

The termination of chain reactions can take place by combination of radicals followed by decomposition of the tetroxide,

$$LO_2^{\cdot} + LO_2^{\cdot} \longrightarrow (LO_2)_2 \quad \text{(tetroxide)}$$

Fig. 15. The propagation of lipid peroxidation

(from Halliwell and Gutteridge, 1985).

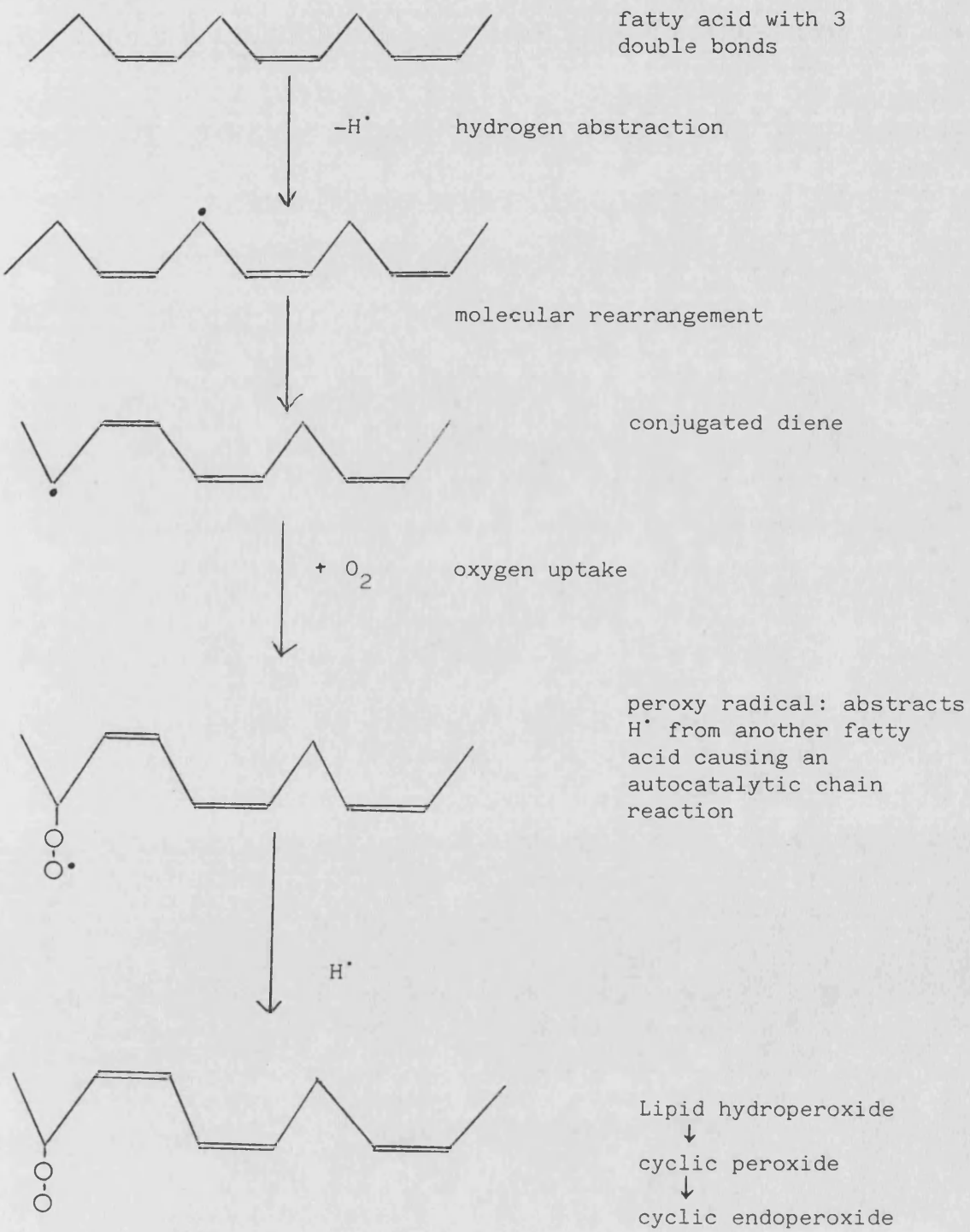

$$(LO_2)_2 \longrightarrow 2LO^{\cdot} + O_2$$

$$LO^{\cdot} + LO^{\cdot} \longrightarrow (LO)_2$$

In a biological situation it is the function of antioxidants (A) to terminate the process by the reaction:

$$LOO^{\cdot} + AOH \longrightarrow AO^{\cdot} + LOOH$$

Vitamin E is such an antioxidant, admirably suited due to its position within the membrane (Fig. 16).

Reaction of vitamin E with the peroxy radical will prevent further $H^{\cdot}$ abstraction:

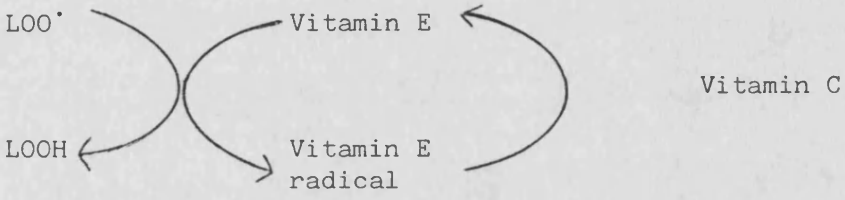

Vitamin C serves to regenerate vitamin E (Tappel, 1968).

The fate of lipid hydroperoxides and consequences to the cell

Pure lipid hydroperoxides are fairly stable molecules at physiological temperatures, but in the presence of transition-metal complexes, their decomposition is catalyzed. Many metal complexes are available *in vivo*, including simple complexes of iron salts with phosphate compounds as well as non-haem proteins. Free haem is effective, as are haemoglobin, myoglobin and cytochromes, but while ferritin catalyzes hydroperoxide decomposition, transferrin and lactoferrin do not. *In vivo* decomposition may be possible, resulting in the formation of alkoxy or peroxy radicals:

$$LOOH + Fe^{2+}\text{-complex} \longrightarrow Fe^{3+}\text{-complex} + OH^{-} + RO^{\cdot}$$

or

$$LOOH + Fe^{3+}\text{-complex} \longrightarrow Fe^{2+}\text{-complex} + ROO^{\cdot}$$

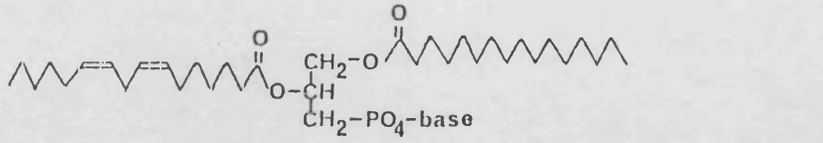

Structure of a phospholipid

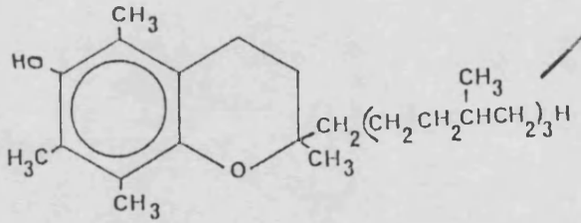

Structure of vitamin E

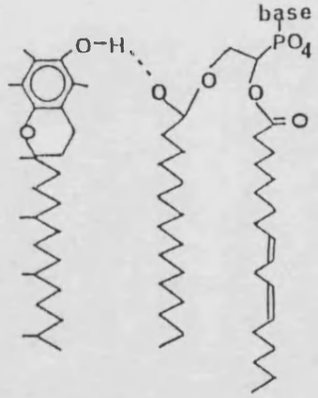

Possible interaction between vitamin E and membrane phospholipids through hydrophobic and hydrogen bondirgs

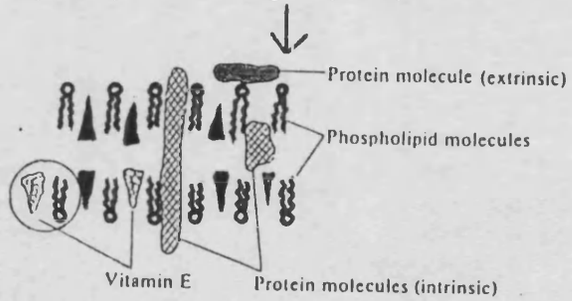

Figure 16

The structure of vitamin E and its possible interaction with a phospholipid in the cell membrane.

These radicals may then propagate further reactions.

UV light has been shown to degrade hydroperoxides in vitro, due to the photolytic cleavage of the relatively weak O-O bond, with the formation of alkoxy and hydroxyl radicals:

$$LOOH + h\nu \longrightarrow LO^{\cdot} + OH^{\cdot}$$

both of which will be involved in propagation reactions. Wavelengths required to initiate such decomposition are below 338 nm (Schieberle and Grosch, 1984) but may have some consequence in solar and broad-band near-UV irradiations.

Further breakdown products have been considered to have a wide range of biological effects (see reviews by Logani, 1980; Slater, 1984; Halliwell and Gutteridge, 1985; Black, 1987). Aldehydes, including malonaldehyde, have variously been reported to attack molecules with -SH or $-NH_2$ groups on proteins, so that enzymes, for example Na^+K^+ATPase and glucose-6-phosphatase, are inhibited by reaction with aldehydes. Aldehydes have also been shown to inhibit protein synthesis and to interfere with bacterial and animal cells in culture, while surface receptors may be inactivated. Free radical intermediates of oxidizing lipids have been shown to be radiomimetic not only in damage caused to amino acids and proteins, but also towards nucleic acids and their bases (Schaich and Borg, 1984). Damage specific to cell membranes as a result of lipid peroxidation has been previously discussed, and while it is in this area that emphasis has been placed during this work, it is evident that events related to lipid peroxidation are not confined to membrane structures.

CELLULAR DEFENCE AGAINST OXYGEN-MEDIATED AND FREE RADICAL SPECIES

At that point in evolution when cyanophytes came into being, free oxygen became available, and while it permitted an increased energy yield to be obtained from foodstuffs by aerobic metabolism, multiple lines of defence were necessarily developed to prevent or minimize unwanted oxidative reactions. Defence mechanisms protecting the cell against attack from reactive oxygen species or free radicals can broadly be classified into enzymatic or quenching systems.

Enzyme systems

A mutually supportive group of enzymes, the superoxide dismutases (SOD), catalases and glutathione peroxidases and reductases work together as follows:

Superoxide dismutases catalytically scavenge the superoxide ion catalyzing its rate of dismutation:

$$O_2^{\cdot -} + O_2^{\cdot -} + 2H^+ \longrightarrow H_2O_2 + O_2$$

The resultant hydrogen peroxide, together with that from other sources, is removed by catalases which catalyze the reaction:

$$2H_2O_2 \longrightarrow 2H_2O + O_2,$$

or by peroxidases which bring about the general reaction:

$$SH_2 + H_2O_2 \longrightarrow S + 2H_2O$$

where SH_2 is a substance which becomes oxidized. One such substance is reduced glutathione (GSH) which, following its oxidation during the process, must be re-reduced by a further enzyme, glutathione reductase, in the presence of NADPH. This sequence of events is shown below:

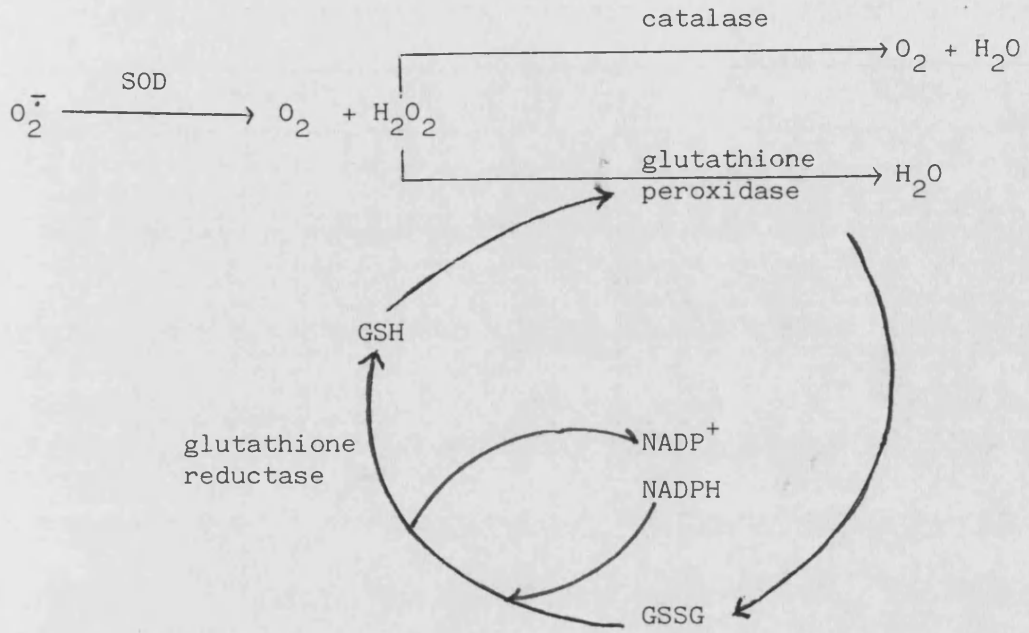

adapted from Proctor and Reynolds (1984).

The subcellular localization of glutathione, glutathione peroxidase and glutathione reductase has been analyzed by Mbemba et al. (1985). GSH was found in all subcellular fractions, whereas the enzymes were restrained to the cytoplasm and mitochondrial fractions. Skin glutathione levels have recently been shown to become depleted by exposure to both mid- and near-UV radiations. Levels are restored within a few hours, compatible with the suggestion that GSH acts as an endogenous photoprotective agent in the skin, but the authors suggest that its depletion may contribute to the production of phototoxicity by these radiations (Connor and Wheeler, 1987).

Endogenous glutathione has been demonstrated to have an important role in the protection of human fibroblasts from 405, 365, 334 and 313 nm radiations, while having no effect on 254 nm-

irradiated cells (Tyrrell and Pidoux, 1986). By comparing the sensitivities of glutathione-depleted cells irradiated with and without cysteamine, a powerful radical scavenger, Tyrrell and Pidoux concluded that glutathione, rather than acting as a radical scavenger, was indeed acting as the hydrogen donor for glutathione peroxidase activity. The transportation of glutathione as an ester into glutathione-deficient fibroblasts has also been shown to offer complete protection against γ-irradiation, particularly when added immediately after irradiation, suggesting a function in repair processes (Wellner et al., 1984). However, Wolters and Konings (1984) could show no such protective effect of GSH in X-irradiated mouse fibroblasts.

There are two forms of glutathione peroxidase, one form contains selenium and is responsible for reactions with both hydrogen peroxide and soluble fatty acid hydroperoxides but is not capable of catalyzing reactions involving complex lipid hydroperoxides (Grossman and Wendel, 1984). The other enzyme does not contain selenium, but has activity towards H_2O_2 and appears to be specific for organic peroxides (Witting, 1980), catalyzing the reaction:

$$2ROOH + 2GSH \longrightarrow 2ROH + GSSG + 2H_2O$$

It was demonstrated by McCay et al. (1976) that while glutathione peroxidase activity inhibits lipid peroxidation in membranes, it does not appear to do so by reducing membrane lipid peroxides to lipid alcohols, neither does it quench autocatalytic propagation steps. The authors considered that the enzyme exerted

its effect by preventing free radical attack on the polyunsaturated fatty acyl groups during the reaction. The mechanism, they suggest, is the reduction by the glutathione peroxidase system, of hydrogen peroxide formed in their reaction systems.

It is considered by Mead (1982) that membranes are further protected against peroxidative damage by the inclusion of saturated fatty acids which slows down the rate of peroxidation. Further, the presence of phospholipases, which remove damaged fatty acids from the phospholipid, ensure their rapid removal and subsequent hydrolysis by hydrolase enzymes.

Agents acting as free radical quenchers

Vitamin E (α-tocopherol) is a fat-soluble molecule which, being hydrophobic, tends to concentrate in the interior of membranes (Fig. 16). Mitochondrial membranes, requiring particular protection against peroxidation, contain about 1 molecule of vitamin E per 2100 molecules of phospholipid. Vitamin E both quenches and reacts with singlet oxygen (Foote, 1978) and could therefore protect the membrane against this species. It also reacts, though slowly, with the superoxide radical (though since this does not initiate lipid peroxidation it may be of less importance here). Most importantly, vitamin E reacts with lipid peroxy radicals to form vitamin E radicals which are insufficiently reactive to abstract $H^{\cdot}$ from the membrane lipids. It thus interrupts the chain reaction of lipid peroxidation by acting as a chain terminator (Halliwell and Gutteridge, 1985). The tocopheryl radicals so formed subsequently react with vitamin C (Tappel, 1968) in order to regenerate vitamin

E. A report in press (McCay et al., through Black, 1987) provides evidence for the use of glutathione in this role.

Vitamin E has recently been described by Ohyashiki (1986) to interact with membrane lipids to decrease membrane fluidity, while the nature of α-tocopherol complexes with fatty acids has been investigated and described (Erin et al., 1985). Vitamin E in conjunction with butylated hydroxytoluene has been shown to suppress the cytotoxicity induced by cholesterol-derived photoproducts, which are known to induce tumour formation (Chan et al., 1980). Chan and Black (1977) had earlier demonstrated that vitamin E, glutathione and vitamin C were all able to reverse UV-induced cytotoxicity, assessed by the restoration of colony forming ability.

Other agents which may act as biological antioxidants include ascorbate, sulphydryl compounds, selenium, carotenoids and mannitol. The role of such antioxidants as photo-protectants has recently been discussed in a review by Black (1987).

SCOPE OF THE PRESENT WORK

The first part of this study was designed to investigate the near-UV sensitivity of the unsaturated fatty acid auxotroph, E. coli K1060 in relation to the unsaturated fatty acids present in the cell membrane. Sensitivity was determined by means of survival curves, and membrane damage as evidenced by the leakage of rubidium. Lipid peroxidation was measured at fluences resulting in membrane damage.

In the second part the investigation was extended to human fibroblasts grown in cell culture, where comparisons were made between a normal and an actinic reticuloid strain. In this section the effect of near-UV radiation on membranes was investigated with reference to their pinocytic activity.

In the final part, preliminary investigations into the peroxidation of unsaturated fatty acids and liposomes during, and following, near-UV irradiation were undertaken.

GENERAL METHODOLOGY

BACTERIOLOGICAL PROCEDURES

1. EQUIPMENT

Glassware

Unless otherwise stated, all glassware was washed with tap water and three rinses of glass distilled water, and dried overnight in a hot air oven. Sterilization was then performed by heating at 160°C for at least 1 hour in an oven. No detergent was used in order to eliminate possible damage to the bacterial membrane by residual detergent (Moss and Smith, 1981).

Aeration apparatus

A forced aeration system standardised the amount of air introduced into culture flasks. Atmospheric air was drawn through a coarse cotton wool filter by a 40 watt Reciprotor piston pump (Edwards High Vacuum Ltd., Sussex), and into a 5 litre bell jar. This was connected to a Rotameter flow meter (Rotameter, Croydon) which monitored the flow rate at 10 ml min^{-1} into each culture vessel. The air was sterilized by passage through a 25 mm diameter Sartorious membrane with a nominal pore size of 0.45 µm as described by Hodges (1979).

Incubation water bath

This was a Gallenkamp immersion bath set at a temperature of 30° and shaking at 100 cycles min^{-1}. The temperature was checked regularly since this affects the fatty acid composition of bacterial lipids (Cronan, 1968).

2. THE ORGANISMS

For the majority of these studies the organism used was E. coli K1060. This strain is an unsaturated fatty acid auxotroph, unable to synthesize or degrade unsaturated fatty acids. The genotype is F^-, fad E62, fab B, lac 160, mel-1, sup E57, sup F58; the organism was obtained from the Medical Research Council, U.K.

The mutations relevant to this study are those relating to fatty acid metabolism. The fad E62 lesion results in an inability to degrade fatty acids via the β-oxidation pathway. The fab B lesion results in a deficiency of the β-ketoacyl-ACP synthetase enzyme, thus preventing unsaturated fatty acid synthesis. These mutations are described further in the Introduction.

Other strains, used for comparison, are shown in Table 2.

3. STORAGE OF ORGANISMS

Master cultures were kept in plastic vials and stored in the vapour phase of a liquid nitrogen refrigerator (Union Carbide Ltd.) at approximately -148°C. These were subcultured into nutrient agar slopes (5 ml of molten nutrient agar containing 0.02% oleic acid poured into 8 ml screw-capped glass vials obtained from Wheaton Scientific, New Jersey, U.S.A.). Inoculated slopes were incubated for 24 h at 37°. One ml of sterile liquid paraffin BP (BDH Ltd.) was aseptically added to each slope to limit evaporation. Liquid paraffin was sterilized in sealed glass 10 ml ampoules by heating at 160°C in a hot air oven for 1 hour. Slopes were kept at room temperature and used routinely for storage of the organism.

Table 2. List of Strains used.

Strain	Lab code number	Relevant genotype	Other genotype	Reference
K-12 JG139 (SR 385)	DV66	+	F^-, rha-5, lacZ53, rps L151, thy A36, deo(C2?)	Kelland (1984)
K-12 AB 1157	DV4	+	F^-, thr, leu, arg, his, pro, ara, lac, gal, mtl, thi, xyl, tsx^r, str^r	Adelberg and Burns (1960)
K-12 SR 362	DV65	uvr A uvr B recA, phr.	F^-, leu, thyR, met, rha, lacZ, str	constructed at Stanford University
B/r	DV132	+	lon, sul	Hill (1964)
CGSC 4401	-	+	wild type	Bachmann (1972)
K1060	DV133	fad E62 fab B	F^-, lac 160, mel-1, sup E57, sup F58	Overath et al. (1970)
SR246	DV51	pol B100	F^-, thy A, thy R, lys, lac Z, su, str	constructed at Stanford University (Kelland, 1984)
B. stearo-thermophilus	-			

4. MEDIA

The preparation of M9 salts solution

M9 salts solution (Anderson, 1946) was used for the washing and dilution of cells, and as a basis for minimal media.

M9A

NH_4Cl	50 g	
$MgSO_4.7H_2O$	10 g	This is a 50x concentrate
water to 1 litre		

M9B

KH_2PO_4	37.5 g	
$Na_2HPO_4.2H_2O$	75 g	This is a 12.5x concentrate
NaCl	6.25 g	
water to 1 litre		

All chemicals were 'Analar' grade obtained from BDH Ltd. Stock concentrates were autoclaved at 121°C for 20 min in 500 ml M.R.C. bottles. For use in washing and dilution the M9 salts solution (subsequently referred to as M9), was prepared by mixing 180 ml M9A, 720 ml M9B and making up to 9 litres with distilled water. Approximately 250 ml volumes were transferred to 300 ml flasks, capped with aluminium foil, and autoclaved at 121°C for 15 mins to sterilize. The pH was routinely checked and was 6.9.

In preparing the minimal growth medium, 20 ml of M9A and some M9B concentrates were mixed with 800 ml distilled water and 80 ml volumes were transferred to 150 ml M.R.C. screw capped bottles and autoclaved for 15 min at 121°C. Immediately prior to use for growth, the growth requirements were added aseptically using laminar flow conditions.

Preparation of growth requirements

a. Glycerol. A stock solution of 10% glycerol (BDH) was made up in distilled water and sterilized through a 25 mm Swinnex unit fitted with a 0.2 μm pore size Sartorius membrane filter disc (V.A. Howe and Co. Ltd., London).

b. Casamino acids. A stock solution of 10% casamino acids (Difco) was made up in distilled water and filtered as above.

c. Thiamine. A stock solution of 1% thiamine HCl (Sigma) was made up in distilled water and filtered as above.

d. Fatty acid. A stock solution of 1% fatty acid was prepared by dissolving the fatty acid in a 10% Brij 58 (Sigma) solution. 10 g Brij 58 was dissolved with heating and stirring in 100 ml distilled water. The fatty acid was added when the Brij was cool, and the solution was filtered as above. Fatty acids used for liquid cultures were linolenic, linoleic or oleic acid (99% pure, from Sigma Ltd.). In preparing plates, oleic acid (BDH) was used.

Growth requirements were added to the prepared M9 described as shown below in Table 3.

Table 3. The preparation of defined growth media.

Growth requirement	Volume added per bottle of M9	Concentration in medium
Glycerol	4 ml	0.4%
Casamino acids	2 ml	0.2%
Thiamine	2 ml	0.02%
Fatty acid	2 ml	0.02%

The prepared defined growth medium was transferred aseptically to a 250 ml Pyrex screw top conical flask for inoculation.

Nutrient Broth medium

This was used routinely as a control to ensure that the E. coli K1060 was maintaining its requirement for an unsaturated fatty acid. Controls were always inoculated in parallel with experimental cultures. The nutrient broth was prepared by dissolving 13 g of powdered nutrient broth (Difco) in distilled water and making the volume up to 1 litre. 100 ml volumes of the broth were transferred to 150 ml M.R.C. bottles and sterilized by autoclaving at 121°C for 15 mins. The pH of the broth media was 7.2-7.4.

5. CULTURES

A loopful of growth from the 24 hour plate was inoculated into a 250 ml flask containing 100 ml defined growth medium prewarmed to 30°C. After connection to the aeration apparatus, this was incubated with shaking in a water bath for 24 hours. This culture is subsequently referred to as the primary culture. On the day of the experiment a primary culture was used to inoculate 100 ml of fresh defined medium by the aseptic transfer of 1 ml of the primary culture. Growth curves were determined under these conditions as shown in Figs. A1 and A2 in the Appendix. From such growth curves the mid-log phase was taken to be 4 hours after inoculation and cells required in this phase of growth were harvested at this time as a standard procedure. Stationary phase cells were harvested 24 hours after inoculation of this culture, referred to subsequently as the secondary culture.

Nutrient agar plates

For routine use, nutrient agar plates supplemented with 0.02% oleic acid were prepared by adding 18.4 g Bacto Nutrient Agar to 784 ml glass distilled water in a flat-bottomed 1 litre flask. After standing for 15 min the agar was brought to the boil and autoclaved at 121°C for 15 min. After cooling to approximately 60°C, 16 ml of 1% oleic acid in 10% Brij 58 was added aseptically. Oleic acid for this purpose was prepared by dissolving 10 g Brij 58 in 100 ml distilled water, heating gently with stirring until the Brij had all dissolved. After cooling 1 ml oleic acid (BDH) was added and stirred well. The solution was then sterilized by filtering through a 25 mm Swinnex unit fitted with a 0.2 μm pore size filter (Millipore). Twenty ml volumes of molten agar were poured into 9 cm diameter sterile petri dishes (Sterilin Ltd., England). Plates were streaked out from a slopes at monthly intervals. Plates for day to day use were subcultured from plate to plate at least weekly and stored at room temperature in an inverted position sealed with adhesive tape. Organisms were not kept in a refrigerator as this reduced viability. For each experiment a plate was streaked out on the day prior to the inoculation of the growth medium and a test plate containing no oleic acid was streaked out to verify the phenotype of the culture for use.

6. HARVESTING OF ORGANISMS

The methods used follow those described by Kelland (1984).

a. Filtration Method

This was used routinely when harvesting log-phase cells, unless the concentration required was greater than 10^7 colony forming units (CFU) ml^{-1}. Briefly, the cells were collected on a washed Sartorius membrane of 0.45 μm pore size using negative pressure Sartorius apparatus. The cells were washed 3 times with 10 ml volumes of M9 salts solution, and resuspended in M9 to give the required concentration of cells.

b. Centrifugation Method

For cells at a concentration higher than 10^7 CFU ml^{-1}, aliquots of the culture were sealed in disposable sterile universal containers (Sterilin, England). After centrifugation at 4000 rpm for 20 min using a Chilspin (MSE, England) centrifuge, the supernatant was removed and the cells resuspended in 20 ml M9 salts, agitated to wash, and recentrifuged. This procedure was repeated twice. The cells were finally resuspended at the required concentration in M9.

When resuspending at a required concentration for experiments, the optical density was measured at 470 nm using a Unicam SP600 spectrophotometer. A previously determined calibration curve is shown in Fig. A2 in the Appendix, where optical density is shown against viable count.

7. ASSESSMENT OF VIABILITY

Cell viability was determined using relative colony forming ability on various solid agar plates.

Plating media

a. Complex medium (YENB)

184 g Difco Bacto Nutrient Agar (Difco, Detroit, U.S.A.) was added to 800 ml distilled water together with 6.0 g Yeast Extract (Difco). After dissolving this was autoclaved at 121°C for 20 mins. After cooling to approximately 60°C, 16 ml 1% oleic acid in Brij 58, prepared as described previously, was added. 20 ml volumes were dispensed into 9 cm sterile petri dishes (Sterilin, England).

b. Defined media

9.6 g Difco Bacto Agar was dissolved in 640 ml distilled water, and autoclaved for 20 min at 121°C. After cooling the growth requirements were added under laminar flow conditions. Where "High salt" medium was required, the M9 salt concentration was decreased 10-fold, and the medium supplemented with 200 mM sodium chloride (Kelland, 1984). The composition of the defined media is shown in Table 4.

All plates were stored at 4°C for up to 1 week. Immediately before use, they were overdried under ventilated conditions at 37°C for 1 hour.

Table 4. Composition of minimal media plates

All weights (g) and volumes (ml) added to each 800 ml agar batch.

Medium	Agar	Distilled water	M9A conc.	M9B conc.	NaCl	Oleic acid (1%)	Thiamine (1%)	Casamino acids (10%)	Glycerol (10%)
Normal	9.6	640	16	64	-	16	16	16	32
High salt	9.6	612	1.6	6.4	100	16	16	16	32

Method of viability assessment

A 0.2 ml sample of bacterial suspension was diluted initially into 3.8 ml M9. After thorough mixing with a Whirlimix (Fison), this suspension was serially diluted 1 in 10 in M9 as required. 0.2 ml of the final dilution was pipetted onto the surface of the agar plates, normally 3 of each type used, and spread over the surface with a sterile glass spreader, a different spreader being used for each plate type. The plates were incubated in an inverted position at 30°C for 48 hours on the complex medium and 72 hours on the minimal media. Colonies were counted after incubation and the mean value of the three plates taken. Taking into account the known dilution factor, the number of viable bacteria in the original suspension was determined.

A range of dilutions was used in order to give plates with 30-200 colonies.

The use of Gilson pipettes in viability assessment

Gilson automatic pipettes were used for dilutions and transfer of diluted cell suspensions to plates. The Pipetman P1000 was used for volumes up to 1 ml, the Pipetman P5000 for volumes between 1 ml and 5 ml. The pipettes were checked to ensure they were delivering accurately and reproducibly. A gravimetric method was used in which 20 replicates of a set volume of water at 20°C were each weighed on an analytical balance. The coefficient of variation was less than one per cent and the deviation from the nominal value was less than 0.5 per cent.

PROCEDURES FOR THE CULTURE OF HUMAN FIBROBLASTS

1. EQUIPMENT

Cell Culture Plasticware

Disposable sterile 80 cm^2 tissue culture flasks (Nunc, Gibco Ltd., Paisley, Scotland), and petri dishes, 90 mm x 15 mm and 50 mm x 10 mm with triple vented lids (Sterilin Ltd.) were all of tissue culture grade polystyrene. Centrifuge tubes (Nunc, Gibco Ltd.) with platic screw tops were washed as for glassware and sterilized by autoclaving at 132°C for 5 mins (Drayton Castle High Vacuum Autoclave).

Glassware

Solutions and media were stored in 125 ml and 500 ml bottles (Flow Laboratories Ltd.) General glassware was obtained from Fisons Ltd.

Washing Procedure

After rinsing in tap water, all used glassware was soaked in 2 per cent v/v RBS 25 detergent (Fisons Ltd.) for 30 min. After thorough cleaning under running water with a China brush it was rinsed in three changes of tap water, being left in the last rinse for 30 min. It was finally left for 1 hour in fresh glass distilled water before drying in a hot air oven. Sterilization was by dry heat at 160°C for at least one hour.

Laminar Flow Facilities

A class I biological safety cabinet (MDH Ltd., Andover) was used for all aseptic manipulations. All surfaces were swabbed with 70 per cent alcohol before use.

Incubators

LEEC PF2 anhydric incubators with forced air circulation (Laboratory and Electrical Engineering Company, Nottingham) were used at 37°C.

Centrifuge

A bench centrifuge (MSE Minor S-61, MSE Scientific Instruments, Crawley) was used.

Freezing Unit

Cells were frozen in a Union Carbide BF-6 biological freezer (Union Carbide, U.K. Ltd.). This was used in a LR-33-10 freezer and cooled up to eight 2 ml ampoules at between 0.5°C and 70° min^{-1} to below -70°C.

Storage freezer

Stock cultures were stored in 2 ml ampoules in a LR-40 freezer (Union Carbide, U.K. Ltd.), in the vapour phase of the liquid N_2 at approximately -148°C.

Microscope

An inverted biological microscope, Wild M40 (Wild Heerbrugg Ltd., Switzerland) was used with phase contrast.

2. CELL CULTURE MATERIALS AND MEDIA

Water

All solutions and media were prepared with double glass distilled water (DDH_2O) obtained from a bi-distillation Fistream still, Model 2903 (Fisons Ltd.), fitted with a Fistream pre-deioniser. DDH_2O was autoclaved in glass bottles (100 ml and 500 ml) for sterilization, and had a pH of 4.5.

Media

Media were prepared using the materials and methods described by Kralli (1987). The medium used was Eagles Minimum Essential Medium (EMEM) with Earle's salts, obtained as a X10 concentrate (Flow Laboratories Ltd.). It was supplemented and diluted as shown below, under aseptic conditions. All additions were obtained from Flow Laboratories.

EMEM x10	40.0 ml
L-glutamine (200 mM)	4.0 ml
Sodium bicarbonate (7.5% w/v)	12.8 ml
Penicillin (5000 $i.u.ml^{-1}$) and streptomycin (5000 $\mu g\ ml^{-1}$)	4.5 ml
Serum: Foetal Calf Serum	68.0 ml
DDH_2O, sterile	340 ml

For storage, EMEM concentrate was stored at 4°C, sodium bicarbonate was stored at room temperature. All other components were stored at -20°C, and thawed in a water bath at 37°C for use. The serum used

in this study was all of the same batch, it was aseptically decanted with sterile 125 ml Flow bottles in 68 ml aliquots for storage at -20°C.

The prepared medium was stored, in the dark, at 4°C and used within one month.

Balanced Salt Solution

Dulbecco's phosphate buffered saline was used. PBS (A) was prepared by dissolving one PBS tablet (Oxoid Ltd., London) in 100 ml freshly prepared DDH_2O and autoclaving at 121°C for 15 min.

PBS (B) was prepared by the addition of 0.5 ml Dulbecco B solution (Oxoid Ltd.) to 100 ml PBS (A). Storage was at room temperature for a maximum of one month. The composition of PBS (B) is shown below.

Component	gl^{-1} DDH_2O
NaCl	8.0
KCl	0.2
Na_2HPO_4	1.15
KH_2PO_4	0.2
$CaCl_2.2H_2O$	0.132
$MgCl_2.6H_2O$	0.1

Trypsin Solution

Trypsin (1:250) was obtained as a sterile 2.5 per cent w/v solution in Hanks balanced salt solution without calcium, magnesium or phenol red, from Flow Laboratories in 100 ml volumes. It was

aseptically diluted to 0.25 per cent with PBS (A) and stored at -20°C until use within four weeks.

The Gassing Procedure

The culture media contained a bicarbonate pH buffer system designed to equilibrate with 5 per cent CO_2 in air. This mixture (supplied as 5 per cent CO_2 and 20 per cent O_2 in N_2, BOC, Bristol) was introduced at a low flow rate by a plugged, sterile Pasteur pipette into gas-tight tissue culture flasks.

Plates were placed in an incubation box (3.25 litre, Gallenkamp, London) and flushed with 150 ml of CO_2 (BOC, Bristol) from a metered supply (Gas Flowmeter, Rotameter Manufacturing Co. Ltd., Croydon).

3. CELL LINES

Two diploid human skin fibroblast lines were used in this study:

GM 730 - from a normal 45 year old female donor, kindly provided by the MRC Cell Mutation Unit, University of Sussex, Brighton; originating from the human genetic Mutant Cell Repository, Camden, New Jersey, U.S.A.

AR6LO - from an actinic reticuloid patient, 55 years old, kindly provided by Dr. F. Giannelli, Guys Medical School, London. Clinical details in Table A1 in Appendix 2.

Maintenance of Cell Lines

Cultures were routinely maintained in culture medium in 80 cm^2

tissue flasks at 37°C, and subcultured routinely to keep cells in a state of active growth.

In order to prevent cross contamination only one cell line was handled at a time and media were labelled for use with one cell line only.

4. CELL STORAGE

Stocks were maintained by the freezing of cells in the exponential stage of growth. Six flasks were trypsinized, the cells resuspended in whole medium and centrifuged. The pellets were pooled and resuspended in 8 ml of growth medium containing 5% DMSO (grade 1, Sigma Ltd.), which was freshly prepared by the aseptic addition of 5 ml filter-sterilized DMSO to 95 ml growth medium. Following aspiration with a sterile Pasteur pipette, 1 ml of suspension was transferred to each of eight sterile 2 ml ampoules. The ampoules were labelled with date, cell line, passage number, and cooled in the BF-6 freezer at 1°C per minute to below -70°C. They were transferred to the shelves of a liquid nitrogen freezer for storage at approximately -148°C.

Recovery from Storage

Ampoules were transferred to a water bath at 37° for quick thawing. The contents were transferred with a sterile Pasteur pipette to a 80 cm^2 flask containing 15 ml growth medium, overgassed with 5% CO_2 in air and incubated at 37°C.

5. THE SUBCULTURE PROCEDURE

The flask to be subcultured was examined to ensure that the medium was free of floating debris, and that the phenol red component indicated a pH which was neither too acidic nor basic. The cells were examined by phase contrast microscopy to ensure that they were of normal appearance.

The medium was removed, and the monolayer rinsed with 5 ml ice-cold trypsin solution (0.25 per cent). This was discarded and replaced by a further 5 ml which was discarded after 1 min. The cells were left for 5 min in the residual trypsin until they were seen to be released from the flask surface. The single cells were resuspended in growth medium, gently aspirated, and the cell density determined using a haemocytometer. 8×10^5 cells were added to 15 ml growth medium in a tissue culture flask. Flasks were overgassed with 5 per cent CO_2 in air delivered at a low flow rate through a sterile Pasteur pipette plugged with non-absorbent cotton wool. The flasks were fully labelled and incubated at 37°C in the dark.

6. THE PREPARATION OF CELL SUSPENSIONS FOR EXPERIMENTAL USE

The procedure was standardised by following a set procedure. Three flasks were each inoculated with 8×10^5 cells with 15 ml growth medium, and incubated at 37°C for 4 days. After this time there was good, but not confluent, growth. Two flasks were used for irradiation, the third was left for three further days and used for subculturing as described above. Cells were thus subcultured once weekly.

Cells required in suspension were trypsinized, and resuspended in 10 ml PBS (B) buffer, to inhibit further tryptic action. The suspension was centrifuged at 1000 rpm for 1 minute, the supernatant removed, and the pellet resuspended in 5 ml PBS (B). The cell density was adjusted to 10^6 cells per ml after counting, by dilution in PBS (B).

7. THE PREPARATION OF MONOLAYERS FOR IRRADIATION

A procedure similar to that for subculture was followed, the flasks being replaced by petri dishes. Cells were added at 3×10^5 in 10 ml medium to the large plates, or 1×10^5 in 4 ml medium to the small plates, and incubated at 37°C. Cells were irradiated before growth reached confluence, usually after 3 days for GM730 cells and 5 to 6 days for AR6LO cells.

THE APPARATUS FOR IRRADIATIONS

1. BROAD-BAND NEAR-UV RADIATION

The Broad-Band Irradiation of Suspensions

The apparatus used, shown in Fig. 17, provided six "Black-Light Blue" (BLB) lamps (Sylvania F15T8, Sylvania Electric Products Inc., Danvers, Mass., U.S.A.), mounted as two vertical banks of three lamps enclosed within a box which provided for twelve Pyrex test tubes (Fisons), positioned between the two banks. Shutters were provided for the screening of the tubes if necessary. A fan maintained the temperature of the irradiated suspensions at 28° ± 1°C. The apparatus, as used by Kelland (1984), allows for similar fluences to be given to all tubes except in the two outermost positions, which were not used. All tubes not in use contained 5 ml water to maintain conditions where reflected light was constant.

The emission spectrum of the original lamps is shown in Fig. 18 (Kelland, 1984). The emission spectrum of the new lamps installed during the course of the work is shown in Fig. 19.

The Broad-Band Irradiation of Fibroblast Monolayers

Fig. 20 illustrates the broad-band irradiation apparatus used for the irradiation of monolayers. Two 18 inch lamps (F15T8, BLB lamps, 15 W, General Electric, Ultraviolet Products) were mounted horizontally in a metal box. The apparatus allowed for the irradiation of two large or six small petri dishes. The emission spectrum for the lamps, as provided by the manufacturers, is shown in Fig. 21a.

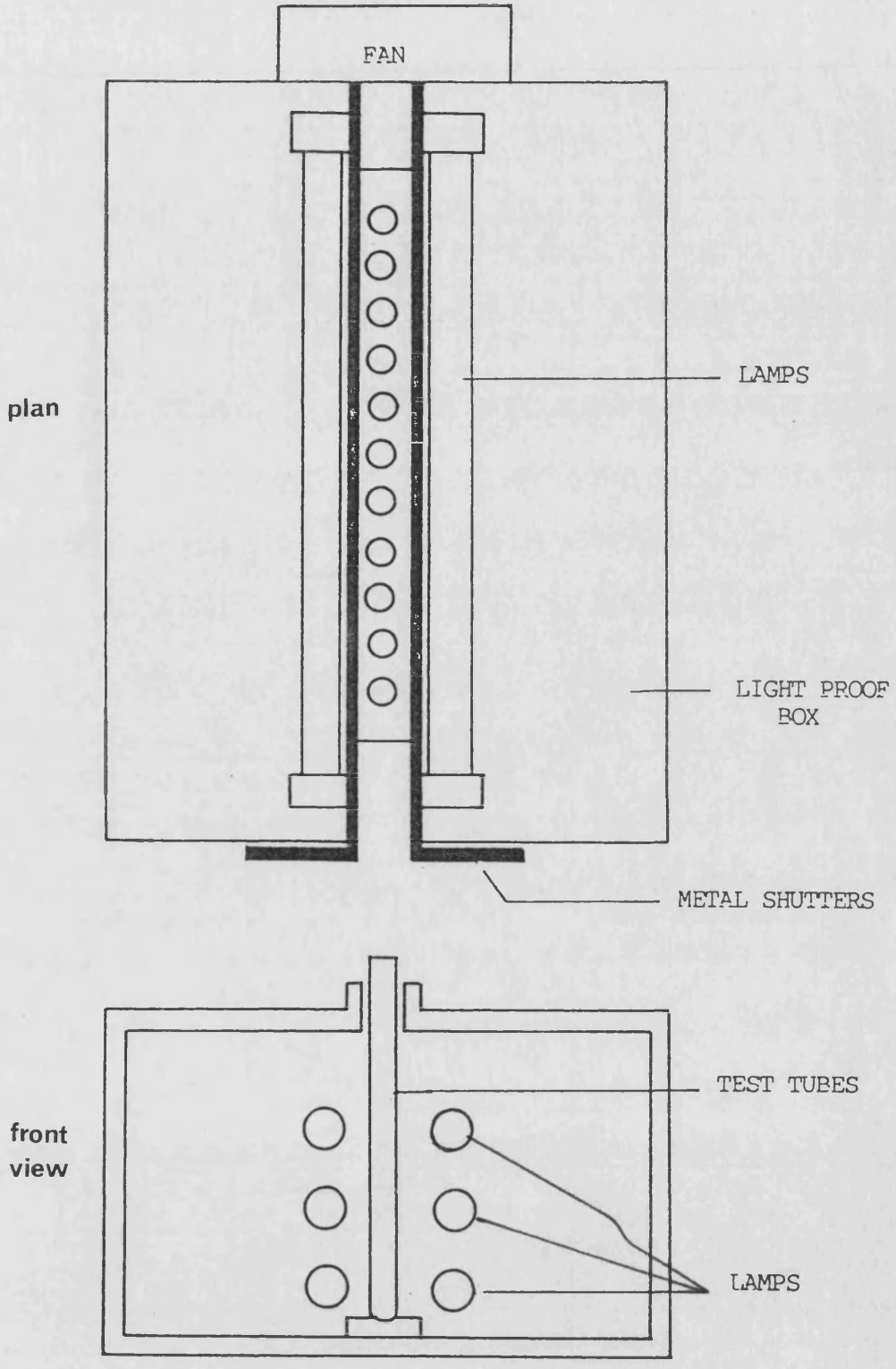

Figure 17

Diagram of the broad-band near-UV (BLB) source.

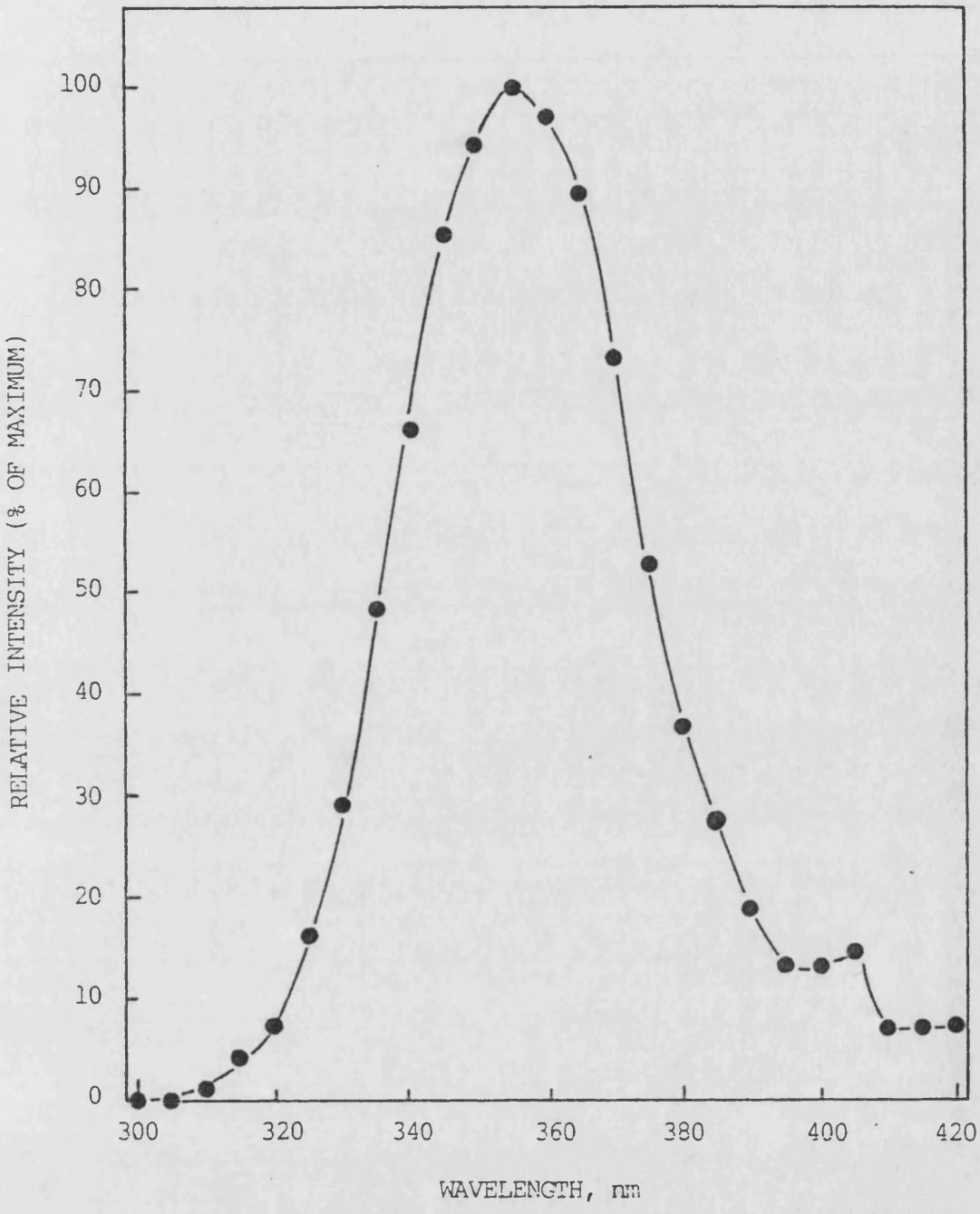

Figure 18

Emission spectrum of near-UV Black-Light Blue fluorescent light source.

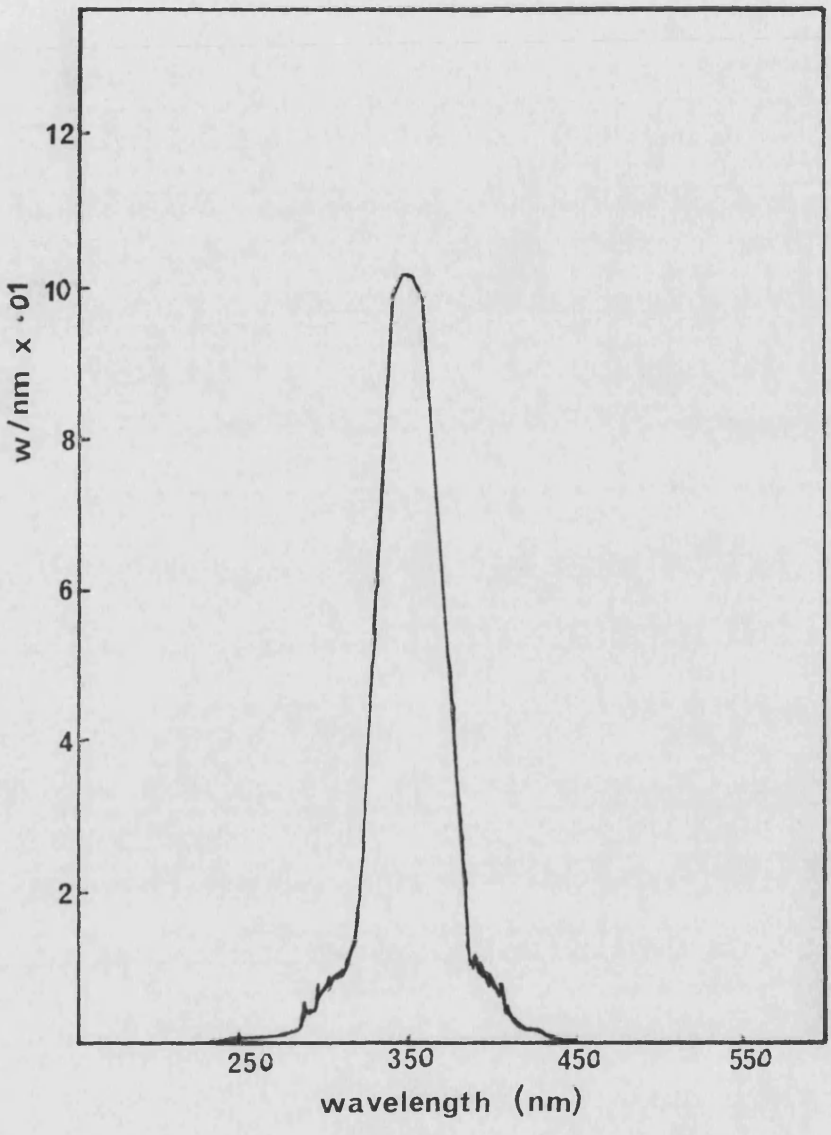

Figure 19

Emission spectrum of near-UV Black-Light Blue fluorescent light source, new lamps.

2. FAR-UV RADIATION

The Far-UV Irradiation of Suspensions

A 5 cm Penray lamp (UV Products Inc.) was fitted with a G-275 filter, providing 95% of the emission at 254 nm. The apparatus is shown in Fig. 22. The irradiation vessel was a straight-sided glass bowl, internal diameter 5 cm, in which 10 ml of sample was irradiated. A flow of humidified, compressed air prevented the build-up of ozone. An iris camera shutter (G.B. Kershaw 630) with a 2 cm aperture was used, fitted with a cable release.

Broad-Band Far-UV Irradiation of Plates

The same housing as that used for the broad-band irradiation of plates (Fig. 19) was used. The apparatus was fitted with two 18 inch G15 T8 (15W, Coast Wave, UV Products) lamps. The emission spectrum, as obtained from the manufacturers, is shown in Fig. 21b.

3. MONOCHROMATIC NEAR-UV RADIATION

Fig. 23 shows the arrangement of the irradiation apparatus as used by Kelland (1984).

The Source

The irradiation source was a Bausch and Lomb SP200, 200 W super pressure mercury vapour lamp (Bausch and Lomb, New York). Lamps were replaced after 100 hours of use when output had fallen and was unstable. New lamps were burned off for 2 hours, or until stable, before use. The lamp was used with a Bausch and Lomb high intensity grating monochromator, fitted with a UV-visible

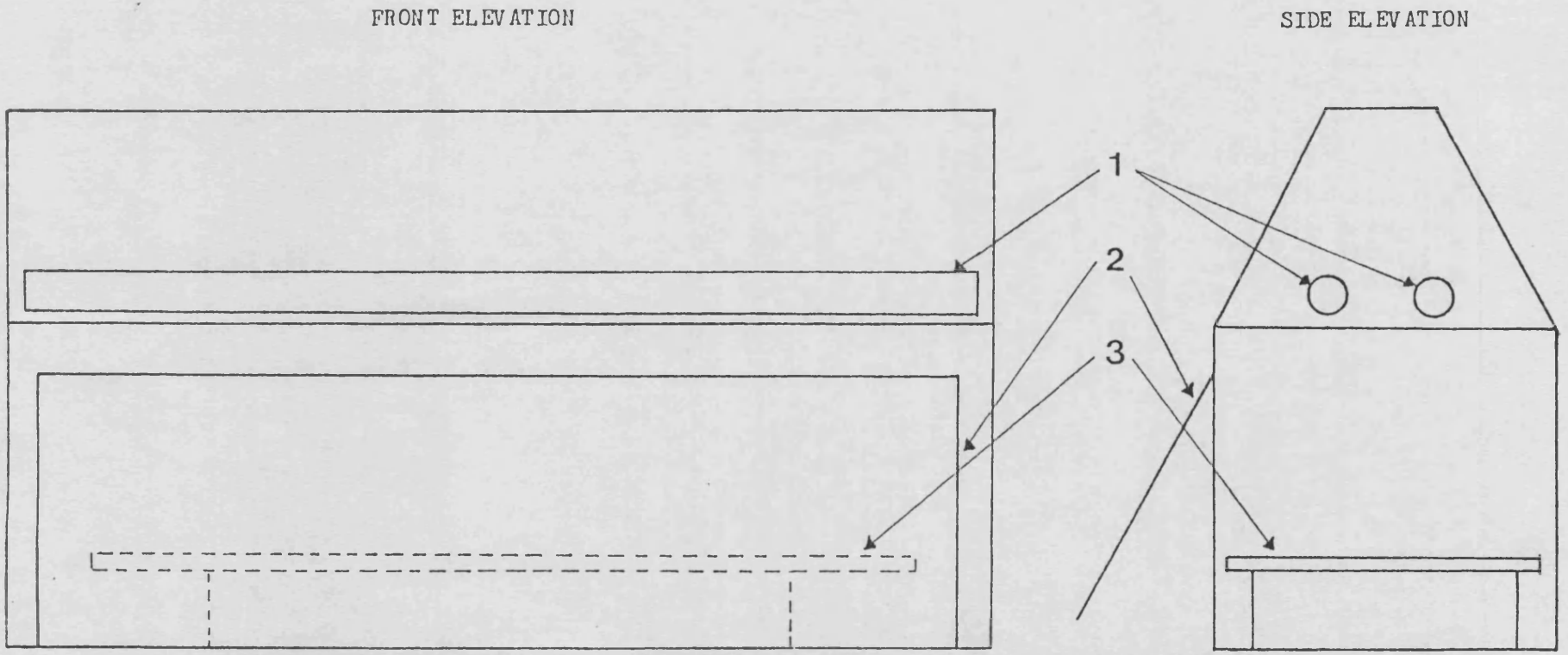

Figure 20 Diagram of the housing used for broad band irradiation of plates
1. Position of lamps
2. Front opening
3. Support for plates

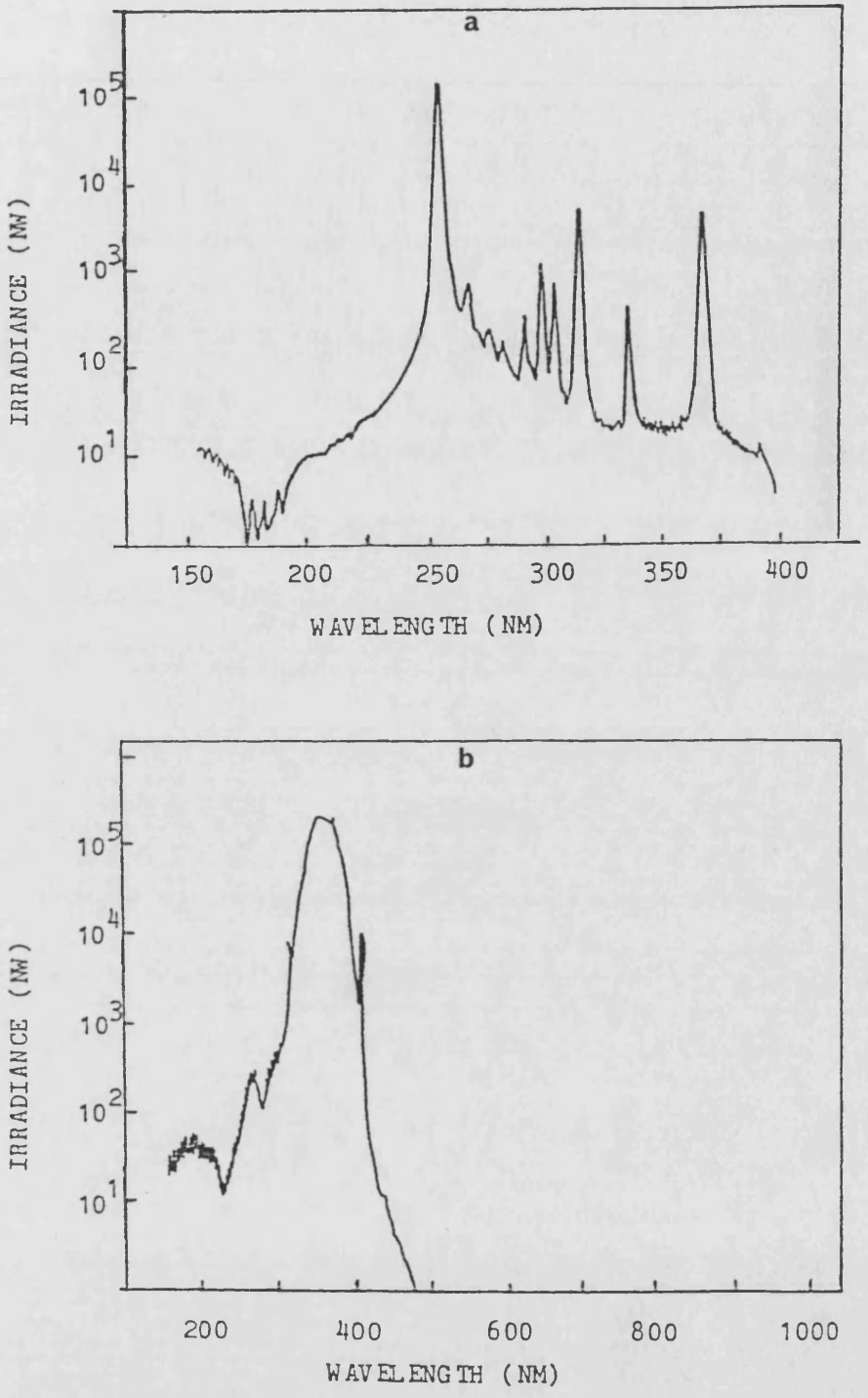

Figure 21

Emission spectra for (a) short wave G15T8 (15W)
(b) long wave F25T8 (15W) lamps

(Instrumentation uncalibrated for wavelengths less than 200nm or greater than 900nm)

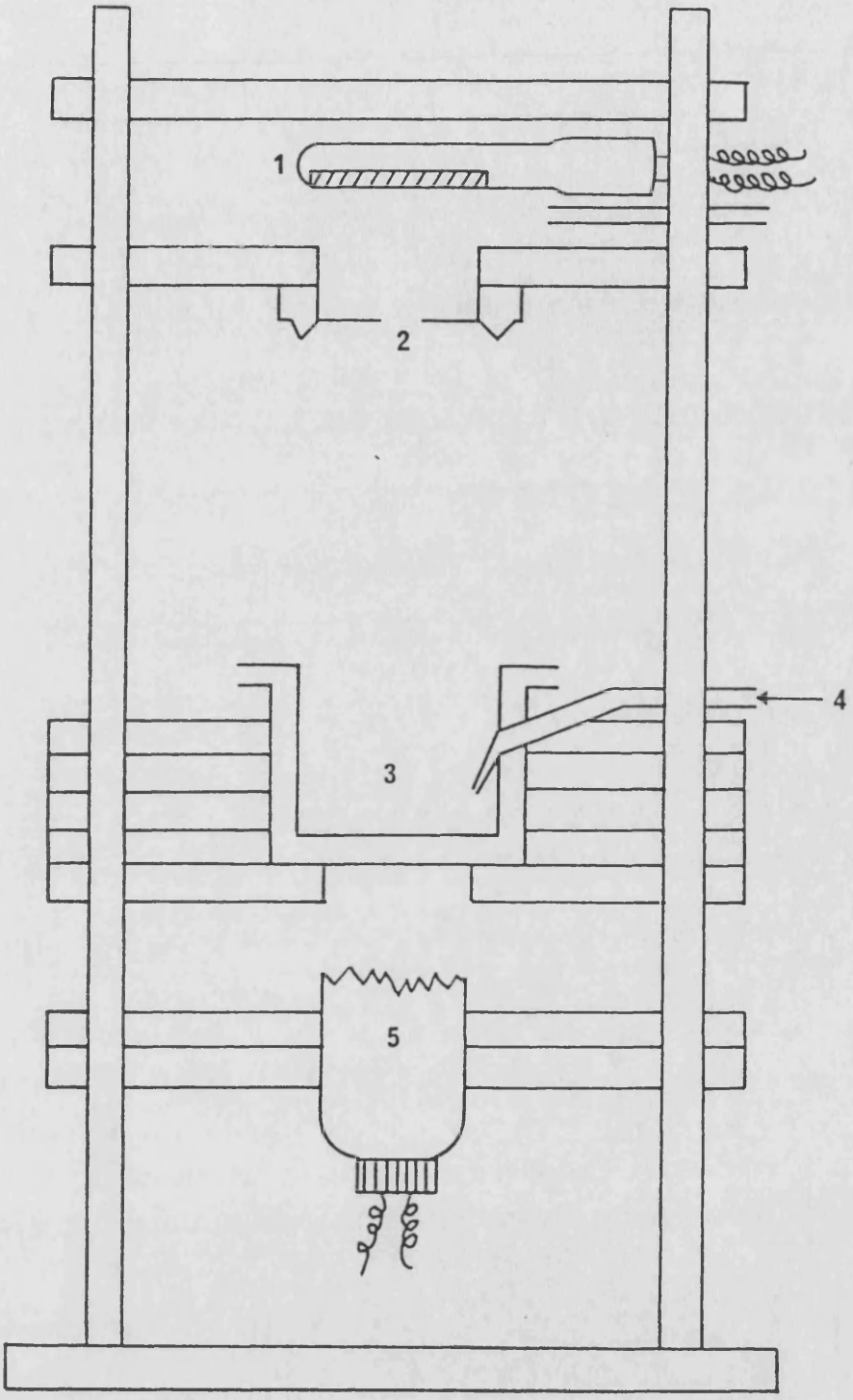

Figure 22

Diagram of apparatus for 254 nm irradiation.

1. UV Source.
2. Shutter.
3. Irradiation Vessel.
4. Air Inlet.
5. Position of Thermopile.

diffraction grating of 1350.0 lines mm^{-1}. Operation is over a wavelength rate of 200-800 nm, with a reciprocal dispersion of 6.4 nm mm^{-1} Matched fixed slit widths were used, the entrance and exit slits being 2.68 mm and 1.5 mm respectively.

The Arrangement of the Apparatus

The UV source and monochromator were arranged at one end of an Ealing Beck optical bench. The remaining components of the system were:

The shutter: An iris camera shutter (G.B. Kershaw 630) with a 2 cm aperture, fitted with a cable release.

The focusing lens: A 40 mm diameter Spectrosil biconvex lens with focal length of 55 mm, producing an inverted, magnified image of the exit slit of the monochromator 3 cm high and 1 cm wide, allowing full illumination of the irradiation cuvette.

Stray light filters: Table 5 shows the details of stray light filters used. These were necessary in order to eliminate light of a shorter wavelength than that required, since shorter wavelengths are more energetic and their inclusion would give erroneous results. Fig. 24 shows the transmission characteristics of the filters used.

The irradiation cuvette: Fig. 25 illustrates the structure of the cuvette, which is a jacketed quartz cuvette, 10 mm wide and with a

Table 5. Details of stray light filters, band widths and approximate fluence rates used in irradiation experiments.

	Wavelength (nm)	Stray light filter	Wavelength 1% transmission on Low side (nm)	% transmission at designated wavelength	Band width at 50% maximum(nm)	Approx. fluence rate $Jm^{-2}sec^{-1}$
*	254	G-275	252	92 without filter (Child's 1962)	4.0	0.05
	290	CORNING 0-56	240	60	13.0	2.2
	300	CORNING 0-53	268	47.9	10.0	4.5
	305	CORNING 0-53	268	56.2	13.5	7.0
	310	CORNING 0-54	302	20	8.5	7.0
*	313	Mylar 2.5 m	301	54	7.0	25
	317	WG 320	296	72.4	9.5	20
	325	CORNING 0-54	302	84	12.5	16
	328	WG 335	314	50	13.0	18
*	334	WG 335	314	68	7.25	14
*	365	CORNING 0-52 (HALF THICKNESS)	332	75	7.0	60
*	365	"	330	72	10.0	95
*	405	CORNING 0-51	362	66	7.0	160

* denotes mercury resonance line.

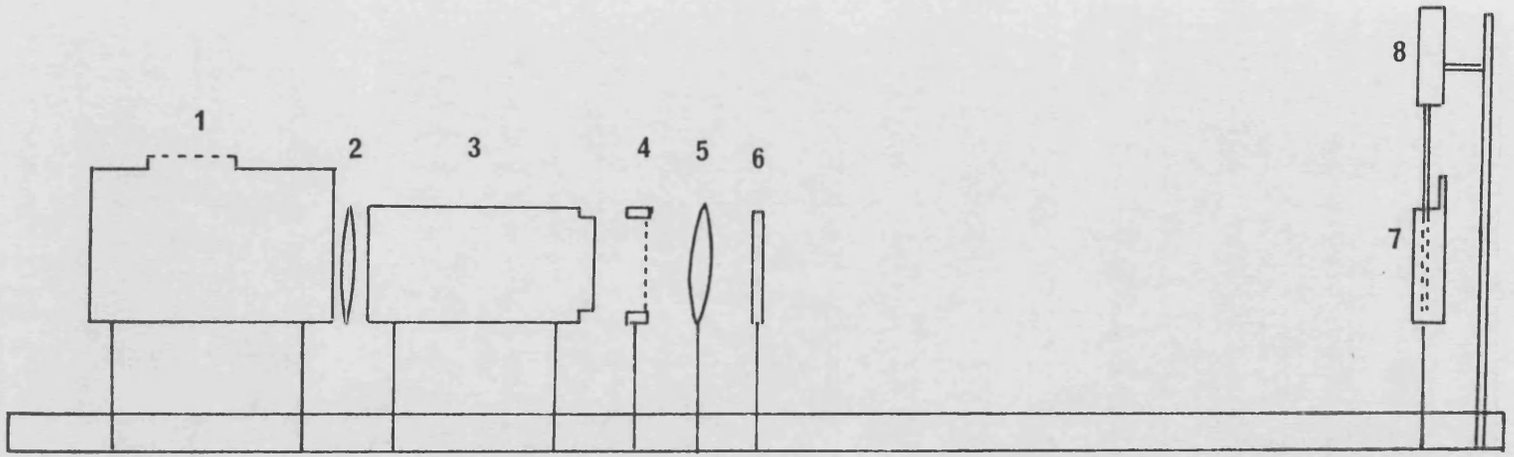

Figure 23 Diagram of apparatus for UV-irradiation of fatty acids and liposomes.

1. Mercury UV source (SP200)
2. Quartz Collective Lens
3. Monochromator
4. Shutter
5. Focusing lens
6. Stray light filter
7. Irradiation cuvette
8. Stirrer

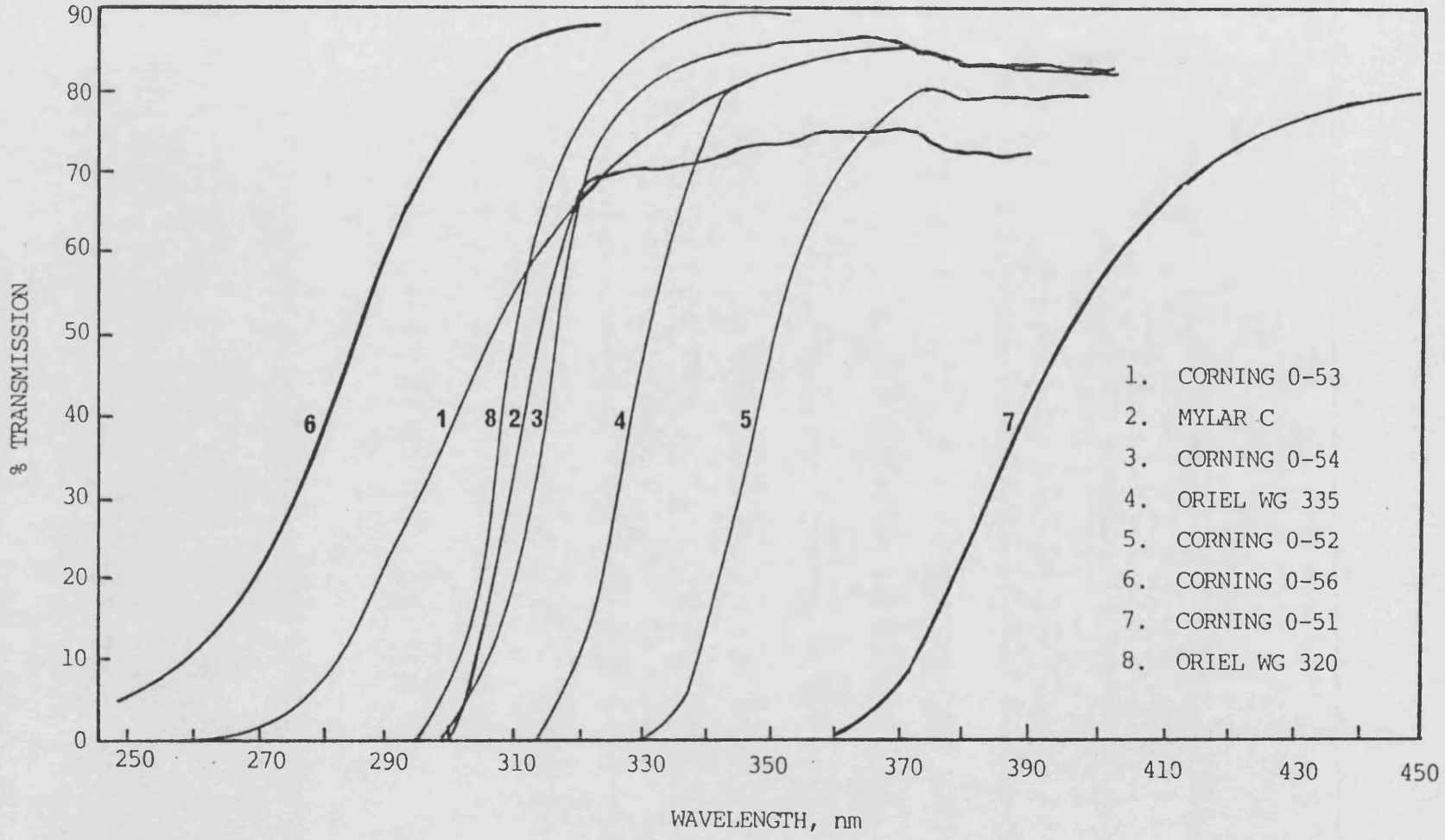

Figure 24 Transmission characeristics of stray light filters

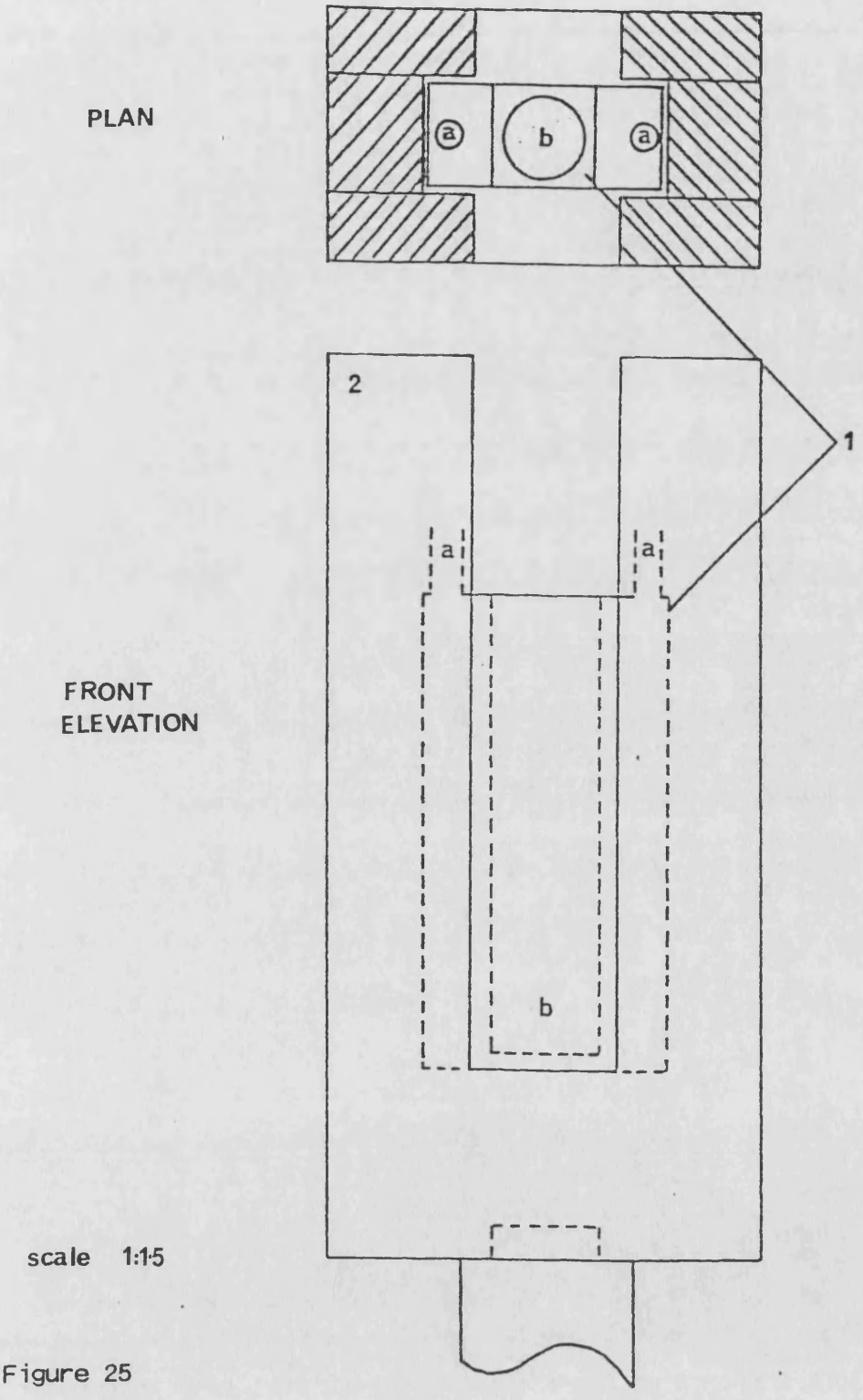

Figure 25

Diagram of the irradiation cuvette
1. Irradiation cuvette
   a. Entrance and exit ports for the circulating fluid
   b. Position of suspension for irradiation
2. Perspex holder

10 mm pathlength (Thermal Syndicate Ltd.). During irradiation the required temperature was maintained by the circulation of a 50% ethylene glycol solution through the jacket. The coolant was held in an insulated bath, cooled when necessary by a U-cool refrigeration unit (Neslab Instruments Inc.) and maintained at the required temperature by a heating coil pump (Grant Instruments Ltd.). Circulation was achieved by a peristaltic pump (Watson Marlow Ltd.). The sample for irradiation was held in the cuvette in the dark for 5 mins to achieve the required temperature. 3.0 ml volumes were irradiated.

The stirrer: A quartz paddle rotated by a laboratory stirrer (Stanhope Seta Ltd.) was used.

Analysis of Emitted Radiation

A second Bausch and Lomb high intensity monochromator was used to scan the spectrum of light emitted from the monochromator system, with the appropriate stray light filter in place. The analysing monochromator was fitted with half-width slit discs, i.e. entrance and exit slits of 1.34 mm and 0.75 mm. Emitted radiation from the standard monochromator was focussed onto its entrance slit, and a calibrated thermopile was used to measure the light passing through. Measurements were made at one nm intervals to ±10 nm from the maximum emission wavelength. The relative intensity was plotted against wavelength, and the bandwidths in nm at half the maximum intensity were calculated. This describes the degree of monochromacity of the source. A typical analysis is shown in Fig. 26.

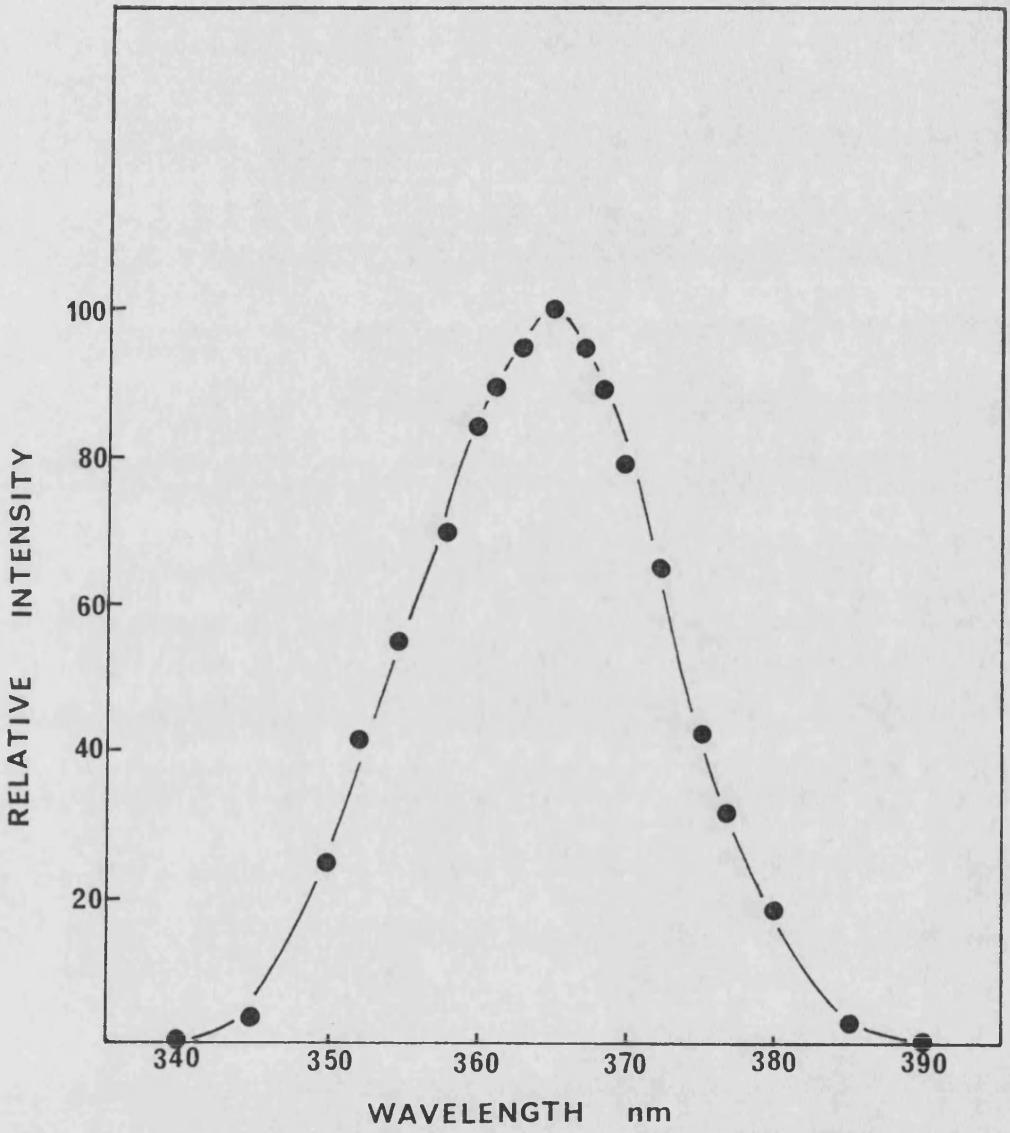

Figure 26

Typical analysis spectrum of emitted 365 radiation from Bausch and Lomb source (plus 0-52 filter)

GENERAL PROCEDURES FOR IRRADIATION

1. BROAD-BAND NEAR-UV RADIATION

The Broad-Band Near-UV Irradiation of Suspensions

A 20 minute warm-up period for the lamps was allowed. 5 ml of the suspension for irradiation, in a sterile Pyrex test tube, was placed in position. Stirring was achieved by the steady bubbling of filtered, humidified air via a Pasteur pipette, except for the stirring of fibroblast suspensions in which case a vertically mounted laboratory stirrer (Stanhope Sera Ltd.) was used, fitted with a quartz paddle. A 5 minute period was allowed to equilibrate the temperature, with the shutters in place. Removal of the shutters allowed exposure to the radiation, and samples were taken at intervals as required for analysis.

The Broad-Band Near-UV Irradiation of Monolayers

After a 20 minute warm-up period the plates were placed on a shelf beneath the lamps at a distance of 8 cm. The lids remained on during the irradiation period.

2. FAR-UV RADIATION

The Far-UV Irradiation of Suspensions

A 20 minute warm-up period was allowed for the Penray lamp. Thermopile readings were used to determine the fluence rate. The sample was placed in the irradiation vessel and the shutter opened for the required time, samples being taken as required for analysis.

The Broad-Band Far-UV Irradiation of Monolayers

After a 20 minute warm-up period two plates at a time were irradiated with the lids off, at a distance of 16 cm from the lamps.

3. MONOCHROMATIC NEAR-UV RADIATION

At least a 30 minute warm-up period was required until the lamp was emitting steadily as shown by the thermopile readings. The cuvette was positioned along the bench and the height adjusted so that the entire face of the cuvette was illuminated. The thermop ile (Oriel 7102) was moved into the beam in place of the cuvette and a number of microvolt readings were taken. The incident fluence was calculated by applying the calibration factor determined by chemical dosimetry. The irradiation cuvette was then replaced, 3 ml of the sample was added and allowed to reach the correct temperature with the coolant circulating and the stirrer on. The shutter was opened for the necessary exposure time and samples taken as required.

4. THE DARK ROOM

All experiments involving irradiation were carried out in a "dark room" under illumination from 80 W red fluorescent tubes (Atlas Ltd.). These lamps emit only light of wavelengths longer than 500 nm.

DETERMINATION OF FLUENCE RATES FOR ULTRAVIOLET RADIATIONS

1. BROAD-BAND NEAR-UV RADIATION SOURCES

Broad-Band Near-UV Source for Suspensions

Following the method of Kelland (1984) a survival curve was obtained for E. coli SR362, which is uvrA, uvrB, recA, phr. By comparison with published data using 365 nm radiation (Brown and Webb, 1972), an approximate fluence rate was calculated and found to be 1.08 $kJm^{-2}s^{-1}$. Later, as the fluence rate was falling, new lamps were installed, and after a burn-off period of 100 hours the fluence rate of these was found to be 1.9 $kJm^{-2}s^{-1}$, as shown in Fig. A3, using cells at the standard concentration of 10^7 ml^{-1}, and also at the higher concentration of 10^9 ml^{-1} used for peroxidation measurements. This was checked periodically and did not alter significantly.

Fluence rates determined by this method assume that most of the radiation emitted is at 365 nm and neglect to take into consideration the more energetic shorter wavelengths. Such determinations are therefore approximate, therefore fluence is expressed as the duration of irradiation rather than as the fluence received.

Broad-Band Near-UV Source for Plates

The fluence rate was determined by means of a radiometer (IL 442A Phototherapy Radiometer, International Light Ltd.) with a spectral sensitivity peak at 357 nm and calibrated for determinations at 366 nm. The fluence rate was found to be 26

$Jm^{-2}s^{-1}$. This compares with a fluence rate determined by chemical actinometry (Kralli, 1987) of 30 $Jm^{-2}s^{-1}$. Again the fluences are approximate and results are expressed relative to the duration of irradiation.

2. FAR-UV RADIATION SOURCES

The Far-UV Source for Suspensions

The fluence rate was determined as described by Kelland (1984) by chemical actinometry. The fluence rate was calculated to be 0.082 $Jm^{-2}s^{-1}$.

The Broad-Band Far-UV Source for Plates

From chemical actinometry the fluence rate was calculated to be 18 $Jm^{-2}s^{-1}$ (Kralli, 1987). Since this is approximate, assuming the radiation to be all at 254 nm, results are expressed relative to the duration of the irradiation rather than as a fluence received.

3. MONOCHROMATIC NEAR-UV SOURCE

The fluence rate was determined using an Oriel 7102 thermophile (Oriel Scientific Ltd.) in conjunction with chemical actinometry. The thermopile was mounted on the optical bench, adjacent to the irradiation cuvette, on a sliding bench saddle. The detector was aligned with the inside front face of the cuvette. When the thermopile was moved across into the radiation beam, output voltages were measured on a microvoltmeter (Keighley Instruments Model 105B).

The thermopile was initially calibrated by potassium ferrioxalate actinometry. A solution of $K_3Fe(C_2O_4)_3$, which absorbs light completely in the UV region, is irradiated, and Fe^{2+} ions are produced during a light-catalysed reaction. The quantum yield of the reaction is practically constant in the UV region, and the yield is independent of the fluence rate.

Actinometry was performed under red light according to the method of Jagger (1967). A calibration curve of optical density at 510 nm against the amount of ferrous ion was determined (Fig. A8 in the Appendix). This was used to ascertain the amount of ferrous ion formed by the radiation. From this a fluence rate was calculated by application of the constants pertaining to the wavelength chosen (Jagger, 1967). The calibration curve for the thermopile is shown in Fig. A9 in Appendix 4.

CHEMICAL ASSAY METHODS

1. THE ASSAY OF LIPID HYDROPEROXIDES BY THE IODOMETRIC METHOD

The method was modified from Asakawa and Matsushita (1980).

Reagents

The reagents below were prepared fresh daily.

Potassium iodide solution: 2% KI (BDH) in 95% ethanol (Analar, BDH)

Aluminium chloride solution: 2% $AlCl_3$ (BDH) with 0.02% o-phenanthroline (BDH) in 95% ethanol.

Hydrochloric acid: 0.01 N HCl (Analar, BDH)

Starch solution: 1% soluble starch (BDH) made up in 10% NaCl (BDH)

Standard potassium iodate solution: 0.05 mM KIO_3 (BDH).

Method

A 0.5 ml volume of the sample to be assayed was added to a test tube containing 0.5 ml KI solution and 0.5 ml $AlCl_3$ reagent. The purpose of the addition of o-phenanthroline (in the $AlCl_3$ reagent) at this stage was to act as an iron chelator to prevent iron-catalyzed free radical chain reactions as described in the Introduction. All samples were assayed in duplicate or triplicate, along with water blanks using 0.5 ml distilled water, and standards using 0.5 ml 0.05 mM KIO_3 solution.

The tubes were incubated in a water bath at 37°C for 5 minutes to allow the catalytic action of the $AlCl_3$; during this time the hydroperoxides reacted with the KI, in the presence of $AlCl_3$, to release iodine.

Following incubation 15.0 ml of 0.01 N HCl were added, followed by 0.5 ml of starch solution. The liberated iodine reacts with the starch, forming a purple-blue colour which was measured by the absorbance at 560 nm. Glass cuvettes with a 4 cm light path were used in a Pye Unicam SP1800 spectrophotometer, or alternatively a Perkin Elmer 5505 spectrophotometer was used with cuvettes of 1 cm light path.

All absorbances were measured relative to distilled water and blank values were subtracted as appropriate. The peroxide value (PV) was then calculated from the formula below, the PV being in m eq/kg^{-1}.

$$PV = \frac{A}{S} \times 0.3$$

where PV = peroxide value

A = absorbance of sample

S = absorbance of standard

This calculation arises as follows (Asakawa and Matsushita, 1980):

Since KIO_3 corresponds to $3I_2$, 0.5 ml 0.05 mM $KIO_3 \equiv 0.075\ \mu mol\ I_2$ and $0.075\ \mu mol\ I_2 \equiv 0.15\ \mu mol$ Active Oxygen (AO).

Since I_2 corresponds to 2AO

then $S \equiv 0.15\ \mu mol$ AO

Since PV = AO (μmol) x $\frac{1}{0.5}$ (sample size)

then PV of standard = $\frac{0.15}{0.5} = 0.3$

$$PV\ sample = 0.3 \times \frac{\text{absorbance sample}}{\text{absorbance standard}}$$

Calibration Curve for the Hydroperoxide Assay

The assay procedure was followed as described, using 0.5 ml aliquots of KIO_3 solutions at various concentrations, and measuring

the absorbance at 560 nm. Fig. A12 in the Appendix shows the calibration curve where the OD_{560} is plotted against the active oxygen per tube.

2. THE MALONDIALDEHYDE ASSAY (TBA-REACTING PRODUCTS ASSAY)

Reagents

2-thiobarbituric acid (TBA): 5 g TBA (Sigma) was dissolved in 5 ml 1N NaOH with gentle heating, then made up to 500 ml with distilled water. This solution was kept in the dark for up to one month. Gentle heating re-dissolved any crystals which formed.

Perchloric acid: Perchloric acid (Analar, BDH) was diluted to 7% in distilled water.

Malondialdehyde (MDA) standard: MDA (Aldrich) was dissolved in distilled water at a concentration of 0.125 µg ml^{-1}.

Method

Duplicate 1 ml samples were added to 1 ml perchloric acid in a disposable universal bottle (Sterilin), followed by the addition of 2 ml TBA solution. The mixture was centrifuted at 4000 rpm for 10 mins (MSE Chilspin Centrifuge) and the bottom 3 ml were removed into a test tube and heated at 100°C in a boiling water bath for 20 min, using a marble as a condenser. After cooling the absorbance at 532 nm was measured, relative to distilled water. Water blanks and MDA standards were run in parallel. The amount of MDA present was determined with reference to a calibration curve, shown in Fig. A13 in Appendix 5.

The TBA test is a common method used for detecting the oxidation of lipids. The assay depends upon the formation of a pink chromophore, a complex formed between malondialdehyde and TBA after heating in an acid medium. An absorption peak is obtained at 532 nm. The chromophore:

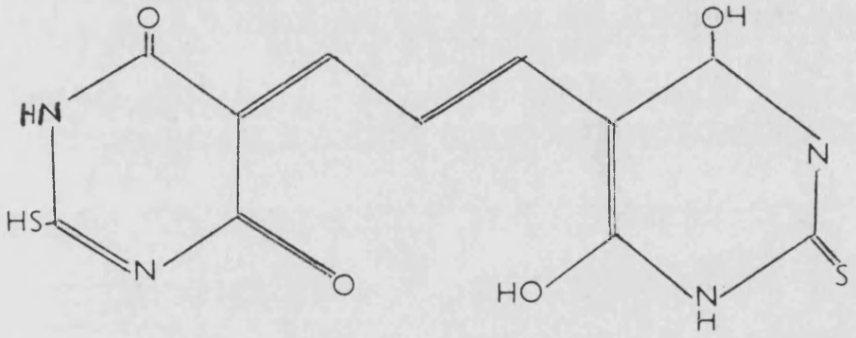

However, this method has long been known to be unspecific. Many lipid oxidation products are known to also react with TBA (Porter et al., 1976; Frankel and Neff, 1983), therefore results are best described as being in "malondialdehyde equivalent" units. Dahle et al. (1962) first proposed a mechanism for the TBA reactant formation, whereby at least 3 unsaturated C=C bonds must be present in a fatty acid, which, upon autoxidation, yields a cyclic peroxide which then, under the conditions of the TBA assay, breaks down to form malondialdehyde. As will be discussed later, the method was initially chosen in view of its wide usage in biological systems, but was subsequently rejected as being less useful than the iodometric assay.

GAS CHROMATOGRAPHIC ANALYSIS OF FATTY ACID METHYL ESTERS

The Chromatograph

A Perkin-Elmer gas chromatograph, Model F33, fitted with a Flame Ionization Detector was used. The chromatograph was combined with a Perkin Elmer 023 chart recorder.

Temperature Programming

To effect adequate separation of the fatty acid methyl esters (FAME) encountered, a temperature programme was used. A 6 min hold at 140°C was followed by a rise at 12° min^{-1} until a temperature of 200°C was reached. This temperature was maintained until the end of the run.

The Column

A glass column, internal diameter 2 mm, length 1 m was used. This was packed with 10% Cp tm Sil 58 on Chromosorb WHP 100-120 mesh support (supplied as a coated packing suitable for FAME analysis by Chrompack, England). The column was filled under pressure and conditioned for 16 hrs at 220°C.

The Carrier Gas

Oxygen-free nitrogen (BOC Bristol) was used at a flow rate of 78 ml min^{-1}.

Materials

Chloroform (Analar, BDH)

Methanol (Analar, BDH)

2% H_2SO_4 (Analar, BDH) in methanol

Diethyl ether (Analar, BDH)

Sodium bicarbonate (BDH), 10% w/v in distilled water

Chromatography standard: Methyl esters of the following fatty acids, supplied 99% pure by Chrompack:

laurate (12:0), myristate (14:0), palmitate (16:0), oleate (18:1), linoleate (18:2), linolenate (18:3).

PREPARATION OF THE SAMPLE

1. Extraction of Total Lipids

The method used was that of Ames (1968), being a modification of the extraction procedure used by Blight and Dyer (1959).

The bacterial culture was harvested by centrifugation at 4000 rpm for 20 min (MSE High Speed Centrifuge). The cells were thoroughly washed by resuspension and centrifugation in three changes of M9 buffer. The final supernatant was removed and the centrifuge tube inverted to drain. The weight of the pellet was calculated by reference to the weight of the empty tube. The extraction method relies on a monophasic system in which methanol, chloroform and water (i.e. bacterial culture) are in the proportion 2 : 1 : 0.8 v/v. On the assumption that a pellet of cells weighing 1 g contains 0.8 ml water, the weight of the pellet was used to calculate the volumes of methanol and chloroform to be added. On addition of the solvents, the tube containing the mixture was placed on ice for 10 min, during which time it was regularly mixed with a vortex mixer (Whirlimix, Fisons Ltd.). At the end of this

period 1 volume of chloroform was added with further mixing. The mixture was then diluted with 1 volume of water and centrifuged at 4000 rpm for 10 min (MSE Chilspin Centrifuge). The dilution procedure creates a biphasic system, the chloroform layer of which contains the lipids, the water-methanol layer, the non-lipids. During centrifugation a pellet of cellular debris forms at the interphase. To remove the lower chloroform layer, a fine Pasteur pipette was introduced through the pellet. The chloroform layer so removed was evaporated to dryness by the vacuum extraction of the solvent, leaving a residue of lipid.

Preparation of Fatty Acid Methyl Esters (FAME)

The lipid extract was dissolved in 1 ml of 2% H_2SO_4, placed in a glass reaction bottle with a close fitting lid, and heated in a water bath at 70°C for 1 hour. This procedure results in the hydrolysis of the phospholipids and the methylation of the resulting fatty acids (Mavis and Vagelos, 1972). Following the dilution of the acidic methanol solution with 1 ml distilled water, 2 ml of diethyl ether was added to extract the FAME.

It was normally necessary to wash the preparation in order to achieve a clean baseline and clear peaks on the chromatogram. Washing was carried out first with 1 ml 10% sodium bicarbonate and then with two washes of 1 ml distilled water. The washing procedure involved addition of the wash to the diethyl ether, followed by gentle agitation and allowing separation of the diethyl ether layer for removal. The washed preparation, if not used immediately, was stored under nitrogen at -20°C.

Preparation of FAME Standards

The chromatography standards were prepared by dilution of the 99% pure Chrompack standards to approximately 1 μg ml^{-1} in diethyl ether. A mixture of these standards was used as required, 2 μl volumes being used for injection. Preliminary runs resulted in the temperature programme described above being selected to give suitable separation of the standards used.

Retention Times

The retention time of each FAME was measured from the time of injection to the time at which the peak was reached, as the FAME was eluted from the column. In practice this time was measured as the distance in mm from the point of injection on the chromatogram. Methyl laurate (12:0) was chosen as the internal standard since this did not occur in the bacterial extracts. The relative retention time was then calculated for each FAME relative to methyl laurate.

Data presented in Appendix 6 shows the reproducibility achieved over 16 chromatograms of mixed standards. Mean relative retention times, and standard deviations, of known standards is calculated. Peaks in bacterial extracts were then identified by reference to the mean relative retention times of two or three chromatograms of standards run on the same day.

Analysis of a Bacterial Extract

The procedure adopted was to begin by injecting a 2 μl sample of standards. 2 μl of bacterial extract was then injected to

confirm the absence of methyl laurate and to check the cleanliness of the sample. If the chromatogram was acceptable, sufficient methyl laurate in diethyl ether was added to the extract to give a peak of comparable height to those in the extract. Two or three chromatograms were then obtained of the extract incorporating the internal standard. Finally, a mixture of standards was again injected to ensure that reproducibility was being maintained.

Retention times of the unknown peaks were measured and relative retention times were calculated with reference to methyl laurate.

Analysis of Dilinoleoyl Lecithin

A sample of dilinoleoyl lecithin (Lipid Products Ltd.) was treated in a manner identical to that described above for the preparation of FAME in order to ascertain the fatty acid composition of the lipid supplied.

THE PREPARATION OF LIPOSOMES

Materials

Dilinoleoyl lecithin (supplied in chloroform : methanol solution by Lipid Products, Redhill).

Method of Preparation

A 0.25 ml volume of the dilinoleoyl lecithin was placed in a 50 ml flask. The solvent was evaporated under a steady stream of nitrogen while the flask was continually rotated. This resulted in the deposition of a thin layer of the lipid on the wall of the flask. Twelve ml glass distilled water was added, followed by vigorous agitation by a vortex mixer (Whirlimix Ltd.) for 20 seconds, followed by a 20 second rest period. This sequence was repeated six times. The water used in this preparation was previously bubbled for 5 minutes with nitrogen, and the flask was flushed with nitrogen before mixing. This was to prevent auto-xidation during the preparation. Immediately before irradiation the suspension was bubbled with air for 3 minutes, to restore oxidative conditions.

GLC Analysis of the Lipid

In order to confirm the presence of linoleic acid and the absence of other fatty acids, GLC analysis was performed on the lipid. The procedure followed was as described in the section concerning GLC analysis. A chromatogram showing the analysis is shown in Fig. A15 in Appendix 7 and confirms linoleic acid as the only fatty acid present.

PREPARATION OF LIPOSOMES FOR ELECTRON MICROSCOPY

Materials

Liposomes prepared as above.

1% osmium tetroxide

acetone (BDH)

gold plating

2% agarose (Sigma)

resin (TAAB, Reading)

uranyl acetate

Reynolds lead citrate

Method 1 for the Scanning Electron Microscope

The liposomes were fixed in 1% osmium tetroxide for 1 hour. The preparation was then centrifuged at 4000 rpm for 10 minutes, then washed in distilled water and recentrifuged twice. The water was removed with a Pasteur pipette and the liposomes were dehydrated by passage through a graded acetone series. After critical point drying they were gold plated using an Edwards Sputter coating apparatus. The liposomes were then observed using a JEOL 100CX electron microscope with a scanning electron microscope attachment (SERC funded).

Method 2 for Sectioning

The liposomes were fixed and washed as described above. The preparation was then mixed rapidly with warm 2% agarose, drawn into a Pasteur pipette and smoothly extruded onto a glass dish. The

resulting cylinder was cut into sections less than 1 mm long which were dehydrated as before. The dried sections were infiltrated with resin and cured at 70°C for 48 hours before ultra-thin sections were prepared using an OMU 3 ultra-microtome (Reichart, Austria). The ultra-thin sections were picked up on copper grids (200 mesh) and stained with 2% aqueous uranyl acetate and subsequently with Reynolds lead citrate. They were then observed using the JEOL 100CX electron microscope.

Photography

Suitable fields of view at various magnifications were photographed using a Polaroid camera; examples of such photographs are shown in Appendix 7. The diameter of the liposomes was determined by measurement from these photographs and multiplication by the magnification factor. Over several fields of view this was found to be 100 nm. Sectioned liposomes indicated the presence of only one or two lipid bilayers.

TREATMENT OF DATA

The survival of irradiated bacteria was expressed graphically by plotting the surviving fraction (N/N_o), on a logarithmic scale, against the amount of radiation received, expressed as the time of exposure for broad-band radiation or as fluence for 254 nm radiation.

In most cases the survival curves obtained consisted of an initial shoulder, followed by an exponential portion, and such curves may be described by the expression:

$$N/N_o = ne^{-kD}$$

where N/N_o is the surviving fraction

D is the UV fluence

k is a measure of the slope of the linear portion of the survivor curve

n is a measure of the extrapolation of the curve with the y axis.

Visual inspection of the curves showed that the width and the extent of the shoulder varied with experimental conditions, such as the treatments applied to the organisms prior to, or during irradiation, and the lamps used. Peroxide values and rubidium leakage from E. coli, and pinocytic activity have been calculated as described in the relevant section, and plotted against irradiation time or fluence.

Each result described in the experimental section of this thesis is represented by a single 'typical' experimental result from a set of two to four experiments. Data pertaining to each

figure are provided in Appendix 8 as a table for each figure, together with data from one of the replicate experiments.

RESULTS AND DISCUSSION

PART 1A

INVESTIGATIONS INTO THE RESPONSE OF E. COLI K1060 TO BROAD-BAND NEAR-UV RADIATION AND THE ROLE OF MEMBRANE FATTY ACIDS

The organism E. coli K1060 is described in the Introduction and Methodology. The organism successfully grows on defined media utilizing any supplied unsaturated or cyclopropane fatty acid. Its fad E62 lesion prevents degradation of the supplied fatty acid, while the fab B lesion prevents de novo synthesis of unsaturated fatty acids.

As previously described, Klamen and Tuveson (1982) demonstrated that the degree of unsaturation of membrane fatty acids determined the sensitivity of exponentially growing cultures of K1060 to broad-band near-UV irradiation. For their investigations, Klamen and Tuveson used 20-carbon fatty acids, while the naturally occurring unsaturated fatty acid in E. coli is the mono-unsaturated 18-carbon cis-vaccenic acid (Cronan and Vagelos, 1972). Since an increase in chain length may lead to a decrease in membrane fluidity it was decided for these studies to use 18-carbon unsaturated fatty acids of the same carboxyl-9 series; oleic (18:1), linoleic (18:2) and linolenic (18:3) acids, and in addition, the cyclopropane derivative of oleic acid, dihydrosterculic acid. The structures of these fatty acids are shown in Table 7.

This section is concerned with the determination of the sensitivity to broad-band near-UV irradiation of K1060 cultures incorporating fatty acids with varying degrees of unsaturation. The dependence of such sensitivity on oxygen and the role of

Table 7. The structure of fatty acids used as supplements for *E. coli* K1060.

cis-vaccenic acid (for comparison)	$CH_3(CH_2)_5.CH=CH(CH_2)_9.COOH$
oleic acid	$CH_3(CH_2)_7.CH=CH(CH_2)_7.COOH$
linolenic acid	$CH_3CH_2.CH=CH.CH_2.CH=CH.CH_2CH=CH(CH_2)_7.COOH$
dihydrosterculic acid	$CH_3(CH_2)_7.\underset{H}{\overset{CH_2}{C}}-\underset{H}{C}(CH_2)_7.COOH$

antioxidants, active oxygen scavengers and irradiation in deuterium oxide was investigated. Where relevant, comparisons were made with sensitivities to far-UV irradiation.

Lipid peroxidation resulting from the near-UV irradiation of K1060 was subsequently determined, using the iodometric hydroperoxide assay described in the Methodology, and compared in cultures incorporating the three unsaturated fatty acids. The effect on lipid peroxidation of oxygen scavengers and deuterium oxide was then investigated.

The leakage of rubidium, as an indicator of radiation-induced membrane damage was measured using the method of Kelland (1984), in cultures incorporating the three unsaturated fatty acids, and the effect of irradiation in deuterium oxide was determined.

1. THE EFFECT OF UNSATURATED FATTY ACID COMPOSITION ON THE SENSITIVITY OF *E. COLI* K1060 TO BROAD-BAND NEAR-UV IRRADIATION

The Sensitivity of Exponential Phase Cells

Cultures of K1060 were grown in media supplemented with oleic, linoleic or linolenic acid. They were harvested in the exponential growth phase and irradiated with the broad-band source as described in the Methodology. Viability was determined on rich media (YENB) or defined media. Gas chromatography analysis of the cultures, as described in a subsequent section of this thesis, confirmed that the organism incorporated the unsaturated fatty acid provided in the growth medium and failed to synthesise other unsaturated fatty acids *de novo*.

Fig. 27 shows examples of survival curves, viability being assessed on YENB. It is evident that day-to-day variation, characteristic of the broad-band irradiation of cells in this phase of growth, presents difficulty in describing sensitivity precisely in terms of the size of the shoulder, or the time taken to reach a level of survival of 10^{-1} or 10^{-2}, for example. However, Fig. 28 illustrates that, even allowing for such variation, there is a clear relationship between sensitivity, expressed in a variety of ways, and the number of C=C bonds in the incorporated fatty acid; the greater the degree of unsaturation, the more sensitive are the cells. Figs. 29 and 30 show viability as determined on a normal salt (Fig. 29) or a high salt (Fig. 30) defined medium.

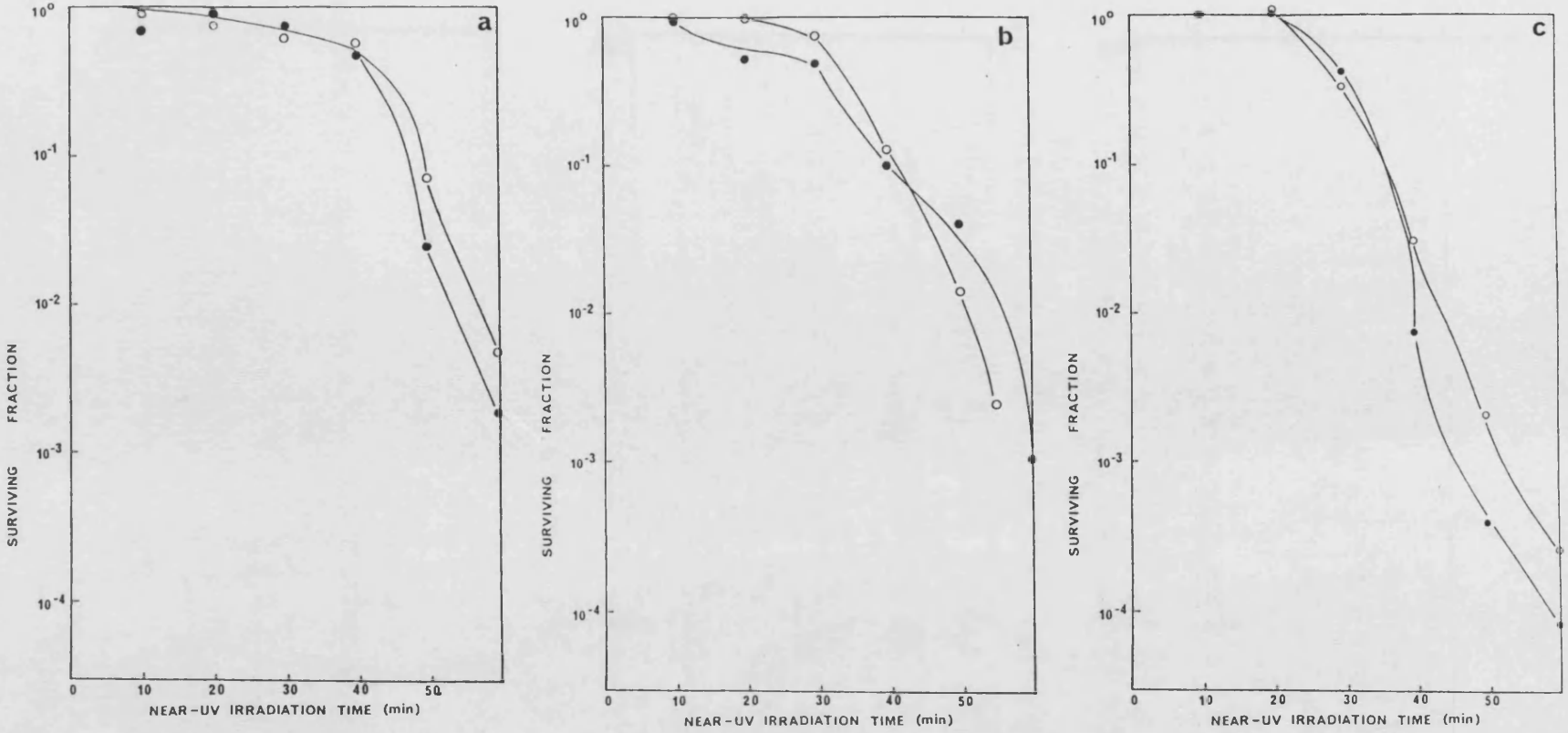

Figure 27
Survival curves for log phase E. coli K1060 incorporating (a) oleic (b) linoleic or (c) linolenic acid, following broad-band near-UV irradiation. Viability assessed on YENB. Open and closed symbols represent replicate experiments performed on different days.

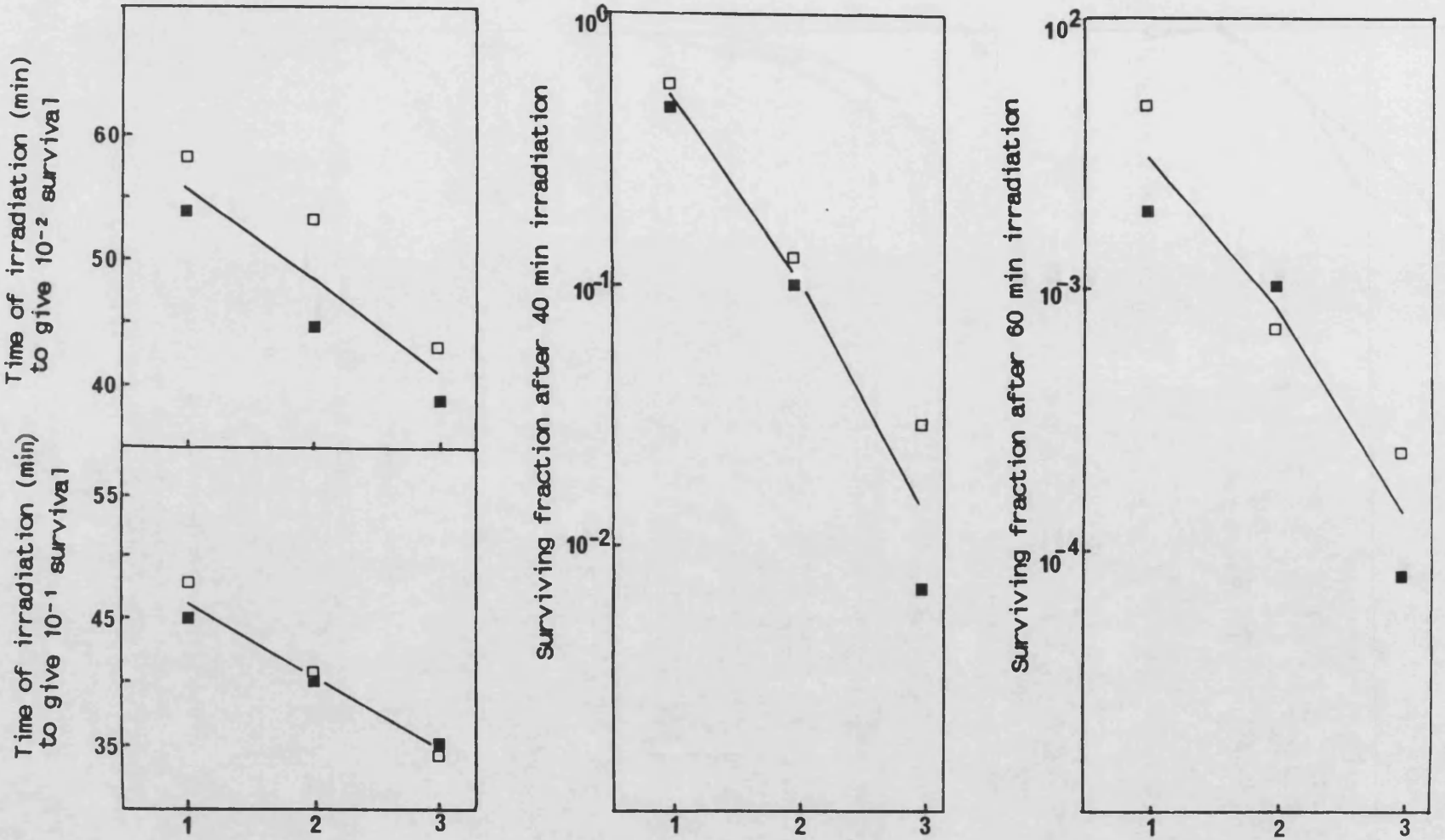

Figure 28 The relationship between the number of unsaturated C=C bonds and survival parameters taken from figure 27.

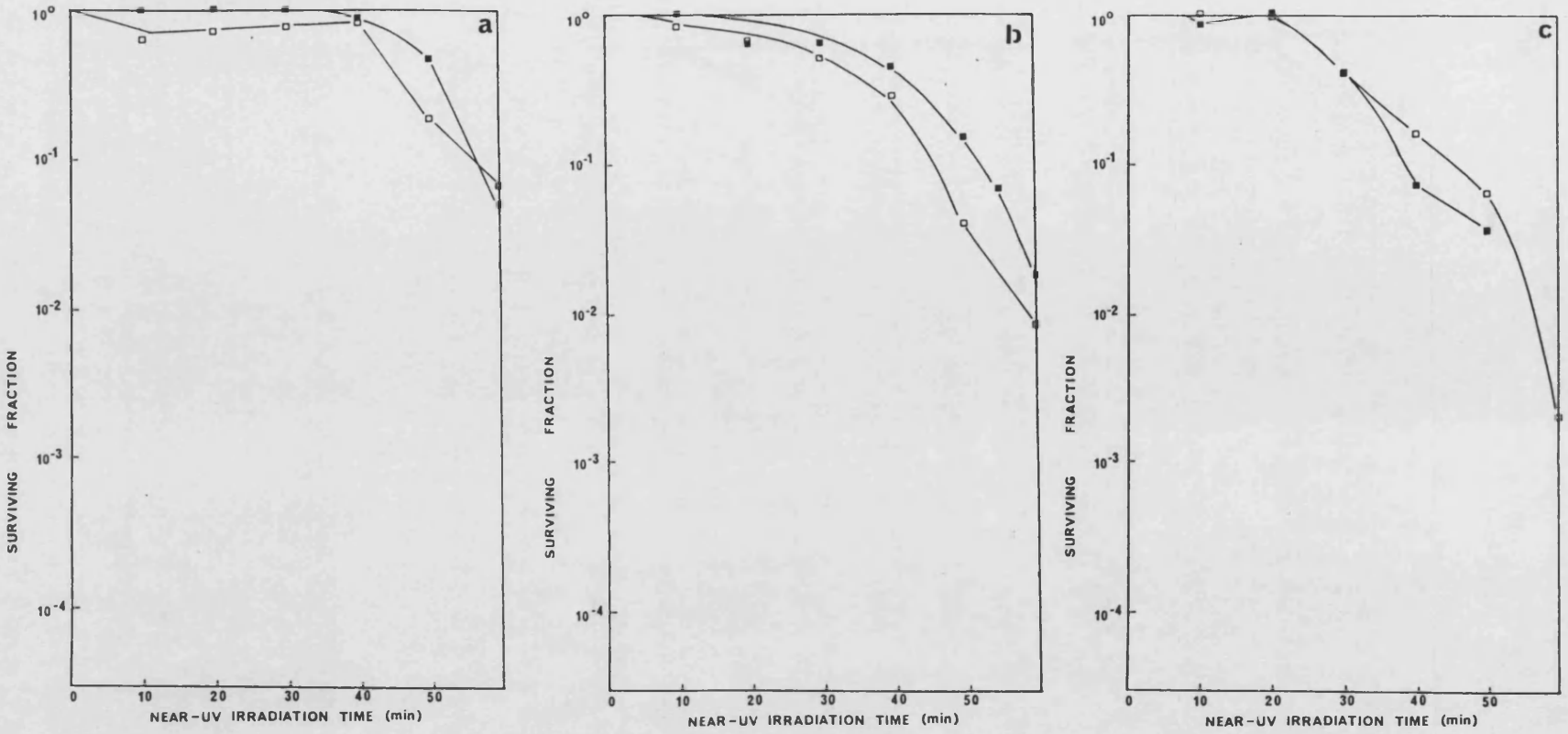

Figure 29
Survival curves for log phase E. coli K1060 incorporating (a) oleic (b) linoleic or (c) linolenic acid, following broad-band near-UV irradiation. Viability assessed on defined medium. Open and closed symbols represent replicate experiments performed on different days.

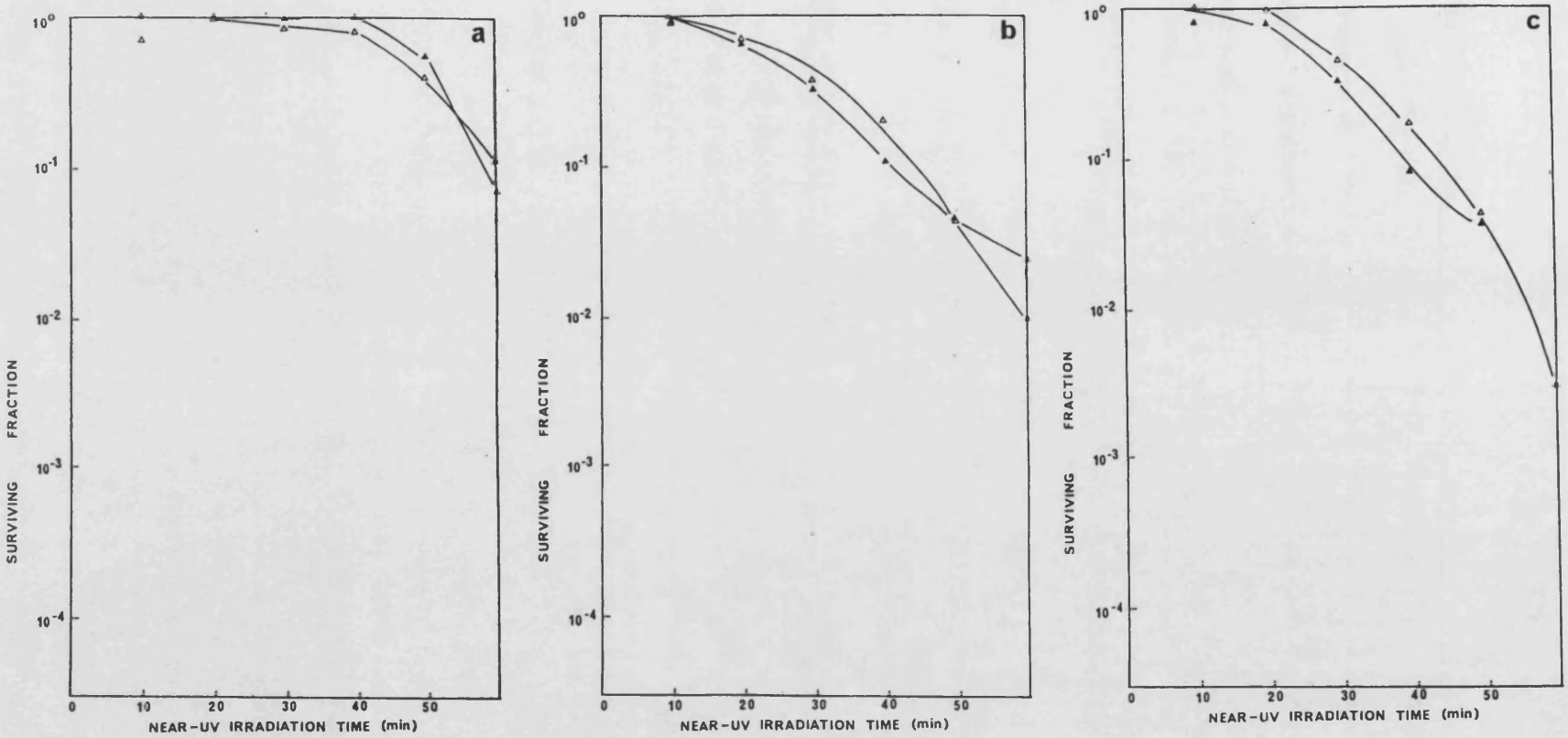

Figure 30
Survival curves for log phase E. coli K1060 incorporating (a) oleic (b) linoleic or (c) linolenic acid, following broad-band near-UV irradiation. Viability assessed on defined medium. Open and closed symbols represent replicate experiments performed on different days.

Replacement of the B L B Lamps

During the course of this work the fluence of the original lamps began to fall, therefore new lamps of the same specification were installed. The fluence rate of the new lamps was determined by biological dosimetry as shown in Fig. A3 in the Appendix. Also presented in Appendix 3 are survival curves for E. coli K1060 incorporating the three unsaturated fatty acids, following irradiation with the new lamps. The effect of fluence rate, since that of the new lamps was approximately double that of the original lamps, is also discussed.

The Sensitivity of Stationary Phase Cells

Similar experiments were performed using stationary phase cells of K1060, harvested after 24 hours growth in appropriately supplemented defined media.

The survival of the cells after broad-band near-UV irradiation did not vary with unsaturated fatty acid content, as Fig. 31 shows.

Survival of E. coli K1060 Cells Incorporating Dihydrosterculic Acid

As exponentially growing bacteria enter the stationary phase of growth, the unsaturated fatty acids are converted to cyclopropane derivatives. This eliminates the C=C bonds, possibly as a protection against lipid peroxidation, while retaining the necessary degree of membrane fluidity.

It is possible to synthesise the cyclopropane derivative of oleic acid in vitro by the method of Kornberg and McConnell (1971). This preparation was carried out very kindly by Dr. M. Coombs

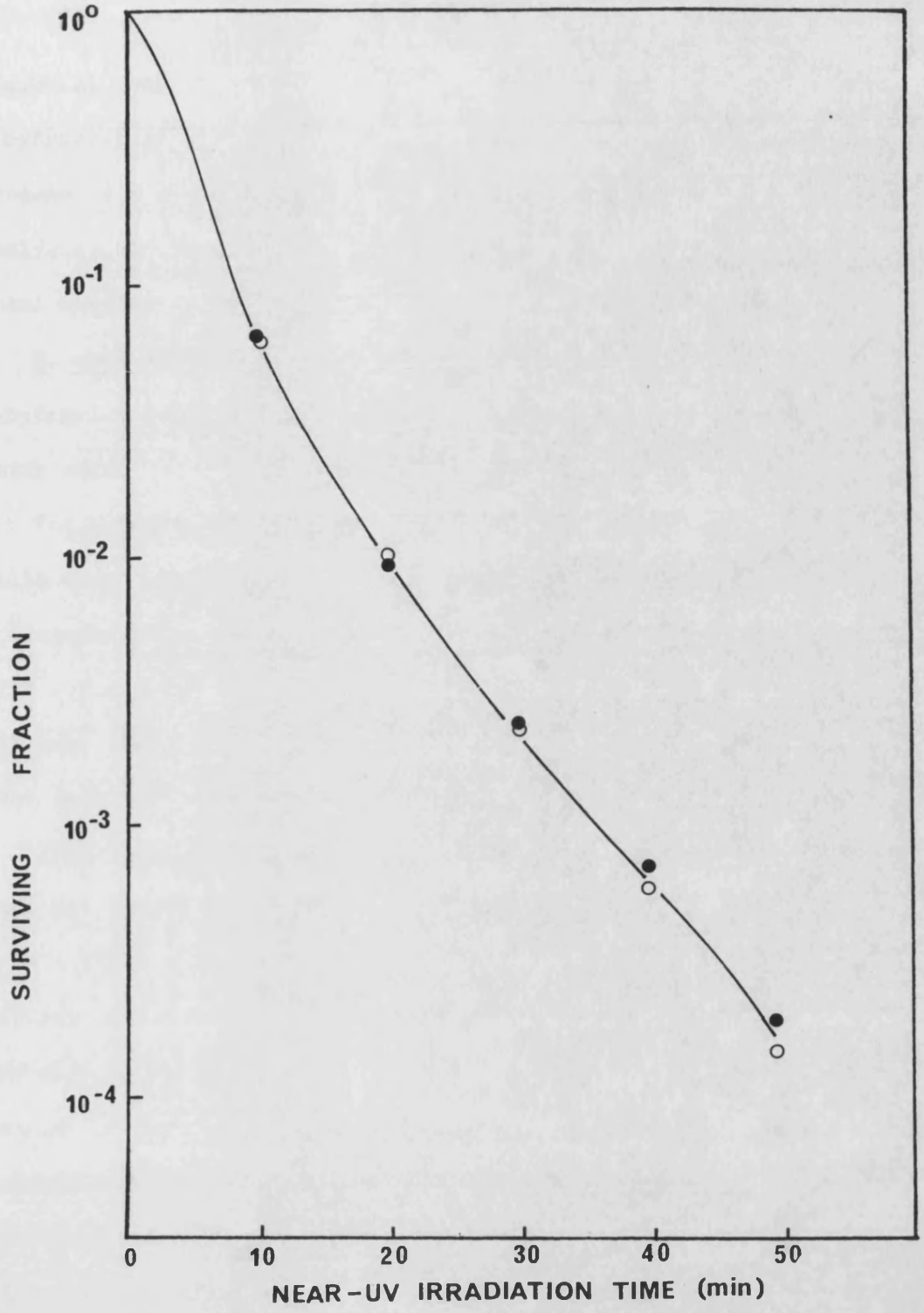

Figure 31
Survival curves for stationary phase E. coli K1060 incorporating oleic (open symbols) or linolenic (closed symbols) acid, following broad-band near-UV irradiation. Viability assessed on YENB.

(Imperial Cancer Research Fund Laboratories). The resulting dihydrosterculic acid was tested for the presence of the cyclopropane ring by both infra-red and nuclear magnetic resonance analysis, and confirmed. The latter technique also established the total absence of C=C double bonds in the sample.

E. coli K1060 grew readily on solid and in liquid media where dihydrosterculic acid was added at 0.02% in place of an unsaturated fatty acid.

Following growth in media supplemented with this fatty acid, cells were harvested in the standard way in the log phase, and irradiated. Fig. 32 shows survival curves of such cells, compared with cells grown in parallel on oleic acid media, and irradiated at the same time. An increase in viability, though small, is apparent (the data for replicate experiments is given in Appendix 8).

These results provide a useful "baseline" against which survival curves of cells incororating oleic, linoleic, or linolenic acid, may be compared. When this fatty acid is incorporated any killing cannot be attributed to lipid peroxidation-mediated events and must therefore be due to other factors, such as DNA or protein damage. It may then be argued that any increased sensitivity exhibited by cells incorporating unsaturated fatty acids may be attributed to the presence of those fatty acids. Since those in turn are only found in the membrane, then this may be considered as evidence of membrane-related contributions to near-UV sensitivity.

Survival of K1060 following Far-UV Irradiation

Near-UV radiation has been observed to differ from Far-UV radiation in terms of radiation-induced membrane damage (Kelland,

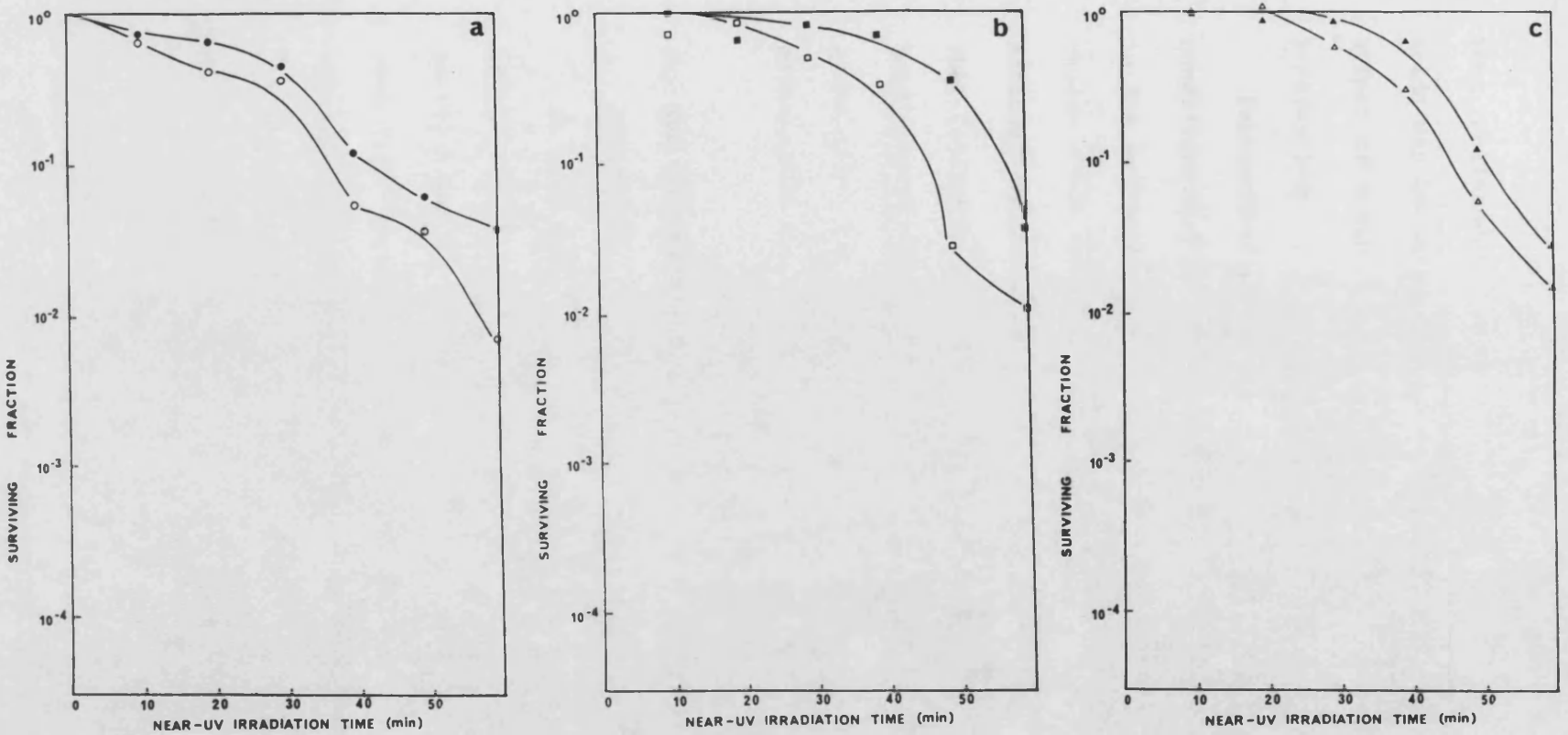

Figure 32
Survival curves for log phase E. coli K1060 incorporating oleic (open symbols) or Dihydrosterculic (closed symbols) acid, following broad-band near-UV irradiation. Viability assessed on (a) YENB (b) defined medium (c) high salt defined medium.

1984, Hollaender, 1943). Since it is suggested that membrane fatty acids may be targets for NUV attack, it is interesting to know the effect of their unsaturation on survival following 254 nm irradiation.

Exponential phase cells were harvested under standard conditions and irradiated with the Penray 254 nm source described in the Methodology prior to assessment of viability. Fluences were chosen which resulted in similar levels of survival to those achieved following near-UV irradiation. Results in Fig. 33 show that following FUV irradiation survival is independent of fatty acid composition. This would be expected, since during FUV irradiation the primary target is DNA, and cell death is principally due to the formation of pyrimidine dimers.

2. THE DEPENDENCE ON OXYGEN FOR KILLING BY BROAD-BAND NEAR-UV RADIATION

As discussed in the Introduction, it is well known that a proportion of damage to cells caused by ultraviolet light, particularly at the longer wavelengths used in broad-band sources such as those used here, is caused by indirect mechanisms involving reactive oxygen species.

While such oxygen-mediated effects would include, for example, single strand breaks in DNA and oxidative damage to proteins, including those of the cell membrane, the unsaturated fatty acyl components of membrane phospholipids may also be a target.

While postulating the peroxidation of membrane fatty acids as a cause of near-UV radiation-induced damage, it is necessary to

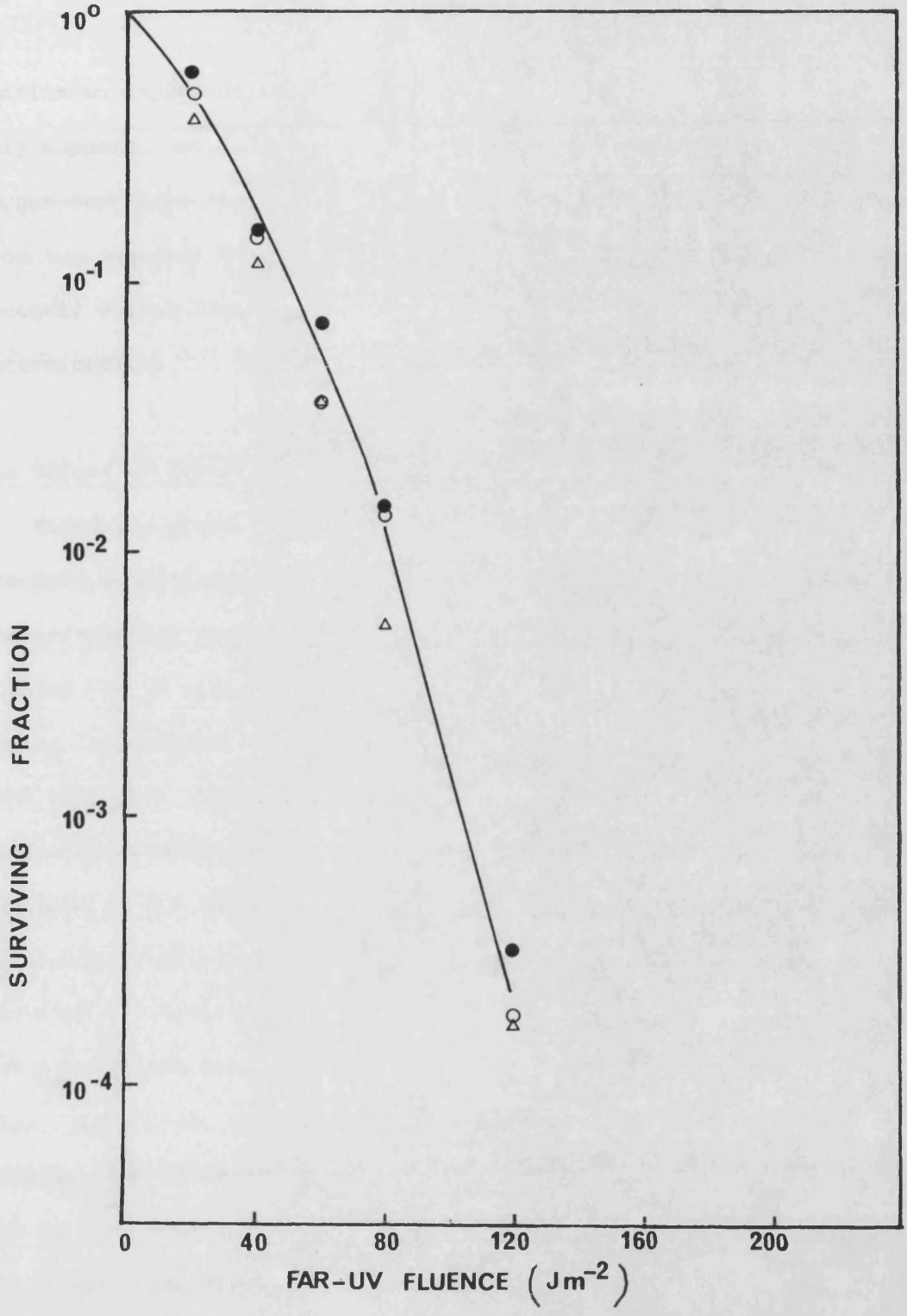

Figure 33
Survival curves for log phase E. coli K1060 incorporating (△) oleic, (●) linoleic or (○) linolenic acid,

following far-UV irradiation.

confirm an oxygen-dependence, even though such dependence would only support, not confirm, such a mechanism, in view of other oxygen-dependent reactions. The necessity for oxygen was considered from two aspects: in the first instance during irradiation, and secondly during incubation of the plates used for viability determination.

The Effect of Irradiation under Aerated or Anoxic Conditions

K1060 was grown and harvested in the exponential phase under standard conditions. The M9 buffer used for resuspending the cells for irradiation was divided into two batches, one of which was bubbled for 20 minutes with oxygen-free nitrogen prior to use. During irradiation this cell suspension was bubbled with oxygen-free nitrogen, while the other batch was aerated normally. Following irradiation with the broad-band source viability was assessed in the usual way. Fig. 34 presents results obtained following irradiation under these conditions. Fig. 34a shows the survival of linolenate-grown cells, where anoxic irradiation results in less killing than irradiation under aerated conditions. Figs. 34b and 34c compare the survival of linolenate- and oleate-grown cells irradiated under these conditions using the new set of BLB lamps installed at this time, as described in Appendix 3. In comparing Figs. 34b and 34c it can be seen that while anoxic irradiation of linolenate-grown cells offers protection after 10-15 minutes exposure, the same effect is not as clearly seen until a longer exposure of 20-25 minutes for oleate-grown cells.

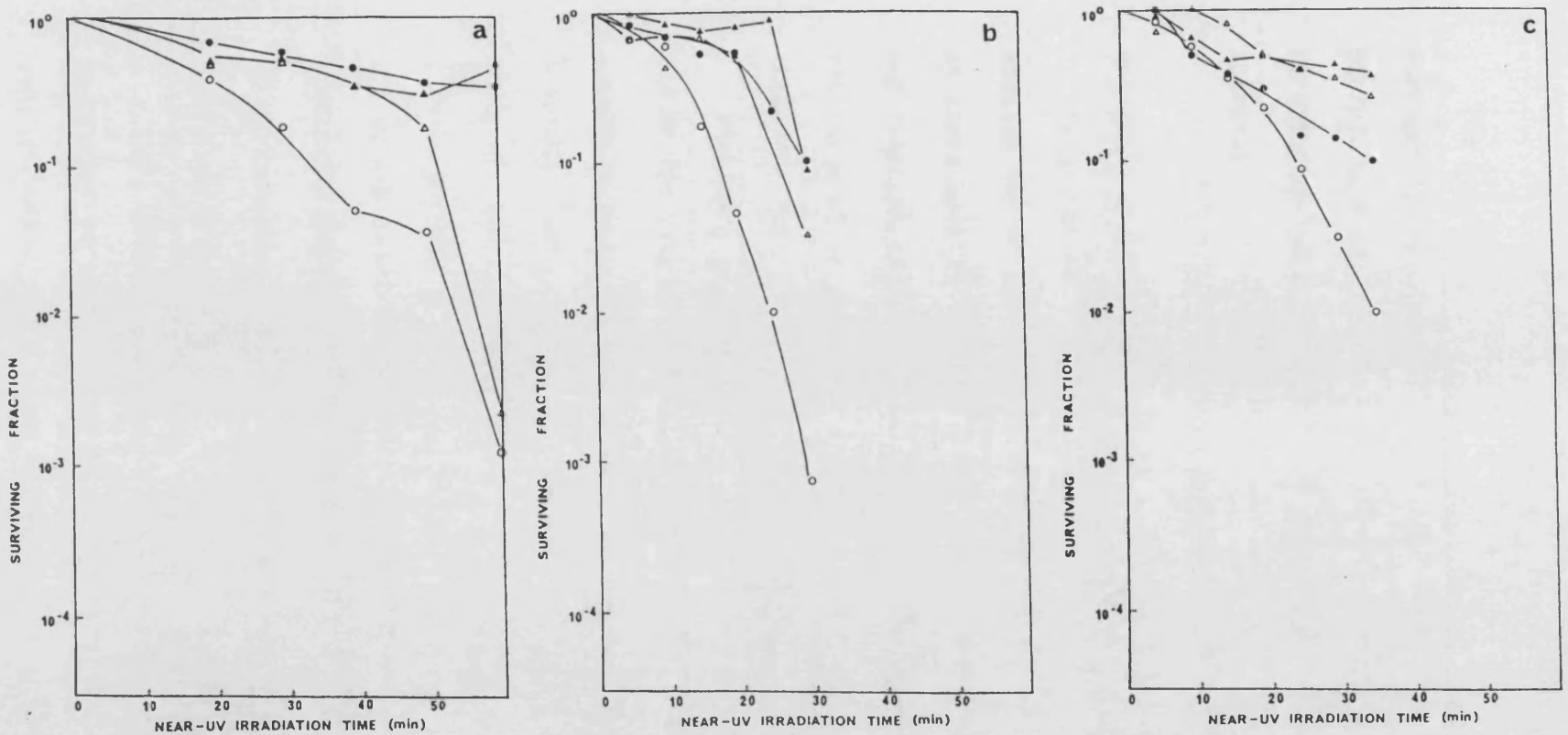

Figure 34 Survival curves forlog phase E.coli K1060 following broad-band near-UV irradiation under aerated (open symbols) or anoxic (closed symbols) conditions. Irradiation with old lamps (a) or new lamps (b,c). Cells incorporating linolenic (a,b) or oleic (c) acid.

The conditions used here are not sufficient to provide for the stringently anoxic conditions used, for example, by Webb and Brown (1979). However, the reduction in available oxygen in the irradiation medium is sufficient to result in an increase in survival.

Anaerobic Incubation of Plates used for Viability Assessment

As discussed in the Introduction, various reactive oxygen species may be formed during irradiation. In addition, propagation of these species and oxygen-dependent propagation of lipid peroxidation may continue after irradiation. The effect of the exclusion of oxygen during incubation following irradiation was therefore investigated.

Following standard irradiation procedures duplicate sets of plates for viability assessment were prepared. One set was incubated under standard conditions. The other set was incubated in anaerobic jars (Gaspack, utilizing Oxoid gas generating kits and anaerobic indicator strips). The anaerobically incubated plates were incubated for 5 or 6 days before colonies were counted, since the growth rate was slow. Fig. 35a shows that while survival of linolenate-grown cells on defined medium is not changed, there is an evident enhancement of survival on the rich medium when viability is assessed following anaerobic incubation.

Post- irradiation oxygen-dependent events may be of minor importance to the cell under the conditions provided by growth on defined media, in contrast to those provided by rich media. This is discussed subsequently.

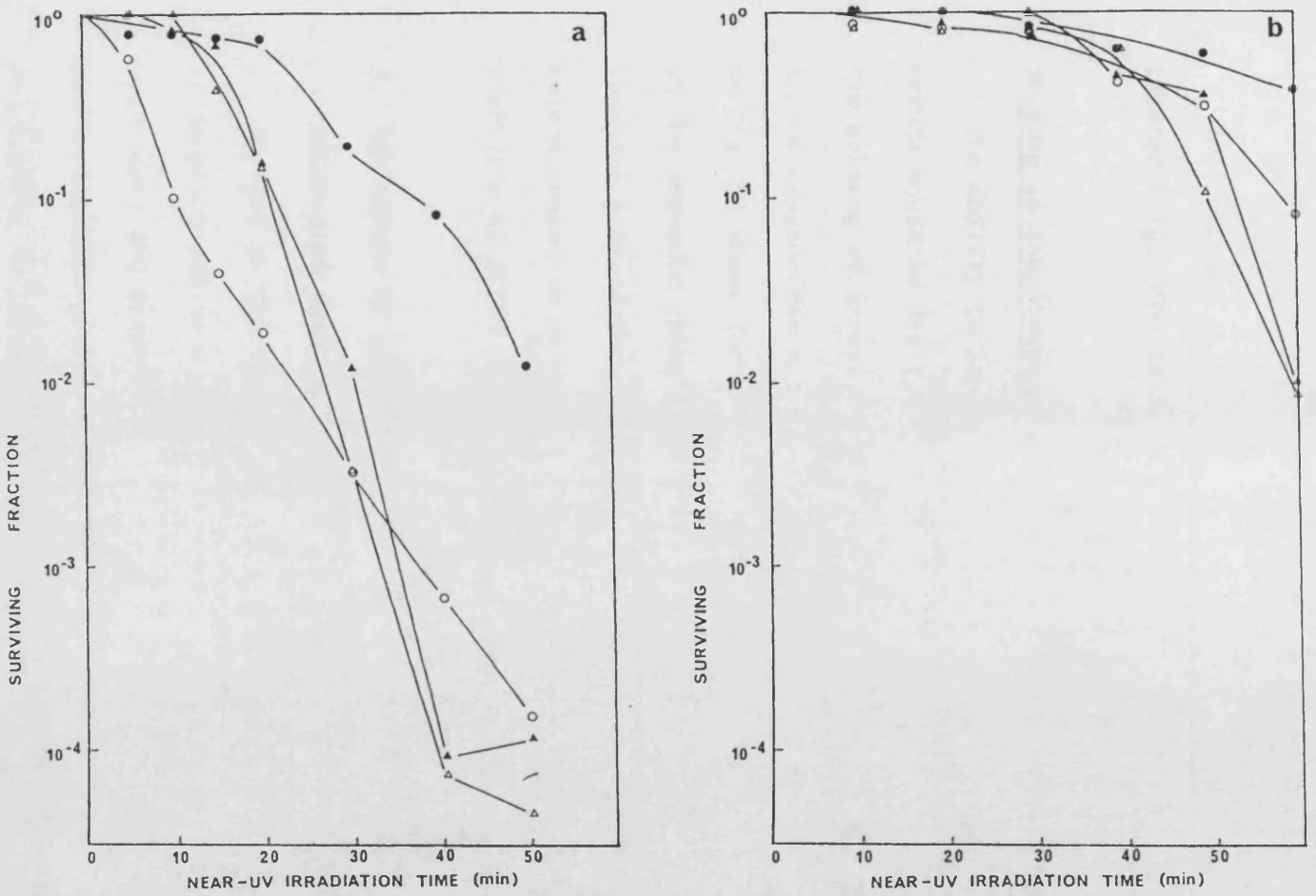

Figure 35 Survival curves for log phase E. coli K1060 following broad-band near-UV irradiation. Viability assessed on YENB (○●) or high salt defined medium (△▲) incubated under aerobic (open symbols) or anaerobic (closed symbols) conditions. Cells incorporating (b) oleic or (a) linolenic acid,

The increase in viability when oleate-grown cells are similarly treated (Fig. 35b) is small.

Holding in the Absence of Oxygen Following Irradiation

The ability to impose a time scale on proposed post-irradiation events would be desirable. However, a preliminary study involving the holding of irradiated cells in M9 while bubbling with either air or oxygen-free nitrogen for 75 minutes showed no oxygen effect, as Fig. 36 shows for cells incorporating linolenic acid. Table 9 in the Appendix shows similar result for cells incorporating linoleic acid. Although this is a limited holding period, the method proved to be unsuitable for longer periods, since the viability of K1060 declined.

3. THE EFFECT OF ANTIOXIDANTS ON THE SURVIVAL OF K1060 FOLLOWING BROAD-BAND NEAR-UV IRRADIATION

In view of the results showing an oxygen effect during irradiation and incubation, various antioxidants, free radical scavengers and enzymes were incorporated into the media used for pre-irradiation growth, and in post-irradiation viability assessment, to investigate whether or not they protected the cells.

Vitamin E is a molecule known for its activity in the termination of lipid peroxidation reactions and radical scavenging action, especially in association with mammalian plasma membranes.

Its effect on the survival of linolenic acid-supplemented K1060 following broad-band NUV irradiation was investigated in two ways. Firstly, it was added to the growth medium for utilization by

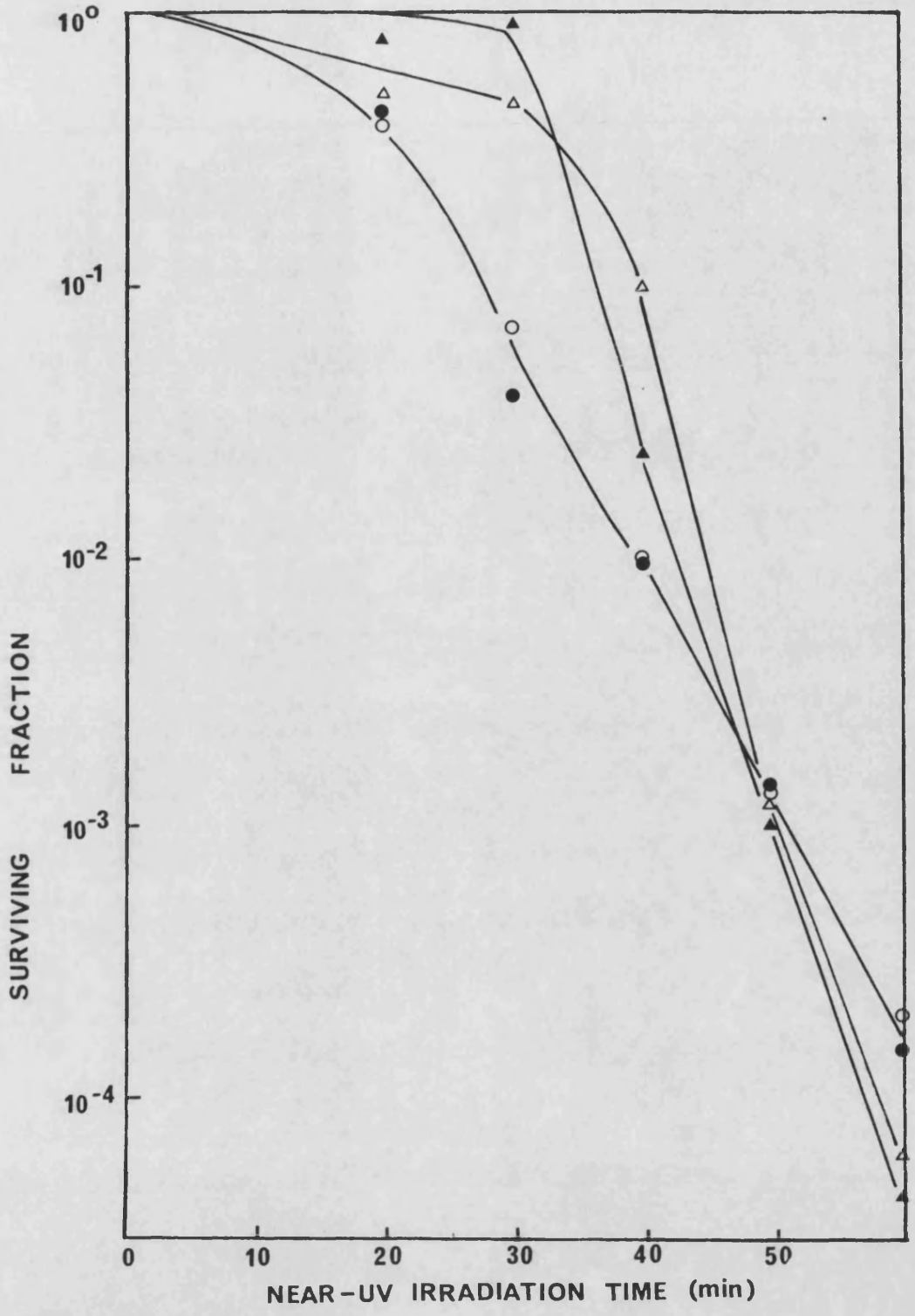

Figure 36
Survival curves for log phase E. coli K1060 incorporating linolenic acid, following broad-band near-UV irradiation. Viability assessed on YENB (O ●) or high salt defined medium (△▲) following 75min bubbling with oxygen-free nitrogen (closed symbols) or air (Open symbols)

the organisms prior to irradiation, secondly it was incorporated into the media used for viability assessment following irradiation of linolenate-grown K1060.

The Effect of Addition of Vitamin E to the Pre-Irradiation Growth Media

Vitamin E was added as α-tocopherol (Sigma, UK) to the pre-irradiation growth media at 100 μg ml^{-1}. It was first solubilized in Brij 58 with the linolenic acid supplement, and sterilized by membrane filtration. Following irradiation with the broad-band source viability was assessed on YENB and high salt minimal media. Fig. 37a shows the result of one such experiment, where it can be seen that supplementation by Vitamin E prior to irradiation offers a low degree of protection.

The Effect of the Addition of Vitamin E to the Plating Medium

In parallel with the previous experiments, the viability of irradiated cells was also assessed on media supplemented with Vitamin E. Such plates were prepared by the aseptic addition of 16ml Brij 58 containing 5 mg ml^{-1} α-tocopherol, in addition to the fatty acid supplement, to a 800 ml batch of agar. This provided a concentration of 2 mg α-tocopherol per plate. Cells grown prior to irradiation in defined media with or without a supplement of α-tocopherol, as described previously, were irradiated and viability assessed on both supplemented and standard media.

Fig. 37b compares survival curves determined in parallel with the experiment depicted in Fig. 37a (shown as the dashed line). The

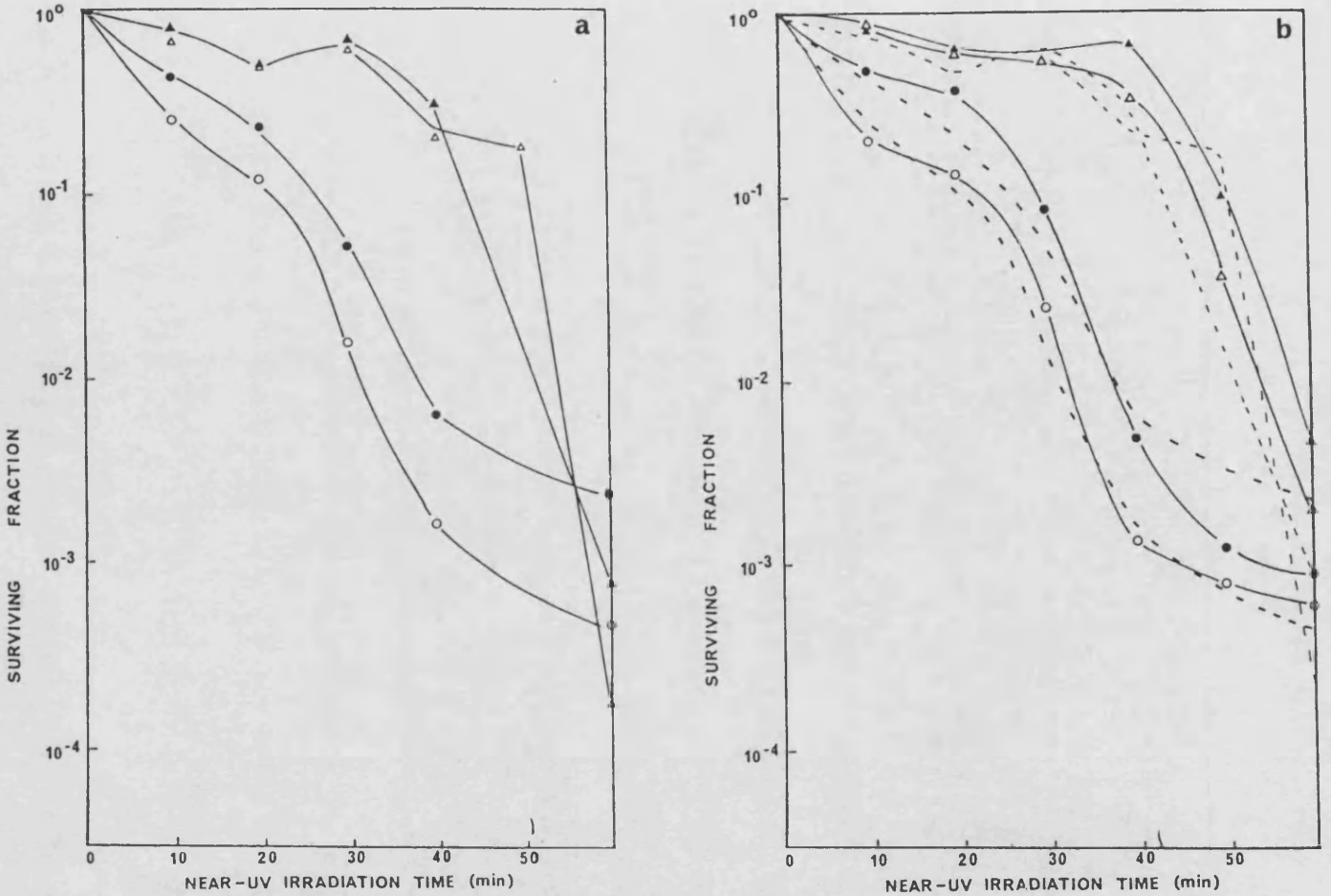

Figure 37

Survival curves for E coli K1060 following broad-band near-UV irradiation after growth in vitamin E-supplemented (closed symbols) or unsupplemented media (open symbols)
(a)Plating media unsupplemented,(b)plating media supplemented with vitamin E. Dashed lines from fig 37a

Viability assessed on YENB (○●) or high salt defined medium(△▲)

addition of α-tocopherol to the plating media does not enhance the survival of cells, whether or not they were supplemented with Vitamin E prior to irradiation.

The Effect of the Addition of Trolox-C to the Plating Medium

Trolox-C is a water-soluble Vitamin E analogue (kindly donated by Hoffman-La Roche Ltd.). When added to the plating media at 2·0 mg per plate, as 16 ml of a 5 mg ml^{-1} solution per 800 ml batch of agar, some degree of protection was observed, as Fig. 38 shows. When Trolox-C was used as a pre-irradiation growth supplement, no reduction in sensitivity was apparent.

Both α-tocopherol and Trolox-C are large molecules, and since they are not nutritional requirements of the organism specific transport systems would not be expected for their uptake. The small protective effect offered by α-tocopherol when provided as a pre-irradiation growth supplement may be accounted for by its diffusion through the cell envelope due to its lipophilic nature. Trolox-C, being water soluble, would not be able to pass the hydrophobic barrier.

4. THE EFFECT OF CATALASE AND SUPEROXIDE DISMUTASE ON SURVIVAL FOLLOWING NEAR-UV IRRADIATION

Superoxide anion ($O_2^{\cdot-}$) is known to result from the NUV-irradiation of NADH and NADPH coenzymes, (Cunningham et al., 1985). Being relatively unreactive compared with hydroxyl radicals, $O_2^{\cdot-}$

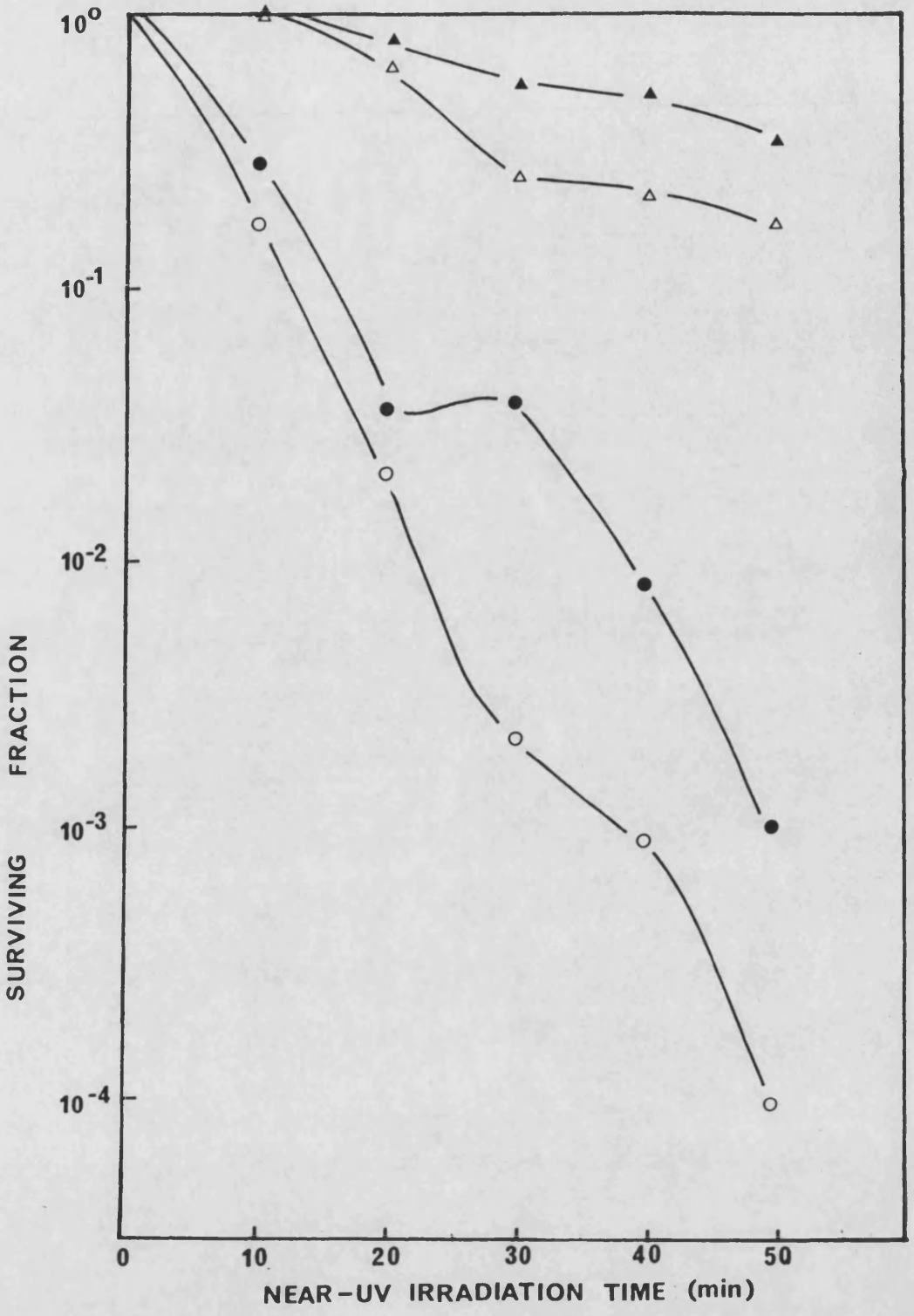

Figure 38
Survival curves for log phase E. coli K1060 incorporating linolenic acid, following broad-band near-UV irradiation. Viability assessed on YENB (○ ●) or high salt defined medium (△ ▲) in the presence (closed symbols) or absence (open symbols) of Trolox-C.

may diffuse away from the site of its production, possibly through the cell envelope, causing damage in its path. When $O_2^{\cdot -}$ is dismutated, a reaction catalysed by superoxide dismutase (SOD), hydrogen peroxide is formed:-

$$O_2^{\cdot -} + O_2^{\cdot -} + 2H^+ \longrightarrow O_2 + H_2O_2$$

Hydrogen peroxide is itself a reactive product, resulting in the formation of the highly reactive $OH^{\cdot}$ upon reaction with further $O_2^{\cdot -}$:

$$H_2O_2 + O_2^{\cdot -} \longrightarrow O_2 + OH^- + OH^{\cdot}$$ (Fridovitch, 1975)

Hydrogen peroxide is also produced during irradiation with NUV sources (McCormick *et al.*, 1976) and moves freely across the membrane. It has been shown to be present in rich media following exposure to light (Mackey and Derrick, 1986). Catalase is the enzyme responsible for the dismutation of hydrogen peroxide:

$$2H_2O_2 \longrightarrow 2H_2O + O_2$$

Mackey and Derrick (1986), detected H_2O_2 in rich media (but not in minimal media) and attributed the reduced survival of cold-shocked *Salm. typhimureum* and *E. coli* to its presence, since the addition of catalase to the rich media restored the viable counts to those obtained on minimal media. Although plates in this laboratory were stored in a cold room until use, it is not unusual for the light to be left on overnight, so that H_2O_2 production in YENB plates is a possibility.

To test whether O_2 or H_2O_2 may be affecting post-irradiation survival on the rich media, SOD or catalase were added to all media prior to plating for viability assessment.

The Effect of SOD and Catalase on Survival

SOD was added to overdried plates as 0.2 ml of SOD (Boehringer) dissolved in M9 to give a concentration of 500 units ml^{-1} (100 units per plate), spread over the surface and dried before use. Catalase was added as 0.2 ml of catalase (Boehringer) diluted in M9 to give a concentration of 500 units ml^{-1} (100 units per plate), spread over the surface and dried before use. The viability of irradiated K1060 cells was then assessed. Fig. 39 shows that the survival on YENB is considerably greater if either SOD (Fig. 39a) or catalase (Fig. 39b) is added, the latter being the more effective.

If hydrogen peroxide contributes to cell killing during post-irradiation incubation, its role may, in part, be considered in terms of its reactions with ferrous ions found in rich media:

$$Fe^{2+} + H_2O_2 \longrightarrow Fe^{3+} + OH^{\cdot} + OH^{-}$$

a reaction which provides for hydroxyl free radical formation, which may challenge and further damage the irradiated cells.

Iron present in media may further be considered in terms of its catalytic action on lipid hydroperoxides, which are shown to be produced during irradiation in the following section.

Lipid hydroperoxides will be catalytically decomposed in the presence of iron:

$$Fe^{3+} + LOOH \longrightarrow Fe^{2+} + LOO^{\cdot} + H^{+}$$

$$Fe^{2+} + LOOH \longrightarrow Fe^{3+} + OH^{-} + LO^{\cdot}$$

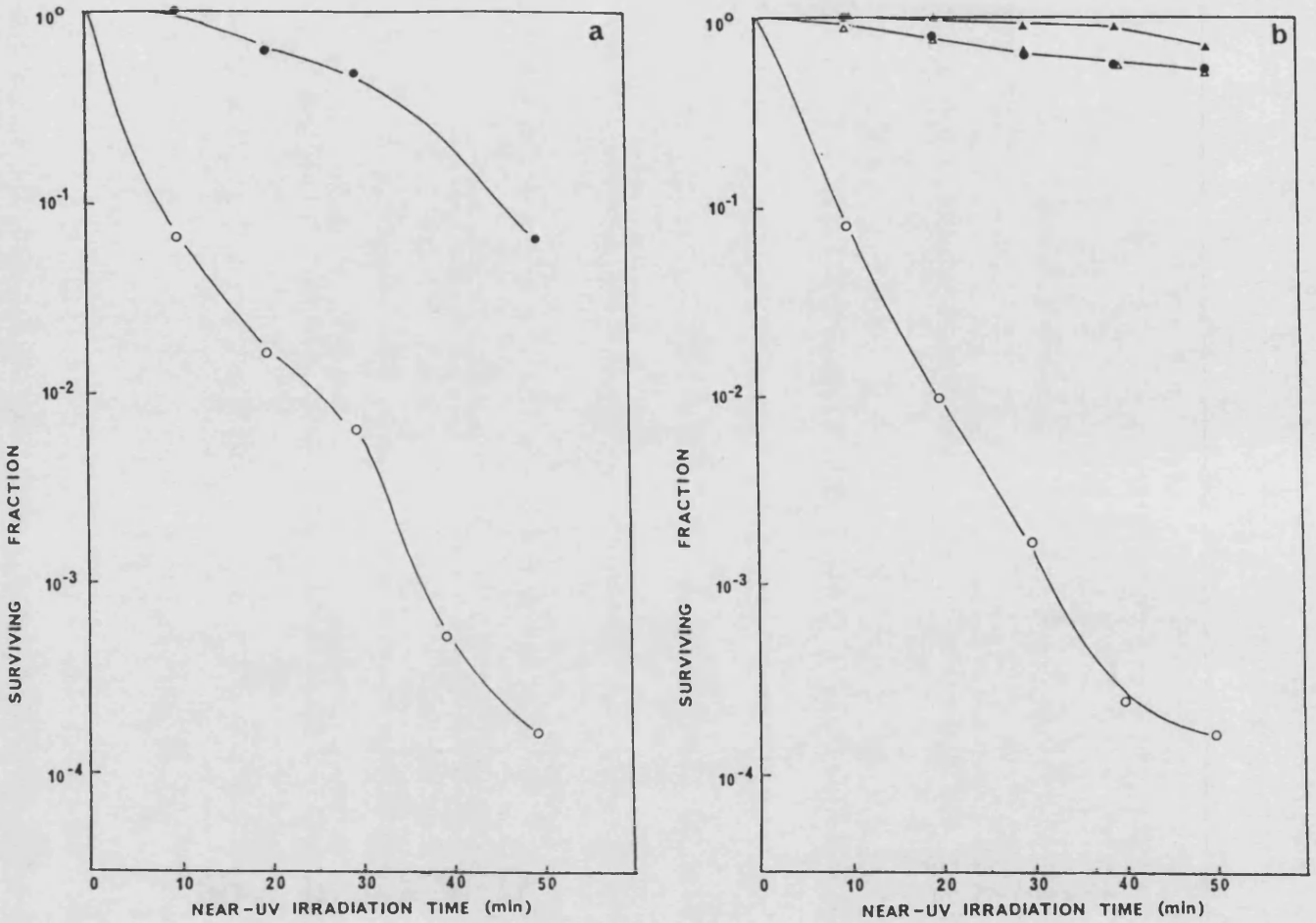

Figure 39
Survival curves for log phase E. coli K1060 incorporating linolenic acid, following broad-band near-UV irradiation. Viability assessed on YENB (○ ●) or high salt defined medium (△ ▲) in the presence (closed symbols) or absence (open symbols) of (a) Superoxide Dismutase (b) Catalase.

The resulting alkoxyl ($LO^{\cdot}$) radicals will then, by propagation reactions, lead to further peroxyl radical formation:

$$LO^{\cdot} + LH \longrightarrow LOH + L^{\cdot} \; (+ O_2 \longrightarrow LOO^{\cdot})$$

Propagation reactions will continue until terminated, for example by reaction with antioxidants to form non-radical products.

It is possible to chelate the iron present in media by the addition of desferrioxamine, so that it is no longer available for participation in such reactions. Desferrioxamine is an extremely efficient chelator (Gutteridge et al., 1979).

5. THE EFFECT OF THE ADDITION OF DESFERRIOXAMINE TO MEDIA USED FOR VIABILITY ASSESSMENT

Desferrioxamine (Ciba) was dissolved in M9 at 10 mg per ml. After filtration to sterilize the solution, 10 ml were added to a batch (800 ml) of YENB agar to provide a final concentration of 0.125 mg ml^{-1}. The degree of protection which the removal of iron from the media offered was consistent but small. The results of one such experiment are shown in Fig. 40 and further data in the Appendix. This leads to the conclusion that the described catalytic role of iron does not apply greatly to the extracellular growth medium. It does not preclude the possibility that cellular iron may play such a part within the cell.

While the results presented here indicated, to varying degrees, an increase in survival when irradiated cells are plated out in the presence of various antioxidants and scavengers, the following points must be remembered:-

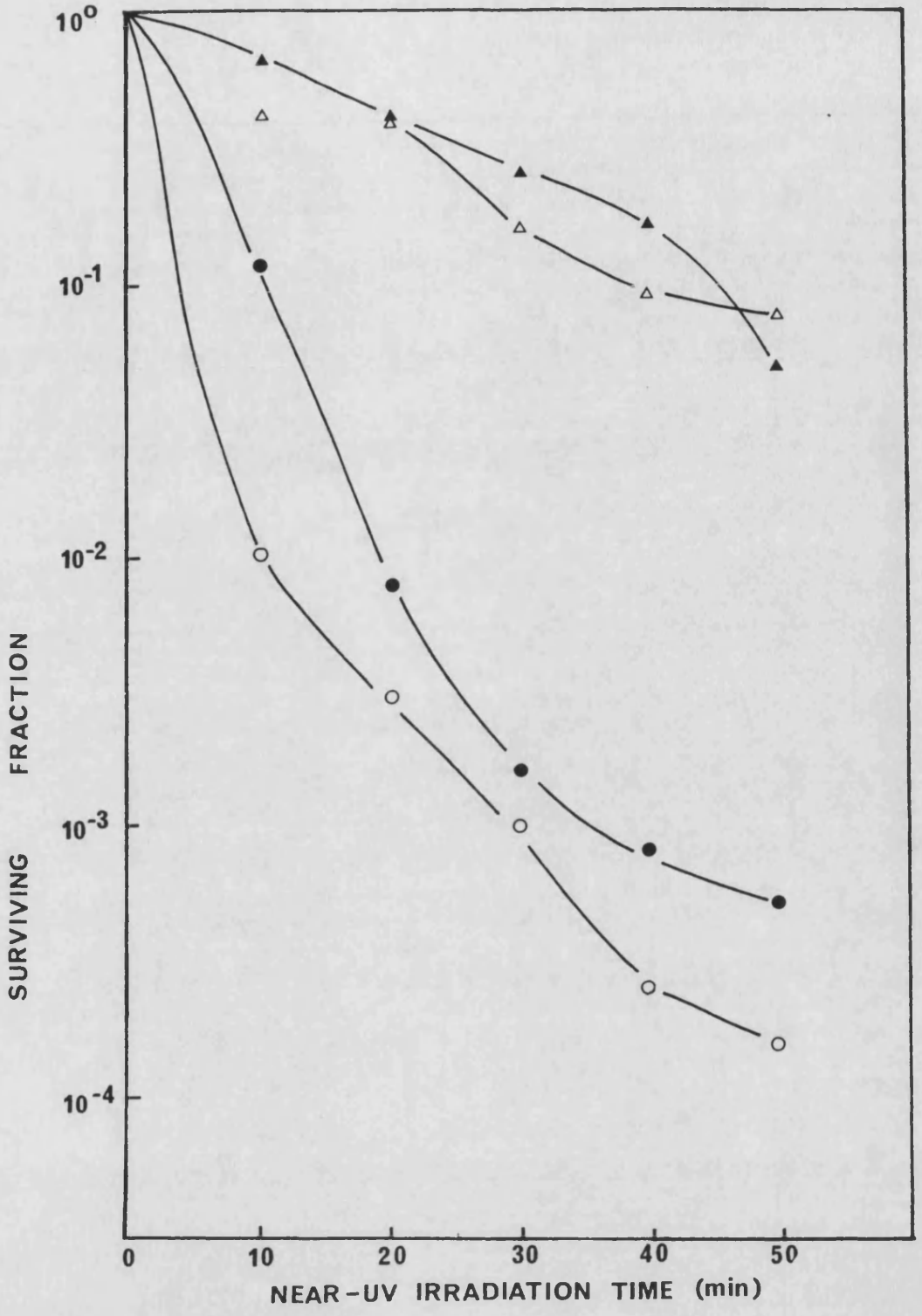

Figure 40
Survival curves for log phase E. coli K1060 incorporating linolenic acid, following broad-band near-UV irradiation. Viability assessed on YENB (○ ●) or high salt defined medium (△ ▲) in the presence (closed symbols) or absence (open symbols) of desferrioxamine.

(i) The propagation reactions of unsaturated fatty acid peroxidation will be within the hydrophobic interior of the cell membrane where the tested scavengers may be unable to reach.

(ii) Once the peroxidation process is proceeding, the major initiators may be alkoxy or peroxy radicals, formed from the decomposition of lipid hydroperoxides. $OH^{\bullet}$ will then not be necessary for the continuation of these reactions.

(iii) $OH^{\bullet}$ radicals have a high and indiscriminate reactivity, they therefore react near the site of their production, and will not diffuse away. With a half life of 10^{-10} seconds (Pryor, 1984) they would be expected to be of importance only during the irradiation period, and not during subsequent incubation unless iron-catalysed decomposition of H_2O_2 or reactions of this with $O_2^{\bullet-}$ provide for their continued production.

If then, intra-cellular reactions are of greater relevance, consideration must be given to the way in which cells normally protect themselves against peroxidative and other irradiation-induced damage. As discussed in the Introduction, the cell is well equipped with protective enzymes and antioxidants.

Glutathione (GSH) is a ubiquitous intracellular thiol, shown in mammalian cells to protect against mid- and near-UV radiations (Tyrrell and Pidoux, 1986). The synthesis of GSH is inhibited by growth of cells in Buthionine sulfoximine (BSO), which prevents λ-gluta yl cysteine synthetase activity (Griffiths et al., 1979).

6. THE EFFECT OF GLUTATHIONE-DEPLETION ON THE SENSITIVITY OF K1060 TO NUV IRRADIATION

Glutathione-Depletion Prior to Irradiation

A solution of BSO was prepared at 2.0 mM in M9. After sterilization by filtration, 10 ml were added to 100 ml of minimal growth media, providing a final concentration of 0.2 mM. E. coli K1060 was grown in this media prior to harvesting and irradiation. BSO supplementation did not affect the growth rate or concentration of cells at harvest. Following irradiation the cells were plated out onto YENB and minimal and high salt minimal media, for assessment of viability.

From Fig. 41a it can be seen that survival is only slightly reduced when assessed on YENB, more so on high salt minimal media when cells were grown prior to irradiation in BSO-supplemented media. (Data of further experiments is shown in the Appendix). When assessed on normal-salt minimal media, viability was not reduced, except after long exposure.

Following the removal of BSO during washing when harvesting and preparing the cells for irradiation, GSH synthesis would be permitted, perhaps even during the course of irradiation, certainly following growth on media following irradiation. This may provide for newly synthesized GSH to function in the detoxification of organic hydroperoxides by acting as the hydrogen donor for glutathione peroxidase (Tyrrell and Pidoux, 1986). In order to prevent de novo synthesis following plating out onto media after irradiation, the following experiments were performed.

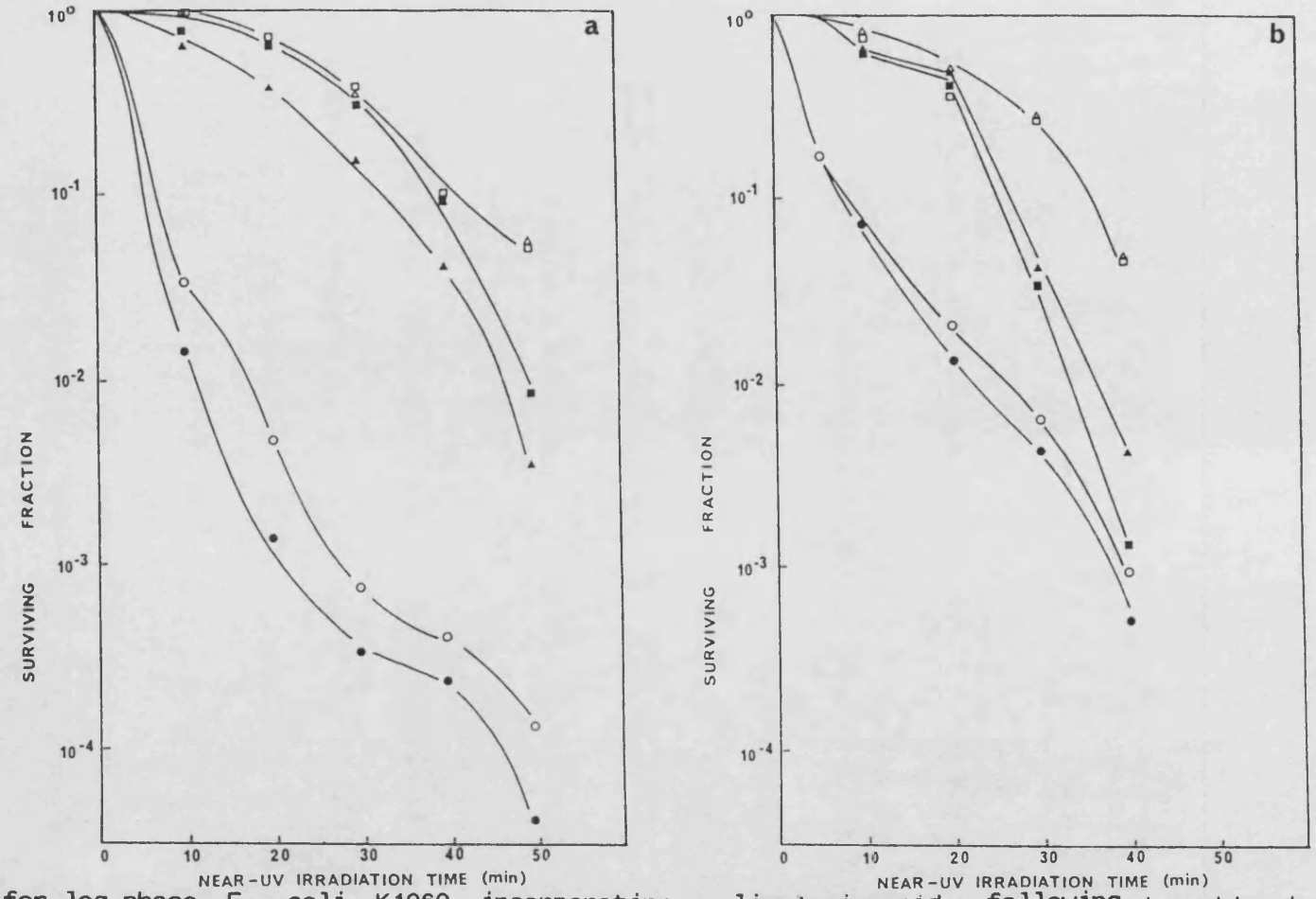

Figure 41
Survival curves for log phase E. coli K1060 incorporating linolenic acid, following broad-band near-UV irradiation. (a) Cells grown in the presence (closed symbols) or absence (open symbols) of BSO. (b) Cells grown with BSO and plated onto media with (closed symbols) or without (open symbols) BSO. Viability assessed on YENB (○ ●) defined (□ ■) or high salt defined medium (△ ▲).

The Effect of the Addition of BSO to the Viability Assessment Media

In addition to its incorporation into the pre-irradiation growth media, as described above, BSO was added to the media used for determining viability. A 0.5 mM solution in M9 was sterilized by filtration. 0.2 ml was added to each plate, spread over the surface and allowed to dry. Viability was assessed on these plates in addition to unsupplemented plates, following irradiation. Unirradiated cells showed no reduction in viability when plated on media supplemented with BSO.

Fig. 41b shows that viability is lower when assessed on BSO-supplemented defined and high-salt defined media. Previous survival curves demonstrate considerably higher viability following growth on defined or high salt defined media, relative to growth on YENB medium. Glutathione-depletion resulting from the continuing presence of BSO reduces such a survival advantage. Glutathione-related protection may therefore be of particular importance to the recovery of cells plated onto defined media following irradiation.

7. THE IMPLICATION OF SINGLET OXYGEN IN NEAR-UV RADIATION-INDUCED KILLING

As discussed in the Introduction, the photosensitized production of singlet oxygen following irradiation of endogenous sensitizers may contribute to cell killing. Evidence for the involvement of this reactive species may be obtained by comparison of the biological effects when irradiation is carried out in the presence of quenchers such as histidine or DABCO and in deuterium oxide.

The Effect of Irradiation in the Presence of 1-4-Diazobicyclo-octane (DABCO)

DABCO has been reported to protect transforming DNA from near-UV inactivation (Peak et al., 1981), and to quench approximately 50% of the singlet oxygen formed when present at 50 mM (Halliwell and Gutteridge, 1985). Ito (1978) reported it to be toxic to Saccharomyces cerevisiae, and it was shown here to be toxic to E. coli K1060 at the concentration used by Peak et al. (100 mM), but not at 10 mM.

DABCO was therefore used at 10 mM, dissolved in M9 and sterilized by membrane filtration, in the irradiation medium. Protection from near-UV irradiation was evident when viability was assessed on both YENB and defined media (Fig. 42). In view of the relatively unreactive nature of DABCO and the low concentration necessarily used here, these results would indicate some importance of active oxygen species. However, as with most singlet oxygen quenchers, DABCO is also a hydroxyl radical scavenger (with a rate constant of approximately 2.5×10^9 $M^{-1}s^{-1}$; Spikes and Swartz, 1978). DABCO may be considered to be active in the irradiation medium rather than intracellularly, being a large molecule.

The Effect of Irradiation in the Presence of Histidine

Histidine is used as a singlet oxygen quencher, reacting with a rate constant of 7.4×10^7 $M^{-1}s^{-1}$ (Lindig and Rodgers, 1981). Histidine was dissolved in M9 at a concentration of 0.1 M and used as the irradiation medium. Fig. 43 shows that survival of K1060 was enhanced when histidine was present during irradiation.

These two sets of results provide evidence for the involvement

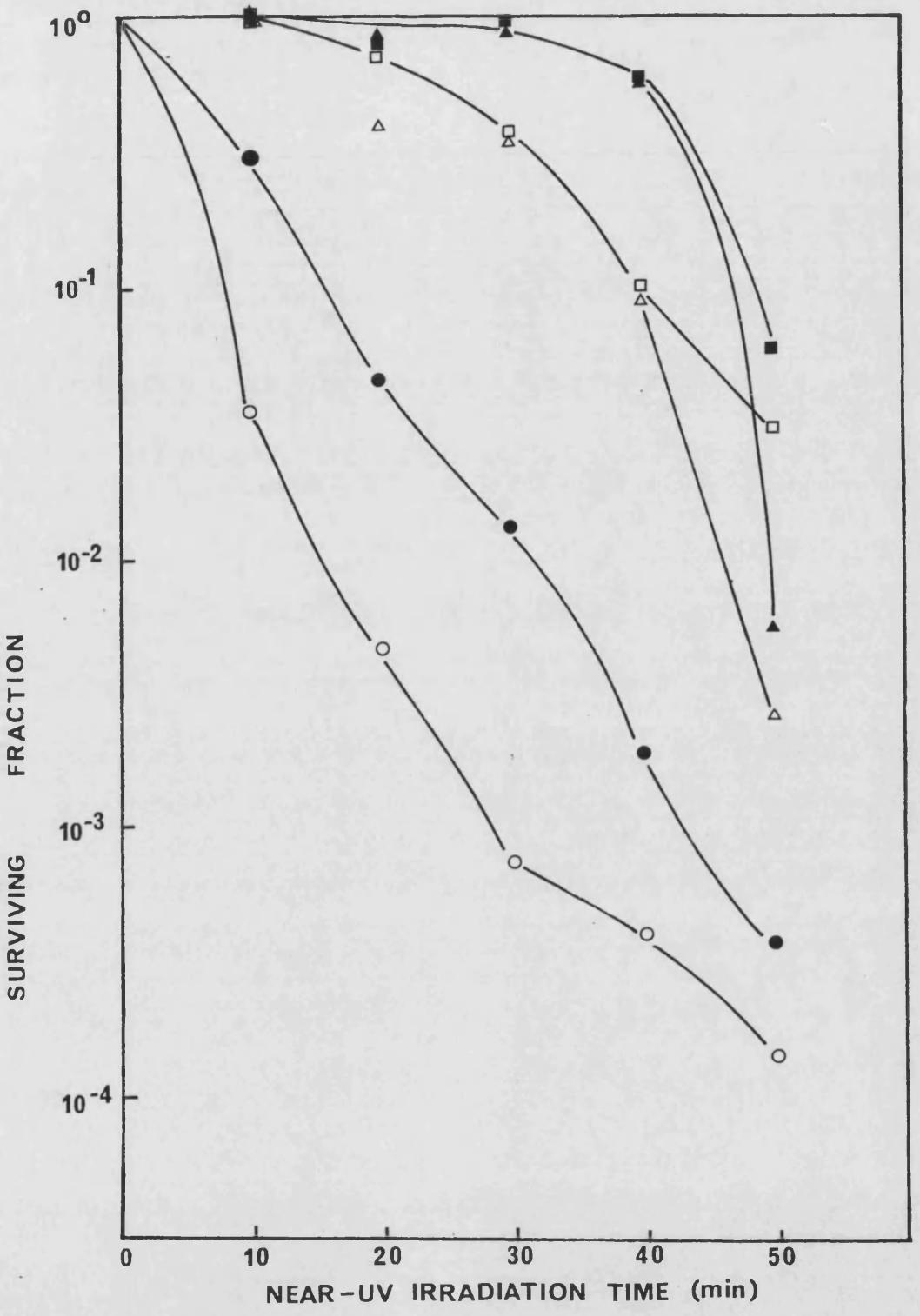

Figure 42
Survival curves for log phase E. coli K1060 incorporating linolenic acid, following broad-band near-UV irradiation in the presence (closed symbols) or absence (open symbols) of DABCO. Viability assessed on YENB (○ ●) defined (□ ■) or high salt defined medium (△ ▲).

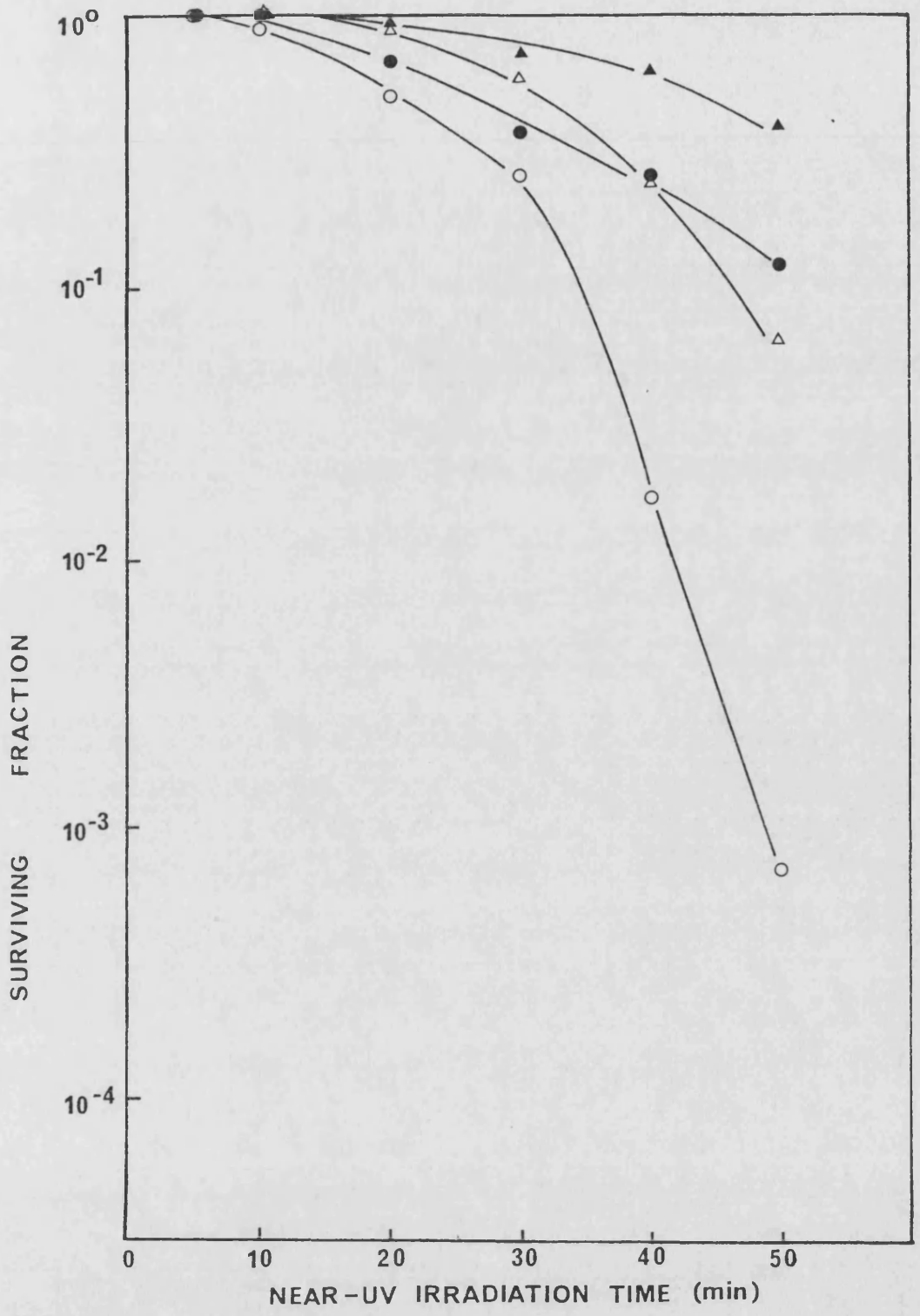

Figure 43
Survival curves for log phase E. coli K1060 incorporating linolenic acid, following broad-band near-UV irradiation in the presence (closed symbols) or absence (open symbols) of Histidine. Viability assessed on YENB (O ●) or high salt defined medium (△▲).

of singlet oxygen, or other active oxygen species during near-UV killing of E. coli K1060.

The Effect of NUV-Irradiation in Deuterium Oxide (D_2O)

The ratio of the decay rate of singlet oxygen in water to that in D_2O is quoted as being 1 : 10, 1 : 14 or 1 : 18 (Spikes and Swartz, 1978). In a situation where singlet oxygen is formed and reacts to cause cell damage, prolongation of its lifetime may result in further damage and perhaps a greater degree of killing.

K1060 cells were irradiated in 75% D_2O buffered with M9 salts to the normal concentration. The dramatic reduction in survival is demonstrated on all media, is shown in Fig. 44. D_2O was shown to be non-toxic to K1060 when they were incubated in its presence in the dark for the period of the experiments.

It is noticeable that, following NUV-irradiation in deuterated medium, viability is the same whether assessed on rich or defined media. This is in contrast to the higher level of survival normally exhibited on defined media.

The observed reduction in survival gives weight to the consideration of singlet oxygen as a mediator of NUV-induced cell killing. It is not, however, conclusive, since D_2O may also prolong the lifetime of superoxide anion, also a product of NUV irradiation (Cunningham et al., 1985).

The Effect of FUV-Irradiation in Deuterium Oxide

There is interest in the differences between NUV- and FUV-radiations as previously described. Therefore the above experiment was performed using 254 nm radiation in place of the broad-band

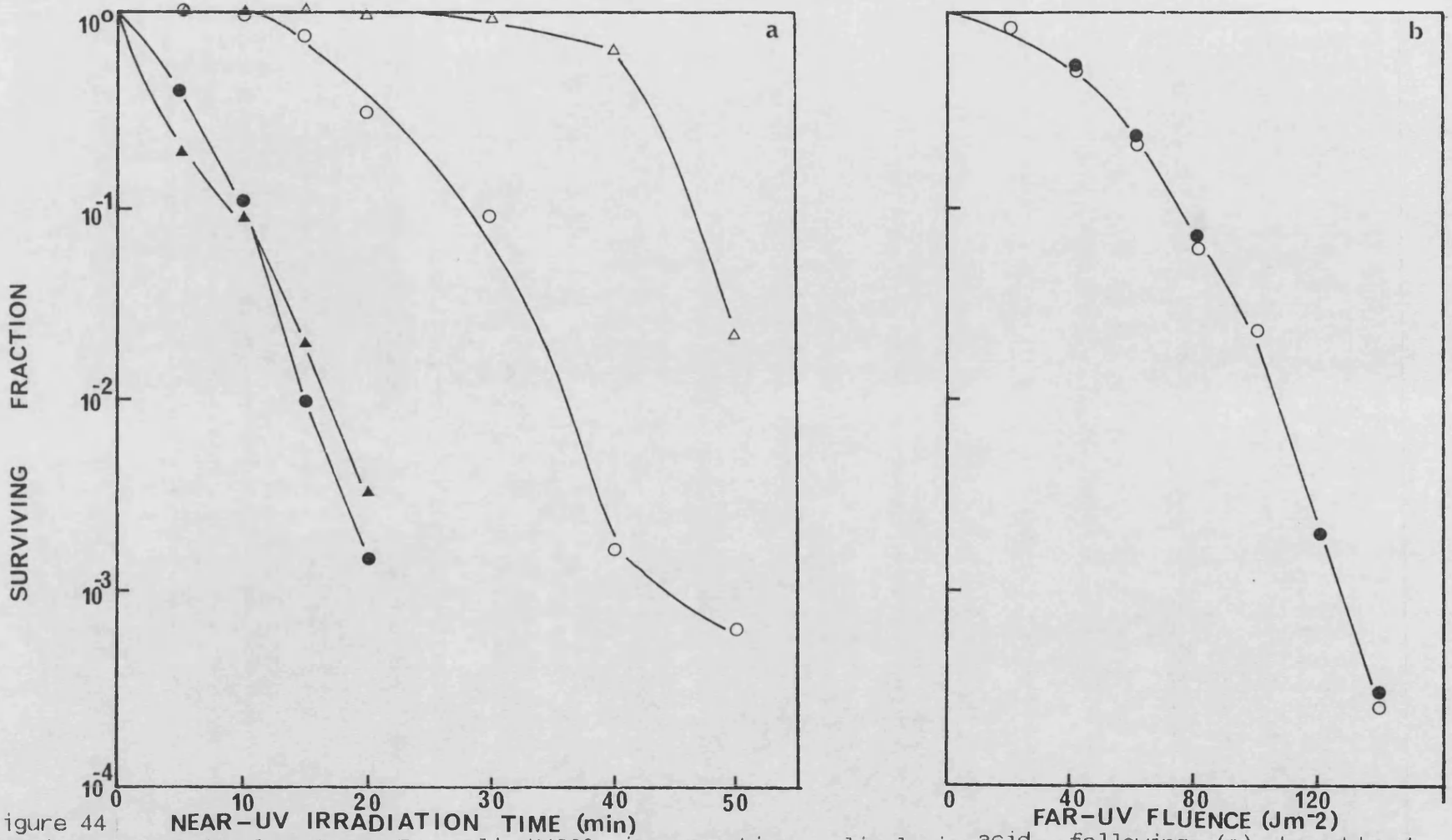

Figure 44 Survival curves for log phase E. coli K1060 incorporating linolenic acid, following (a) broad-band near-UV (b) far-UV irradiation in the presence (closed symbols) or absence (open symbols) of Deuterium oxide. Viability assessed on YENB (O ●) or high salt defined medium (△▲).

source, using fluences which resulted in the same degree of killing. Fig. 44b shows that no D_2O effect was observed in such experiments at this wavelength. This would be expected in view of the predominance of DNA damage during 254 nm irradiation.

SUMMARY OF SURVIVAL RESULTS

The sensitivity of exponential phase, but not stationary phase, E. coli K1060 cells to near-UV irradiation has been shown to be correlated with the unsaturation of membrane phospholipids. The survival of far-UV-irradiated cells is not dependent upon fatty acid composition.

Evidence for the involvement of oxygen, during both irradiation and post-irradiation incubation has been presented, since the exclusion of oxygen results in an increase in survival. Vitamin E, but not Trolox-C, offers a limited degree of protection when provided as a pre-irradiation growth supplement, while the depletion of cellular glutathione by growth in BSO-medium, reduces survival. Both catalase and superoxide dismutase, when added to the plating media, result in greatly increased survival, while the iron-chelator desferrioxamine offers limited protection.

The involvement of reactive oxygen species, particularly singlet oxygen is implicated by the reduction in survival following irradiation in D_2O, and an increase in survival when irradiated in DABCO and histidine.

NEAR-UV IRRADIATION-INDUCED LIPID PEROXIDATION IN E. COLI K1060

The sensitivity of exponentially growing K1060 cells to NUV radiation has been shown to increase with increasing unsaturation of the membrane phospholipids, using both 18-carbon fatty acids (in the previous section of this thesis) and 20-carbon fatty acids (Klamen and Tuveson, 1982). Survival following NUV irradiation has been demonstrated to be enhanced when active oxygen quenchers are present, while reduced when irradiation takes place in a deuterated medium. Results of these experiments indicate that lipid peroxidation should be investigated as a mechanism for NUV-induced lethality.

The series of experiments described in this section were designed to determine whether lipid peroxidation could be detected in irradiated K1060 cells, and to assess whether factors affecting survival also affected such peroxidation.

The Measurement of Lipid Peroxidation in E. coli K1060

The method used for measurement of lipid peroxidation in E. coli was the method for the assay of total hydroperoxides described in the methodology. The method depends upon the catalyzed reaction between hydroperoxides and potassium iodide, where iodine is released. Its subsequent reaction with soluble starch forms a purple colour, the absorbance of which is measured spectrophotometrically. The method was chosen instead of the often used malondialdehyde (MDA), otherwise known as the Thiobarbituric acid (TBA), method for several reasons:

1. The production of MDA depends upon the presence of at least 3 unsaturated bonds in the fatty acid (Dahle et al., 1962). Comparisons were, however, required here between K1060 cells incorporating oleic (18:1) or linoleic (18:2) acid in addition to those incorporating linolenic acid (18:3). The chosen method determines all hydroperoxides, regardless of the level of unsaturation of the fatty acids used.
2. Substances which react, under test conditions, with TBA are varied (Gutteridge, 1981) and such substances may be present in the cell suspensions tested here; for example free-radical-damaged amino acids and carbohydrates have been shown to give positive TBA-reactive products (Gutteridge, 1981).
3. The determination of lipid peroxides by the TBA method depends upon the decomposition of hydroperoxides present to their secondary products during the heating procedure required. This has been shown to be incomplete (Asakawa and Matsushita, 1979).

The method used here is sensitive and reasonably specific for hydroperoxides (Asakawa and Matsushita, 1980). Results are expressed as a Peroxide Value (PV) in meq kg^{-1} which is calculated with reference to a potassium iodate standard run in parallel with the tests, as described in the Methodology.

Additional Methodology Applicable to Measurements with Whole Cells

In order to achieve suitable measurements, K1060 cells were irradiated at a concentration of 10^9 ml^{-1}. The hydroperoxide assay was always performed immediately after irradiation. Before taking

optical density measurements the preparation was centrifuged, immediately after the addition of the starch reagent, (MSE bench centrifuge, 4000 rpm for 10 mins). The coloured supernatant was used for measurements, the cell pellet being discarded. In all cases the PV was calculated with reference to an unirradiated control cell suspension, thereby giving an indication that an increase in colour observed in the irradiated samples was a result of the irradiation. The PV was then expressed as a PV per 10^6 cells.

1. NUV-RADIATION-INDUCED LIPID PEROXIDATION AND THE EFFECT OF THE DEGREE OF UNSATURATION OF THE FATTY ACID INCORPORATED BY K1060

Figure 45 shows that hydroperoxides were detectable in cells incorporating linolenic acid after 60 minutes exposure to broad-band NUV radiation. Higher fluences result in peroxidation in cells incorporating oleic or linoleic acid. Peroxidation then increases with increasing fluence. Following an irradiation period of 195 minutes the PV of cells grown on linoleic acid is greater than those grown on oleic acid by a factor of 2.7, for linolenic acid-grown cells the factor is 4.1.

The results clearly show that peroxidation of membrane lipids occurs during NUV-irradiation, and that the degree of peroxidation is related to the degree of unsaturation of the fatty acids incorporated, increasing with increasing fluence.

No peroxidation was detectable when cell suspensions were bubbled with oxygen-free nitrogen, instead of air, throughout irradiation.

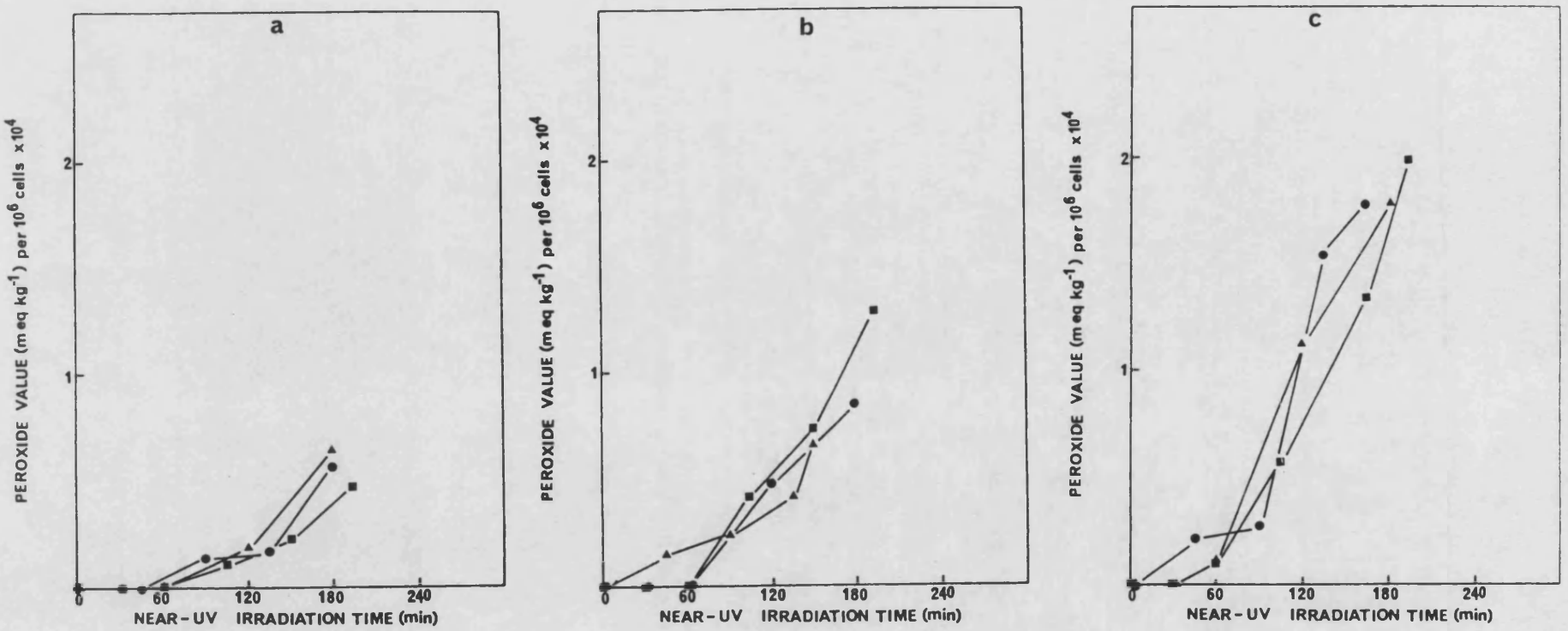

Figure 45 The Peroxide Value (PV) of E.coli K1060 cells following broad-band near-UV irradiation. Cells incorporating (a) oleic (b) linoleic (c) linolenic acid. Different symbols represent replicate experiments.

2. POST-IRRADIATION LEVELS OF HYDROPEROXIDES IN K1060 CELLS

Lipid peroxidation, once initiated, may proceed by free radical reactions until a termination reaction halts the process. Consideration was therefore given to the possibility that peroxidation may continue, after irradiation.

Cell suspensions were irradiated as previously described. The level of hydroperoxides was determined at the end of irradiation and for up to 3 hours subsequently. During this period the cell suspensions were kept in the dark, under aerated conditions, in the same M9 in which irradiation took place, thus maintaining the cells in a non-dividing state. However, as Fig. 46 shows, no significant further peroxidation took place in the post-irradiation period, neither do the cells reduce the hydroperoxides present.

3. THE EFFECT OF GLUTATHIONE-DEPLETION ON LIPID PEROXIDATION FOLLOWING NUV IRRADIATION OF K1060

Reference to Fig. 41 shows that K1060 grown in media supplemented with BSO, known to inhibit the synthesis of glutathione, is more sensitive to NUV radiation than untreated cells. One function of cellular glutathione is to detoxify organic hydroperoxides by acting as the hydrogen donor for glutathione peroxidase (Tyrrell and Pidoux, 1986). If this process takes place during irradiation, it may be expected that the detectable level of hydroperoxides would be higher in glutathione-depleted cells.

This was tested by growing K1060 on media supplemented with 0.2 mM BSO prior to harvest and irradiation. Comparisons were made with untreated cells grown, harvested and irradiated in parallel.

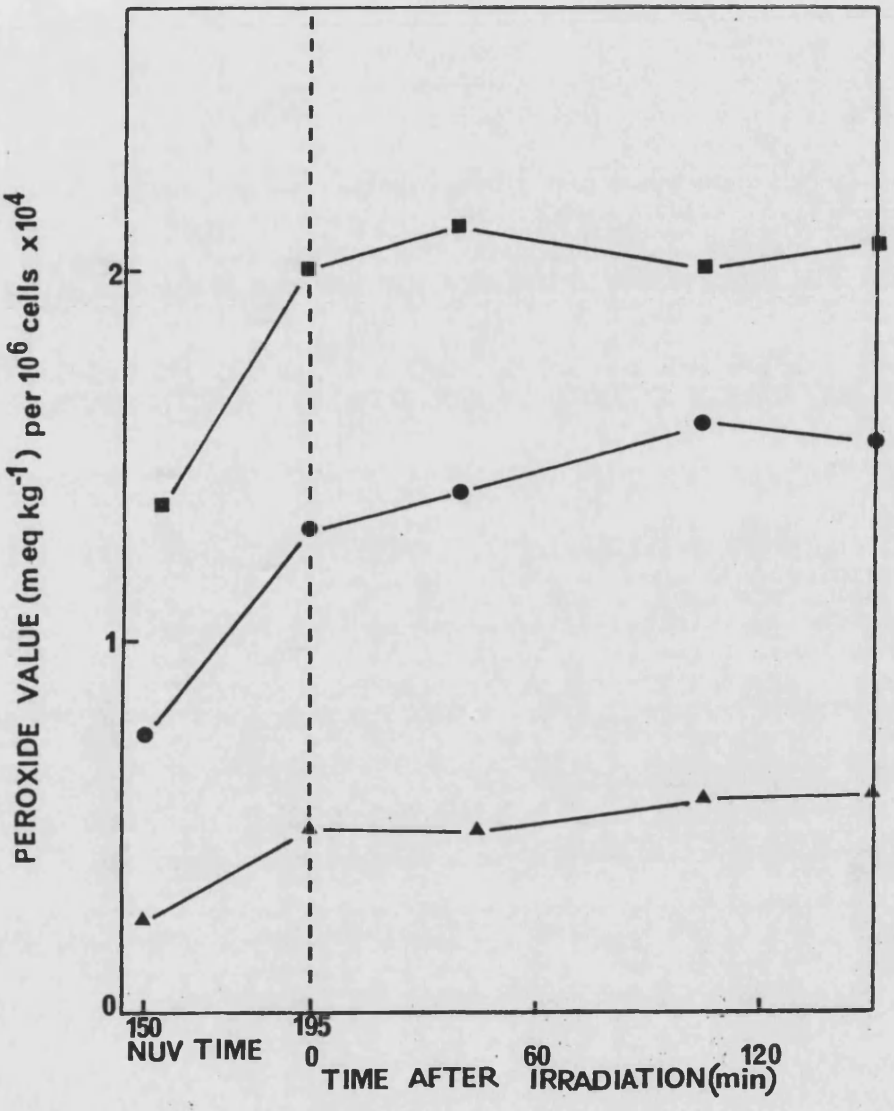

Figure 46

The Peroxide Value (PV) of E.coli K1060 cells in the post-irradiation period following broad-band near-UV irradiation. Cells incorporating (a) oleic (b) linoleic (c) linolenic acid.

Fig. 47a shows that after each fluence the BSO-treated cells exhibit a higher level of peroxidation than untreated cells.

4. THE EFFECT OF IRRADIATION IN THE PRESENCE OF DABCO ON LIPID PEROXIDATION

When E. coli K1060 is irradiated in the presence of DABCO, a free radical and singlet oxygen scavenger, viability is increased (Fig. 42). It would be expected that DABCO would also reduce the rate of lipid peroxidation by virtue of this scavenging ability.

Harvested linolenate-grown K1060 were resuspended in either M9, or in 0.01 M DABCO, and lipid peroxidation was measured, following broad-band NUV irradiation of the two sets in parallel. There was a substantial decrease in the detectable level of hydroperoxides, as shown in Fig. 47d.

5. THE EFFECT OF IRRADIATION IN THE PRESENCE OF HISTIDINE ON LIPID PEROXIDATION

Histidine, a singlet oxygen quencher, when present in the irradiation medium, results in an increase in survival (Fig. 43). Its effect on lipid peroxidation was determined by resuspending K1060 cells in either 0.1 M histidine or in M9. Lipid peroxidation was measured following irradiation. There was a reduction in the level of hydroperoxides (Fig. 47c) when histidine was present.

6. THE EFFECT OF IRRADIATION IN D_2O ON LIPID PEROXIDATION

Lipid peroxidation was measured in K1060 cells which had been irradiated in 75% D_2O under conditions which resulted in a decrease

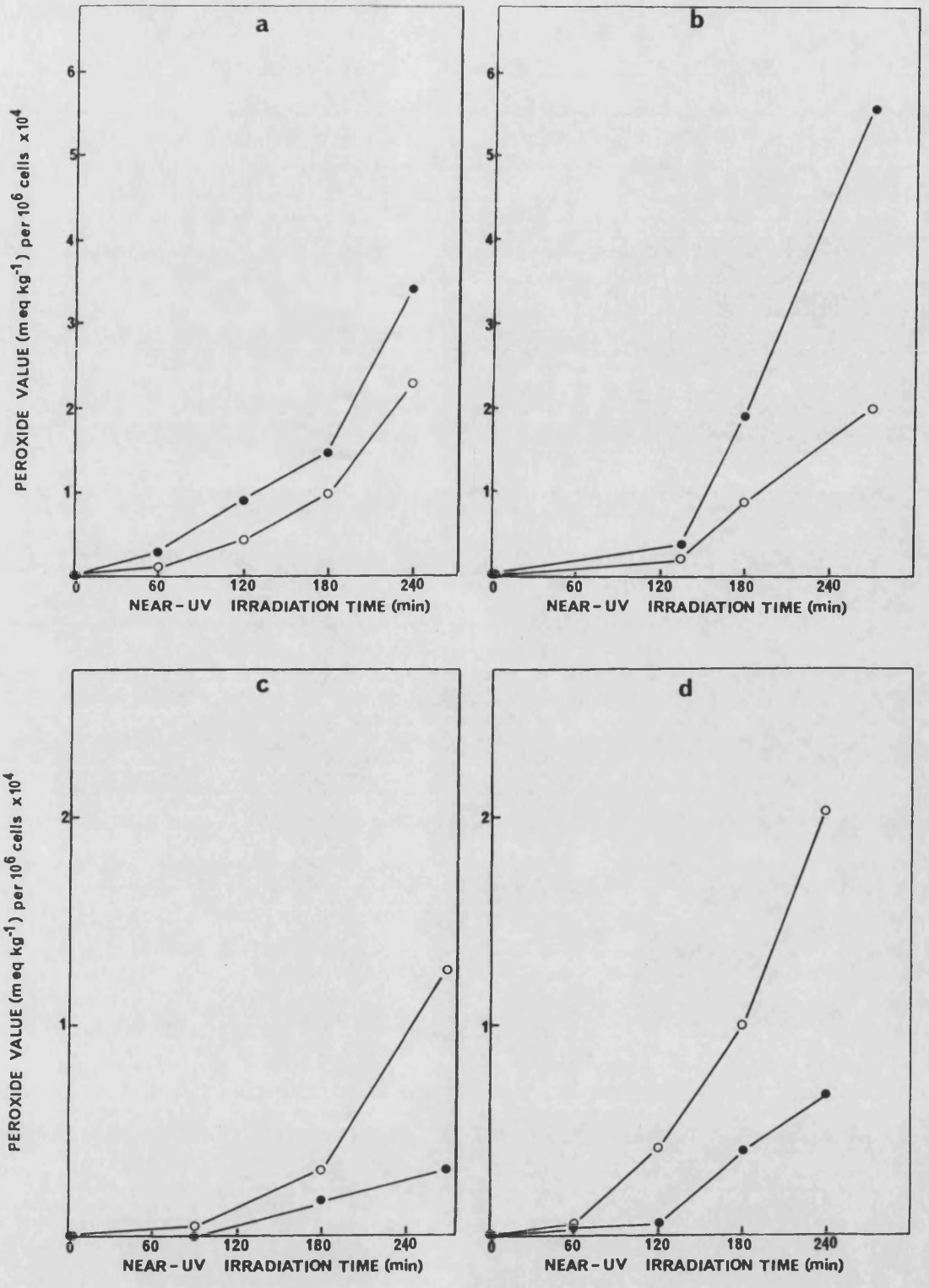

Figure 47

The Peroxide Value (PV) of E. coli K1060 cells following broad-band near-UV irradiation. (a) Cells grown prior to irradiation with (●) or without (○) BSO. (b) Cells irradiated in the presence (closed symbols) or absence (open symbols) of D_2O. (c) Cells irradiated in the presence (closed symbols) or absence (open symbols) of histidine. (d) Cells irradiated in the presence (closed symbols) or absence (open symbols) of DABCO.

in survival (Fig. 44). Clearly, lipid peroxidation is increased when irradiation takes place in deuterated medium, by a factor of up to 2.6 after 180 minutes irradiation (Fig. 47d).

SUMMARY OF LIPID PEROXIDATION RESULTS

Lipid peroxidation has been demonstrated in irradiated suspensions of E. coli K1060 cells, and has been shown to depend upon the unsaturation of the fatty acids incorporated into the bacterial membrane. Since no residual pool of fatty acid remains in the cells of such auxotrophs (Nunn and Cronan, 1974) any hydroperoxides measured must be associated with membrane phospholipids.

Peroxidation is increased in cells irradiated following glutathione-depletion, and in deuterated media. Histidine and DABCO reduce the level of hydroperoxides formed during irradiation. The results demonstrate that NUV irradiation-induced lipid peroxidation may, in part, be due to singlet oxygen attack, although other reactive species may be involved. The cells' natural glutathione content is of evident importance in dealing with the peroxidative process.

However, the question of the relevance to the cell of this peroxidation must be considered. The manipulation of the cell membrane to incorporate a polyunsaturated fatty acid clearly results in peroxidation at relatively low fluences, whereas in the cells incorporating oleic acid, simulating the natural state of unsaturation of the membrane, hydroperoxide levels remain fairly low even after considerable exposure. It must be borne in mind that

very low levels of hydroperoxides will not be detectable by the method, even though slight peroxidative damage may impair membrane functions or integrity to some degree. As discussed elsewhere, a measurement of events occurring immediately following irradiation does not necessarily relate to viability as assessed by colony forming ability. A cell may be alive and functioning, though suffering peroxidative or membrane damage, but fail to divide due to DNA malfunction. Alternatively, at higher fluences the membrane may be grossly damaged, leaking or even causing cell lysis. The leakage of rubidium from cells is an accepted method for demonstrating membrane damage and an investigation of this is found in the following section.

NEAR-UV-INDUCED MEMBRANE DAMAGE IN E. COLI K1060 AS DEMONSTRATED BY RUBIDIUM LEAKAGE

The leakage of rubidium ($^{86}Rb^+$), a potassium analogue, has been used to demonstrate near-UV induced membrane damage in stationary-phase cells of E. coli strains (SR 385, AB 1157, B/r), (Kelland, 1984; Kelland et al., 1984). Leakage of $^{86}Rb^+$ from both near- and far- UV irradiated E. coli cells, incorporating each of the three fatty acids, has been investigated and is described here.

Additional Methodology

(i) K^+-free M9 salts solution

M9 salts solution was prepared replacing the K^+ content mole for mole with Na^+ as NaH_2PO_4. M9B concentrate was therefore prepared with NaH_2PO_4 at 49.2 g/l replacing KH_2PO_4 at 37.5 g/l. This concentrate was sterilized and used as described for normal M9B. All media and dilutions requiring M9 were made with K^+-free M9, to ensure maximum uptake of rubidium by the cells.

(ii) KCl Solution

A 0.4 M solution was prepared from 2.982 g KCl (BDH Ltd.) dissolved in 100 ml distilled water before autoclaving at 121°C for 15 min.

(iii) $CaCl_2$ Solution

A 1 mM solution was prepared by dissolving 111 mg $CaCl_2$

fused, granular (BDH Ltd.) in 100 ml distilled water, and autoclaved at 121°C for 25 min.

Radioactive Labelling of E. coli K1060

Minimal growth medium was prepared as shown in the Table below:

Ingredient	**Quantity (ml)**
glycerol 40%	0.8
casamino acids 10%	0.4
fatty acid 1% in 10% Brij 58	0.4
thiamine 1%	0.4
water*	15.54
M9A	0.4
M9B (K^+ free)	1.6
KCl 0.4 M	0.2
$CaCl_2$ 1 mM	0.2
$^{86}RbCl$*	0.06

* The volume of $^{86}RbCl$ added was sufficient to give a concentration of 0.111 MBq ml^{-1}. The $^{86}RbCl$ was obtained as a sterile aqueous solution of radioactive concentration 37.0 MBq ml^{-1}, from Amersham International plc, specific activity 37-29 MBq mg^{-1} rubidium. As $^{86}RbCl$ has a radioactivity half-life of 18.66 days, the volume of $^{86}RbCl$ added was adjusted by calculating the amount of decay from the date when the activity was determined, so that approximately 0.111 MBq ml^{-1} was always added. A corresponding adjustment to the volume of water was made, to give a final volume of 20 ml.

Cultures were grown by the inoculation of 10 ml volumes of the media described above, and were incubated for 16 hours. A 0.1 ml volume of this culture was used to inoculate a further 10 ml volume, and grown to mid-log phase. When harvested, the cells were resuspended in K^+-free M9 at a concentration of 1 x 10^8 cells ml^{-1}, in order to give reasonable scintillation counts. It was felt necessary to assess whether this concentration of cells, and growth in a low K^+ medium in the presence of $^{86}RbCl$ affected sensitivity to BLB radiation, since potassium is known to be required for the activation of some enzymes (Epstein and Davies, 1970). Fig. 48 shows that the sensitivity of the organism grown on all three fatty acids is similar in normal or low K^+ media, (compare with Figs. A4, A5, and A6).

The Measurement of $^{86}Rb^+$ leakage from cells

Scintillation Counting

Rubidium leaked from the cells was measured by liquid scintillation counting. The method involves placing the sample containing the radioactive label in an appropriate medium, the scintillation cocktail, which converts radioactive energy into a pulse of light energy. This pulse is detected by means of a synchronized photocathode and is converted to an electrical pulse by a photomultiplier. During liquid scintillation counting the following energy steps occur between the radioactive sample (Rs) and the constituents of the scintillation cocktail:

$$Rs \xrightarrow{1} \text{solvent} \xrightarrow{2} \text{solute} \xrightarrow{3} \text{photocathode}$$

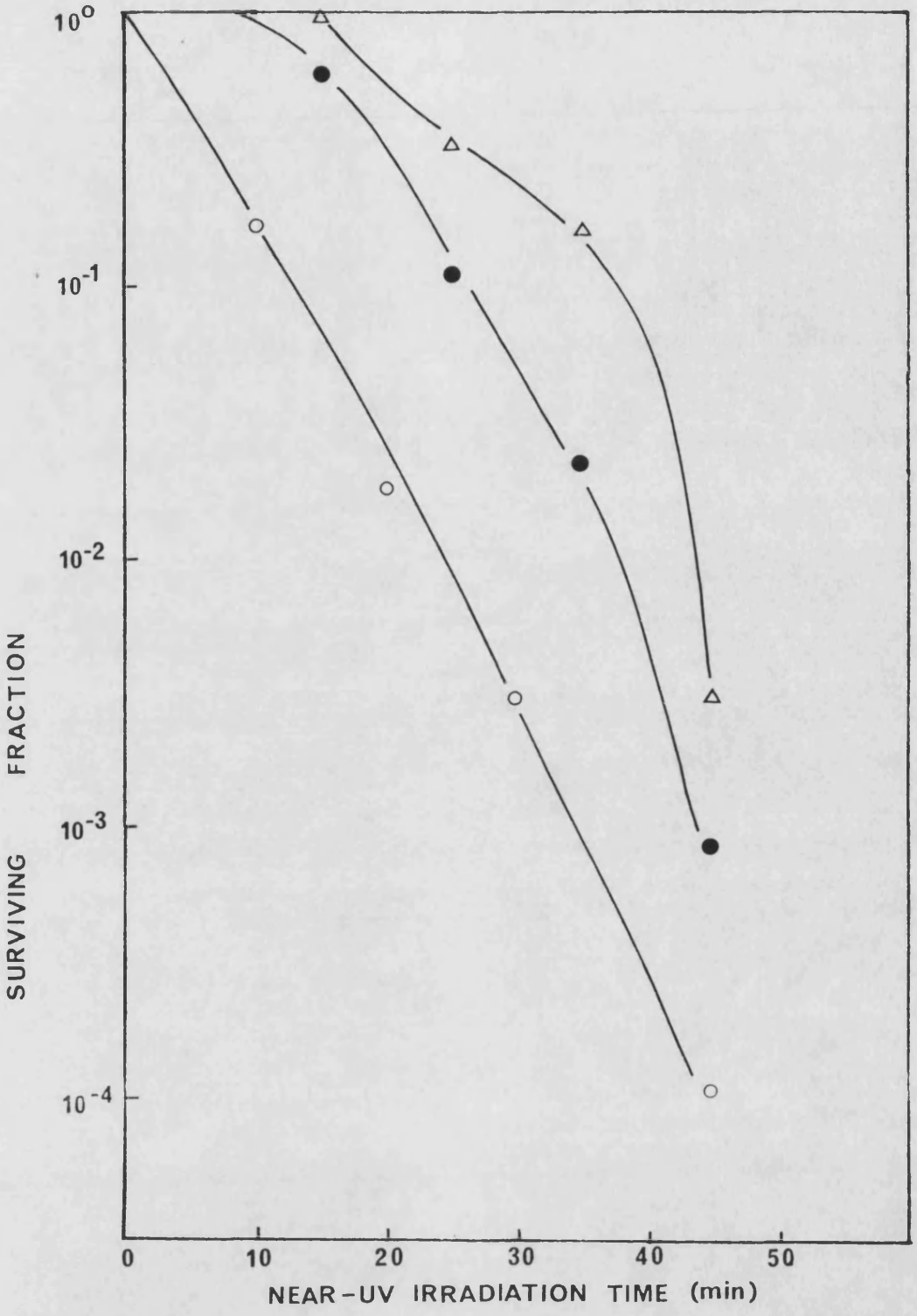

Figure 48
Survival curves of E. coli K1060 following broad-band near- UV irradiation after growth in low- potassium- medium. Cells incorporating (△) oleic (●) linoleic (○) linolenic acid.

At each of these energy transfer steps there is a probability that an incomplete energy transfer will occur, due to the nature of the scintillation cocktail. Interference may arise from photon, chemical or colour quenching. Therefore the extent of this quenching affects the ability of the photocathode to detect the light pulses. The quantification of the radioactivity is expressed in counts per minute (cpm), this being a characteristic of a particular liquid scintillation counter and scintillation cocktail. To convert cpm to an absolute quantity of radioactivity, a quench curve must be constructed so that the efficiency of the counting process may be estimated, thus taking into account interferences in energy transfer. From the efficiency measurement the absolute value of disintegrations per minute (dpm) may be determined. Therefore dpm = cpm x efficiency.

To construct a quench curve the external standard channels ratio method was used, being most convenient for the scintillation counter used. (1215 Rackbeta, LKB Wallac, Turku, Finland). The scintillant used was xylene-based Aqua Luma (Lumac Systems, AG, Basle, Switzerland). The method involves adding 4 ml of Aqua Luma to a series of 7 plastic mini-vials each containing a capsule of known radioactivity. To each sample, 0.2 ml distilled water was added to simulate the emulsion system found under experimental conditions. Increasing amounts from 0 to 40 µl of carbon tetrachloride were added to provide quenching. The samples were then loaded onto the counter, which had been programmed to count the samples and automatically construct a quench curve. The quench curve is included in Appendix 5, Fig. A14. The quench curve is

stored in the counter's memory and dpms for all samples were then calculated automatically. Samples were placed at 4° in the counter immediately after preparation in order to minimise absorption of xylene which, by reducing the effective volume of scintillant, produces a continuous drift in the external standard ratio.

Preparation of Samples for Scintillation Counting

The harvested cells, resuspended in K^+-free M9 were divided into two batches. One was used as an unirradiated control and was kept in a Pyrex test tube, bubbled with air in parallel with the irradiated samples, the second batch was irradiated under standard conditions. At each sample time 0.7 ml was removed from both the control and the irradiated suspensions, and centrifuged for 3 min using a MSE Microcentaur centrifuge and Ependorf polypropylene tubes. Duplicate 0.2 ml samples were added to 4 ml of aqua luma, for scintillation counting. Leakage was then calculated as dpm per cell. In addition to a sample taken as above before irradiation, a total cell count was taken by the direct counting of 0.2 ml of uncentrifuged suspension in 4 ml scintillant, as a measure of the $^{86}Rb^+$ taken in by the cells.

1. THE EFFECT OF MEMBRANE FATTY ACID UNSATURATION ON THE LEAKAGE OF ^{86}Rb FROM IRRADIATED LOG-PHASE K1060 CELLS

Cultures of K1060 cells incorporating the three fatty acids were irradiated under standard conditions. From Fig. 49 showing dpm with time, it is clear that although the control cells leak $^{86}Rb^{+}$ steadily over the period of the experiment, the irradiated cells leak to a greater extent. It is apparent that with increasing unsaturation of the incorporated fatty acid not only do the cells leak more $^{86}Rb^{+}$ after each exposure time, but the time of irradiation needed to cause the excess leakage becomes shorter.

In order to express the leakage from the irradiated cells relative to that from control cells, the results were also plotted showing the ratio of dpm irradiated cells to dpm control cells, as shown in Fig. 50. however, where counts are low, slight variation in counts can be seen to distort the results which are less clear at lower fluences.

2. RUBIDIUM LEAKAGE FROM STATIONARY PHASE K1060 CELLS FOLLOWING NEAR-UV IRRADIATION

E. coli K1060 cultures were grown to stationary phase in the labelled medium. $^{86}Rb^{+}$ was measured following irradiation as described. It is evident from Figs. 51 and 52, that cells in this growth phase also leak $^{86}Rb^{+}$ at a higher rate than control, unirradiated cells. However, stationary phase cells leak rapidly, within the first 30 minutes of exposure, and thereafter leak at a steady rate. This is in contrast to cells harvested and irradiated

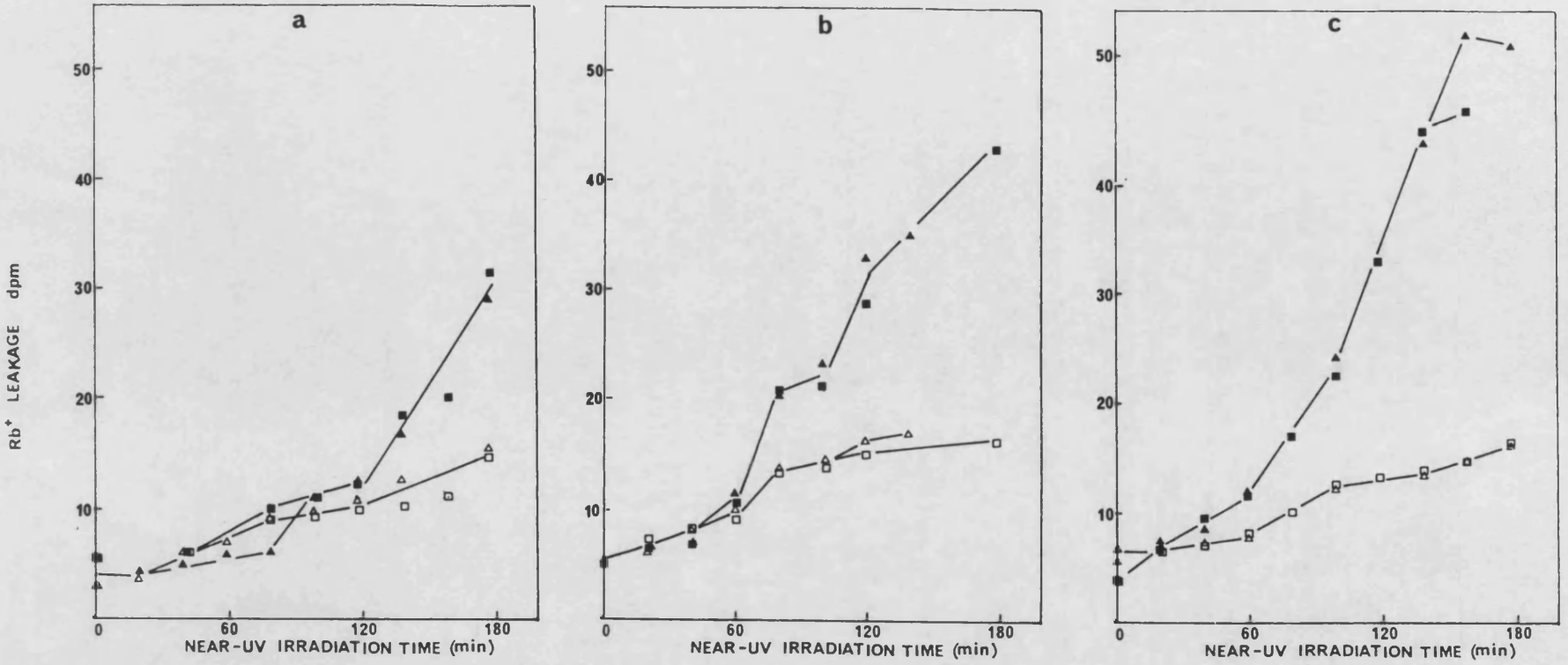

Figure 49 The leakage of $^{86}Rb^{+}$ from log phase E. coli K1060 following broad-band near-UV irradiation (closed symbols) or unirradiated controls (open symbols). Cells incorporating (a) oleic (b) linoleic (c) linolenic acid. Alternate symbols represent replicate experiments. Leakage expressed as d.p.m. per cell $x10^{6}$.

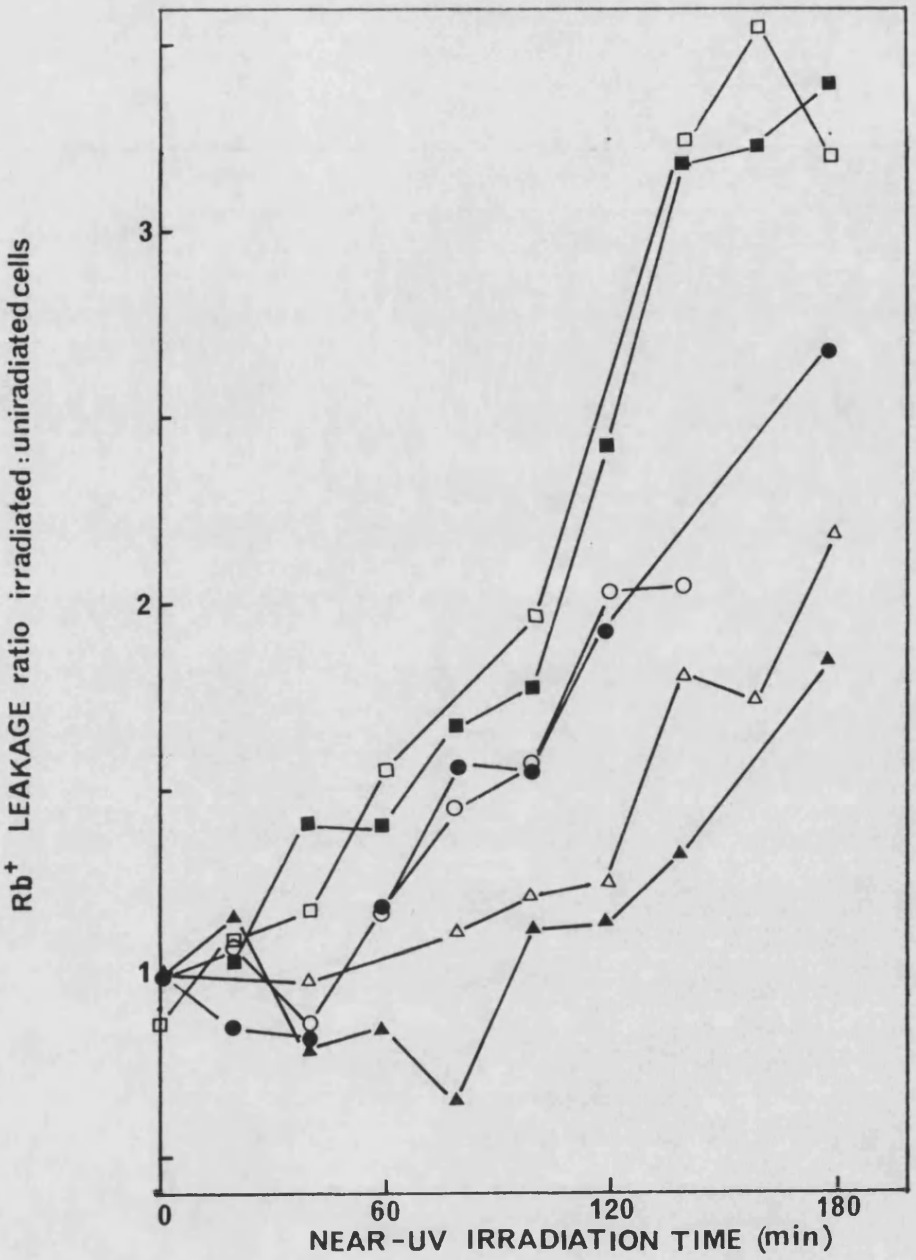

Figure 50
The leakage of $^{86}Rb^{+}$ from log phase E. coli K1060 following broad-band near-UV irradiation (closed symbols) or unirradiated controls (open symbols). Cells incorporating (△▲) oleic, (○●) linoleic, (□■) linolenic acid. Leakage expressed as ratio d.p.m. irradiated cells : d.p.m. unirradiated cells. (Data from figure 49).

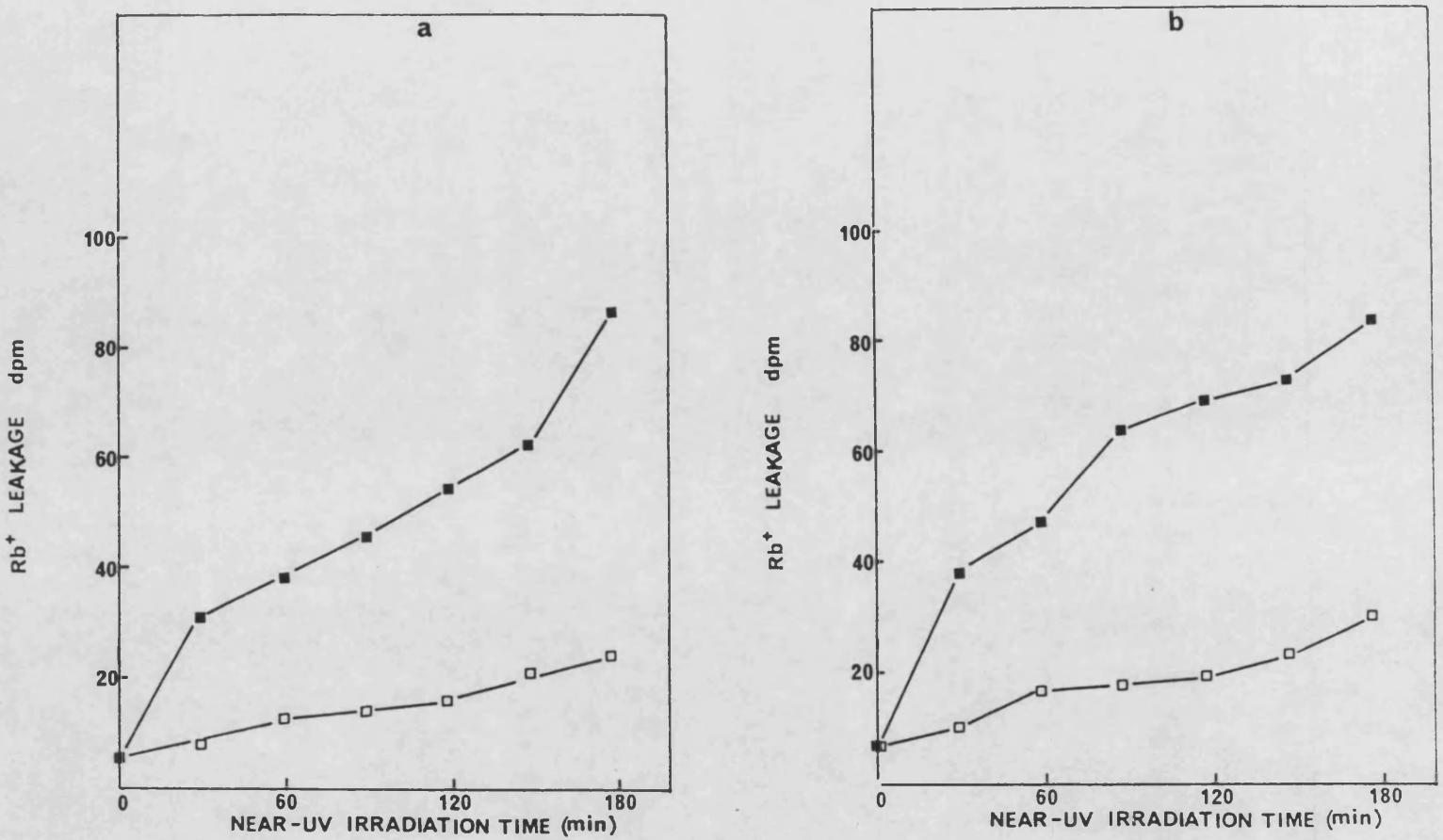

Figure 51 The leakage of $^{86}Rb^{+}$ from stationary phase E. coli K1060 following broad-band near-UV irradiation (closed symbols) or unirradiated controls (open symbols). Cells incorporating (a) oleic or (b) linolenic acid. Alternate symbols represent replicate experiments. Leakage expressed as d.p.m. per cell x 10^{6}.

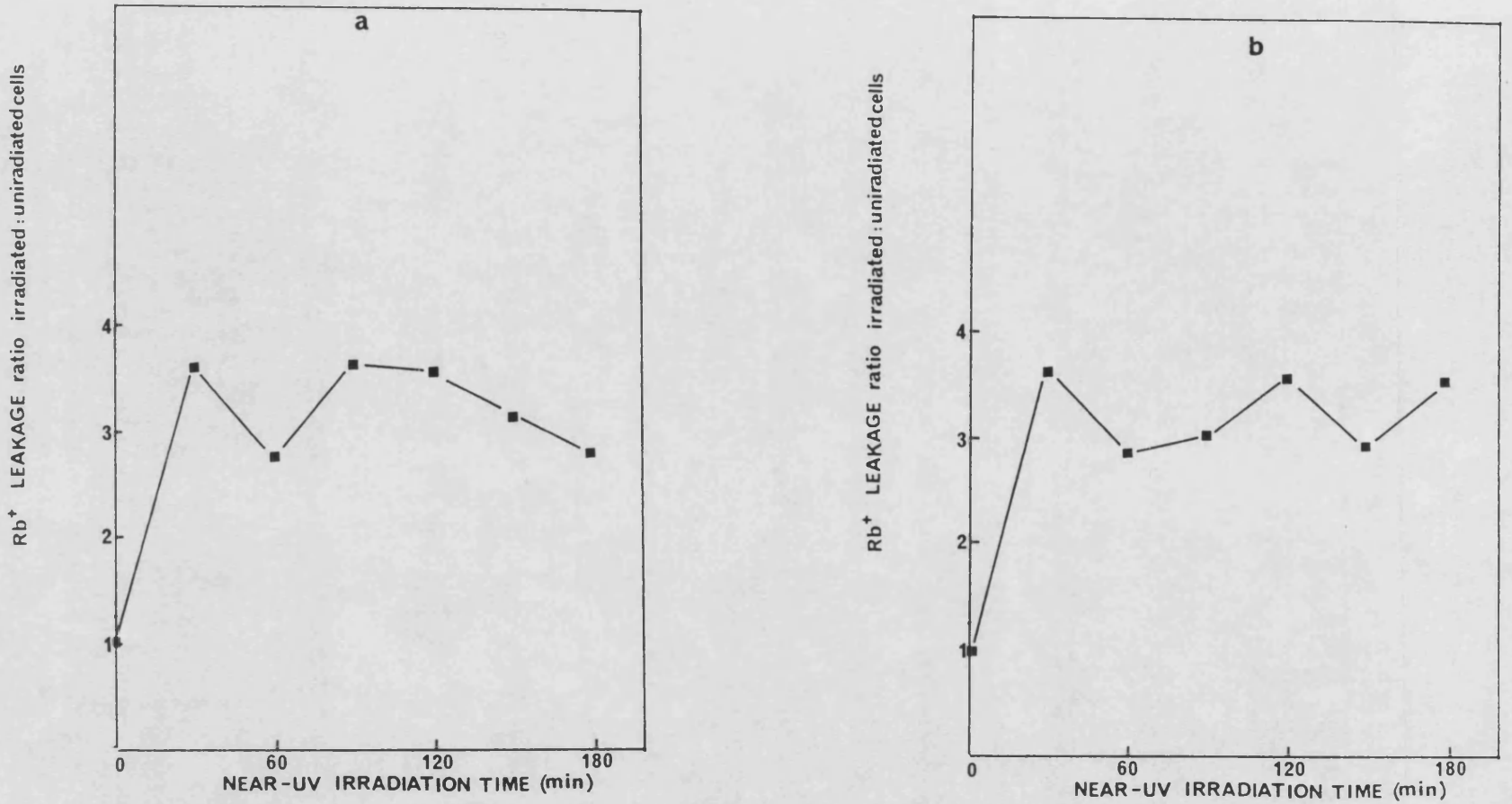

Figure 52 The leakage of $^{86}Rb^{+}$ from stationary phase E. coli K1060 following broad-band near-UV irradiation (closed symbols) or unirradiated controls (open symbols). Cells incorporating (a) oleic,or (b) linolenic acid. Leakage expressed as ratio d.p.m. irradiated cells : d.p.m. unirradiated cells. (Data from figure 51).

in the log phase of growth, where a lag period is apparent before leakage is demonstrable, (Fig. 49). Also in contrast is the similar profile of leakage with irradiation time from cells grown in oleate- or linolenate-supplemented medium. Fatty acid unsaturation does not appear to be correlated with leakage in stationary phase cells, reflecting the lack of correlation between sensitivity and fatty acid composition in these cells (Fig. 31).

It is possible that the rapid, initial leakage from stationary phase cells contributes to their greater sensitivity to near-UV radiation when compared with log phase cells (Figs. 28 and 31).

3. RUBIDIUM LEAKAGE FROM K1060 FOLLOWING FAR-UV IRRADIATION

It has been shown that the survival of log-phase K1060 cells following near-UV (Fig. 28) but not for far-UV (Fig. 33) irradiation is related to the unsaturated fatty acid content of the membrane. Experiments were therefore performed in order to determine whether membrane leakage was induced by far-UV (254 nm) irradiation, and whether the fatty acid content of the cell affected any such leakage. Fluences were chosen so that survival of the irradiated cells was reduced to similar levels achieved by the near-UV fluences used.

There was no evidence of leakge from the far-UV irradiated cells in excess of that measured from unirradiated cells (Fig. 53), even after fluences resulting in a surviving fraction of 5×10^{-6}. An increase in fatty acid unsaturation did not cause any far-UV-induced leakage.

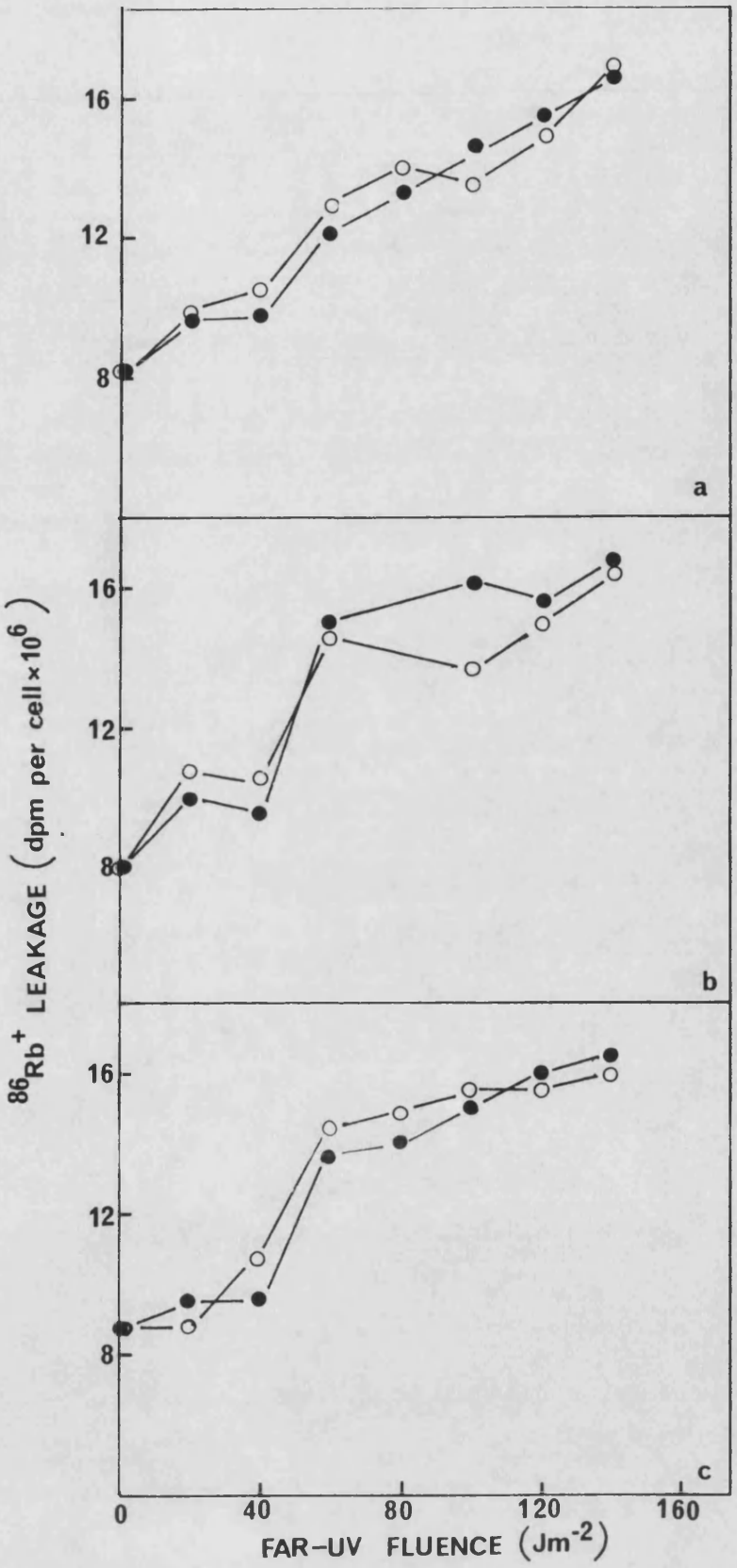

Figure 53

The leakage of $^{86}Rb^{+}$ from log phase E. coli K1060 following far-UV irradiation (closed symbols) or unirradiated controls (open symbols). Cells incorporating (a) oleic (b) linoleic (c) linolenic acid.

It is of interest to express the leakage of $^{86}Rb^{+}$ from irradiated cells as a function of the surviving fraction. Fig. 54 shows survival curves obtained over the long exposures used in leakage experiments, and Fig. 55 relates leakage to these survivals. It can be seen that while near-UV-induced leakage increases as the surviving fraction decreases, a corresponding reduction in survival following far-UV irradiation is not accompanied by an increase in leakage.

It has been shown that irradiation in D_2O reduces the survival of K1060 following near-UV but not far-UV irradiation (Fig. 44). Such an increase in sensitivity has been discussed in terms of the possible involvement of reactive oxygen species particularly with reference to lipid peroxidation (Fig. 47d). The enhancement of cell killing and lipid peroxidation in deuterated medium may be reflected in an increase in membrane damage, therefore $^{86}Rb^{+}$ leakage was measured from cells irradiated in D_2O.

4. THE LEAKAGE OF $^{86}Rb^{+}$ FROM LOG PHASE K1060 CELLS IRRADIATED IN D_2O

Harvested cells were divided into two batches and resuspended in either K^{+}-free M9 or 75% D_2O made isotonic with K^{+}-free M9 salts. The cells were irradiated and $^{86}Rb^{+}$ leakage measured.

The results of such an experiment are shown in Fig. 56a. It is apparent that cells irradiated in D_2O leak to a greater extent than those irradiated in M9. Leakage expressed as the ratio of dpm irradiated cells : dpm control cells (Fig. 56b) reduces the apparent effect since unirradiated cells in D_2O also leak more than control cells.

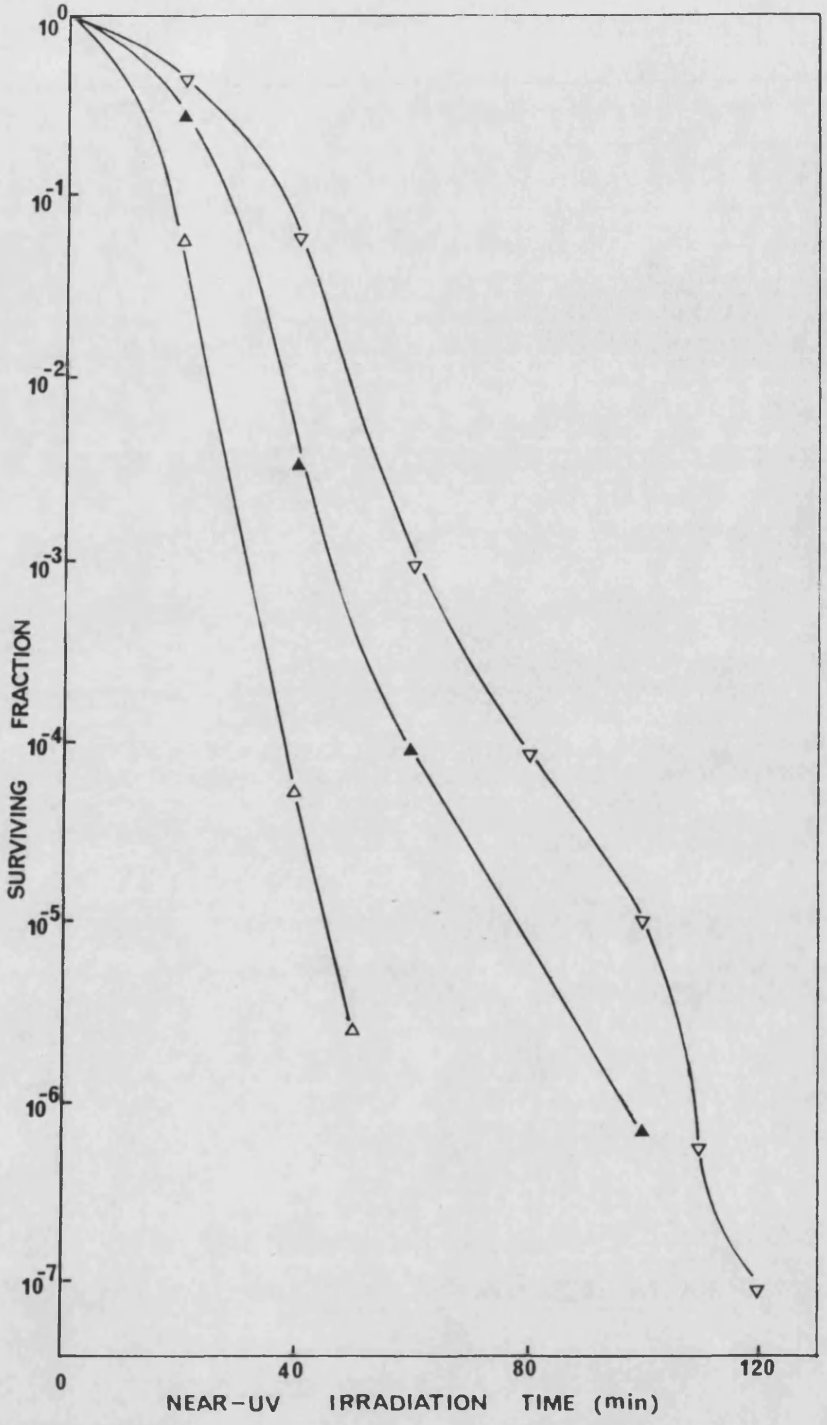

Figure 54
Survival curves of E. coli K1060 following broad-band near- UV irradiation.
Cells incorporating (▽) oleic (▲) linoleic (△) linolenic acid.

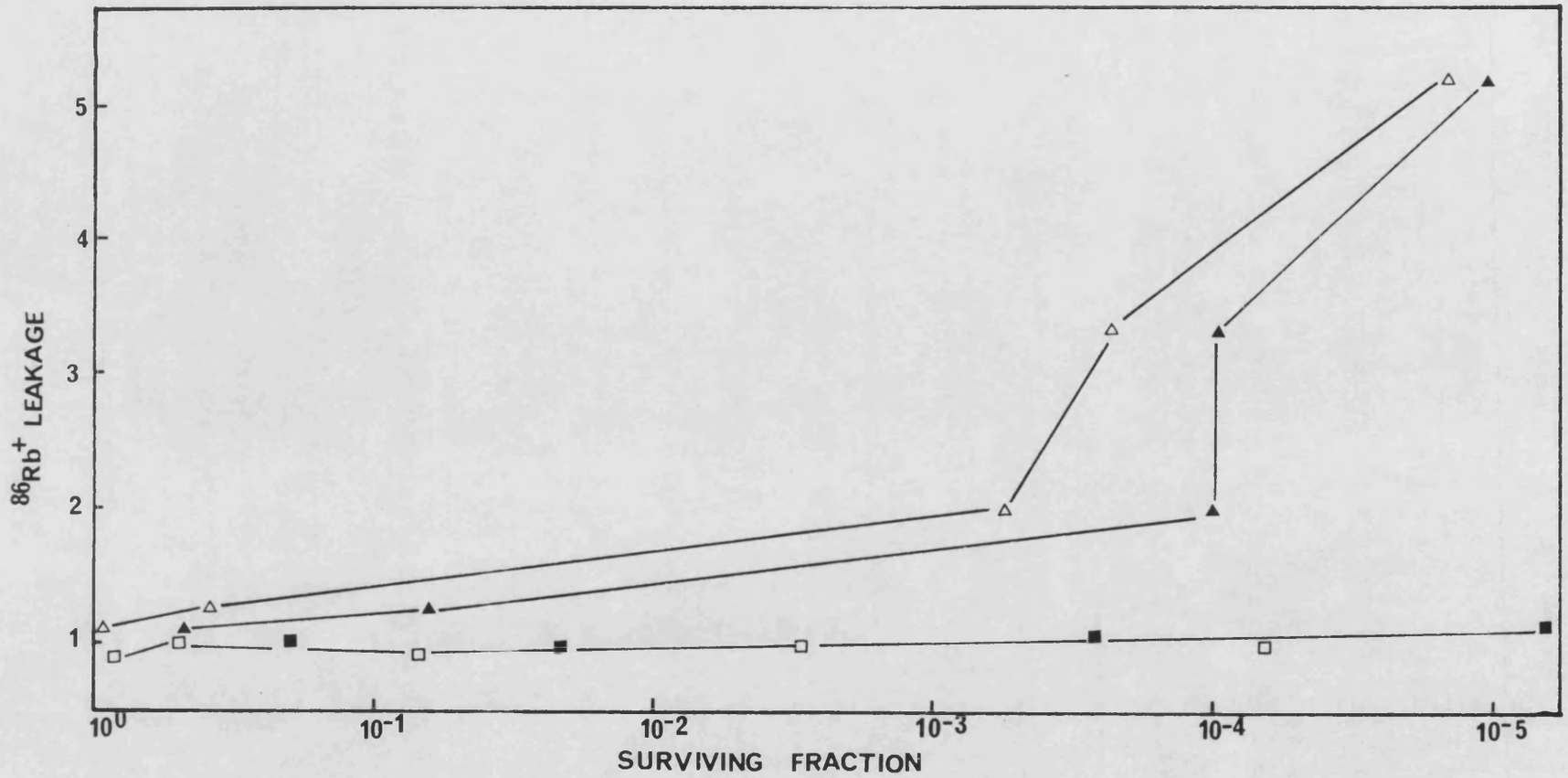

Figure 55
The effect of far-UV (□ ■) or near-UV (△ ▲) irradiation on the leakage of $^{86}Rb^{+}$ from log phase E. coli K1060 expressed in relation to surviving fractions. Alternate symbols represent replicate experiments.

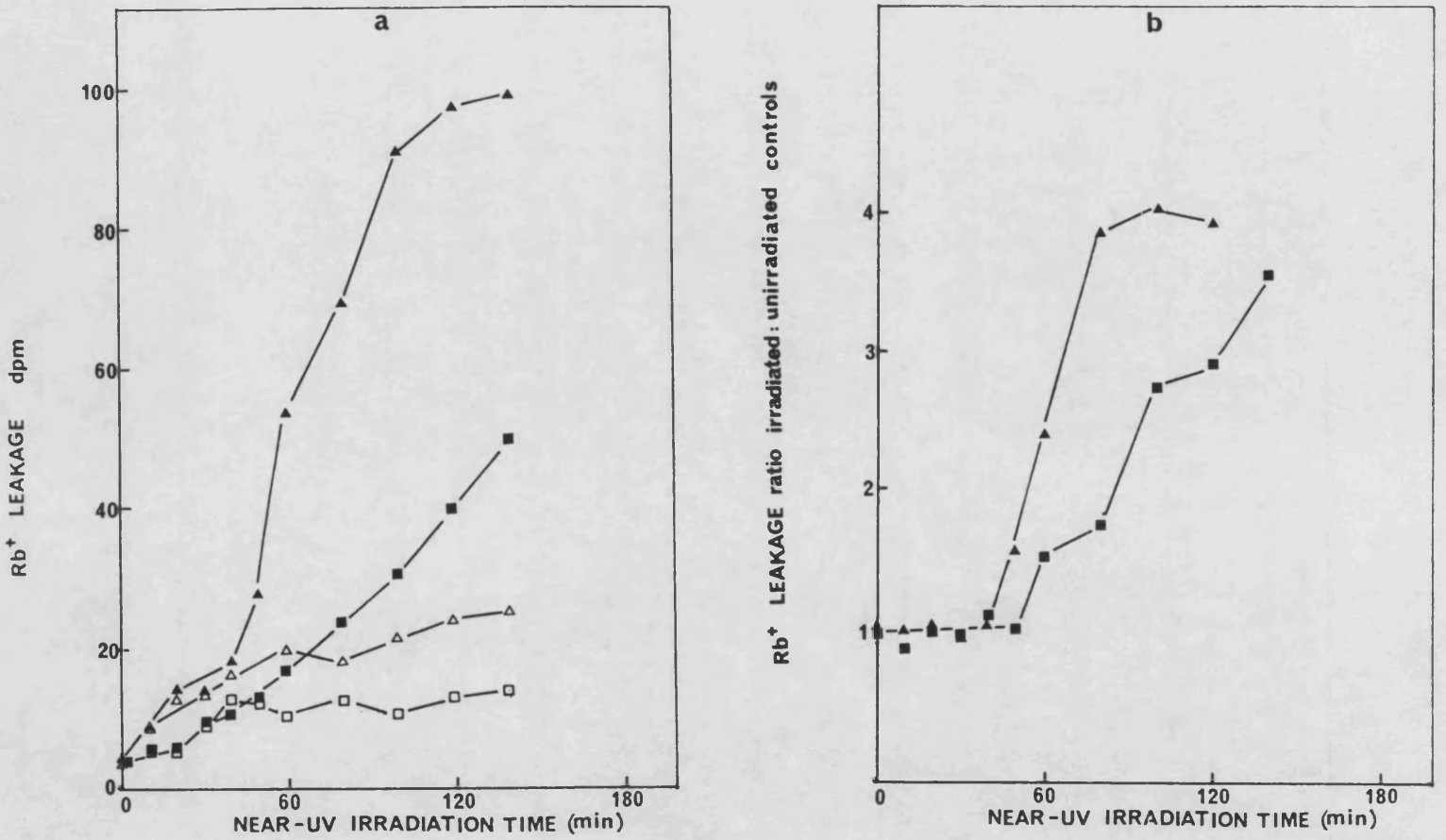

Figure 56
The leakage of $^{86}Rb^+$ from log phase E. coli K1060 following broad-band near-UV irradiation (closed symbols) or unirradiated controls (open symbols) in the presence (△▲) or absence (□■) of D_2O.

The data presented in Figs. 44, 47b and 56 provide evidence supporting membrane fatty acids as targets for attack by radiation-induced singlet oxygen attack.

Vitamin E was shown to reduce the sensitivity of K1060, to a low degree, to near-UV irradiation (Fig. 37) when provided as a supplement in the pre-irradiation growth medium, while Trolox-C had no such effect. It was of interest to determine whether these antioxidants would protect against leakage of rubidium from irradiated cells.

5. THE EFFECT OF VITAMIN E ON $^{86}Rb^{+}$ LEAKAGE FROM NEAR-UV IRRADIATED CELLS

Vitamin E was provided in the pre-irradiation growth medium at 100 μg ml^{-1}. Supplemented and standard cultures were grown in parallel, then were harvested, irradiated and $^{86}Rb^{+}$ leakage was determined in parallel.

Fig. 57 shows that while leakage from the unirradiated cells is similar whether or not they were supplemented with Vitamin E, the irradiation-induced $^{86}Rb^{+}$ leakage from supplemented cells is delayed, indicating a protective effect.

6. THE EFFECT OF TROLOX-C ON $^{86}Rb^{+}$ LEAKAGE FOLLOWING NEAR-UV IRRADIATION

Although Trolox-C did not protect irradiated K1060 when used as a pre-irradiation growth supplement, it was decided to determine whether leakage from irradiated, supplemented cells was also unaffected. Trolox-C was used as a supplement in the growth medium

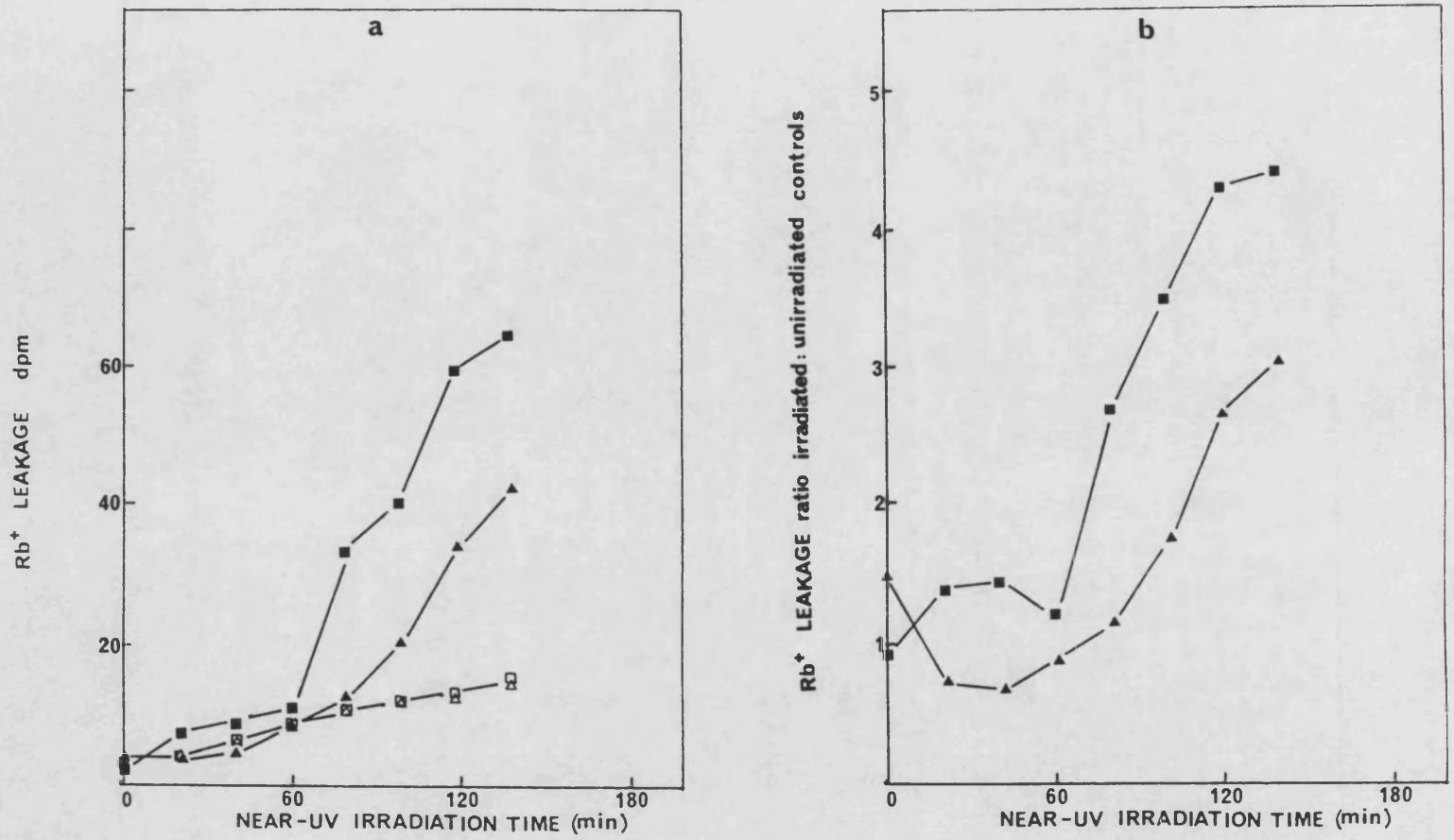

Figure 57
The leakage of $^{86}Rb^{+}$ from log phase E. coli K1060 following broad-band near-UV irradiation (closed symbols) or unirradiated controls (open symbols) following growth with (△▲) or without (□■) vitamin E.

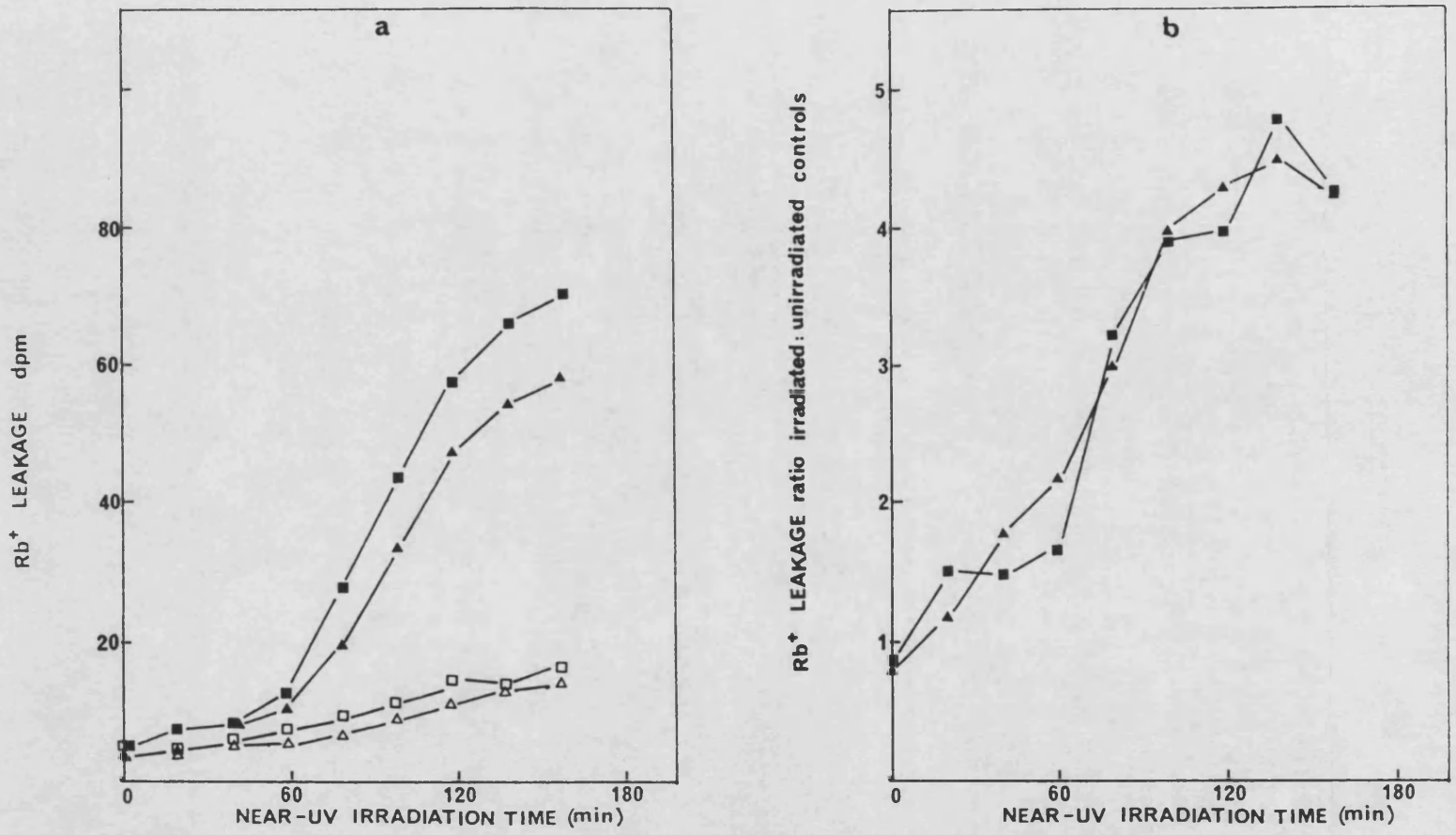

Figure 58
The leakage of $^{86}Rb^{+}$ from log phase E. coli K1060 following broad-band near-UV irradiation (closed symbols) or unirradiated controls (open symbols) following growth with (△▲) or without (□■) Trolox-C.

at a concentration of 100 μg ml^{-1}, prior to harvesting and irradiation. Unsupplemented cells were grown and irradiated in parallel. Fig. 58 shows that there is no reduction in leakage attributable to Trolox-C supplementation.

SUMMARY OF RUBIDIUM LEAKAGE RESULTS

Membrane damage, as assessed by the leakage of $^{86}Rb^{+}$ from irradiated K1060 cells relative to unirradiated cells, has been shown to occur following near-UV but not far-UV irradiation. Such leakage occurs after lower fluences, and more rapidly with increasing unsaturation of membrane lipids. Irradiation in D_2O, known to prolong the lifetime of reactive oxygen species, results in an increase in leakage, while Vitamin E, but not Trolox-C, protect against the radiation-induced damage.

Leakiness is measurable in linolenate-grown cells after fluences resulting in a surviving fraction of betweeen 10^{-2} and 10^{-3}. Such leakage occurs in linolenate-grown cells where survival is reduced to 10^{-4}, and in oleate-grown cells to 10^{-7}. Although these survival levels, particularly from oleate-grown cells, are low, two factors should be considered. (1) Even at such low survival levels far-UV irradiation does not result in $^{86}Rb^{+}$ leakage, (2) low levels of leakage, beyond the range of detection, may occur and be relevant to survival and (3) leakage, being measured immediately after irradiation, may not directly correlate with survival if the degree of membrane damage is sufficiently limited to allow subsequent repair.

DISCUSSION

As described in the Introduction, there is clear evidence for damage to DNA and DNA repair mechanisms by near-UV radiation, and these account for much of the lethality ascribed to such radiation (for reviews see Jagger, 1985 and Webb, 1977). However, since the review by Webb in 1977 there has been accumulating evidence for other near-UV-induced lesions, particularly to the membrane.

The investigations in this section were encouraged by the published work of Klamen and Tuveson (1982), who hypothesised the singlet oxygen-mediated attack of unsaturated C=C bonds of membrane fatty acids as a contributory factor in the near-UV killing of E. coli K1060. The investigations here were intended to extend their published results by providing evidence for the involvement of singlet oxygen and the peroxidation of membrane lipids, and to demonstrate membrane damage by rubidium-leakage experiments.

Initial results confirmed the correlation between fatty acid unsaturation and near-UV sensitivity using fatty acids of 18-carbon chain length rather than the 20-carbon fatty acids used by Klamen and Tuveson (Figs. 27-30). In order to eliminate the possibility of oxidative attack on unsaturated membrane fatty acids, logarithmically growing K1060 cells were supplemented with dihydrosterculic acid, the cyclopropane derivative of oleic acid. In such cells there were no unsaturated fatty acids present in the membrane. These cells were shown to be considerably less sensitive to near-UV radiation than cells incorporating polyunsaturated fatty acids (Fig. 32). These survival curves indicate that the proportion

of lethal damage which may be attributed to factors other than the unsaturation of the membrane fatty acids is low at the fluences used. Membrane fluidity may be altered as a result of the incorporation of polyunsaturated fatty acids, although the organism incorporates less of a polyunsaturated fatty acid in order to compensate for such alterations, as shown in Table 9 in a subsequent section relating to GLC analysis. It would therefore be interesting to synthesise the cyclopropane derivatives of linoleic and linolenic acids, incorporate them into logarithmically growing K1060 cells, and to investigate the effect on near-UV sensitivity. The influence of membrane fluidity, rather than the role of oxidative attack, may then be determined.

Stationary phase K1060 cells show no correlation between near-UV sensitivity and unsaturated fatty acid composition (Fig. 30) even though GLC analysis demonstrated that the organism inefficiently converts unsaturated fatty acids to their cyclopropane derivatives (shown subsequently in Figs. 67-72). Such a lack of correlation indicates that in stationary phase cells factors other than the unsaturation of membrane fatty acids are of particular importance.

The importance of oxygen during the irradiation of log phase cells is evident (Fig. 34), and necessarily so when proposing oxidative attack on unsaturated membrane fatty acids. These results are in accord with copious published data, where oxygen-dependence has been demonstrated for near-UV-induced lesions such as single-strand breaks in DNA (Tyrrell *et al.*, 1974; Peak and Peak, 1982), and killing of bacterial cells (Webb and Lorenz, 1970). These and

other oxygen-dependent lesions have been reviewed recently by Jagger (1985).

The exclusion of oxygen following irradiation, by the anaerobic incubation of plates for viability assessment, also proved to be effective in offering protection (Fig. 35). This suggests that oxidative damage may continue during the post-irradiation period under normal conditions. While post-irradiation peroxidation was not increased during a holding period in M9 (Fig. 46) this does not exclude the possibility that it may be favoured in rich media.

Both cellular activity and extra-cellular events must be considered to play some part in the determination of whether or not an irradiated cell survives and successfully divides to form a colony. The prevention of cellular synthesis of glutathione caused a decrease in survival, and while glutathione-depleted cells show some increased sensitivity, the effect is much more evident if post-irradiation synthesis is also prevented, particularly when viability is assessed on defined media (Fig. 41).

Under standard conditions K1060 exhibits considerably lower levels of survival when assessed on rich media (YENB) as shown in Figs. 27, 29 and 30. Some insight into the causes of this disadvantage to irradiated cells may be gained from the following considerations.

1. The effect is increasingly apparent as the unsaturation of the incorporated fatty acid increases (Figs. 27, 29, 30).
2. The discrepancy is reduced when irradiation takes places under nitrogen, (Fig. 36).
3. Anaerobic incubation for viability assessment increases the

levels of survival on YENB but not on defined media (Fig. 35).

4. The addition of either catalase or superoxide dismutase to YENB plates restores viability to those levels obtained on defined media (Fig. 39).
5. Irradiation in D_2O reduces viability to the same level on both media (Fig. 44).
6. Growth on rich media is considerably more rapid than on defined media, colonies being visible within 16 hours on the former, and up to 36 hours on the latter.

Therefore oxygen-mediated events are evidently more important to those cells growing aerobically under the conditions provided by rich media, both hydrogen peroxide and superoxide anion being implicated. Peroxidative damage and free radical propagation may be maximized in rich media under aerobic conditions causing further stress to an already damaged cell, which is subsequently unable to divide and form a colony.

Mackey and Derrick (1986) detected hydrogen peroxide in rich media plates at levels which were apparently high enough to reduce the viability of cold-shocked E. coli and Salm. typhimureum. They proposed mechanisms which may be suitably considered here, since membrane damage is evident in both cases:

1. Damaged membranes are more permeable to H_2O_2 which therefore diffuses more rapidly to sensitive sites in the cell.
2. Surface located catalase is lost. To this may be added the observation that catalase is inactivated by near-UV radiation (Cheng et al., 1981).
3. Co-factors required for DNA repair enzymes are lost from the

cell (Sato and Takanashi, 1970).

4. Reduced thiols which protect against oxidation damage are lost from the cell.
5. A conformational change of the DNA/membrane attachment sites sensitizes DNA to peroxidative attack.

Such mechanisms may be relevant to irradiated K1060 cells, in view not only of the demonstrated lipid peroxidation, but also of the effective protection afforded by catalase. It should also be considered that H_2O_2 may react with superoxide anion to produce reactive and damaging hydroxyl radicals as described previously.

In addition to Mackey and Derrick's work, Sammartano and Tuveson (1984) have also demonstrated the protection afforded by catalase when provided in the plating medium.

Sensitivity (Fig. 44), peroxidation (Fig. 47d) and leakage (Fig. 56) have all been shown to be increased when cells are irradiated in D_2O, leading to the speculation that type II photosensitizations, following the absorption of near-UV radiation by endogenous photosensitizerss, contribute to cell killing. These are not surprising results, since endogenous photosensitizers are ubiquitous (Jagger, 1985; Webb, 1977). The attack by such oxygen species, when enhanced by irradiation in D_2O, may be considered to damage the cells to such an extent that, not only is survival reduced on rich media, but the previously evident survival advantage promoted by growth on defined media is lost. Consideration could be given therefore, to the role of growth rate in determining survival, since under conditions where growth rate is reduced (on defined media and under anaerobic conditions)

survival is higher. Such a lowered growth rate may allow time for repair mechanisms to operate before cell division proceeds. Such mechanisms would then include the reactions of glutathione. Where damage is more severe, for example after irradiation in D_2O, the repair mechanisms may be inadequate. Further evidence in support of this is presented in the following section.

Lipid peroxidation has been demonstrated to result from the near-UV irradiation of K1060, the lowest fluence resulting in measurable peroxidation decreasing as the degree of unsaturation of the incorporated fatty acid increases (Fig. 45). Singlet oxygen may be proposed as a mediator of this peroxidation, since it is enhanced in D_2O and reduced in histidine and DABCO. Its relevance to survival should be considered by comparison with survival curves determined over similar exposure times and under similar conditions, where a correlation is evident between lipid peroxidation and sensitivity.

Where, at lower fluences, peroxidation is undetectable account should be made of the fact that the assay method may not detect hydroperoxides which are, nevertheless, present in quantities sufficient to moderate membrane activity, perhaps in localized areas. Such damage may contribute to cell killing in addition to DNA lesions suffered by the cell. It would be expected that lipid hydroperoxides would cause disorder in the lipid bilayer of the membrane, affecting permeability and other properties, even if only in localized areas. Membrane-associated enzymes, including those of transport systems, particularly those responding to changes in fatty acid composition, may have their function impaired as lipids are peroxidized .

The leakage of rubidium from near-UV irradiated cells occurs at fluences similar to those resulting in lipid peroxidation (Fig. 49). After far-UV irradiation resulting in levels of survival achieved by these fluences no such leakage occurs (Fig. 53) demonstrating a difference in the mechanisms involved in cell killing. Correlation is apparent between fatty acid unsaturation and $^{86}Rb^{+}$ leakage (Fig. 49) indicating that a more unsaturated membrane suffers a greater degree of near-UV-induced damage. Such a correlation makes it unlikely that $^{86}Rb^{+}$ efflux is a result of inactivation of the proton-K^{+} pump, unless the operation of this pump is dependent upon local lipid structure. Irradiation in D_2O, which was shown to increase sensitivity and lipid peroxidation, also increased leakage of rubidium (Fig. 56).

Peak et al. (1987) provided evidence for porphyrin derivatives as mediators of oxygen-dependent near-UV-irradiation-induced damaged to the cytomembrane, as demonstrated by $^{86}Rb^{+}$ leakage. Although they used monochromatic 334 nm and 405 nm radiations, the broad-band near-UV radiation to which K1060 was exposed would be in the range capable of causing such photosensitized reactions. These authors discounted DNA breaks as being the target for such reactions, and it would be useful to investigate lipid peroxidation in their hem A8 mutant strain under their experimental conditions.

Evidence for membrane damage has been presented as a sensitivity of irradiated cells to high salt concentrations (Moss and Smith, 1981; Kelland et al., 1983a, 1983b). In this present study with K1060 a high salt defined medium was used in order to express membrane damage in a similar way and comparisons were made

with survival on YENB (which is a low salt medium) and a defined medium with normal salt concentration. The result was entirely unexpected, namely that survival on YENB was always lower than on either defined medium (Figs. 27, 29, 30). A comparison between normal and high salt defined media showed reduced survival on the latter only after glutathione depletion (Fig. 41). This indicates that the near-UV sensitivity of K1060, and the leakage of $^{86}Rb^{+}$ demonstrated here, may be due to different mechanisms from those in the SR385 strain employed by Kelland et al. (1983a, 1983b), and Kelland (1984). Alternatively, K1060 may have inherent differences in its response to membrane damage, perhaps by way of membrane repair or in its osmotic tolerance. This is investigated further in the following section.

In summary, the results in this section have related the unsaturation of membrane fatty acids to the sensitivity of K1060 to near-UV irradiation. Lipid peroxidation and leakage of rubidium have been shown to occur at similar fluences, and both increase with the increasing unsaturation of membrane fatty acids. This provides evidence for unsaturated phospholipids as targets for near-UV-induced attack, and since factors which modify peroxidation also modify survival, and within the limited range tested similarly modify leakage, it is tempting to speculate upon a causal relationship.

RESULTS AND DISCUSSION

PART 1B

FACTORS DETERMINING THE POST-IRRADIATION SURVIVAL OF E. COLI K1060

Work in this laboratory by Kelland (1984), as discussed in the Introduction, showed a NUV-induced sensitivity to high salt concentrations by E. coli SR385 and other strains. This was interpreted as NUV-induced membrane damage, a hypothesis supported by the subsequent demonstration of leakage of rubidium and other substances from irradiated cells. Klamen and Tuveson (1982) proposed the attack by singlet oxygen on unsaturated fatty acids in the bacterial membrane during exposure to NUV radiation. This proposal followed the demonstration of increasing sensitivity to NUV irradiation as the degree of unsaturation of membrane fatty acids increased. These results were obtained using E. coli K1060, which was therefore considered to be a useful organism for investigations into NUV-induced membrane damage and its possible causes, particularly in relation to lipid peroxidation.

It was hoped that constructive comparisons might be made with Kelland's results, since radiation sources and irradiation procedures would be the same.

Following initial survival determinations after NUV-irradiation it was apparent that K1060 differed from SR385 as follows:

1. SR385: Survival assessed on YENB was always higher than on defined media.

   K1060: Survival assessed on YENB was always lower than on defined media.

2. SR385: Survival on high salt defined media was always lower than on low salt defined media.

   K1060: No salt sensitivity was demonstrable.

Several experiments were performed to investigate the differing response of K1060, particularly since, having demonstrated NUV-induced $^{86}Rb^{+}$ leakage, parallel salt-sensitivity was not evident. Initial experiments investigated the composition of media used for the assessment of viability.

1. THE EFFECT OF VARIATIONS IN THE COMPOSITION OF MEDIA USED TO ASSESS VIABILITY FOLLOWING NUV IRRADIATION

Survival on YENB Relative to Minimal Media

In the first set of experiments the relative survivals on defined and rich media of the two strains, K1060 and SR385, were compared. Figs. 59a and 59b demonstrate the relative survivals and confirm Kelland's results where SR385 exhibits enhanced viability on rich media.

Survival on Minimal Media Containing Normal or High Concentrations of Sodium Chloride

When viability is assessed on normal or high salt defined media SR385 shows a NUV-induced salt sensitivity (Fig. 59b). K1060 shows no such sensitivity (Fig. 59a). This result is discussed at the end of this section.

The Effect of Variations in Media Components

Variations are summarised in Table 8, together with a summary of the reasons for the modification and the results obtained. The significant results are those obtained when either sodium chloride

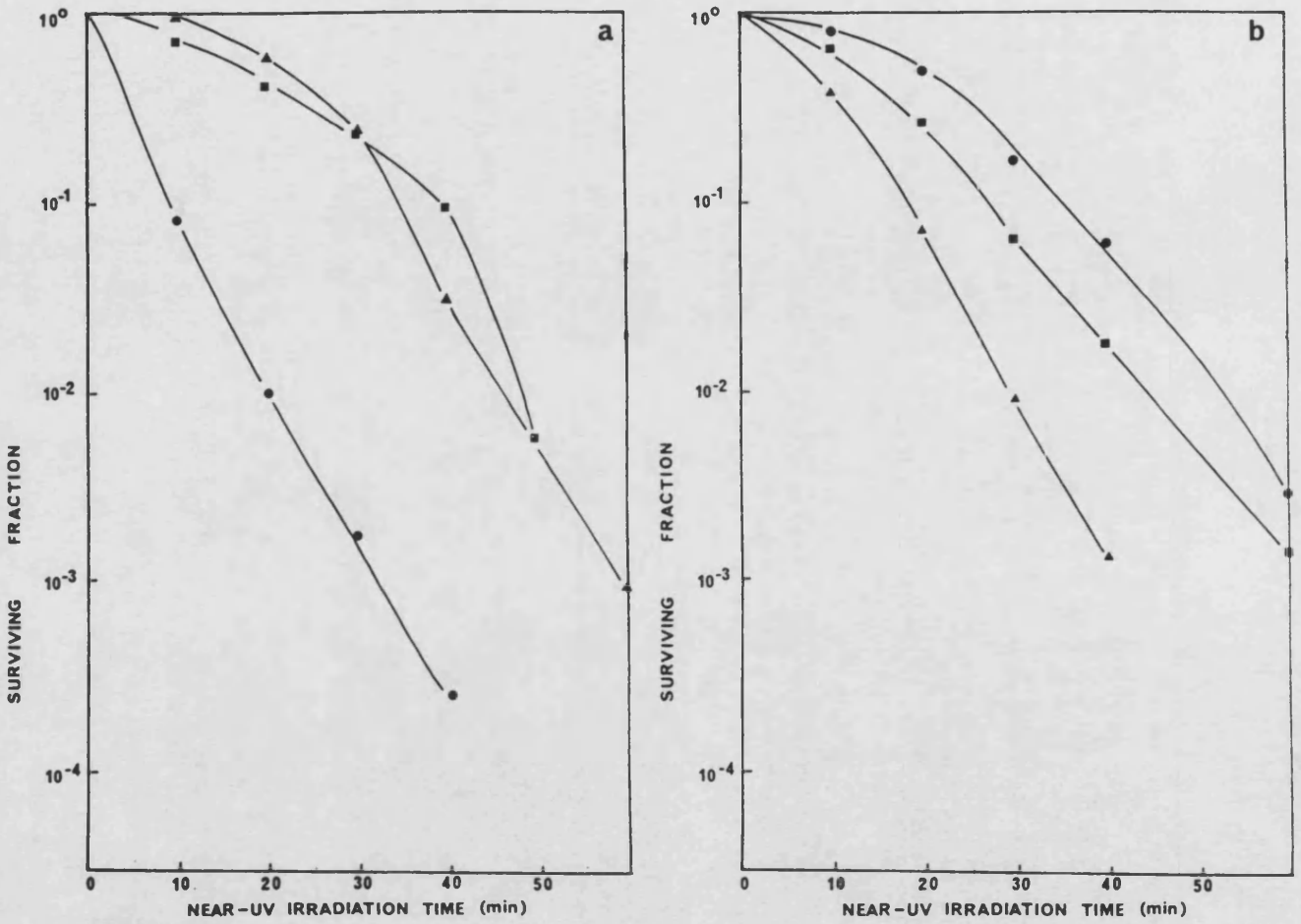

Figure 59
Survival curves for E. coli (a) K1060 (b) SR385 following broad-band near-UV irradiation. Viability assessed on YENB (●) normal salt defined medium (■) or high salt defined medium (▲).

or M9 salts were added to YENB. Both resulted in higher survivals, and this is discussed at the end of this section.

2. THE EFFECT OF PRE-IRRADIATION GROWTH MEDIA

E. coli K1060 is conventionally grown in glycerol in contrast to glucose, used for SR385. It has been shown that alternative carbon sources, including glucose and glycerol, have no effect either on fatty acid composition nor on the amount or proportion of phospholipids (Damoglou and Dawes, 1968).

For comparison with SR385, glycerol was replaced by glucose at the same concentration (0.4%) in the pre-irradiation growth medium. Following irradiation in parallel with cultures grown in glycerol-medium, viability was increased when assessed on YENB following growth in glucose-medium (Fig. 63a). In the converse of this experiment, where SR385 was grown in glycerol- rather than glucose-supplemented medium, no such change in survival was demonstrated (Fig. 63b), and it can be seen that salt sensitivity is apparent.

3. THE EFFECT OF INOCULUM SIZE AND AGE OF CELLS AT HARVEST PRIOR TO IRRADIATION

As explained previously, there is day to day variation in the sensitivity of exponentially growing E. coli cells to broad-band NUV-irradiation. Cells were normally harvested 4 hours after inoculation of the medium, at which time reference to Fig. A1 shows the cells to be well into the log phase. Although inoculum size (1 ml) and the age of cells at harvest, (4 hours), were standardized, variations were introduced in the following type of

Table 8. Modifications to the media used for assessment of viability following NUV irradiation of K1060

Normal Component	Variation (DM=defined medium)	Reason	Effect on Survival	Fig.
Glycerol 0.4%	replaced by 0.4% glucose in DM	SR385 grown on glucose	none	60
Casamino acids	omitted from DM	shown to protect SR385 (Kelland, 1984)	none	60
Difco Bacto-agar	replaced by Oxoid No. 3 agar in DM	Oxoid agar used for SR385 (Kelland, 1984)	none	61a
Yeast Extract	omitted from YENB	Rich source of B-complex vitamins, which, as co-factors for respiratory enzymes may increase oxidative stress to the cells	none	61b
	added to DM		some reduction in survival	
Beef extract present at 0.3% in Difco YENB	a beef-extract free YENB was made up: 5 g peptone 15 g Bacto Agar 6 g yeast extract 16 ml 1% oleic acid to 1 ℓ water.	may increase the iron content of YENB, causing iron-catalysed reactions as discussed elsewhere	none	61c
	sodium chloride added to YENB at 200 mM	for comparison with high salt defined media	increase in survival	62

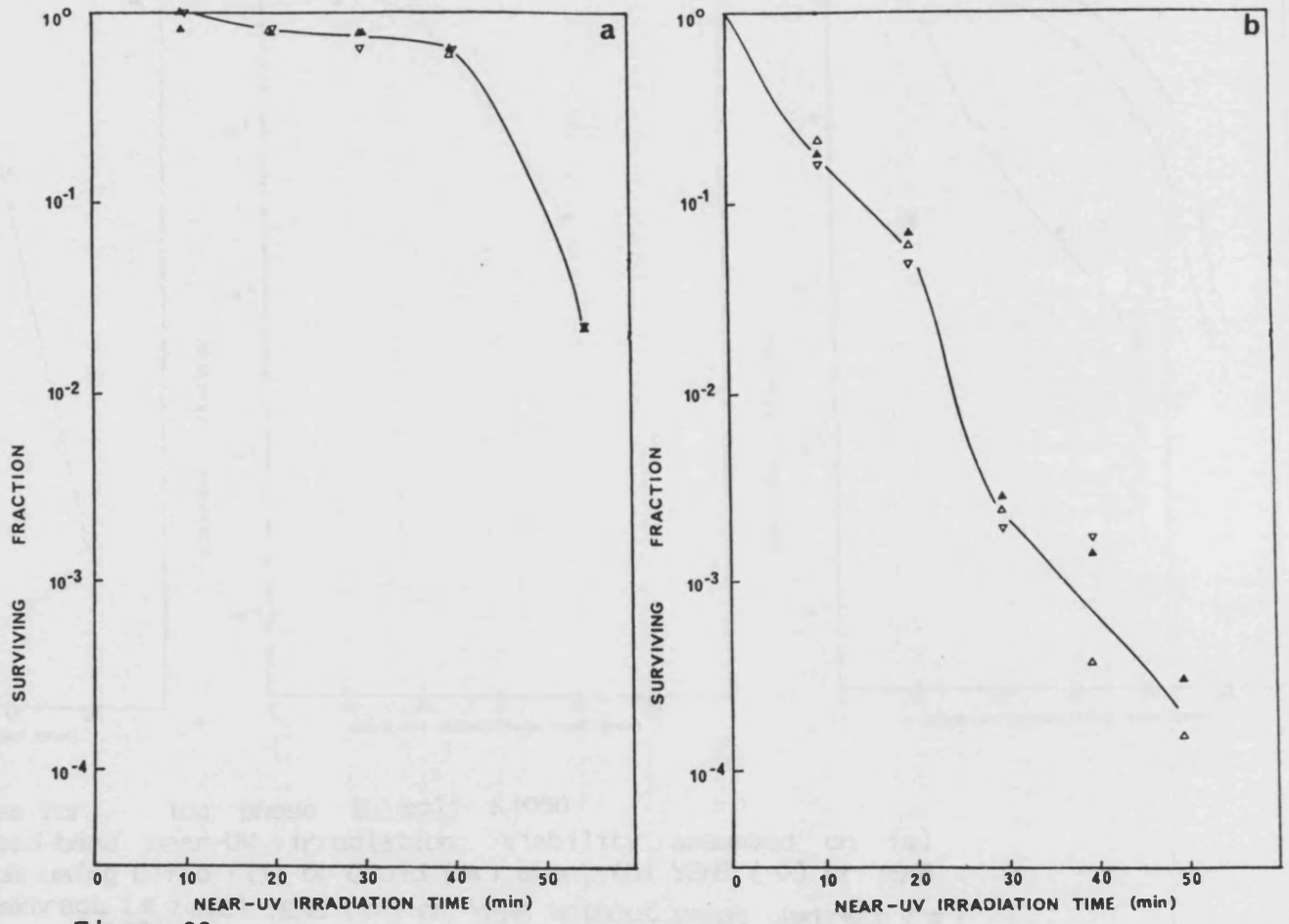

Figure 60
Survival curves for (a) log phase (b) stationary phase E. coli K1060 following broad-band near-UV irradiation. Viability assessed on high salt defined medium with (▲) glucose replacing glycerol, (▽) no casamino acids, (△) standard medium.

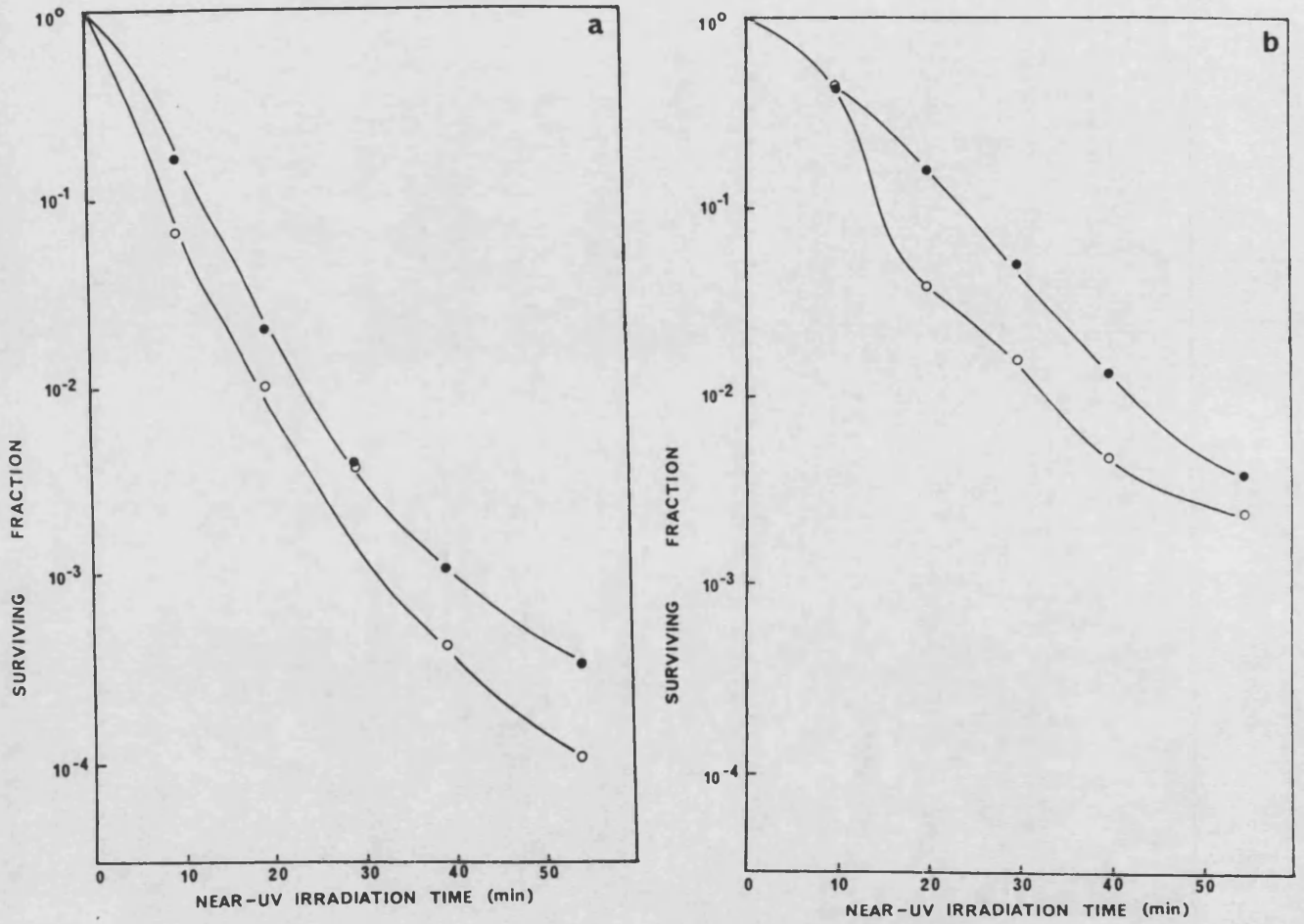

Figure 62
Survival curves for (a) log phase (b) stationary phase E. coli K1060 following broad-band near-UV irradiation. Viability assessed on (○)YENB or (a) YENB plus NaCl (●), (b) YENB plus M9 salts (●).

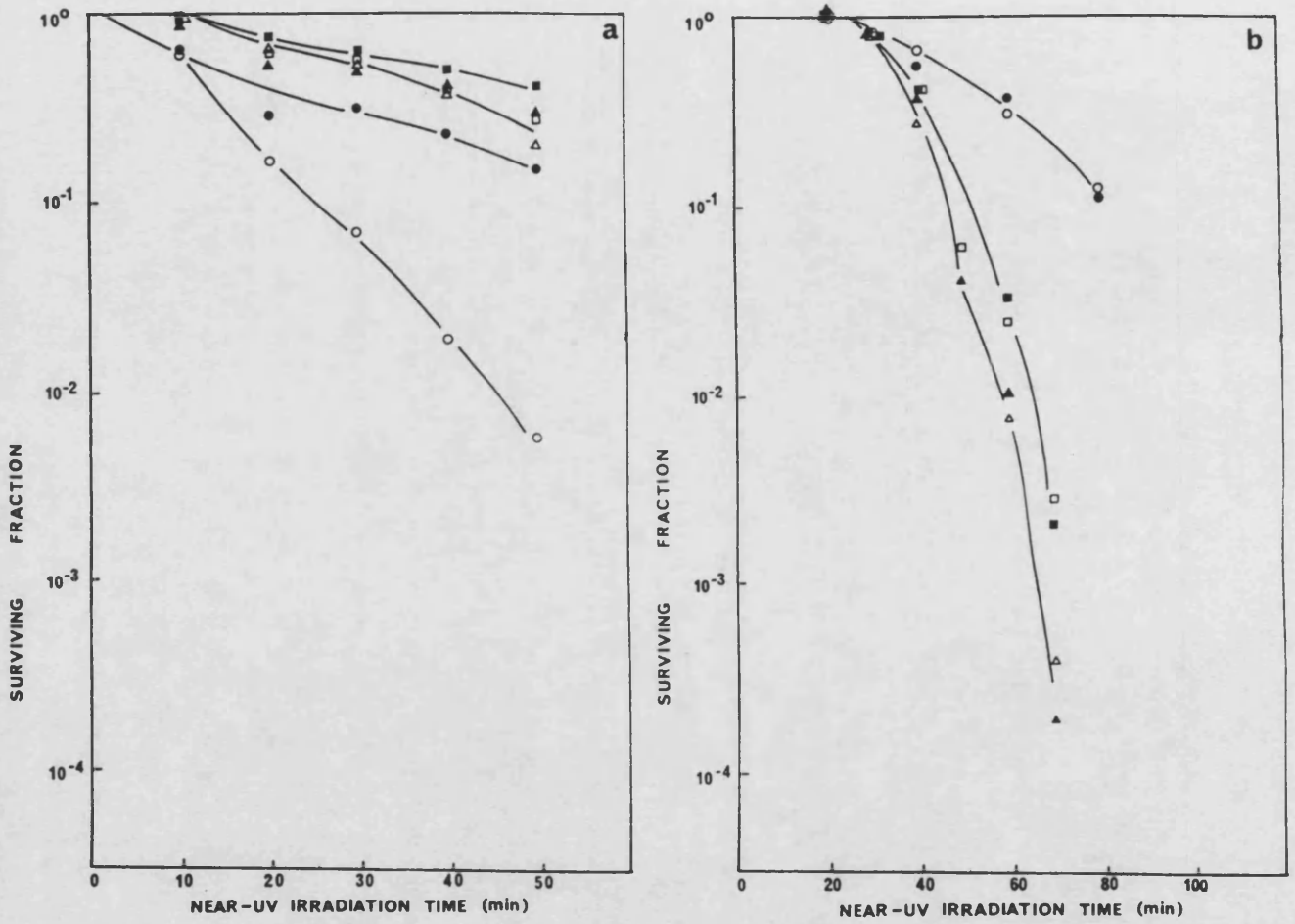

Figure 63
Survival curves for E. coli (a) K1060 (b) SR385 following broad-band near-UV irradiation. Growth prior to irradiation in standard (open symbols) or alternate (closed symbols) carbon source. Viability assessed on YENB (○●) Normal salt defined medium (□ ■) or high salt defined medium (△ ▲).

experiment in order to assess possible effects on sensitivity.

A single 24 hour culture was used to inoculate two batches of growth medium; one batch was inoculated with 1 ml, the other with 0.5 ml. Both cultures were grown into the log phase. Cells from the first culture were harvested at 120 and 240 minutes, cells from the second were harvested at 180 and 360 minutes. These variations were therefore well outside those introduced by error in the day to day handling of cultures. Figs. 64a and 64b show that the age of cells at harvest from each culture did not affect survival. The inoculum size of cells made insignificant difference to survival after lower fluences. After 20 minutes' exposure the cells from the culture having the large inoculum size are increasingly more resistant to irradiation.

4. THE EFFECT OF INCUBATION TEMPERATURE ON ASSESSMENT OF VIABILITY FOLLOWING NUV-IRRADIATION

Plates for determination of viability were routinely incubated at 30°C when using K1060; SR385 was incubated by Kelland at 37°C. The effect of incubation temperature was therefore investigated. Following irradiation, duplicate sets of plates were prepared, one set was incubated at 37°C, the other at 30°C. While no alteration in survival as assessed on YENB was demonstrated, Fig. 65 shows that on both high salt and normal salt defined media survival is reduced following incubation at 37°C.

5. A COMPARISON WITH *E. COLI* K12

E. coli K1060 has been shown to differ from SR385 in several

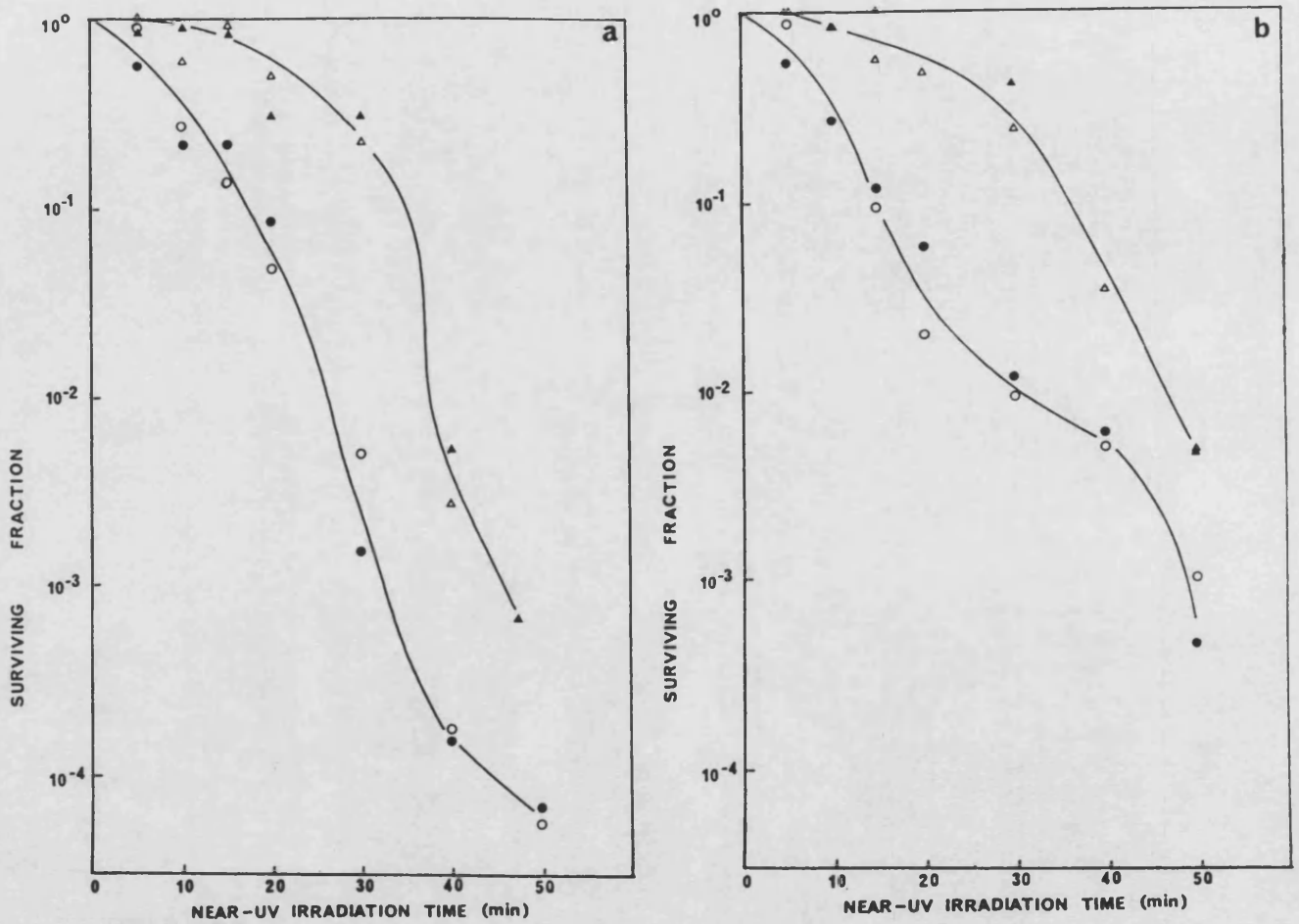

Figure 64

Survival curves for E. coli K1060 following broad-band near- UV irradiation. (a) 0.5ml inoculum, cells harvested at (○△) 3h or 6h (●▲), (b) 1.0ml inoculum, cells harvested at 2h (○△) or 4h (●▲). Viability assessed on YENB (○●) or high salt defined medium (▲△).

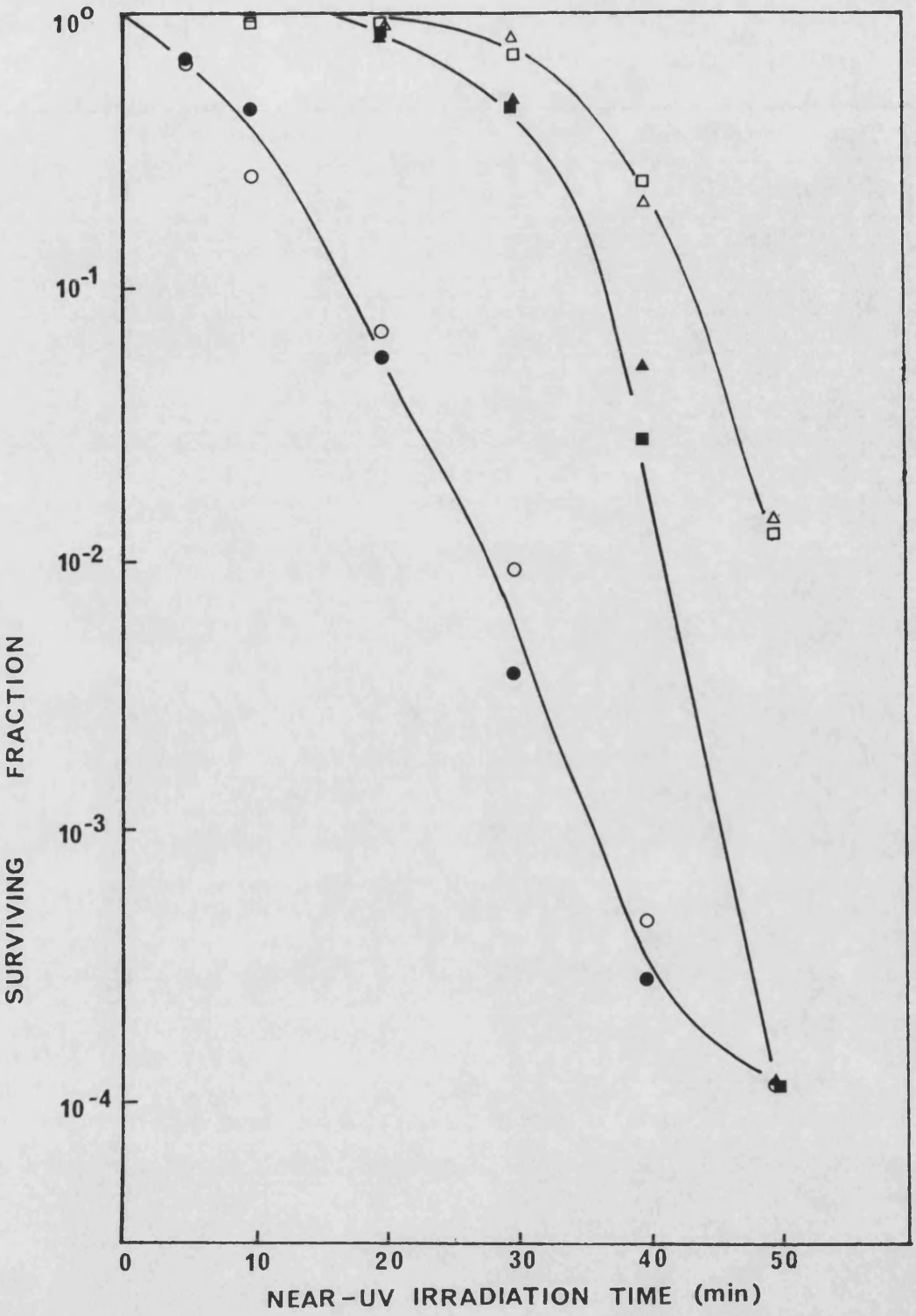

Figure 65
Survival curves for E. coli K1060 following broad-band near- UV irradiation. Viability assessed on YENB (○ ●), Normal salt defined medium (△ ▲) or high salt defined medium (□ ■) after incubation at 30°C (open symbols or 37°C (closed symbols).

respects with regard to survival following irradiation with BLB. While results shown in this section show the survival of organisms incorporating linolenic acid (18:3) in order to maximise any effects which may be attributed to changes in the membrane, the same relative survival on YENB, minimal media or high salt defined media, is exhibited by cells incorporating oleic or linoleic acids (Figs. 27, 29, 30). While the membrane of the oleic acid-grown cells should be similar in respects of fluidity and fatty acid unsaturation to the membrane of SR385, it is evident that other factors may be responsible for the observed differences. Both K1060 and SR385 are derivatives of E. coli K12 (Overath et al., 1970; Kelland, 1984) and so a comparison with this strain was thought to be useful.

The organism was grown in a defined medium as used for K1060, with the exclusion of the unrequired fatty acid. After irradiation its survival was assessed on YENB, normal and high salt defined media. The results (Fig. 66) show that this parent organism, with no membrane modification, responds to BLB radiation in a similar way to SR385, in exhibiting salt sensitivity, though survival on YENB is reduced (as for K1060). This result, together with the survival of E. coli K1060 incorporating dihydrosterculic acid into the membrane (as discussed elsewhere), indicate that while the unsaturation of membrane fatty acids contributes to killing by BLB radiation, the enhanced sensitivity shown by plating onto rich media (or increased viability on defined media) must be otherwise accounted for.

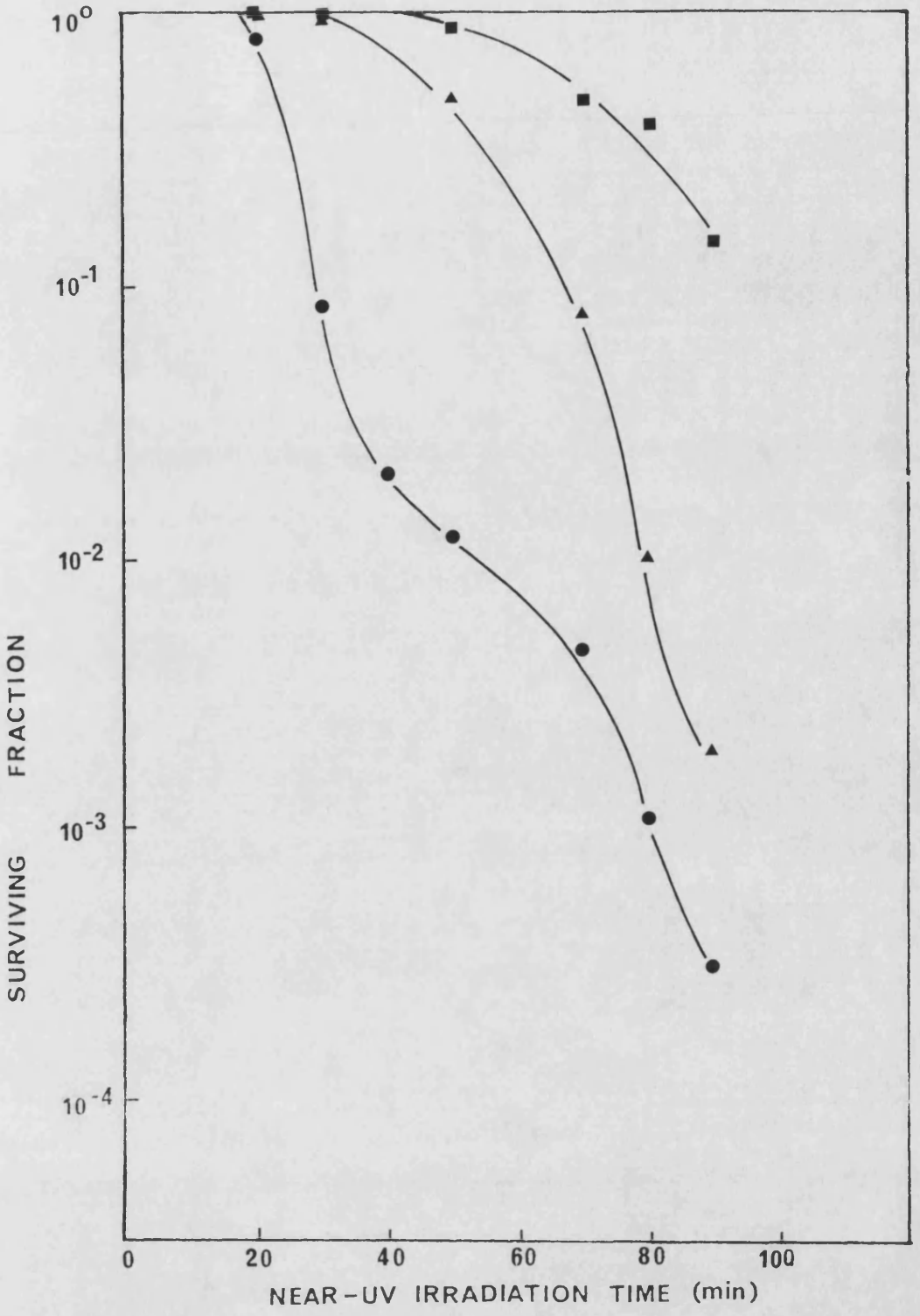

Figure 66
Survival curves for stationary phase E. coli K12 following broad-band near-UV irradiation. Viability assessed on YENB (●), Normal salt defined medium (■) or high salt defined medium (▲).

DISCUSSION

From this limited survey of factors which might influence the survival of irradiated cells the following conclusions may be drawn:-

1. The composition of the media used to assess viability has little effect of survival other than that in rich media result in a lower survival than defined media (Table 8).
2. The addition of salts to rich media increases viability, whether added as sodium chloride or M9 salts (Fig. 62).
3. Pre-irradiation growth in glucose-media results in a reduced level of sensitivity to NUV-irradiation (Fig. 63).
4. Post-irradiation incubation at 37°C results in lower survivals than incubation at 30°, as assessed on defined media (Fig. 65).

None of these results explains the differences between SR385 and K1060, since in no case was the relative survival of K1060 on YENB or defined media reversed to match that of SR385. However, the results raise several interesting points.

It has been shown (Schulz *et al.*, 1969) that the fatty acid synthesizing enzymes of *E. coli* are stimulated by salts, particularly by high concentrations of sodium chloride and potassium phosphate, and low concentrations of magnesium chloride, the cations being responsible. Normal strength defined medium contains the following salts: 22 mM KH_2PO_4, 34 mM $Na_2HPO_4.2H_2O$, 19 mM NH_4Cl, 0.9 mM $MgSO_4.7H_2O$ and 9 mM NaCl. High salt defined media, while reducing the concentrations of these salts to one tenth, has NaCl added at 200 mM. These media may then both provide for

stimulation of any residual activity of the fab B enzyme of K1060.

It has also been shown that temperature-sensitive fab B mutants of E. coli are able to grow in non-permissive conditions providing that the osmotic pressure of the medium is high. The cells growing under such conditions have unusually high proportions of saturated fatty acids (Broekman and Steenbakkers, 1973). It was later demonstrated that in high osmotic pressure media, unsaturated fatty acid synthesis is significantly increased in fab B mutants (Broekman and Steenbakkers, 1974).

It is therefore feasible that irradiated cells, having suffered peroxidative damage to membrane lipids, are able to grow on defined and high salt media by stimulated fatty acid synthesis allowing repair of the damaged membrane. The addition of NaCl or M9 salts to rich media may facilitate such repair to some degree, resulting in the increased viability shown, even though oxygen or hydrogen peroxide-related attack has been shown to be a cause of lower survival on YENB.

In several types of experiments conditions resulting in a lower growth rate increased viability. When K1060 is incubated at 37°C following irradiation, survival is lower than at 30°C. There is a noticeable difference in the growth rate at these two temperatures, being higher at 37°C. Experiments discussed in the previous section showed that anaerobic incubation resulted in higher survival than aerobic incubation. Under anaerobic conditions the growth rate is reduced considerably. Consistently through this work survival has been higher on all minimal media used, where growth is slower.

These results imply that in such experiments a lower growth rate is important in increasing viability, independently of the conditions imposed which lowered the growth rate. When growing rapidly due to the rich nutrient conditions provided by YENB there may not be time for repair processes to eliminate irradiation-induced lesions. Rapidly growing cells may undergo the type of death and lysis due to a protein synthesis-requiring process (inferred to be membrane synthesis) as exhibited by oleate-starved fatty acid auxotrophs (Henning et al., 1969).

The metabolic state of the cells prior to irradiation is known to be a factor in determining near-UV sensitivity since this alters through the growth phases of the culture (see in a review, Webb, 1977; Kelland, 1984). The replacement of glycerol by glucose, a simple easily metabolised carbon source, may alter metabolism in some way sufficiently to alter near-UV sensitivity, as shown in Fig. 63.

In summary, this section illustrates the difficulty in comparing different strains of E. coli, and leads to the conclusion that comparisons should be interpreted with care. K1060 was chosen since its membrane is easily manipulated to provide a model in which the effect of membrane phospholipid unsaturation could be studied. Although the leakage of rubidium and lipid peroxidation have been demonstrated, the organism failed to exhibit salt sensitivity. A suggestion has been put forward that this may be explained in terms of membrane repair and modification by salt-stimulated metabolism. This is proposed to be favoured under conditions where growth is slow, a condition which also facilitates

repair even on rich media, where viability is enhanced if the growth rate is lower.

It is probable that a combination of factors is responsible for the viability of irradiated cells. No consideration has been given in this study to near-UV irradiation-induced DNA lesions or damage to proteins, either cytosolic or membrane. The changes induced in the K1060 membrane by supplementation with polyunsaturated fatty acids may extend beyond the change in the fatty acyl moieties. Overath et al. (1970) suggested that K1060 exhibits a general change in cellular permeability and physiology when various fatty acids are incorporated in the membrane. It has also been demonstrated that protein distribution in the membrane of unsaturated fatty acid auxotrophs differs from that in wild type strains. Such observations, based on freeze-fracture electron microscopy are summarised in a review by Cronan and Gelmann (1975) and may account for the difference between K1060 and the wild type in their salt sensitivities. Further studies to include membrane protein content may help to elucidate the reasons for the variety of sensitivity patterns exhibited by these strains and those used by Kelland (1984).

RESULTS AND DISCUSSION

PART 1C

THE FATTY ACID ANALYSIS OF E. COLI STRAINS DETERMINED BY GAS-LIQUID CHROMATOGRAPHY

The entire lipid content of E. coli is found in the cell envelope and consists mainly of phospholipid. The remaining small amount of fatty acid is found covalently bound to galactosamine moieties of the polysaccharides as lipid A; such fatty acids are saturated. The unsaturated fatty acid composition determined therefore represents the unsaturated fatty acid content of membrane phospholipids.

It was the purpose of experiments described in Section 1A to investigate the effect of alterations in the unsaturation of membrane fatty acids on survival, lipid peroxidation and membrane leakage following near-UV irradiation. E. coli K1060, being an unsaturated fatty acid auxotroph has been widely used by workers investigating membrane-related effects and is known to incorporate the unsaturated fatty acid provided in the culture medium (Overath et al., 1970).

It was felt necessary to analyse the fatty acid composition of E. coli K1060 here for various reasons:

1. Both log phase and stationary phase cultures were used. Documentation generally refers to stationary phase cells (except Klamen and Tuveson, 1982, where fatty acids other than those used here were reported).
2. Culture conditions, notably temperature, vary in reported work. Since these affect fatty acid composition (e.g. Marr and Ingraham, 1962) reported compositions may differ from those

achieved here.

3. Having established the method it was used for determining the fatty acid compositions of other strains used in this laboratory as described subsequently, for comparison with K1060.
4. The method was also suitable for confirming the fatty acids composition of lipids used for liposomes.

Additional Methodology

Cultures from defined media were harvested either in stationary or mid-log phase for analysis. 200 ml stationary phase cultures or 1 litre log phase cultures were used. After centrifuging at 4000 rpm for 20 min (MSE High Speed 18 Centrifuge) the pellet was washed three times by resuspension in M9 buffer followed by centrifugation. The final pellet was drained of supernatant and weighed. The procedure for extraction of total lipids followed by the preparation of methyl esters of the fatty acids for GLC analysis is described in the Methodology. Methyl laurate (12:0) was used as an internal standard after confirmation that this fatty acid did not appear in bacterial extracts. Retention times were calculated relative to that of methyl laurate and identified by reference to standards run under the same conditions.

A typical trace showing the separation of standard fatty acids used is shown in Appendix 6, together with pertinent data. GLC traces of E. coli K1060 are shown in Figs. 67-72, where the composition of logarithmic and stationary phase cultures following growth on media supplemented with the three unsaturated fatty acids

(18:1, 18:2, 18:3) may be compared. Various other strains used in experiments described in this thesis and by other workers in the laboratory are included for comparison (Figs. 73-77).

The relative proportions of the fatty acid constituents was estimated by the measurement of peak heights. These data is shown in Table 9.

Retention times and relative retention times of peaks from bacterial extracts are presented in Appendix 6.

E. coli K1060:

In all cases the chromatograms confirm that the only unsaturated fatty acid incorporated into the bacterial lipids is the one supplied in the growth medium. In accordance with expectations, the higher the degree of unsaturation in the fatty acid, the less of it is required (in order to maintain the correct degree of membrane fluidity), in which case the proportion of palmitic acid (16:0) increases. Cells grown to exponential phase on oleic acid (18:1) contain a much higher proportion of this fatty acid than stationary phase cells. Some conversion to the cyclopropane derivative (19:0) takes place, but the cells evidently change to palmitic acid synthesis for the stationary phase of growth, since the proportion of this is increased here. E. coli K1060 retains a higher proportion of unsaturated fatty acid than other strains.

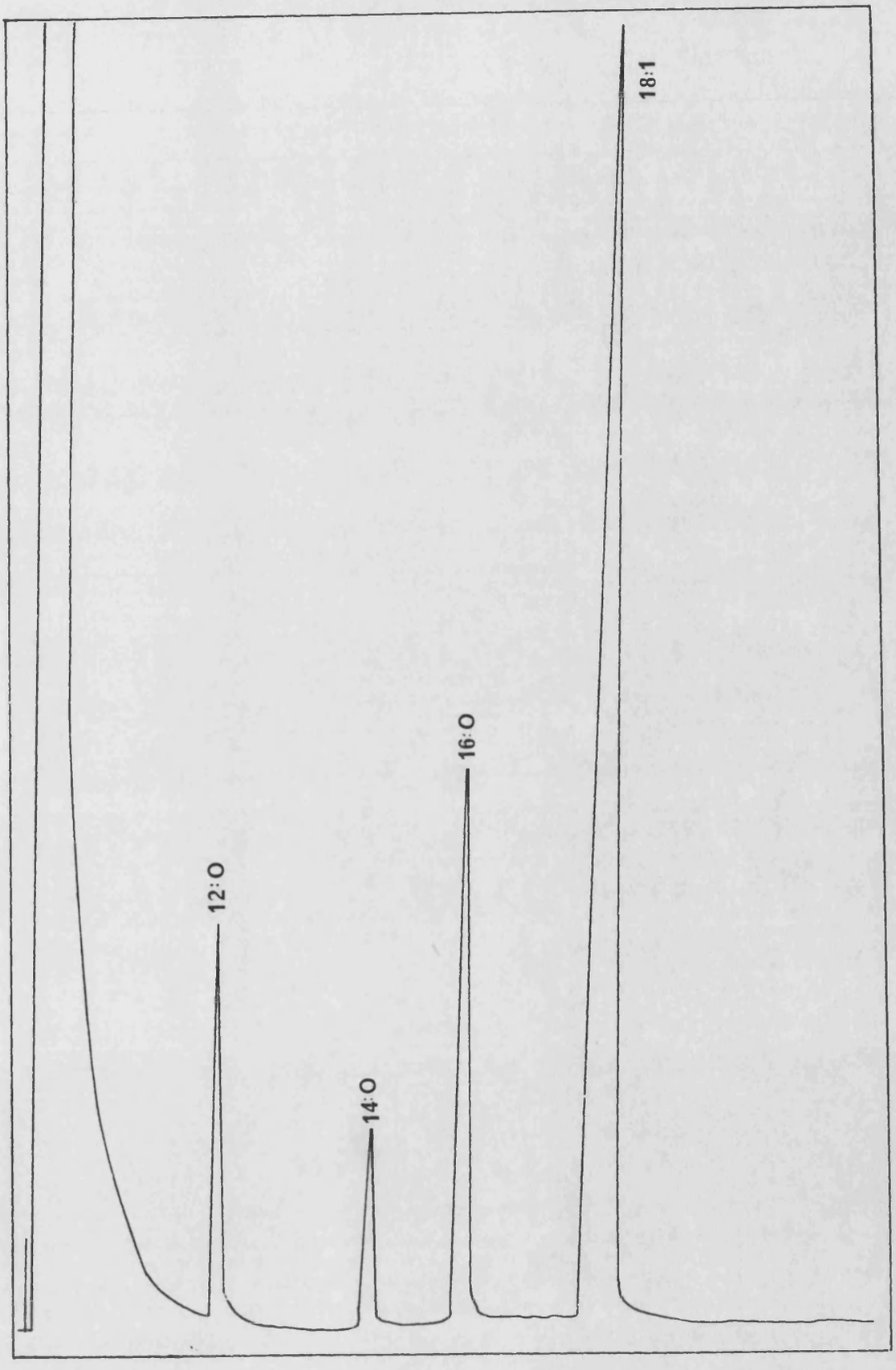

Figure 67
GLC trace for E. coli K1060 (18:1) , log phase.

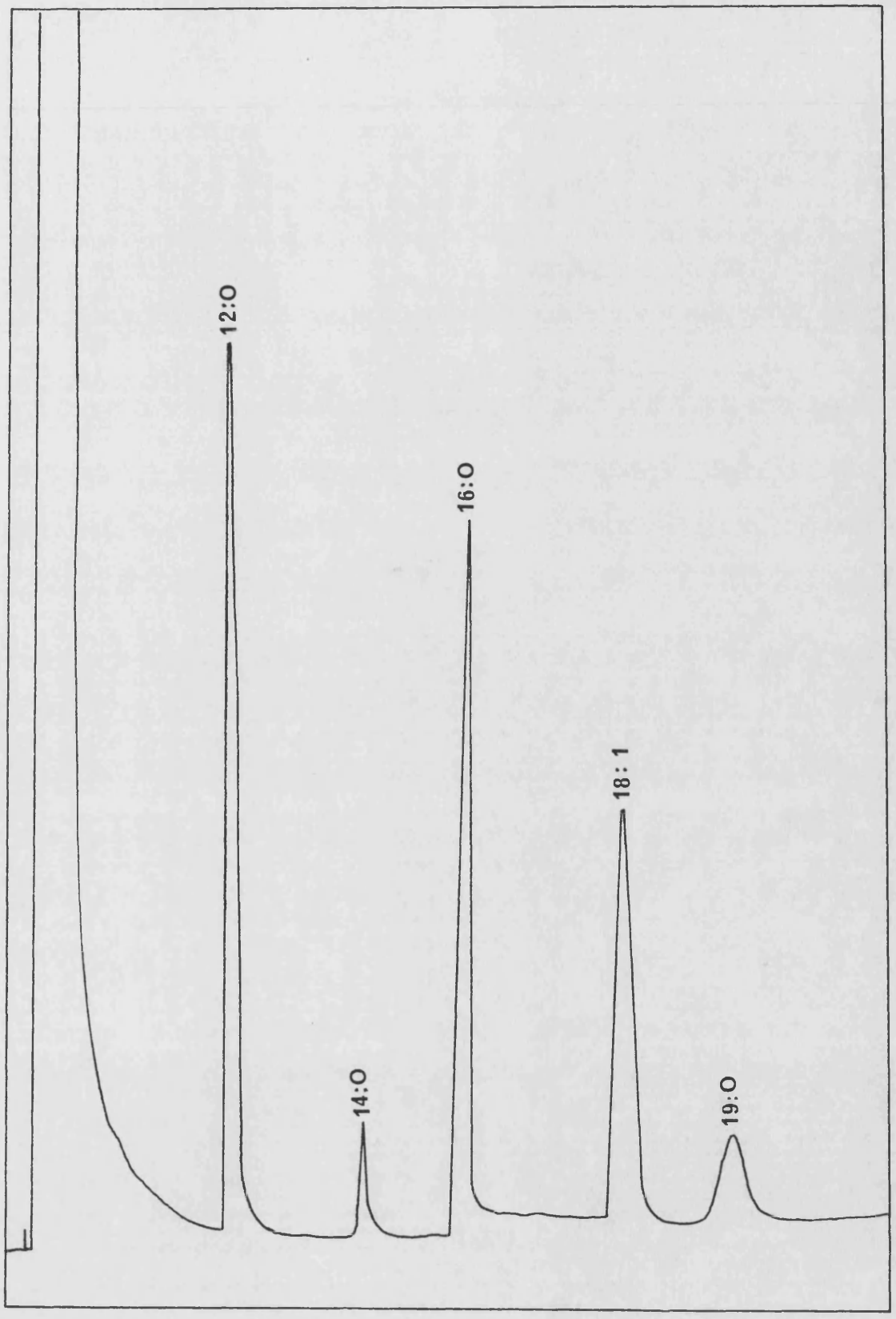

Figure 68
GLC trace for E. coli K1060 (18:1) ,stationary phase.

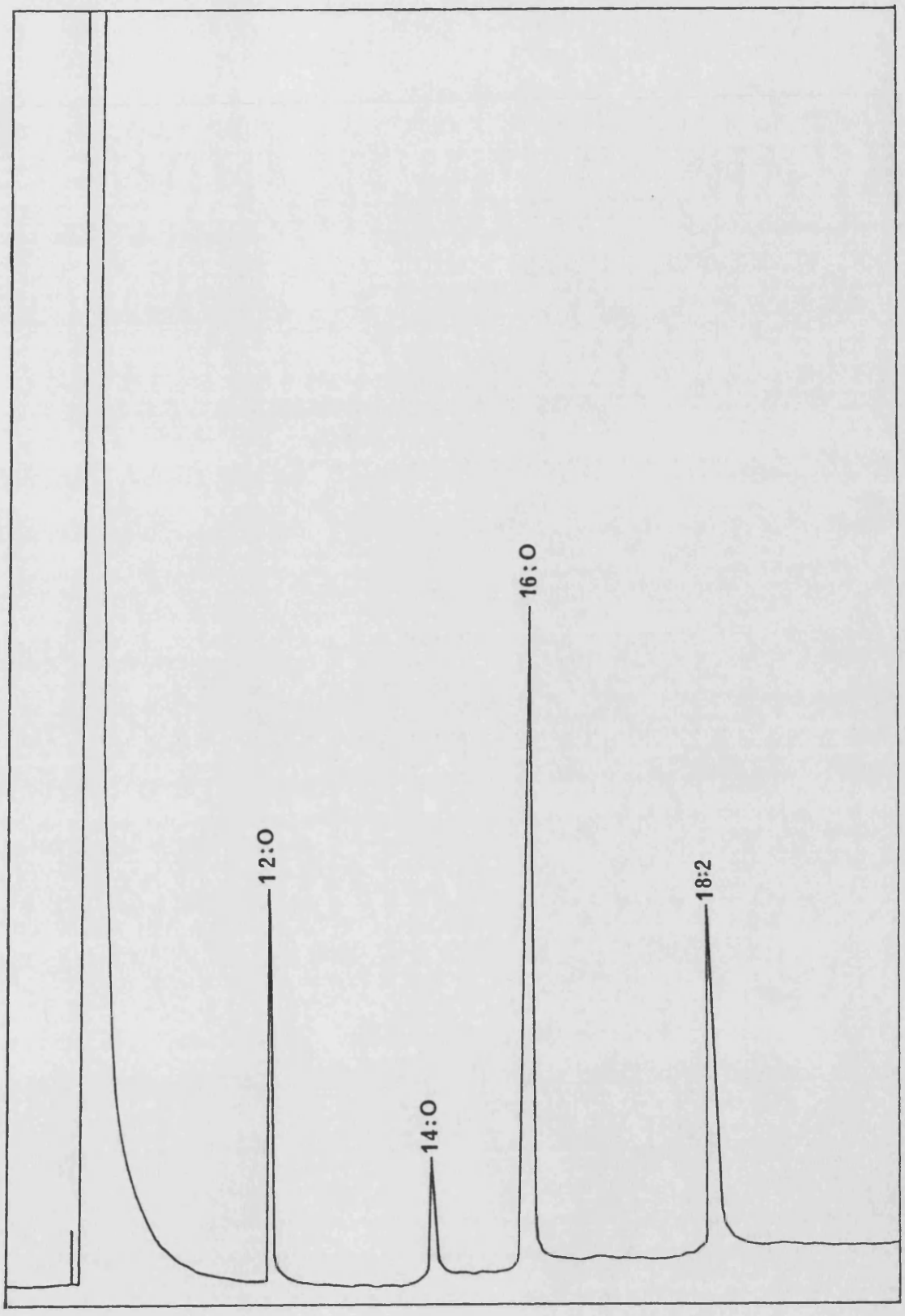

Figure 69
GLC trace for E. coli K1060 (18:2), log phase.

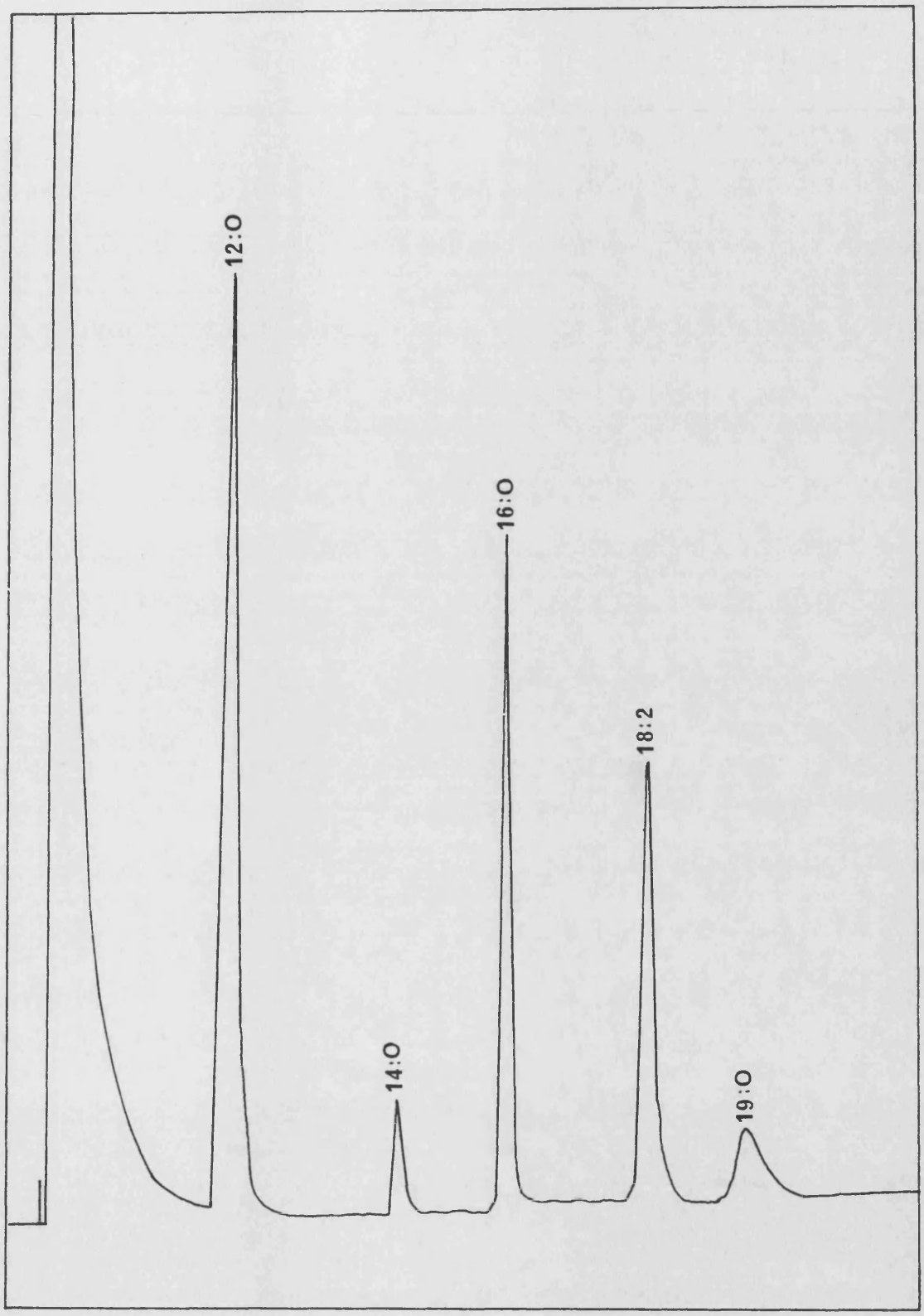

Figure 70
GLC trace for E. coli K1060 (18:2), stationary phase.

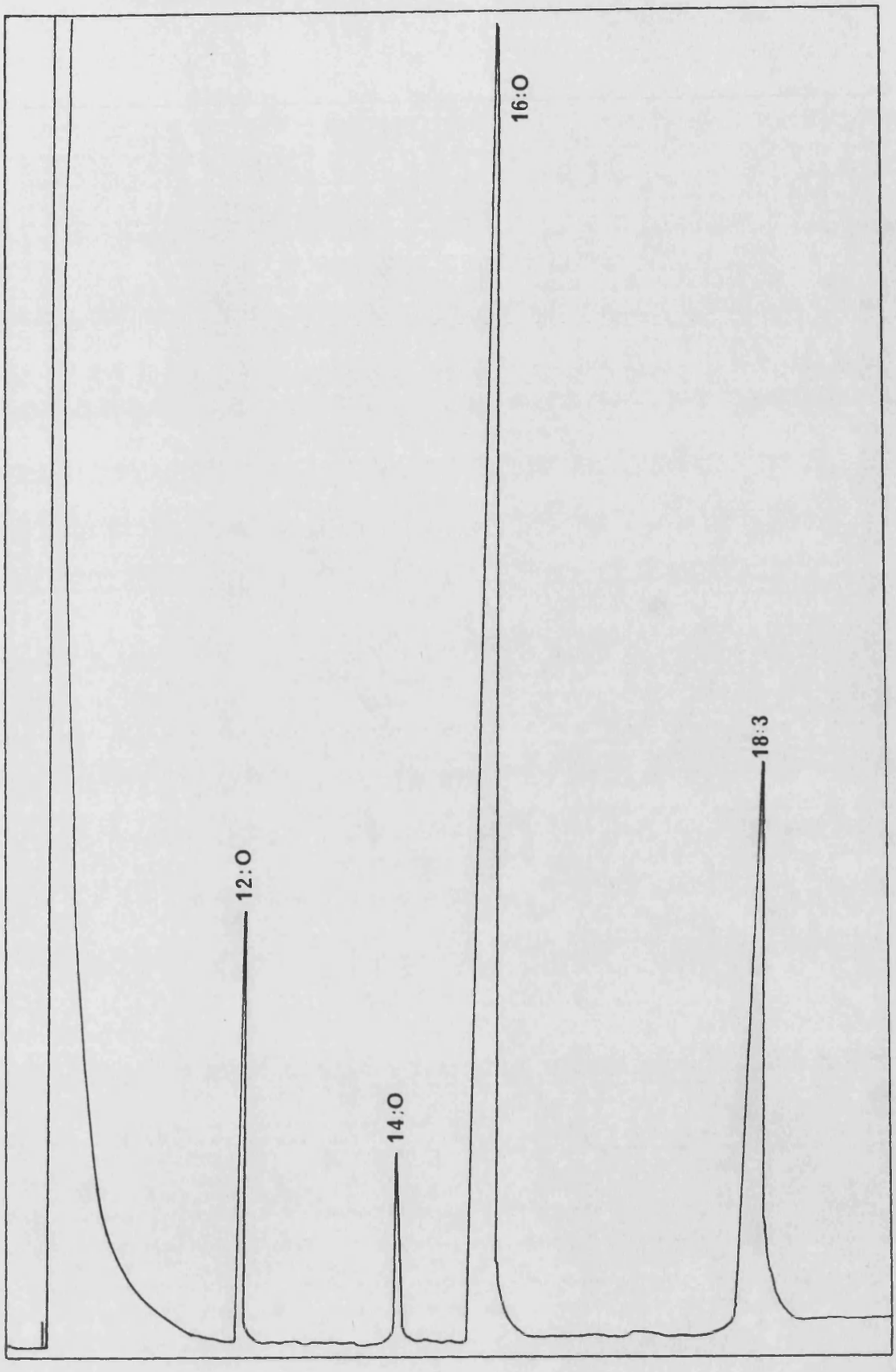

Figure 71
GLC trace for E. coli K1060 (18:3), log phase.

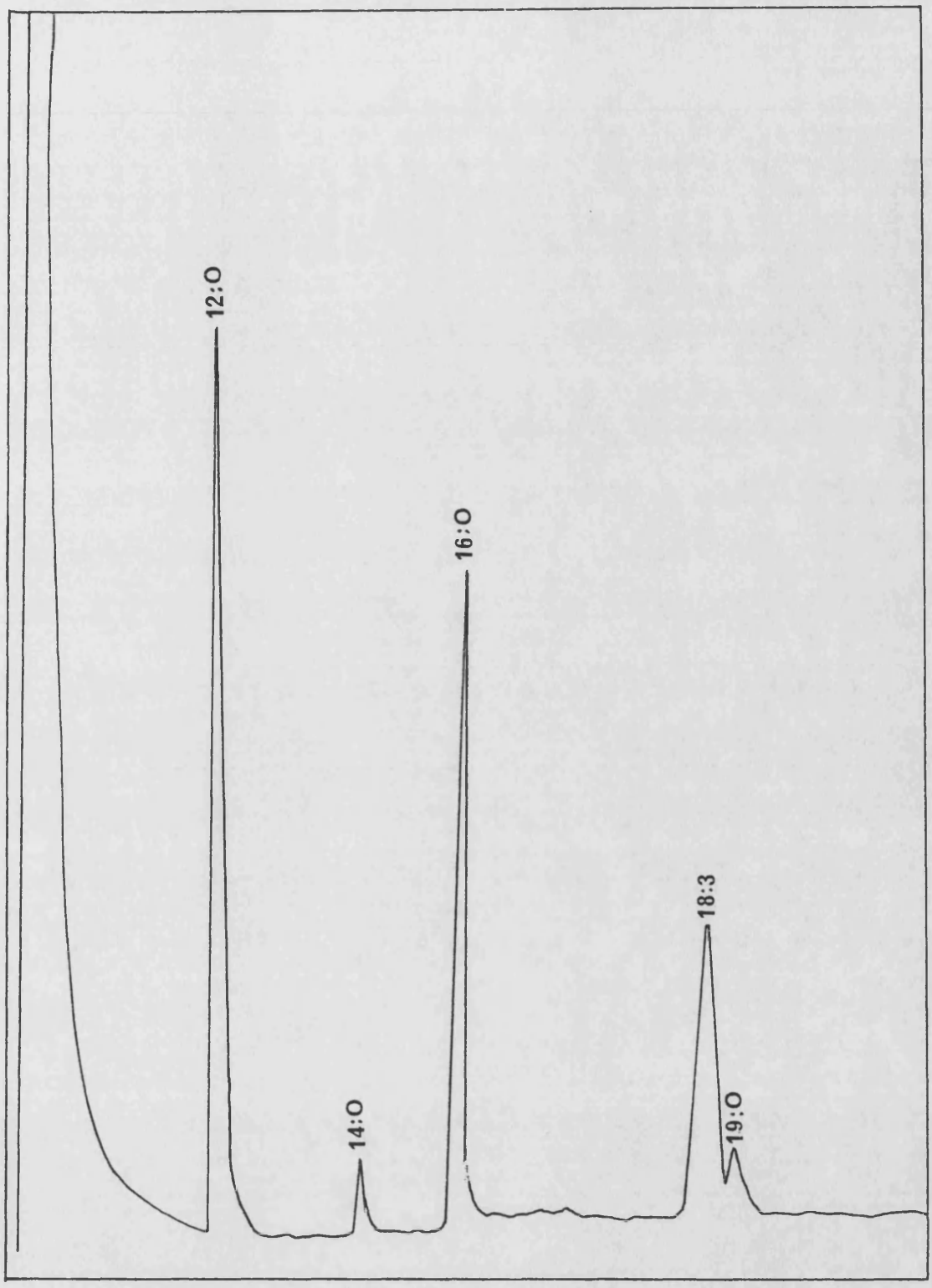

Figure 72
GLC trace for E. coli K1060 (18:3), stationary phase.

Table 9. The fatty acid composition of E. coli strains

Strain	Growth phase	% FATTY ACID 14:0	16:0	16:1	17:0	18:0	18:1	18:2	18:3	19:0	Unidentified	% Sat	% Unsat
SR362	Stat	6.2	53.1	9.9	18.5		12.3					77.8	22.2
SR246 (DM)	S	12.3	41.1	20.5	6.1	8.5	4.1			4.1	3.4	72.1	24.6
SR246 (Y)	S	5.0	39.7	19.7	19.3	1.3	13.1			1.7		67.0	32.8
B/r	S	7.5	56.5		4.7	4.7	7.5	7.8		1.6	9.6	70.3	15.3
AB1157	S	5.6	55.4	8.7	20.7		5.9			2.4	1.2	84.1	14.6
SR385	S	6.1	59.2	3.2	24.5		2.7			4.2		94.0	5.9
K-12	S	3.8	46.1	17.9			28.2			3.8		53.9	46.1
K1060	L	10.7	23.0				66.1					33.7	66.1
(18:1)	S	9.0	52.7				31.5			6.7		68.4	31.5
K1060	L	10.8	58.9					30.2				69.7	30.2
(18:2)	S	8.9	51.8					33.9		5.2		65.8	33.9
K1060	L	9.2	63.7						27.1			72.9	27.1
(18:3)	S	6.8	59.6						27.2	6.2		72.6	27.2
B. Stearo.	S	14.5	21.5		2.9	18.0	9.8			33		89.9	9.8

DM - defined medium Y - YENB

Other strains:

SR362 is the repair deficient strain used in biological dosimetry measurements. Its fatty acid composition is typical of the species.

B/r, (Fig. 73), AB 1157 (Fig. 74) and SR385 (Fig. 75b) have all been shown to have varying NUV-sensitivities and indications of NUV-induced membrane damage (Kelland, 1984). B/r exhibited several unidentifiable peaks, even following washing of the extract. The proportion of cyclopropane (17:0) fatty acids is lower than that of AB1157, SR385 and SR362, but of a similar level to that found in SR362.

SR246 is a strain which has been shown to be more sensitive to NUV irradiation following growth in rich media than when grown in minimal media. It exhibits the same relative sensitivities when irradiated with green light in the presence of Rose Bengal, which results in the production of singlet oxygen. Two chromatographs are shown, from stationary phase cells grown in rich (Fig. 77a), or defined (Fig. 76) media. The proportion of unsaturated fatty acids, due to a higher level of cis-vaccenic acid (18:1), is greater when grown in rich media.

The wild-type K-12 has a higher level of cis-vaccenic acid than the other strains analysed (Fig. 76b), resulting in an overall greater level of unsaturation.

B. stearothermophilus is a particularly heat- resistant bacteria, and has an absence of palmitoleic acid (16:1), and a high level of cyclopropane fatty acid (19:0) (Fig.77b).

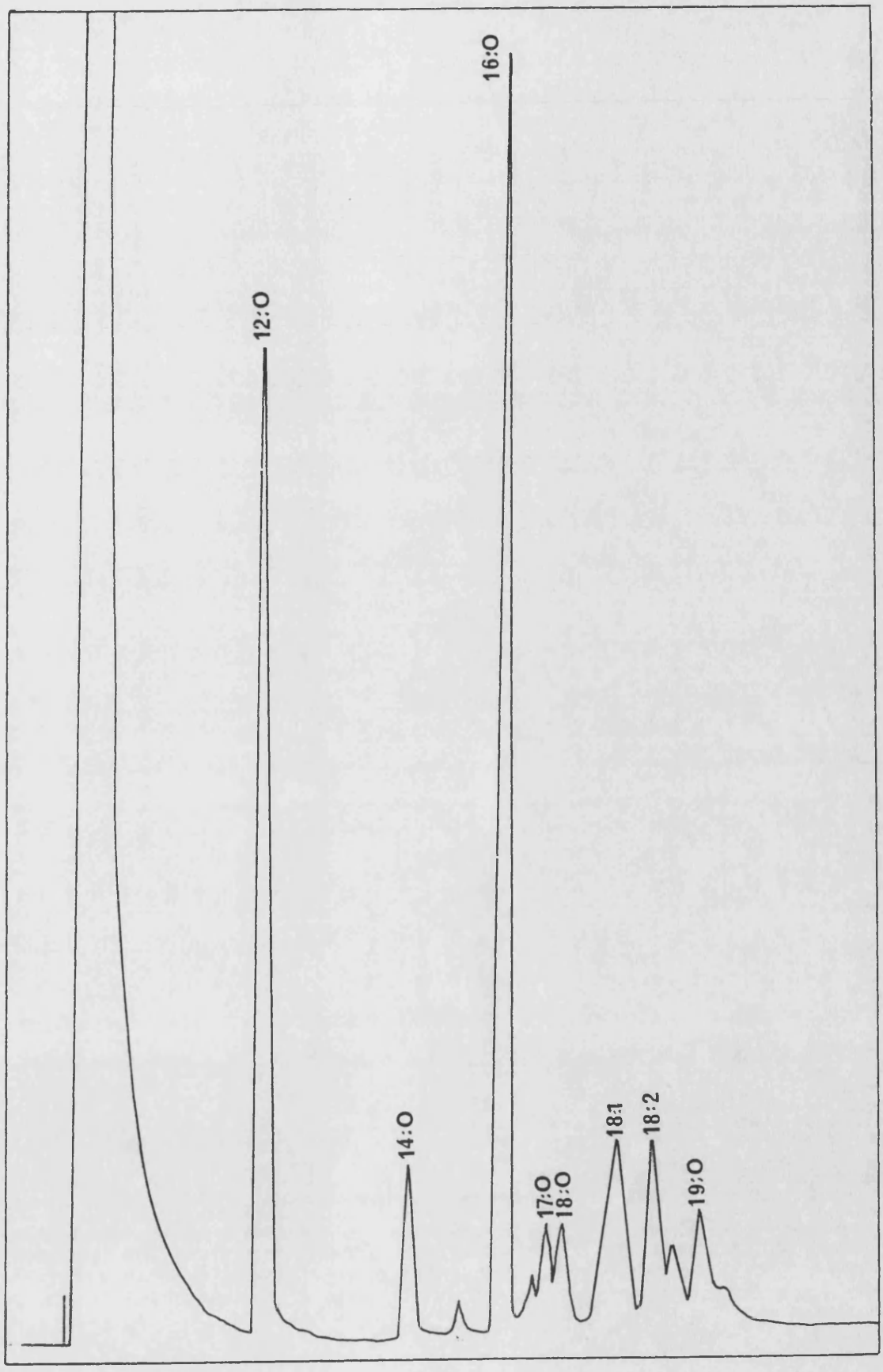

Figure 73
GLC trace for E. coli B/r, stationary phase.

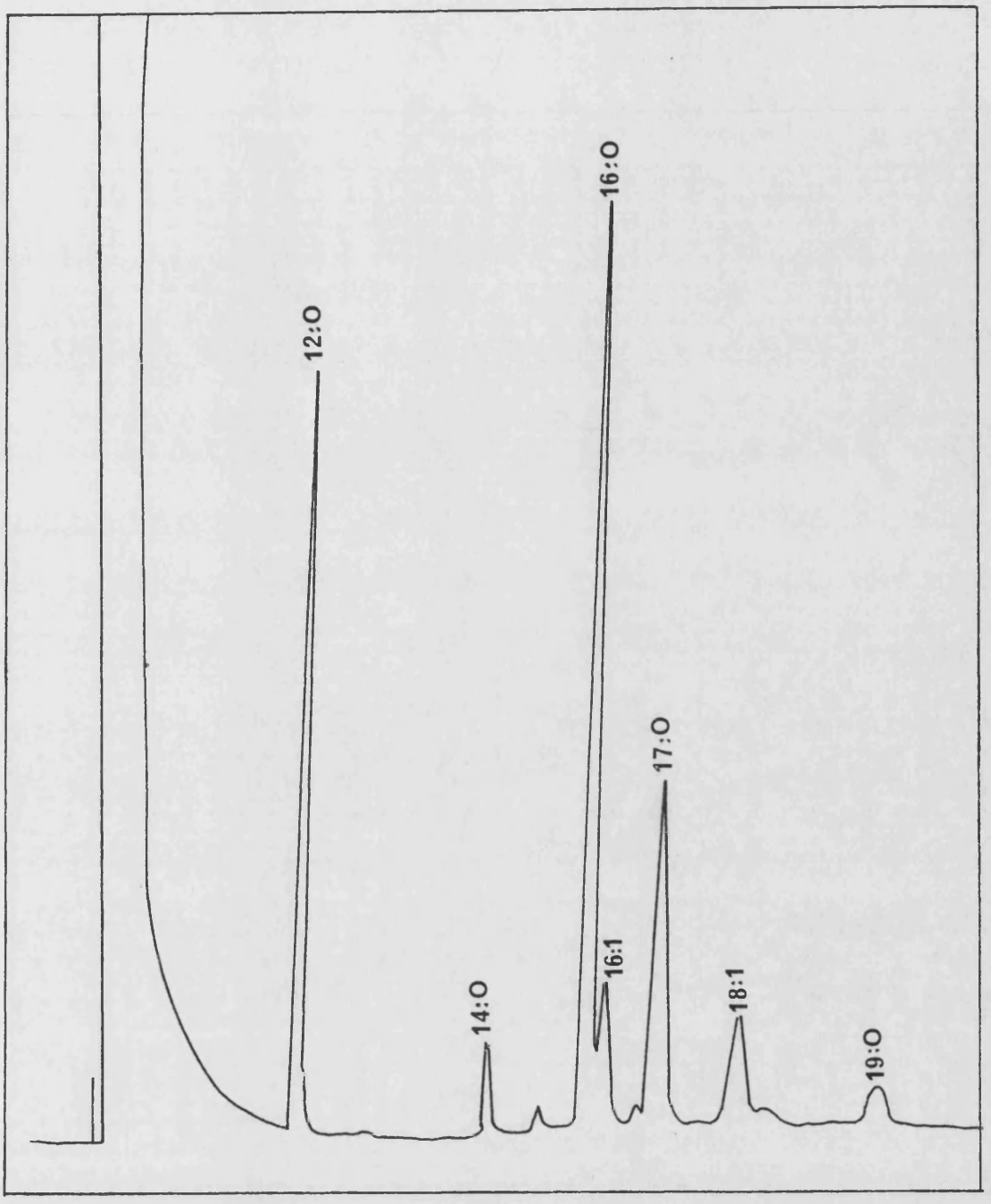

Figure 74

GLC trace for E. coli AB 1157 stationary phase.

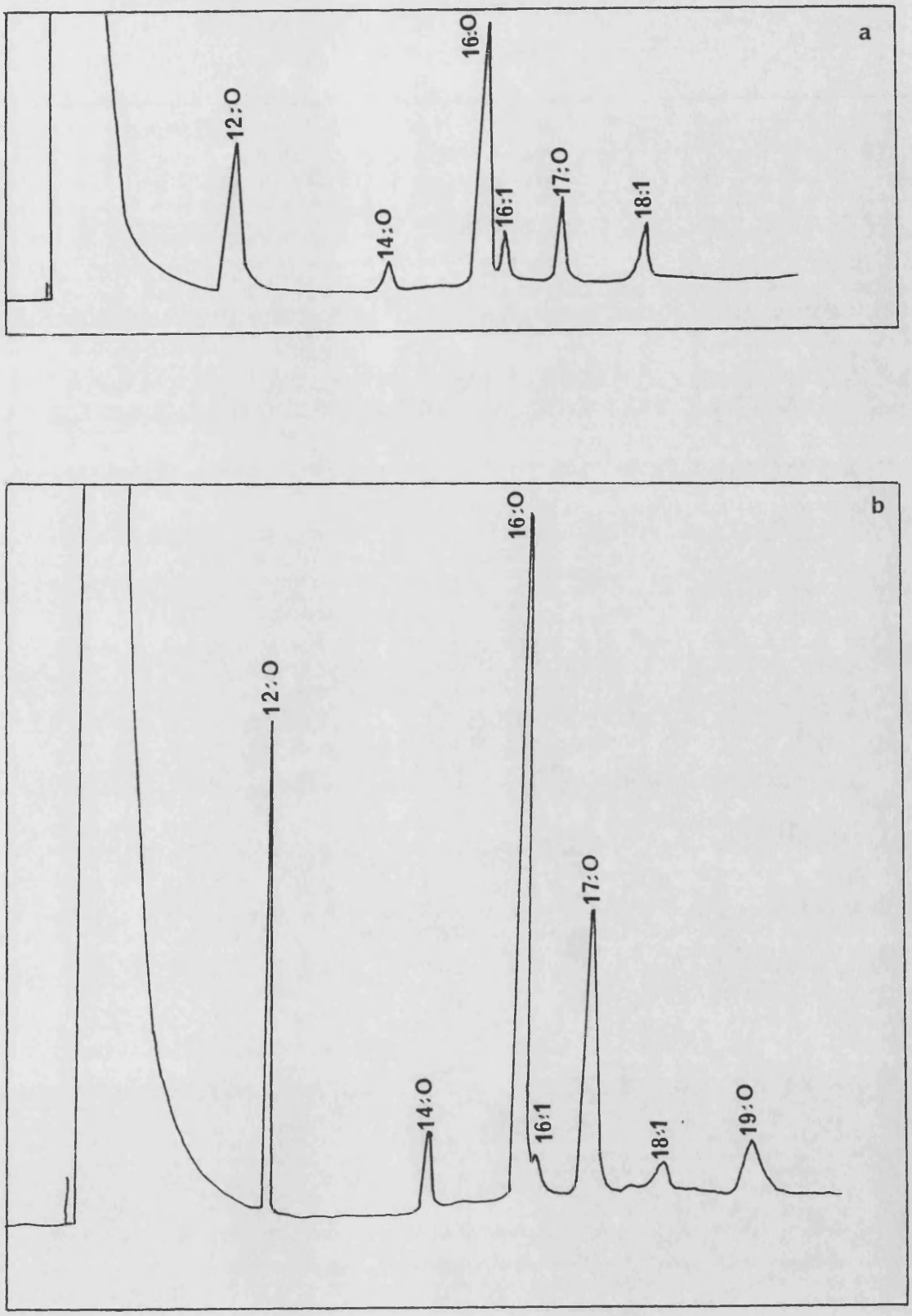

Figure 75
(a)GLC trace for E. coli SR 362 stationary phase

(b)GLC trace for E. coli SR 385 stationary phase.

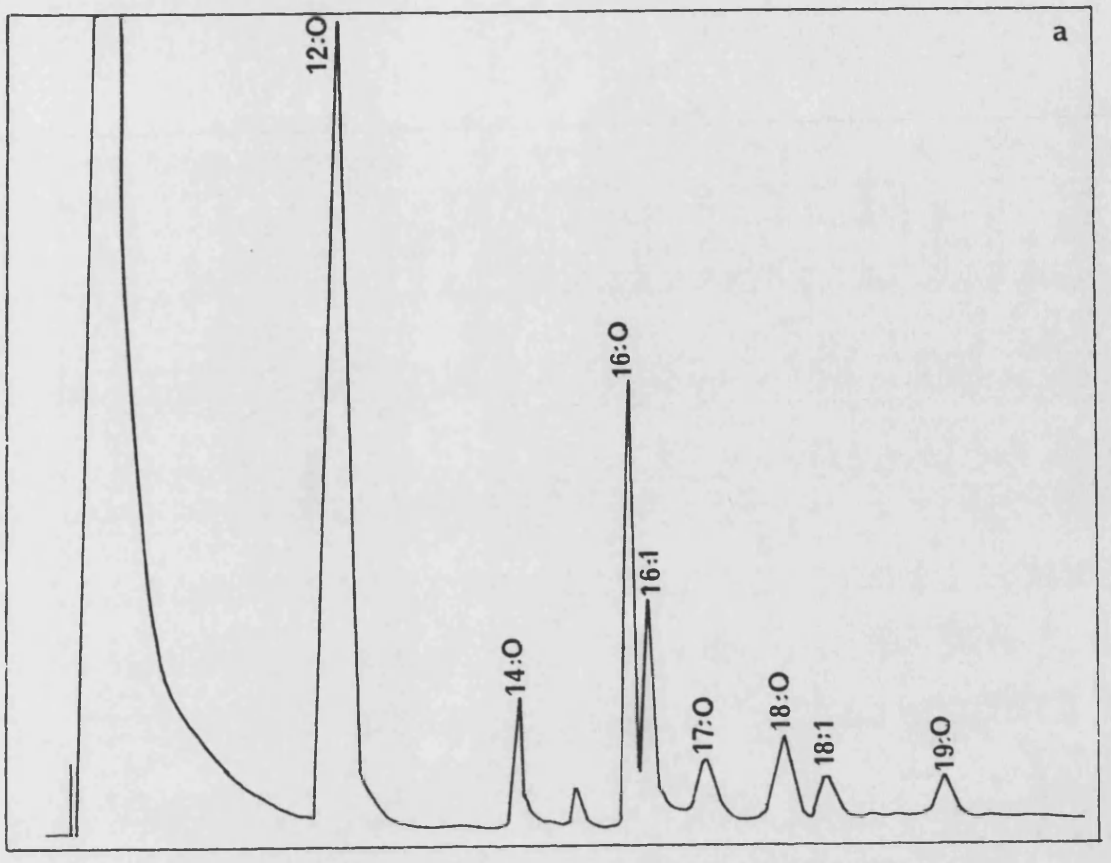

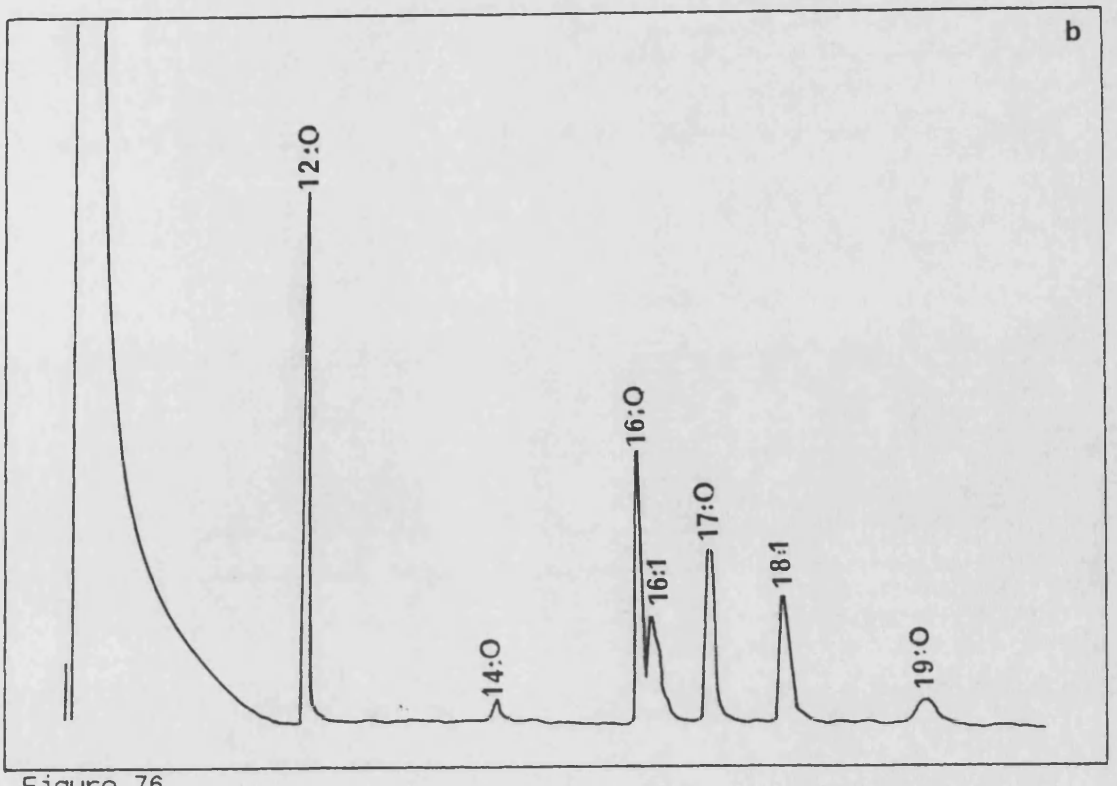

Figure 76
(a)GLC trace for E. coli 246 (defined medium) stationary phase.
(b)GLC trace for E. coli K12 stationary phase.

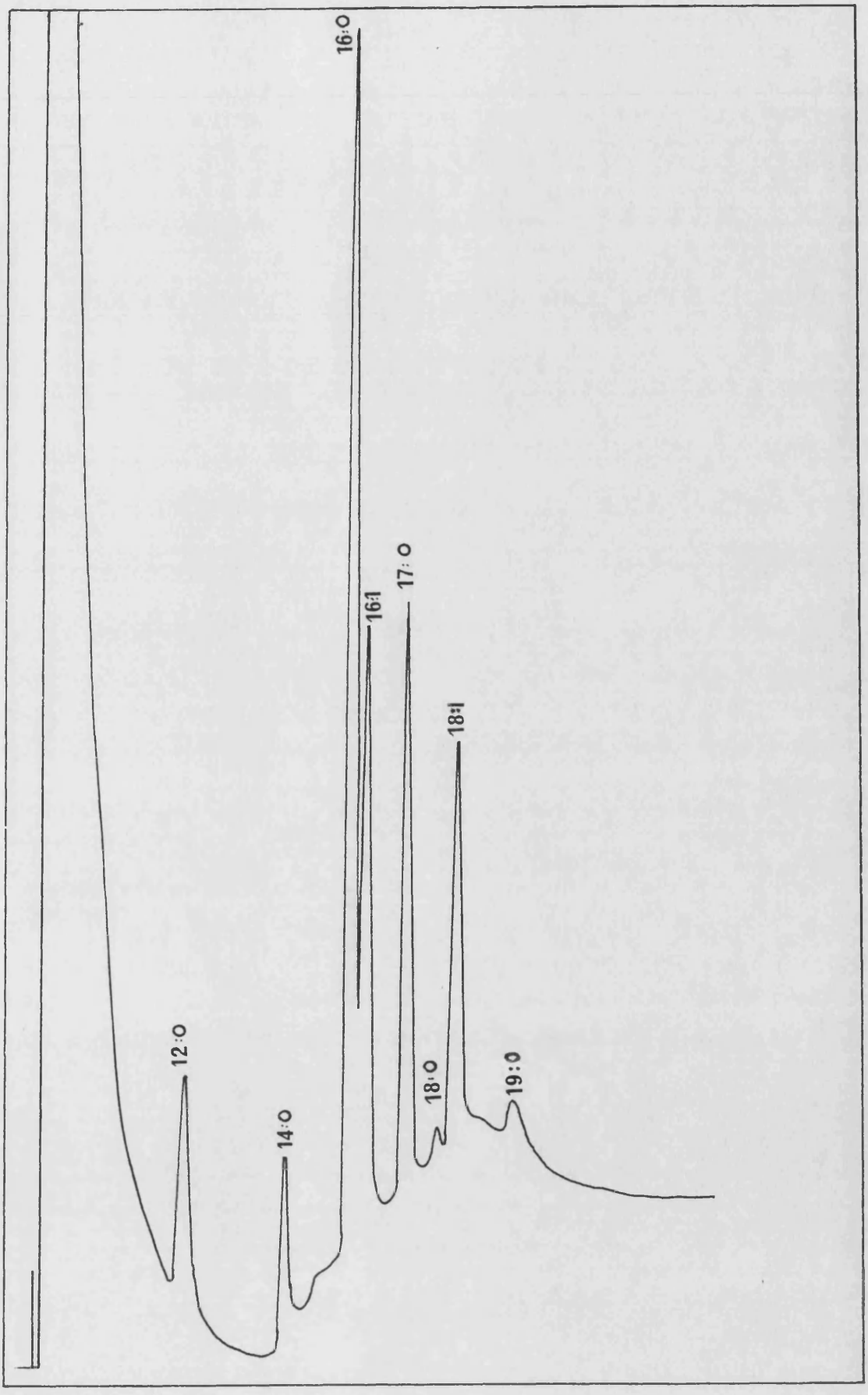

Figure 77a
GLC trace for E. coli 246 (YENB) stationary phase

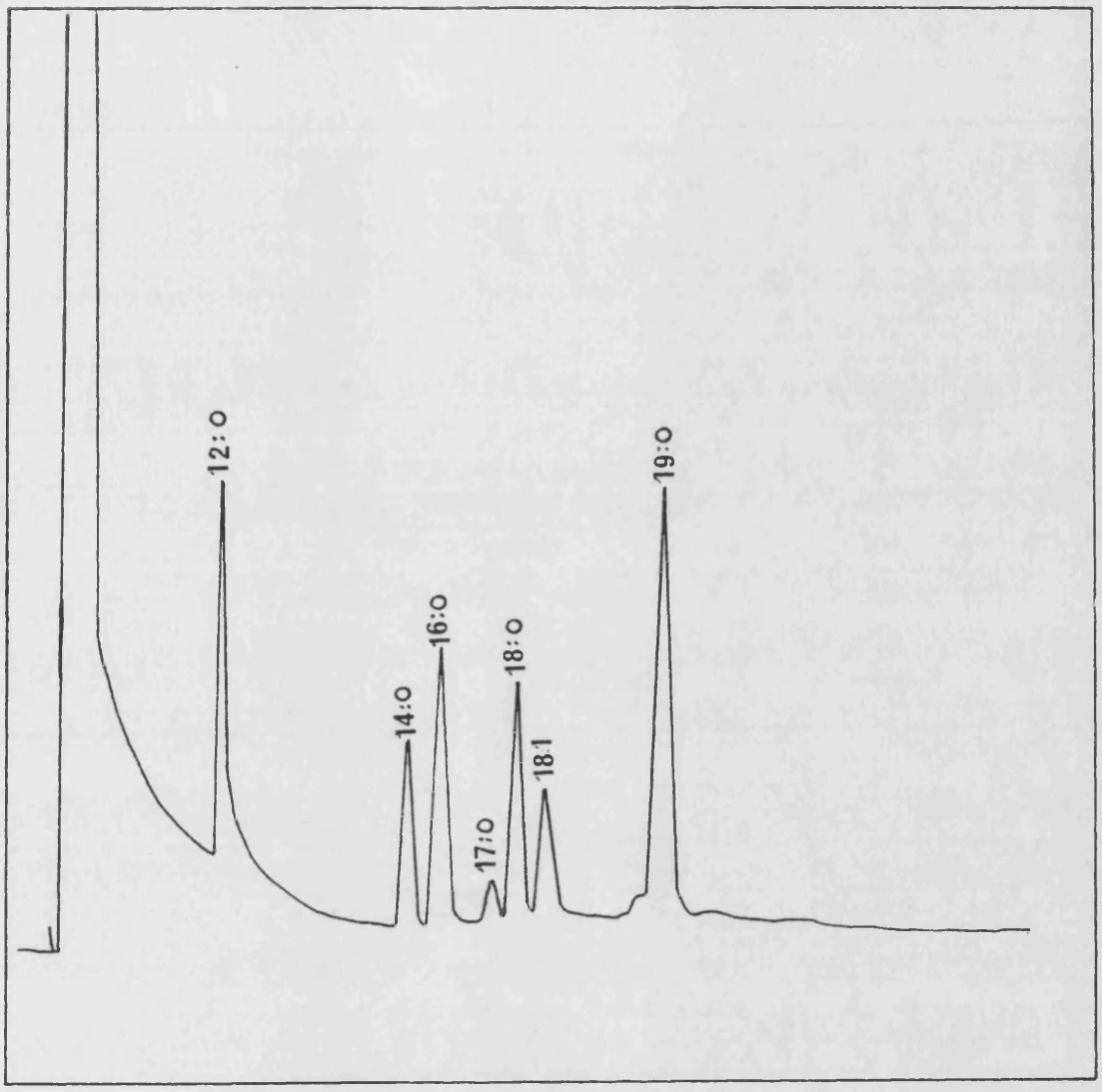

Figure 77b
GLC trace for B. stearothermophilus, stationary phase.

SUMMARY

In summary, it has been confirmed that E. coli K1060 incorporated the unsaturated fatty acid which was supplied in the growth medium. The conversion of unsaturated fatty acids to their cyclopropane derivatives has been shown to be inefficient when compared with other strains, thus a high proportion of unsaturated fatty acid remains in stationary phase cells.

The fatty acid analysis of other strains shows no remarkable differences which may be associated with near-UV sensitivity, with the exception of the SR246 strain which, following growth in rich medium, has a high proportion of unsaturated fatty acids, an interesting fact in view of its increased near-UV sensitivity following growth in such media.

RESULTS AND DISCUSSION

PART 2A

INVESTIGATIONS INTO NEAR-UV IRRADIATION-INDUCED LIPID PEROXIDATION IN HUMAN FIBROBLASTS

Results in Part 1 demonstrated lipid peroxidation and concomitant membrane leakage in E. coli K1060 cells. Mammalian cell membranes might be expected to show similar, or perhaps more evident, lipid peroxidation, since they include arachidonic acid (20:4) a polyunsaturated fatty acid, in addition to oleic (18:1) and linoleic (18:2) acids.(McAleer et al., 1987, reported the fatty acid composition of the GM730 strain of fibroblasts used here).

Sakanashi et al. (1986) described a delayed alteration in membrane fluidity due to the metabolism of lipid peroxidation products in B-16 melanoma cells following mid-UV irradiation. Earlier work showed near-UV-induced lipid peroxidation associated with membrane damage in erythrocytes and liposomes (Roschupkin et al., 1975), in lysosomes (Desai et al., 1965) and in liposomes (Mandal and Chatterjee, 1980). It was felt to be useful to investigate the phenomenon in fibroblasts since near-UV radiation is known to kill such cells (e.g. Keyse et al., 1983). Tyrrell and Pidoux (1986) have demonstrated a clear sensitivity of glutathione-depleted human skin fibroblasts to radiation of wavelengths ranging from 313 to 405 nm, indicating an important role of peroxidase damage.

In the first series of experiments, cells harvested from monolayers were irradiated in suspension in buffer, under conditions similar to those described for E. coli. Lipid hydroperoxides were assayed following broad-band near-UV

irradiation.

Comparisons were made throughout between GM730, a normal human skin fibroblast strain, and AR6L0, an actinic reticuloid strain, since the latter have been shown to exhibit *in vitro* cellular sensitivity to broad-spectrum near-UV irradiation (Giannelli *et al.*, 1983; Botcherby *et al.*, 1984) and to monochromatic 365 nm near-UV (Kralli and Moss, 1987). Trolox-C has been shown to reduce this sensitivity (Kralli and Moss, 1987) at 25°C, indicating a deficiency on the part of this cell line in overcoming oxidative damage.

1. THE NEAR-UV IRRADIATION OF FIBROBLASTS IN SUSPENSION AND DETERMINATION OF LIPID PEROXIDATION

Cells were irradiated in suspension in PBS (B) buffer in order to preclude the formation of toxic photoproducts during irradiation (Wang *et al.*, 1974). The broad-band NUV source used is described in the Methodology. Lipid hydroperoxides were measured on the whole suspension, and a peroxide value (PV) was calculated with reference to control, unirradiated suspensions. Due to the turbidity of the suspensions they were centrifuged (MSE Bench Centrifuge, 4000 rpm x 5 mins) before optical density measurements were taken.

Fig. 78a shows the results of 3 experiments where lipid peroxidation was measured in GM730 fibroblasts following long exposures to broad-band NUV radiation.

From Fig. 78b it can be seen that AR6L0 cells undergo similar peroxidation.

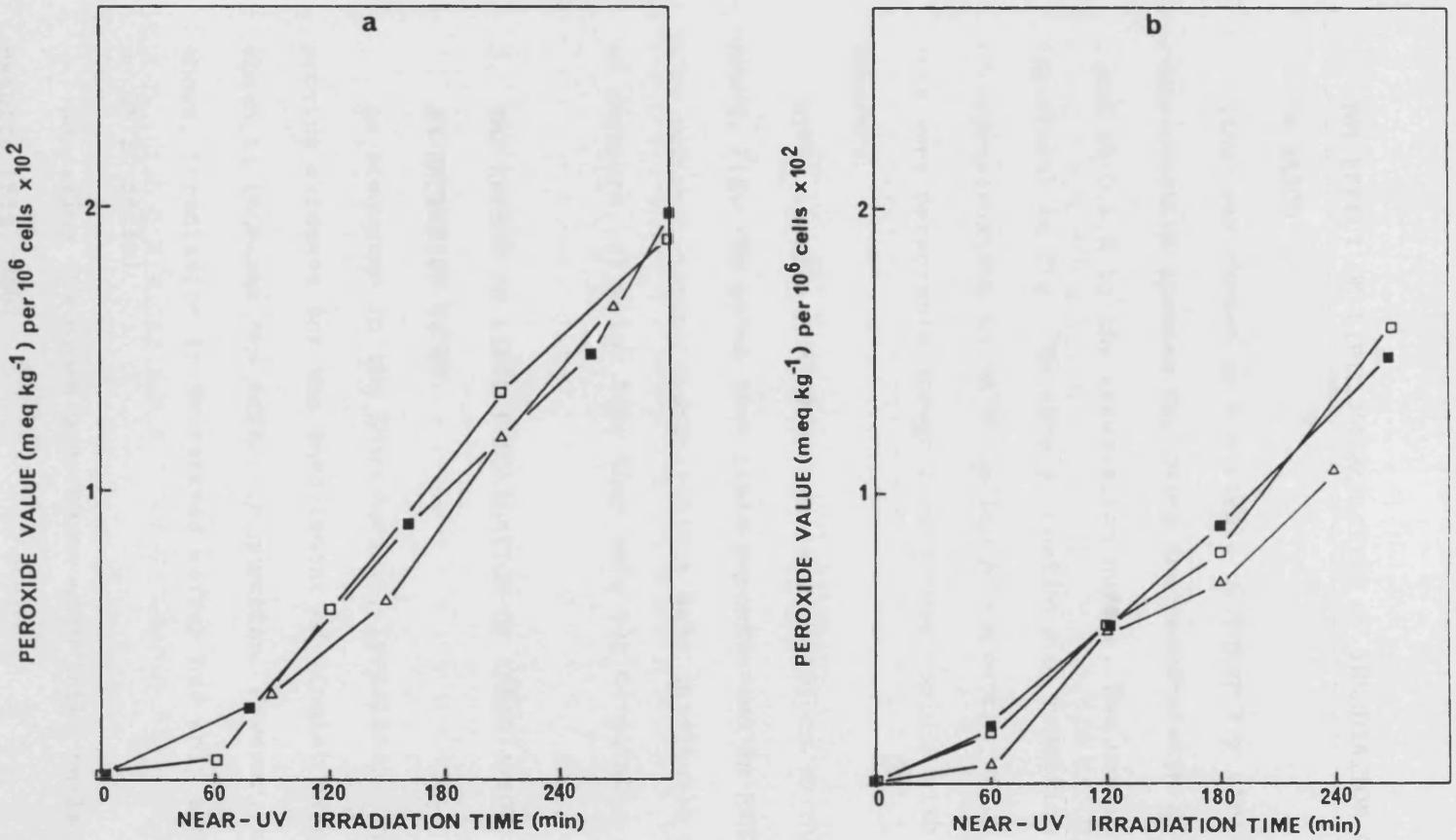

Figure 78 Lipid peroxidation in (a) GM730 (b) AR6L0 fibroblasts following near-UV irradiation. Alternate symbols represent replicate experiments.

2. THE EFFECT ON LIPID PEROXIDATION OF IRRADIATION OF FIBROBLASTS IN DABCO

DABCO was chosen as a suitable quencher for singlet oxygen or other reactive species following the results with E. coli. It was added at 0.1 M to the irradiation buffer. The results of such an experiment in Fig. 79a show a considerable reduction in the level of hydroperoxides in GM730 cells. At exposures of up to 150 min none were detectable though levels rose rapidly with further exposure.

After irradiation under similar conditions to those described above, Fig. 79b shows that lipid peroxidation in AR6LO cells is also reduced, though hydroperoxides were detectable after 120 min of exposure, at which time they were not detectable in GM730 cells.

3. THE EFFECT ON LIPID PEROXIDATION OF IRRADIATION OF FIBROBLASTS IN DEUTERIUM OXIDE

As discussed in the Introduction, irradiation in D_2O may provide evidence for the invovlement of singlet oxygen if it is shown to increase the effect in question. However, as Fig. 80a shows, irradiation in deuterated buffer had only a marginal effect on GM730 cells.

Repeating the above experiment with AR6LO cells yielded similar results (Fig. 80b).

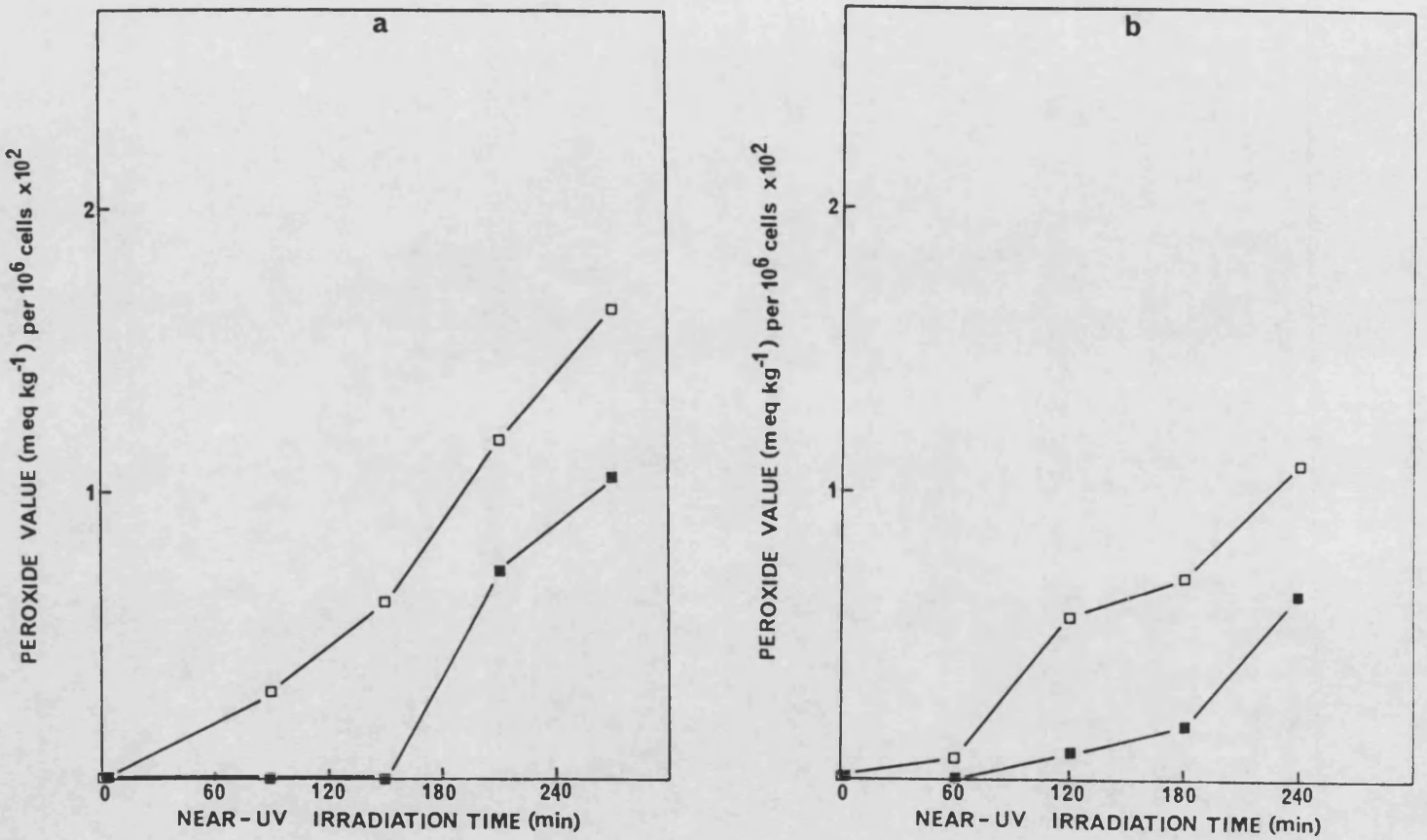

Figure 79 Lipid peroxidation in (a) GM730 (b) AR6L0 fibroblasts following near-UV irradiation in the presence (■) or absence (□) of DABCO.

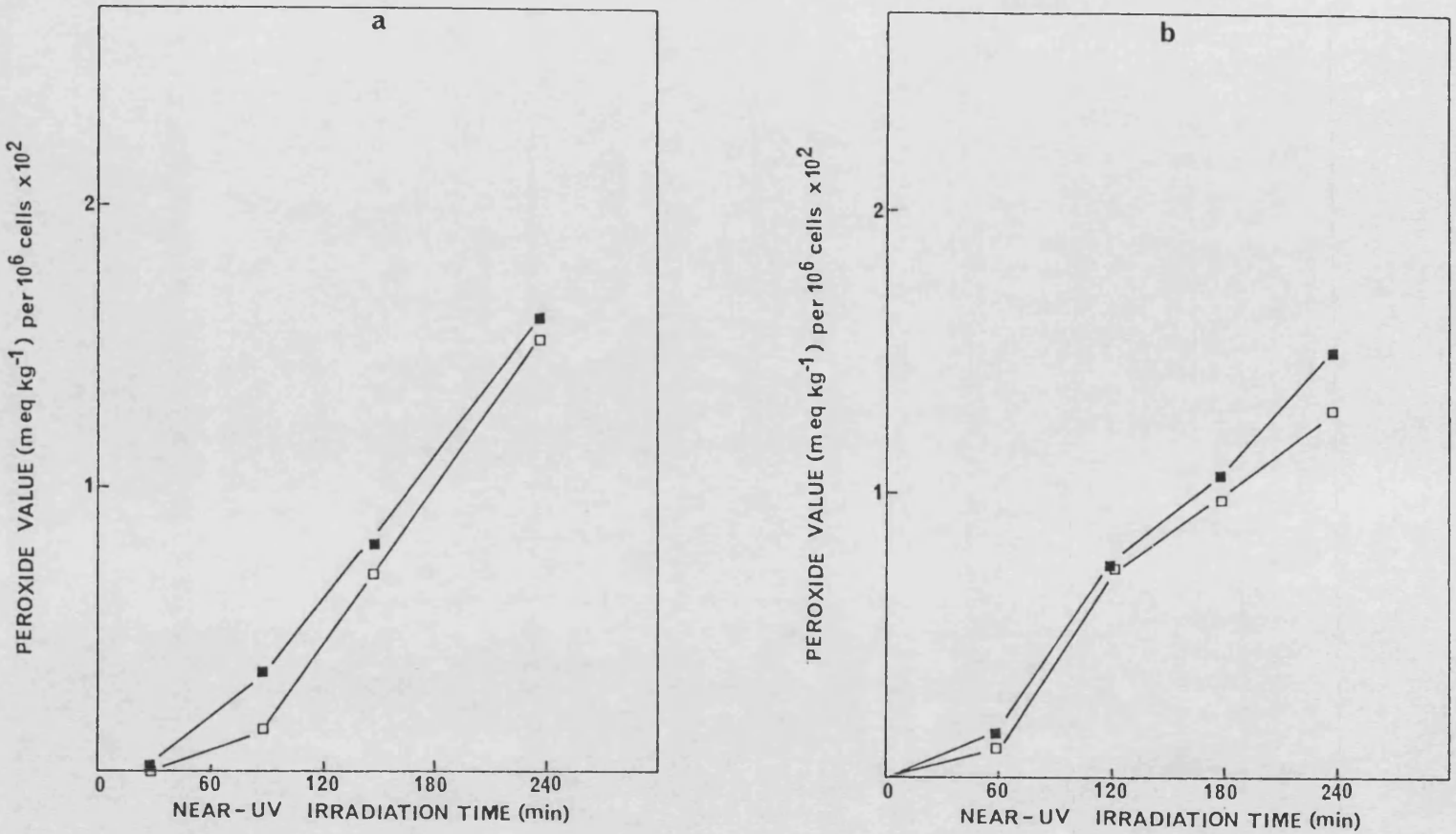

Figure 80 Lipid peroxidation in (a) GM730 (b) AR6L0 fibroblasts following near-UV irradiation in the presence (■) or absence (□) of D_2O.

4. THE EFFECT OF GLUTATHIONE-DEPLETION ON NUV-INDUCED LIPID PEROXIDATION IN FIBROBLASTS

As previously discussed, growth in Buthionine sulfoximine (BSO) depletes cells of intracellular glutathione. As reported by Tyrrell and Pidoux (1986) this results in the sensitization of human skin fibroblasts to both mid- and near-UV monochromatic radiations, apparently due to the inability of glutathione peroxidase to function in the absence of glutathione. To investigate the effect of such depletion on the irradiation-induced peroxidation in fibroblasts, BSO was added, as a sterile solution at 500 mM, to the media of plates which had been subcultured 3 days previously.

Cells were trypsinized for use the following day (i.e. after at least 18 hours incubation with BSO). It is documented that this reduces the levels of intracellular glutathione to about 5% of the normal level (Tyrrell and Pidoux, 1986). Cells were subsequently treated in the standard way. Lipid peroxidation was found to be increased (Fig. 81a) at all fluences, using GM730 cells.

Fig. 81b shows that AR6LO cells also exhibit an increased level of lipid peroxidation.

5. POST-IRRADIATION LEVELS OF HYDROPEROXIDES IN FIBROBLASTS

Irradiated cells may be subjected to peroxidative stress with which they are adequately able to deal. Sakanashi et al. (1986) demonstrated TBA-reacting materials following mid-UV irradiation of melanoma cells. The level of those products was found to decrease to normal levels within three hours, and in the following three hours had reached levels of 20 per cent lower than control levels.

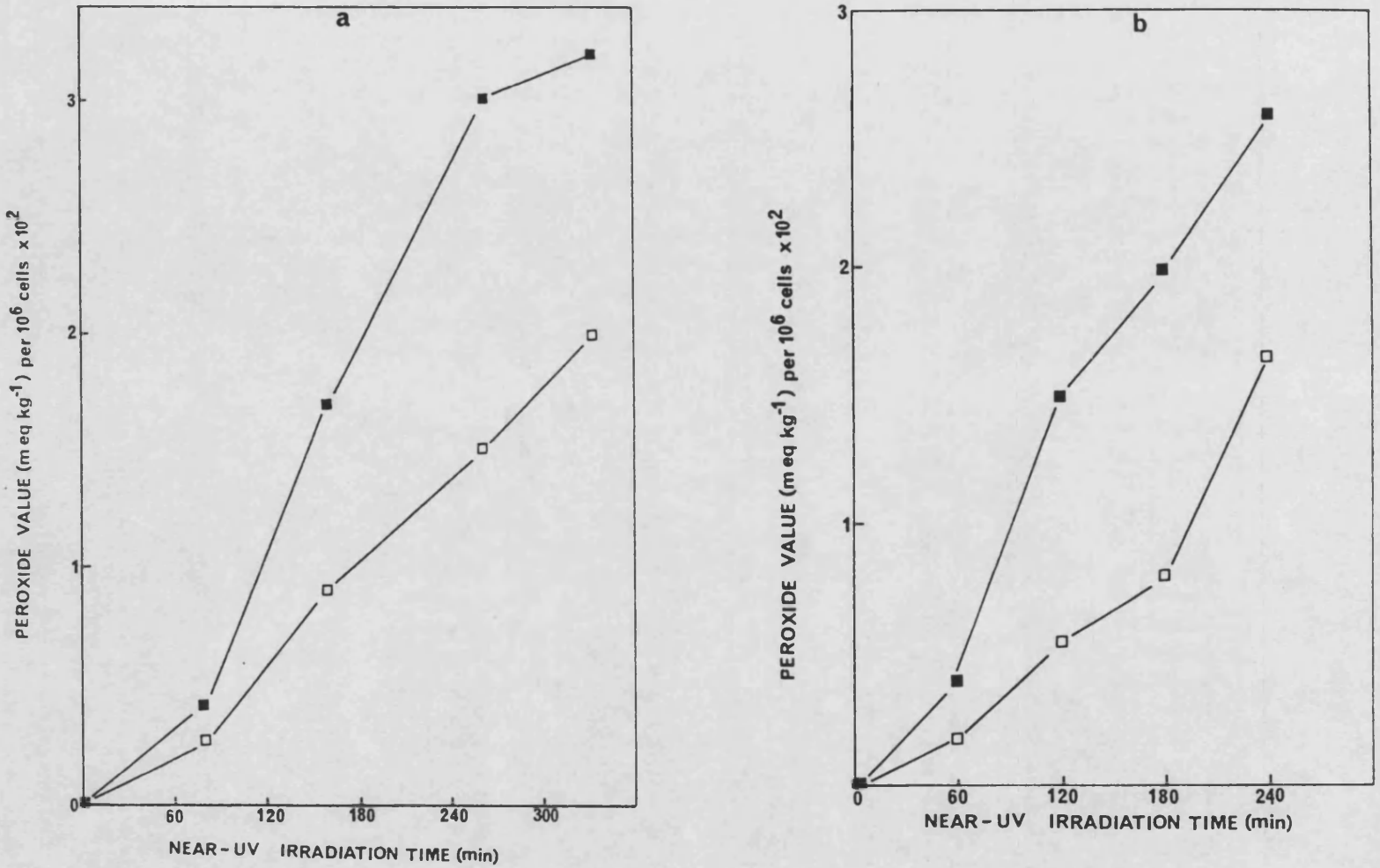

Figure 81 Lipid peroxidation in (a) GM730 (b) AR6L0 fibroblasts following near-UV irradiation after growth in the presence (■) or absence (□) of BSO.

Experiments were carried out on suspensions of GM730 and AR6L0 fibroblasts, where the PV was determined immediately following irradiation and over a subsequent period where cells were incubated, in the irradiation buffer, at 37°C.

From the results of such experiments, presented in Table 10, it is evident that the level of hydroperoxides does decrease in the post-irradiation period, within 30 mins. The degree of reduction is variable, however, though BSO-treated cells are clearly less able to reduce the hydroperoxides. This line of investigation was not pursued for the same reasons as those discussed below.

Table 10. The Peroxide Value (PV) of irradiated fibroblasts in the hour subsequent to the end of broad-band near-UV irradiation

Cell Type/ Conditions	PV per 10^6 cells determined at times indicated after irradiation		
	0 min	30 min	60 min
AR6L0	.020	.010	.010
AR6L0	.019	.0069	.0047
AR6L0	.022	.0037	-
GM730	.030	.010	.010
GM730	.008	.0055	.0011
GM730+	.053	.0055	-
GM730+	.053	.0055	-
GM730*	.058	-	.016
GM730 + BSO	.032	.055	.02
GM730 + BSO	.071	.039	.031

* or + represent matched cells.

SUMMARY

The results clearly indicate that lipid peroxidation results from the broad-band near-UV irradiation of both lines of fibroblasts. While DABCO reduces the degree of peroxidation, irradiation in D_2O does not result in an increase. It is therefore not possible to implicate singlet oxygen as the mediator of lipid peroxidation in these cells, where perhaps free radical reactions should be considered as an alternative. It is, however, surprising that irradiation in D_2O did not result in an increase in peroxidation. Repeat experiments were performed on separate batches of cells over a period of 4 months, and while it was always evident that hydroperoxides were present in irradiated cells, unirradiated control cells in D_2O also showed similar peroxidation. Problems were also experienced due to the clumping together of cells when irradiated in D_2O.

The depletion of glutathione by growth in BSO-medium resulted in increased peroxidation, which may contribute to the increased sensitivity of such cells to near-UV irradiation as reported by Tyrrell and Pidoux (1986). A Peroxide Value (PV) of 1.0 for a sample of 10^6 cells represents 3×10^{11} molecules of active oxygen, that is hydroperoxide molecules, per cell. The degree of disorder caused by this level of peroxidation is difficult to relate to the survival of, or stress to a cell, particularly as the hydroperoxides are subsequently reduced. In addition, fatty acids are not confined to membranes in the eukaryotic cell grown in culture, where they may be found in intracellular pools as triacylglycerides (King and Spector, 1981), so that lipid peroxidation may not necessarily reflect membrane damage.

It can be seen that the exposures required to achieve measurable lipid peroxidation are long, and would, by extrapolation from Kralli's data (1987) have reduced the population by several orders of magnitude as shown in Fig. 82. If near-UV-induced effects are detectable at fluences which do not result in overkill, their biological importance may be more positively assessed. However, the inability to demonstrate an effect, for example lipid peroxidation, at such fluences does not preclude the importance of that effect. The limits of the assay method may not allow detection of a biologically important level of lipid hydroperoxides.

Kralli (1987), while determining the majority of survival curves from cells irradiated in suspension, also reported the leakage of rubidium from AR6L0, but not GM730 fibroblasts, irradiated as monolayers with broad-band near-UV light. An important consideration during the irradiation of cells as a monolayer is the relative exposure of membrane and nucleus as shown below, due to the different shapes assumed by the cells.

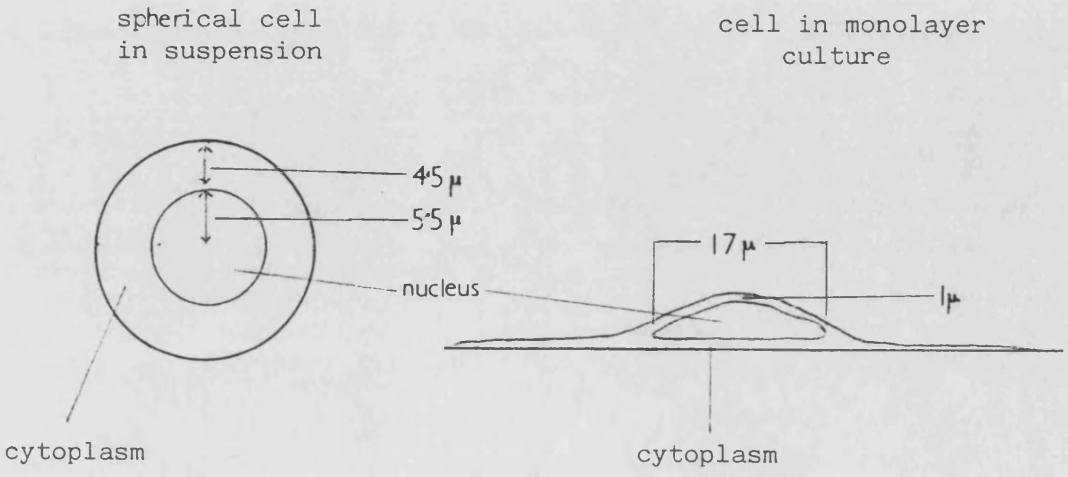

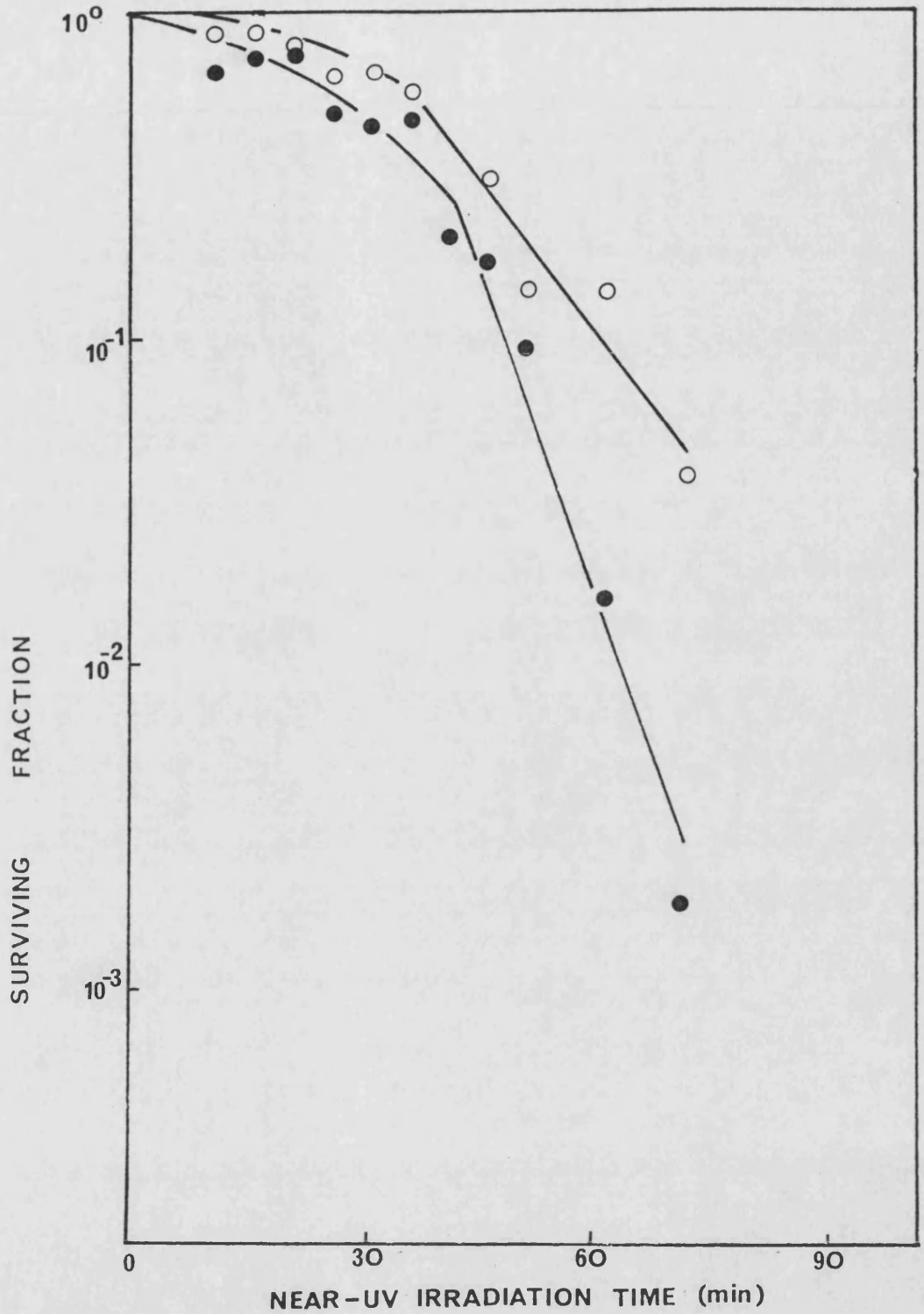

Figure 82

The inactivation of AR6L0 (●) and GM730 (○) cells as a function of near-UV irradiation time. (From Kralli, 1987).

Cells attached and growing as a monolayer obviously expose, not only the nucleus, but a constantly greater surface area of membrane to a unidirectional radiation source. Comparisons are therefore difficult between data where cells were irradiated in suspension or as a monolayer. In addition, the process of trypsinization must damage the membrane to some extent even before irradiation. This was confirmed when rubidium leakage experiments were performed on trypsinized cells, resulting in total, immediate loss of $^{86}Rb^{+}$ after trypsinization. It was intended that experiments here should allow comparison with Kralli's data (Kralli, 1987), therefore subsequent work was confined to the irradiation of cells as monolayers, using moderate fluences.

THE MEASUREMENT OF LIPID PEROXIDATION IN IRRADIATED MONOLAYERS

Monolayers were used at 4 to 5 days old, when growth had just reached confluence. The medium was removed with a Pasteur pipette, and the monolayer was washed 3 times with 10 ml PBS (B). Ten ml PBS (B) were then added to the plate, which was irradiated with the lid on, using the light source described. Two plates could be irradiated simultaneously. At the end of the irradiation period 0.5 ml aliquots of the buffer were removed and lipid hydroperoxides were measured. The irradiation volume was maintained by replacing the sample with fresh PBS (B).

Matched plates were always used as unirradiated controls, being kept wrapped in foil to exclude light during the time of the experiment. Cell numbers were determined by trypsinization at the end of the experiment and counting with a haemocytometer.

Results, however, were negative. No peroxidation was detectable until cells had been exposed for approximately 4½ hours. After such exposure the monolayer was observed microscropically, and was noticeably abnormal, and even after 2½ hours irradiation AR6LO cells were shrivelled, their processes withdrawn, and dark cytoplasmic inclusions were evident.

Attention was therefore given to the effect which near-UV irradiation might have on membrane function as assessed by changes in the rate of pinocytosis, as described in the following section.

RESULTS AND DISCUSSION

PART 2B

INVESTIGATIONS INTO CHANGES IN PINOCYTOSIS INDUCED BY THE NEAR-UV IRRADIATION OF HUMAN FIBROBLASTS

As described in the Introduction endo- and exocytosis occur extensively in fibroblasts, being responsible for the internalization of an amount of cell surface membrane equal to 180 per cent of the cell surface every hour (Steinman et al., 1976). Although no data was available in the literature relating to changes in membrane function in terms of pinocytic activity following near-UV irradiation, Maisin (1974) reported an increase in the number of pinocytic vesicles in mouse lung capillaries after 20 Grays of X-irradiation.

The following series of experiments were designed to investigate the rate of endocytosis in irradiated and unirradiated fibroblasts, and the subsequent exocytosis of internalized labelled marker. GM730 and AR6L0 fibroblasts were compared, and the effect of antioxidants, D_2O and glutathione-depletion were investigated.

The Measurement of Endocytic Uptake of ^{14}C-Sucrose from the Medium

The technique used was based on that of Besterman et al. (1981). Cells were grown in 50 mm tissue culture flasks (Nunc) until growth was approaching confluence. When ready for use the medium was removed, the cells were washed three times with 5 ml PBS (B) buffer, and 5 ml fresh PBS (B) buffer added. The cells were either irradiated with the broad-band sources described, or kept as unirradiated controls. Following preliminary experiments an exposure time of 40 min to broad-band near-UV radiation was chosen;

this fluence results in survival levels in excess of 30 per cent (Kralli, 1987). Following the irradiation period the buffer was drained and 5 ml of pre-warmed growth medium containing 0.0185 M Bq ml^{-1} of ^{14}C sucrose was added. ^{14}C sucrose was obtained as a sterile solution of radioactive concentration 7.40 MBq ml^{-1}, specific activity 60.3 MBq mg^{-1} from Amersham International plc, Amersham. In order to obtain a radioactive count representing the labelled material adhering to the plate and cell surfaces, the medium was removed immediately from one pair of plates. The remaining plates were incubated at 37° in a gassed plastic box. This was to provide optimum conditions for the cells during the incubation period during which the cells took up the medium by endocytosis. Pairs of plates (one irradiated, one control) were removed at intervals, and the labelled medium was removed with a Pasteur pipette. Immediately afterwards the cells were washed rapidly six times with 5 ml of ice-cold PBS (B), and inverted on paper towelling to dry. The cells were then solubilized by the addition of 2.0 ml of 1% Dodecyl sulphate (SDS; Sigma) and after 5 minutes two samples were taken for scintillation counting. The technique of scintillation counting is described previously.

An appropriate quench curve was constructed for ^{14}C as shown in Fig. A15 in Appendix 5, and results were expressed as disintegrations per minute (dpm). The total cell number per plate was estimated by the trypsinization of cells from one plate from the same batch, and counted with a haemocytometer. Results could then be expressed as dpm per cell, following correction of the total dpm by subtraction of the zero time value. Results were

plotted as dpm per cell with time of incubation in the labelled medium.

1. ENDOCYTIC UPTAKE OF ^{14}C SUCROSE BY FIBROBLASTS

GM730 fibroblasts

Typical results are shown in Fig. 83a where the uptake of ^{14}C sucrose by irradiated and control cells is shown over a period of up to 90 minutes. It is clear that irradiated cells are more active in their endocytic activity, since they accumulate the labelled medium to a greater extent than unirradiated control cells.

It may be argued that the irradiated cells appear to accumulate more label when alternatively it may be that the membrane has been damaged to the extent that ^{14}C sucrose is able to penetrate the cells. Similar experiments were therefore undertaken where the incubation with labelled medium took place on ice in a refrigerator. Pinocytic activity is halted, or greatly reduced, at such temperatures. Fig. 83b shows that no uptake was evident by either control or irradiated cells.

It can be concluded, therefore, that during the incubation period the labelled sucrose is internalised endocytically, to a greater extent by irradiated cells.

AR6LO Fibroblasts

Experiments with AR6LO fibroblasts showed similar results, as shown in Fig. 84a and 84b. The unirradiated cells are generally more active than GM730 cells, the irradiated cells however have a slightly lower overall rate of uptake.

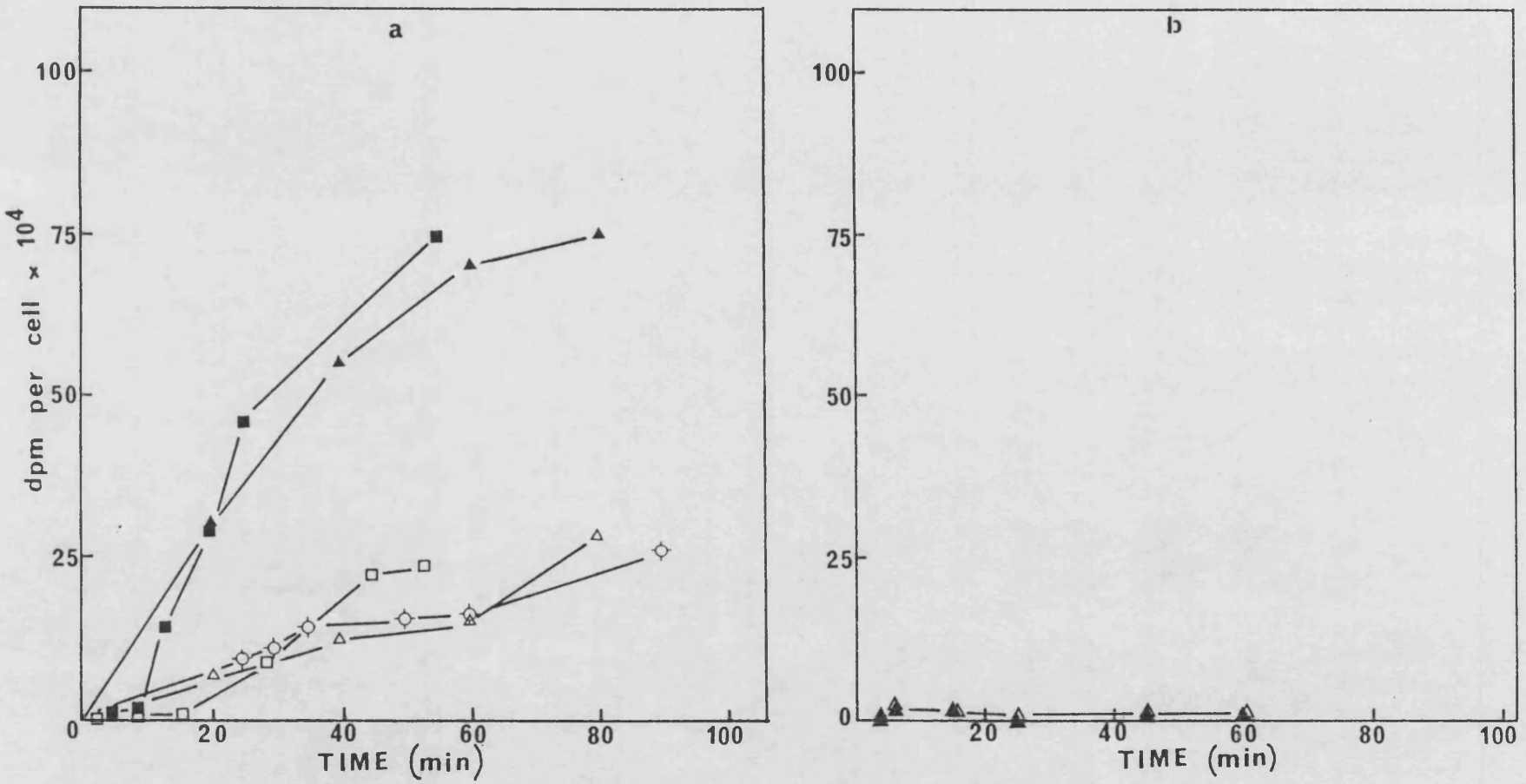

Figure 83 The uptake of ^{14}C-sucrose by GM730 fibroblasts at (a) 37°C (b) 4°C. Open symbols represent unirradiated cells, closed symbols represent cells irradiated for 40min with broad-band near-UV light. Alternate symbols represent replicate experiments.

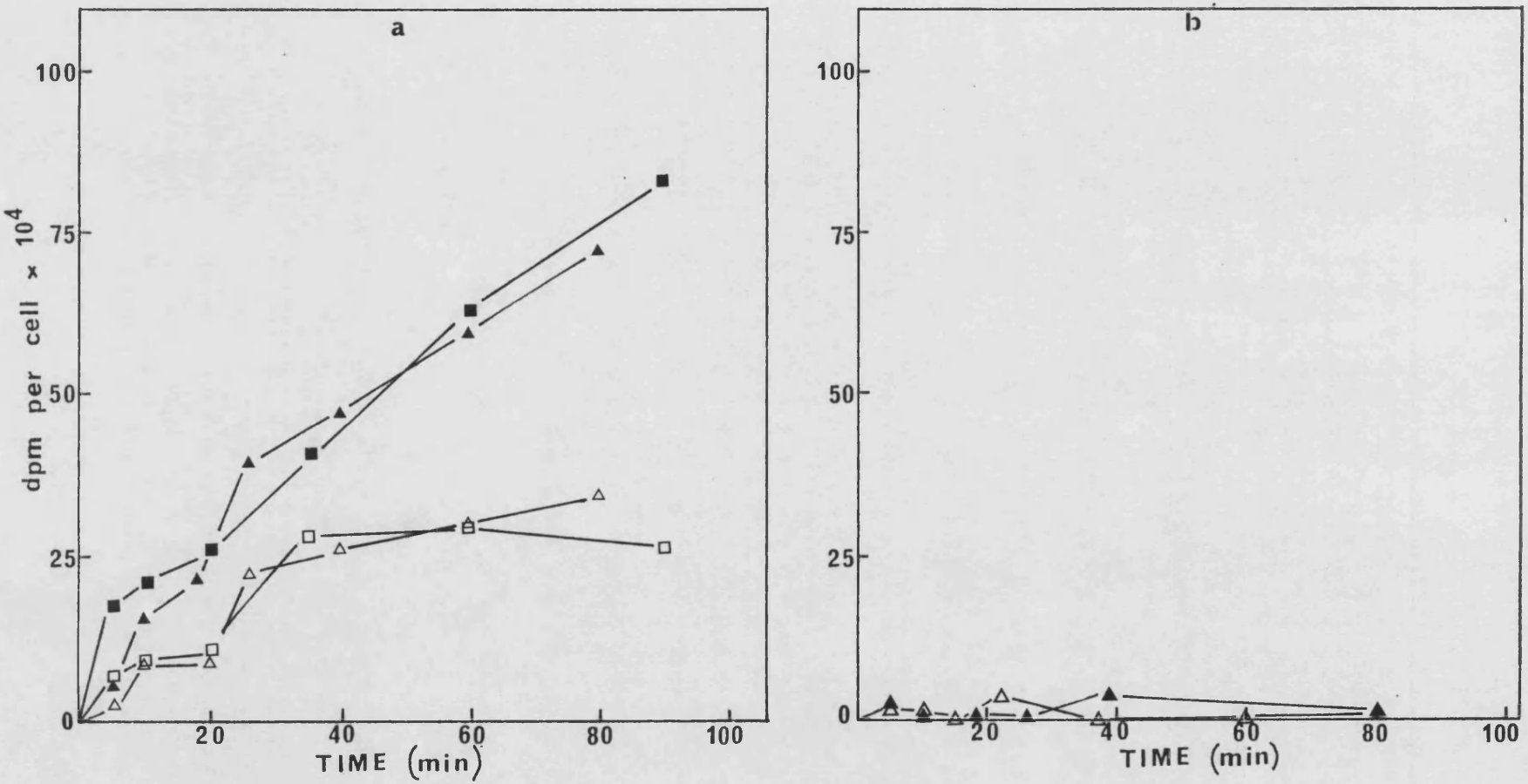

Figure 84 The uptake of ^{14}C-sucrose by AR6L0 fibroblasts at (a) 37°C (b) 4°C. Open symbols represent unirradiated cells, closed symbols represent cells irradiated for 40min with broad-band near-UV light. Alternate symbols represent replicate experiments.

2. THE EFFECT OF VITAMIN E ON THE RATE OF ENDOCYTOSIS

Since Vitamin E has been shown to reduce the sensitivity of AR6L0 cells, and to reduce near-UV irradiation-induced $^{86}Rb^{+}$ leakage, (Kralli, 1987), it was decided to investigate its effect on endocytosis. 100 µg/ml alpha-tocopherol acetate was included in the growth medium. Fig. 85a shows that although the supplemented cells exhibit an increase in endocytic activity, it is not as pronounced as in the unsupplemented cells. By contrast, no such effect is seen when GM730 fibroblasts are similarly treated (Fig. 85b).

An alternative method of estimating membrane activity determines the rate of exocytosis of a previously endocytosed labelled substance. It has been shown (Besterman et al., 1981) that the majority of fluid internalized in pinocytic vesicles is rapidly returned to the extracellular medium via exocytosis. This phenomenon is apparent even within the first few minutes of incubation with the labelled medium. It is possible to allow cells to internalize labelled medium, then to follow its subsequent release, by exocytosis, into fresh, unlabelled media. This gives an indication of the rate of exocytosis (and hence membrane activity) and allows determination of the amount of endocytosed label. It was decided to use this method as the method involving determination of endocytosis was of limited use for the following reasons.

1. The space available in the near-UV irradiation apparatus was limited, allowing the irradiation of a maximum of 6 small

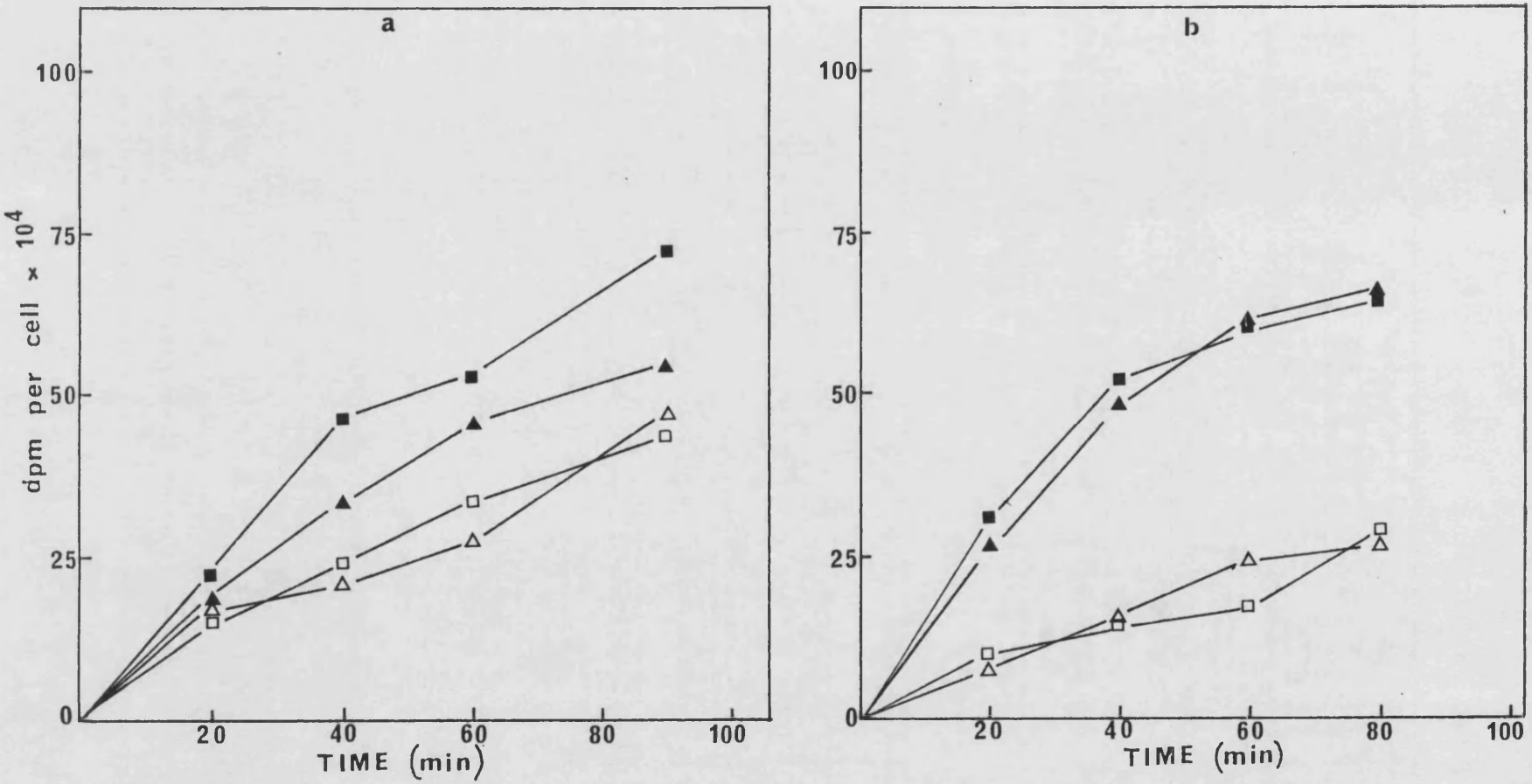

Figure 85 The uptake of ^{14}C-sucrose by (a) AR6L0 (b) GM730 fibroblasts grown (Δ ▲) with or (□ ■) without vitamin E. Open symbols represent unirradiated cells, closed symbols represent cells irradiated for 40min with broad-band near-UV light.

plates at any time.

2. The dpm achieved are low, due to the low cell number on small plates.
3. It was felt that it might be useful to extend the period of observation following irradiation, this being more easily applied to the study of exocytosis.

The Measurement of Exocytosis of Pinocytosed ^{14}C Sucrose in Fibroblasts

The method is based on that of Besterman et al. (1981). Tissue culture dishes (90 mm, Nunc), were seeded in the normal way and incubated for 2 to 3 days. The medium was removed, the monolayers washed twice with PBS (B) buffer, and 10 ml fresh PBS (B) buffer added. The lids were replaced and the cells were either irradiated or kept in the dark as controls. Immediately following irradiation the buffer was removed and replaced with 10 ml pre-warmed growth medium containing 0.0185 MBq ^{14}C sucrose. ^{14}C-sucrose was obtained as a sterile solution of radioactive concentration 7.40 MBq ml^{-1}, specific activity 60.3 MBq mg^{-1}, from Amersham International plc, Amersham. The plates were placed in an incubation box, gassed in the usual way and incubated at 37°C for 1 hour. During this time the cells (as previously shown) internalized the labelled medium. At the end of incubation the labelled medium was removed with a Pasteur pipette. The monolayers were rapidly but gently washed six times with 10 ml ice-cold PBS (B) buffer, and inverted to drain momentarily before the addition of 10 ml of pre-warmed medium at

37°C. This medium was removed immediately for a zero-time count, and fresh medium added to the plate. After incubation at 37°C for a chosen period, this procedure of the removal and replacement of the medium was repeated, scintillation counts being obtained on the removed media. In this way the amount of label released into the medium over the period of incubation could be measured. After subtraction of the zero-time count (correcting for ^{14}C sucrose absorbed to the surfaces and providing a check for washing efficiency), the scintillation count, as dpm per cell, was calculated by reference to the cell count from a plate from the same batch. The accumulated dpm per cell was plotted with the time of re-incubation. Any residual label associated with the monolayer could be measured by the solubilization of the cells with 1% SDS for scintillation counting. In practice this was low after the three hours of re-incubation allowed. The accumulation of the labelled sucrose in the re- incubation medium from irradiated and unirradiated GM730 and AR6L0 fibroblasts were compared. Various modifications in growth media or irradiation conditions were then made for further comparisons.

3. EXOCYTOSIS OF ^{14}C SUCROSE FROM FIBROBLASTS

GM730 Fibroblasts

Following 40 minutes' irradiation with the broad-band near-UV source, ^{14}C sucrose accumulated in the medium at a faster rate, and reaching higher levels, from the irradiated cells than from unirradiated cells (Fig. 86a).

The higher levels achieved overall from irradiated cells is an

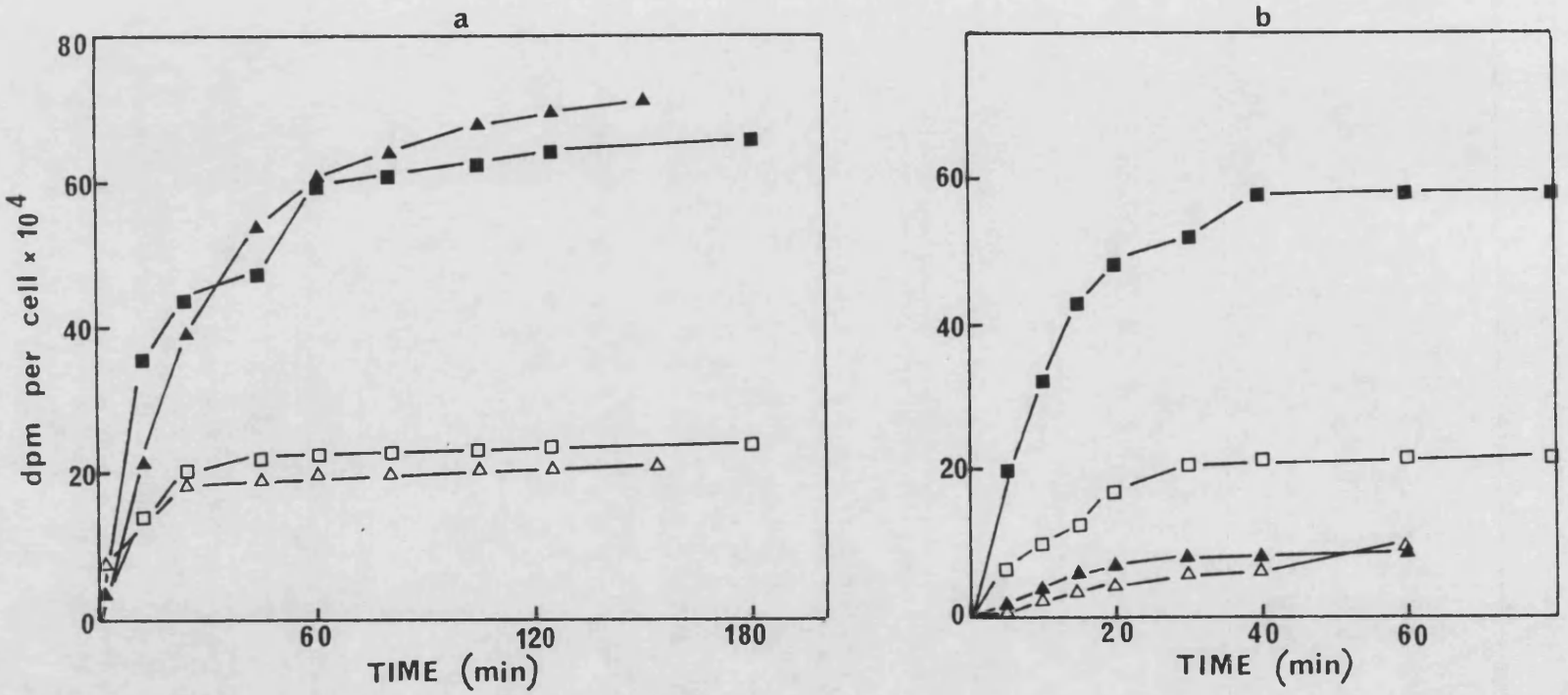

Figure 86 The accumulation of ^{14}C-sucrose in the medium by GM730 fibroblasts at 37 (a) or (b) 37°C (□■)(△▲) 4°C. Open symbols represent unirradiated cells, closed symbols represent cells irradiated for 40min with broad-band near-UV light. Alternate symbols represent replicate experiments.

indication that more ^{14}C sucrose was taken into the cells during the post-irradiation incubation period, as a result of the increase in endocytic activity demonstrated previously. In order to confirm that the measured ^{14}C sucrose was reaching the medium by way of exocytosis rather than leakage through a damaged membrane, measurements were made at 4°C, since pinocytic activity is halted at this temperature.

The Measurement of ^{14}C Sucrose Accumulation at 4° and 37° from GM730 Fibroblasts

Four matched plates were used for each experiment. Two were irradiated for 40 min, two were kept as controls. Following irradiation all plates were incubated with ^{14}C sucrose medium and washed under standard conditions. During the subsequent accumulation measurements one pair of plates was incubated at 37°C while the other pair was kept on ice in a refrigerator.

Replacement media was kept on ice until use. From Fig. 86b it can be seen that both control and irradiated cells, when kept at 4°C release only very low amounts of ^{14}C sucrose. Such levels may be consistent with surface-absorbed label being subsequently washed off by the media, or with a low level of pinocytic activity. It is not due to irradiation-induced membrane damage, since control and irradiated cells follow the same accumulation curve.

AR6L0 Fibroblasts

Experiments with AR6L0 fibroblasts showed similar results (Fig. 87a). Irradiated cells consistently exhibited higher levels of

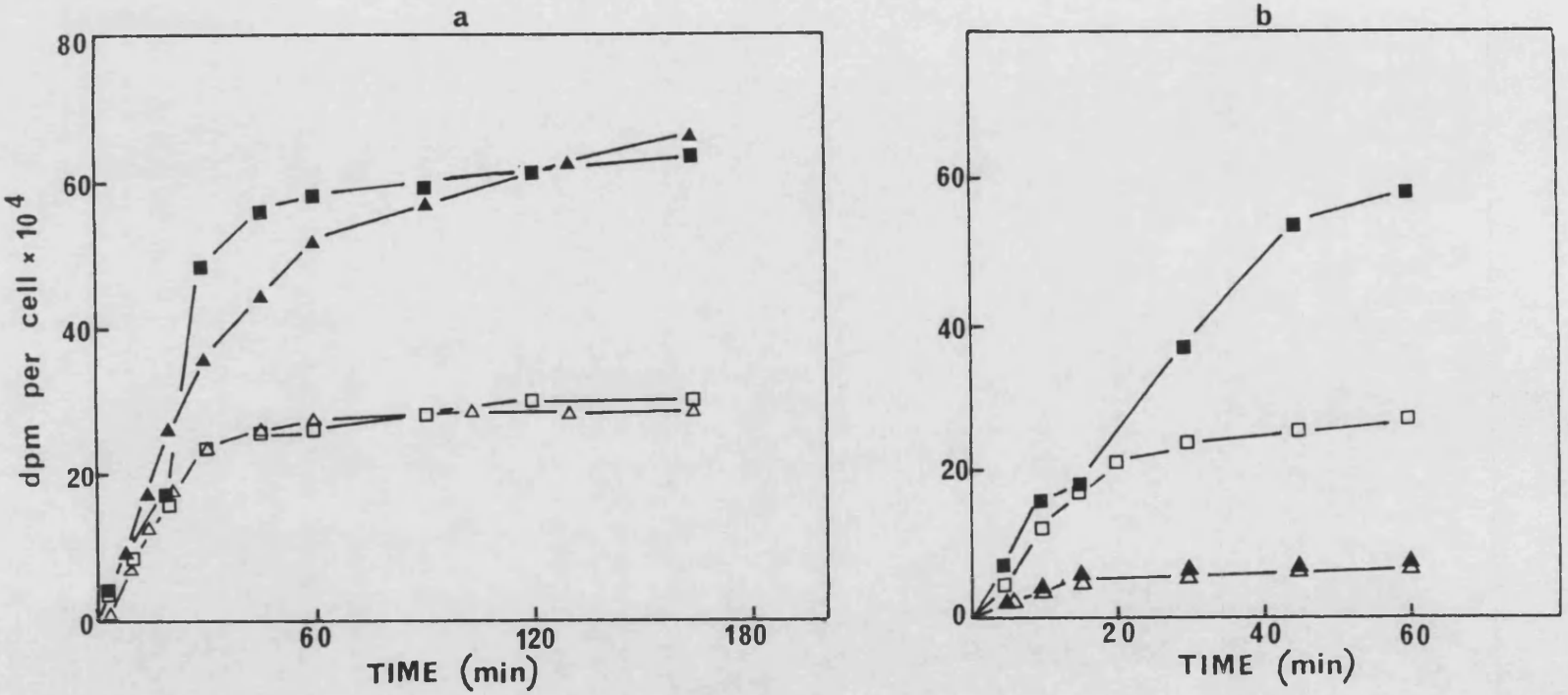

Figure 87 The accumulation of ^{14}C-sucrose in the medium by AR6LO fibroblasts at (a) 37°C (b) 37°C (□■) or 4°C (△▲) Open symbols represent unirradiated cells, closed symbols represent cells irradiated for 40min with broad-band near-UV light. Alternate symbols represent replicate experiments.

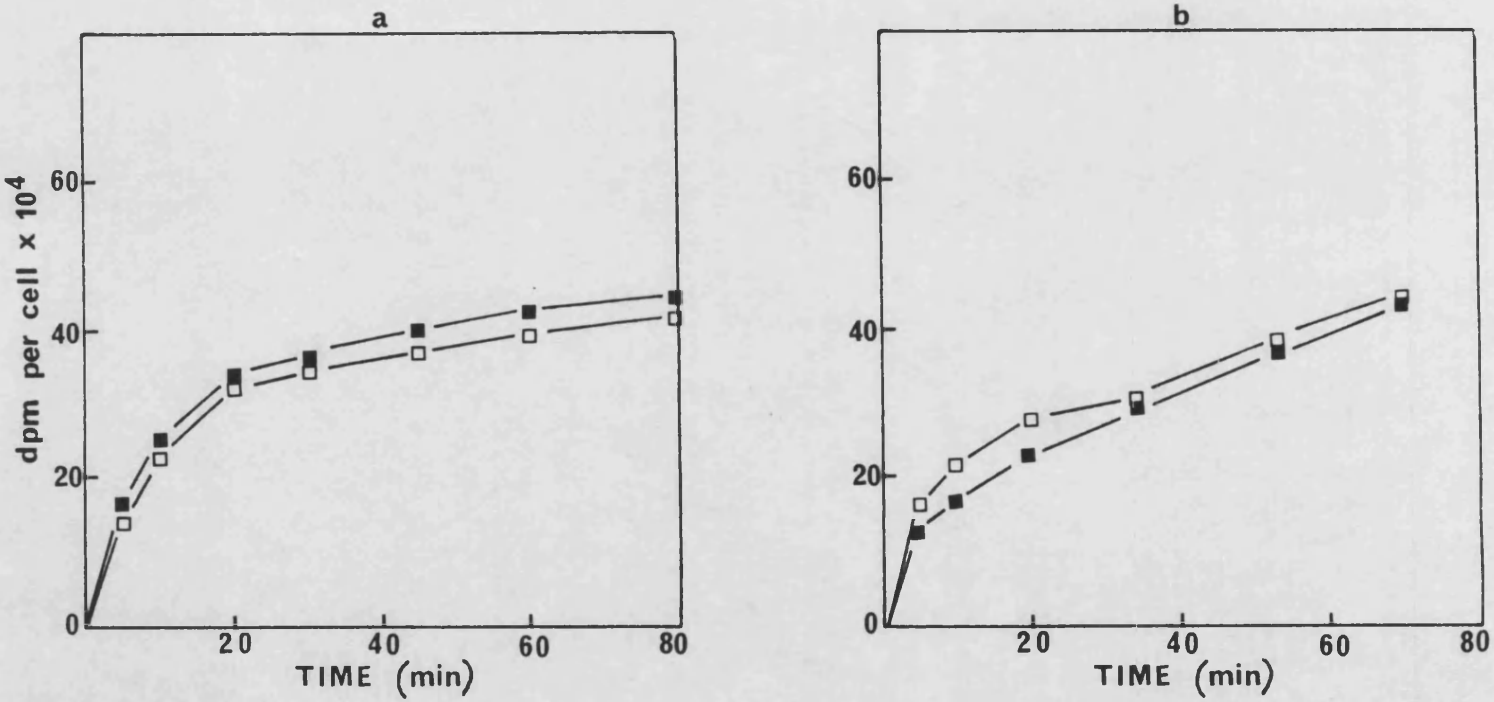

Figure 88 The accumulation of ^{14}C-sucrose in the medium by (a) GM730 fibroblasts (b) AR6LO fibroblasts. Open symbols represent unirradiated cells, closed symbols represent cells irradiated with 2.16 kJm^{-2} broad band far-UV light.

pinocytic activity than the unirradiated controls, as demonstrated by the increased levels of label in the re-incubation medium.

The Measurement of ^{14}C Sucrose Accumulation at 4° and 37°C From AR6LO Fibroblasts

In parallel with similar experiments with GM730 fibroblasts, exocytic activity is shown in Fig. 87b to be reduced to similar levels when the monolayers are incubated at 4°C.

4. EXOCYTOSIS FOLLOWING FAR-UV IRRADIATION OF GM730 AND AR6LO FIBROBLASTS

The above results provided interesting evidence of changes in membrane activity following broad-band near-UV irradiation. Previous work has shown several membrane effects to result from near-UV, but not far-UV irradiation. Therefore similar measurements were undertaken following irradiation by broad-band far-UV radiation using the source described in the Methodology. Both cell lines were irradiated for two minutes, a fluence reported to be 2-3 orders of magnitude larger than is required for lethality (Kralli, 1987). Even at such fluences there is no evidence of any increased pinocytic activity by far-UV-irradiated cells (Fig. 88a).

Although the fluence given (2.16 kJm^{-2}) is lethal to both types of cell, it is obvious that membrane activity continues within the time of this experiment (i.e. 1 hour incubation with ^{14}C sucrose medium, plus 80 min re-incubation while measuring the accumulation of ^{14}C sucrose).

5 . THE EFFECT OF FLUENCE ON THE NEAR-UV IRRADIATION-INDUCED INCREASE IN PINOCYTIC ACTIVITY

In view of the clear irradiation-induced increase in pinocytic activity in both cell lines, it was decided to investigate whether the increase varied with the fluence given. A set of matched plates was used for each experiment, one being kept as an unirradiated control, the others being exposed for various times to the broad-band near-UV radiation. The results of four such experiments are shown in Figs. 89a and 89b. (GM730 fibroblasts) and Figs. 90a and 90b (AR6L0 fibroblasts). While shorter exposures have little or no effect, long exposures result in up to four times as much release of label into the medium, indicating a corresponding pinocytic uptake of label. The relationship is not linear however. Fig. 91 shows the increase in accumulated label, after 40 minutes re-incubation, following irradiation for various times, relative to unirradiated controls.

After one hour of re-incubation in fresh media GM730 fibroblasts irradiated for 60 min have released 3.8 times as much ^{14}C sucrose than control cells. This compares with values of 3.4 after 50 mins and 3.5 after 55 mins for AR6L0 fibroblasts. These increases are therefore of the same order, even though a comparison with survival curves shown in Fig. 82, (Kralli, 1987) shows that after 50 min exposure the survival of AR6L0 cells is only one third of that of GM730 cells. By 60 mins the level of survival of AR6L0 cells is less than that of GM730 cells by a factor of 9. It is therefore unclear how such an increase in pinocytic activity may, if at all, be related to survival following irradiation.

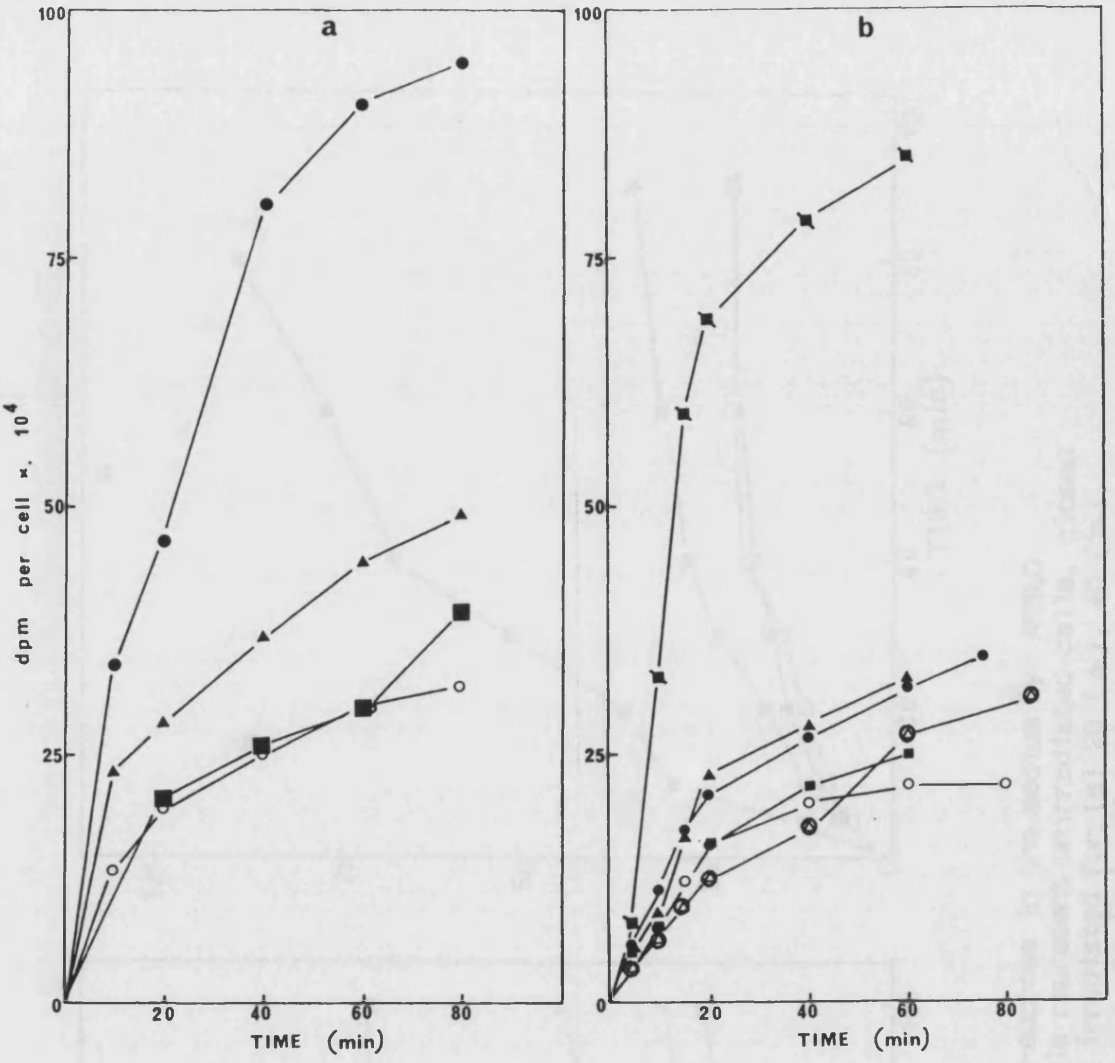

Figure 89

The accumulation of ^{14}C-sucrose in the medium by GM730 fibroblasts. Open symbols represent unirradiated cells, closed symbols represent cells irradiated for (a) 20 (■), 30 (▲), 50 (●) min, (b) 10 (■), 15 (●), 20 (●), 25 (▲), 60 (■) mins, broad-band near-UV light.

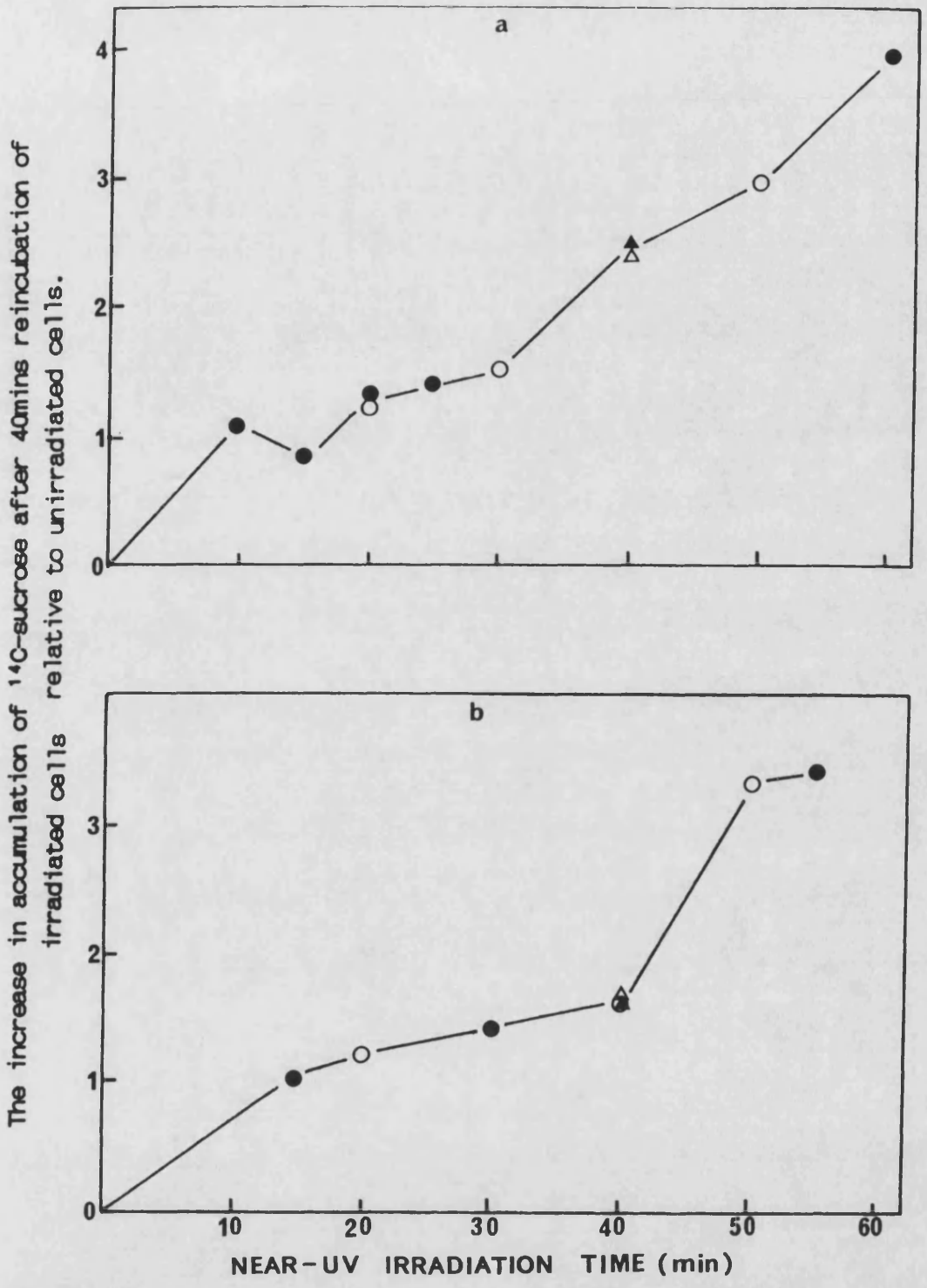

Figure 91

The increase in accumulation of ^{14}C-sucrose after 40 mins reincubation of irradiated cells, relative to unirradiated cells.
(a) GM730 cells, data taken from figs. 89a (●), 89b (○) and 86a (△▲).
(b) AR6LO cells, data taken from figs. 90a (●), 90b (◕) and 87a (△▲).

It was of interest to know whether or not certain factors would affect this irradiation-induced change in membrane activity, in view of their demonstrated effects on survival, $^{86}Rb^{+}$ leakage and/or lipid peroxidation. Experiments were therefore performed where the effects of Trolox-C, Vitamin E, DABCO, D_2O and glutathione-depletion were investigated.

6. THE EFFECT OF VITAMIN E ON EXOCYTOSIS FOLLOWING NEAR-UV IRRADIATION

Vitamin E was added to the growth media as 100 μg per ml of alpha-tocopherol acetate. The cells were irradiated with broad-band near-UV radiation for 45 minutes, incubated with labelled medium for 1 hour, and the accumulation of ^{14}C sucrose in the reincubation medium was measured. Typical results are shown in Fig. 92, where GM730 and AR6L0 cells may be compared. Growth in Vitamin E has no effect on exocytosis by GM730 fibroblasts. AR6L0 cells from non-supplemented medium show an increase in the level of label of 1.9 by the end of 100 min re-incubation. The Vitamin E supplemented cells, however show an increase of only 1.4, thus some effect is evident.

7. THE EFFECT OF TROLOX-C ON EXOCYTOSIS FOLLOWING BROAD-BAND NUV IRRADIATION

Similar experiments were performed using 100 μg per ml Trolox-C as a growth supplement. Results seen in Fig. 93a show a minimal reduction in the accumulation of label in the medium from supplemented GM730 cells. However, Fig. 93b shows a remarkable

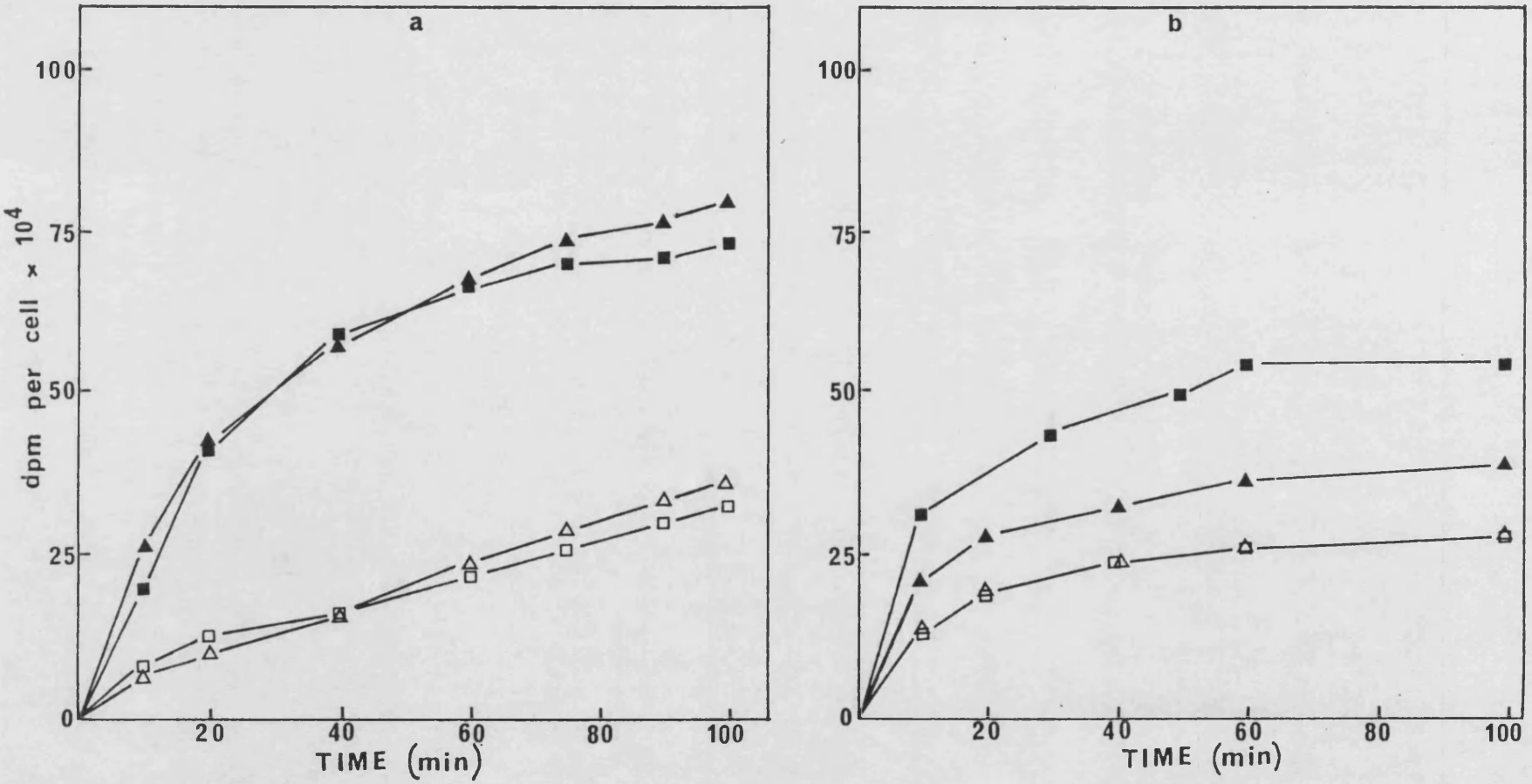

Figure 92 The accumulation of ^{14}C-sucrose in the medium by (a) GM730 fibroblasts (b) AR6LO fibroblasts. Open symbols represent unirradiated cells, closed symbols represent cells irradiated for 45mins with broad band near-UV light, following growth with (Δ ▲) or without (□ ■) vitamin E.

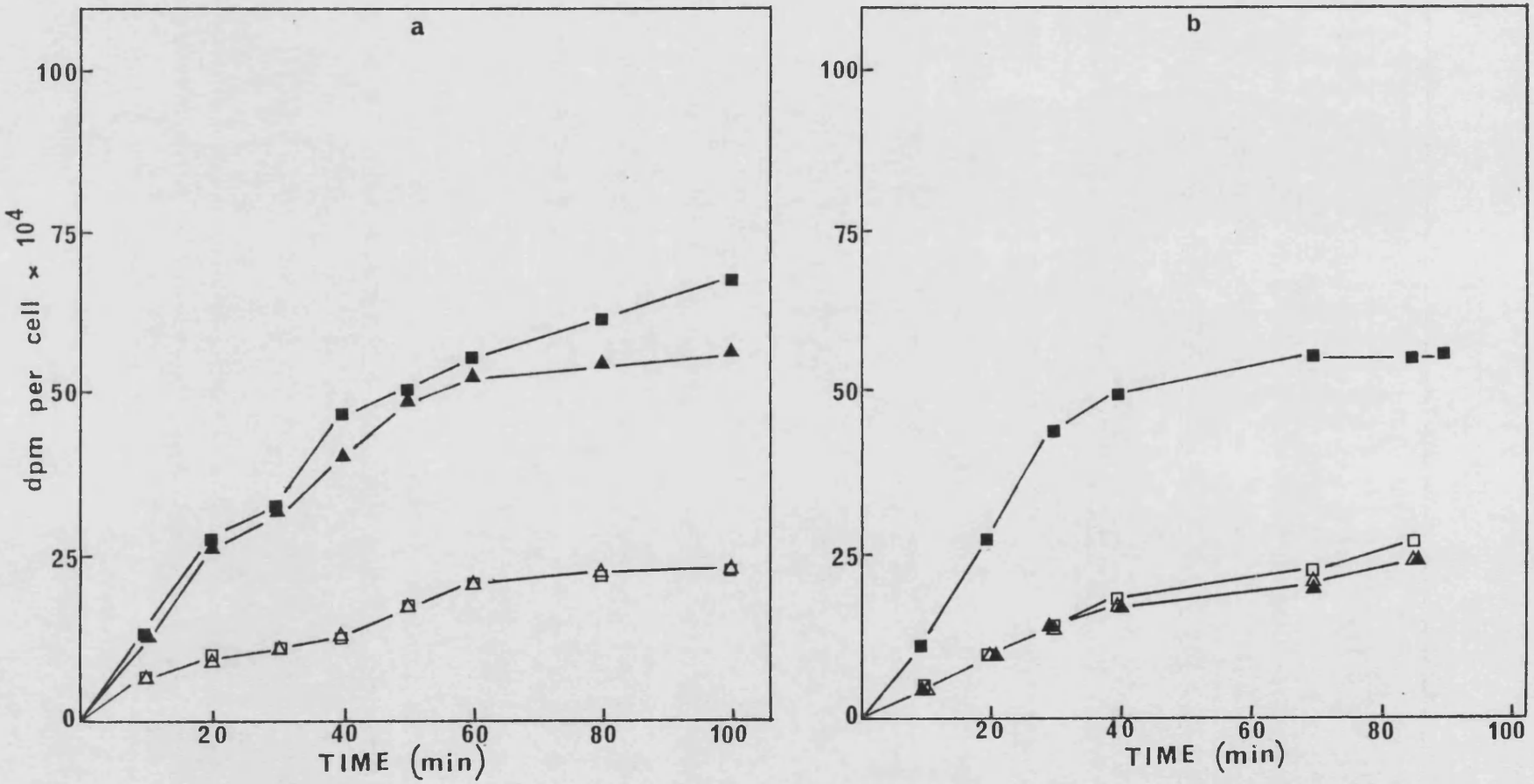

Figure 93 The accumulation of ^{14}C-sucrose in the medium by (a) GM730 fibroblasts (b) AR6LO fibroblasts. Open symbols represent unirradiated cells, closed symbols represent cells irradiated for 45mins with broad band near-UV light, following growth with (△ ▲) or without (□ ■) Trolox-C.

effect on AR6LO cells, where there is no increase in pinocytic activity evident in the supplemented, irradiated cells.

This result is interesting since Kralli (1987) showed that Trolox-C offered such protection to AR6LO fibroblasts that their survival after irradiation was increased to levels similar to those of GM730 cells. Trolox-C was also shown to inhibit near-UV irradiation-induced $^{86}Rb^{+}$ leakage from AR6LO cells.

8. THE EFFECT OF IRRADIATION IN D_2O ON EXOCYTOSIS IN GM730 AND AR6LO FIBROBLASTS

If reactive oxygen species are of particular importance to AR6LO fibroblasts, it would be expected that irradiation in deuterated buffer would enhance radiation-induced damage. Kralli (1987) showed that survival of both cell lines was decreased under these conditions. Both types of cell were irradiated in 75% buffered D_2O, following a 20 min incubation period for equilibration, with broad-band near-UV radiation for 30 min, representing a fluence resulting in a moderate increase in pinocytic activity (Figs. 89 and 90). It was necessary to choose a short exposure time, since after the standard 40 minute period cells were very easily detached during the washing procedure with ice-cold PBS (B) buffer following irradiation in deuterated buffer. The results in Fig. 94 show a slight increase in the activity of both types of cell following irradiation in 75% D_2O. GM730 cells show an accumulation of label in the medium which is greater by a factor of 1.2 for cells irradiated in buffer, and of 1.4 for cells

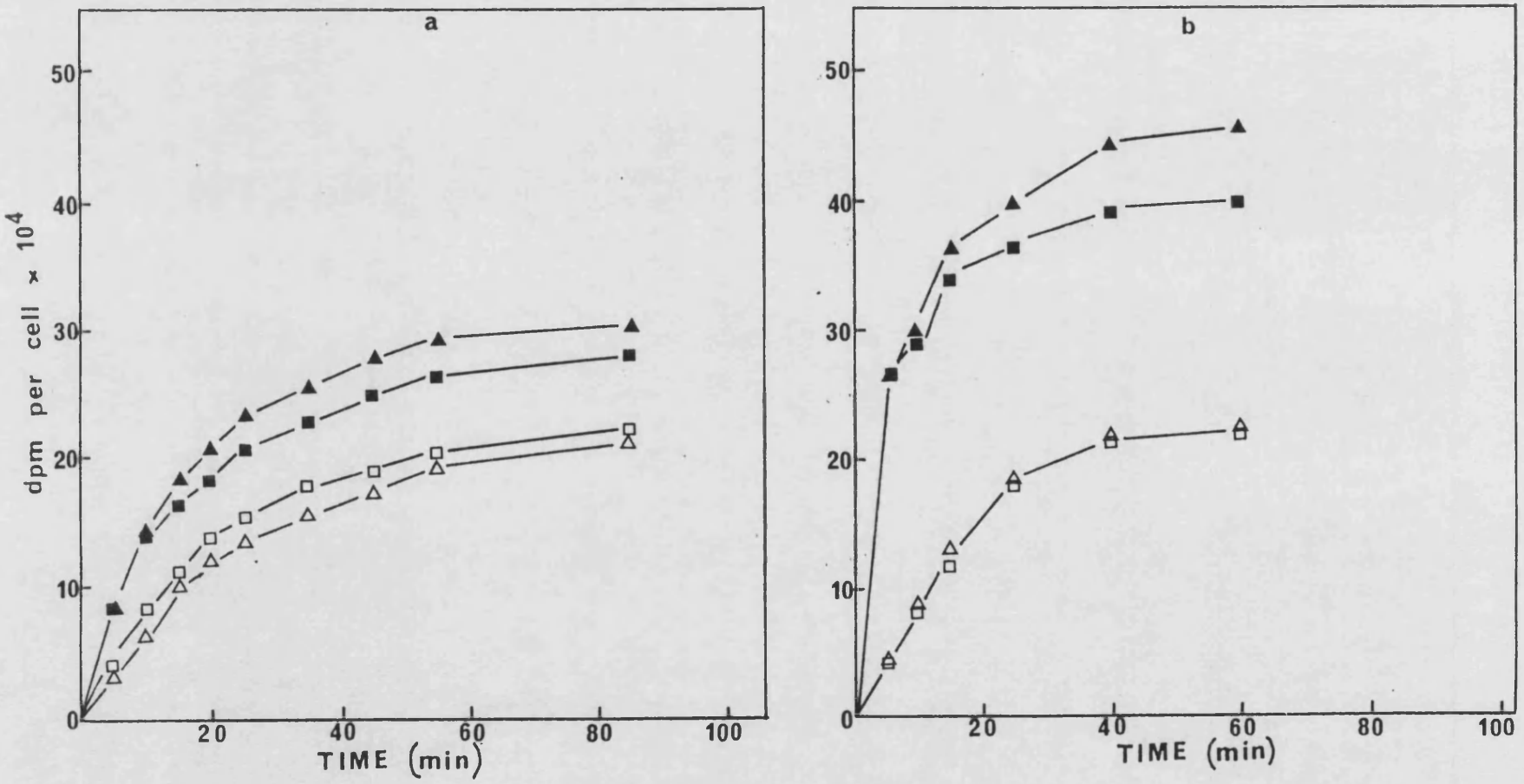

Figure 94 The accumulation of ^{14}C-sucrose in the medium by (a) GM730 fibroblasts (b) AR6LO fibroblasts. Open symbols represent unirradiated cells, closed symbols represent cells irradiated for 30mins with broad band near-UV light in the absence (□ ■) or presence (△ ▲) of D_2O

irradiated in D_2O. The equivalent values for AR6LO cells are 1.8 and 2.3. Therefore, while the effect of D_2O is small on GM730 cells, it is more evident on AR6LO cells.

9. THE EFFECT OF GLUTATHIONE DEPLETION ON IRRADIATION-INDUCED PINOCYTIC ACTIVITY

When one of the normal defence mechanisms against oxidative damage, i.e. glutathione, is deficient, it has been shown that lipid peroxidation is increased, Fig. 81a and 81b, and that survival of similar fibroblasts is reduced (Tyrrell and Pidoux, 1986). It was interesting, therefore, to investigate the result of glutathione deficiency on the irradiation-induced increase in pinocytosis.

Cells were depleted of glutathione by incubation in 500 mM BSO as previously described, prior to irradiation. Shorter exposure times were again chosen, in parallel with the previous experiments. Fig. 95 shows the results of such an experiment on each cell line. Glutathione-depleted GM730 cells responded by a marked increase in pinocytic activity. The increase, above the normal level, of accumulation of label from the unirradiated cells should be noted, however, so that after 100 min the glutathione-depleted cells exhibit a real increase of 2.1 compared with that of normal cells of 1.8.

The AR6LO cells grown in the BSO-medium, however, show exactly the same response as normal cells.

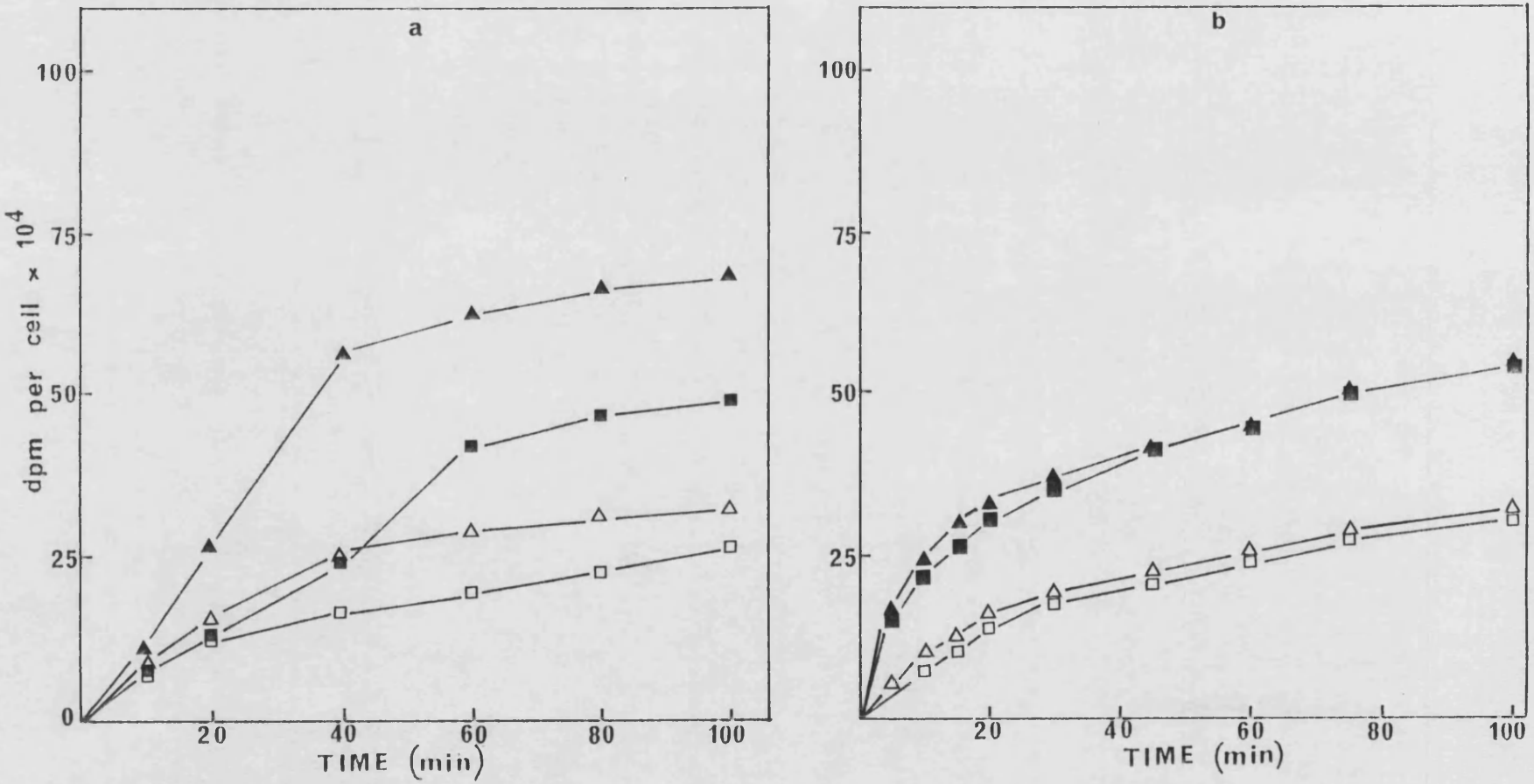

Figure 95 The accumulation of ^{14}C-sucrose in the medium by (a) GM730 fibroblasts (b) AR6LO fibroblasts. Open symbols represent unirradiated cells, closed symbols represent cells irradiated for 30mins with broad band near-UV light, following growth with (△ ▲) or without (□ ■) BSO.

SUMMARY AND DISCUSSION

The measurement of endocytic uptake of labelled medium has demonstrated that irradiated fibroblasts internalize the medium to a greater extent than unirradiated cells (Figs. 83 and 84). The increase in activity exhibited by irradiated AR6LO cells is reduced when they are previously grown in vitamin E supplemented medium, though this has no effect on GM730 cells (Fig. 85).

Internalized ^{14}C-sucrose subsequently returned to the medium has also been measured and the results reflect those described above, (Figs. 86 and 87). The enhancement of pinocytic activity increases with increasing fluence following near-UV irradiation for exposures of up to 60 minutes (Figs. 89 and 90). The levels of survival of the two cell lines following such fluences differ by a factor of 9, the AR6LO cells being the more sensitive (Fig. 82). However, the increase in membrane activity relative to unirradiated controls, is similar for both. No direct correlation is therefore evident between sensitivity and increased pinocytic activity.

When cells are supplemented with vitamin E during pre-irradiation growth, the irradiation-induced increase in activity is reduced in AR6LO cells but not GM730 cells (Fig. 92). Trolox-C, used similarly as a supplement, prevents any irradiation-induced increase in AR6LO cells (Fig. 93).

Kralli and Moss (1987) demonstrated that vitamin E and Trolox-C protected AR6LO cells from 365 nm-induced lethality to such an extent that they were as resistant as GM730 cells. In view of this finding the association between the phenomenon of increased

pinocytic activity and sensitivity to near-UV irradiation, as mentioned above, must be carefully considered. If an increase in pinocytosis is a means by which the membrane can be repaired, then a decrease in such activity would be expected to reduce survival. It may be considered, however, that such a radiation-induced increase in membrane turnover depletes the cell's resources, causing added stress to metabolic activity, which may contribute to cell killing. It was suggested by Kralli and Moss (1987) that AR6LO cells may be deficient in enzyme activity, resulting in an inadequacy in dealing with oxidative damage. Trolox-C and vitamin E may then reduce such damage to a level with which the residual enzyme activity can cope. The result of antioxidant supplementation should then be to restore AR6LO cells to the state of competence found in GM730 cells, and therefore any difference in GM730 cells and supplemented AR6LO cells must indicate diverse responses to near-UV radiation.

Irradiation in D_2O was shown by Kralli (1987) to result in the sensitization of both cell lines to near-UV radiation. As indicated, cells were easily detached from the plates by the washing procedure after fluences which had no such effect in buffer. The effect of D_2O on irradiation-induced pinocytic activity was to increase it to a small degree in both cell lines. This result would indicate that by prolonging the active lifetime of reactive oxygen species during the irradiation period the cell reacts subsequently by increasing pinocytic activity. This may be an amplification of the situation in non-deuterated buffer, where the production of such oxygen species contributes to damage at the

cell membrane, the response of the cell being to repair the membrane during the enhanced recycling process. This offers further explanation of the protective action of Trolox-C and vitamin E, where the reduction of oxidative damage negates the necessity for extra membrane recycling, and substantiates evidence that AR6LO cells are deficient in endogenous antioxidants. The ineffective action of these antioxidants in the protection of GM730 cells may then reflect that the cells are already maximally protected by endogenous antioxidants. The depletion of cellular glutathione, with a resulting increase in hydroperoxide accumulation, would on the basis of the above speculation, lead to a more rapid membrane turnover to repair the damage. This is indeed the case for GM730 cells, but there is no evident increase in AR6LO cells. BSO has been widely used as a potent inhibitor of glutathione synthesis since its description by Griffith and Meister (1979), and it is unlikely that AR6LO cells are not affected in the usual way. Indeed an increase in lipid peroxidation has been demonstrated in BSO-treated AR6LO cells (Fig. 81b). Normal fibroblasts have been shown to be sensitized to near-UV radiation following growth in BSO-supplemented medium (Tyrrell and Pidoux, 1986). It would be interesting to determine the effect of such treatment on the survival of AR6LO cells.

Since the response of each cell line may differ following a particular treatment, perhaps the activity of unirradiated cells should be examined more closely. Reference to Fig. 83a and 84a shows that untreated AR6LO cells internalize the medium more rapidly than GM730 cells, indicating a higher degree of pinocytic

activity. This could explain Kralli's observations that unirradiated AR6L0 cells leaked rubidium more than GM730 cells (Kralli, 1987) if the rubidium was being exocytosed from the interior, as opposed to 'leaking' out. Although unirradiated AR6L0 cells are more active than GM730 cells the position is reversed following irradiation so that the relative increase in activity by AR6L0 cells is lower than for GM730 cells, perhaps reflecting a reduced ability to recycle damaged membrane, which may in turn contribute to the greater sensitivity of AR6L0 cells.

The results presented here form a complex picture, where an irradiation-induced effect has clearly been demonstrated, yet its implications are unclear.

Pinocytosis has been the subject of many reviews (e.g. Besterman and Low, 1983) and quantitative studies (e.g. Williams et al., 1975; Steinman et al., 1976; Steinman et al., 1981). Its role in the recycling of plasma membranes has been discussed (Steinman et al., 1983) and books devoted to the subject (e.g. Pastan and Willingham, 1985). The literature indicates agreement that one function of pinocytosis may be the recycling of the membrane as a homeostatic measure, while providing the cell with proteins and other nutrients as macromolecules from the media. It is conceivable that parts of the membrane, having been damaged during irradiation, are removed, modified by lysosomal action to remove unwanted components, repaired by additions via the endoplasmic reticulum and returned by exocytosis to the cell surface. Whether the increase in activity as indicated by these

experiments is of benefit or detriment to the cell in terms of survival remains unclear. It would be useful to subject fibroblasts to other treatments, known to damage the membrane, and to determine their effect on pinocytosis. It would also be interesting to follow this phenomenon over longer periods of time, perhaps until cell division had occurred, and to correlate precisely the survival of treated cells with the degree of enhanced pinocytic activity observed. More detailed studies could determine the fate of the internalised membrane and any modifications which are made prior to its reinsertion at the cell surface.

Clearly these studies, while providing evidence for changes in membrane activity, are preliminary, and leave many questions unanswered. While such events may occur in cell culture, their relevance or application to cells irradiated *in vivo* should be considered, and may be extended to studies of *in vivo* situations where pinocytosis is known to occur and how it may be affected by detrimental treatments.

RESULTS AND DISCUSSION

PART 3

PRELIMINARY INVESTIGATIONS INTO THE EFFECTS OF NEAR-UV RADIATION ON FREE FATTY ACIDS AND LIPOSOMES

Lipid peroxidation has been demonstrated to result from the near-UV irradiation of human skin, and it has been suggested that such peroxidation may be, in part, responsible for ageing and some pathological conditions of the skin (Meffert et al., 1976). Although consideration is generally given to the peroxidation of lipid components of the cellular membrane, there are free fatty acids associated with the skin. The human stratum corneum consists of lipid-depleted cells embedded in a neutral lipid-rich interstitium. The composition of this lipid layer, found in a lamellar form segregated in the intercellular spaces, is reported to be a mixture of lipids and sterols with free fatty acids. The unsaturated free fatty acids include 18:1 and 18:2, while unsaturated fatty acids associated with the lipid components include 14:1, 16:1, 18:1, 18:2, 20:2, 20:3, 20:4, 22:1, 24:1 and 24:2 (Lampe et al., 1983; Elias et al., 1979). Since such fatty acids and lipids, being situated extracellularly, may not benefit from the antioxidative protective devices within the cell, any factor promoting peroxidation may do so unhindered.

The immediate concern in the investigations for this thesis, was of the in vivo importance of lipid peroxidation. However, it was thought that a preliminary in vitro study of the effects of near-UV irradiation on the unsaturated fatty acids used in the bacteriological studies in this thesis, and in cell culture investigations in this laboratory (McAleer et al., 1987) would be of interest. The preliminary nature of the experimental work

included here imposes constraints upon the interpretation of results. Parameters such as dose rate effects, the role of free radicals, the importance of pre-existing peroxides present as contaminants in the sample and the role of iron-catalysed reactions due to contaminating iron in laboratory distilled water have not been investigated or controlled. The effects of such factors have been widely studied in the in vitro peroxidation of fatty acids and lipids induced by means other than near-UV irradiation (Halliwell and Gutteridge, 1985; Gutteridge, 1984), and reviewed by Frankel (1985, 1986); these serve to emphasise the limits of the work presented there.

Additional Methodology

Materials: oleic (18:1), linoleic (18:2), linolenic (18:3) acids, (99% pure, Sigma U.K. Ltd.), stored under nitrogen at -20°C when not in use. Ethanol (95%; Analar, BDH).

The Preparation of fatty acid dispersions for irradiation

The fatty acid was dissolved in 95% ethanol at a concentration of 10^{-2} M and diluted with distilled water to 10^{-3} M. The dispersions were used immediately for irradiation.

Absorption spectra of the fatty acid dispersions

The dispersions at the concentration used were slightly opaque and therefore part of the radiation became absorbed or scattered. This would have resulted in the molecules at the rear of the cuvette receiving a lower fluence than those at the front. Rapid

stirring eliminates this non-uniformity but overall the fluence received by the fatty acids was lower than that calculated by dosimetry. In order to calculate a correction factor which could be applied to the fluence, an absorption spectrum was obtained for each fatty acid. Normally determination of the optical density would be made using a spectrophotometer, but as Jagger et al. (1975), described, if the light is scattered appreciably by the sample, then a photon which has traversed most or all of the sample may be scattered sufficiently to miss the detector, due to the large sample-detector distance. Therefore determination of the optical density was made utilizing a thermopile (Oriel 7102, Oriel Corp. of America) positioned directly against the back of the cuvette, reducing the sample-detector distance to about 3 mm. Thermopile readings were taken with and without the sample in position and the per cent transmission through the sample was calculated. From this figure the optical density was calculated. Measurements were taken between 290 nm and 405 nm and plotted as shown in Fig. A10 and A11 in Appendix 5.

The dose correction factor

A dose correction factor was calculated for each wavelength used experimentally using the formula from Morowitz (1950) and applied to the fluence determined by thermopile readings in each experiment (as described in the General Methodology). The fluence absorbed by the sample was thus obtained.

The irradiation of fatty acids

Irradiations were generally performed using monochromatic near-UV radiation, as described in the Methodology. Where fluences reasonably achieved using monochromatic light were inadequate, some irradiations were performed using the broad-band (BLB) source as indicated.

Determination of the products of peroxidation

Immediately after irradiation samples were taken for the TBA-reacting products assay and/or the hydroperoxide assay. Unirradiated controls, which had been held under similar conditions of temperature and stirring were always similarly assayed in parallel. Results are expressed relative to values obtained from unirradiated controls, so that values shown indicate peroxidation products arising as a result of the irradiation.

1. The dose-response for the peroxidation of linolenic acid

It was first necessary to determine whether, at a constant fluence rate, detectable peroxidation products increased linearly with the fluence received. This was performed using 303 nm monochromatic radiation and broad-band radiation, using linolenic acid. The results are shown in Figs. 96a and 96b. With both sources of radiation the lines deviate from linearity at longer exposure times. It is evident that following irradiation with the monochromatic source there is an increasing disparity between the results obtained using the two assay methods.

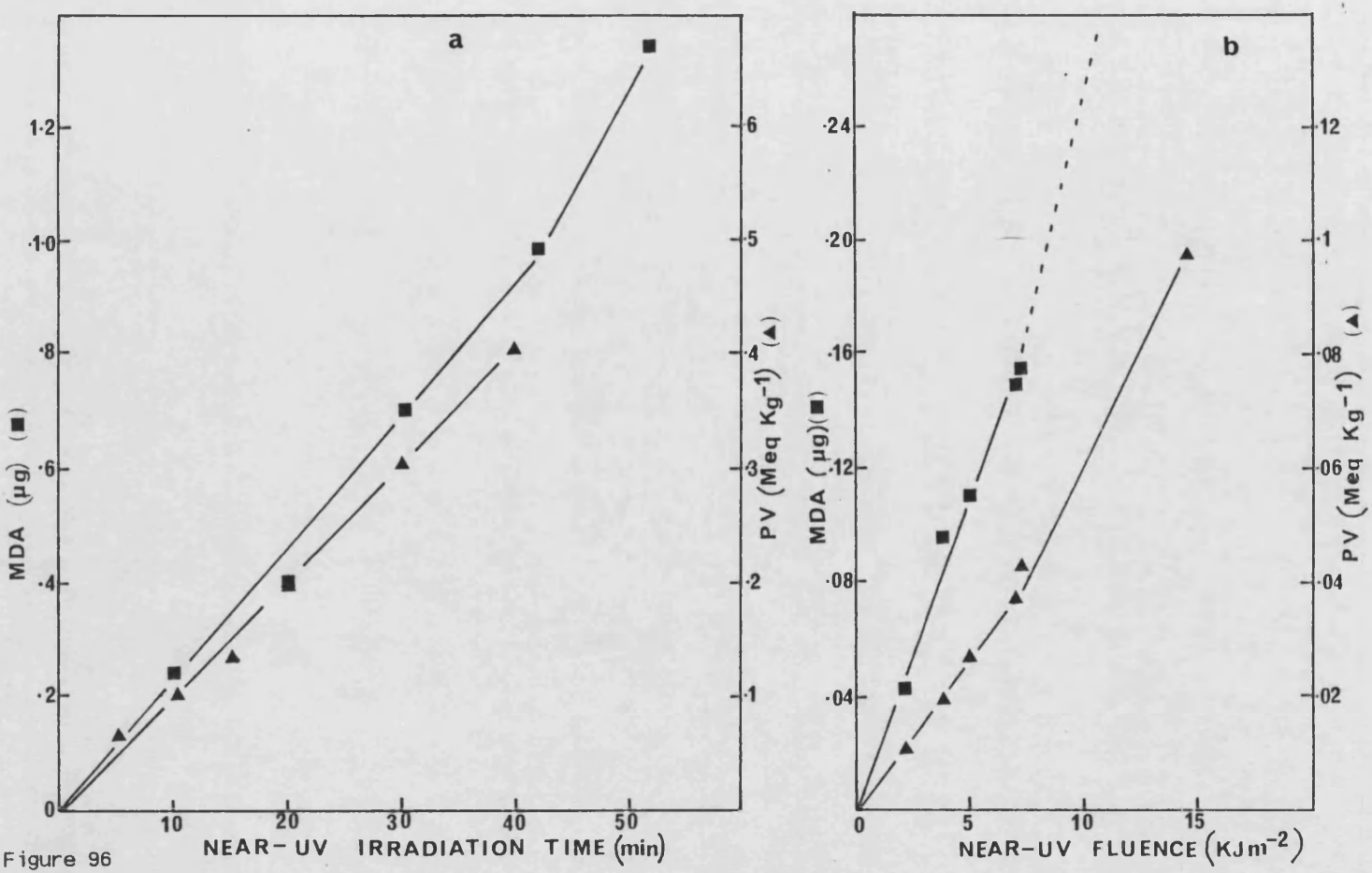

Figure 96

The production of MDA and hydroperoxides by the irradiation of 1x10-3 M linolenic acid by (a)broad-band (b)monochromatic 303nm radiation. Results expressed relative to unirradiated controls.

The dose-response of three concentrations of linolenic acid was determined (Fig. 97). A concentration of 10^{-3} M was chosen for subsequent experiments since it was sufficient to yield easily measurable peroxidation products, while higher concentrations produced very turbid mixtures.

2. The peroxidation of fatty acids at monochromatic wavelengths

Linolenic and linoleic acids were irradiated at various wavelengths and assayed for hydroperoxides and TBA-reacting products. This was a brief survey, intended to ascertain the relative efficiencies of the various wavelengths in catalyzing the peroxidative reactions. Most of the data shown in this section are therefore the result of single determinations at each wavelength (though duplicate samples were used for each chemical assay).

Results are expressed in Table 12 and are expressed as the yield of MDA in $\mu g ml^{-1}$ and the PV (meq kg^{-1}) of the irradiated sample, measured relative to unirradiated controls. The fluence in Jm^{-2} at each wavelength is corrected with reference to the quanta per joule at that wavelength, to give the quanta per square metre.

MDA determinations were carried out on all samples, however values achieved for irradiated linoleic acid were extremely low. The TBA-reacting products derived from autoxidising linolenic and linoleic acids were reported by Gutteridge et al. (1974). They reported that linolenic acid yielded 9 TBA-positive substances, and that linoleic acid yielded 7, at a lower rate, even though theoretically linoleic acid should not yield MDA. The MDA values presented in Table 12 are included for reference, but felt to be

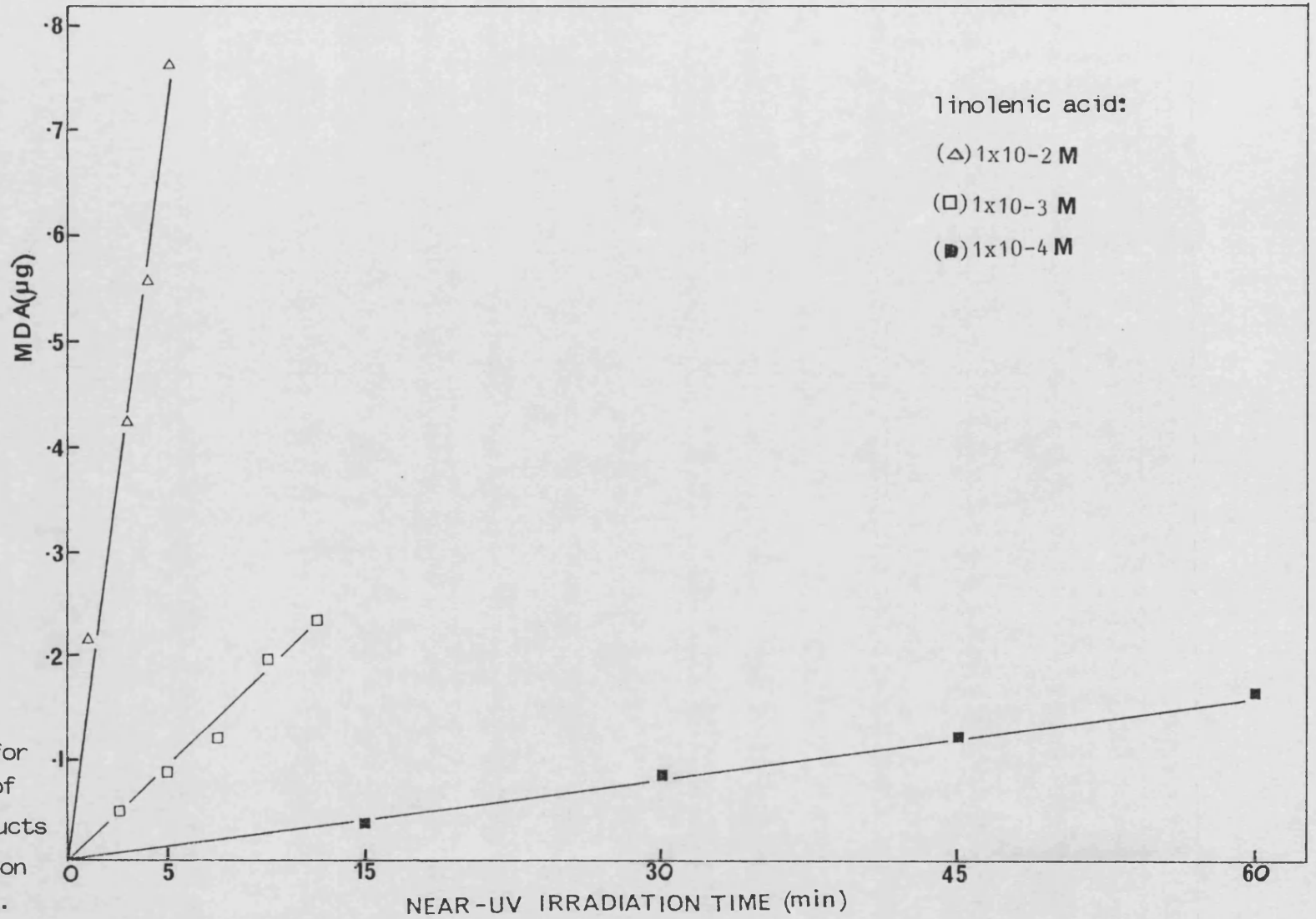

Figure 97

Dose response for the production of TBA-reacting products during irradiation with BLB source.

Table 12. The products of peroxidation of 1 mM linoleic acid and 1 mM linolenic acid after the quantum doses given at the wavelengths used

Wavelength (nm)	Linoleic acid			Linolenic acid		
	Fluence (Qm^{-2})	PV ($meqkg^{-1}$)	MDA (μgml^{-1})	Fluence (Qm^{-2})	PV ($meqkg^{-1}$)	MDA (μgml^{-1})
290	$1.0x10^{22}$	0.087	0.083	$7.3x10^{20}$	0.030	0.195
303	$1.8x10^{22}$	0.126	0.020	$1.8x10^{21}$	0.019	0.164
313	$1.9x10^{22}$	0.056	0.036	$4.6x10^{21}$	0.023	0.258
325	$1.8x10^{22}$	0.012	0.012	-	-	-
334	$3.6x10^{22}$	0.024	0.040	$1.0x10^{22}$	0.017	0.287
345	$2.2x10^{22}$	0.010	0.005	$8.0x10^{21}$	0.025	0.139
350	-	-	-	$1.7x10^{22}$	0.019	0.200
365	$8.3x10^{22}$	0.009	0.078	$3.1x10^{22}$	0.016	0.206
375	$1.1x10^{23}$	0.006	0.111	-	-	-
385	$4.7x10^{22}$	0.002	-	$2.6x10^{22}$	0.007	0.092

subject to unacceptable variation, as evidenced when plotted against the quantum fluence of radiation used.

Oleic acid, under similar irradiation conditions did not undergo any significant peroxidation. The low fluences achieved with the monochromatic source did not result in detectable peroxidation. Irradiation with the broad-band source for 245 nm yielded a PV of 0.06 $meqkg^{-1}$, but no TBA-reacting products.

Action spectra for the NUV irradiation-induced peroxidation of fatty acids

In order to determine the relative efficiencies of the various wavelengths in causing peroxidation, action spectra would be plotted. An action spectrum is a plot of the reciprocal of the fluence required to produce a given effect, against wavelength.

In order that an action spectrum be valid, certain criteria should be met. One such criterion is reciprocity of time and fluence rate, so that the effect obtained is shown to be a function of total fluence, and not of the time during which irradiation occurs. In experiments here, the times of irradiation required to achieve a result at longer, less energetic wavelengths, were longer than those required at shorter wavelengths. Unirradiated controls were always used to give blank values for optical density measurement, thus correcting for autoxidation products formed over the duration of the experiment. However, any such reactions proceeding over long periods were felt to complicate the results, therefore exposure times were kept as low as possible by using the highest fluence rates obtainable. To test the effect of lower fluence rates and consequently longer exposure times, a comparison

was made with 365 nm radiation between 4 different rates used for increasing periods. The results are shown below (Table 13).

Table 13. The effect of fluence rate on peroxidation of linolenic acid by 365 nm radiation

Fluence rate ($Jm^{-2}s^{-1}$)	Fluence (Jm^{-2})	Time of irradiation (min)	MDA (μgml^{-1})	PV ($meqkg^{-1}$)
11.8	$3.4x10^4$	48	0.145	0.040
8.8	$3.4x10^4$	64	0.240	0.075
7.3	$3.4x10^4$	79	0.252	0.080
5.8	$3.4x10^4$	98	0.268	0.089

This result indicates that although the same fluence was given, the amount of MDA and hydroperoxides increased with increasing time necessary to give that fluence. This relationship invalidates the plotting of an action spectrum.

Further comparisons are shown below in Table 14, where at 334 nm and 313 nm various fluences and fluence rates were used during different experiments. When the yield of MDA per Jm^{-2} is calculated, it is not consistent except in that the yield per Jm^{-2} increases with increasing exposure time.

As previously discussed, it was not the intention in this preliminary study to investigate factors which might contribute to the near-UV radiation-induced peroxidation of the unsaturated fatty acids. However, it became evident that in the period following irradiation peroxidation of the fatty acids continued. This phenomenon was given further consideration, as it may be pertinent to post-irradiation events *in vivo*.

Table 14. The yield of TBA-reacting products, "MDA", at various fluences and fluence rates

Wavelength (nm)	Fluence rate ($Jm^{-2}s^{-1}$)	Fluence (Jm^{-2})	Time (min)	MDA (μgml^{-1})	MDA per Jm^{-2}
334	0.9	$3.85x10^{3}$	70	0.049	$1.27x10^{-5}$
	1.5	$2.30x10^{4}$	245	1.220	$5.30x10^{-5}$
	2.3	$1.39x10^{4}$	100	0.287	$2.06x10^{-5}$
313	1.7	$2.2x10^{4}$	215	1.01	$4.5x10^{-5}$
	1.8	$2.4x10^{4}$	215	1.03	$4.3x10^{-5}$
	2.1	$8.3x10^{3}$	66	0.258	$3.1x10^{-5}$

3. Post-irradiation peroxidation of linoleic acid

Linoleic acid was irradiated as described above. Immediately following irradiation the hydroperoxide assay was performed. The irradiated samples, unirradiated controls and water blanks were divided into two batches. One was bubbled gently with air, through narrow polyethylene tubing, the other batch was bubbled with oxygen-free nitrogen. The optical density was measured at intervals and the peroxide value calculated.

During the hours following cessation of irradiation the peroxide value of the irradiated samples increased more than that of unirradiated samples. Fig. 98 depicts the optical densities obtained during one such experiment, following 2.78×10^{22} Qm^{-2} of 303 nm radiation. Peroxide values of the irradiated fatty acids, calculated relative to the appropriate unirradiated controls were

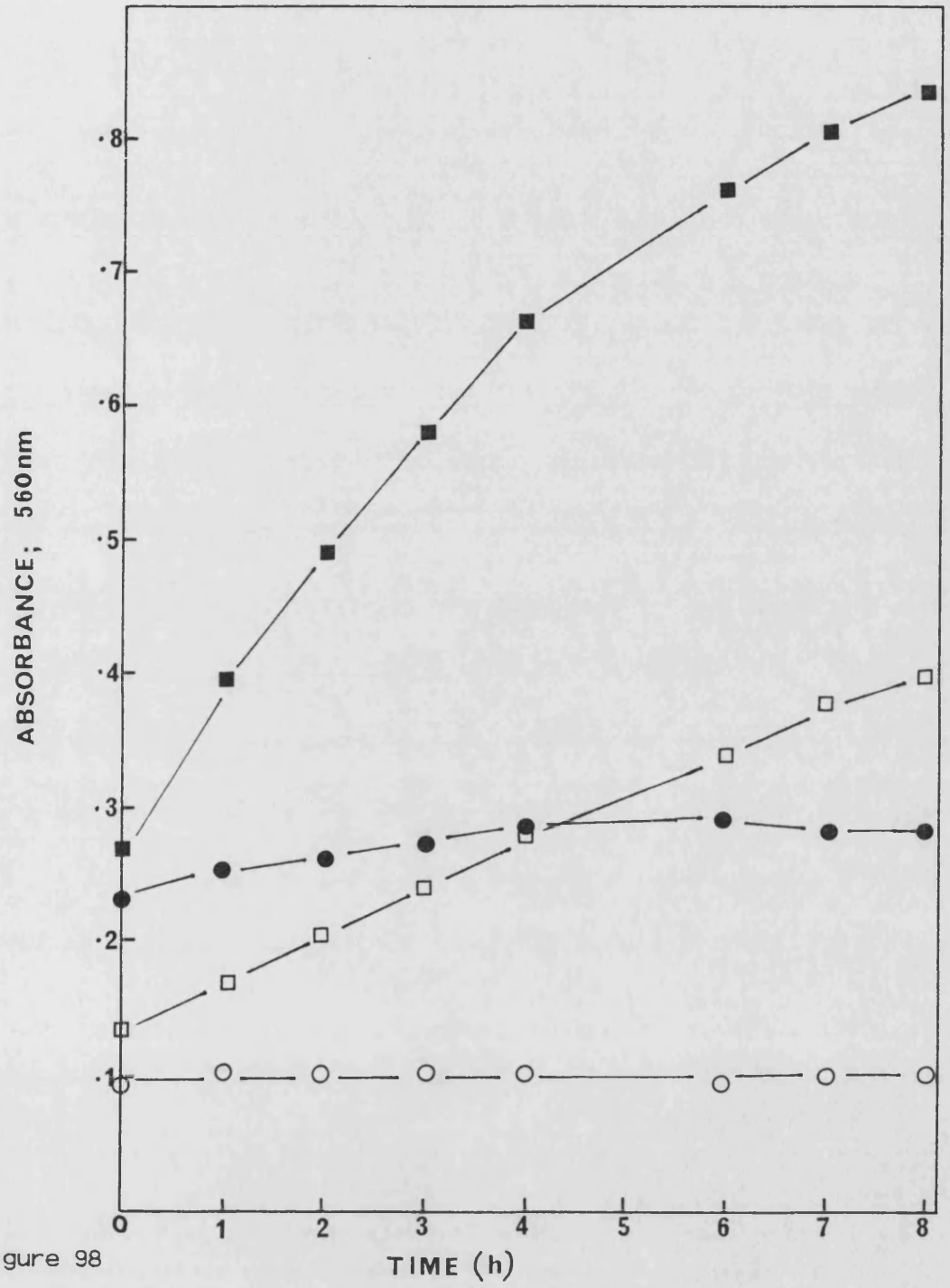

Figure 98

The optical density of unirradiated (open symbols) and irradiated (closed symbols) linoleic acid during the hours following irradiation at 303nm(2.78×10^{22} Q m-2.)

Samples bubbled with air (□■) or nitrogen(○●).

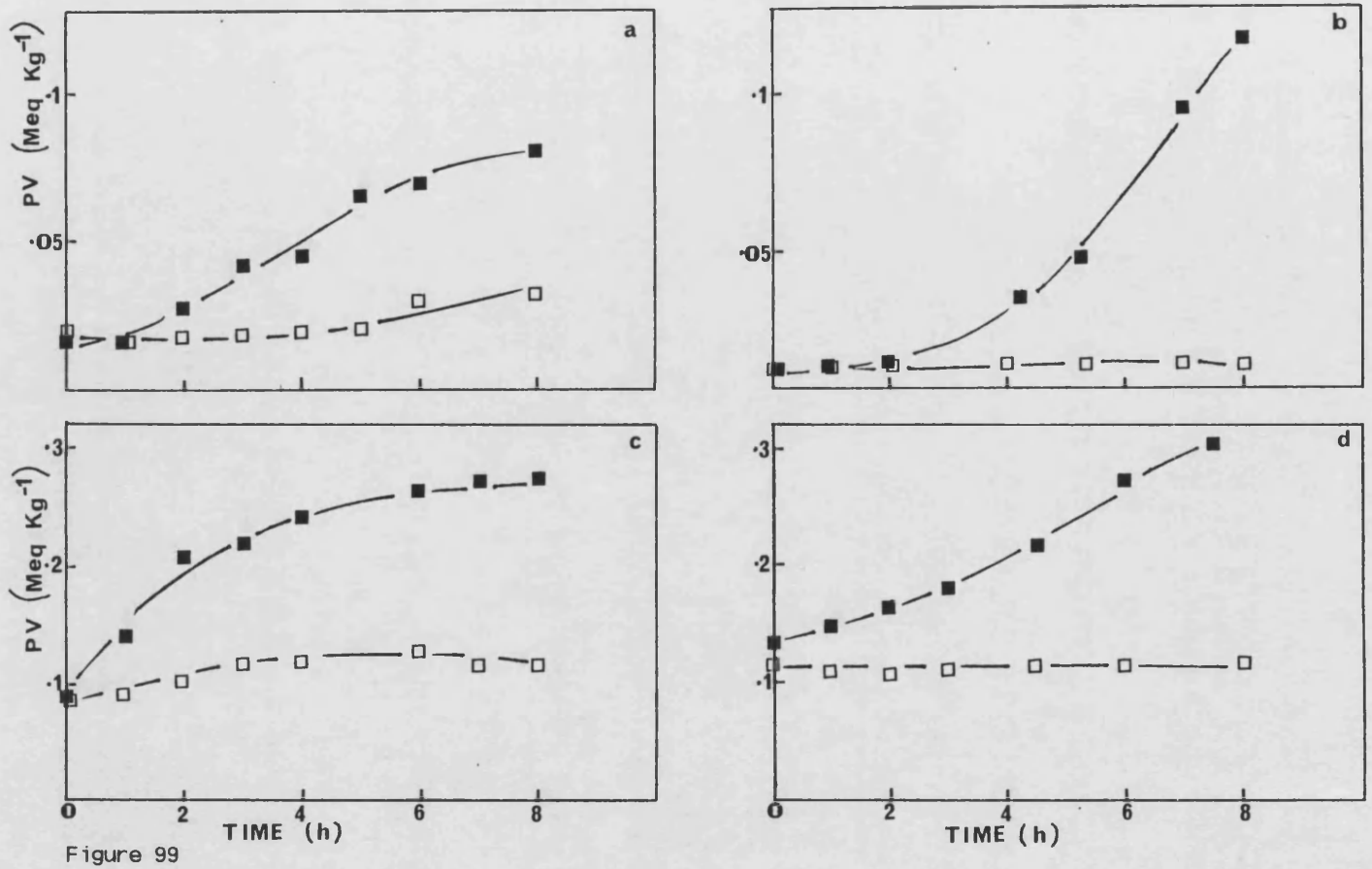

Figure 99

The PV of irradiated linoleic acid in the hours following irradiation with (a)334nm:$3.0\times10^{22}Qm^{-2}$ (b)303nm:$1.4\times10^{22}Qm^{-2}$ (c)303nm:$2.8\times10^{22}Qm^{-2}$ (d)303nm:$4.4\times10^{22}Qm^{-2}$. Samples bubbled with air (closed symbols) or nitrogen (open symbols).

plotted with time as shown in Fig. 99. The data presented in Fig. 99c shows the data plotted in Fig. 98. Fig. 99b and 99d show the peroxide values following lower fluences of 303 nm radiation, while Fig. 99a shows values following 334 nm irradiation.

As expected, the nitrogen-bubbled samples showed little or no peroxidation, whether or not they had been irradiated, during this post-irradiation period. Such samples maintained a constant optical density as shown in Fig. 98.

4. The near-UV irradiation of liposomes

Liposomes may be considered to provide a highly simplified model depicting the arrangement of lipid molecules within a biological membrane. The spatial configuration of the molecules in a liposomal membrane, where the arrangement of fatty acid chains within the hydrophobic interior of the bilayer in close proximity to each other may facilitate propagation steps of peroxidative reactions.

Lecithin containing two linoleic acid moieties per molecule was available, though a lecithin containing linolenic acid was not. Therefore liposomes were prepared using dilinoleoyl lecithin as described in the Methodology, and shown in Appendix 7. Liposomes were prepared so that the concentration of linoleic acid was equivalent to the concentration of the free fatty acid used in the previously described experiments. Suspensions of the liposomes were irradiated with the monochromatic source as described in the Methodology.

Initial levels of hydroperoxides were extremely low, if detectable at all, immediately after irradiation.

When liposomes were bubbled with air during the post-irradiation period, the observed level of hydroperoxides increased rapidly following a lag period during which there was no such increase. Fig. 100 shows the optical density measurements following the hydroperoxide assay for irradiated and unirradiated liposomes bubbled after irradiation with either air or oxygen-free nitrogen.

The PV of the aerated, irradiated liposomes was calculated relative to the unirradiated liposomes and plotted with the post-irradiation time, as shown in Figs. 101-103. Nitrogen-bubbled liposomes underwent no peroxidation, as shown in the data relating to these experiments in the appendix (Table 55). Four wavelengths were used, various fluences being given at those wavelengths.

It is clear that following higher fluences at one wavelength the post-irradiation peroxidation proceeds at a faster rate, reaching a higher level over the period of the experiment. When similar quantum fluences are used at different wavelengths, the lower wavelength results in higher levels of hydroperoxides. This would be expected in consideration of the inverse relationship between the energy of a quantum and the wavelength of the radiation.

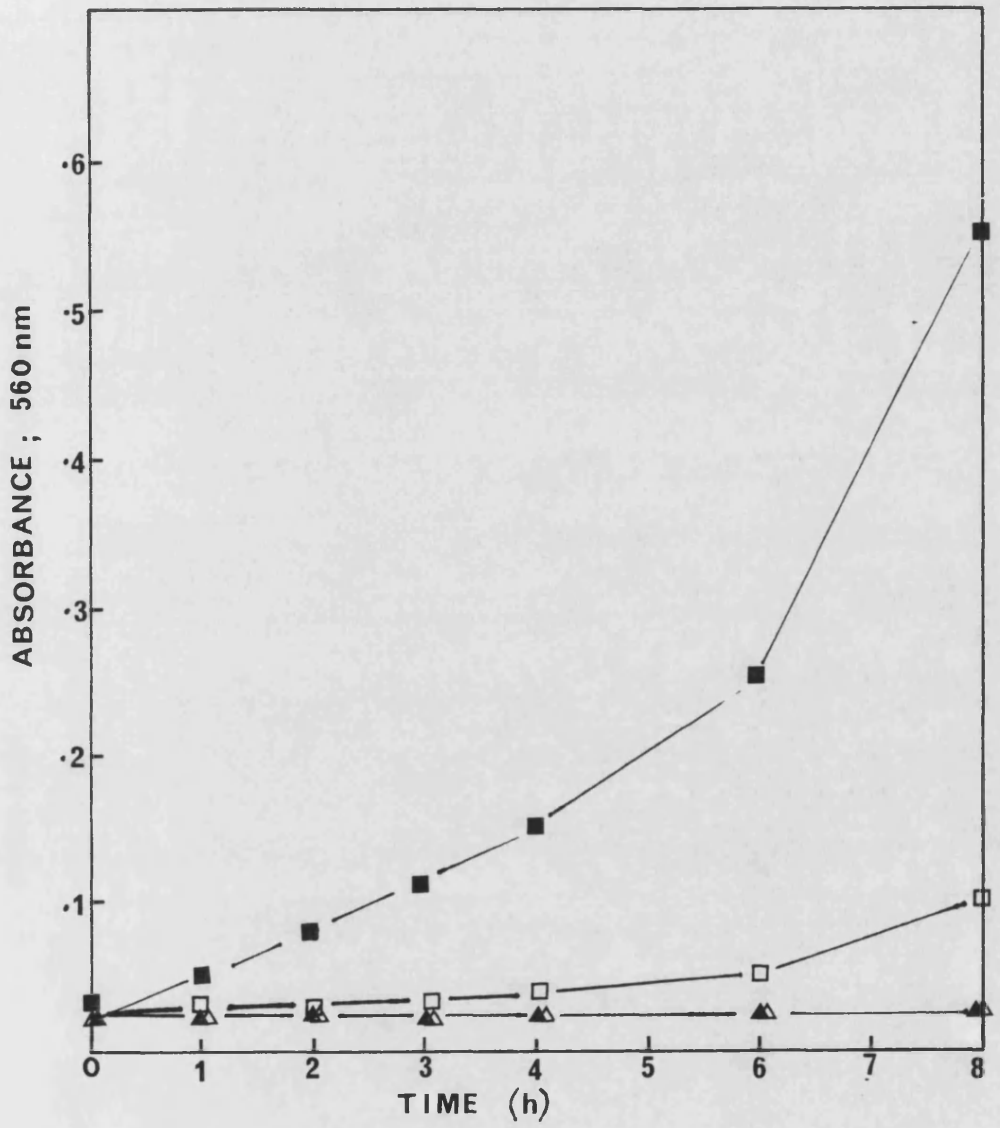

Figure 100

Optical density (560nm) of unirradiated (open symbols) and irradiated (closed symbols) liposomes during the hours following irradiation at 303nm (3.0×10^{22} Qm-2). Samples bubbled with air (□■) or nitrogen (△▲).

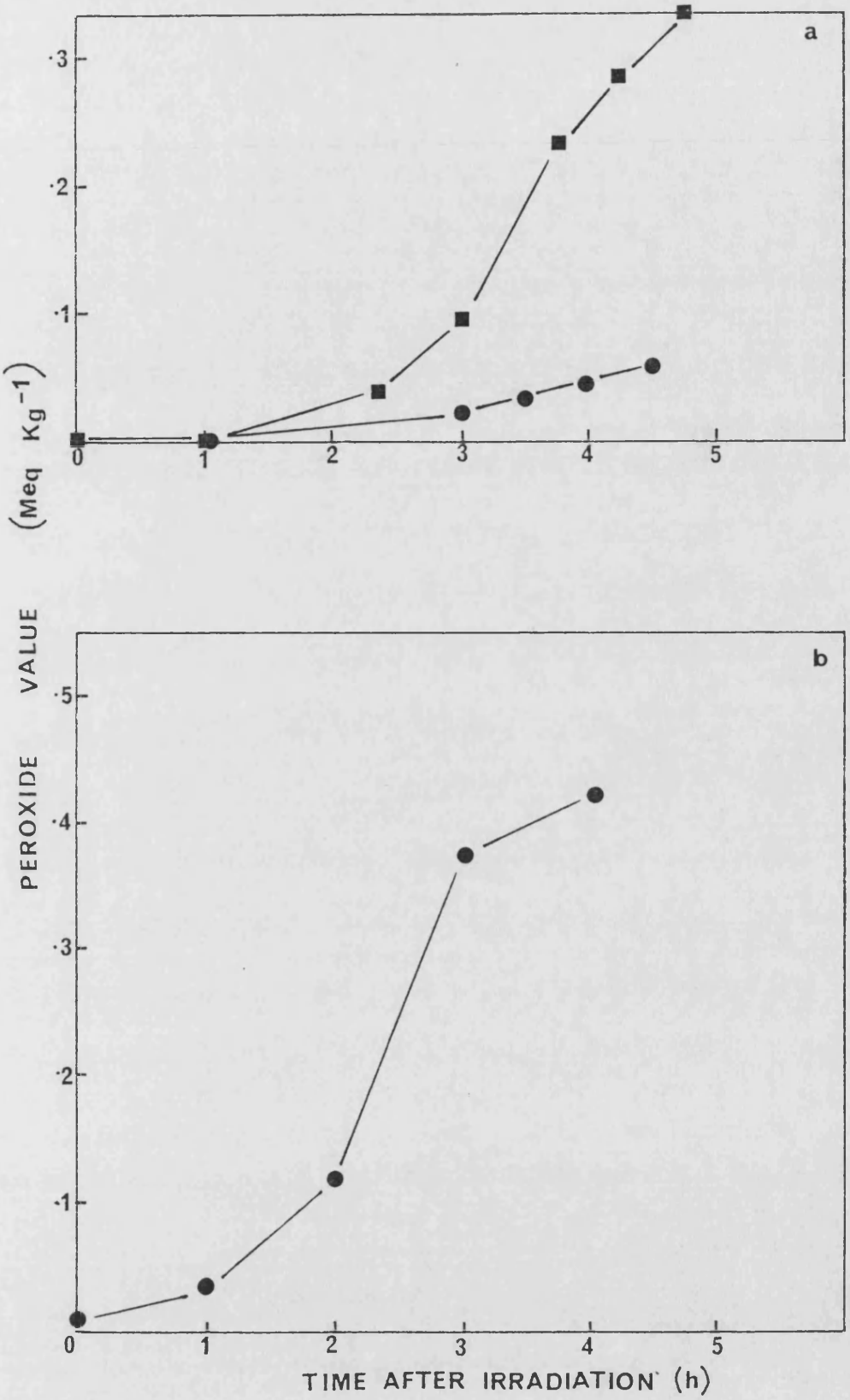

Figure 101

Post-irradiation peroxidation of dilinoleoyl Lecithin Liposomes after irradiation at a) 290 nm, fluences (■) $1.1 \times 10^{22} Qm^{-2}$ (●) $8.5 \times 10^{21} Qm^{-2}$. b) 297 nm, fluence $2.3 \times 10^{22} QM^{-2}$

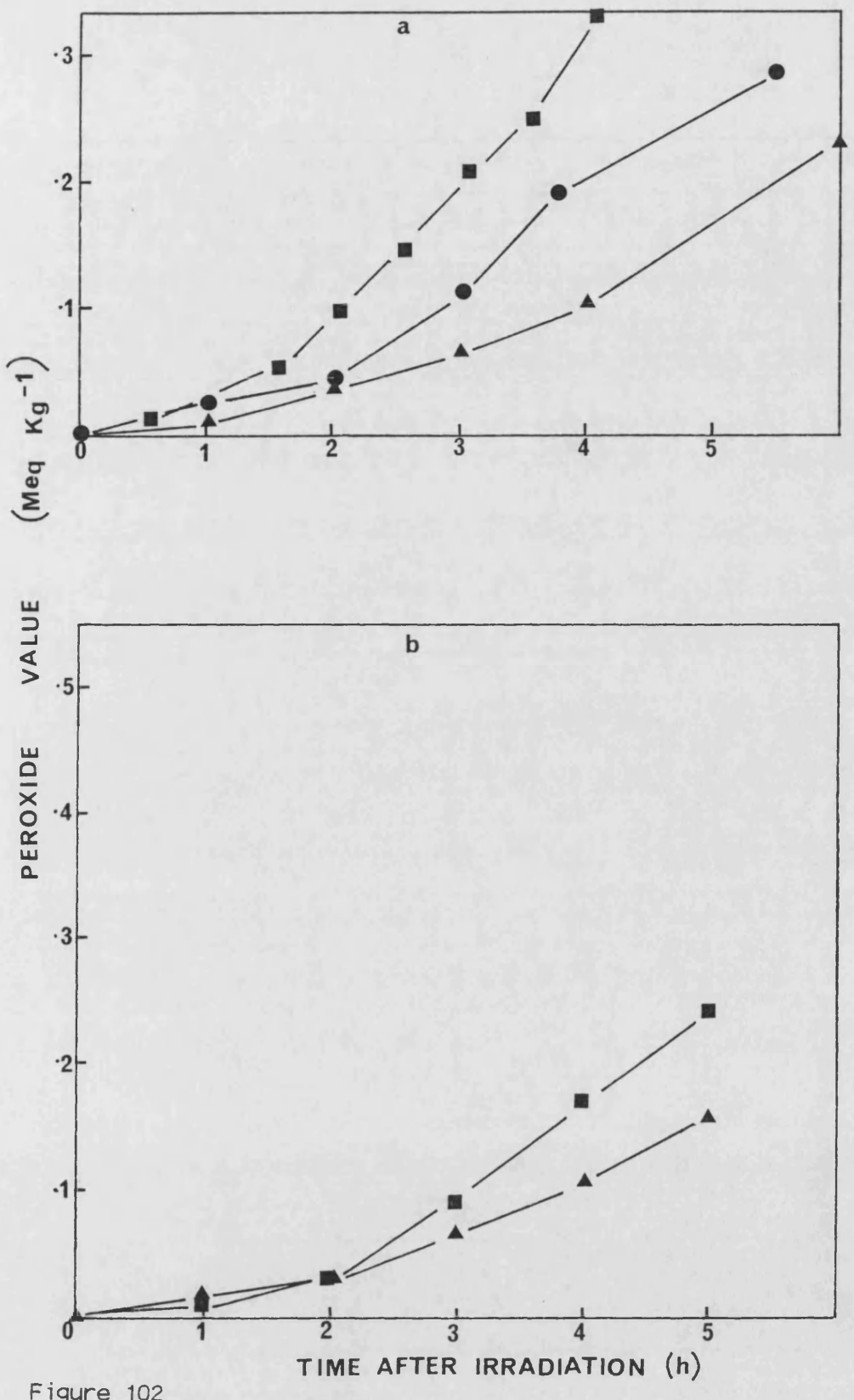

Figure 102 Post-irradiation peroxidation of dilinoleoyl Lecithin Liposomes after irradiation at

a) 303 nm, (■) $7.2 \times 10^{22} Qm^{-2}$ (▲) $3 \times 10^{22} Qm^{-2}$ (●) $6.3 \times 10^{22} Qm^{-2}$

b) 303 nm, (■) $5.8 \times 10^{22} Qm^{-2}$ (▲) $2.8 \times 10^{22} Qm^{-2}$

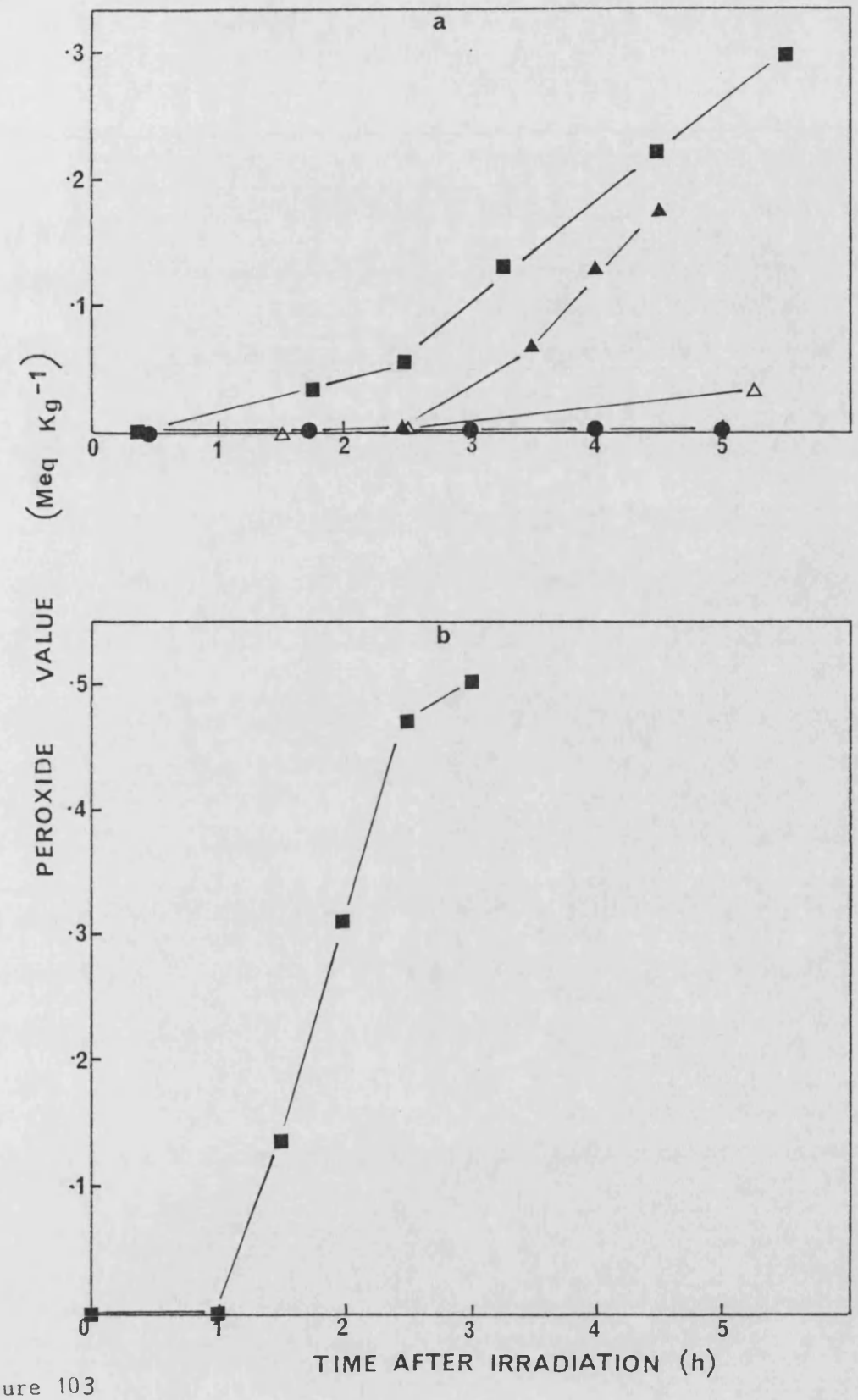

Figure 103

Post-irradiation peroxidation of dilinoleoyl Lecithin Liposomes after irradiation at a) 334 nm, fluences (■) 6.6×10^{22} Qm^{-2} (▲) 5.9×10^{22} Qm^{-2} (●) 3.1×10^{22} Qm^{-2} (△) 4.2×10^{22} Qm^{-2} b) 365 nm, fluence 4.3×10^{23} Qm^{-2}

SUMMARY AND DISCUSSION

In this preliminary series of experiments commercial preparations of fatty acids and dilinoleoyl lecithin have been shown to undergo peroxidation during exposure to near-UV irradiation (Figs. 96 and 97), and in the hours following irradiation (Figs. 98-103). Schieberle and Grosch (1984) demonstrated the photolysis of unsaturated fatty acid hydroperoxides at wavelengths below 338 nm. While their irradiation system involved various polar and non-polar solvents, they confirmed that the hydroperoxides were photolytically cleaved at the relatively weak O-O bond with the formation of alkoxy and hydroxy radicals. It is perhaps the most reasonable explanation of the results obtained in this series of experiments that lipid or fatty acid hydroperoxides, present as low-level contaminants of the preparation, were degraded in this fashion. The resulting radicals may then have taken part in propagation reactions both during and after irradiation, resulting in the levels of peroxidation observed. Such reactions would reasonably be expected to be catalysed by iron, present as a contaminant of the laboratory water supply (Halliwell and Gutteridge, 1985), and such parameters could be further investigated and controlled. As previously described, the human stratum corneum contains unsaturated free fatty acids, which may be susceptible to autoxidation if not protected by antioxidants within the layer. An investigation into the level of hydroperoxides, and perhaps available iron, in this layer, and the effects of solar radiation upon them and the fatty acids *per se*,

may provide useful information about the biological relevance of the results presented above.

APPENDICES

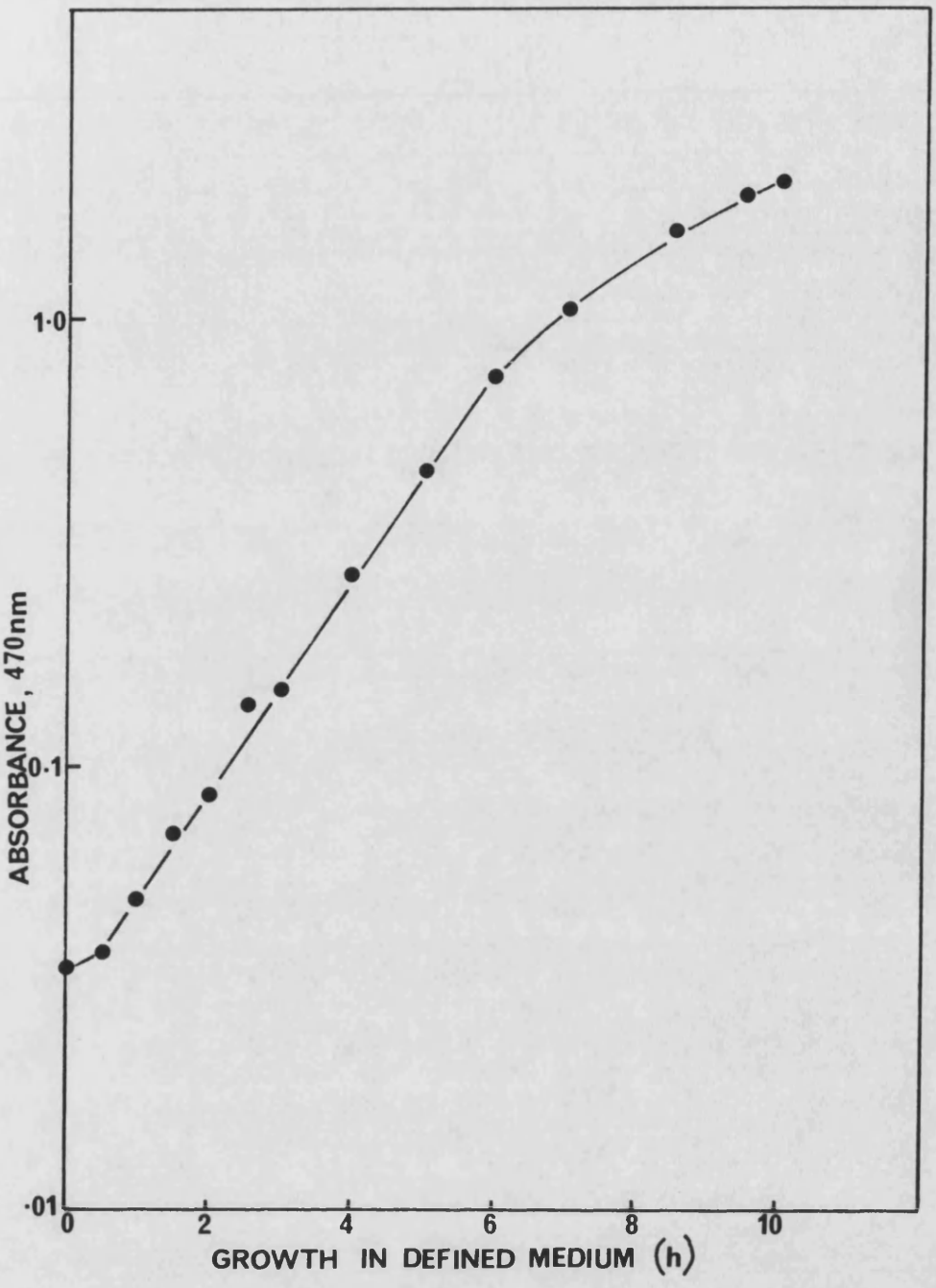

Figure A1

Growth curve of E. coli K1060 in defined growth medium.

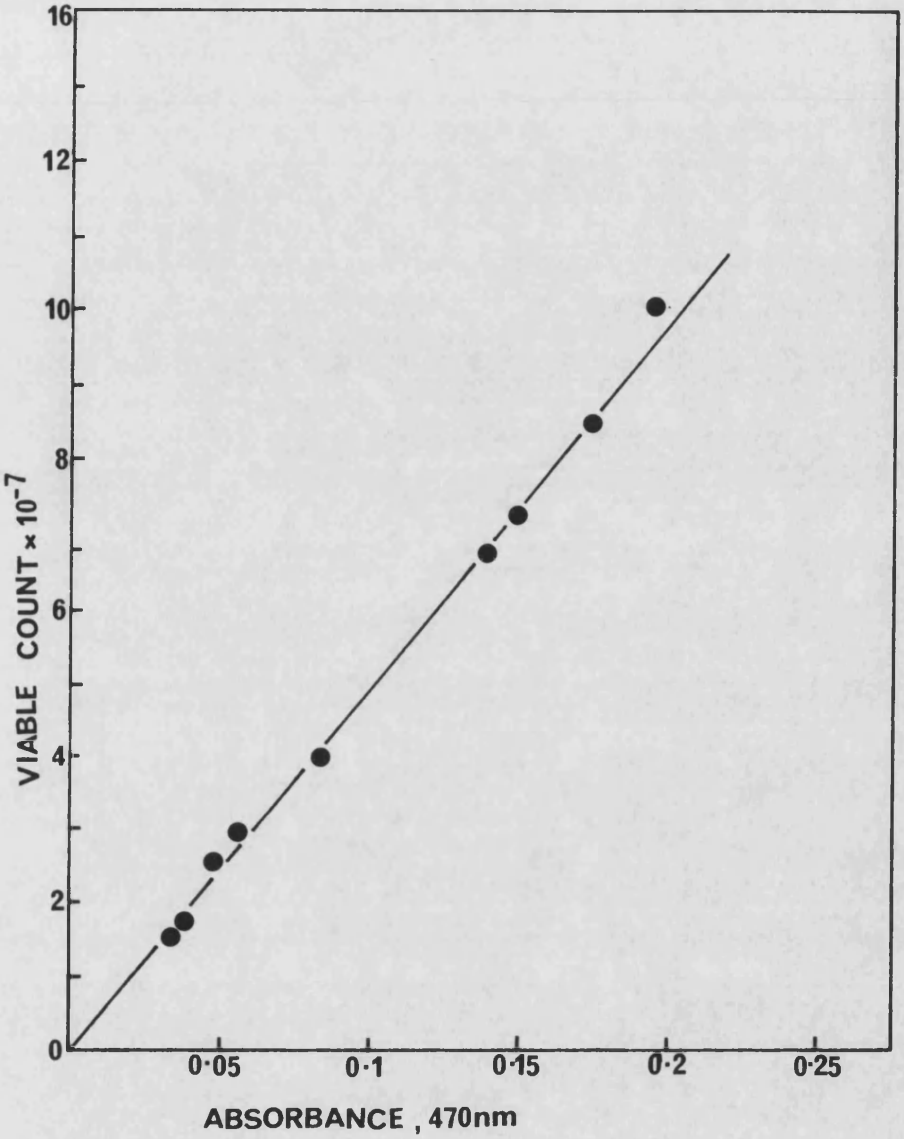

Figure A2

Optical density at 470nm : viable count calibration graph for E. coli K1060

Appendix 2

Table A1 CLINICAL HISTORY OF PATIENT FROM WHICH AR6LO CELLS ORIGINATED

From the Institute of Dermatology, St. John's Hospital Hoverton Grove, London

Date of Birth:	4.10.1932
Sex:	Male
History:	Started 1978, back of hands; 1979 noticed relationship of rash to solar exposure
Monochromator tests	April 1980, monochromator light tests showed abnormal photosensitivity out to 400 nm. Threshold doses for abnormal morphological responses at 300, 307.5 nm were 10 $mJcm^{-2}$, at 320 nm 0.5Jcm^{-2} and at 340 nm 10 Jcm^{-2}; abnormal morphological responses also obtained with 360 and 400 nm; threshold doses not determined.
Other tests:	April, 1980, photo-patch tests done to:

hexachlorophene	-ve
tribromsalicylanilide	-ve
bithionol	-ve
trichlorcarbanilide	-ve
chlorpromazine	+ve

There were weak questionable patch test reactions to a number of substances, e.g. oak moss, "perfume-mix", potassium dichromate, balsam of peru.

Normal (116%) UDS and post-replication repair.

On examination: April, 1980, erythemato-papular eruption on back of hands, face, scalp and neck

APPENDIX 3

THE INSTALLATION OF NEW BROAD-BAND NEAR-UV LAMPS (BLB)

As the fluence rate of the original lamps was falling, new B-L-B lamps, of the same specification, were installed during the course of this work.

The fluence rate of the new lamps, determined by biological dosimetry as previously described, was approximately twice that of the old lamps (Fig. A3 shows the result of such a dosimetry determination).

Survival curves were plotted for E. coli K1060 incorporating each of the three unsaturated fatty acids used in this work. Viability was assessed on YENB, and normal or high salt defined media. The results of replicate experiments are shown in Fig. A4, A5 and A6. A comparison with Figs. 27, 29 and 30 shows that as a result of the higher fluence rate, the survival of K1060 incorporating linolenic acid (18;3), when assessed on YENB is considerably reduced, the shoulder of the survival curve being minimal. The effect is less evident for linoleate-grown cells, while being absent for oleate-grown cells.

The reduction in survival of linolenate-grown cells is less evident when plated onto defined media (either normal or high salt).

The effect of fluence rate was therefore determined, by irradiating linolenate-grown K1060 from the same culture batch with either 6 lamps or 3 lamps, the latter effectively reducing the fluence rate to that of the original lamps.

Fig. A7 shows the results where, following exposure to the same

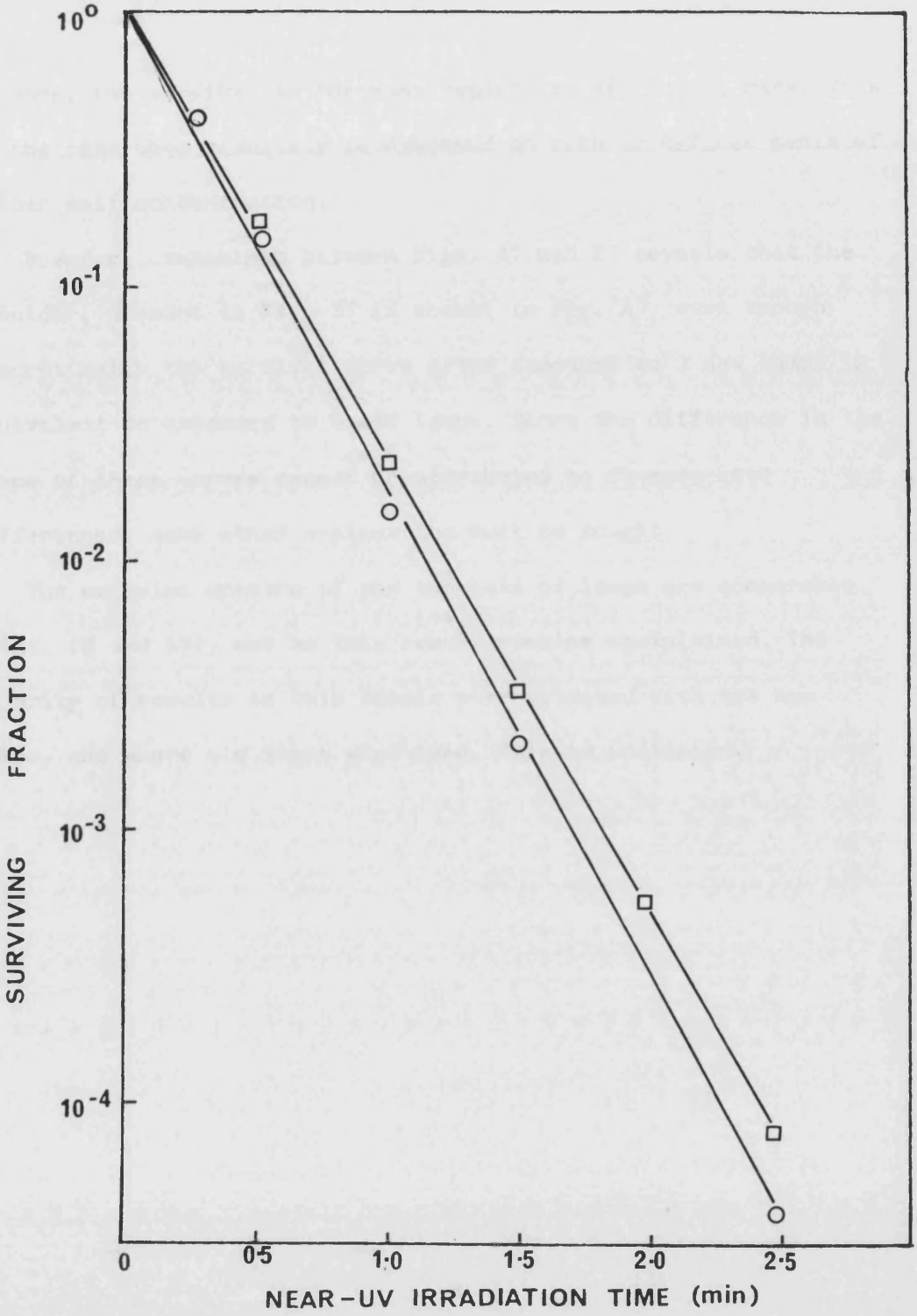

Figure A3

Biological dosimetry for the broad-band near-UV lamps using E. coli K1060 at a concentration of (□) 10^9 (○) 10^7 cells ml^{-1}. Calculated fluence rate (□) 1.7×10^3 $Jm^{-2}s^{-1}$
(○) 1.9×10^3 $Jm^{-2}s^{-1}$

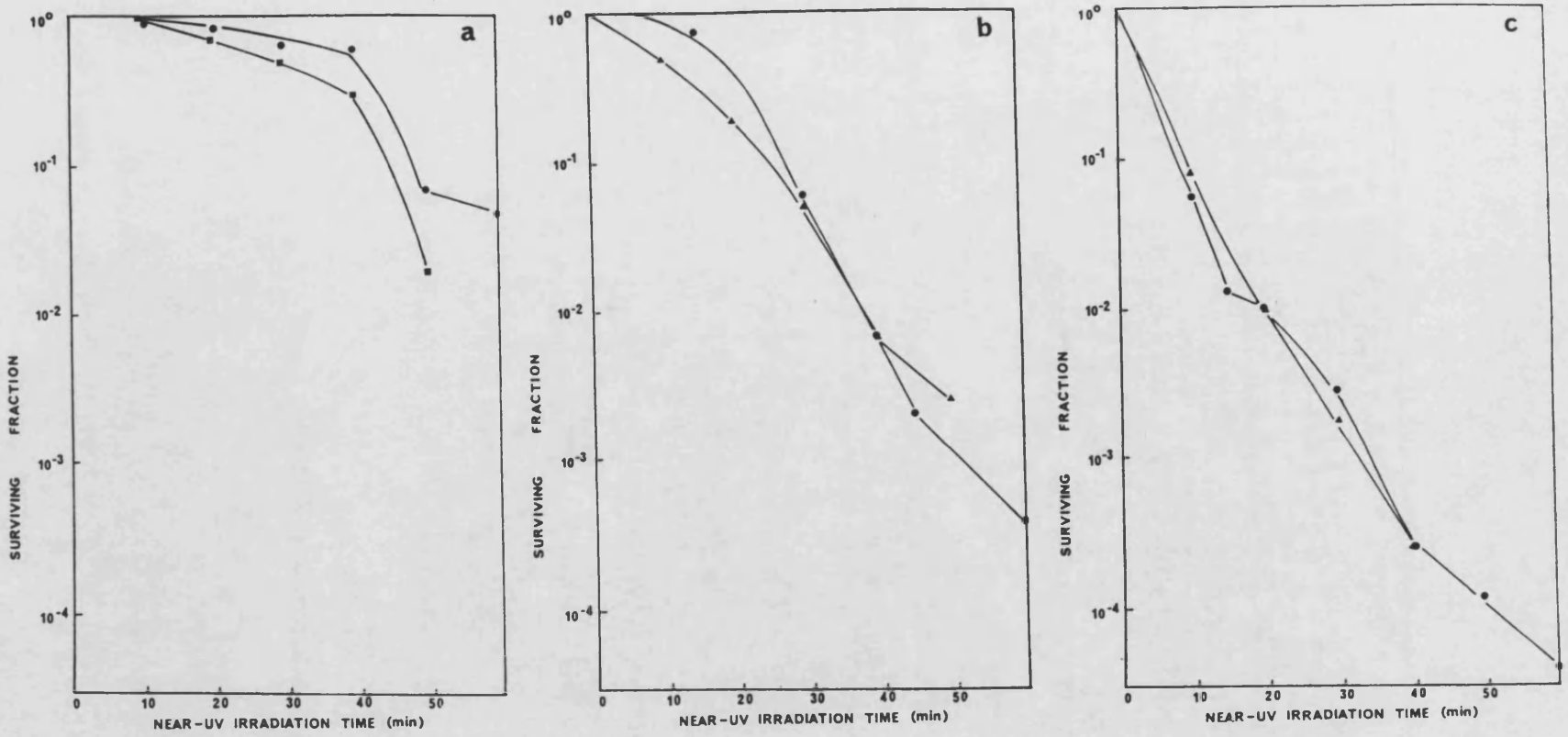

Figure A4
Survival curves for log phase E. coli K1060 incorporating (a) oleic (b) linoleic or (c) linolenic acid, following broad-band near-UV irradiation with the new lamps. Viability assessed on YENB. Open and closed symbols represent replicate experiments performed on different days.

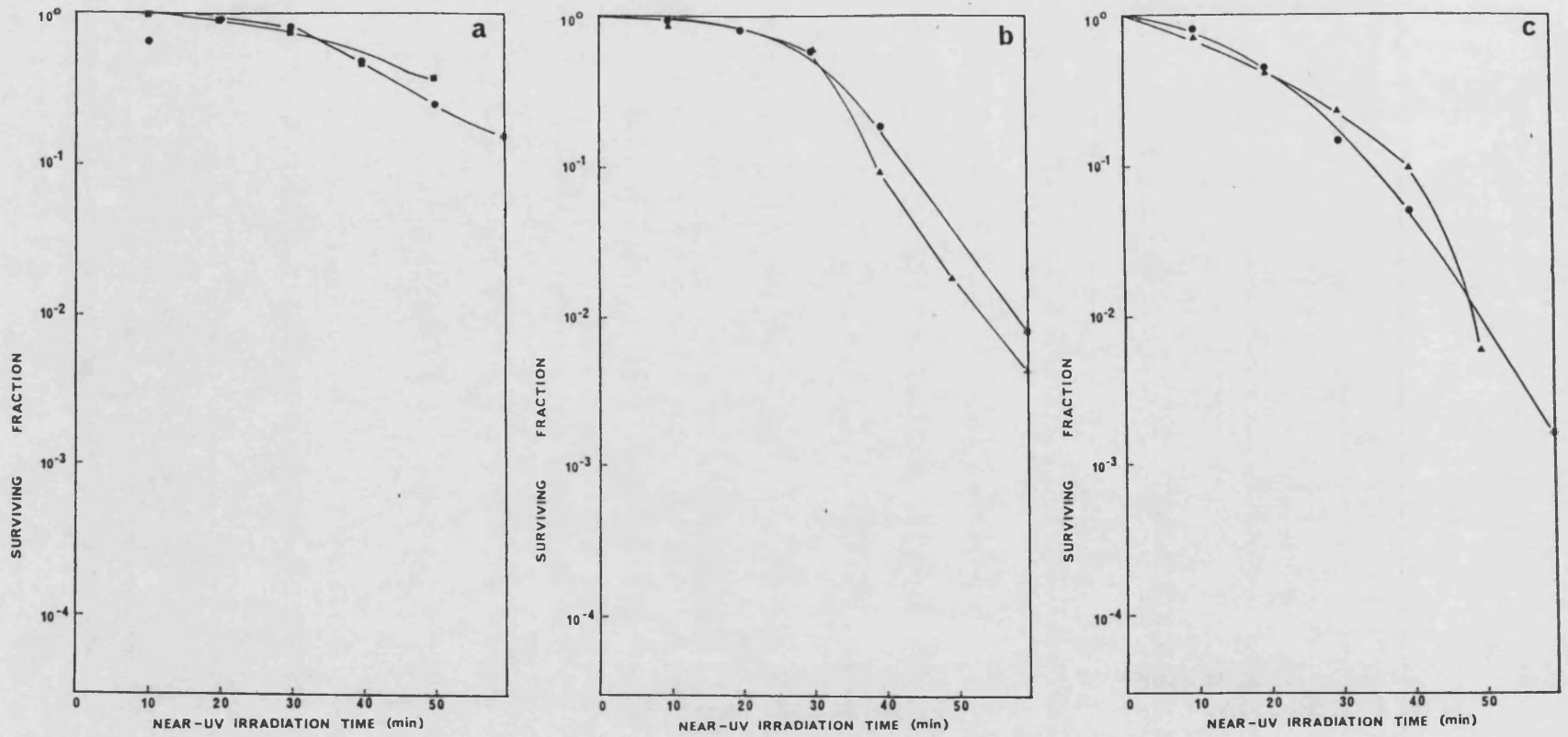

Figure A5 Survival curves for log phase E. coli K1060 incorporating (a) oleic (b) linoleic or (c) linolenic acid, following broad-band near-UV irradiation. Viability assessed on defined medium. Open and closed symbols represent replicate experiments performed on different days.

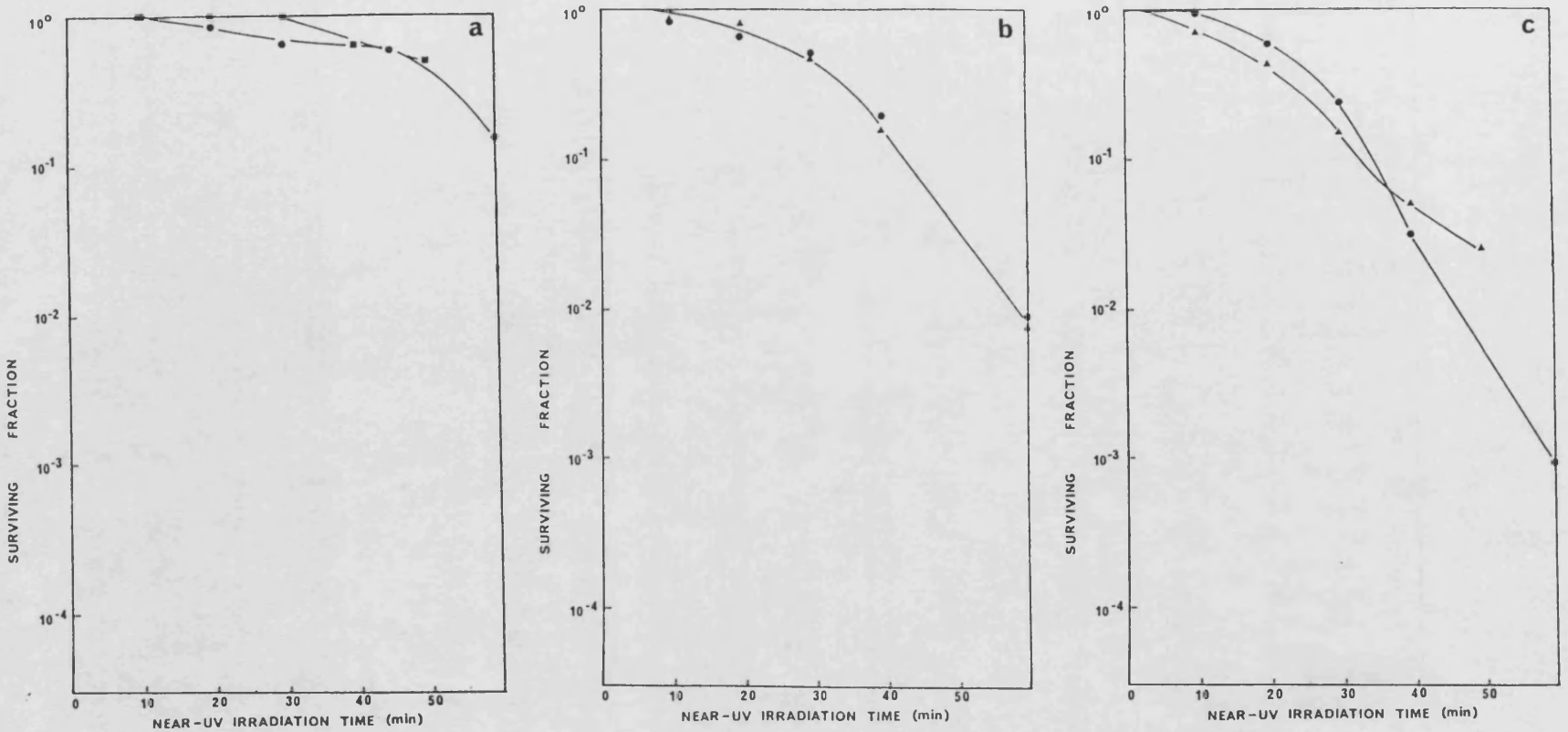

Figure A6 Survival curves for log phase E. coli K1060 incorporating (a) oleic (b) linoleic or (c) linolenic acid, following broad-band near-UV irradiation Viability assessed on high salt defined medium. Open and closed symbols represent experiments performed on different days.

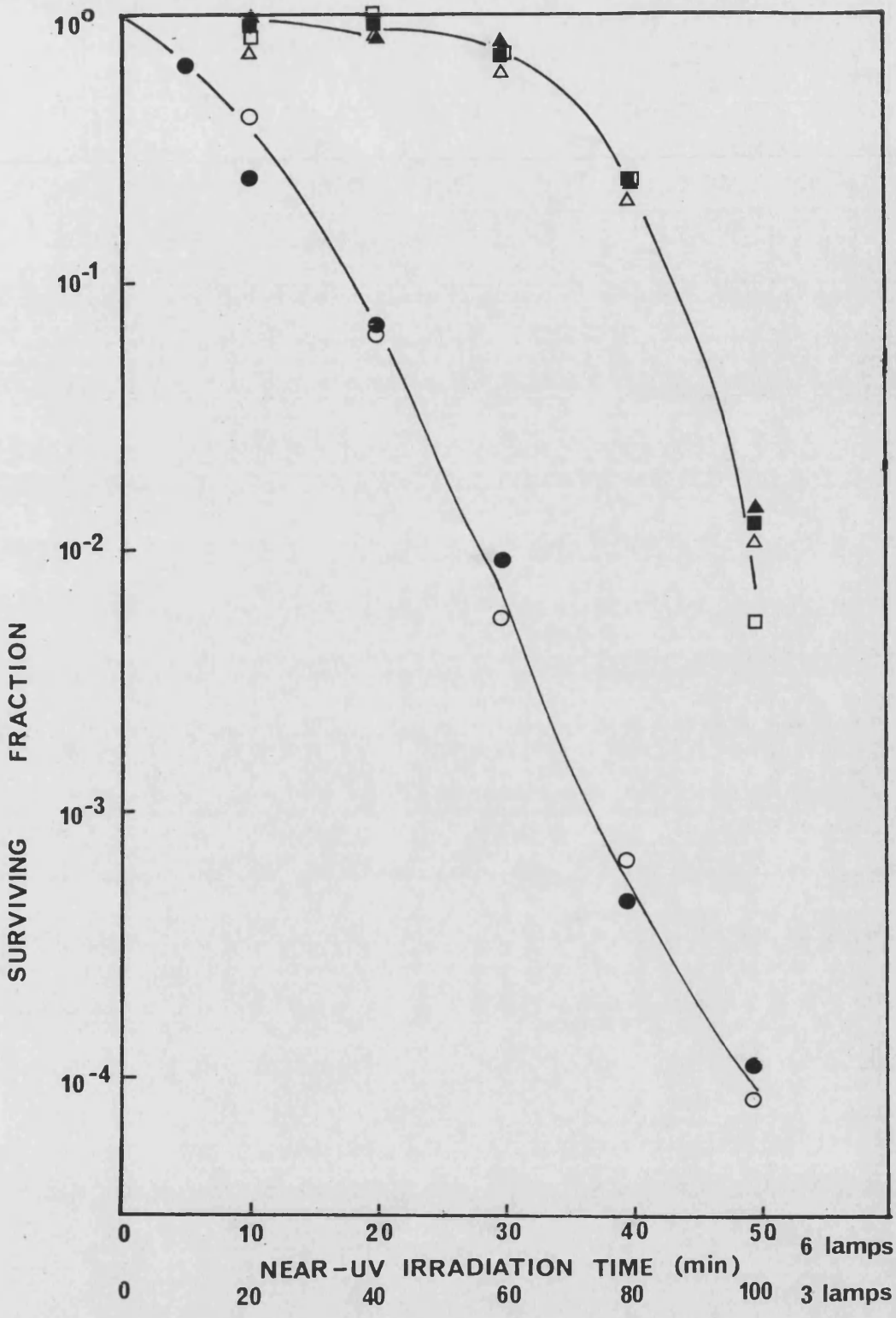

Figure A7
Survival curves for E. coli K1060 following irradiation with 3 (open symbols) or 6 (closed symbols) new BLB lamps. Viability assessed on YENB (○●), normal salt (□■) or high salt (△▲) medium.

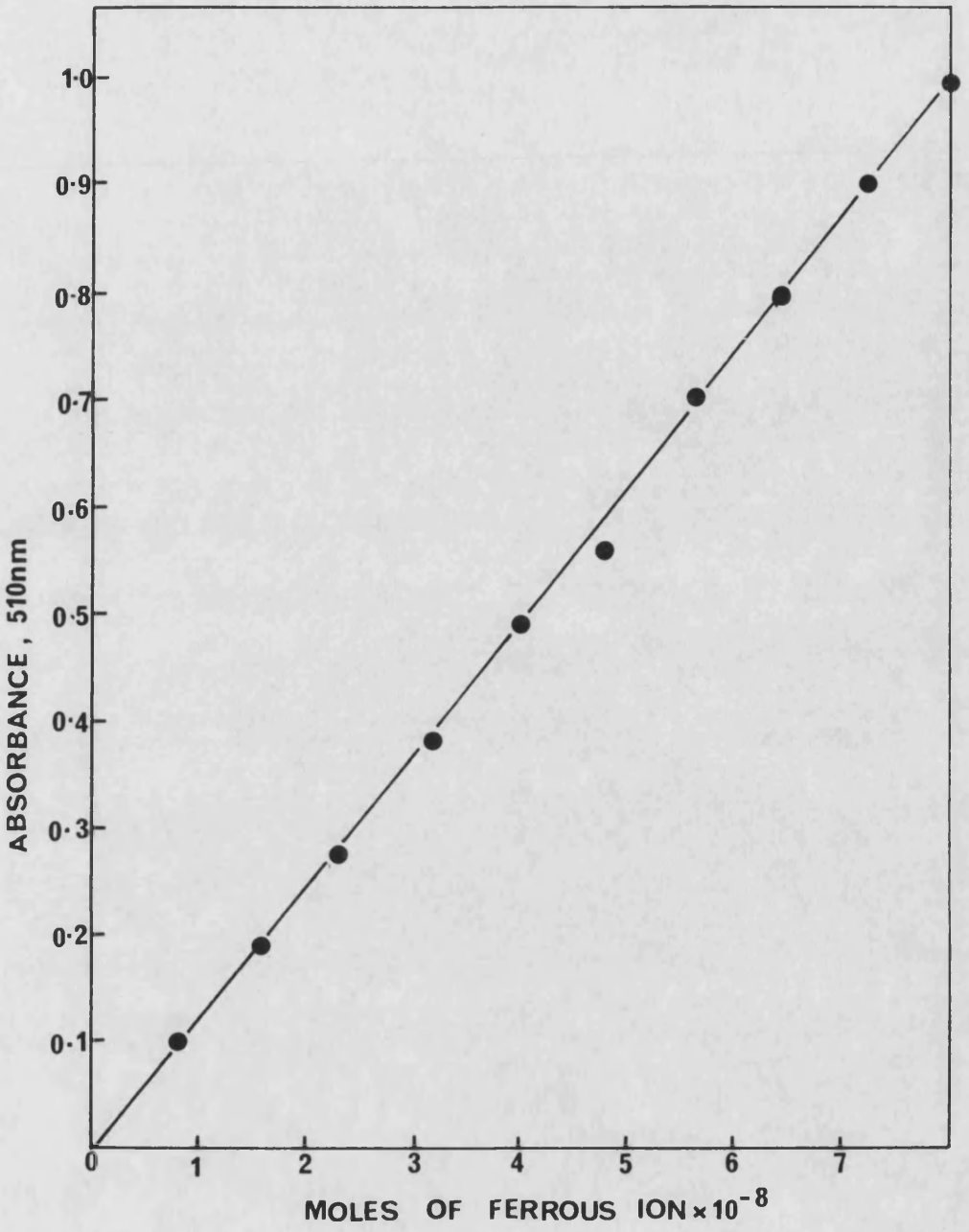

Figure A8

Calibration Curve for the conversion of optical density to amount of ferrous ion.

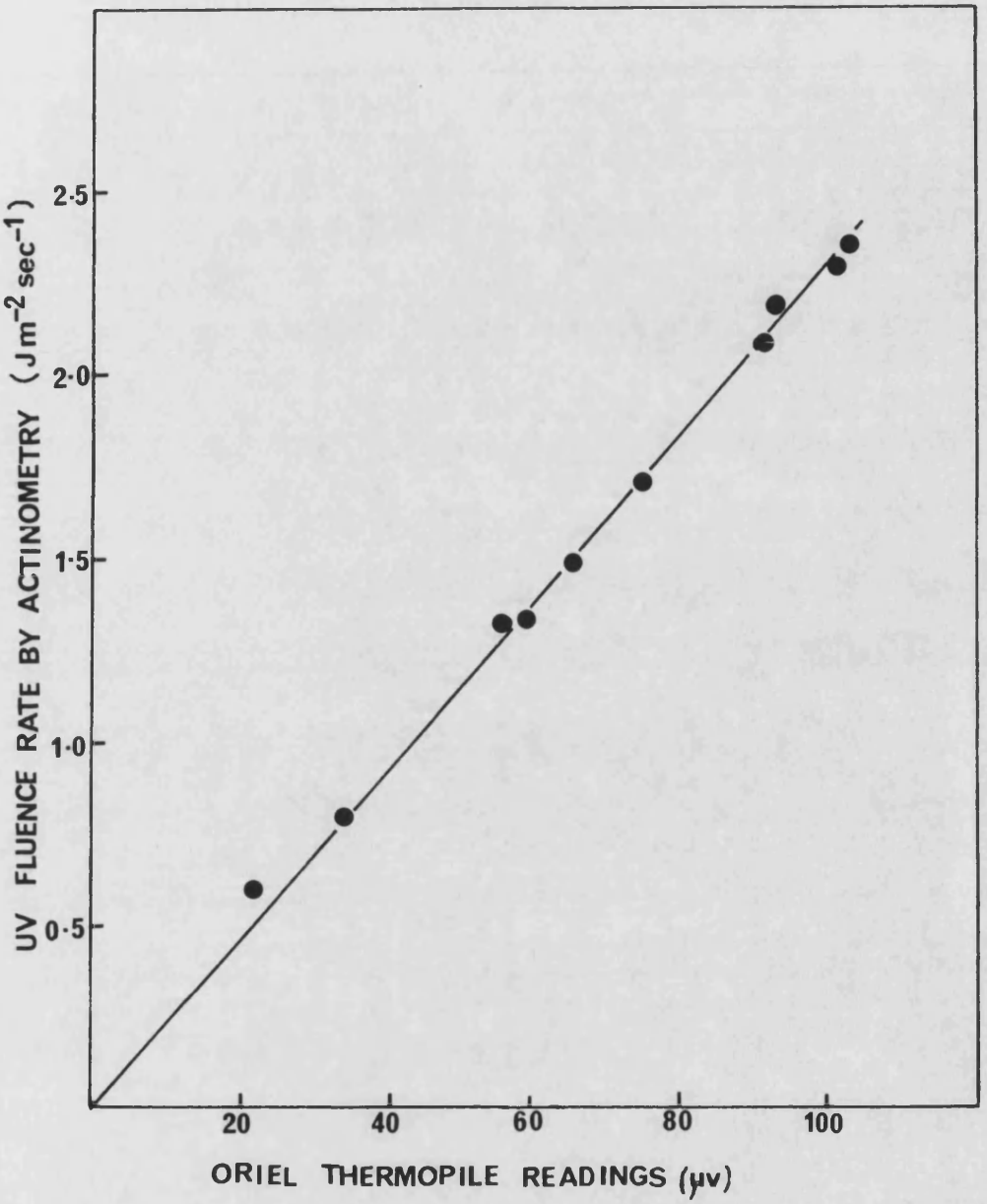

Figure A9

Thermopile readings (Oriel 7102) in microvolts, plotted against UV fluence rate obtained by potassium ferrioxalate actinometry.
Slope by linear regression analysis = 0.023
Correlation Coefficient = 0.995

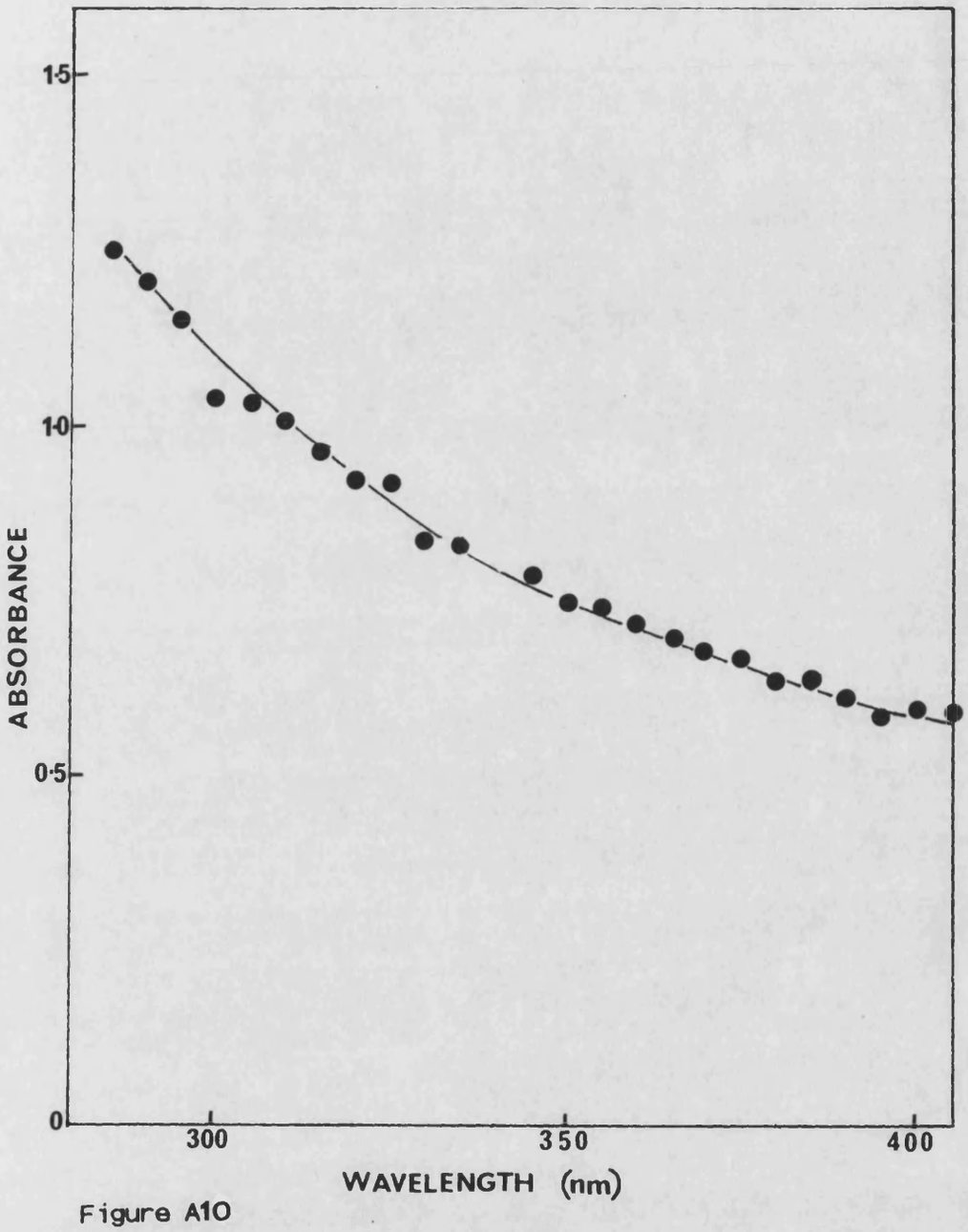

Figure A10

The absorbance of 1.0×10^{-3}M linoleic acid, calculated from %Transmission measurements taken using themopile readings,

where: $A = 2 - \log T$

A = Absorbance
T = Transmission

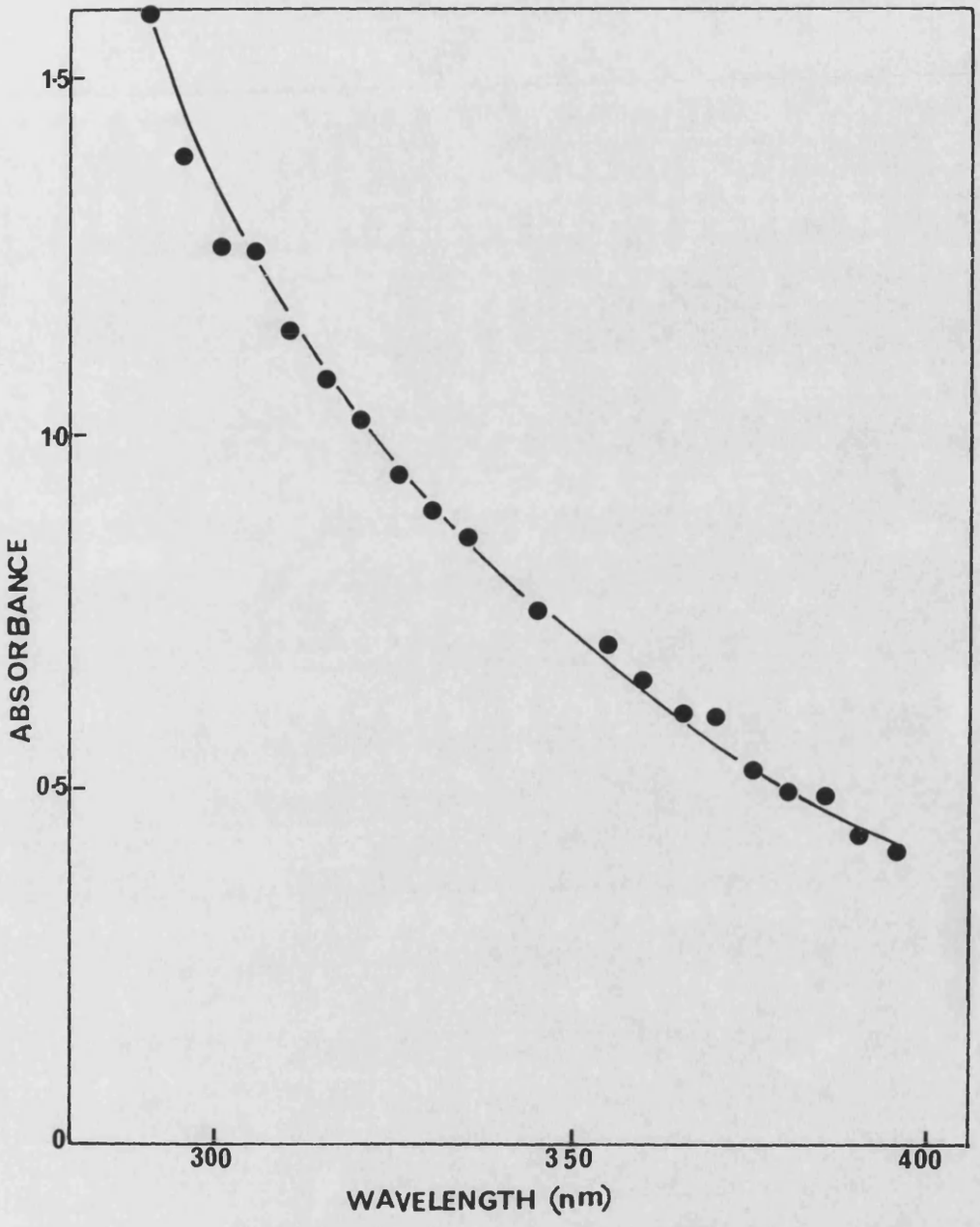

Figure A11

The absorbance of 1.0×10^{-3}M linolenic acid, calculated from %Transmission measurements taken using themopile readings,
where: A = 2 - logT
A = Absorbance
T = Transmission

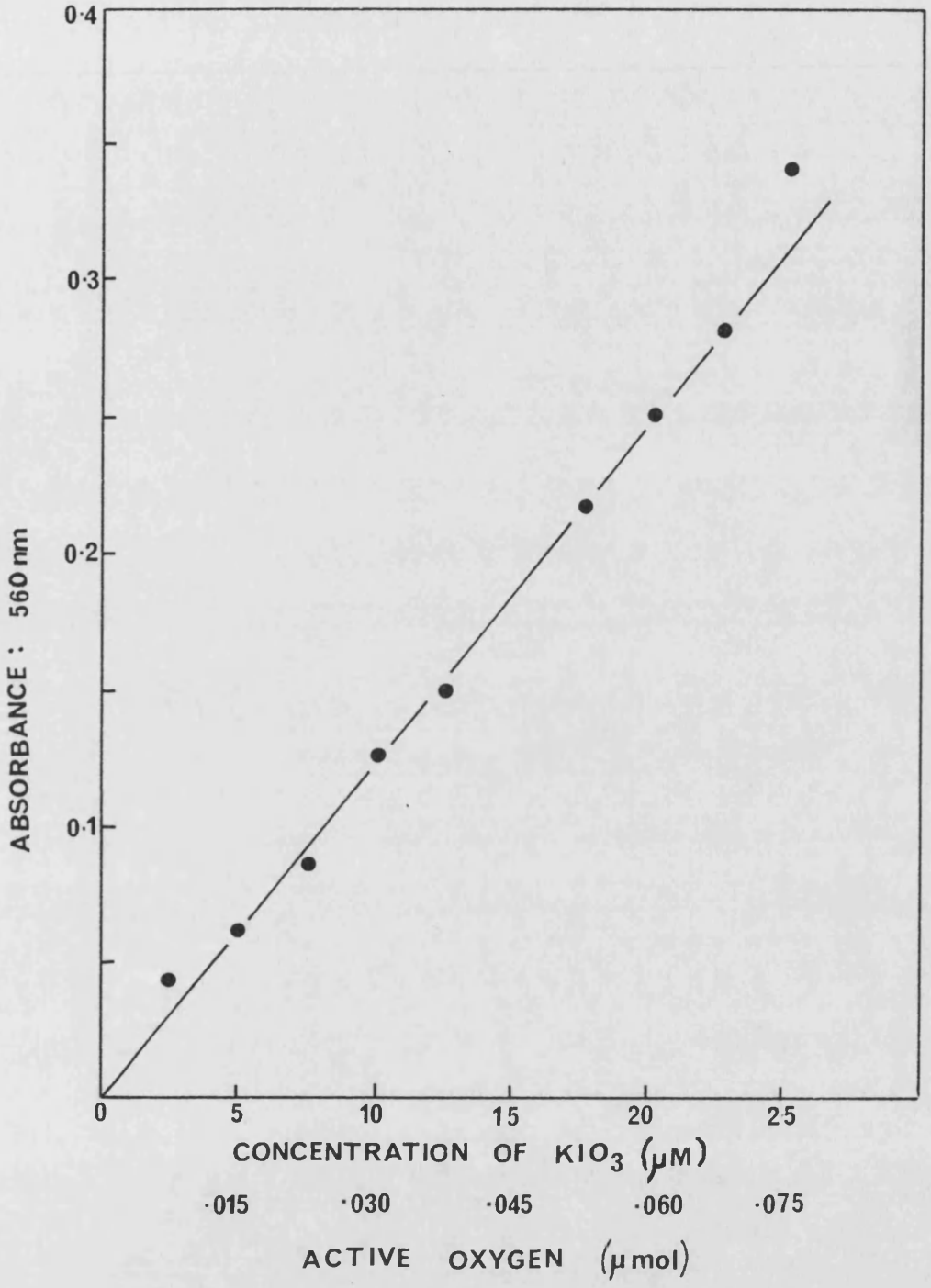

Figure A12

The calibration curve for the hydroperoxide assay.

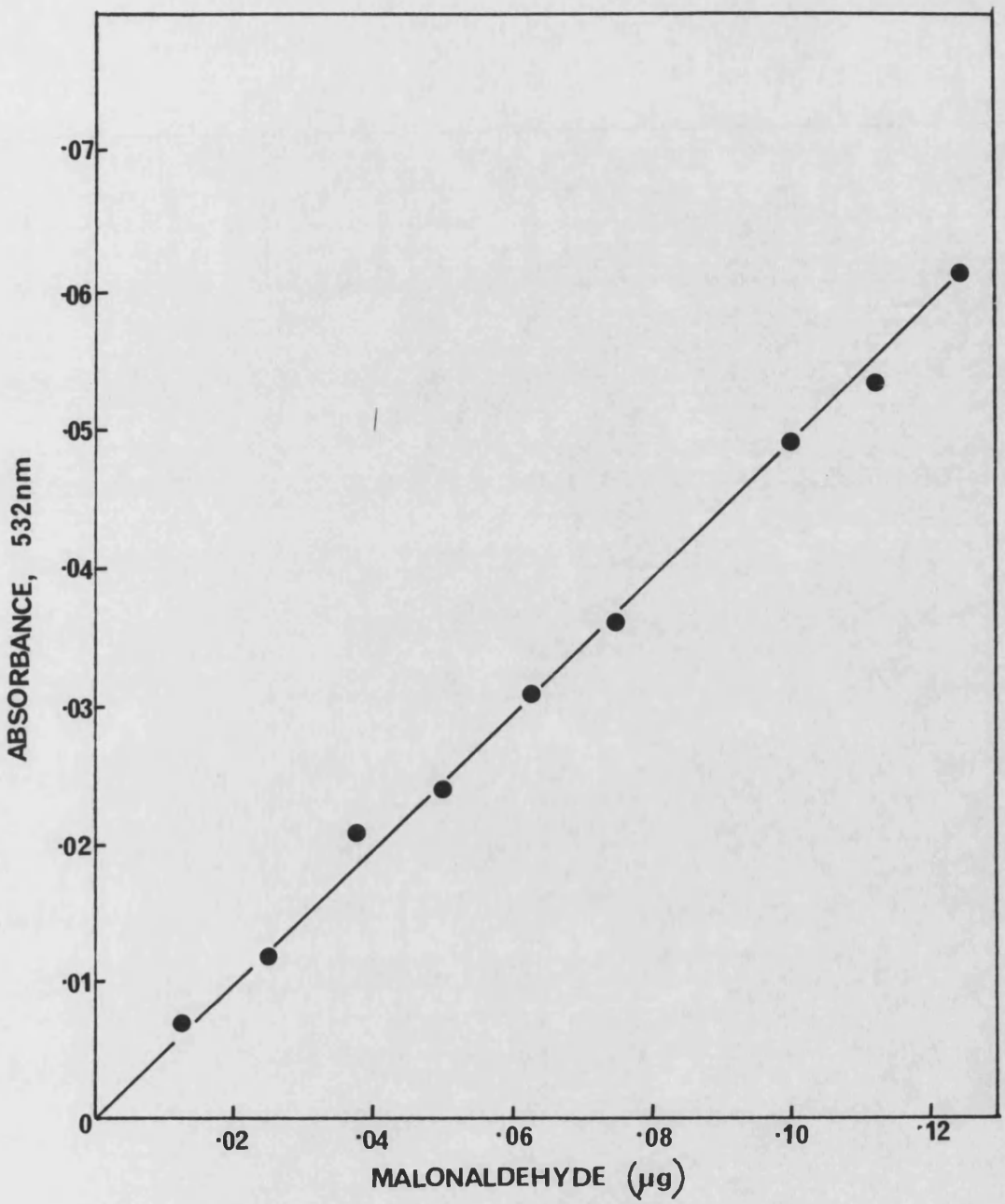

Figure A13

Calibration curve for the assay of Malonaldehyde.
Slope by linear regression analysis = 0.4863
Correlation Coefficient = 0.987

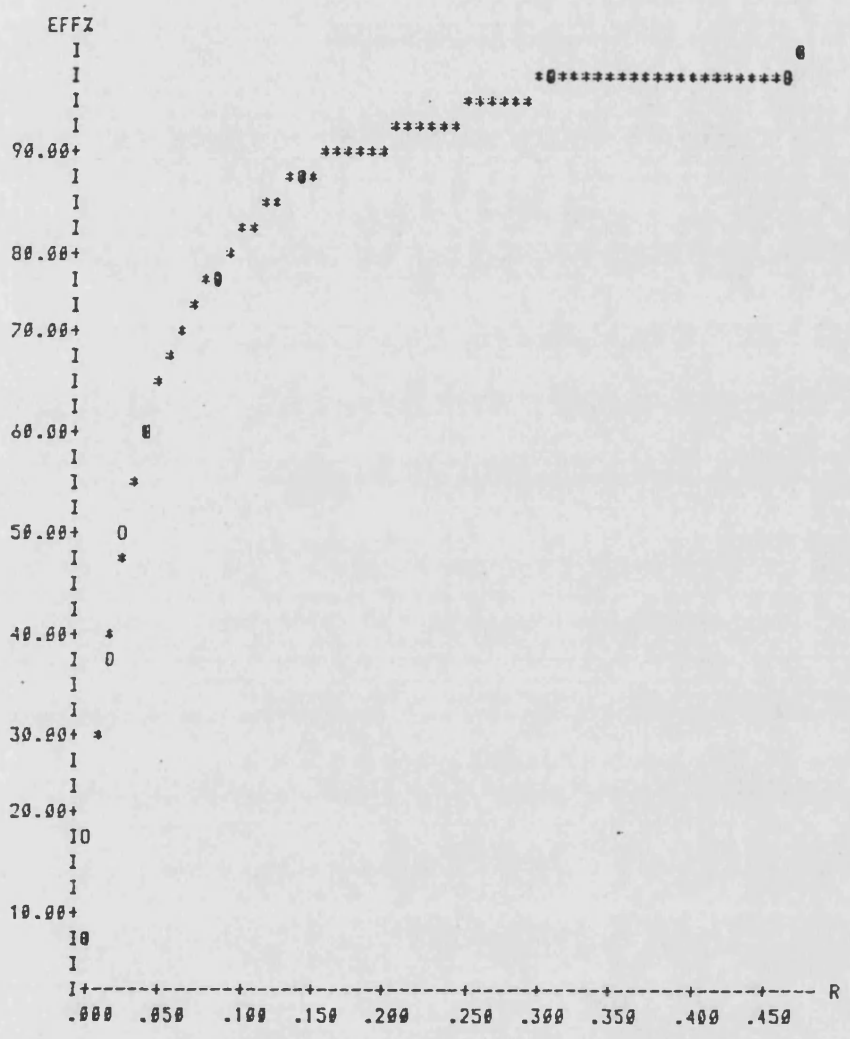

Figure A14 Quench curve for $^{86}Rb^{+}$ determined by the LKB Rackbeta 1215 liquid scintillation counter.

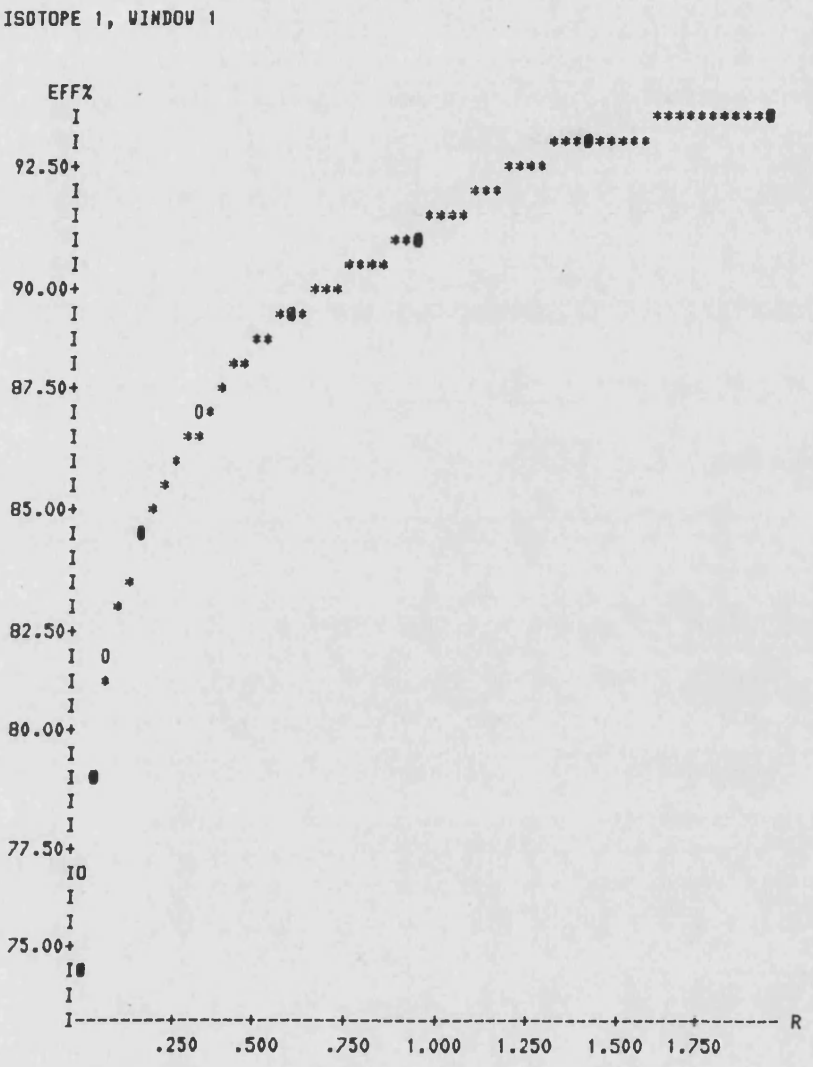

Figure A15
Quench curve for ^{14}C Sucrose

APPENDIX 6 (1)

The Retention Times (Rt) and Retention Times Relative to 12:0 (r) for 16 GLC Chromatograms using a Mixture of FAME Standards

FAME	Rt	r	Rt	r	Rt	r	Rt	r
12:0	30	-	28.0	-	30.5	-	29.5	-
14:0								
16:0								
18:1	89	2.96	83.5	2.98	87.5	2.86	86	2.91
18:2	96	3.20	90.5	3.23	94.5	3.09	93	3.15
18:3	106.5	3.55	100.5	3.59	105	3.44	103.5	3.50
12:0	30.5	-	29.0	-	33.5	-	29	-
14:0	55.5	1.82	50.0	1.72	58.5	1.75	53	1.82
16:0	71.5	2.34	69.0	2.37	75	2.23	68.5	2.36
18:1	92.0	3.01	89.5	3.08	98.5	2.94	88.5	3.05
18:2	98.5	3.23	95.5	3.29	106	3.16	94	3.24
18:3	108.0	3.54	104.5	3.60	117	3.49	102.5	3.53
12:0	33	-	34	-	27.5	-	30.5	-
14:0	57	1.72	60.5	1.77	50	1.82	57.5	1.88
16:0	78	2.36	76	2.23	67	2.43	74	2.42
18:1	92	2.78	98	2.88	84	3.05	93.0	3.05
18:2	98	2.96	106	3.11	89	3.23	99	3.24
18:3	107	3.24	116	3.41	95.5	3.47	115	3.77
12:0	27.5	-	27.5	-	26.5	-	28	-
14:0	50	1.81	48	1.74	45.0	1.69	53	1.89
16:0	67	2.43	66	2.40	64.5	2.43	69	2.46
18:1	85	3.09	84.5	3.07	83.0	3.13	88	3.14
18:2	90	3.27	90	3.27	88.5	3.34	94	3.35
18:3	97.5	3.54	97.5	3.54	96	3.62	103	3.67

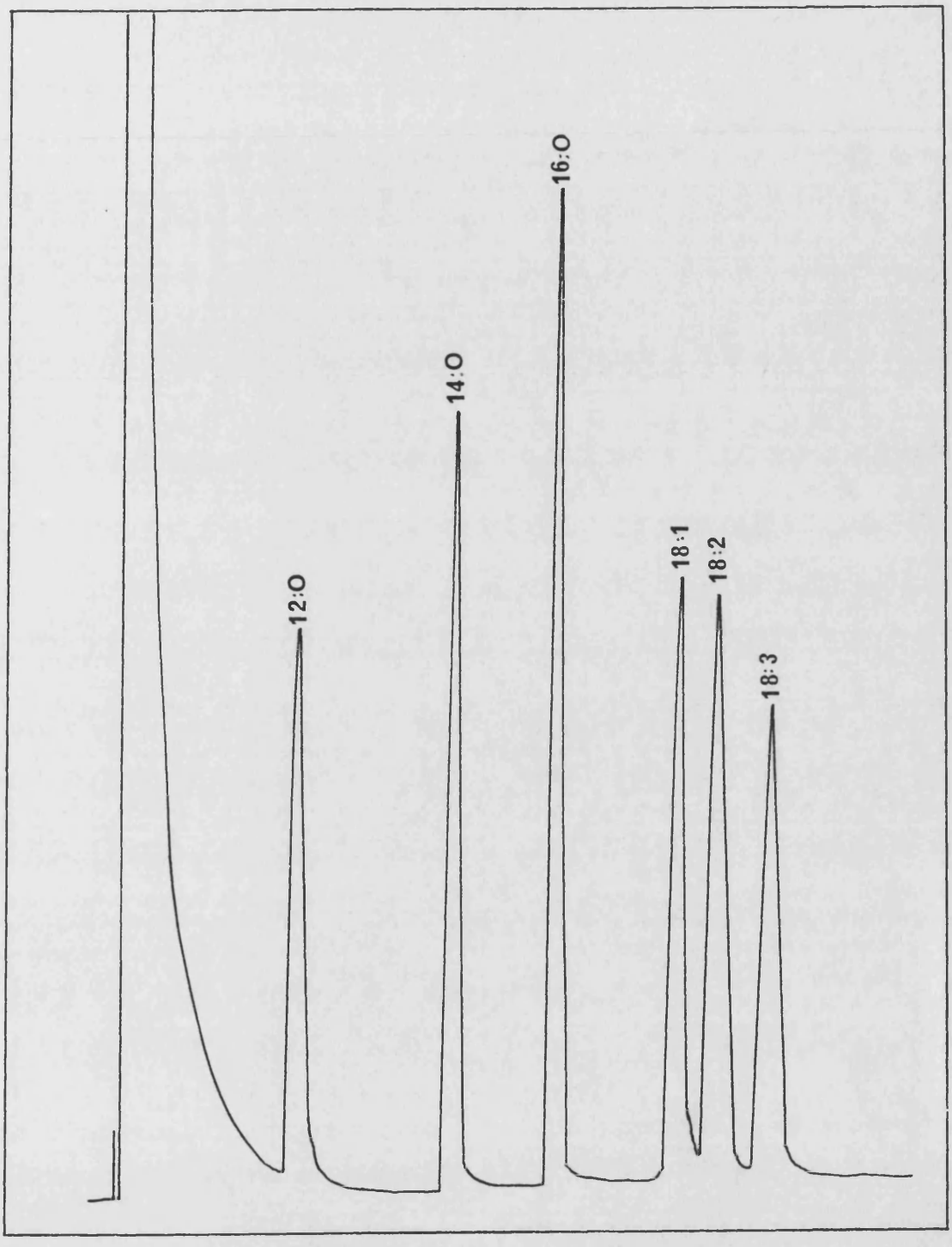

Figure A16

GLC trace of fatty acid standards

The Separation of Oleic, Linoleic and Linolenic Acids

Since these three fatty acids are close together on the chromatogram, the efficiency of their separation was determined as shown below:

$$R = \frac{\Delta RT}{\bar{\omega}} = \frac{2(Rt_2 - Rt_1)}{\omega_1 + \omega_2}$$

where R = resolution

ΔRt = distance between the 2 peaks

$\bar{\omega}$ = mean base width of the 2 peaks

For the separation of 18:1 and 18:2

$$R = \frac{2 \times (94.5 - 88.5)}{6 + 5}$$

$$= 1.09$$

If R = 1.0 the separation is taken to be 98%.

For the separation of 18:2 and 18:3

$$R = \frac{2 \times (102.7 - 94.5)}{5 + 6}$$

$$= 1.49$$

If R = 1.5 the separation is taken to be 99.7%.

These three 18C fatty acids are therefore separated to a satisfactory degree.

APPENDIX 6 (2)

The Retention Times (Rt) and Relative Retention Times (r) of Peaks from Bacterial Extracts; Their Identification, Peak Height and Proportion (%)

r is measured relative to Rt laurate (12:0).

Rt	r	fatty acid	peak ht.	%
AB1157				
32	-	12:0		
60.5	1.89	14:0	14	5.57
68	2.12		3	1.19
75	2.34	16:0	13.9	55.38
77.5	2.42	16:1	22	8.76
86	2.68	17:0	52	20.72
98.5	3.07	18:1	15	5.97
119	3.72	19:0	6	2.39
SR385				
32		12:0		
60	12.87	14:0	11.5	6.13
75	2.34	16:0	111	59.20
77	2.40	16:1	6	3.20
86	2.68	17:0	46	24.53
98	3.06	18:1	5	2.66
112.5	3.51	19:0	8	4.26
K12				
31.5		12:0		
57.5	1.82	14:0	3	3.8
76	2.41	16:0	36	46.1
78	2.47	16:1	14	17.9
95.5	3.03	18:1	22	28.2
115	3.65	19:0	3	3.8

Appendix 6(2) continued

Rt	r	fatty acid	peak ht.	%
SR362				
32.5		12:0		
58.5	1.80	14:0	5	6.17
75	2.30	16:0	43	53.08
77	2.37	16:1	8	9.87
87	2.67	17:0	15	18.52
100	3.07	18:1	10	12.34
SR246				
32.5		12:0		
59.5	1.83	14:0	18	12.33
67.5	2.07	?	5	3.42
72.5	2.23	16:0	60	41.09
76.5	2.35	16:1	30	20.55
85	2.61	17:0	9	6.16
95	2.92	18:0	12.5	8.56
101	3.10	18:1	6	4.11
117	3.6	19:0	6	4.11
B/r				
31.0		12:0		
57.5	1.85	14:0	29	7.55
67.0	2.16		5	1.30
73.0	2.35	16:0	217	56.51
79	2.54		9	2.34
81	2.61	17:0	18	4.68
84	2.70	18:0	18	4.68
93.5	3.01	18:1	29	7.55
99	3.19	18:2	30	7.81
102.5	3.30		13	3.38
107.0	3.45		19	2.60
111.0	3.58	19:0	6	1.56
K1060 18:1 Log				
33		12:0		
59.5	1.80	14:0	36	10.77
75.5	2.28	16:0	77	23.05
99.5	3.01	18:1	221	66.16

Appendix 6(2) continued

Rt	r	fatty acid	peak ht.	%
K1060 18:1 Stat				
33		12:0		
56	1.69	14:0	20	9.01
74	2.24	16:0	117	52.70
99.5	3.01	18:1	70	31.53
118	3.57	19:0	15	6.75
K1060 18:2 Log				
32		12:0		
60	1.87	14:0	20	10.8
75	2.34	16:0	109	68.9
104.5	3.26	18:2	56	30.2
K1060 18:2 Stat				
30		12:0		
57	1.90	14:0	19	8.9
74	2.46	16:0	110	51.8
97.5	3.25	18:2	72	33.9
103.2	3.77	19:0	11	5.2
K1060 18:3 Log				
33.5		12:0		
59	1.76	14:0	32	9.22
75	2.23	16:0	221	63.69
120.5	3.59	18:3	94	27.09
K1060 18:3 Stat.				
31		12:0		
56	1.80	14:0	12	6.8
72	2.32	16:0	105	59.6
111	3.58	18:3	48	27.2
116	3.74	19:0	11	6.2
B. stearothermophilus				
21.5				
47	2.18	14:0	25	14.5
51.5	2.39	16:0	37	21.5
58.5	2.72	17:0	5	2.9
62	2.88	18:0	31	18.0
65.5	3.04	18:1	17	9.8
81	3.76	19:0	57	33

Appendix 6(2) concluded

Rt	r	fatty acid	peak ht.	%
246 YENB				
26				
51.5	1.98	14:0	27	5.06
60.5	2.32	16:0	212	39.7
64	2.46	16:1	105	19.69
70.5	2.71	17:0	103	19.32
77.5	2.98	18:0	7	1.31
80.0	3.07	18:1	70	13.1
91.5	3.52	(18:3)	9	1.68

Appendix 7

Liposomes — electron micrographs

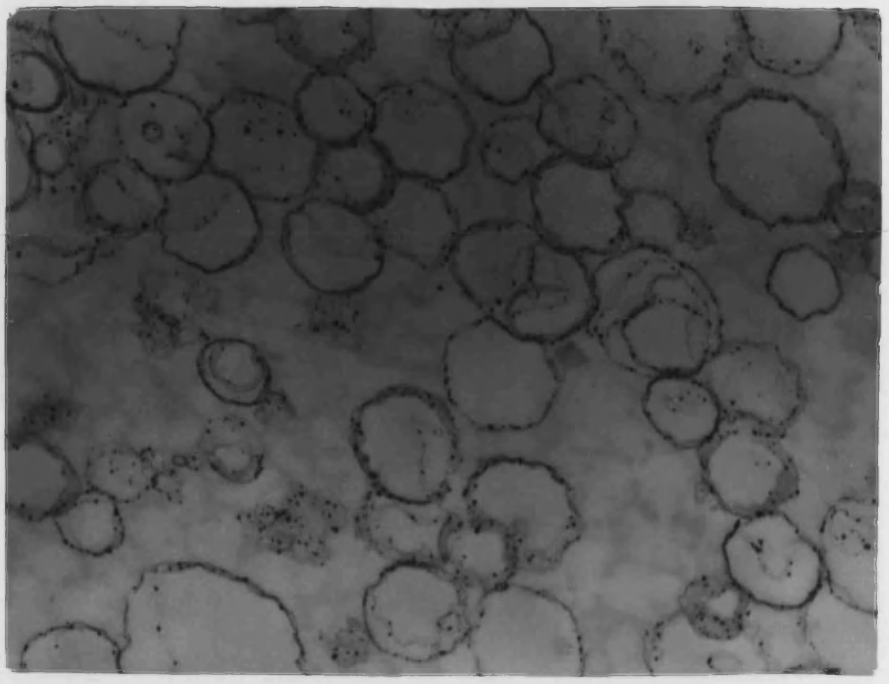

x 10^4

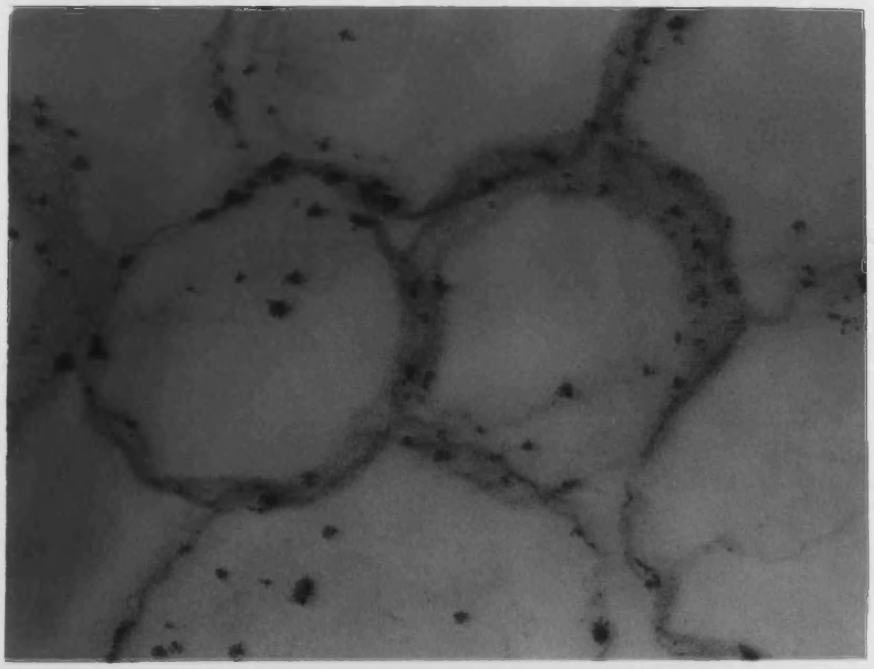

x 10^5

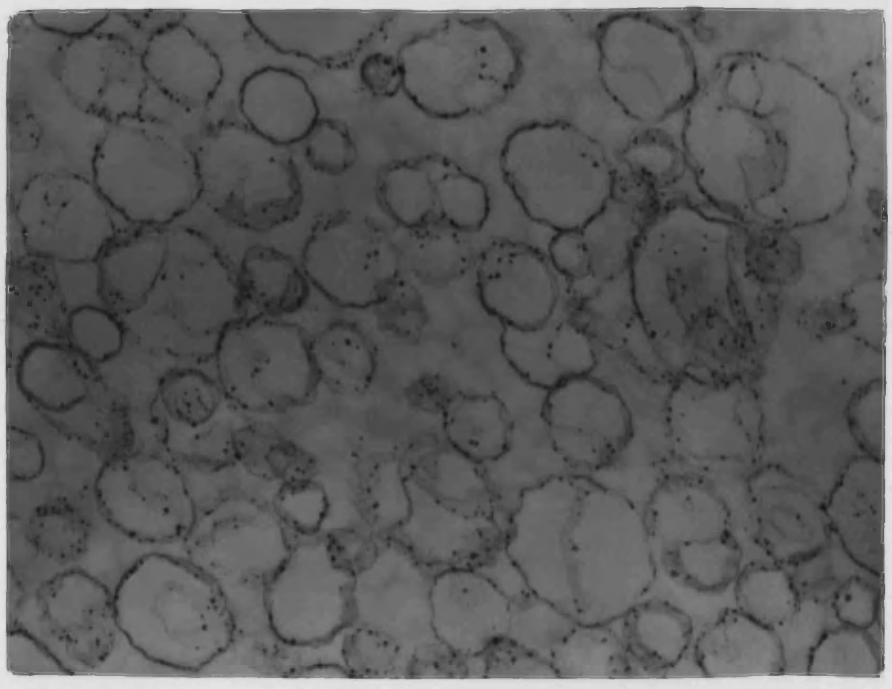

x 1·5 × 10^4

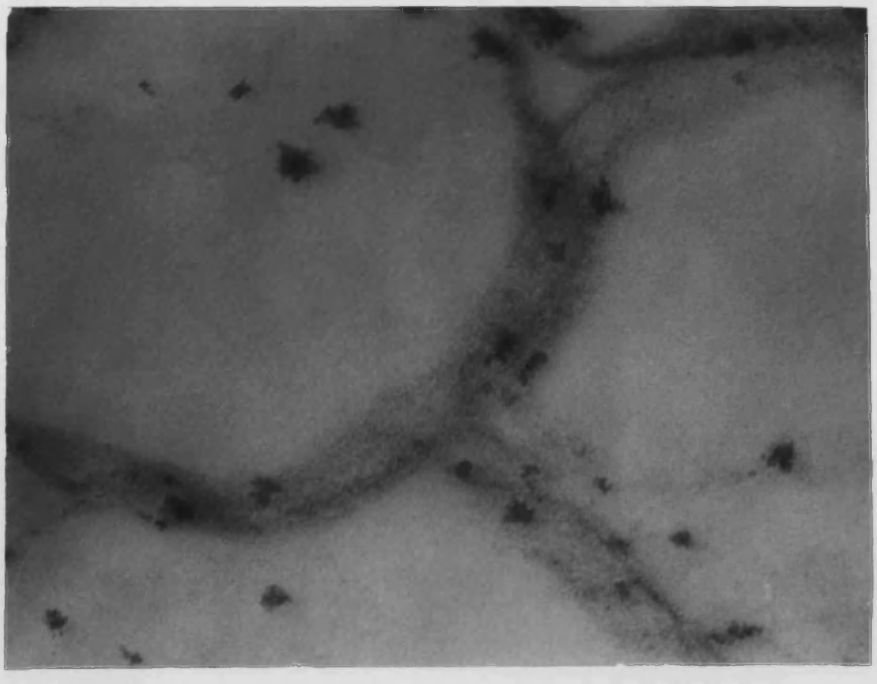

× 4 × 10^4

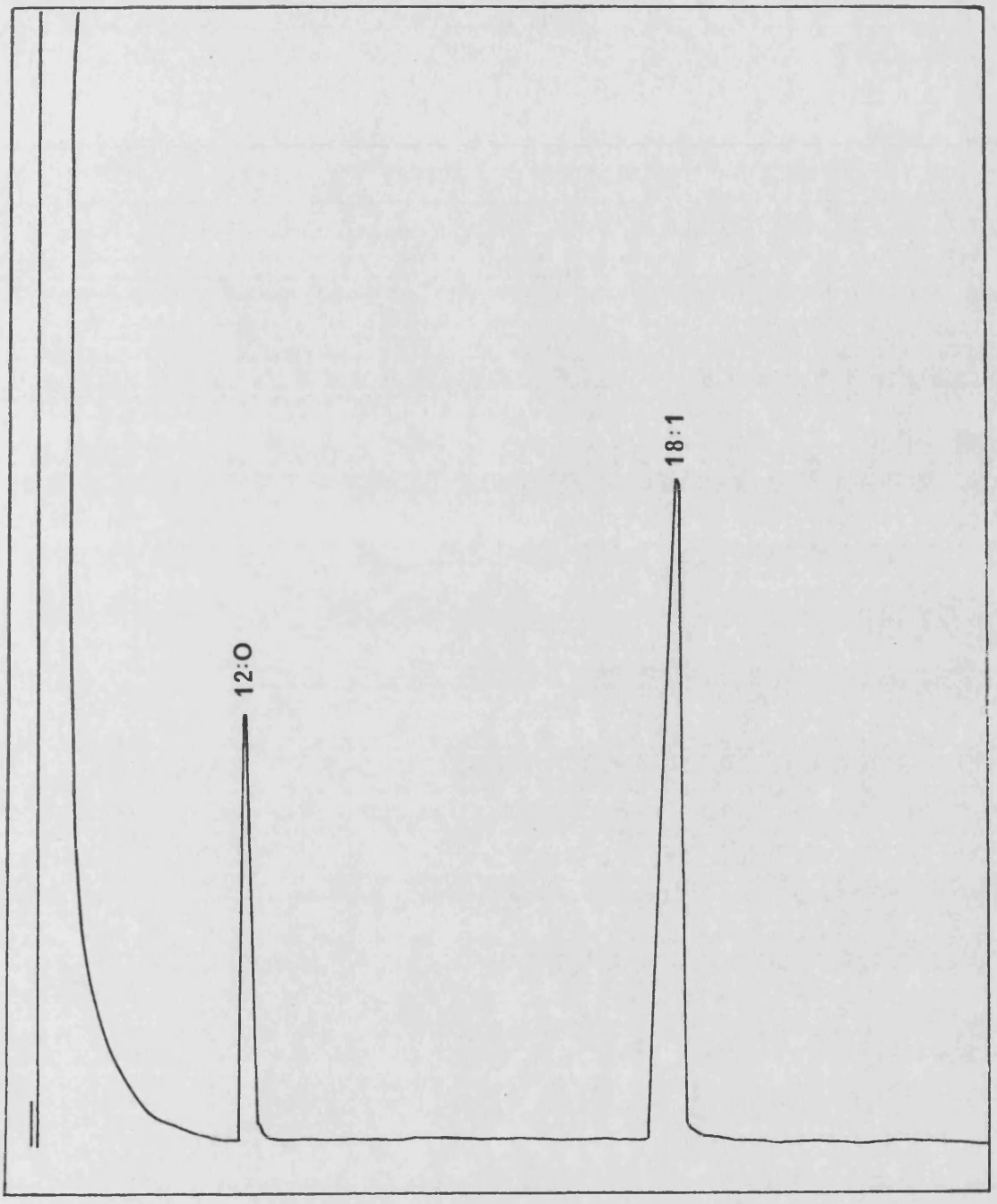

Figure A17
GLC trace for dilinoleoyl lecithin liposomes.

APPENDIX 8

Data pertaining to Figures 27–103

and Figures A4–A7

Table 1: Fig. 27. The survival of E. coli K1060 following broad-band near-UV irradiation (Original lamps).

NUV Exposure Time (min)	Surviving fraction, assessed on YENB					
	Fatty acid incorporated					
	(a) oleic acid		(b) linoleic acid		(c) linolenic acid	
	(i)	(ii)	(i)	(ii)	(i)	(ii)
0	$\underline{1.88\times10^{7}}$	$\underline{1.74\times10^{7}}$	$\underline{8.70\times10^{6}}$	$\underline{9.68\times10^{6}}$	$\underline{1.35\times10^{7}}$	$\underline{1.01\times10^{7}}$
10	9.20×10^{-1}	6.49×10^{-1}	9.60×10^{-1}	1.01×10^{0}	1.01×10^{0}	1.10×10^{0}
20	7.82×10^{-1}	9.19×10^{-1}	5.37×10^{-1}	1.00×10^{0}	1.17×10^{0}	1.21×10^{0}
30	6.64×10^{-1}	7.93×10^{-1}	4.92×10^{-1}	7.49×10^{-1}	4.31×10^{-1}	3.31×10^{-1}
40	6.33×10^{-1}	4.82×10^{-1}	9.95×10^{-2}	1.32×10^{-1}	7.35×10^{-3}	2.95×10^{-2}
50	7.28×10^{-2}	2.47×10^{-2}	3.95×10^{-2}	1.39×10^{-2}	3.71×10^{-4}	2.00×10^{-3}
55				2.36×10^{-3}		
60	4.87×10^{-3}	1.95×10^{-3}	1.02×10^{-3}		8.02×10^{-5}	2.42×10^{-4}
70	1.01×10^{-4}	6.30×10^{-5}	1.01×10^{-4}	1.19×10^{-4}		

Underlined values represent mean viable count of unirradiated controls.
(i) and (ii) represents results of replicate experiments.

Table 2. Fig. 29. The survival of E. coli K1060 following broad-band near-UV irradiation (original lamps.

NUV Exposure Time (min)	Surviving fraction, assessed on defined medium					
	Fatty acid incorporated					
	(a) oleic acid		(b) linoleic acid		(c) linolenic acid	
	(i)	(ii)	(i)	(ii)	(i)	(ii)
0	$\underline{1.07\times10^{7}}$	$\underline{1.01\times10^{7}}$	$\underline{8.70\times10^{6}}$	$\underline{2.68\times10^{6}}$	$\underline{1.45\times10^{7}}$	$\underline{1.37\times10^{7}}$
10	6.45×10^{-1}	1.05×10^{0}	8.72×10^{-1}	1.10×10^{0}	1.10×10^{0}	8.90×10^{-1}
20	7.43×10^{-1}	1.10×10^{0}	6.84×10^{-1}	6.52×10^{-1}	1.00×10^{0}	1.17×10^{0}
30	7.70×10^{-1}	1.09×10^{0}	4.98×10^{-1}	6.50×10^{-1}	4.31×10^{-1}	4.31×10^{-1}
40	8.51×10^{-1}	9.01×10^{-1}	2.71×10^{-1}	4.52×10^{-1}	1.66×10^{-1}	7.39×10^{-2}
50	1.80×10^{-1}	4.72×10^{-1}	3.90×10^{-2}	1.48×10^{-1}	6.40×10^{-2}	3.65×10^{-2}
60	6.72×10^{-2}	5.00×10^{-2}	8.50×10^{-3}	1.75×10^{-2}	2.11×10^{-3}	-

Underlined values represent mean viable count of unirradiated controls.
(i) and (ii) represents results of replicate experiments.

Table 3. Fig. 30 Survival of E. coli K1060 following broad-band near-UV irradiation (original lamps).

NUV Exposure time (min)	Surviving fraction, assessed on high salt defined medium Fatty acid incorporated					
	(a) oleic acid		(b) linoleic acid		(c) linolenic acid	
	(i)	(ii)	(i)	(ii)	(i)	(ii)
0	$\underline{9.351 \times 10^{6}}$	$\underline{1.03 \times 10^{7}}$	$\underline{9.05 \times 10^{6}}$	$\underline{3.30 \times 10^{7}}$	$\underline{1.49 \times 10^{7}}$	$\underline{1.35 \times 10^{7}}$
10	7.30×10^{-1}	1.09×10^{0}	9.24×10^{-1}	9.54×10^{-1}	1.01×10^{0}	8.23×10^{-1}
20	1.01×10^{0}	1.07×10^{0}	7.31×10^{-1}	6.60×10^{-1}	9.99×10^{-1}	8.09×10^{-1}
30	8.42×10^{-1}	1.00×10^{0}	3.68×10^{-1}	3.20×10^{-1}	4.56×10^{-1}	3.39×10^{-1}
40	8.00×10^{-1}	1.04×10^{0}	2.00×10^{-1}	1.00×10^{-1}	1.73×10^{-1}	8.02×10^{-2}
50	4.02×10^{-1}	5.51×10^{-1}	4.25×10^{-2}	4.50×10^{-2}	4.32×10^{-2}	3.60×10^{-2}
60	1.09×10^{-1}	6.95×10^{-2}	9.26×10^{-3}	2.40×10^{-2}	2.96×10^{-3}	-

Underlined values represent mean viable count of unirradiated controls.
(i) and (ii) represents results of replicate experiments.

Table 4. Fig. 31. The survival of stationary phase E. coli K1060 following broad-band near-UV irradiation.

NUV exposure Time (min)	Viability assessed on YENB Fatty acid incorporated	
	Oleic acid	Linolenic acid
0	$\underline{3.30\text{x}10^{7}}$	$\underline{3.05\text{x}10^{7}}$
10	$6.61\text{x}10^{-3}$	$6.20\text{x}10^{-2}$
20	$9.02\text{x}10^{-3}$	$1.00\text{x}10^{-2}$
30	$2.40\text{x}10^{-3}$	$2.24\text{x}10^{-3}$
40	$6.91\text{x}10^{-4}$	$5.63\text{x}1-^{-4}$
50	$1.85\text{x}10^{-4}$	$1.39\text{x}10^{-4}$
60	$7.56\text{x}10^{-5}$	$3.98\text{x}10^{-5}$
70	$1.53\text{x}10^{-5}$	$1.55\text{x}10^{-5}$

Underlined values represent mean viable count of unirradiated controls.

Table 5. Fig. 32. Survival of E. coli K1060 following broad-band near-UV irradiation

NUV Exposure Time (min)	Surviving fraction, viability assessed on: (a) YENB		(b) defined medium		(c) high salt medium	
	Fatty acid incorporated: DS acid	oleic acid	DS acid	oleic acid	DS acid	oleic acid
(i)						
0	$\underline{6.50\times10^{6}}$	$\underline{2.19\times10^{7}}$	$\underline{6.75\times10^{6}}$	$\underline{2.75\times10^{7}}$	$\underline{6.15\times10^{6}}$	$\underline{2.70\times10^{7}}$
10	7.70×10^{-1}	6.69×10^{-1}	1.01×10^{0}	7.45×10^{-1}	9.85×10^{-1}	1.02×10^{0}
20	6.72×10^{-1}	4.46×10^{-1}	6.92×10^{-1}	8.43×10^{-1}	8.95×10^{-1}	1.20×10^{0}
30	4.59×10^{-1}	3.87×10^{-1}	8.61×10^{-1}	5.04×10^{-1}	8.80×10^{-1}	5.81×10^{-1}
40	1.19×10^{-1}	5.46×10^{-2}	7.07×10^{-1}	3.27×10^{-1}	6.56×10^{-1}	3.13×10^{-1}
50	6.39×10^{-2}	3.69×10^{-2}	5.53×10^{-1}	2.65×10^{-2}	1.22×10^{-1}	5.60×10^{-2}
60	3.77×10^{-2}	7.28×10^{-3}	3.38×10^{-2}	9.82×10^{-3}	5.82×10^{-2}	1.49×10^{-2}

DS acid = Dihydrosterculic acid.
(i) and (ii) represent data from two replicate experiments.
Underlined values represent mean viable counts of unirradiated controls.

Table 5. continued.

NUV Exposure Time (min)	Surviving fraction, viability assessed on: (a) YENB		(b) defined medium		(c) high salt medium	
	Fatty acid incorporated					
	DS acid	oleic acid	DS acid	oleic acid	DS acid	oleic acid
(ii)						
0	$\underline{1.16\times10^{7}}$	$\underline{9.65\times10^{6}}$	$\underline{1.29\times10^{7}}$	$\underline{1.00\times10^{7}}$	$\underline{1.27\times10^{7}}$	$\underline{1.01\times10^{7}}$
10	7.32×10^{-1}	5.49×10^{-1}	1.00×10^{0}	9.70×10^{-1}	1.04×10^{0}	9.85×10^{-1}
20	5.86×10^{-1}	3.68×10^{-1}	1.00×10^{0}	9.60×10^{-1}	1.01×10^{0}	9.55×10^{-1}
30	4.01×10^{-1}	1.84×10^{-1}	9.84×10^{-1}	7.06×10^{-1}	1.03×10^{0}	7.07×10^{-1}
40	1.99×10^{-1}	9.68×10^{-2}	5.40×10^{-1}	2.90×10^{-1}	5.82×10^{-1}	9.30×10^{-1}
50	9.82×10^{-2}	1.30×10^{-2}	9.92×10^{-2}	5.32×10^{-2}	1.02×10^{-1}	5.49×10^{-2}
60	4.91×10^{-2}	6.42×10^{-2}	5.15×10^{-2}	2.32×10^{-2}	5.90×10^{-2}	3.61×10^{-2}

DS acid = Dihydrosterculic acid.
(i) and (ii) represent data from two replicate experiments.
Underlined values represent mean viable counts of unirradiated controls.

Table 6. Fig. 33. The survival of E. coli K1060 following far-UV irradiation.

Far UV fluence (Jm^{-2})	Fatty acid incorporated		
	oleic acid	linoleic acid	linolenic acid
0	$\underline{9.15 \times 10^{6}}$	$\underline{9.35 \times 10^{6}}$	$\underline{8.76 \times 10^{6}}$
20	4.15×10^{-1}	6.20×10^{-1}	5.12×10^{-1}
40	1.20×10^{-1}	1.61×10^{-1}	1.46×10^{-1}
60	3.61×10^{-2}	7.23×10^{-2}	3.68×10^{-2}
80	5.30×10^{-3}	1.51×10^{-2}	1.37×10^{-2}
120	1.64×10^{-4}	3.20×10^{-4}	1.84×10^{-4}

Underlined values represent mean viable counts of unirradiated controls.

Table 7. Fig. 34. the survival of E. coli K1060 following broad-band near-UV irradiation under oxic or anoxic conditions.

34a. E. coli K1060 incoporating linolenic acid, irradiated with original lamps.

NUV Exposure time (min)	Viability assessed on YENB. Cell suspensions bubbled during irradiation with: Air	N_2	high salt defined medium. Air	N_2
0	7.03×10^{6}	7.06×10^{6}	9.66×10^{6}	9.10×10^{6}
20	3.90×10^{-1}	7.16×10^{-1}	4.90×10^{-1}	5.26×10^{-1}
30	1.83×10^{-1}	5.98×10^{-1}	5.51×10^{-1}	5.32×10^{-1}
40	5.03×10^{-2}	4.63×10^{-1}	-	3.36×10^{-1}
50	3.62×10^{-2}	3.70×10^{-1}	1.86×10^{-1}	3.09×10^{-1}
60	1.25×10^{-2}	3.49×10^{-1}	2.27×10^{-3}	4.87×10^{-1}
70	1.25×10^{-3}	1.70×10^{-1}	2.50×10^{-4}	2.53×10^{-1}

34b, E. coli K1060 incorporating linolenic acid, irradiated with new lamps.

NUV Exposure time (min)	Viability assessed on YENB. Bubbled after irradiation with: Air	N_2	high salt defined medium. Air	N_2
0	1.56×10^{7}	1.54×10^{7}	1.58×10^{7}	1.58×10^{7}
5	6.70×10^{-1}	8.53×10^{-1}	6.73×10^{-1}	9.85×10^{-1}
10	6.21×10^{-1}	7.09×10^{-1}	4.42×10^{-1}	8.36×10^{-1}
15	1.82×10^{-1}	5.36×10^{-1}	7.00×10^{-1}	7.59×10^{-1}
20	4.73×10^{-2}	5.53×10^{-1}	5.36×10^{-1}	7.92×10^{-1}
25	9.99×10^{-3}	2.25×10^{-1}	-	8.92×10^{-1}
30	7.41×10^{-4}	1.01×10^{-1}	3.33×10^{-2}	8.71×10^{-2}

Table 7. continued

34c, E. coli K1060 incorporating linolenic acid, irradiated with new lamps.

NUV Exposure time (min)	Viability assessed on YENB Bubbled after irradiation with Air	N_2	high salt defined medium Air	N_2
0	$\underline{5.75\times10^{6}}$	$\underline{5.45\times10^{6}}$	$\underline{6.05\times10^{6}}$	$\underline{5.15\times10^{6}}$
5	8.50×10^{-1}	1.00×10^{0}	7.32×10^{-1}	9.29×10^{-1}
10	5.73×10^{-1}	5.00×10^{-1}	1.02×10^{0}	7.68×10^{-1}
15	3.51×10^{-1}	3.84×10^{-1}	8.20×10^{-1}	4.73×10^{-1}
20	2.25×10^{-1}	3.02×10^{-1}	5.13×10^{-1}	4.95×10^{-1}
25	8.72×10^{-2}	1.38×10^{-1}	3.96×10^{-1}	3.92×10^{-1}
30	2.87×10^{-3}	1.38×10^{-1}	3.29×10^{-1}	4.40×10^{-1}
35	9.23×10^{-3}	9.82×10^{-2}	2.45×10^{-1}	3.46×10^{-1}

Underlined values represent mean viable counts of unirradiated controls.

Table 8. Fig. 35. Survival of E. coli K1060 (a) incorporating linolenic acid, (b) incorporating oleic acid, following broad-band near-UV irradiation.

(a) 18:3

NUV Exposure time (min)	Viability assessed on YENB		high salt defined medium	
	Conditions of incubation			
	Aerobic	Anaerobic	Aerobic	Anaerobic
(i)				
0	$\underline{6.25\times10^{6}}$	$\underline{6.55\times10^{6}}$	$\underline{6.25\times10^{6}}$	$\underline{6.20\times10^{6}}$
5	6.02×10^{-1}	8.34×10^{-1}	1.02×10^{0}	1.04×10^{0}
10	1.04×10^{-1}	8.40×10^{-1}	1.12×10^{0}	8.65×10^{0}
15	4.00×10^{-2}	7.74×10^{-1}	4.81×10^{-1}	7.05×10^{-1}
20	1.91×10^{-2}	7.70×10^{-1}	1.45×10^{-1}	1.65×10^{-1}
30	3.30×10^{-3}	2.00×10^{-1}	3.20×10^{-3}	1.21×10^{-2}
40	6.88×10^{-4}	8.36×10^{-2}	7.25×10^{-5}	9.00×10^{-5}
50	1.48×10^{-4}	1.21×10^{-2}	4.41×1^{-5}	1.24×10^{-4}
(ii)				
0	$\underline{2.85\times10^{6}}$	$\underline{3.72\times10^{6}}$	$\underline{2.65\times10^{6}}$	$\underline{1.25\times10^{6}}$
5	5.76×10^{-1}	9.06×10^{-1}	5.79×10^{-1}	1.04×10^{0}
10	1.42×10^{-1}	8.00×10^{-1}	5.40×10^{-1}	1.04×10^{-1}
15	6.02×10^{-2}	5.55×10^{-1}	2.01×10^{-1}	7.07×10^{-1}
20	3.83×10^{-2}	-	-	-
25	2.44×10^{-2}	1.11×10^{-1}	2.45×10^{-2}	9.65×10^{-2}
30	1.70×10^{-2}	1.11×10^{-1}	8.09×10^{-3}	8.20×10^{-2}
35	-	2.54×10^{-1}	-	-

(i) and (ii) show data from separate experiments. Data from (i) is plotted in Fig. 35a.
Underlined values represent mean viable counts of unirradiated controls.

Table 8. (continued)

(b) 18:1

NUV Exposure time (min)	Viability assessed on YENB Conditions of incubation Aerobic	Anaerobic	high salt defined medium Aerobic	Anaerobic
(i)				
0	$\underline{1.37\times10^{7}}$	$\underline{9.60\times10^{6}}$	$\underline{1.09\times10^{7}}$	$\underline{1.13\times10^{7}}$
10	8.79×10^{-1}	1.10×10^{0}	8.50×10^{-1}	1.10×10^{0}
20	8.45×10^{-1}	1.04×10^{0}	8.25×10^{-1}	8.99×10^{0}
30	8.20×10^{-1}	8.50×10^{-1}	8.16×10^{-1}	1.00×10^{0}
40	4.20×10^{-1}	6.50×10^{-1}	6.45×10^{-1}	4.75×10^{-1}
50	3.14×10^{-1}	6.21×10^{-1}	1.07×1^{-1}	3.83×10^{-1}
60	8.00×10^{-2}	4.05×10^{-1}	8.73×10^{-3}	1.00×10^{-2}

Underlined values represent mean viable counts of unirradiated controls.

Table 9. Fig. 36. The survival of E. coli K1060 following broad-band near-UV irradiation (original lamps). Survival assessed after bubbling for 75 min with nitrogen.

NUV Exposure time (min)	Viability assessed on YENB Bubbled after irradiation with Air	Viability assessed on YENB Bubbled after irradiation with N_2	Viability assessed on high salt defined medium Bubbled after irradiation with Air	Viability assessed on high salt defined medium Bubbled after irradiation with N_2
(i)				
0	$\underline{1.25\times10^{7}}$	$\underline{1.06\times10^{7}}$	$\underline{1.33\times10^{7}}$	$\underline{1.05\times10^{7}}$
20	3.91×10^{-1}	4.45×10^{-1}	5.10×10^{-1}	8.16×10^{-1}
30	7.21×10^{-2}	4.19×10^{-2}	4.55×10^{-1}	9.43×10^{-1}
40	1.00×10^{-2}	9.41×10^{-3}	1.01×10^{-1}	2.53×10^{-1}
50	1.32×10^{-3}	1.42×10^{-3}	1.20×10^{-3}	1.01×10^{-3}
60	3.71×10^{-4}	5.15×10^{-4}	6.02×10^{-5}	4.15×10^{-5}
70	2.00×10^{-5}	1.50×10^{-5}	-	1.38×10^{-5}
(ii)				
0	$\underline{9.55\times10^{6}}$	$\underline{9.20\times10^{6}}$	$\underline{9.75\times10^{6}}$	$\underline{8.75\times10^{6}}$
20	7.50×10^{-1}	9.82×10^{-1}	5.62×10^{-1}	1.07×10^{0}
30	8.13×10^{-1}	8.32×10^{-1}	7.82×10^{-1}	9.62×10^{-1}
40	5.01×10^{-2}	7.00×10^{-2}	6.91×10^{-1}	8.81×10^{-1}
50	-	1.91×10^{-3}	8.98×10^{-2}	1.49×10^{-3}
60	-	2.75×10^{-2}	4.71×10^{-2}	5.23×10^{-2}

(i) Fatty acid incorporated = linolenic acid
(ii) A similar experiment, fatty acid incorporated = linoleic acid.

Underlined values represent mean viable counts of unirradiated controls.

Table 10(i). Fig. 37a. Survival of E. coli K1060 following broad-band near-UV irradiation after growth with or without vitamin E.

NUV Exposure time (min)	Viability assessed on YENB Presence of Vitamin E in growth medium +	YENB −	high salt defined medium +	high salt defined medium −
(i)				
0	$\underline{8.65\times10^{6}}$	$\underline{8.25\times10^{6}}$	$\underline{9.25\times10^{6}}$	$\underline{9.85\times10^{6}}$
10	4.42×10^{-1}	2.54×10^{-1}	8.10×10^{-1}	6.66×10^{-1}
20	2.30×10^{-1}	1.18×10^{-1}	5.40×10^{-1}	4.92×10^{-1}
30	5.08×10^{-2}	1.57×10^{-2}	7.05×10^{-1}	6.20×10^{-1}
40	6.41×10^{-3}	1.63×10^{-3}	3.15×10^{-1}	2.00×10^{-1}
50	−	−	−	1.81×10^{-1}
60	2.39×10^{-3}	4.72×10^{-4}	7.89×10^{-3}	1.74×10^{-4}
(ii)				
0	$\underline{1.02\times10^{7}}$	$\underline{1.01\times10^{7}}$	$\underline{1.06\times10^{7}}$	$\underline{1.13\times10^{7}}$
10	5.19×10^{-1}	1.86×10^{-1}	7.80×10^{-1}	7.92×10^{-1}
20	2.28×10^{-1}	8.43×10^{-3}	5.47×10^{-1}	5.42×10^{-1}
30	5.19×10^{-2}	4.11×10^{-3}	2.90×10^{-1}	2.69×10^{-1}
40	5.00×10^{-3}	1.96×10^{-3}	9.24×10^{-2}	1.32×10^{-1}
50	2.74×10^{-3}	9.70×10^{-4}	5.31×10^{-2}	4.46×10^{-2}
60	1.35×10^{-3}	4.80×10^{-4}	2.51×10^{-3}	1.96×10^{-3}

Underlined values represent mean viable counts of unirradiated controls.

Table 10. continued.

(ii) Fig. 37b. Survival of E. coli K1060 with Vitamin E in plates following growth with or without Vitamin E.

NUV Exposure time (min)	Viability assessed on YENB		high salt defined medium	
	Presence of Vitamin E in growth medium			
	+	-	+	-
(i)				
0	$\underline{8.765\times10^{6}}$	$\underline{8.205\times10^{6}}$	$\underline{1.08\times10^{7}}$	$\underline{8.75\times10^{6}}$
10	4.91×10^{-1}	2.07×10^{-1}	8.31×10^{-1}	8.80×10^{-1}
20	3.88×10^{-1}	1.34×10^{-1}	6.66×10^{-1}	5.93×10^{-1}
30	8.45×10^{-2}	2.50×10^{-2}	-	5.50×10^{-1}
40	4.80×10^{-3}	1.34×10^{-3}	6.70×10^{-1}	3.36×10^{-1}
50	1.24×10^{-3}	7.91×10^{-4}	1.00×10^{-1}	3.65×10^{-2}
60	8.91×10^{-4}	6.09×10^{-4}	4.61×10^{-3}	1.98×10^{-3}
(ii)				
0	$\underline{9.26\times10^{6}}$	$\underline{9.39\times10^{6}}$	$\underline{1.01\times10^{7}}$	$\underline{1.03\times10^{7}}$
10	5.86×10^{-1}	5.71×10^{-1}	9.51×10^{-1}	9.42×10^{-1}
20	2.95×10^{-1}	2.56×10^{-1}	8.69×10^{-1}	8.53×10^{-1}
30	6.98×10^{-2}	6.75×10^{-2}	5.01×10^{-1}	4.98×10^{-1}
40	4.10×10^{-3}	6.19×10^{-3}	3.25×10^{-1}	3.01×10^{-1}
50	1.01×10^{-3}	1.09×10^{-3}	4.36×10^{-2}	4.42×10^{-2}
60	6.00×10^{-4}	9.59×10^{-4}	4.01×10^{-3}	4.99×10^{-3}

Underlined values represent mean viable counts for unirradiated controls.

i) and (ii) show data from separate experiments. Data from (i) is plotted in Fig. 37a and 37b.

Table 11. Fig. 38. Survival of E. coli K1060 with Trolox-C in the plating medium following irradiation.

NUV Exposure time (min)	Surviving fraction, Viability assessed on YENB		high salt defined medium	
	Presence of Trolox in growth medium			
	+	-	+	-
(i)				
0	$\underline{8.50\times10^{6}}$	$\underline{1.02\times10^{7}}$	$\underline{2.35\times10^{7}}$	$\underline{2.25\times10^{7}}$
10	2.94×10^{-1}	1.72×10^{-1}	1.06×10^{0}	9.70×10^{-1}
20	3.64×10^{-2}	2.13×10^{-2}	8.11×10^{-1}	6.43×10^{-1}
30	5.08×10^{-2}	1.57×10^{-2}	5.65×10^{-1}	2.45×10^{-1}
40	8.00×10^{-3}	9.04×10^{-4}	5.10×10^{-1}	2.10×10^{-1}
50	1.00×10^{-3}	9.31×10^{-5}	3.52×10^{-1}	1.76×10^{-1}
(ii)				
0	$\underline{1.93\times10^{7}}$	$\underline{1.82\times10^{7}}$	$\underline{1.93\times10^{7}}$	$\underline{2.08\times10^{7}}$
10	3.79×10^{-1}	2.81×10^{-1}	1.02×10^{0}	1.02×10^{0}
20	2.58×10^{-1}	2.03×10^{-2}	8.06×10^{-1}	5.75×10^{-1}
30	2.30×10^{-1}	2.03×10^{-3}	3.96×10^{-1}	2.60×10^{-1}
40	1.35×10^{-1}	1.40×10^{-3}	2.62×10^{-1}	1.72×10^{-1}
50	6.22×10^{-2}	5.44×10^{-4}	7.39×10^{-2}	4.08×10^{-2}

Underlined values represent mean viable counts of unirradiated controls.

(i) and (ii) show data from separate experiments. Data from (i) is plotted in Fig. 38.

Table 12. Fig. 39a. Survival of E. coli K1060 on YENB with SOD following irradiation.

NUV Exposure time (min)	Surviving fraction Presence of SOD on plates (i) +	(i) −	(ii) +	(ii) −
0	$\underline{6.20\times10^{6}}$	$\underline{6.60\times10^{6}}$	$\underline{1.49\times10^{7}}$	$\underline{1.44\times10^{7}}$
10	1.05×10^{0}	6.75×10^{-2}	5.03×10^{-1}	6.94×10^{-1}
20	6.45×10^{-1}	1.66×10^{-2}	1.74×10^{-1}	6.94×10^{-2}
30	5.00×10^{-1}	6.51×10^{-3}	1.11×10^{-1}	1.11×10^{-2}
40	−	5.30×10^{-4}	1.02×10^{-1}	1.51×10^{-3}
50	6.77×10^{-2}	1.66×10^{-4}	−	1.90×10^{-4}

Underlined values represent mean viable counts of unirradiated controls.

Table 12. continued

39b. Survival of E. coli K1060 with catalase on the plates following irradiation.

NUV Exposure time (min)	Surviving fraction, viability assesssed on YENB		high salt defined medium	
	Presence of catalase			
	+	-	+	-
(i)				
0	$\underline{6.30\times10^{6}}$	$\underline{6.20\times10^{6}}$	$\underline{6.60\times10^{6}}$	$\underline{6.35\times10^{6}}$
10	1.09×10^{0}	8.01×10^{-2}	1.03×10^{0}	8.81×10^{-1}
20	8.22×10^{-1}	9.51×10^{-3}	9.74×10^{-1}	7.73×10^{-1}
30	6.40×10^{-1}	1.73×10^{-3}	9.21×10^{-1}	6.80×10^{-1}
40	5.62×10^{-1}	2.63×10^{-4}	9.01×10^{-1}	5.72×10^{-1}
50	5.31×10^{-1}	1.62×10^{-4}	6.92×10^{-1}	5.01×10^{-1}
(ii)				
0	$\underline{1.06\times10^{7}}$	$\underline{1.04\times10^{7}}$	$\underline{1.15\times10^{7}}$	$\underline{1.12\times10^{7}}$
10	9.90×10^{-1}	7.78×10^{-1}	1.01×10^{0}	9.37×10^{-1}
20	7.83×10^{-1}	4.71×10^{-1}	9.47×10^{-1}	8.28×10^{-1}
30	6.03×10^{-1}	2.59×10^{-2}	7.14×10^{-1}	4.21×10^{-1}
40	5.28×10^{-1}	1.05×10^{-2}	4.12×10^{-1}	3.59×10^{-1}
50	3.96×10^{-1}	1.82×10^{-3}	1.14×10^{-1}	1.01×10^{-1}

Underlined values represent mean viable counts of unirradiated controls.

(i) and (ii) show data from separate experiments. Data from (i) is plotted in Fig. 39a and 39b.

Table 13. Fig. 40. The survival of E. coli K1060 with deferrioxamine in the plates following irradiation.

NUV Exposure time (min)	Surviving fraction, viability assesssed on YENB Presence of desferrioxamine +	YENB -	high salt defined medium +	high salt defined medium -
(i)				
0	$\underline{9.56\times10^{6}}$	$\underline{9.73\times10^{6}}$	$\underline{1.13\times10^{7}}$	$\underline{1.07\times10^{7}}$
10	1.18×10^{-1}	1.01×10^{-2}	6.81×10^{-1}	4.39×10^{-1}
20	7.73×10^{-3}	3.18×10^{-3}	4.16×10^{-1}	4.01×10^{-1}
30	1.67×10^{-3}	1.04×10^{-3}	2.65×10^{-1}	1.58×10^{-1}
40	8.25×10^{-4}	2.46×10^{-4}	1.76×10^{-1}	9.62×10^{-2}
50	5.22×10^{-4}	1.64×10^{-4}	4.95×10^{-2}	7.75×10^{-2}
(ii)				
0	$\underline{1.13\times10^{7}}$	$\underline{1.04\times10^{7}}$	$\underline{1.21\times10^{7}}$	$\underline{1.05\times10^{7}}$
10	9.97310^{-2}	7.96×10^{-2}	8.95×10^{-1}	7.34×10^{-1}
20	2.74×10^{-2}	8.76×10^{-3}	5.26×10^{-1}	3.92×10^{-1}
30	5.48×10^{-3}	1.63×10^{-3}	4.52×10^{-1}	2.86×10^{-1}
40	8.49×10^{-4}	2.21×10^{-4}	3.03×10^{-1}	2.00×10^{-1}
50	3.36×10^{-4}	1.50×10^{-4}	7.39×10^{-2}	5.31×10^{-2}
(iii)				
0	$\underline{1.58\times10^{7}}$	$\underline{1.44\times10^{7}}$		
10	$5.4^{4\times10^{-1}}$	3.40×10^{-1}		
20	1.70×10^{-1}	6.94×10^{-2}		
30	1.52×10^{-1}	1.11×10^{-2}		
40	1.35×10^{-1}	1.51×10^{-3}		
50	6.89×10^{-2}	1.90×10^{-4}		

Underlined values represent mean viable counts of unirradiated controls.

(i), (ii) and (iii) represent duplicate experiments. Data from (i) is plotted in Fig. 40.

Table 14. Fig. 41. The survival of E. coli K1060 following irradiation after growth in BSO-medium.

41a.

NUV exposure time (min)	Surviving fraction, viability assessed on: YENB		defined medium		high salt medium	
	Presence of BSO in growth medium					
	+	−	+	−	+	−
(i)						
0	1.22×10^{7}	1.04×10^{7}	1.25×10^{7}	1.02×10^{7}	1.37×10^{7}	1.04×10^{7}
10	1.39×10^{-1}	3.46×10^{-2}	7.80×10^{-1}	9.80×10^{-1}	6.39×10^{-1}	9.70×10^{-1}
20	1.39×10^{-3}	4.71×10^{-3}	6.48×10^{-1}	7.35×10^{-1}	3.86×10^{-1}	4.11×10^{-1}
30	2.42×10^{-4}	7.50×10^{-4}	3.14×10^{-1}	3.82×10^{-1}	1.52×10^{-1}	3.52×10^{-1}
40	3.36×10^{-4}	4.04×10^{-4}	9.44×10^{-2}	1.05×10^{-1}	4.01×10^{-2}	9.11×10^{-1}
50	4.26×10^{-5}	1.44×10^{-4}	8.56×10^{-3}	5.09×10^{-2}	3.57×10^{-3}	5.58×10^{-2}
(ii)						
0	9.45×10^{6}	1.21×10^{7}	1.02×10^{7}	1.28×10^{7}	1.03×10^{7}	1.29×10^{7}
10	1.60×10^{-1}	4.17×10^{-1}	1.10×10^{0}	8.33×10^{-1}	9.02×10^{-1}	1.01×10^{0}
20	3.70×10^{-2}	6.98×10^{-2}	8.72×10^{-1}	6.95×10^{-1}	6.58×10^{-1}	7.44×10^{-1}
30	1.00×10^{-2}	3.30×10^{-2}	2.10×10^{-1}	3.39×10^{-1}	2.27×10^{-1}	3.48×10^{-1}
40	4.92×10^{-4}	2.81×10^{-3}	9.20×10^{-2}	1.03×10^{-1}	3.01×10^{-2}	1.11×10^{-1}
50	1.01×10^{-4}	3.01×10^{-4}	5.19×10^{-2}	4.49×10^{-2}	4.13×10^{-3}	4.88×10^{-2}

Table 14. (continued)

41b. Survival of E. coli K1060 with BSO in plates following irradiation.

NUV exposure time (min)	Surviving fraction, viability assessed on: YENB		defined medium		high salt medium	
	Presence of BSO in growth medium					
	+	-	+	-	+	-
(i)						
0	$\underline{1.45\times10^{7}}$	$\underline{1.51\times10^{7}}$	$\underline{1.47\times10^{7}}$	$\underline{1.53\times10^{7}}$	$\underline{1.46\times10^{7}}$	1.53×10^{7}
5		1.75×10^{-1}				
10	7.24×10^{-2}	-	6.05×10^{-1}	7.19×10^{-1}	6.57×10^{-1}	8.17×10^{-1}
20	1.38×10^{-2}	2.05×10^{-2}	4.08×10^{-1}	3.53×10^{-1}	5.06×10^{-1}	4.12×10^{-1}
30	4.34×10^{-3}	6.22×10^{-3}	3.33×10^{-2}	2.48×10^{-1}	4.17×10^{-2}	2.81×10^{-1}
40	4.96×10^{-4}	9.27×10^{-4}	1.26×10^{-3}	4.31×10^{-2}	4.24×10^{-3}	4.57×10^{-2}
50	-	4.11×10^{-4}	-	2.09×10^{-3}	-	1.50×10^{-3}
(ii)						
0	$\underline{1.30\times10^{7}}$	$\underline{1.01\times10^{7}}$	$\underline{1.39\times10^{7}}$	$\underline{1.13\times10^{7}}$	$\underline{1.40\times10^{7}}$	$\underline{1.04\times10^{7}}$
5	5.07×10^{-1}	6.00×10^{-1}	-	-	-	-
10	2.11×10^{-1}	2.67×10^{-1}	9.06×10^{-1}	9.38×10^{1}	8.56×10^{-1}	9.32×10^{-1}
20	1.01×10^{-2}	7.92×10^{-2}	8.48×10^{-1}	9.55×10^{-1}	7.16×10^{-1}	7.69×10^{-1}
30	1.07×10^{-3}	2.06×10^{-2}	5.83×10^{-1}	7.17×10^{-1}	5.25×10^{-1}	7.69×10^{-1}
40	2.15×10^{-5}	4.95×10^{-4}	1.69×10^{-1}	2.47×10^{-1}	7.08×10^{-2}	1.92×10^{-1}
50	-	1.18×10^{-4}	1.24×10^{-2}	7.41×10^{-2}	1.01×10^{-2}	6.39×10^{-2}

Underlined values represent mean viable counts of unirradiated controls.
(i) and (ii) show data from separate experiments. Data from (i) is plotted in Fig. 41a and 41b.

Table 15. Fig. 42. Survival of E. coli K1060 following irradiation in DABCO.

NUV exposure time (min)	Surviving fraction, viability assessed on: YENB		defined medium		high salt medium	
	Presence of BSO in growth medium					
	+	-	+	-	+	-
(i)						
0	$\underline{1.53\times10^{7}}$	$\underline{1.04\times10^{7}}$	$\underline{1.53\times10^{7}}$	$\underline{1.02\times10^{7}}$	$\underline{1.65\times10^{7}}$	$\underline{1.04\times10^{7}}$
10	3.07×10^{-1}	3.46×10^{-2}	9.74×10^{-1}	9.80×10^{-1}	1.14×10^{0}	9.52×10^{-1}
20	4.70×10^{-2}	4.71×10^{-3}	8.23×10^{-1}	7.35×10^{-1}	8.60×10^{-1}	3.46×10^{-1}
30	1.30×10^{-2}	7.50×10^{-4}	9.67×10^{-1}	3.82×10^{-1}	8.60×10^{-1}	3.46×10^{-1}
40	1.84×10^{-3}	4.04×10^{-4}	6.16×10^{-1}	1.05×10^{-1}	5.87×10^{-1}	8.94×10^{-2}
50	3.66×10^{-4}	1.44×10^{-4}	5.90×10^{-2}	3.04×10^{-2}	5.57×10^{-3}	2.62×10^{-3}
(ii)						
0	$\underline{1.13\times10^{7}}$	$\underline{1.04\times10^{7}}$			$\underline{1.13\times10^{7}}$	$\underline{1.07\times10^{7}}$
10	9.60×10^{-1}	7.78×10^{-1}			7.10×10^{-1}	7.11×10^{-1}
20	5.19×10^{-1}	4.71×10^{-1}			4.45×10^{-1}	4.36×10^{-1}
30	1.58×10^{-1}	1.25×10^{-1}			2.42×10^{-1}	2.31×10^{-1}
40	3.46×10^{-2}	1.05×10^{-2}			9.70×10^{-2}	5.50×10^{-2}
50	4.22×10^{-3}	1.82×10^{-3}			5.83×10^{-2}	2.50×10^{-2}

Underlined values represent mean viable counts of unirradiated controls.

Table 16. Fig. 43. The survival of E. coli K1060 following irradiation in the presence of histidine.

NUV Exposure time (min)	Surviving fraction, viability assesssed on YENB		high salt defined medium	
	Presence of histidine			
	+	-	+	-
(i)				
0	$\underline{3.96\times10^{6}}$	$\underline{3.90\times10^{6}}$	$\underline{4.13\times10^{6}}$	$\underline{4.60\times10^{6}}$
5	1.00×10^{0}	1.17×10^{0}		
10	1.01×10^{0}	9.17×10^{-1}	1.02×10^{0}	1.06×10^{0}
20	6.81×10^{-1}	5.13×10^{-1}	9.51×10^{-1}	7.95×10^{-1}
30	3.83×10^{-1}	2.56×10^{-1}	7.49×10^{-1}	6.01×10^{-1}
40	2.62×10^{-1}	1.71×10^{-2}	6.41×10^{-1}	2.39×10^{-1}
50	1.27×10^{-1}	6.92×10^{-4}	4.02×10^{-1}	6.42×10^{-2}
(ii)				
0	$\underline{7.95\times10^{6}}$	$\underline{7.80\times10^{6}}$	$\underline{8.70\times10^{6}}$	$\underline{8.30\times10^{6}}$
10	8.99×10^{-1}	8.48×10^{-1}	1.00×10^{0}	9.75×10^{-1}
20	7.79×10^{-1}	4.17×10^{-1}	1.00×10^{0}	8.55×10^{-1}
30	2.07×10^{-1}	1.20×10^{-2}	8.39×10^{-1}	4.87×10^{-1}
40	3.01×10^{-2}	2.02×10^{-3}	6.55×10^{-1}	1.45×10^{-1}
50	2.26×10^{-3}	1.51×10^{-4}	1.55×10^{-1}	8.07×10^{-2}

Underlined values represent mean viable counts of unirradiated controls.

(i) and (ii) represent duplicate experiments. Data from (i) is plotted in Fig. 43.

Table 17. Fig. 44. Survival of E. coli K1060 following irradiation in D_2O

NUV Exposure time (min)	Surviving fraction, viability assesssed on YENB		high salt defined medium	
	Presence of D_2O			
	+	-	+	-
(i)				
0	$\underline{5.90\times10^{6}}$	$\underline{7.00\times10^{6}}$	$\underline{5.70\times10^{6}}$	$\underline{6.80\times10^{6}}$
5	3.89×10^{-1}	1.10×10^{-1}	1.86×10^{-1}	1.00×10^{0}
10	1.15×10^{-1}	9.51×10^{-1}	8.80×10^{-2}	1.00×10^{0}
15	1.01×10^{-2}	7.82×10^{-1}	2.03×10^{-2}	1.10×10^{0}
20	1.52×10^{-3}	3.14×10^{-1}	3.38×10^{-3}	9.77×10^{-1}
30	-	9.42×10^{-2}	-	9.26×10^{-1}
40	-	1.71×10^{-3}	-	6.61×10^{-1}
50	-	6.57×10^{-4}	-	3.23×10^{-2}
60	-	5.71×10^{-4}	-	2.35×10^{-4}
(ii)				
0	$\underline{4.60\times10^{7}}$	$\underline{3.93\times10^{7}}$	$\underline{4.43\times10^{7}}$	$\underline{5.50\times10^{7}}$
20	7.39×10^{-2}	3.56×10^{-1}	1.77×10^{-1}	8.00×10^{-1}
40	1.89×10^{-4}	3.56×10^{-1}	1.72×10^{-4}	2.25×10^{-1}
60	5.65×10^{-5}	1.50×10^{-3}	7.91×10^{-5}	-
80	4.34×10^{-5}	7.63×10^{-5}	5.95×10^{-5}	5.09×10^{-5}

Underlined values represent mean viable counts of unirradiated controls.
(i) and (ii) represent duplicate experiments. Data from (i) is plotted in Fig. 44

Table 17. (continued)

Fig. 44b. Survival following far-UV irradiation, viability assessed on YENB.

Far UV Fluence	Surviving fraction	
(Jm^{-2})	+ D_2O	- D_2O
0	$\underline{9.68 \times 10^{6}}$	$\underline{1.02 \times 10^{7}}$
20		8.39×10^{-1}
40	5.01×10^{-1}	4.80×10^{-1}
60	2.32×10^{-1}	1.97×10^{-1}
80	6.98×10^{-2}	5.81×10^{-2}
100	-	2.32×10^{-2}
120	1.99×10^{-3}	-
140	3.00×10^{-4}	2.46×10^{-4}

Underlined values represent mean viable counts of unirradiated controls.

Table 18 . Fig. 45. The Peroxide Values (PV) of E. coli K1060 incorporating various fatty acids following near-UV irradiation

Near-UV exposure time (min)	PV (meq kg^{-1}) per 10^6 cells x 10^4 fatty acid incorporated		
	(a) oleic	(b) linoleic	(c) linolenic
(i)			
0	0	0	0
30	0	0	0
60	0	0	0.104
105	0.126	0.420	0.580
150	0.240	0.740	1.360
195	0.480	1.300	2.000
(ii)			
0	0	0	0
30	0	0	0
60	0	0	0.120
120	0.200	0.480	1.140
180	0.660	0.860	1.800
(iii)			
0	0	0	0
45	0	0.150	0.220
90	0.156	0.240	0.280
135	0.180	0.420	1.560
150	–	0.660	1.800
180	0.580	–	–

(i), (ii) and (iii) show data from separate experiments.

Table 19. Fig. 46. The Peroxide Value (PV) of E. coli K1060 during the post-irradiation period following near-UV irradiation (various fatty acids incorporated as shown).

Near-UV exposure time (min)	PV (meq kg^{-1}) per 10^6 cells x 10^4 fatty acid incorporated		
	(a) oleic	(b) linoleic	(c) linolenic
(i)			
150	0.240	0.740	1.360
195	0.480	1.300	2.000
Time after irradiation (min			
0	0.480	1.300	2.000
45	0.480	1.400	2.120
105	0.560	1.580	2.000
150	0.580	1.540	2.060
(ii)			
NUV exposure time (min)			
180	0.660	0.860	1.800
Time after irradiation (min)			
0	0.660	0.860	1.800
60	0.600	0.850	1.800
120	0.580	0.750	1.800
180	0.600	0.820	1.600

Table 20. Fig. 47. Lipid peroxidation in E. coli K1060 (18:3) following near-UV irradiation

	(a)		(d)	
Treatment	Following growth in BSO		Irradiated in DABCO	
NUV exposure time (min)	PV (meq kg^{-1}) per 10^6 cells x 10^4		PV (meq kg-1) per 10^6 cells x 10^4	
	BSO	+BSO	-DABCO	+DABCO
60	0.058	0.280	0.058	0.040
120	0.420	0.860	0.420	0.056
180	0.980	1.480	0.980	0.400
240	2.300	3.400	2.300	0.680

	(c)		(b)	
Treatment	Irradiated in histidine		Irradiated in D_2O	
NUV exposure time (min)	PV (meq kg^{-1}) per 10^6 cells x 10^4		PV (meq kg^{-1} per 10^6 cells x 10^4	
	-His	+His	$-D_2O$	$+D_2O$
90	0.048	0	-	-
135	-	-	0.046	0.078
180	0.320	0.180	0.920	1.920
270	1.280	0.330	2.120	5.580

Table 21. Fig. 48. survival of E. coli K1060, grown in low potassium-medium following near-UV irradiation

Near UV exposure time (min)	Surviving fraction, viability assessed on YENB fatty acid incorporated		
	oleic	linoleic	linolenic
0	3.70×10^{7}	1.80×10^{7}	1.90×10^{7}
10	-	-	1.60×10^{-1}
15	9.59×10^{-1}	6.02×10^{-1}	-
20	-	-	1.76×10^{-2}
25	3.30×10^{-1}	1.12×10^{-1}	-
30	-	-	2.87×10^{-3}
35	1.61×10^{-1}	2.26×10^{-2}	-
45	3.00×10^{-3}	8.46×10^{-4}	1.06×10^{-4}

Table 22 . Fig. 49. The leakage of $^{86}Rb^{+}$ from E. coli K1060 incorporating various fatty acids, following near-UV irradiation.

Time (min)	dpm per cell x 10^6 fatty acid incorporated					
	(a) oleic		(b) linoleic		(c) linolenic	
	Irradiated	Unirradiated	Irradiated	Unirradiated	Irradiated	Unirradiated
(i)						
0	3.28	3.28	4.80	4.82	3.80	3.84
20	4.28	3.68	6.40	7.44	7.28	6.76
40	4.80	6.16	6.88	8.28	9.52	6.80
60	6.00	7.04	10.80	9.20	11.52	8.20
80	6.16	9.40	21.00	13.28	16.68	10.12
100	11.12	9.80	21.40	13.80	22.48	12.6
120	12.40	10.88	29.00	15.04	33.00	13.21
140	17.00	12.80	-	-	44.96	14.08
160	-	-	-	-	47.20	14.68
180	29.64	15.88	43.40	16.20	55.64	16.40

Table 22 . (continued)

Time (min)	dpm per cell x 10^6 fatty acid incorporated					
	(a) oleic		(b) linoleic		(c) linolenic	
	Irradiated	Unirradiated	Irradiated	Unirradiated	Irradiated	Unirradiated
(ii)						
0	5.80	5.80	5.31	5.40	5.46	6.31
20			6.49	6.02	7.19	6.53
40	5.91	6.10	6.96	8.01	8.25	6.94
60	-	-	11.52	9.89	11.86	7.59
80	10.12	9.20	20.50	13.95	-	-
100	11.15	9.30	23.14	14.62	24.01	12.24
120	12.60	10.15	33.16	16.14	-	-
140	18.95	10.60	35.24	17.01	43.52	13.34
160	20.12	11.60	-	-	51.79	14.59
180	32.20	14.80	-	-	50.93	15.83

(i) and (ii) show data from separate experiments.

Table 23. Fig. 51. Leakage of $^{86}Rb^{+}$ from stationary phase E. coli K1060 following near-UV irradiation

Time (min)	dpm per cell x 10^6 fatty acid incorporated			
	oleic		linolenic	
	Irradiated	Unirradiated	Irradiated	Unirradiated
0	6.68	6.68	6.28	6.28
30	38.24	10.44	31.56	8.68
60	46.96	17.00	38.2	13.16
90	63.84	17.68	45.32	14.72
120	68.76	19.39	54.01	15.32
150	72.16	23.56	62.48	21.08
180	83.83	30.20	86.16	24.60
210	88.08	31.20	84.32	30.76

Table 24 . Fig. 53. The leakage of $^{86}Rb^{+}$ from E. coli K1060 incorporating various fatty acids, following far-UV (254 nm) irradiation.

Far-UV fluence (Jm^{-2})	dpm per cell x 10^6 fatty acid incorporated					
	(a) oleic		(b) linoleic		(c) linolenic	
	Irradiated	Unirradiated	Irradiated	Unirradiated	Irradiated	Unirradiated
0	8.20	8.20	7.88	7.88	8.68	8.72
20	9.68	9.88	9.88	10.68	9.60	8.80
40	9.80	10.48	9.48	10.48	9.60	10.68
60	12.16	13.00	15.00	14.48	13.68	14.40
80	13.28	13.96	12.48	11.28	14.08	14.88
100	14.60	13.48	16.20	13.68	15.00	15.48
120	15.48	14.88	15.60	15.00	16.00	15.60
140	16.48	16.88	16.80	16.40	16.60	16.00

Table 25. Fig. 54. The survival of E. coli K1060 following long exposure to irradiation viability assessed on YENB.

NUV exposure time (min)	Viability assessed on: YENB	high salt medium
(a) Oleate-grown cells		
0	$\underline{1.01\times10^{8}}$	$\underline{1.30\times10^{8}}$
20	4.81×10^{-1}	9.15×10^{-1}
40	6.52×10^{-2}	3.78×10^{-1}
60	9.81×10^{-4}	5.41×10^{-3}
80	9.38×10^{-5}	2.42×10^{-4}
100	1.09×10^{-5}	1.46×10^{-5}
110	5.86×10^{-7}	2.20×10^{-8}
120	9.89×10^{-8}	6.09×10^{-7}
(b) Linoleate-grown cells		
0	$\underline{7.29\times10^{7}}$	$\underline{7.28\times10^{7}}$
20	3.21×10^{-1}	7.63×10^{-1}
40	3.73×10^{-3}	1.38×10^{-1}
60	9.75×10^{-5}	5.52×10^{-5}
80	-	2.73×10^{-6}
100	7.59×10^{-7}	1.02×10^{-6}
(c) Linolenate-grown cells		
0	$\underline{8.97\times10^{7}}$	
20	6.23×10^{-2}	
40	5.82×10^{-5}	
50	2.69×10^{-6}	

Table 26. Fig. 56a. The leakage of $^{86}Rb^{+}$ from E. coli K1060 following irradiation in D_2O.

Time (min)	dpm per cell x 10^6			
	Irradiated		Unirradiated	
	$-D_2O$	$+D_2O$	$-D_2O$	$+D_2O$
(i)				
0	3.40	4.24	3.12	3.60
10	5.44	9.76	5.88	9.40
20	6.28	14.16	5.76	13.00
30	9.80	13.44	9.52	13.36
40	13.12	18.32	10.84	16.20
50	13.36	28.08	12.08	16.80
60	16.88	54.48	10.40	19.96
80	24.00	71.48	13.00	18.00
100	30.92	91.32	10.84	22.12
120	40.16	98.36	13.24	24.32
140	50.88	99.76	13.80	25.28
(ii)				
0	2.52	2.48	2.52	2.48
20	3.20	6.32	2.84	4.23
40	10.63	14.04	5.32	5.96
60	14.16	23.64	6.68	6.96
80	20.72	50.12	9.28	10.89
100	23.14	61.26	10.56	16.32
120	30.20	89.48	12.32	18.91
140	33.56	99.98	14.10	19.58

(i) and (ii) show data from separate experiments. Data from (1) is plotted in Fig. 56.

Table 27. Fig. 57. The effect of growth in Vitamin E on leakage of $^{86}Rb^{+}$ from E. coli K1060 following near-UV irradiation.

Time (min)	dpm per cell x 10^6			
	Irradiated		Unirradiated	
	-Vit E	+ Vit E	-Vit E	+Vit E
(i)				
0	2.78	4.00	2.98	2.64
20	7.01	3.88	4.96	5.00
40	9.25	4.56	6.42	6.36
60	11.63	8.20	9.53	9.32
80	31.52	12.88	11.62	11.12
100	41.69	20.72	12.43	11.84
120	59.81	33.80	13.82	12.72
140	65.76	43.28	14.86	14.16
(ii)				
0	3.52	3.02	3.14	3.62
20	8.52	4.13	3.98	3.86
40	9.65	4.92	4.56	4.12
60	12.32	7.68	5.85	5.05
80	18.98	10.32	10.89	9.67
100	26.95	20.01	12.14	11.52
120	38.86	32.95	13.32	12.86
140	49.72	41.56	15.20	14.96

(i) and (ii) show data from separate experiments. Data from (1) is plotted in Fig. 57.

Table 28. Fig. 58. The effect of growth in Trolox-C on leakage of $^{86}Rb^{+}$ from E. coli K1060 following near-UV irradiation.

Time (min)	dpm per cell x 10^6			
	Irradiated		Unirradiated	
	-Trolox-C	+Trolox-C	-Trolox-C	+Trolox-C
(i)				
0	3.52	3.24	4.08	4.08
20	7.04	3.68	4.60	3.12
40	8.56	8.04	5.76	4.48
60	12.48	10.52	7.44	4.76
80	28.08	19.64	8.76	6.44
100	43.80	33.08	11.24	8.36
120	57.68	47.04	14.48	10.92
140	66.04	55.24	13.80	12.28
160	70.40	59.28	16.48	14.08
(ii)				
0	1.68	1.80	1.40	2.00
20	3.36	3.29	3.48	3.36
40	6.68	5.87	4.04	3.98
60	8.04	6.96	4.88	4.56
80	16.80	14.32	5.40	5.32
100	36.16	32.56	10.96	9.58
120	47.92	45.68	12.67	11.29
140	55.32	53.19	12.98	12.05

(i) and (ii) show data from separate experiments. Data from (1) is plotted in Fig. 58

Table 29. Fig. 59b. Survival of E. coli SR 385 following near-UV irradiation.

NUV exposure time (min)	Surviving fraction, viability assessed on: YENB	Normal salt	High salt
0	$\underline{1.36\times10^{7}}$	$\underline{1.40\times10^{7}}$	$\underline{1.39\times10^{7}}$
20	8.39×10^{-1}	6.62×10^{-1}	3.96×10^{-1}
40	5.23×10^{-1}	2.75×10^{-1}	7.51×10^{-2}
60	1.65×10^{-1}	6.43×10^{-2}	9.38×10^{-3}
80	6.30×10^{-2}	1.84×10^{-2}	1.36×10^{-3}
120	2.91×10^{-3}	1.42×10^{-3}	-

Table 30. Fig. 60. Survival of (a) log phase; (b) stationary phase E. coli K1060.

	NUV exposure time (min)	Surviving fraction, viability assessed on defined media: Standard	+ glucose	- casamino acids
(a)	0	$\underline{1.13\times10^{7}}$	$\underline{1.01\times10^{7}}$	$\underline{1.17\times10^{7}}$
	10	1.04×10^{0}	8.49×10^{-1}	1.09×10^{0}
	20	8.41×10^{-1}	7.95×10^{-1}	8.50×10^{-1}
	30	7.78×10^{-1}	8.00×10^{-1}	6.57×10^{-1}
	40	6.00×10^{-1}	6.51×10^{-1}	6.49×10^{-1}
	60	2.20×10^{-2}	-	2.21×10^{-2}
b)	0	$\underline{1.04\times10^{7}}$	$\underline{1.05\times10^{7}}$	$\underline{1.04\times10^{7}}$
	10	2.21×10^{-1}	1.79×10^{-1}	1.60×10^{-1}
	20	6.01×10^{-2}	6.99×10^{-1}	4.91×10^{-1}
	30	2.42×10^{-3}	2.81×10^{-3}	1.90×10^{-3}
	40	3.79×10^{-4}	1.38×10^{-3}	1.70×10^{-3}
	50	1.51×10^{-4}	3.00×10^{-4}	-

Underlined values represent mean viable counts of unirradiated controls.

Table 31. Fig. 61. The effect of media modifications on the survival of *E. coli* K1060 following near-UV irradiation.

NUV exposure time (min)	Surviving fraction, viability assessed on modified media	
	Difco agar, defined	Oxoid agar, defined
61a) 0	$\underline{1.37\times10^{7}}$	$\underline{1.29\times10^{7}}$
10	9.86×10^{-1}	7.99×10^{-1}
15	1.10×10^{0}	9.10×10^{-1}
20	8.82×10^{-1}	5.88×10^{-1}
30	3.71×10^{-1}	3.10×10^{-1}
40	4.00×10^{-2}	6.60×10^{-2}
50	3.41×10^{-4}	2.92×10^{-4}
60	8.09×10^{-5}	7.30×10^{-5}

61c)	YENB		Defined medium	
	standard	minus yeast	standard	plus yeast
0	$\underline{1.29\times10^{7}}$	$\underline{1.21\times10^{7}}$	$\underline{1.31\times10^{7}}$	$\underline{1.29\times10^{7}}$
10	6.53×10^{-1}	7.35×10^{-1}	1.02×10^{0}	9.59×10^{-1}
20	7.19×10^{-2}	9.52×10^{-2}	9.56×10^{-1}	7.30×10^{-1}
30	1.78×10^{-2}	2.11×10^{-2}	-	-
40	4.92×10^{-3}	4.05×10^{-3}	2.85×10^{-1}	1.10×10^{-1}
50	-	-	8.98×10^{-3}	4.09×10^{-3}

61b)	YENB (standard)	YENB, no beef extract
0	$\underline{9.50\times10^{6}}$	$\underline{1.01\times10^{7}}$
5	8.81×10^{-1}	9.48×10^{-1}
10	7.63×10^{-1}	6.78×10^{-1}
20	6.70×10^{-1}	5.76×10^{-1}
30	1.29×10^{-1}	1.48×10^{-1}
40	3.00×10^{-2}	2.98×10^{-2}

Underlined values represent mean viable count of unirradiated controls.

Table 32. Fig. 62. The effect of salts on the survival of E. coli K1060 following near-UV irradiation.

NUV exposure time (min)	Surviving fraction, viability assessed on YENB			
	Fig. 62a		Fig. 62b	
	standard	+NaCl	standard	+M9 salts
(i)				
0	$\underline{1.65\times10^{7}}$	$\underline{1.42\times10^{7}}$	$\underline{1.07\times10^{7}}$	$\underline{1.08\times10^{7}}$
10	6.85×10^{-2}	1.62×10^{-1}	4.69×10^{-1}	4.55×10^{-1}
20	1.00×10^{-2}	2.01×10^{-2}	3.91×10^{-2}	1.62×10^{-1}
30	3.62×10^{-3}	3.91×10^{-3}	1.61×10^{-2}	5.05×10^{-2}
40	4.12×10^{-4}	1.06×10^{-3}	4.64×10^{-3}	1.31×10^{-2}
50	1.06×10^{-4}	3.25×10^{-4}	2.40×10^{-3}	3.74×10^{-3}
(ii)				
0	$\underline{8.45\times10^{6}}$	$\underline{8.55\times10^{6}}$	$\underline{1.13\times10^{7}}$	$\underline{1.23\times10^{7}}$
10	6.91×10^{-2}	9.42×10^{-2}	1.51×10^{-1}	3.89×10^{-1}
20	7.13×10^{-3}	1.24×10^{-2}	2.56×10^{-2}	3.00×10^{-2}
30	5.45×10^{-4}	1.00×10^{-2}	1.82×10^{-3}	7.85×10^{-3}
40	1.54×10^{-4}	2.70×10^{-3}	5.39×10^{-4}	1.82×10^{-3}
50	1.19×10^{-4}	4.13×10^{-4}	8.80×10^{-5}	1.11×10^{-3}

Underlined values represent mean viable counts of unirradiated controls.
(i) and (ii) are data from separate experiments. Data from (i) is plotted in Fig. 62.

Table 33. Fig. 63. The survival of E. coli (a) K1060, (b) SR 385 following near-UV irradiation after growth in either glucose or glycerol media.

NUV exposure time (min)	Surviving fraction, viability assessed on: Carbon source in growth medium					
	YENB		DM		HS DM	
	glucose	glycerol	glucose	glycerol	glucose	glycerol
63a)						
0	$\underline{6.55\times10^{6}}$	$\underline{1.66\times10^{7}}$	$\underline{6.60\times10^{6}}$	$\underline{1.62\times10^{7}}$	$\underline{6.65\times10^{6}}$	$\underline{1.65\times10^{7}}$
10	6.51×10^{-1}	6.32×10^{-1}	9.20×10^{-1}	9.81×10^{-1}	8.56×10^{-1}	9.54×10^{-1}
20	3.93×10^{-1}	1.73×10^{-1}	7.72×10^{-1}	6.32×10^{-1}	5.43×10^{-1}	6.10×10^{-1}
30	3.35×10^{-1}	7.22×10^{-2}	6.56×10^{-1}	5.82×10^{-1}	5.00×10^{-1}	5.61×10^{-1}
40	2.46×10^{-1}	1.90×10^{-2}	5.13×10^{-1}	4.01×10^{-1}	4.26×10^{-1}	3.86×10^{-1}
50	1.52×10^{-1}	5.92×10^{-3}	4.24×10^{-1}	2.82×10^{-1}	3.02×10^{-1}	2.16×10^{-1}
63b)						
0	$\underline{1.01\times10^{7}}$	$\underline{1.65\times10^{7}}$	$\underline{1.22\times10^{7}}$	$\underline{1.76\times10^{7}}$	$\underline{1.20\times10^{7}}$	$\underline{1.75\times10^{7}}$
20	9.92×10^{-1}	9.91×10^{-1}	1.01×10^{0}	1.35×10^{0}	1.10×10^{0}	1.30×10^{0}
30	8.56×10^{-1}	8.49×10^{-1}	8.01×10^{-1}	8.12×10^{-1}	7.95×10^{-1}	7.82×10^{-1}
40	5.51×10^{-1}	6.65×10^{-1}	4.15×10^{-1}	4.20×10^{-1}	3.85×10^{-1}	2.80×10^{-1}
50	-	-	-	6.19×10^{-2}	-	4.20×10^{-2}
60	3.66×10^{-1}	3.02×10^{-1}	2.49×10^{-2}	3.28×10^{-2}	1.01×10^{-2}	7.48×10^{-3}
70			2.02×10^{-3}	2.85×10^{-3}	1.89×10^{-4}	3.85×10^{-4}
80	1.10×10^{-1}	1.26×10^{-1}	-	-	-	-

Underlined values represent mean viable counts of unirradiated controls.

Table 34. Fig. 64. The survival of E. coli K1060 following near-UV irradiation after (a) 0.5 ml and (b) 1.0 ml inoculum size of culture used for irradiation.

NUV exposure time (min)	Surviving fraction, viability assessed on: YENB		Defined medium	
	Time cells harvested for irradiation			
	3h	6h	3h	6h
64a)				
0	$\underline{5.21\times10^{6}}$	$\underline{1.93\times10^{6}}$	$\underline{6.13\times10^{6}}$	$\underline{2.33\times10^{6}}$
5	9.14×10^{-1}	6.80×10^{-1}	1.09×10^{0}	8.42×10^{-1}
10	2.69×10^{-1}	2.31×10^{-1}	6.05×10^{-1}	9.20×10^{-1}
15	1.43×10^{-1}	2.20×10^{-1}	9.50×10^{-1}	8.51×10^{-1}
20	4.81×10^{-2}	8.92×10^{-2}	5.13×10^{-1}	3.10×10^{-1}
30	5.05×10^{-3}	1.52×10^{-3}	2.32×10^{-1}	3.19×10^{-1}
40	1.72×10^{-4}	1.50×10^{-4}	2.72×10^{-3}	5.29×10^{-3}
50	5.51×10^{-5}	6.80×10^{-5}	-	6.78×10^{-4}
64b)	2h	4h	2h	4h
0	$\underline{9.16\times10^{6}}$	$\underline{9.62\times10^{6}}$	$\underline{1.24\times10^{7}}$	$\underline{1.13\times10^{7}}$
5	8.89×10^{-1}	5.41×10^{-1}	1.02×10^{0}	1.12×10^{0}
10	-	2.73×10^{-1}	8.42×10^{-1}	8.39×10^{-1}
15	9.39×10^{-2}	1.21×10^{-1}	5.73×10^{-1}	1.01×10^{0}
20	2.04×10^{-2}	6.00×10^{-2}	4.89×10^{-1}	-
30	9.25×10^{-3}	1.18×10^{-2}	2.39×10^{-1}	4.33×10^{-1}
40	5.05×10^{-3}	6.03×10^{-3}	3.40×10^{-2}	-
50	1.03×10^{-3}	4.26×10^{-4}	4.76×10^{-3}	4.49×10^{-4}

Underlined values represent mean viable counts of unirradiated controls.

Table 35. Fig. 65. The effect of incubation temperature on the survival of E. coli K1060 following near-UV irradiation

NUV exposure time (min)	YENB		Defined medium		High salt medium	
	Incubation temperature					
	30°	37°	30°	37°	30°	37°
(i)						
0	1.07×10^{7}	1.10×10^{7}	1.13×10^{7}	1.12×10^{7}	1.00×10^{7}	1.02×10^{7}
5	6.61×10^{-1}	6.92×10^{-1}				
10	2.52×10^{-1}	4.50×10^{-1}	9.43×10^{-1}	-	9.70×10^{-1}	-
20	7.05×10^{-2}	5.49×10^{-1}	9.52×10^{-1}	8.51×10^{-1}	8.98×10^{-1}	8.01×10^{-1}
30	9.01×10^{-3}	3.72x10-3	7.15×10^{-1}	4.61×10^{-1}	8.02×10^{-1}	4.81×10^{-1}
40	4.62×10^{-4}	2.75×10^{-4}	2.43×10^{-1}	2.70×10^{-2}	2.03×10^{-1}	5.01×10^{-2}
50	1.11×10^{-4}	2.20×10^{-5}	1.21×10^{-2}	1.00×10^{-4}	1.43×10^{-2}	1.11×10^{-4}
(ii)						
0	8.41×10^{6}	8.50×10^{6}	8.51×10^{6}	8.78×10^{6}	7.82×10^{6}	7.36×10^{6}
10	6.95×10^{-2}	6.31×10^{-1}	8.90×10^{-1}	8.70×10^{-1}	8.65×10^{-1}	8.50×10^{-1}
20	7.12×10^{-3}	1.75×10^{-3}	1.34×10^{-1}	9.70×10^{-2}	4.20×10^{-1}	1.00×10^{-1}
30	5.46×10^{-4}	5.00×10^{-4}	3.05×10^{-2}	1.87×10^{-2}	4.25x1-$^{-2}$	9.00×10^{-3}
40	1.19×10^{-4}	2.32×10^{-4}	1.40×10^{-2}	2.51×10^{-3}	3.10×10^{-2}	4.56×10^{-3}
50	1.50×10^{-4}	1.30×10^{-4}	2.86×10^{-3}	1.95×10^{-4}	3.58×10^{-3}	3.29×10^{-4}

(i) and (ii) are data from separate excperiments. Data from (i) is plotted in Fig. 65.

Table 36. Fig. 66. The survival of E coli K-12 following near-UV irradiation

NUV exposure time (min)	Surviving fraction, viability assessed on: YENB	normal salt	high salt
0	$\underline{1.95 \times 10^{7}}$	$\underline{2.06 \times 10^{7}}$	$\underline{2.01 \times 10^{7}}$
20	8.32×10^{-1}	1.01×10^{0}	9.95×10^{-1}
30	8.61×10^{-2}	9.98×10^{-1}	9.53×10^{-1}
40	2.05×10^{-2}	-	-
50	1.22×10^{-2}	9.02×10^{-1}	4.97×10^{-1}
60	-	-	-
70	4.61×10^{-3}	4.98×10^{-1}	8.05×10^{-2}
80	1.14×10^{-3}	2.91×10^{-1}	1.00×10^{-2}
90	3.15×10^{-4}	1.54×10^{-1}	1.88×10^{-3}

Underlined values represent mean viable counts in unirradiated controls.

Table 37. Fig. 78. Lipid peroxidation in irradiated fibroblasts following near-UV irradiation of GM 730 (78a) or AR6L0 (78b) fibroblasts.

	NUV exposure time (min)	PV per 10^6 cells (meq kg^{-1})	NUV time	PV per 10^6 cells (meq kg^{-1})	NUV time	PV per 10^6 cells (meq kg^{-1})
		(i) 9.85×10^5*		(ii) 3.0×10^6*		(iii) 1.6×10^6*
78a)	90	0.0030	80	0.0025	60	0.0007
	150	0.0063	160	0.0090	120	0.0060
	210	0.0120	260	0.0150	210	0.0137
	270	0.0167	300	0.0200	300	0.0190
		(i) 1.7×10^6*		(ii) 6.0×10^5*		(iii) 1.5×10^6
78b)	60	0.0006	60	0.0018	60	0.0020
	120	0.0056	120	0.0056	180	0.0090
	180	0.0070	180	0.0081	270	0.0150
	240	0.0110	270	0.0166	120	0.0057

* Cell concentration (ml^{-1})
(i), (ii),(iii) are data from separate experiments with each fibroblast strain.

Table 38. Fig. 79. The effect of DABCO on lipid peroxidation during near-UV irradiation of GM 730 (79a) or AR6LO (79b) fibroblasts.

NUV exposure time (min)	PV per 10^6 cells (meq kg^{-1})			
	-DABCO	+DABCO	-DABCO	+DABCO
79a)	(i) 9.8 x 10^5*		(ii) 1.6x10^6*	
60	-	-	0.0006	0
90	0.0030	0	-	-
120	-	-	0.0070	0.0003
150	0.0062	0	-	-
210	0.0120	0.0074	0.0136	0.0031
240	-	-	0.0160	0.0096
270	0.0167	0.0107	-	-
79b)	(i) 1.7x10^6*		(ii) 1.0x10^6*	
60	0.0006	0	0.0009	0
120	0.0056	0.0007	0.0051	0.0006
180	0.0070	0.0018	-	-
210	-	-	0.0105	0.0025
240	0.0110	0.0064	0.0132	0.0086

* cell concentration (ml^{-1})

(i) and (ii) are data from separate experiments. Data from (i) is plotted in Fig. 79a and 79b.

Table [39]. Fig. 80. The effect of D_2O on lipid peroxidation during near-UV irradiation of GM730 (80a) or AR6LO (80b) fibroblasts.

NUV exposure time (min)	PV per 10^6 cells (meq kg^{-1})			
	$-D_2O$	$+D_2O$	$-D_2O$	$+D_2O$
80a)	(i) 1.5 x 10^6*		(ii) 3.3x10^6*	
30	0	0.0002	-	-
90	0.0015	0.0034	-	-
120	-	-	0.0021	0.0039
150	0.0070	0.0080	-	-
180	-	-	0.0096	0.0109
240	0.0153	0.0162	0.0142	0.0159
80b)	(i) 2.0x10^6*		(ii) 2.4x10^6*	
60	0.0015	0.0016	0.0019	0.0022
120	0.0075	0.0075	0.0082	0.0099
180	0.0098	0.0107	0.0120	0.0133
240	0.0130	0.0150	0.0151	0.0172

* cell concentration (ml^{-1})

(i) and (ii) are data from separate experiments. Data from (i) is plotted in Fig. 80a and 80b.

Table 40. Fig. 81. The effect of growth in BSO medium on lipid peroxidation during near-UV irradiation of GM730 (81a) or AR6LO (81b) fibroblasts.

NUV exposure time (min)	PV per 10^6 cells (meq kg^{-1})			
	- BSO	+ BSO	- BSO	+ BSO
81a)	(i) 3.0 x 10^6*		(ii) 1.6x10^6*	
60	-	-	0.0011	0.0047
80	0.0025	0.0040	-	-
120	-	-	0.0071	0.0096
160	0.0090	0.0170	-	-
200	-	-	0.0220	0.0335
260	0.0150	0.0300	-	-
330	0.0200	0.0320	-	-
81b)	(i) 2.4x10^6*		(ii) 2.9x10^6*	
60	0.0017	0.0040	0.0020	0.0036
120	0.0055	0.0150	0.0059	0.0162
180	0.0081	0.0200	0.0095	0.0210
240	0.0166	0.0259	0.0170	0.0265

* cell concentration (ml^{-1})

(i) and (ii) are data from separate experiments. Data from (i) is plotted in Fig. 81a and 81b.

Table 41. Fig. 83. Endocytosis of ^{14}C-sucrose by GM730 fibroblasts at 37°C (83a) and 4°C (83b)

	Irradiated cells		Unirradiated controls	
	Time (min)	dpm per cell x10^4	Time (min)	dpm per cell x10^4
(i) 2.0x10^5*				
83a	5	0.9	3	0
	9	0.9	9	0
	13	13.6	16	0.7
	20	28.9	29	9.3
	25	44.8	45	22.3
	55	74.4	53	23.1
(ii) 2.4x10^5*				
	20	30.4	20	6.9
	40	55.4	40	12.4
	60	70.1	60	14.7
	80	75.5	80	28.5
(iii) 1.9x10^5*				
			25	8.7
			30	10.5
			35	13.9
			50	14.9
			60	16.3
			90	26.6
83b (i) 2.0x10^5*				
	4	1.05	4	0.15
	6	1.80	6	2.25
	15	0.15	15	1.35
	25	0	25	0.15
	45	0.30	45	1.65
	60	0.60	60	1.0

(i), (ii) and (iii) are data from 3 separate experiments.

* cell count, per plate.

Table 42. Fig. 84. Endocytosis of ^{14}C-sucrose by AR6LO fibroblasts at 37° (84a) and 4° (84b).

	Irradiated cells		Unirradiated controls	
	Time (min)	dpm per cell x10^4	Time (min)	dpm per cell x10^4
(i) 3.0x10^5*				
84a	5	18.2	5	7.7
	10	22.0	10	10.4
	20	27.0	20	10.9
	35	42.0	35	29.3
	60	64.1	60	29.7
	90	83.8	90	26.4
(ii) 3.5x10^5*				
	5	6.0	5	3.2
	10	16.0	10	9.5
	18	22.0	18	9.8
	26	40.0	26	23.1
	40	48.0	40	27.3
	60	59.0	60	31.4
	80	73.0	80	35.0
(i) 1.5x10^5*				
84b	5	2.6	5	1.8
	10	1.4	10	1.4
	18	1.1	15	0
	26	0.4	22	3.6
	39	3.4	37	0
	80	1.0	60	0

* cell count, per plate

(i) and (ii) show data from 2 separate experiments

Table 43. Fig. 85. The effect of growth in vitamin E on endocytosis of ^{14}C-sucrose following near-UV irradiation of AR6LO (85a) or GM730 (85b) fibroblasts.

NUV exposure time (min)	dpm per cell x 10^4 Irradiated cells - Vit E	Irradiated cells + Vit E	Unirradiated cells - Vit E	Unirradiated cells + Vit E
85a) (i) 2.2 x 10^5*				
20	21.9	18.5	15.0	17.0
40	46.1	33.1	23.5	21.0
60	52.2	44.8	33.7	27.6
90	71.7	54.1	43.3	46.9
(ii) 1.8x10^5*				
30	20.9	17.5	10.9	10.1
60	37.6	30.2	15.8	14.9
90	58.8	55.6	25.3	25.9
120	71.8	65.2	32.4	33.2
85b) (i) 2.3x10^5*				
20	30.3	26.4	9.6	7.4
40	52.1	48.1	14.2	15.2
60	59.6	60.9	16.4	23.8
80	64.1	65.6	28.4	26.1
(ii) 1.3x10^5				
20	31.4	28.0	13.1	11.2
40	50.6	47.3	17.2	18.1
60	57.4	58.6	26.8	25.7
80	61.4	62.7	29.7	27.7

* cell concentration (ml^{-1})
(i) and (ii) are data from separate experiments. Data from (i) is plotted in Fig. 85a and 85b.

Table 44. Fig. 86. Exocytosis of ^{14}C-sucrose by GM730 fibroblasts following near-UV irradiation. Incubation at 37° (86a) and 37° and 4° (86b).

Time (min)	dpm per cell x 10^4 Irradiated cells	Unirradiated controls
86a) (i) 7.2×10^5*		
2	2.7	7.6
12	21.1	14.1
25	39.7	18.0
45	53.8	18.9
60	61.4	19.3
80	64.3	19.7
105	67.9	20.0
125	69.4	20.5
150	71.6	21.1
(ii) 1.0×10^6*		
12	35.3	14.1
25	43.1	20.3
45	46.7	21.6
60	58.9	22.1
80	61.0	22.5
105	63.3	22.8
125	64.4	23.3
180	66.0	23.9

86b) (i) 9.0×10^5*				
	4°C	37°C	4°C	37°C
5	1.4	19.0	1.0	6.5
10	4.6	32.6	2.6	9.5
15	7.0	43.3	3.6	12.5
20	7.7	48.1	4.7	17.0
30	8.3	52.7	5.7	20.5
40	8.7	57.6	7.0	21.4
60	8.7	57.7	10.2	21.4
80	-	59.2	-	22.1

* Cell concentration (per plate)
(i) and (ii) show data from separate experiments.

Table 45. Fig. 87. Exocytosis of ^{14}C-sucrose by AR6L0 cells following near-UV irradiation. Incubation at 37° (87a) and 37° and 4° (87b).

Time (min)	dpm per cell x 10^4 irradiated cells	unirradiated controls
87a. (i) 6.6×10^5*		
5	4.2	3.8
10	8.1	7.7
20	17.1	15.6
30	48.5	23.5
45	56.4	25.3
60	57.7	26.0
90	58.9	27.8
120	61.6	29.6
165	63.9	30.4
(ii) 1.1×10^6*		
3	2.2	1.4
9	9.0	6.7
15	17.5	12.3
20	26.2	17.8
30	35.8	23.6
45	44.5	25.7
60	52.6	27.8
105	58.5	28.2
130	63.0	28.3
165	66.0	28.4

87b. (i) 1.1×10^6*

	4°	37°	4°	37°
5	2.6	7.7	2.6	5.4
10	5.0	16.3	3.9	12.2
15	6.4	18.2	5.4	17.8
20	-	-	-	21.9
30	7.2	37.2	6.0	23.8
45	8.0	54.5	6.8	24.7
60	8.6	59.2	7.8	25.7

* cell concentration (per plate)
(i) and (ii) show data from two separate experiments.

Table 46. Fig. 88. Exocytosis of ^{14}Csucrose by fibroblasts following far-UV irradiation of GM730 (88a) and AR6L0 (88b) fibroblasts.

Time (min)	dpm per cell x 10^4 Irradiated cells	Unirradiated cells
88a. 1.6×10^6*		
5	8.3	7.0
10	12.7	11.5
20	17.0	15.9
30	18.1	17.2
45	19.7	18.3
60	21.2	19.5
80	21.9	20.5
88b. 2.1×10^6*		
5	6.4	8.3
10	8.6	10.8
20	11.4	14.0
34	14.9	17.3
53	18.4	19.6
70	21.9	22.2

* cell concentration (per plate)

Table 47. Fig. 89. The dose response of exocytosis of ^{14}C sucrose by GM730 fibroblasts with increasing fluences of near-UV radiation.

89a. cell concentration 9.5 x 10^5 (per plate)

Time (min)	dpm per cell x 10^4 Time of irradiation (min) 20	30	50	unirradiated
5	14.3	23.6	34.4	13.6
10	20.9	28.5	46.4	18.7
20	26.3	36.8	80.6	25.1
30	29.9	44.7	90.8	29.9
40	39.9	49.2	95.0	32.0

89b cell concentration 1.9 x 10^6 (per plate

Time (min)	dpm per cell x 10^4 Time of irradiation (min) 10	15	20	25	60	unirradiated
5	3.2	4.9	6.0	5.2	8.0	3.6
10	6.4	7.4	11.4	8.8	33.2	7.3
15	9.4	12.1	17.6	16.6	59.3	12.4
20	12.5	16.0	21.0	23.0	69.2	16.1
40	17.7	21.7	26.7	28.1	79.2	19.9
60	26.9	24.9	31.8	32.7	85.1	21.9
75	-	-	34.9	-	-	-
85	30.9	-	-	-	-	22.0

Table 48 . Fig.90. The dose-response of exocytosis of ^{14}C-sucrose by AR6LO cells with near-UV irradiation.

Fig. 90a. Cell concentration 1.6 x 10^6 (per plate).

Time (min)	dpm per cell x 10^4 Time of irradiation (min) 20	40	50	Unirradiated
5	8.7	8.2	13.4	4.7
10	16.3	14.5	23.4	6.8
20	20.2	20.0	44.5	11.6
30	21.7	27.4	54.2	16.0
45	23.9	32.0	63.9	18.0
60	25.6	36.0	67.5	18.8
75	28.5	40.0	69.0	20.5
100	31.3	45.0	71.0	24.7

Fig. 90b. Cell concentration 1.0 x 10^6 (per plate).

Time (min)	dpm per cell x 10^4 Time of irradiation (min) 15	30	55	Unirradiated
5	7.4	7.8	12.1	5.8
10	10.3	12.0	30.0	8.9
20	14.5	17.8	37.0	13.0
30	16.9	24.0	52.5	15.0
40	19.2	28.1	68.7	20.8
60	21.4	32.0	77.7	21.2
90	22.0	36.1	89.1	22.0

Table 49. Fig. 92. The effect of growth in Vitamin E on the exocytosis of ^{14}C-sucrose by GM730 cells (92a) and AR6LO (92b) following near-UV irradiation.

Time (min)	dpm per cell x 10^4 irradiated cells - Vit E	irradiated cells + Vit E	unirradiated controls - Vit E	unirradiated controls + Vit E
92a. (i) 1.5 x 10^6*				
10	26.8	20.0	6.6	8,2
20	43.4	41.5	10.1	13.0
40	57.6	59.6	15.5	16.2
60	68.8	66.7	24.3	22.0
75	74.3	70.4	29.4	26.0
90	77.4	71.6	34.0	30.2
100	80.0	73.9	36.9	33.6
(ii) 5.5 x 10^5*				
10	24.9	25.3	8.2	8.0
20	42.0	40.9	9.4	11.4
30	56.9	53.1	10.7	13.3
40	59.0	58.0	14.0	16.5
50	74.3	66.2	15.4	18.3
60	77.6	72.2	25.4	25.2
70	80.1	77.6	27.6	26.9
100	84.9	82.0	30.0	28.9
92b. (i) 2.2 x 10^6*				
10	31.8	21.3	13.7	14.2
30	44.2	28.0	19.2	20.5
40	50.0	32.9	24.2	24.4
60	54.9	36.6	25.9	26.5
100	54.7	39.7	28.2	28.7
(ii) 2.8 x 10^6*				
10	25.3	18.5	12.5	10.7
20	31.8	23.2	16.1	15.0
30	41.8	30.7	18.9	17.5
45	51.7	38.9	22.1	21.1
60	60.0	43.2	25.0	24.3
75	62.9	53.2	28.2	28.2
90	65.0	55.7	28.5	28.9

* cell concentration (per plate)
(i) and (ii) show data from separate experiments. Data from (i) is plotted in Fig. 92a and 92b.

Table 50. Fig. 93. The effect of growth in Trolox-C on the exocytosis of ^{14}C-sucrose by GM730 cells (93a) and AR6LO (93b) following near-UV irradiation.

Time (min)	dpm per cell x 10^4 irradiated cells - Trolox-C	irradiated cells + Trolox-C	unirradiated controls - Trolox-C	unirradiated controls + Trolox-C
93a. (i) 2.0 x 10^6*				
10	13.1	12.9	6.5	7.1
20	28.2	25.8	10.0	9.5
30	32.9	31.5	18.8	11.2
40	47.8	40.7	12.6	13.3
50	50.7	49.6	18.0	17.9
60	56.4	53.2	20.7	21.6
80	62.6	54.6	22.6	23.4
100	68.2	57.5	23.4	23.6
(ii) 1.7 x 10^6*				
10	13.8	16.1	7.7	8.9
20	30.0	30.5	10.0	10.5
30	33.8	32.7	10.5	12.2
40	48.8	41.6	13.3	12.7
50	52.7	47.7	19.4	16.1
60	58.8	51.1	21.1	20.5
70	62.2	55.0	23.3	23.9
80	66.6	58.3	27.2	26.1
93b. (i) 1.3 x 10^6*				
10	11.6	4.9	5.7	6.2
20	27.8	10.0	9.7	11.4
30	44.9	14.3	14.4	14.4
40	50.6	17.7	18.7	17.5
70	56.9	21.0	23.6	22.1
85	57.1	25.3	27.9	25.7
(ii) 1.9 x 10^6*				
20	25.7	10.1	11.0	9.8
40	50.3	13.9	15.1	13.2
60	55.1	18.1	19.0	16.8
80	78.5	21.7	24.0	21.3
100	82.1	28.1	26.0	26.6

* cell concentration (per plate)
(i) and (ii) show data from separate experiments. Data from (i) is plotted in Fig. 93a and 93b.

Table 51. Fig. 94. The effect of irradiation in D_2O on the exocytosis of ^{14}C-sucrose by GM730 cells (94a) and AR6L0 (94b) fibroblasts following near-UV irradiation.

Time (min)	dpm per cell x 10^4 irradiated cells − D_2O	irradiated cells + D_2O	unirradiated controls − D_2O	unirradiated controls + D_2
94a. (i) 1.2 x 10^6*				
5	8.4	8.4	4.2	3.4
10	13.9	14.7	8.5	6.4
15	16.4	18.5	11.5	10.2
20	18.4	21.0	14.0	12.2
25	20.7	23.4	15.4	14.4
35	22.9	25.5	17.8	15.8
45	25.1	27.7	19.0	17.2
55	26.5	29.2	20.7	19.5
85	27.8	30.6	22.4	21.4
(ii) 2.0 x 10^6*				
10	13.5	13.9	8.9	9.1
20	19.0	22.1	14.3	14.6
30	22.1	26.5	17.5	17.2
40	25.5	28.2	18.8	18.9
50	27.1	32.4	19.7	20.1
60	27.9	33.2	20.9	21.2
70	28.2	34.1	21.5	22.0
80	28.5	34.6	22.0	23.2
94b. (i) 1.9 x 10^6*				
5	26.5	26.6	4.1	4.3
10	29.0	29.9	8.2	7.8
15	33.9	36.4	11.8	13.1
25	36.4	39.8	17.9	18.3
40	39.2	44.6	21.5	21.9
60	39.9	46.7	22.0	22.2
(ii) 1.5 x 10^6*				
10	27.5	29.8	9.2	8.9
20	3.23	38.7	14.9	14.5
30	36.5	42.5	20.1	19.8
45	39.2	46.3	20.6	20.5
60	41.3	47.2	20.9	21.2
70	42.0	48.1	21.2	21.6

* cell concentration (per plate)
(i) and (ii) show data from separate experiments. Data from (i) is plotted in Fig. 94a and 94b.

Table 52. Fig. 95. The effect of growth in BSO-medium on the exocytosis of ^{14}C-sucrose by GM730 cells (95a) and AR6LO (95b) following near-UV irradiation.

Time (min)	dpm per cell x 10^4 irradiated cells - BSO	irradiated cells + BSO	unirradiated controls - BSO	unirradiated controls + BSO
95a. (i) + BSO: 3.2 x 10^6, - BSO: 4.0 x 10^6*				
10	6.6	11.0	6.2	9.0
20	12.2	26.1	11.4	15.5
40	23.4	56.3	16.5	24.7
60	41.6	62.3	19.2	28.5
80	46.5	66.5	22.4	31.5
100	49.0	69.0	26.1	32.0
(ii) + BSO: 1.2 x 10^6, - BSO, 1.9 x 10^6*				
10	15.1	18.2	9.0	6.9
20	21.0	30.1	13.0	11.9
30	31.1	43.1	18.9	15.1
40	41.6	58.8	22.0	19.0
50	51.7	66.5	25.0	22.0
60	52.9	68.8	29.1	22.6
80	53.4	69.9	30.2	22.9
100	54.0	71.8	30.5	23.1
95b. (i) + BSO: 1.5 x 10^6, - BSO: 1.7 x 10^6*				
5	14.9	17.0	4.3	6.0
10	21.0	24.6	7.0	10.2
15	26.2	29.6	10.5	12.5
20	30.4	33.4	14.0	16.0
30	35.2	36.8	17.6	19.4
45	41.8	41.6	21.0	22.8
60	45.7	45.4	23.8	26.0
75	49.5	50.2	27.3	29.0
100	53.8	55.0	30.7	32.2
(ii) + BSO: 1.1 x 10^6, - BSO: 1.5 x 10^6*				
10	20.2	20.8	11.9	13.8
20	34.1	35.1	17.4	19.1
30	39.0	40.2	20.0	21.2
40	42.0	42.4	23.0	24.2
50	43.0	43.4	26.7	27.1
60	44.4	45.3	30.7	31.0
80	45.1	45.6	32.4	32.6
100	46.0	46.6	32.7	32.9

* cell concentration (per plate)
(i) and (ii) show data from separate experiments. Data from (i) is plotted in Fig. 95a and 95b.

Table 53. Fig. 96. The production of MDA or hydrop-eroxides after BLB (96a) or 303 nm (96b) irradiation

	Time (min)	MDA (μg)	Time (min)	PV ($meqkg^{-1}$)
96a)				
	10	0.24	5	0.067
	20	0.4	10	0.10
	30	0.70	15	0.13
	42	0.98	20	0.19
	52	1.37	30	0.30
96b)	Fluence	MDA (μg)	Fluence	PV ($meqkg^{-1}$)
	2.1	.042	2.1	0.010
	3.7	.095	3.7	0.019
	5.0	.108	5.0	0.026
	6.9	.148	6.9	0.036
	7.2	.152	7.2	0.042
	14.6	0.42	14.6	0.097

Table 54. Fig. 97. Dose response, linolenic acid, TBA-reacting products.

(a) $1x10^{-2}$ M Linolenic acid		(b) $1x10^{-3}$ M Linolenic acid		(c) $1x10^{-4}$ M Linolenic acid	
Time of irradiation (min)	MDA (µg)	Time of irradiation (min)	MDA (µg)	Time of irradiation (min)	MDA (µg)
1	0.217	2.5	0.050	15	0.003
3	0.437	5	0.085	30	0.080
4	0.575	7.5	0.117	45	0.120
5	0.785	10	0.195	60	0.165
		12.5	0.235		

Table 55. Figs. 98 and 100. The optical densities (560 nm) following the hydroperoxide assay of linoleic acid (Fig. 98) or liposomes (Fig. 100), either irradiated (I) or unirradiated (C) samples, bubbled with air or nitrogen.

Time after irradiation (hours)	Sample	Linoleic acid		Liposomes	
		N_2	Air	N_2	Air
0	I	0.230	0.267	0.022	0.030
	C	0.093	0.130	0.022	0.022
1	I	0.251	0.398	0.023	0.053
	C	0.102	0.168	0.024	0.033
2	I	0.265	0.490	0.022	0.082
	C	0.103	0.207	0.023	0.027
3	I	0.272	0.580	0.022	0.113
	C	0.102	0.240	0.023	0.027
4	I	0.287	0.665	0.025	0.150
	C	0.101	0.280	0.024	0.038
5	I	-	-	-	-
	C	-	-	-	-
6	I	0.293	0.761	0.026	0.253
	C	0.095	0.342	0.023	0.050
7	I	0.279	0.805	-	-
	C	0.100	0.379	-	-
8	I	0.278	0.836	0.015	0.500
	C	0.101	0.400	0.026	0.100

Table 56 . Fig. 99. Peroxide values of irradiated linoleic acid.

	Time following irradiation (hours)	PV meq kg^{-1} Bubbled with N_2	Air
99a)	0	0.012	0.015
	1	0.017	0.017
	2	0.018	0.027
	3	0.018	0.042
	4	0.019	0.045
	5	0.021	0.066
	6	0.030	0.070
	8	0.032	0.081
99b	0	0.0095	0.0095
	1	0.0093	0.0094
	2	0.0093	0.0093
	4.25	0.0094	0.031
	5.25	0.0094	0.041
	7	0.0095	0.097
	8	0.0095	0.120
99c	0	0.087	0.088
	1	0.092	0.142
	2	0.102	0.209
	3	0.118	0.217
	4	0.119	0.245
	6	0.127	0.264
	7	0.114	0.271
	8	0.113	0.275
99d	0	0.117	0.134
	1	0.111	0.148
	2	0.111	0.165
	3	0.113	0.180
	4.5	0.115	0.217
	6	0.115	0.274
	7.75	0.116	0.305

Table 57. Figs. 101-103. PV of liposomes in post-irradiation period.

Time after irradiation (hours)	Fig. 101a λ = 290 nm		Fig. 101b λ = 297 nm
	(1.1×10^{22} Qm^{-2})	(8.5×10^{21} Qm^{-2})	(2.26×10^{22} Qm^{-2})
0	0	0	0.008
1	0	0	0.031
2	-	-	0.117
2.3	0.040	-	-
3	0.094	0.023	0.376
3.5	-	0.0033	-
3.75	0.233	-	-
4	-	0.046	0.419
4.25	0.287	-	-
4.5	-	0.060	-
4.75	0.338	-	-

Fig. 102a: λ = 303 nm

	(6.3×10^{22} Qm^{-2})	(3.0×10^{22} Qm^{-2})	(7.2×10^{22} Qm^{-2})
0	0.028	0	0
0.5	-	-	0.020
1	-	0.015	-
1.5	-	-	0.044
2	0.046	0.041	0.089
2.5	-	-	0.140
3	0.112	0.068	0.204
3.5	-	-	0.245
3.75	0.189	-	-
4	-	0.105	0.330
5	-	-	-
5.5	0.283	-	-
6	-	0.228	-
7	-	-	-

Table 58.

Fig. 102b: λ = 313 nm

Time after irradiation (hours)	($5.78 \times 10^{22} Qm^{-2}$)	($2.75 \times 10^{22} Qm^{-2}$)
0	0	0.004
0.5	-	-
1	0.015	0.022
1.5	-	-
2	0.036	0.034
2.5	-	-
3	0.096	0.069
3.5	-	-
3.75	-	-
4	0.173	0.110
5	0.244	0.159
5.5	-	-
6	-	-
7	0.470	0.392

Table 59.

Time after irradiation (hours)	Fig. 103a: λ = 334 nm			Fig. 103b: λ = 365 nm	
	(3.1×10^{22} Qm^{-2})	(4.2×10^{22} Qm^{-2})	(6.6×10^{22} Qm^{-2})	5.9×10^{22} Qm^{-2})	(4.35×10^{23} Qm^{-2})
0	0	0	0	0	0
0.3	–	–	0	–	–
0.5	0.003	0.001	–	0	–
1.0	–	–	–	–	0.006
1.3	–	–	0.007	–	–
1.5	–	0.001	–	0	0.140
1.75	0.003	–	–	–	–
2.0	–	–	–	–	0.314
2.5	–	–	0.055	0.003	0.475
3.0	0.004	–	–	–	0.507
3.25	–	–	0.130	–	–
3.5	–	–	–	0.069	–
4.0	0.004	–	–	0.129	–
4.5	–	–	0.225	0.178	–
5.0	0.004	–	–	–	–
5.25	–	0.032	–	–	–
5.5	–	–	0.300	–	–

Table 60. Fig. A4. Survival of E. coli K1060 following irradiation with new lamps, viability assessed on YENB.

NUV exposure time (min)	Fatty acid incorporated: oleic (i)	oleic (ii)	linoleic (i)	linoleic (ii)	linolenic (i)	linolenic (ii)
0	6.85×10^{6}	1.88×10^{7}	7.01×10^{6}	7.91×10^{6}	1.15×10^{7}	1.04×10^{7}
10	9.81×10^{-1}	9.21×10^{-1}	-	5.32×10^{-1}	5.51×10^{-2}	8.09×10^{-2}
15	-	-	7.51×10^{-1}	-	1.32×10^{-2}	-
20	7.23×10^{-1}	7.92×10^{-1}	-	1.95×10^{-1}	1.00×10^{-2}	9.52×10^{-3}
30	5.21×10^{-1}	6.66×10^{-1}	6.00×10^{-2}	4.93×10^{-2}	2.74×10^{-3}	1.76×10^{-3}
40	3.10×10^{-1}	6.30×10^{-1}	7.62×10^{-3}	6.49×10^{-3}	2.43×10^{-4}	2.41×10^{-4}
45	-	-	1.99×10^{-3}	-	-	-
50	1.92×10^{-1}	7.32×10^{-2}	-	2.53×10^{-3}	1.12×10^{-4}	1.60×10^{-4}
60	-	4.85×10^{-3}	3.71×10^{-4}	-	3.70×10^{-5}	-
70	-	1.01×10^{-4}	-	-	-	-

Table 61. Fig. A5. Survival of E. coli K1060 following irradiation with new lamps, viability assessed on defined medium (normal salt).

NUV exposure time (min)	Fatty acid incorporated: oleic (i)	oleic (ii)	linoleic (i)	linoleic (ii)	linolenic (i)	linolenic (ii)
0	6.80×10^{6}	1.74×10^{7}	9.86×10^{6}	7.89×10^{6}	1.25×10^{7}	1.13×10^{7}
10	9.65×10^{-1}	6.51×10^{-1}	9.50×10^{-1}	8.82×1^{-1}	8.21×10^{-1}	7.19×10^{-1}
20	9.00×10^{-1}	9.20×10^{-1}	8.09×10^{-1}	-	4.62×10^{-1}	4.32×10^{-1}
30	7.66×10^{-1}	7.92×10^{-1}	6.01×10^{-1}	6.05×10^{-1}	1.51×10^{-1}	2.30×10^{-1}
40	4.71×10^{-1}	4.83×10^{-1}	1.85×10^{-1}	9.09×10^{-2}	5.00×10^{-2}	9.70×10^{-2}
50	3.84×10^{-1}	2.51×10^{-1}	-	1.81×10^{-2}	-	5.83×10^{-2}
60	-	1.91×10^{-2}	7.65×10^{-3}	4.10×10^{-3}	1.61×10^{-3}	-
70	-	6.30×10^{-5}	-	-	-	-

Table 62. Fig. A6. Survival of E. coli K1060 following irradiation with new lamps, viability assessed on high salt defined medium.

NUV exposure time (min)	Fatty acid incorporated: oleic (i)	oleic (ii)	linoleic (i)	linoleic (ii)	linolenic (i)	linolenic (ii)
0	6.75×10^{6}	8.20×10^{6}	6.95×10^{6}	9.60×10^{6}	1.30×10^{7}	1.07×10^{7}
10	1.00×10^{0}	1.00×10^{0}-	8.33×10^{-1}	7.97×1^{-1}	9.65×10^{-1}	7.16×10^{-1}
20	1.00×10^{0}	8.39×10^{-1}	6.75×10^{-1}	8.33×10^{-1}	5.86×10^{-1}	4.44×10^{-1}
30	9.93×10^{-1}	6.44×10^{-1}	5.29×10^{-1}	4.68×10^{-1}	2.34×10^{-1}	1.49×10^{-1}
40	6.24×10^{-1}	-	1.95×10^{-1}	1.56×10^{-1}	3.06×10^{-2}	5.16×10^{-2}
45	-	5.91×10^{-1}	-	-	-	-
50	5.10×10^{-1}	-	-	-	-	2.59×10^{-2}
60	-	1.53×10^{-1}	8.62×10^{-3}	7.41×10^{-2}	9.23×10^{-4}	-

Table 63. Fig. A7. Survival of E coli K1060 following irradiation with the new BLB lamps (a) 3 lamps, (b) 6 lamps

	NUV exposure time (min)	YENB	Surviving fraction normal salt defined medium	high salt defined medium
(a)	0	$\underline{1.34\times10^{7}}$	$\underline{1.35\times10^{7}}$	$\underline{1.37\times10^{7}}$
	20	4.32×10^{-1}	8.61×10^{-1}	7.09×10^{-1}
	40	6.63×10^{-2}	1.08×10^{0}	8.36×10^{-1}
	60	5.62×10^{-3}	7.31×10^{-1}	6.17×10^{-1}
	80	6.70×10^{-4}	2.43×10^{-1}	2.45×10^{-1}
	100	8.41×10^{-5}	5.36×10^{-3}	1.01×10^{-2}
(b)	0	$\underline{1.07\times10^{7}}$	$\underline{1.13\times10^{7}}$	$\underline{1.00\times10^{7}}$
	5	6.66×10^{-1}	-	-
	10	2.51×10^{-1}	9.43×10^{-1}	98.70×10^{-1}
	20	7.00×10^{-2}	9.51×1010^{-1}	8.09×10^{-1}
	30	9.02×10^{-3}	7.15×10^{-1}	8.00×10^{-1}
	40	4.62×10^{-4}	2.40×10^{-1}	2.03×10^{-1}
	50	1.11×10^{-4}	1.23×10^{-2}	1.41×10^{-2}

Underlined values represent mean viable counts of unirradiated controls.

REFERENCES

REFERENCES

Adelberg, E.A. and Burns, S.N. (1960). Genetic variation in the sex factor of E. coli. J. Bacteriol. **79**: 321-330.

Ahmad, S.I. (1981). The near-UV conversion of hydrogen peroxide to superoxide anion. Photochem. Photophys. **2**: 173.

Akamatsu, Y. (1974). Osmotic stabilization of unsaturated fatty acid auxotrophs of E. coli. J. Biochem. **76**: 553-561.

Ames, F.G. (1968). Lipids of Salm. typhimureum and E. coli: structure and metabolism. J. Bacteriol. **95**: 833-843.

Anderson, E.H. (1946). Growth requirements of virus-resistant mutants of E. coli strain B. Proc. Natl. Acad. Sci. (USA) **32**: 120-128.

Anderson, S.M. and Krinsky, N.I. (1973). Protective action of carotenoid pigments against photodynamic damage to liposomes. Photochem. Photobiol. **18**: 403-408.

Asakawa, T. and Matsushita, S. (1979). TBA test for detecting lipid peroxides. Lipids **14**: 401-406.

Asakawa, T. and Matsushita, S. (1980). A colorimetric micro-determination of peroxide values utilizing $AlCl_3$ as the catalyst. Lipids. **15**: 965-967.

Bachmann, B. (1972). Pedigrees of some mutant strains of E. coli. Bacteriol. Reviews **36**: 525-557.

Benga, G. (1986). In: "Structure and Properties of Cell Membranes". Volume III, Benga, G. Ed. CRC Press.

Besterman, J.M. and Low, R.B. (1983). Endocytosis. Biochem. J. **210**: 1-13.

Besterman, J.M., Airhart, J.A., Woodworth, R.C. and Low, R.B. (1981). Exocytosis of Pinocytosed fluid in cultured cells: kinetic evidence for rapid turnover and compartmentation. J. Cell. Biology. **91**: 716-727.

Black, H.S. (1987). Potential involvement of free radical reactions in ultraviolet light - mediated cutaneous dmamage. Photochem. Photobiol. **346**: 213-221.

Bligh, E.G. and Dyer, W.J. (1959). A rapid method of total lipid extraction and purification. Can. J. Biochem. Physiol. **37**: 911-917.

Botcherby, P.K., Magnus, I.A., Marimo, B. and Gianelli, F. (1984). Actinic reticuloid - An idiopathic photodermatosis with cellular sensitivity to near-ultraviolet radiation. Photoehcm. Photobiol. **39**: 641-649.

Bretscher, M.S. (1986). The moleculesof the cell membrane. Scientific American. August 1986.

Bretscher, M.S. and Raff. M.C. (1975). Mammalian Plasma Membranes. Nature **158**: 43-49.

Broekman, J.H.F.F. and Steenbackkers, J.F. (1973). Growth in high osmotic medium of an unsaturated fatty acid auxotroph of E. coli K-12. J. Bacteriol. **116**: 285-289.

Broekman, J.H.F.F. and Steenbakkers, J.F. (1974). Effects of the osmotic pressure of the growth medium in fab B mutants of E. coli. J. Bacteriol. **117**: 971-977.

Brown, M.S. and Webb, R.B. (1972). Photoreactivation of 365 nm inactivation in Escherichia coli. Mutat. Res. **15**: 348-352.

Carruthers, A. and Melchior, D.L. (1986). How bilayer lipids affect membrane protein activity. TIBS II. August 1986: 331-335.

Chan, J.T. and Black, H.S. (1977). Antioxidant-mediated reversal of ultraviolet light cytotoxicity. J. Invest. Dermatol. **68**: 366-368.

Chan, J.T., Chan, E.Y., Black. H.S. and Wyborny, L.E. (1980). Effects of lipid soluble antioxidants on cytoxoticity induced by photochemical products of cholesterol. Experientia **36**: 439-440.

Cohn, Z.A. and Steinman, R.M. (1982). In "Membrane Recycling", D. Evered and G.M. Collins, Ed. Pitman, U.K. Ltd.

Connor, M.J. and Wheeler, L.A. (1987). Depletion of cutaneous glutathione by ultraviolet radiation. Photochem. Photobiol. **46**: 239-245.

Coombs, A.M.L. and Moss, S.H. (1987). Effects of peroxide and catalase on near ultraviolet radiation sensitivity in E. coli strains. Int. J. Radiat. Biol. **51**: 493-503.

Cronan, J.E. (1968). Phospholipid alterations during growth of E. coli. J. Bacteriol. **95**: 2054-2061.

Cronan, J.E. and Gelmann, E.P. (1975). Physical properties of membrane lipids: Biological relevance and regulation. Bacteriol. Reviews **39**: 232-256.

Cronan, J.E. and Vagelos, P.R. (1972). Membrane phospholipids of E. coli. Biochim. Biophys. Acta **265**: 25-60.

Cunningham, M.L., Johnson, J.S., Giovanazzi, S.M. and Peak, M.J. (1985). Photosensitized production of superoxide anion by

monochromatic (290-405 nm) UV irradiaton of NADH and NADPH coenzymes. Photochem. Photobiol. **42**: 125-128.

Czapski, G. (1984). Reactions of $^{\cdot}OH$ in "Methods in Enzymology" 105. L. Packer, Ed. Academic Press, N.Y. pp. 210-215.

Dahle, L.D., Hill, E.G. and Holman, R.T. (1962). The thiobarbituric acid reaction and the autoxidations of polyunsaturated fatty acid methyl esters. Arch. Biochem. Biophys. **98**: 253-261.

Damoglou, A.P. and Dawes, E.A. (1968). Studies on the lipid content and phospholipid regulation of glucose. Biochem. J. **110**: 775-783.

Danpure, H.J. and Tyrrell, R.M. (1976). Oxygen-dependence of near-UV (365 nm) lethality and the interaction of near-UV and X-rays in two mammalian cell lines. Photochem. Photobiol. **23**: 171-177.

D'Aoust, J.Y., Giroux, J., Barran, L.R., Schneider, H. and Martin, W.G. (1974). Some effects of light on E. coli. J. Bacteriology. **120**: 799-804.

Davis, B.D., Dulbecco, R., Eisen, H.N. and Ginsberg, H.S. (1980). In "Microbiology" 3rd Ed. pp. 73-110. Harper and Row, Hagerstown.

DeLeo, V.A., Hanson, D., Weinstein, I.B. and Harber, L.C. (1985). U-V radiation stimulates the release of arachidonic acid from mammalian cells in culture. Photochem. Photobiol. **41**: 51-56.

DeLeo, V.A., Horlick, H., Hanson, D., Eisinger, M. and Harber, L.C. (1984). Ultraviolet radiation induces changes in membrane metabolism of human keratinocytes in culture. J. Invest. Dermatol. **83**: 323-326.

Desai, I.D., Sawant, P.L. and Tappel, A.L. (1964). Peroxidative and radiation damage to isolated lysosomes. Biochem. Biophys. Acta **86**: 277-285.

Dearden, S.J. and Hunter, T.F. (1981). Bilayer microviscosity changes due to O_2 ($^1\Delta g$) peroxidation in lipid vesicles. Chem. Phys. Lett. **81**: 606-609.

Dearden, S.J., Hunter, T.F. and Philp, J. (1985). Fatty acid analysis as a function of photo-oxidation in egg yolk lecithin vesicles. Photochem. Photobiol. **41**: 213-215.

Dennis, W.H. and Yatvin, M.B. (1981). Correlation of hyperthermic sensitivity and membrane microviscosity in E. coli K1060. Int. J. Radiat. **39**: 265-271.

Dobretsov, G.E., Borschevskaya, T.A., Petrov, V.A. and Vladimirov, Yn.A. (1977). The increase of phospholipid bilayer rigidity after lipid peroxidation. FEBS Letters **84**: 125-128.

Eichenberger, K., Bohni, P., Winterhalter, K.H., Kawato, S. and Richter, C. (1982). Microsomal lipid peroxidation causes an increase in the order of the membrane lipid domain. FEBS Letters **142**: 59-62.

Elias, P.M., Goerke, J. and Friend, D.S. (1977). Mammalian epidermal barrier layer lipids: composition and influence on structure. J. Invest. Dermatol. **69**: 535-546.

Epstein, W. and Davies, M. (1970). Potassium-dependent mutants of E. coli K12. J. Bacteriol. **101**: 836-843.

Erin, A.N., Skrypin, V.V. and Kagan, V.E. (1985). Formation of α-tocopherol complexes with fatty acids. Biochim. Biophys. Acta **815**: 209-214.

Filho, F., Elias, C.A. and deSouza, W. (1986). Effect of far-UV and near-UV radiation on the cell surface charge of the protozoan Trichomonas foetus. Photochem. Photobiol. **43**: 505-507.

Foote, C.S. (1979). Quenching of singlet oxygen. In: "Singlet Oxygen" H.H. Wasserman and R.W. Murray, Eds., Academic Press, New York, pp. 139-167.

Foote, C.S., Clough, R.L. and Yee, B.G. (1978). Photooxidation of tocopherols. In: "Tocopherol, Oxygen and Biomembranes". De Duve, C. and Hayaishi, O., eds.

Fralick, J.A. and Lark, K.G. (1973). Evidence for the involvement of unsaturated fatty acid in initiating the chromosome replication of E. coli. J. Mol. Biol. **80**: 459-475.

Frankel, E.N. (1984). Lipid oxidation: Mechanisms, products and biological significance. JAOCS **61**: 1908-1917.

Frankel, E.N. (1985). Chemistry of free radical and singlet oxidation of lipids. Prog. Lipid Res. **23**: 197-221.

Frankel, E.N. (1986). Lipid oxidation: Mechanisms, products and biological significance. J. Am. Oil Chemists Soc. **61**: 1908-1917.

Frankel, E.N. and Neff, W.E. (1983). Formation of malonaldehyde from lipid oxidation products. Biochim. Biophys. Acta **754**: 264-270.

Freeman, B.A. (1984). Biological sites and mechanisms of free radical production. In: "Free Radicals in Molecular Biology, Aging and Disease" D. Armstrong et al., Eds. Raven Press, New York.

Fridovich, I. (1975). Superoxide Dismutases. Ann. Rev. Biochem. **44**: 147-159.

Gange, R.W. and Rosen, C.F. (1986). UVA effects on mammalian skin and cells. Photochem. Photobiol. **43**: 701-705.

Giannelli, F., Botcherby, P.K., Marimo, B. and Magnus, I.A. (1983). Cellular hypersensitivity to UV-A: A clue to the aetiology of actinic reticuloid? Lancet **1**: 88-91.

Girotti, A.W., Thomas, J.P. and Jordan, J.E. (1985). Prooxidant and antioxidant effects of ascorbate on photosensitized peroxidation of lipids in erythrocyte membranes. Photochem. Photobiol. **41**: 267-276.

Goldstein, J.L., Anderson, R.G.W. and Brown, M.S. (1979). Coated pits, coated vesicles and receptor-mediated endocytosis. Nature **279**: 679-685.

Goni, F.M., Ondarroa, M., Azpiazu, I. and Macarulla, J.M. (1985). Phospholipid oxidation catalysed by cytochrome C in liposomes. Biochim. Biophys. Acta **835**: 549-556.

Griffith, D.W. and Meister, A. (1979). Potent and specific inhibition of glutathione synthesis by BSO. J. Biol. Chem. **254**: 7558-7560.

Grossman, A. and Wendel, A. (1984). Phospholipid hydroperoxides are not substrates for selenium-dependent glutathione peroxidase. In: "Oxygen Radicals in Chemistry and Biology" Walter de Gruyter and Co., Berlin.

Gutteridge, J.H.C., Stocks, J. and Dormandy, T.L. (1974). Thiobarbituric Acid reacting substances derived from

autoxidizing linoleic and linolenic acids. Analytica Chimica Acta **70:** 107-111.

Gutteridge, J.M. (1981). TBA reactivity following iron-dependent free-radical damage to amino acids and carbohydrates. FEBS Letters **128:** 343-348.

Gutteridge, J.M.C., Richmond, R., Halliwell, B. (1979). Inhibition of the iron-catalysed formation of hydroxyl radicals from superoxide and of lipid peroxidation by desferrioxamine. Biochem. J. **184:** 469-472.

Hakomori, S. (1986). Glycosphingolipids. Sci. American. 32-41.

Halliwell, B. and Gutteridge, J. (1984). Oxygen toxicity, oxygen radicals, transition metals and disease. Biochem. J. **219:** 1-14.

Halliwell, B. and Gutteridge, J.M.C. (1985). In: "Free Radicals in Biology and Medicine" Clarendon Press, Oxford.

Hansen, S. (1984). In: "Lipids of Plants and Microbes". Harwood, J.L. and Russel, N.J., Eds. Allen Unwin.

Hartman, P.S. and Eisenstark, A. (1978). Synergistic killing of E. coli by near-UV radiation and hydrogen peroxide: Distinction between recA-repairable and recA-nonrepairable damage. J. Bacteriol. **133:** 769-774.

Hartman, P.S., Eisenstark, A. and Pauw, P.G. (1979). Near-UV radiation plus hydrogen peroxide inactivation of phage T7: DNA-protein crosslinks prevent DNA injection. Proc. Natl. Acad. Sci. **76:** 3228-3232.

Harwood, J.L. and Russel, N.J. (1984). In: "Lipids of Plants and Microbes". Allen Unwin.

Henning, U., Dennert, G., Rehn, K. and Deppe, G. (1969). Effects of oleate starvation in a FA auxotroph of E. coli K12. J. Bacteriol. 98: 784-796.

Hill, R.F. and Feiner, R.R. (1964). Further studies of UV sensitive mutants of E. coli strain B. J. Gen. Microbiol. 35: 105-114.

Hodges, N.D.M. (1979). PhD Thesis, University of Bath.

Hoffman, M.E. and Meneghini, R. (1979). Action of hydrogen peroxide on human fibroblasts in culture. Photochem. Photobiol. 30: 151-155.

Hollaender, A. (1943). The effect of long ultraviolet and short visible radiation (3500-4900 A) on Escherichia coli. J. Bacteriol. 46: 531-541.

Ingledew, W.J. and Poole, R.K. (1984). The respiratory chains of E. coli. Microbiological Reviews 48: 222-271.

Ito, T. (1978). Cellular and subcellular mechanisms of photodynamic action: The $^1O_2$ hypothesis as a driving force in recent research. Photochem. Photobiol. 28: 493-508.

Ito, T. (1983). Photodynamic agents as tools for cell biology. In: "Photochemical and Photobiological Reviews" 7 Smith, K.C., Ed. Plenum Publishing Corporation. pp. 141-186.

Ito, A. and Ito, T. (1983). Possible involvement of membrane damage in the inactivation by broad-band near-UV radiation in Sacch. cerevisiae cells. Photochem. Photobiol. 37: 395-401.

Jacobson, A.F. and Yatvin, M.B. (1976). Changes in phospholipid composition of E. coli following and UV-irradiation. Rad. Res. 66: 247-266.

Jagger, J. (1967). In: "Introduction to research in ultraviolet photobiology" Prentice-Hall Inc., Englewood Cliffs, New Jersey. pp. 137-139.

Jagger, J. (1983). Physiological effects of near-ultraviolet radiation on bacteria. In: "Photochemical and Photobiological Reviews **7**, K.C. Smith, Ed. Plenum Press, New York, pp. 1-75.

Jagger, J. (1985). In: "Solar - UV Actions on Living Cells" Praeger Publishers, New York.

Jagger, J., Fossum, T. and McCaul, S. (1975). UV irradiation of suspensions of micro-organisms: Possible errors involved in the estimation of average fluence per cell. Photochem. Photobiol. **21**: 379-382.

Jones, C.W. (1982). In: "Bacterial Respiration and Photosynthesis" American Society for Microbiology, Washington D.C.

Kelland, L.R. (1984). PhD Thesis, University of Bath.

Kelland, L.R., Moss, S.H. and Davies, D.J.G. (1983a). An action spectrum for UV radiation-induced membrane damage in E. coli K12. Photochem. Photobiol. **37**: 301-306.

Kelland, L.R., Moss, S.H. and Davies, D.J.G. (1983b). Recovery of E. coli K12 from NUV radiation-induced membrane damage. Photochem. Photobiol. **37**: 617-622.

Kelland, L.R., Moss, S.H. and Davies, D.J.G. (1984). Leakage of $^{86}Rb^{+}$ after ultraviolet irradiation of E. coli K12. Photochem. Photobiol. **39**: 329-335.

Keyse, S.M., Moss, S.H. and Davies, D.J.G. (1983). Action spectra for the inactivation of normal and Xeroderma Pigmentosum human

skin fibroblasts by UV radiations. Photochem. Photobiol. **37:** 307-312.

King, M. and Spector, A. (1981). Lipid metabolism in cultured cells. In: "The growth requirements of vertebrate cells in vitro". R. Waymouth, P. Ham and N. Chapple, Eds. Cambridge University Press, pp. 293-312.

Klamen, D.L. and Tuveson, R.W. (1982). The effect of membrane fatty acid composition in the near UV (300-400 nm) sensitivity of E. coli K1060. Photochem. Photobiol. **35:** 167-173.

Kobayashi, K. and Ito, T. (1976). Further in vivo studies on the participation of singlet oxygen in the photodynamic inactivation and induction of genetic changes in Sacch. cerevisiae. Photochem. Photobiol. **23:** 21-28.

Koch, W.H. and Chedekel, M.R. (1987). Photochemistry and photobiology of melanogenic metabolites: formation of free radicals. Photochem. Photobiol. **46:** 229-238.

Konings, A.W.T. (1984). Lipid peroxidation in liposomes. In: "Liposome Technology Vol. I" G. Gregoradis, Ed. CRC Press.

Kornberg, R.D. and McConnell, H.M. (1971). Lateral diffusion of phospholipids in a vesicle membrane. Proc. Nat. Acad. Sci. U.S.A. **68:** 2564-2568.

Kralli, A. (1987). PhD Thesis, University of Bath.

Kralli, A. and Moss, S.H. (1987). The sensitivity of an actinic reticuloid cell strain to near-ultraviolet radiation and its modification by Trolox-C, a vitamin E analogue. British J. Dermatol. **116:** 761-772.

Krinski, N.I. (1985). Detection and biological function of active oxygen species. Photochem. Photobiol. **41**: 965.

Lagarde, M., Sicard, B., Guichardant, M., Felisi, O., and Dechavanne, M. (1984). Fatty acid composition in native and cultured human endothelial cells. In Vitro **20**: 33-37.

Lamola, A.A. (1977). Photodegradation of biomembranes. In: "Research in Photobiology" A. Castellani, Ed. Plenum Press, N.Y. pp. 53-63.

Lampe, M.A., Burlingame, A.L., Whitney, J., Williams, M.L., Brown, B.E., Roitman, E. and Elias, P.M. (1983). Human stratum corneum lipids: characterization and regional variations. J. Lipid Research **24**: 120-130.

Leyko, W. and Bartosz, G. (1986). Membrane effects of ionizing radiation and hyperthermia. Int. J. Radiat. Biol. **49**: 743-770.

Lindig, B.A. and Rodgers, M.A.J. (1981). Rate parameters for the quenching of $^1O_2$ by water soluble and lipid soluble substrates in aqueous and micellar systems. Photochem. Photobiol. **33**: 627-634.

Logani, M.K. and Davies, R.E. (1980). Lipid oxidation. Biological effects and antioxidants - A review. Lipids **15**(6): 485-495.

Machtiger, N.A. and Fox, F.C. (1973). Biochemistry of bacterial membranes. Ann. Rev. Biochem. **833**: 575-595.

Mackey, B.M. and Derrick, C.M. (1986). Peroxide sensitivity of cold-shocked Salm. typhimureum and E. coli and its relationship to minimal medium recovery. J. Appl. Bacteriol. **60**: 501-511.

Maisin, J.R. (1974). The influence of radiation on blood vessels and circulation: Chapter II: Ultrastructure of the vessel wall. Curr. topics in Radiation Res. Quarterly **10**: 29-57.

Mandal, T.K. and Chatterjee, S.N. (1980). UV and sunlight-induced lipid peroxidation in liposomal membranes. Radiat. Res. **83**: 290-302.

Marr, A.G. and Ingraham, J.L. (1962). Effect of temperature on the composition of fatty acids in E. coli. J. Bacteriol. **84**: 1260-1267.

Mavis, R.D. and Vagelos, P.R. (1972). The effect of phospholipid fatty acid composition on membranous enzymes in E. coli. J. Biol. Chem. **247**: 652-659.

Mbemba, F., Houbion, A., Raes, M. and Remacle, J. (1985). Sub-cellular localisation and modification with ageing of glutathione, glutathione peroxidase and glutathione reductase activities in human fibroblasts. Biochim. Biophys. Acta **838**: 211-220.

McAleer, M.A., Moore, S.P. and Moss, S.H. (1987). Effect of growth temperature on lipid composition and ultraviolet sensitivity of human cells. Photochem. Photobiol. **46**: 31-37.

McCay, P.B., Gibson, D.D., Fong, K. and Hornbrook, K.R. (1976). Effect of glutathione peroxidase activity on lipid peroxidation in biological membranes. Biochim. Biophys. Acta **431**: 459-468.

McCay, P.B., Li, E.K., Brueggemann, G. and Powell, S.R. (1987). A biological antioxidant function for vitamin E: Electron shuttling for a membrane-bound 'Free Radical Reductase'. In: "Advanced Technologies and their Nutritional Implications in

the Production of Edible Fats" NATO Advanced Research Workshop, Plenum Press, New York.

McCormick, J.P., Fischer, J.R., Pachlatko, J.P. and Eisenstark, A. (1976). Characterization of a cell-lethal product from the photooxidation of tryptophan: hydrogen peroxide. Science **191**: 468-469.

Mead, J.F. (1982). Mechanism of protection against membrane peroxidation. In: "Lipid Peroxides in Biology and Medicine" Yagi, K., Ed. Academic Press.

Meister, A. and Anderson, M.E. (1983). Glutathione. Ann. Rev. Biochem. **52**: 711-760.

Meffert, H., Diezel, W., Sonnichsen, N. (1976). Stable lipid peroxidation products in human skin: Detection, UV light-induced increase, pathogenic importance. Experientia **32**: 1397-1398.

Merkel, P.B., Nilsson, R. and Kearns, D.R. (1972). Deuterium effects on singlet oxygen lifetimes in solutions. A new test of singlet oxygen reactions. J. Am. Chem. Soc. **94**: 1030-1032.

Midden, W.R. (1985). Is singlet oxygen responsible for superoxide toxicity? Photochem. Photobiol. **41**: 805.

Minotti, G. and D'Aoust, S. (1987). The requirement for Iron (III) in the initiation of lipid peroxidation by Iron (II) and hydrogen peroxide. J. Biol. Chem. **262**: 1096-1104.

Morowitz, M.J. (1950). Absorption effects in volume irradiation of microorganisms. Science **111**: 229-230.

Moss, S.H. and Smith, K.C. (1981). Membrane damage can be a significant factor in the inactivation of E. coli by NUV

irradiation. Photochem. Photobiol. **33**: 203-210.

Munro, G.F. and Bell, C.A. (1973). Effects of external osmolarity on phospholipid metabolism in E. coli B. J. Bacteriol. **73**: 257-262.

Nunn, W.D. and Cronan, J.E. (1974). Unsaturated fatty acid synthesis is not required for induction of lactose transport in E. coli. J. Biol. Chem. **249**: 724-731.

Ohyashiki, T., Ushiro, H. and Mohri, T. (1986). Effects of α-tocopherol on the lipid peroxidation and fluidity of procine intestinal brush-border membranes. Biochim. Biophys. Acta **858**: 294-300.

Overath, P., Schairer, H.V. and Stoffel, W. (1970). Correlation of in vivo and in vitro phase transitions of membrane lipids in E. coli. Proc. Natl. Acad. Sci. (USA) **67**: 606-612.

Pastan, I. and Willingham, M.C. (1985). "Endocytosis" Plenum Press, New York.

Patrick, G. (1977). The effects of radiation on cell membranes. In: "Mammalian Cell Membranes" Vol. 5. G.A. Jamieson and D.M. Robinson, Eds. Butterworth, London, pp. 72-100.

Peak, M.J. and Peak, J.G. (1973). Protection by histidine from inactivation of DNA transforming activity by NUV light (365 nm) compared with far UV light (254 nm). Photochem. Photobiol. **18**: 525-527.

Peak, M.J. and Peak, J.G. (1980). Protection by glycerol against the biological actions of near-UV light. Radiat. Res. **83**: 553-558.

Peak, M.J. and Peak, J.G. (1982). Single strand breaks induced in Bacillus subtilis DNA by ultraviolet light. Action spectrum and properties. Photochem. Photobiol. **35**: 675-680.

Peak, J.G., Foote, C.S. and Peak, M.J. (1981). Protection by DABCO against inactivation of transforming DNA by NUV light: Action spectra and implications for the involvement of singlet oxygen. Photochem. Photobiol. **34**: 45-49.

Peak, M.J., Johnson, J.S., Tuveson, R.W. and Peak, J.G. (1987). Inactivation by monochromatic near-UV radiation of an E. coli hem A8 mutant grown with and without δ-ALA. The role of DNA vs. membrane damage. Photochem. Photobiol. **45**: 473-478.

Peak, M.J., Peak, J.G. and Cunningham, M.L. (1985). Solar-UV radiation generates superoxide anion after interaction with naturally occurring cellular photosensitizers. Photochem. Photobiol. **41**: 865.

Peak, J.G., Peak, M.J. and Foote, C.S. (1986). Observations on the photosensitized breakage of DNA by 2-thiouracil and 334 nm radiation. Photochem. Photobiol. **44**: 111-116.

Peak, J.G., Peak, M.J. and MacCoss, M. (1984). DNA breakage caused by 334 nm ultraviolet light is enhanced by naturally occurring nucleic acid components and nucleotide coenzymes. Photochem. Photobiol. **39**: 713-716.

Pearse, B.M.F. and Bretsher, M.S. (1981). Membrane recycling by coated vesicles. Ann. Rev. Biochem. **50**: 85-101.

Pereira, O.M., Smith, J.R. and Packer, L. (1976). Photosensitization of human diploid cell cultures by intracellular flavins

and protection by antioxidants. Photochem. Photobiol. **24**: 237-242.

Pooler, J.P. and Valenzeno, D.P. (1979). The role of singlet oxygen in photooxidation of excitable cell membranes. Photochem. Photobiol. **31**: 581-584.

Porter, N.A., Nixon, J. and Isaac, R. (1976). Cyclic peroxides and the TBA assay. Biochim. and Biophys. Acta **441**: 506-512.

Proctor, P.H. and Reynolds, E.S. (1984). Free radicals and disease in man. Physiol. Chem. Phys. Med. NMR **16**: 175-195.

Putvinsky, A.V., Sokolov, A.V., Roshchupkin, D.I. and Vladimorov, Y.A. (1979). Electric breakdown of bilayer phospholipid membranes under UV irradiation-induced lipid peroxidation. FEBS Letters **106**: 53-55.

Raleigh, J.A. and Kremers, W. (1978). Promotion of radiation peroxidation in models of lipid membranes by caesium and rubidium counter-ions. Int. J. Radiat. Biol. **34**: 439-446.

Redpath, J.L. and Patterson, L.K. (1978). The effect of membrane fatty acid composition on the radiosensitivity of E. coli K1060. Radiat. Research **75**: 443-447.

Rock, C.O. and Jackowski, S. (1985). Pathways for the incorporation of exogenous fatty acids into phosphatidylethanolamine in E. coli. J. Biol. Chem. **260**: 12720-12724.

Roshchupkin, D.I., Pelenitsyn, A.B., Potapenko, A.Y., Talitsky, V.V. and Vladimirov, Y.A. (1975). Study of the effects of UV light on biomembranes IV. The effect of oxygen on UV induced haemolysis and lipid photoperosication in rat erythrocytes and liposomes. Photochem. and Photobiol. **21**: 63-69.

Rosenfeld, I.S., D'Agnolo, G. and Vagelos, P.R. (1973). Synthesis of unsaturated fatty acids and the lesion in fab B mutants. J. Biol. Chem. **248:** 2452-2460.

Rosenstein, B.S., Ducore, J.M. and Cummings, S.W. (1983). The mechanism of bilirubin-photosensitized DNA strand breakage in human cells exposed to phototherapy light. Mutation Res. **112:** 397-406.

Roza, L., van der Schans, G.P. and Lohman, P.H. (1985). The induction and repair of DNA damage and its influence on cell death in primary human fibroblasts exposed to UVA or UVC radiation. Mutat. Res. **146:** 89-98.

Sakanashi, T., Sugiyama, M., Suematsu, T., Hidaka, T. and Ogura, R. (1986). Delayed alteration of membrane fluidity in intact cultured B-16 melanoma cells affected by UV irradiation. Biochemistry International **12:** 341-346.

Salet, C., Bazin, M., Moreno, G. and Favre, A. (1985). 4-Thiouridine as a photodynamic agent. Photochem. Photobiol. **41:** 617-619.

Sammartano, L.J. and Tuveson, R.W. (1984). The effects of exogenous catalase on broad spectrum near-UV (300-400 nm) treated Escherichia coli cells. Photochem. Photobiol. **40:** 607-612.

Sammartano, L.J. and Tuveson, R.W. (1985). Hydrogen peroxide induced resistance to broad spectrum near-ultraviolet (300-400 nm) inactivation in Escherichia coli. Photochem. Photobiol. **41:** 367-370.

Sanderman, H. (1978). Regulation of membrane enzymes by lipids. Biochim. Biophys. Acta **515:** 209-237.

Sato, M. and Takanashi, H. (1970). Cold shock of bacteria IV. Involvement of DNA ligase reaction in recovery of E. coli from cold shock. J. Gen. and App. Microbiology **16**: 279-290.

Schaich, K.M. and Borg, D.C. (1984). Radiomimetic effects of peroxidizing lipids on nucleic acids and their bases. In: "Oxygen Radicals in Chemistry and Biology" Walter de Gruyter and Co. Publishers, Berlin.

Schairer, H.U. and Overath, P. (1969). Lipids containing trans-unsaturated fatty acids change the temperature characteristics of thiomethylgalactoside accumulation in E. coli. J. Mol. Biol. **44**: 209-214.

Schieberle, P. and Grosch, W. (1985). Photolysis of unsaturated fatty acid hydroperoxides (2). Chemistry and Physics of Lipids. **37**: 99-114.

Schulz, H., Weeks, G., Toomey, R.E., Shapiro, M. and Wakil, S.J. (1969). Studies on the mechanism of fatty acid synthesis. J. Biol. Chem. **244**: 6577-6583.

Scott, J.A., Khaw, B., Homcy, C.J., Rabito, C.A. (1987). Oxygen radicals alter the cell membrane potential in a renal cell line. Biochim. Biophys. Acta **897**: 25-32.

Silverstein, S.C., Steinman, R.M. and Cohn, Z.A. (1977). Endocytosis. Ann. Rev. Biochem. **46**: 669-722.

Slater, T.F. (1976). In: "Recent Advnces in Biochemical Pathology: Toxic Liver Injury". Dianzani, M.U., Ugazio, G. and Sena, L.M. Eds. Minerva Medica. Turin.

Slater, T.F. (1984). Free-radical mechanisms in tissue injury. Biochem. J. **222**: 1-15.

Spikes, J.D. and Swartz, H.M. (1978). Review and general discussion from the international conference on singlet oxygen and related species in chemistry and biology. Photochem. Photobiol. **28**: 921-933.

Sprott, G.D., Martin, W.G. and Schneider, H. (1976). Differential effects of near-UV and visible light on the active transport and other membrane processes in E. coli. Photochem. Photobiol. **24**: 21-27.

Sprott, G.D. and Usher, J.R. (1977). The electrochemical proton gradient and phenylalanine transport in E. coli irradiated with near-ultraviolet light. Can. J. Microbiol. **23**: 1683-1688.

Steinman, R.M., Brodie, S.E. and Cohn, Z.A. (1976). Membrane flow during pinocytosis. J. Cell. Biol. **68**: 665-687.

Steinman, R.M., Mellman, I.S., Muller, W.A. and Cohn, Z.A. (1983). Endocytosis and the recycling of the plasma membrane. J. Cell. Biol. **96**: 1-27.

Steinman, R.M., Silver, J.M. and Cohn, Z.A. (1974). Pinocytosis in fibroblasts. J. Cell. Biol. **63**: 949-969.

Stoein, J.D. and Wang, R.J. (1974). Effect of near ultraviolet and visible light on mammalian cells in culture. II. Formation of toxic photoproducts in tissue culture medium by blacklight. Proc. Natl. Acad. Sci. (USA) **71**: 3961-3965.

Stubbs, C.D. and Smith, A.D. (1984). The modification of mammalian membrane polyunsaturated fatty acid composition in relation to membrane fluidity and function. Biochim. Biophys. Acta **779**: 89-137.

Sunamoto, J., Baba, Y., Iwamoto, K. and Kondo, H. (1985). Liposomal membranes XX. Autooxidation of unsaturated fatty acids in liposomal membranes. Biochim. Biophys. Acta **833**: 144-150.

Sutherland, J.C. and Griffin, K.P. (1981). Absorption spectrum of DNA for wavelengths greater than 300 nm. Radiation Res. **86**: 399-409.

Taber, H., Pomerantz, B.J. and Halfenger, G.M. (1978). Near-ultraviolet induction of growth delay studied in a menaquinone-deficient mutant of Bacillus subtilis. Photochem. Photobiol. **28**: 191-196.

Tappel, A.L. (1968). Will antioxidant nutrients slow aging processes? Geriatrics **23**: 97-105.

Taylor, F. and Cronan, J.E. 91976). J. Bacteriol. **125**: 518-523.

Thomas, J.M., Mehl, K.S. and Pryor, W.A. (1978). The role of superoxide anion in the xanthine oxidase-induced autooxidation of linoleic acid. Biochem. Biophys. Res. Comm. **83**: 927-936.

Tsai, S.C. and Jagger, J. (1981). The roles of the rel^+ gene and of 4-thiouridine in killing and photoprotection of E. coli by near-ultraviolet radiation. Photochem. Photobiol. **33**: 825-834.

Tuveson, R.W. and Sammartano, L.J. (1986). Sensitivity of hem A mutant E. coli cells to inactivation by near UV light depends on the level of supplementation with delta-amino levulinic acid. Photochem. Photobiol. **43**: 621-626.

Tyrrell, R.M. (1979). Lethal cellular changes induced by near ultraviolet radiation. Acta. Biol. Med. Germ. **38**: 1259-1269.

Tyrrell, R.M. (1985). A common pathway for protection of bacteria against damage by solar UVA (334 nm, 365 nm) and an oxidising

agent (H_2O_2). Mutation Research **145:** 129-136.

Tyrrell, R.M., Ley, R.D. and Webb, R.G. (1974). Induction of single strand breaks (alkali-labile bonds) in bacterial and phage DNA by near-UV (365 nm) radiation. Photochem. Photobiol. **20:** 395-398.

Tyrrell, R.M. and Pidoux, M. (1986). Endogenous glutathione protects human skin fibroblasts against the cytotoxic action of UVB, UVA and near-visible radiations. Photochem. Photobiol. **44:** 561-564.

Valenzeno, D.P. (1987). Photomodification of biological membranes with emphasis on singlet oxygen mechanisms. Photochem. Photobiol. **46:** 147-160.

Van der Zee, J., Dubbleman, T. and Steveninck, J. (1985). Peroxide-induced membrane damage in human erythrocytes. Biochim. Biophys. Acta **818:** 38-44.

Wagner, S., Feldman, A. and Snipes, W. (1982). Recovery from damage induced by acridine plus NUV light in E. coli. Photochem. Photobiol. **35:** 73-81.

Wagner, S., Taylor, W.D., Keith, A. and Snipes, W. (1980). Effects of acridine plus NUV light on E. coli membranes and DNA in vivo. Photochem. Photobiol. **32:** 771-779.

Wagner, S. and Snipes, W. (1982). Effects of acridine plus near-UV light on the outer membrane of E. coli. Photochem. Photobiol. **36:** 255-258.

Wang, R.J., Stoien, J.D. and Landa, F. (1974). Lethal effect of near-ultraviolet irradiation on mammalian cells in culture. Nature **1247:** 43-45.

Webb, R.B. (1977). Lethal and mutagenic effects of near-ultraviolet radiation. In: "Photochemical and Photobiological Reviews" K.C. Smith, Ed., Vol. 2, pp. 169-261. New York Plenum Press.

Webb, R.B. (1978). Near-UV mutagenesis: Photoreactivation of 365 nm-induced mutational lesions in E. coli WP2S. J. Bacteriol. **133**: 860-866.

Webb, R.B. and Brown, M.S. (1979). Action spectra for oxygen-dependent and independent inactivation of E. coli WP2s from 254 nm to 460 nm. Photochem. Photobiol. **29**: 407-409.

Webb, R.B. and Lorenz, J.R. (1970). Oxygen dependence and repair of lethal effects of near ultraviolet and visible light. Photochem. Photobiol. **12**: 283-289.

Wellner, V.P., Anderson, M.E., Puri, R.N., Jensen, G.L. and Meister, A. (1984). Radioprotection by glutathione ester. Transport of glutathione ester into human lymphoid cells and fibroblasts. Proc. natl. Acad. Sci. USA **81**: 4732-4735.

Wilbur, K.M., Bernheim, F. and Shapiro, O.W. (1949). The thiobarbituric acid reagent as a test for the oxidation of unsaturated fatty acids by various reagents. Arch. Biochem. **24**: 305-313.

Williams, K.E., Kidston, E.M., Beck, F. and Lloyd, J.B. (1975). Quantitative Studies of Pinocytosis. J. Cell. Biology **64**: 113-122.

Witting, L.A. (1980). Vitamin E and lipid antioxidants in free-radical-initiated reactions. In: "Free Radicals in Biology" W.A. Pryor, Ed. Vol. 4, Academic Press, N.Y., pp. 295-319.

Wolff, S.L. (1981). In: "Biology of the Cell" Wadsworth Publishing

Company Inc. Belmont, California.

Wolff, S., Garner, A. and Dean, R.T. (1986). Free radicals, lipids and protein degradation. TIBS II. January 1986: 27-31.

Wolters, H. and Konings, A.W.T. (1984). Radiosensitivity of normal and polyunsaturated fatty acid supplemented fibroblasts after depletion of glutathione. Int. J. Radiat. Biol. **46**: 161-168.

Yamamoto, Y., Niki, E., Kamiya, Y. and Shimasaki, H. (1984). Oxidation of lipids 7. Oxidation of phosphatidylcholines in homogenous solution and in water dispersion. Biochem. Biophys. Acta **795**: 332-340.

Yatvin, M.B. (1976). Evidence that survival of γ-irradiated E. coli is influenced by membrane fluidity. Int. J. Radiat. Biol. **30**: 571-575.

Yoshikawa, W., Akutsu, H., Kyogoku, Y. and Akamatsu, Y. (1985). An essential role of phosphatidylglycerol in the formation of the osmotically stable liposomes of E. coli phospholipids **821**: 277-285.